# Techniques and Instrumentation for Structure Determination

# Contents

## Articles

# References



# Article Licenses

# I.C. Baianu, Ph.D.,M.Inst.P., Editor (with listed contributors)

# Principles

## Crystal

A **crystal** or **crystalline solid** is a solid material whose constituent atoms, molecules, or ions are arranged in an orderly repeating pattern extending in all three spatial dimensions. The scientific study of crystals and crystal formation is known as crystallography. The process of crystal formation via mechanisms of crystal growth is called crystallization or solidification. The word *crystal* is derived from the Ancient Greek word κρύσταλλος (*krustallos*), meaning "rock-crystal" but also "ice",[1] from κρύος (*kruos*), "icy cold, frost".[2] [3] The word once referred particularly to quartz, or "rock crystal".

Quartz crystal. The individual grains of this polycrystalline mineral sample are clearly visible.

Most metals encountered in everyday life are polycrystals. Crystals are often symmetrically intergrown to form crystal twins.

### Crystal structure

The process of forming a crystalline structure from a fluid or from materials dissolved in the fluid is often referred to as the **crystallization** process. In the old example referenced by the root meaning of the word crystal, water being cooled undergoes a phase change from liquid to solid beginning with small ice crystals that grow until they fuse, forming a polycrystalline structure. The physical properties of the ice depend on the size and arrangement of the individual crystals, or grains, and the same may be said of metals solidifying from a molten state.

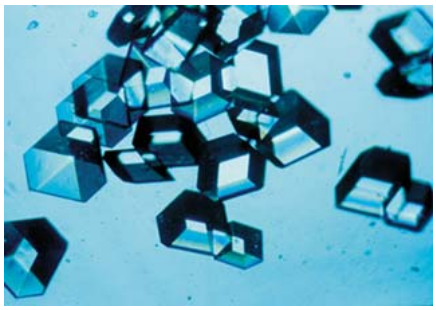

Insulin crystals grown in outer space

Which crystal structure the fluid will form depends on the chemistry of the fluid, the conditions under which it is being solidified, and also on the ambient pressure. While the cooling process usually results in the generation of a crystalline material, under certain conditions, the fluid may be frozen in a noncrystalline state. In most cases, this involves cooling the fluid so rapidly that atoms cannot travel to their lattice sites before they lose mobility. A noncrystalline material, which has no long-range order, is called an amorphous, vitreous, or glassy material. It is also often referred to as an amorphous solid, although there are distinct differences between crystalline solids and amorphous solids: most notably, the process of forming a glass does not release the latent heat of fusion.

Halite (sodium chloride) - a single, large crystal.

Crystalline structures occur in all classes of materials, with all types of chemical bonds. Almost all metal exists in a polycrystalline state; amorphous or single-crystal metals must be

produced synthetically, often with great difficulty. Ionically bonded crystals can form upon solidification of salts, either from a molten fluid or upon crystallization from a solution. Covalently bonded crystals are also very common, notable examples being diamond, silica, and graphite. Polymer materials generally will form crystalline regions, but the lengths of the molecules usually prevent complete crystallization. Weak van der Waals forces can also play a role in a crystal structure; for example, this type of bonding loosely holds together the hexagonal-patterned sheets in graphite.

Most crystalline materials have a variety of crystallographic defects. The types and structures of these defects can contain a profound effect on the properties of the materials.

## Crystalline phases

- Polymorphism is the ability of a solid to exist in more than one crystal form. For example, water ice is ordinarily found in the hexagonal form Ice $I_h$, but can also exist as the cubic Ice $I_c$, the rhombohedral ice II, and many other forms.
- Amorphous phases are also possible with the same molecule, such as amorphous ice. In this case, the phenomenon is known as polyamorphism.
- For pure chemical elements, polymorphism is known as allotropy. For example, diamond, graphite, and fullerenes are different allotropes of carbon.

## Special cases

Since the initial discovery of crystal-like individual arrays of atoms that are not regularly repeated, made in 1982 by Dan Shechtman, the acceptance of the concept and the word quasicrystal have led the International Union of Crystallography to redefine the term crystal to mean "any solid having an essentially discrete diffraction diagram", thereby shifting the essential attribute of crystallinity from position space to Fourier space. Within the family of crystals one distinguishes between traditional crystals, which are periodic, or repeating, at the atomic scale, and aperiodic (incommensurate) crystals which are not. This broader definition adopted in 1996 reflects the current understanding that microscopic periodicity is a sufficient but not a necessary condition for crystals.

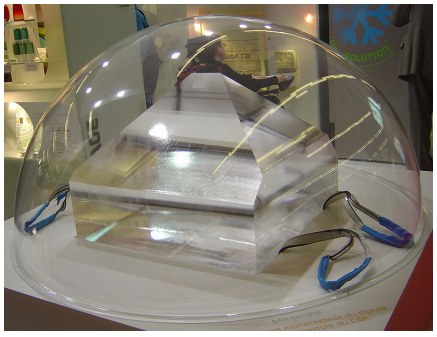

A large monocrystal of potassium dihydrogen phosphate grown from solution by Saint-Gobain for the megajoule laser of CEA.

While the term "crystal" has a precise meaning within materials science and solid-state physics, colloquially "crystal" refers to solid objects that exhibit well-defined and often pleasing geometric shapes. In this sense of the word, many types of crystals are found in nature. The shape of these crystals is dependent on the types of molecular bonds between the atoms to determine the structure, as well as on the conditions under which they formed. Snowflakes, diamonds, and table salt are common examples of crystals.

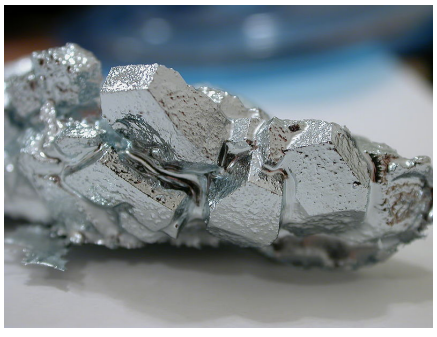

Gallium, a metal that easily forms large single crystals

Some crystalline materials may exhibit special electrical properties such as the ferroelectric effect or the piezoelectric effect. Additionally, light passing through a crystal is often refracted or bent in different directions, producing an array of colors; crystal optics is the study of these effects. In periodic dielectric structures a range of unique optical properties can be expected as seen in photonic crystals.

## Crystalline rocks

Ice crystals

Fossil shell with calcite crystals

Inorganic matter, if free to take that physical state in which it is most stable, tends to crystallize. There is no practical limit to the size a crystal may attain under the right conditions, and selenite single crystals in excess of 10 m are found in the Cave of the Crystals in Naica, Mexico.[4]

Crystalline rock masses have consolidated from aqueous solution or from molten magma. The vast majority of igneous rocks belong to this group and the degree of crystallization depends primarily on the conditions under which they solidified. Such rocks as granite, which have cooled very slowly and under great pressures, have completely crystallized, but many lavas were poured out at the surface and cooled very rapidly; in this latter group a small amount of amorphous or glassy matter is frequent. Other crystalline rocks, the evaporites such as rock salt, gypsum and some limestones have been deposited from aqueous solution, mostly owing to evaporation in arid climates. Still another group, the metamorphic rocks which includes the marbles, mica-schists and quartzites; are recrystallized, that is to say, they were at first fragmental rocks, like limestone, shale and sandstone and have never been in a molten condition nor entirely in solution. The high temperature and pressure conditions of metamorphism have acted on them erasing their original structures, and inducing recrystallization in the solid state.[]

## Properties

| Crystal | Particles | Attractive forces | Melting point | Other properties |
|---|---|---|---|---|
| Ionic | Positive and negative ions | Electrostatic attractions | High | Hard, brittle, good electrical conductor in molten state |
| Molecular | Polar molecules | London force and dipole-dipole attraction | Low | Soft, non-conductor or extremely poor conductor of electricity in liquid state |
| Molecular | Non-polar molecules | London force | Low | Soft conductor |

## See also

- Atomic packing factor
- Colloidal crystal
- Crystal growth
- Crystal habit
- Crystal oscillator
- Crystal system
- Crystallite
- Crystallographic database
- Liquid crystal
- Quasicrystal

## References

[1] κρύσταλλος (http://www.perseus.tufts.edu/hopper/text?doc=Perseus:text:1999.04.0057:entry=kru/stallos), Henry George Liddell, Robert Scott, *A Greek-English Lexicon*, on Perseus Digital Library

[2] κρύος (http://www.perseus.tufts.edu/hopper/text?doc=Perseus:text:1999.04.0057:entry=kru/os), Henry George Liddell, Robert Scott, *A Greek-English Lexicon*, on Perseus Digital Library

[3] "kreus-" (http://www.bartleby.com/61/roots/IE243.html). *The American Heritage Dictionary of the English Language: Fourth Edition: Appendix I: Indo-European Roots*. 2000. .

[4] National Geographic, 2008. Cavern of Crystal Giants (http://ngm.nationalgeographic.com/2008/11/crystal-giants/shea-text)

### Further reading

- Howard, J. Michael; Darcy Howard (Illustrator) (1998). "Introduction to Crystallography and Mineral Crystal Systems" (http://www.rockhounds.com/rockshop/xtal/index.html). Bob's Rock Shop. Retrieved 2008-04-20.
- Krassmann, Thomas (2005–2008). "The Giant Crystal Project" (http://giantcrystals.strahlen.org). Krassmann. Retrieved 2008-04-20.
- Various authors (2007). "Teaching Pamphlets" (http://www.iucr.ac.uk/iucr-top/comm/cteach/pamphlets.html). Commission on Crystallographic Teaching. Retrieved 2008-04-20.
- Various authors (2004). "Crystal Lattice Structures:Index by Space Group" (http://cst-www.nrl.navy.mil/lattice/spcgrp/). U.S. Naval Research Laboratory, Center for Computational Materials Science. Retrieved 2008-04-20.
- Various authors (2010). "Crystallography" (http://www.xtal.iqfr.csic.es/Cristalografia/index-en.html). Spanish National Research Council, Department of Crystallography. Retrieved 2010-01-08.

# Diffraction

**Diffraction** refers to various phenomena which occur when a wave encounters an obstacle. In classical physics, it is described as the apparent bending of waves around small obstacles and the spreading out of waves past small openings. Similar effects occur when light waves travel through a medium with a varying refractive index or a sound wave through one with varying acoustic impedance. Diffraction occurs with all waves, including sound waves, water waves, and electromagnetic waves such as visible light, x-rays and radio waves. As physical objects have wave-like properties (at the atomic level), diffraction also occurs with matter and can be studied according to the principles of quantum mechanics.

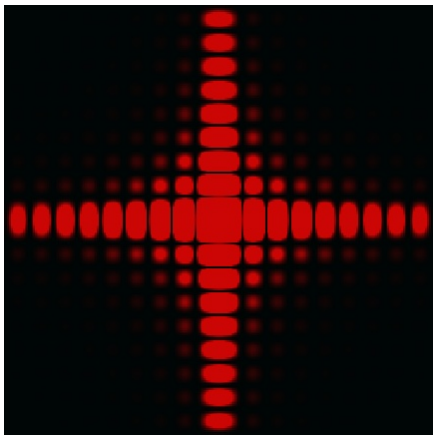

The intensity pattern formed on a screen by diffraction from a square aperture

While diffraction occurs whenever propagating waves encounter such changes, its effects are generally most pronounced for waves where the wavelength is on the order of the size of the diffracting objects. If the obstructing object provides multiple, closely-spaced openings, a complex pattern of varying intensity can result. This is due to the superposition, or interference, of different parts of a wave that traveled to the observer by different paths (see diffraction grating).

The formalism of diffraction can also describe the way in which waves of finite extent propagate in free space. For example, the expanding

profile of a laser beam, the beam shape of a radar antenna and the field of view of an ultrasonic transducer are all explained by diffraction theory.

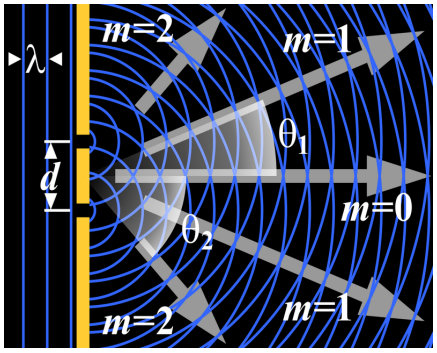


Generation of an interference pattern from two-slit diffraction

Colors seen in a spider web are partially due to diffraction, according to some analyses.[1]

## Examples

The effects of diffraction are regularly seen in everyday life. The most colorful examples of diffraction are those involving light; for example, the closely spaced tracks on a CD or DVD act as a diffraction grating to form the familiar rainbow pattern seen when looking at a disk. This principle can be extended to engineer a grating with a structure such that it will produce any diffraction pattern desired; the hologram on a credit card is an example. Diffraction in the atmosphere by small particles can cause a bright ring to be visible around a bright light source like the sun or the moon. A shadow of a solid object, using light from a compact source, shows small fringes near its edges. The speckle pattern which is observed when laser light falls on an optically rough surface is also a diffraction phenomenon. All these effects are a consequence of the fact that light propagates as a wave.

Solar glory at the steam from hot springs. A **glory** is an optical phenomenon produced by light backscattered (a combination of diffraction, reflection and refraction) towards its source by a cloud of uniformly-sized water droplets.

Diffraction can occur with any kind of wave. Ocean waves diffract around jetties and other obstacles. Sound waves can diffract around objects, which is why one can still hear someone calling even when hiding behind a tree.[2] Diffraction can also be a concern in some technical applications; it sets a fundamental limit to the resolution of a camera, telescope, or microscope.

## History

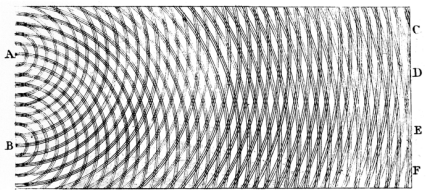

Thomas Young's sketch of two-slit diffraction, which he presented to the Royal Society in 1803

The effects of diffraction of light were first carefully observed and characterized by Francesco Maria Grimaldi, who also coined the term *diffraction*, from the Latin *diffringere*, 'to break into pieces', referring to light breaking up into different directions. The results of Grimaldi's observations were published posthumously in 1665.[3] [4] [5] Isaac Newton studied these effects and attributed them to *inflexion* of light rays. James Gregory (1638–1675) observed the diffraction patterns caused by a bird feather, which was effectively the first diffraction grating to be discovered.[6] Thomas Young performed a celebrated experiment in 1803 demonstrating interference from two closely spaced slits.[7] Explaining his results by interference of the waves emanating from the two different slits, he deduced that light must propagate as waves. Augustin-Jean Fresnel did more definitive studies and calculations of diffraction, made public in 1815[8] and 1818,[9] and thereby gave great support to the wave theory of light that had been advanced by Christiaan Huygens[10] and reinvigorated by Young, against Newton's particle theory.

## The mechanism of diffraction

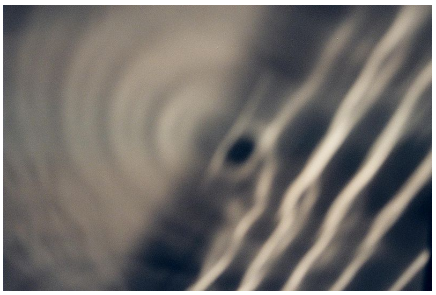
Photograph of single-slit diffraction in a circular ripple tank

Diffraction arises because of the way in which waves propagate; this is described by the Huygens–Fresnel principle. The propagation of a wave can be visualized by considering every point on a wavefront as a point source for a secondary radial wave. The subsequent propagation and addition of all these radial waves form the new wavefront. When waves are added together, their sum is determined by the relative phases as well as the amplitudes of the individual waves, an effect which is often known as wave interference. The summed amplitude of the waves can have any value between zero and the sum of the individual amplitudes. Hence, diffraction patterns usually have a series of maxima and minima.

The form of a diffraction pattern can be determined from the sum of the phases and amplitudes of the Huygens wavelets at each point in space. There are various analytical models which can be used to do this including the Fraunhofer diffraction equation for the far field and the Fresnel diffraction equation for the near field. Most configurations cannot be solved analytically, but can yield numerical solutions through finite element and boundary element methods.

## Diffraction systems

It is possible to obtain a qualitative understanding of many diffraction phenomena by considering how the relative phases of the individual secondary wave sources vary, and in particular, the conditions in which the phase difference equals half a cycle in which case waves will cancel one another out.

The simplest descriptions of diffraction are those in which the situation can be reduced to a two-dimensional problem. For water waves, this is already the case, water waves propagate only on the surface of the water. For light, we can often neglect one direction if the diffracting object extends in that direction over a distance far greater than the wavelength. In the case of light shining through small circular holes we will have to take into account the full three dimensional nature of the problem.

Some of the simpler cases of diffraction are considered below.

## Single-slit diffraction

A long slit of infinitesimal width which is illuminated by light diffracts the light into a series of circular waves and the wavefront which emerges from the slit is a cylindrical wave of uniform intensity.

A slit which is wider than a wavelength has a large number of point sources spaced evenly across the width of the slit. The light at a given angle is made up of contributions from each of these point sources and if the relative phases of these contributions vary by 2π or more, we expect to find minima and maxima in the diffracted light.

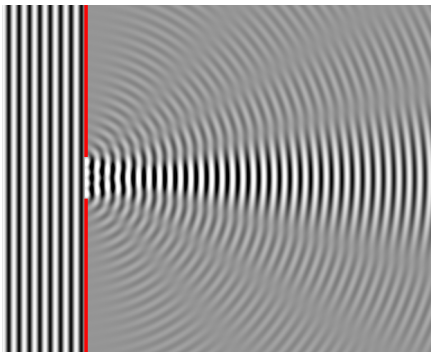

Numerical approximation of diffraction pattern from a slit of width four wavelengths with an incident plane wave. The main central beam, nulls, and phase reversals are apparent.

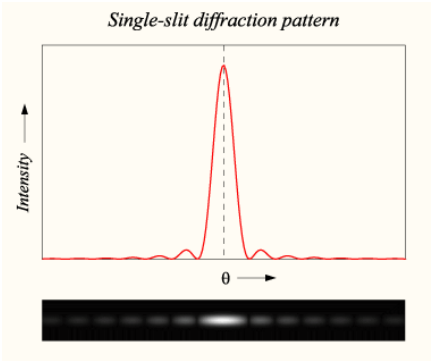


Graph and image of single-slit diffraction

We can find the angle at which a first minimum is obtained in the diffracted light by the following reasoning. The light from a source located at the top edge of the slit interferes destructively with a source located at the middle of the slit, when the path difference between them is equal to $\lambda/2$. Similarly, the source just below the top of the slit will interfere destructively with the source located just below the middle of the slit at the same angle. We can continue this reasoning along the entire height of the slit to conclude that the condition for destructive interference for the entire slit is the same as the condition for destructive interference between two narrow slits a distance apart that is half the width of the slit. The path difference is given by $\frac{d\sin(\theta)}{2}$ so that the minimum intensity occurs at an angle $\theta_{\text{min}}$ given by

$$d\,\sin\theta_{\min} = \lambda$$

where $d$ is the width of the slit.

A similar argument can be used to show that if we imagine the slit to be divided into four, six, eight parts, etc., minima are obtained at angles $\theta_n$ given by

$$d\,\sin\theta_n = n\lambda$$

where $n$ is an integer other than zero.

There is no such simple argument to enable us to find the maxima of the diffraction pattern. The intensity profile can be calculated using the Fraunhofer diffraction integral as

$$I(\theta) = I_0\,\mathrm{sinc}^2(d\sin\theta/\lambda)$$

where the sinc function is given by $\mathrm{sinc}(x) = \sin(\pi x)/(\pi x)$ if $x \neq 0$, and $\mathrm{sinc}(0) = 1$.

This analysis applies only to the far field, that is, at a distance much larger than the width of the slit.

## Diffraction grating

A diffraction grating is an optical component with a regular pattern. The form of the light diffracted by a grating depends on the structure of the elements and the number of elements present, but all gratings have intensity maxima at angles $\theta_m$ which are given by the grating equation

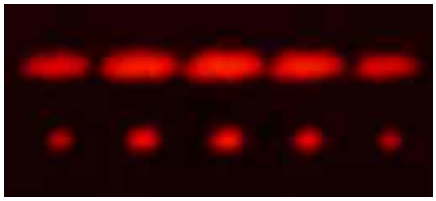

2-slit (top) and 5-slit diffraction of red laser light

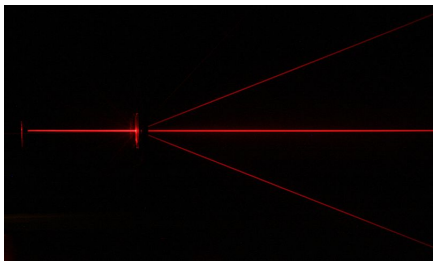

Diffraction of a red laser using a diffraction grating

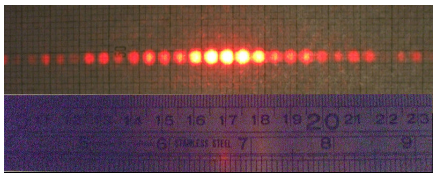

A diffraction pattern of a 633 nm laser through a grid of 150 slits

$$d\left(\sin\theta_m + \sin\theta_i\right) = m\lambda.$$

where $\theta_i$ is the angle at which the light is incident, $d$ is the separation of grating elements and $m$ is an integer which can be positive or negative.

The light diffracted by a grating is found by summing the light diffracted from each of the elements, and is essentially a convolution of diffraction and interference patterns.

The figure shows the light diffracted by 2-element and 5-element gratings where the grating spacings are the same; it can be seen that the maxima are in the same position, but the detailed structures of the intensities are different.

## Diffraction by a circular aperture

The far-field diffraction of a plane wave incident on a circular aperture is often referred to as the Airy Disk. The variation in intensity with angle is given by

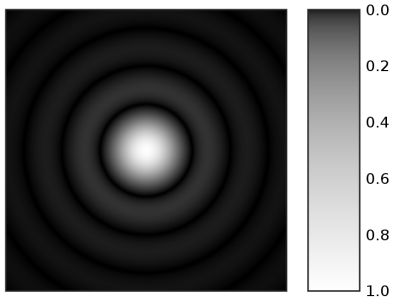


A computer-generated image of an **Airy disk**

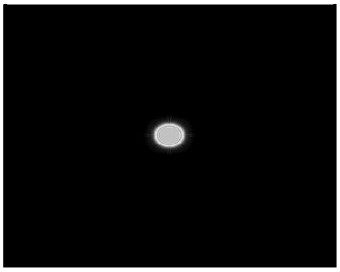

Computer generated light diffraction pattern from a circular aperture of diameter 0.5 micrometre at a wavelength of 0.6 micrometre (red-light) at distances of 0.1 cm – 1 cm in steps of 0.1 cm. One can see the image moving from the Fresnel region into the Fraunhofer region where the Airy pattern is seen.

$$I(\theta) = I_0 \left( \frac{2J_1(ka \sin\theta)}{ka \sin\theta} \right)^2$$

where $a$ is the radius of the circular aperture, $k$ is equal to $2\pi/\lambda$ and $J_1$ is a Bessel function. The smaller the aperture, the larger the spot size at a given distance, and the greater the divergence of the diffracted beams.

## Propagation of a laser beam

The way in which the profile of a laser beam changes as it propagates is determined by diffraction. The output mirror of the laser is an aperture, and the subsequent beam shape is determined by that aperture. Hence, the smaller the output beam, the quicker it diverges. Diode lasers have much greater divergence than He–Ne lasers for this reason.

Paradoxically, it is possible to reduce the divergence of a laser beam by first expanding it with one convex lens, and then collimating it with a second convex lens whose focal point is coincident with that of the first lens. The resulting beam has a larger aperture, and hence a lower divergence.

## Diffraction-limited imaging

The ability of an imaging system to resolve detail is ultimately limited by diffraction. This is because a plane wave incident on a circular lens or mirror is diffracted as described above. The light is not focused to a point but forms an Airy disk having a central spot in the focal plane with radius to first null of

The Airy disk around each of the stars from the 2.56 m telescope aperture can be seen in this *lucky image* of the binary star zeta Boötis.

$$d = 1.22\lambda N,$$

where λ is the wavelength of the light and *N* is the f-number (focal length divided by diameter) of the imaging optics. In object space, the corresponding angular resolution is

$$\sin\theta = 1.22\frac{\lambda}{D},$$

where *D* is the diameter of the entrance pupil of the imaging lens (e.g., of a telescope's main mirror).

Two point sources will each produce an Airy pattern – see the photo of a binary star. As the point sources move closer together, the patterns will start to overlap, and ultimately they will merge to form a single pattern, in which case the two point sources cannot be resolved in the image. The Rayleigh criterion specifies that two point sources can be considered to be resolvable if the separation of the two images is at least the radius of the Airy disk, i.e. if the first minimum of one coincides with the maximum of the other.

Thus, the larger the aperture of the lens, and the smaller the wavelength, the finer the resolution of an imaging system. This is why telescopes have very large lenses or mirrors, and why optical microscopes are limited in the detail which they can see.

### Speckle patterns

The speckle pattern which is seen when using a laser pointer is another diffraction phenomenon. It is a result of the superpostion of many waves with different phases, which are produced when a laser beam illuminates a rough surface. They add together to give a resultant wave whose amplitude, and therefore intensity varies randomly.

## Common features of diffraction patterns

Several qualitative observations can be made of diffraction in general:

- The angular spacing of the features in the diffraction pattern is inversely proportional to the dimensions of the object causing the diffraction. In other words: The smaller the diffracting object, the 'wider' the resulting diffraction pattern, and vice versa. (More precisely, this is true of the sines of the angles.)
- The diffraction angles are invariant under scaling; that is, they depend only on the ratio of the wavelength to the size of the diffracting object.
- When the diffracting object has a periodic structure, for example in a diffraction grating, the features generally become sharper. The third figure, for example, shows a comparison of a double-slit pattern with a pattern formed by five slits, both sets of slits having the same spacing, between the center of one slit and the next.

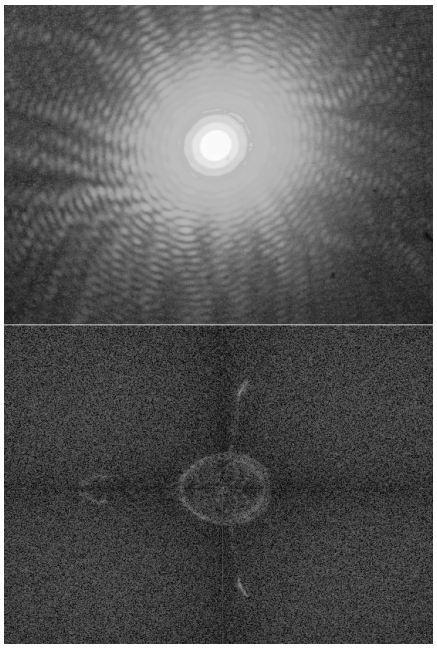

The upper half of this image shows a diffraction pattern of He-Ne laser beam on an elliptic aperture. The lower half is its 2D Fourier transform approximately reconstructing the shape of the aperture.

## Particle diffraction

Quantum theory tells us that every particle exhibits wave properties. In particular, massive particles can interfere and therefore diffract. Diffraction of electrons and neutrons stood as one of the powerful arguments in favor of quantum mechanics. The wavelength associated with a particle is the de Broglie wavelength

$$\lambda = \frac{h}{p}$$

where $h$ is Planck's constant and $p$ is the momentum of the particle (mass × velocity for slow-moving particles). For most macroscopic objects, this wavelength is so short that it is not meaningful to assign a wavelength to them. A sodium atom traveling at about 30,000 m/s would have a De Broglie wavelength of about 50 pico meters.

Because the wavelength for even the smallest of macroscopic objects is extremely small, diffraction of matter waves is only visible for small particles, like electrons, neutrons, atoms and small molecules. The short wavelength of these matter waves makes them ideally suited to study the atomic crystal structure of solids and large molecules like proteins.

Relatively larger molecules like buckyballs were also shown to diffract.[11]

## Bragg diffraction

Diffraction from a three dimensional periodic structure such as atoms in a crystal is called Bragg diffraction. It is similar to what occurs when waves are scattered from a diffraction grating. Bragg diffraction is a consequence of interference between waves reflecting from different crystal planes. The condition of constructive interference is given by *Bragg's law*:

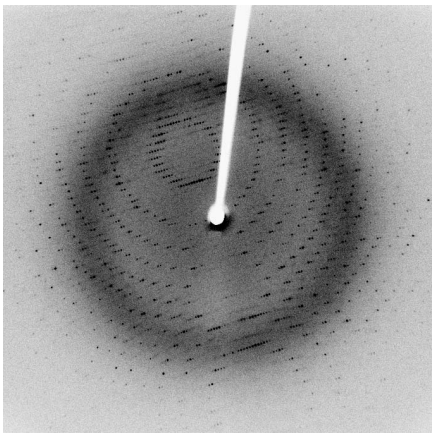

Following Bragg's law, each dot (or *reflection*), in this diffraction pattern forms from the constructive interference of X-rays passing through a crystal. The data can be used to determine the crystal's atomic structure.

$$m\lambda = 2d\sin\theta$$

where

λ is the wavelength,

*d* is the distance between crystal planes,

θ is the angle of the diffracted wave.

and *m* is an integer known as the *order* of the diffracted beam.

Bragg diffraction may be carried out using either light of very short wavelength like x-rays or matter waves like neutrons (and electrons) whose wavelength is on the order of (or much smaller than) the atomic spacing[12] . The pattern produced gives information of the separations of crystallographic planes *d*, allowing one to deduce the crystal structure. Diffraction contrast, in electron microscopes and x-topography devices in particular, is also a powerful tool for examining individual defects and local strain fields in crystals.

## Coherence

The description of diffraction relies on the interference of waves emanating from the same source taking different paths to the same point on a screen. In this description, the difference in phase between waves that took different paths is only dependent on the effective path length. This does not take into account the fact that waves that arrive at the screen at the same time were emitted by the source at different times. The initial phase with which the source emits waves can change over time in an unpredictable way. This means that waves emitted by the source at times that are too far apart can no longer form a constant interference pattern since the relation between their phases is no longer time independent.

The length over which the phase in a beam of light is correlated, is called the coherence length. In order for interference to occur, the path length difference must be smaller than the coherence length. This is sometimes referred to as spectral coherence, as it is related to the presence of different frequency components in the wave. In the case of light emitted by an atomic transition, the coherence length is related to the lifetime of the excited state from which the atom made its transition.

If waves are emitted from an extended source, this can lead to incoherence in the transversal direction. When looking at a cross section of a beam of light, the length over which the phase is correlated is called the transverse coherence length. In the case of Young's double slit experiment, this would mean that if the transverse coherence length is smaller than the spacing between the two slits, the resulting pattern on a screen would look like two single slit diffraction patterns.

In the case of particles like electrons, neutrons and atoms, the coherence length is related to the spatial extent of the wave function that describes the particle.

## See also

- Atmospheric diffraction
- Bragg diffraction
- Brocken spectre
- Cloud iridescence
- Diffraction formalism
- Diffraction grating
- Diffraction limit
- Diffractometer
- Dynamical theory of diffraction
- Electron diffraction
- Fraunhofer diffraction
- Fresnel diffraction
- Fresnel imager
- Fresnel number
- Fresnel zone
- Neutron diffraction
- Prism
- Powder diffraction
- Refraction
- Schaefer–Bergmann diffraction
- Thinned array curse
- X-ray scattering techniques

## References

[1] Dietrich Zawischa. "Optical effects on spider webs" (http://www.itp.uni-hannover.de/~zawischa/ITP/spiderweb.html). . Retrieved 2007-09-21.

[2] Andrew Norton (2000). *Dynamic fields and waves* (http://books.google.com/?id=XRRMxjr24pwC&pg=PA102&dq=sound+wave+diffraction+behind+tree). CRC Press. p. 102. ISBN 9780750307192. .

[3] Francesco Maria Grimaldi, *Physico-mathesis de lumine, coloribus, et iride, aliisque adnexis...* [The physical mathematics of light, color, and the rainbow, and other things appended...] (Bologna ("Bonomia"), Italy: Vittorio Bonati, 1665), pages 1-11 (http://books.google.com/books?id=FzYVAAAAQAAJ&pg=PA1&source=gbs_toc_r&cad=3#v=onepage&q&f=false): "Propositio I. Lumen propagatur seu diffunditur non solum directe, refracte, ac reflexe, sed etiam alio quodam quarto modo, diffracte." (Proposition 1. Light propagates or spreads not only in a straight line, by refraction, and by reflection, but also by another, certain fourth way: by diffraction.)

[4] Jean Louis Aubert (1760). *Memoires pour l'histoire des sciences et des beaux arts* (http://books.google.com/?id=3OgDAAAAMAAJ&pg=PP151&lpg=PP151&dq=grimaldi+diffraction+date:0-1800). Paris: Impr. de S. A. S.; Chez E. Ganeau. pp. 149. .

[5] Sir David Brewster (1831). *A Treatise on Optics* (http://books.google.com/?id=opYAAAAAMAAJ&pg=RA1-PA95&lpg=RA1-PA95&dq=grimaldi+diffraction+date:0-1840). London: Longman, Rees, Orme, Brown & Green and John Taylor. pp. 95. .

[6] Letter from James Gregory to John Collins, dated 13 May 1673. Reprinted in: *Correspondence of Scientific Men of the Seventeenth Century....*, ed. Stephen Jordan Rigaud (Oxford, England: Oxford University Press, 1841), vol. 2, pages 251-255; see especially page 254. Available on-line at: Books.Google.com (http://books.google.com/books?id=0h45L_66bcYC&pg=PA254&dq=feather+ovals&

ei=5jlaSsLQKJnkygTi1Lz8CA&ie=ISO-8859-1&output=html).

[7] Young, Thomas (1804-01-01). "The Bakerian Lecture: Experiments and calculations relative to physical optics" (http://books.google.com/?id=7AZGAAAAMAAJ&pg=PA1). *Philosophical Transactions of the Royal Society of London* (Royal Society of London.) **94**: 1–16. doi:10.1098/rstl.1804.0001. . (Note: This lecture was presented before the Royal Society on 24 November 1803.)

[8] Augustin-Jean Fresnel (1816) "Mémoire sur la diffraction de la lumière … ," *Annales de la Chemie et de Physique*, 2nd series, vol. 1, pages 239-281. (Presented before *l'Académie des sciences* on 15 October 1815.) Available on-line at: Bibnum.education.fr (http://www.bibnum.education.fr/physique/optique/premier-memoire-sur-la-diffraction-de-la-lumiere) **(French)**

[9] Augustin-Jean Fresnel (1826) "Mémoire sur la diffraction de la lumière," *Mémoires de l'Académie des Sciences (Paris)*, vol. 5, pages 33-475. (Summitted to *l'Académie des sciences* of Paris on 20 April 1818.)

[10] Christiaan Huygens, *Traité de la lumiere* (Leiden, Netherlands: Pieter van der Aa, 1690), Chapter 1. (Note: Huygens published his *Traité* in 1690; however, in the preface to his book, Huygens states that in 1678 he first communicated his book to the French Royal Academy of Sciences.)

[11] Brezger, B.; Hackermüller, L.; Uttenthaler, S.; Petschinka, J.; Arndt, M.; Zeilinger, A. (February 2002). "Matter–Wave Interferometer for Large Molecules" (http://homepage.univie.ac.at/Lucia.Hackermueller/unsereArtikel/Brezger2002a.pdf) (reprint). *Physical Review Letters* **88** (10): 100404. doi:10.1103/PhysRevLett.88.100404. PMID 11909334. . Retrieved 2007-04-30.

[12] John M. Cowley (1975) *Diffraction physics* (North-Holland, Amsterdam) ISBN 0 444 10791 6

## External links

- Diffraction and Crystallography for beginners (http://www.xtal.iqfr.csic.es/Cristalografia/index-en.html)
- Do Sensors “Outresolve” Lenses? (http://luminous-landscape.com/tutorials/resolution.shtml); on lens and sensor resolution interaction.
- Diffraction and acoustics. (http://www.acoustics.salford.ac.uk/feschools/waves/diffract.htm)
- Diffraction in photography. (http://www.johnsankey.ca/diffraction.html)
- On Diffraction (http://www.mathpages.com/home/kmath636/kmath636.htm) at MathPages.
- Diffraction pattern calculators (http://demonstrations.wolfram.com/search.html?query=diffraction) at The Wolfram Demonstrations Project
- Wave Optics (http://www.lightandmatter.com/html_books/5op/ch05/ch05.html) – A chapter of an online textbook.
- 2-D wave Java applet (http://www.falstad.com/wave2d/) – Displays diffraction patterns of various slit configurations.
- Diffraction Java applet (http://www.falstad.com/diffraction/) – Displays diffraction patterns of various 2-D apertures.
- Diffraction approximations illustrated (http://www.mit.edu/~birge/diffraction/) – MIT site that illustrates the various approximations in diffraction and intuitively explains the Fraunhofer regime from the perspective of linear system theory.
- Gap (http://www.phy.hk/wiki/englishhtm/Diffraction.htm) Obstacle (http://www.phy.hk/wiki/englishhtm/Diffraction2.htm) Corner (http://www.phy.hk/wiki/englishhtm/Diffraction3.htm) – Java simulation of diffraction of water wave.
- Google Maps (http://maps.google.com/maps?q=Panama+canal&hl=en&ie=UTF8&om=1&z=16&ll=9.385048,-79.918799&spn=0.015539,0.027122&t=k&iwloc=addr) – Satellite image of Panama Canal entry ocean wave diffraction.
- Google Maps (http://maps.google.com/maps?f=q&source=s_q&hl=en&geocode=&q=&sll=52.788632,1.609969&sspn=0.010472,0.016093&ie=UTF8&t=h&ll=52.788217,1.606772&spn=0.010472,0.016093&z=16) and Bing Maps (http://www.bing.com/maps/?v=2&cp=52.788763840321245~1.6073888540267944&lvl=16&sty=h&eo=0) - Aerial photo of waves diffracting through sea barriers at Sea Palling in Norfolk, UK.
- Diffraction Effects (http://www.cvimellesgriot.com/products/Documents/TechnicalGuide/Diffraction_Effects.pdf)
- An Introduction to The Wigner Distribution in Geometric Optics (http://scripts.mit.edu/~raskar/lightfields/index.php?title=An_Introduction_to_The_Wigner_Distribution_in_Geometric_Optics)

- DoITPoMS Teaching and Learning Package - Diffraction and Imaging (http://www.doitpoms.ac.uk/tlplib/diffraction/index.php)

# Uniform theory of diffraction

In numerical analysis, the **uniform geometrical theory of diffraction** (**UTD**) is a high frequency method for solving electromagnetic scattering problems from electrically small discontinuities or discontinuities in more than one dimension at the same point. [1] UTD is an extension of Joseph Keller's *geometrical theory of diffraction* (GTD). [2]

The uniform theory of diffraction approximates near field electromagnetic fields as quasi optical and uses ray diffraction to determine diffraction coefficients for each diffracting object-source combination. These coefficients are then used to calculate the field strength and phase for each direction away from the diffracting point.

These fields are then added to the incident fields and reflected fields to obtain a total solution.

## See also

- Electromagnetic modeling

## References

[1] R. G. Kouyoumjian and P. H. Pathak, "A uniform geometrical theory of diffraction for an edge in a perfectly conducting surface," *Proc. IEEE*, vol. 62, pp. 1448-1461, November 1974.

[2] J. B. Keller, "Geometrical theory of diffraction" (http://www.opticsinfobase.org/abstract.cfm?URI=josa-52-2-116), *J. Opt. Soc. Am.*, vol. 52, no. 2, pp. 116-130, 1962.

## External links

- Overview of Asymptotic Expansion Methods in Electromagnetics (http://www.cvel.clemson.edu/modeling/tutorials/techniques/gtd-utd/gtd-utd.html)

# Crystallography

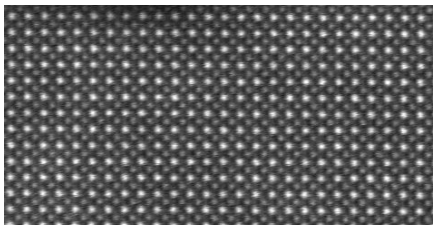

A crystalline solid: atomic resolution image of strontium titanate. Brighter atoms are Sr and darker ones are Ti.

**Crystallography** is the experimental science of the arrangement of atoms in solids. The word "crystallography" derives from the Greek words *crystallon* = cold drop / frozen drop, with its meaning extending to all solids with some degree of transparency, and *grapho* = write.

Before the development of X-ray diffraction crystallography (see below), the study of crystals was based on their geometry. This involves measuring the angles of crystal faces relative to theoretical reference axes (crystallographic axes), and establishing the symmetry of the crystal in question. The former is carried out using a goniometer. The position in 3D space of each crystal face is plotted on a stereographic net, e.g. Wulff net or Lambert net. In fact, the pole to each face is plotted on the net. Each point is labelled with its Miller index. The final plot allows the symmetry of the crystal to be established.

Crystallographic methods now depend on the analysis of the diffraction patterns of a sample targeted by a beam of some type. Although X-rays are most commonly used, the beam is not always electromagnetic radiation. For some purposes electrons or neutrons are used. This is facilitated by the wave properties of the particles. Crystallographers often explicitly state the type of illumination used when referring to a method, as with the terms *X-ray diffraction, neutron diffraction* and *electron diffraction.*

These three types of radiation interact with the specimen in different ways. X-rays interact with the spatial distribution of the valence electrons, while electrons are charged particles and therefore feel the total charge distribution of both the atomic nuclei and the surrounding electrons. Neutrons are scattered by the atomic nuclei through the strong nuclear forces, but in addition, the magnetic moment of neutrons is non-zero. They are therefore also scattered by magnetic fields. When neutrons are scattered from hydrogen-containing materials, they produce diffraction patterns with high noise levels. However, the material can sometimes be treated to substitute hydrogen for deuterium. Because of these different forms of interaction, the three types of radiation are suitable for different crystallographic studies.

## Theory

Generally, an image of a small object is made using a lens to focus the illuminating radiation, as is done with the rays of the visible spectrum in light microscopy. However, the wavelength of visible light (about 4000 to 7000 angstroms) is three orders of magnitude longer than the length of typical atomic bonds and atoms themselves (about 1 to 2 angstroms). Therefore, obtaining information about the spatial arrangement of atoms requires the use of radiation with shorter wavelengths, such as X-rays. Employing shorter wavelengths implied abandoning microscopy and true imaging, however, because there exists no material from which a lens capable of focusing this type of radiation can be created. (That said, scientists have had some success focusing X-rays with microscopic Fresnel zone plates made from gold, and by critical-angle reflection inside long tapered capillaries.)[1] Diffracted x-ray beams cannot be focused to produce images, so the sample structure must be reconstructed from the diffraction pattern. Sharp features in the diffraction pattern arise from periodic, repeating structure in the sample, which are often very strong due to coherent reflection of many photons from many regularly spaced instances of similar structure, while non-periodic components of the structure result in diffuse (and usually weak) diffraction features.

Because of their highly ordered and repetitive structure, crystals give diffraction patterns of sharp Bragg reflection spots, and are ideal for analyzing the structure of solids.

## Notation

- Coordinates in *square brackets* such as **[100]** denote a direction vector (in real space).
- Coordinates in *angle brackets* or *chevrons* such as **<100>** denote a *family* of directions which are related by symmetry operations. In the cubic crystal system for example, **<100>** would mean [100], [010], [001] or the negative of any of those directions.
- Miller indices in *parentheses* such as **(100)** denote a plane of the crystal structure, and regular repetitions of that plane with a particular spacing. In the cubic system, the normal to the (hkl) plane is the direction [hkl], but in lower-symmetry cases, the normal to (hkl) is not parallel to [hkl].
- Indices in *curly brackets* or *braces* such as **{100}** denote a family of planes and their normals which are equivalent in cubic materials due to symmetry operations, much the way angle brackets denote a family of directions. In non-cubic materials, <hkl> is not necessarily perpendicular to {hkl}.

## Technique

Some materials studied using crystallography, proteins for example, do not occur naturally as crystals. Typically, such molecules are placed in solution and allowed to crystallize over days, weeks, or months through vapor diffusion. A drop of solution containing the molecule, buffer, and precipitants is sealed in a container with a reservoir containing a hygroscopic solution. Water in the drop diffuses to the reservoir, slowly increasing the concentration and allowing a crystal to form. If the concentration were to rise more quickly, the molecule would simply precipitate out of solution, resulting in disorderly granules rather than an orderly and hence usable crystal.

Once a crystal is obtained, data can be collected using a beam of radiation. Although many universities that engage in crystallographic research have their own X-ray producing equipment, synchrotrons are often used as X-ray sources, because of the purer and more complete patterns such sources can generate. Synchrotron sources also have a much higher intensity of X-ray beams, so data collection takes a fraction of the time normally necessary at weaker sources.

Producing an image from a diffraction pattern requires sophisticated mathematics and often an iterative process of **modelling and refinement.** In this process, the mathematically predicted diffraction patterns of an hypothesized or "model" structure are compared to the actual pattern generated by the crystalline sample. Ideally, researchers make several initial guesses, which through refinement all converge on the same answer. Models are refined until their predicted patterns match to as great a degree as can be achieved without radical revision of the model. This is a painstaking process, made much easier today by computers.

The mathematical methods for the analysis of diffraction data only apply to *patterns,* which in turn result only when waves diffract from orderly arrays. Hence crystallography applies for the most part only to crystals, or to molecules which can be coaxed to crystallize for the sake of measurement. In spite of this, a certain amount of molecular information can be deduced from the patterns that are generated by fibers and powders, which while not as perfect as a solid crystal, may exhibit a degree of order. This level of order can be sufficient to deduce the structure of simple molecules, or to determine the coarse features of more complicated molecules. For example, the double-helical structure of DNA was deduced from an X-ray diffraction pattern that had been generated by a fibrous sample).

## Crystallography in materials engineering

Crystallography is a tool that is often employed by materials scientists. In single crystals, the effects of the crystalline arrangement of atoms is often easy to see macroscopically, because the natural shapes of crystals reflect the atomic structure. In addition, physical properties are often controlled by crystalline defects. The understanding of crystal structures is an important prerequisite for understanding crystallographic defects. Mostly, materials do not occur in a single crystalline, but poly-crystalline form, such that the powder diffraction method plays a most important role in structural determination.

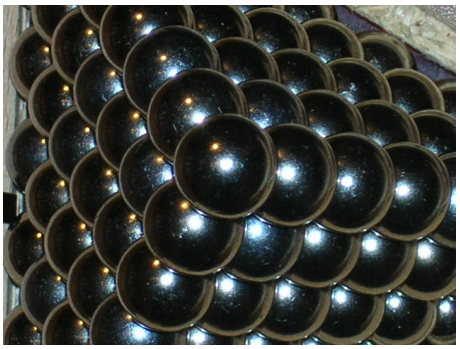

An example of a cubic lattice

A number of other physical properties are linked to crystallography. For example, the minerals in clay form small, flat, platelike structures. Clay can be easily deformed because the platelike particles can slip along each other in the plane of the plates, yet remain strongly connected in the direction perpendicular to the plates. Such mechanisms can be studied by crystallographic texture measurements.

In another example, iron transforms from a body-centered cubic (bcc) structure to a face-centered cubic (fcc) structure called austenite when it is heated. The fcc structure is a close-packed structure, and the bcc structure is not, which explains why the volume of the iron decreases when this transformation occurs.

Crystallography is useful in phase identification. When performing any process on a material, it may be desired to find out what compounds and what phases are present in the material. Each phase has a characteristic arrangement of atoms. Techniques like X-ray diffraction can be used to identify which patterns are present in the material, and thus which compounds are present.

Crystallography covers the enumeration of the symmetry patterns which can be formed by atoms in a crystal and for this reason has a relation to group theory and geometry. See symmetry group.

## Biology

X-ray crystallography is the primary method for determining the molecular conformations of biological macromolecules, particularly protein and nucleic acids such as DNA and RNA. In fact, the double-helical structure of DNA was deduced from crystallographic data. The first crystal structure of a macromolecule was solved in 1958 [2] A three-dimensional model of the myoglobin molecule obtained by X-ray analysis.[3] The Protein Data Bank (PDB) is a freely accessible repository for the structures of proteins and other biological macromolecules. Computer programs like RasMol or Pymol can be used to visualize biological molecular structures.

Electron crystallography has been used to determine some protein structures, most notably membrane proteins and viral capsids.

## Scientists of note

- William Barlow
- John Desmond Bernal
- William Henry Bragg
- William Lawrence Bragg
- Auguste Bravais
- Martin Julian Buerger
- Francis Crick
- Pierre Curie
- Peter Debye
- Boris Delone
- Paul Peter Ewald
- Evgraf Stepanovich Fedorov
- Rosalind Franklin
- Georges Friedel
- Paul Heinrich von Groth
- René Just Haüy
- Carl Hermann
- Johann Friedrich Christian Hessel
- Dorothy Crowfoot Hodgkin
- Robert Huber
- Aaron Klug
- Max von Laue
- Kathleen Lonsdale
- Ernest-François Mallard
- Charles-Victor Mauguin
- William Hallowes Miller
- Friedrich Mohs
- Paul Niggli
- Arthur Lindo Patterson
- Max Perutz
- Hugo Rietveld
- Jean-Baptiste L. Romé de l'Isle
- Paul Scherrer
- Arthur Moritz Schönflies
- Constance Tipper
- Don Craig Wiley
- Ada Yonath
- Rajagopala Chidambaram
- Tej P. Singh
- Christian Samuel Weiss
- Ralph Walter Graystone Wyckoff

## See also

- Atomic packing factor
- Condensed matter physics
- Crystal engineering
- Crystal growth
- Crystal optics
- Crystal system
- Crystal
- Crystallite
- Crystallization processes
- Crystallographic database
- Crystallographic group
- Dynamical theory of diffraction
- Electron crystallography
- Euclidean plane isometry
- Fixed points of isometry groups in Euclidean space
- Fractional coordinates
- Group action
- Laser-heated pedestal growth
- Materials science
- Metallurgy
- Mineralogy
- Neutron crystallography
- Neutron diffraction at OPAL
- Permutation group
- Point group
- Solid state chemistry
- Space group
- Symmetric group

## References

[1] A. Snigirev *et al.* (2007). "Two-step hard X-ray focusing combining Fresnel zone plate and single-bounce ellipsoidal capillary". *Journal of Synchrotron Radiation* **14** (Pt 4): 326–330. doi:10.1107/S0909049507025174. PMID 17587657.

[2] Kendrew, J.C. et al. (1958)

[3] (*Nature* 181, 662–666). (http://www.nature.com/physics/looking-back/kendrew/kendrew.pdf)

## Further reading

- Burns, G.; Glazer, A.M. (1990). *Space Groups for Scientists and Engineers* (2nd ed.). Boston: Academic Press, Inc. ISBN 0-12-145761-3.
- Clegg, W (1998). *Crystal Structure Determination (Oxford Chemistry Primer)*. Oxford: Oxford University Press. ISBN 0-19-855-901-1.
- Drenth, J (1999). *Principles of Protein X-Ray Crystallography*. New York: Springer-Verlag. ISBN 0-387-98587-5.
- Giacovazzo, C; Monaco HL, Viterbo D, Scordari F, Gilli G, Zanotti G, and Catti M (1992). *Fundamentals of Crystallography*. Oxford: Oxford University Press. ISBN 0-19-855578-4.
- Glusker, JP; Lewis M, Rossi M (1994). *Crystal Structure Analysis for Chemists and Biologists*. New York: VCH Publishers. ISBN 0-471-18543-4.

- O'Keeffe, M.; Hyde, B.G. (1996). *Crystal Structures; I. Patterns and Symmetry*. Washington, DC: Mineralogical Society of America, *Monograph Series*. ISBN 0-939950-40-5.

**Applied Computational Powder Diffraction Data Analysis**

- Edited by R. A. Young (1993). Young, R.A.. ed. *The Rietveld Method*. Oxford: Oxford University Press & International Union of Crystallography. ISBN 0-19-855577-6.


## External links

- American Crystallographic Association (http://www.AmerCrystalAssn.org/)
- Learning Crystallography (http://www.xtal.iqfr.csic.es/Cristalografia/index-en.html)
- Crystal Lattice Structures (http://cst-www.nrl.navy.mil/lattice/spcgrp/)
- Vega Science Trust Interviews on Crystallography (http://www.vega.org.uk) Freeview video interviews with Max Pertuz, Rober Huber and Aaron Klug.
- Commission on Crystallographic Teaching, Pamphlets (http://www.iucr.org/iucr-top/comm/cteach/pamphlets.html)
- Ames Laboratory, US DOE Crystallography Research Resources (http://www.mcbmm.ameslab.gov/index.html)

# Paracrystalline

**Paracrystalline** materials are defined as having short and medium range ordering in their lattice (similar to the liquid crystal phases) but lacking long-range ordering at least in one direction.[1]

Ordering is the regularity in which atoms appear in a predictable lattice, as measured from one point. In a highly ordered, perfectly crystalline material, or single crystal, the location of every atom in the structure can be described exactly measuring out from a single origin. Conversely, in a disordered structure such as a liquid or amorphous solid, the location of the first and perhaps second nearest neighbors can be described from an origin (with some degree of uncertainty) and the ability to predict locations decreases rapidly from there out. The distance at which atom locations can be predicted is referred to as the correlation length $\xi$. A paracrystalline material exhibits correlation somewhere between the fully amorphous and fully crystalline.

The primary, most accessible source of crystallinity information is X-ray diffraction, although other techniques may be needed to observe the complex structure of paracrystalline materials, such as fluctuation electron microscopy [2] in combination with Density of states modeling[3] of electronic and vibrational states.

## Paracrystalline Model

The paracrystalline model is a revision of the Continuous Random Network model first proposed by W. H. Zachariasen in 1932 [4] . The paracrystal model is defined as highly strained, microcrystalline grains surrounded by fully amorphous material [5] . This is a higher energy state then the continuous random network model. The important distinction between this model and the microcrystalline phases is the lack of defined grain boundaries and highly strained lattice parameters, which makes calculations of molecular and lattice dynamics difficult. A general theory of paracrystals has been formulated in a basic textbook[6] , and then further developed/refined by various authors. An example of a paracrystalline, or partially disordered lattice is showin in the following figure.

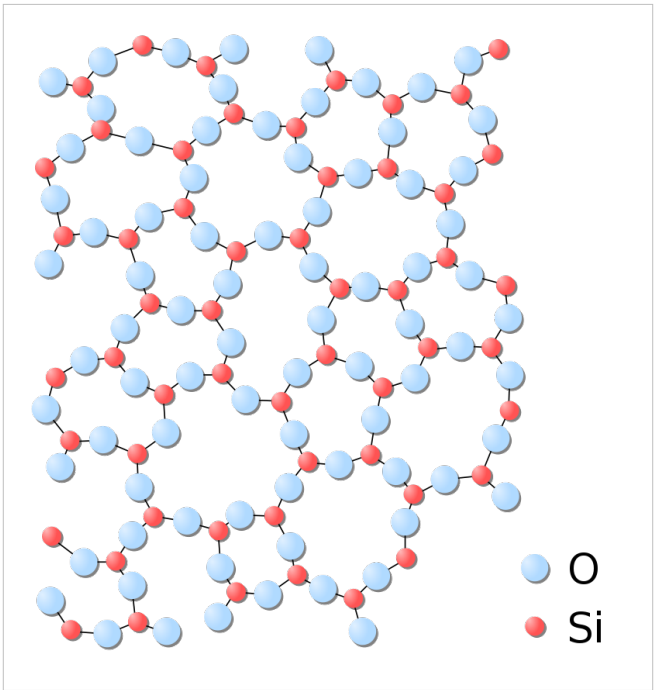


## Applications

The paracrystal model has been useful, for example, in describing the state of partially amorphous semiconductor materials after deposition. It has also been successfully applied to synthetic polymers, liquid crystals, biopoloymers[7] [8] , and biomembranes[9] .

## See also

- X-ray scattering
- Amorphous solid
- Single Crystal
- Polycrystalline
- Crystallography
- DNA
- X-ray pattern of a B-DNA Paracrystal [10]

## Notes

[1] Voyles, et al. Structure and physical properties of paracrystalline atomistic models of amorphous silicon. *J. Ap. Phys.*, **90**(2001) 4437, doi: 10.1063/1.1407319

[2] Biswas, P, et al. *J. Phys.:Condens. Matter*, **19** (2007) 455202, doi:10.1088/0953-8984/19/45/455202

[3] Nakhmanson, Voyles, Mousseau, Barkema, and Drabold. *Phys. Rev. B* **63**(2001) 235207. doi: 10.1103/PhysRevB.63.235207

[4] Zachariasen, W.H., *J. Am. Chem. Soc.*, **54**(1932) 3841.

[5] J.M. Cowley, Diffraction Studies on Non-Cryst. Substan. 13 (1981)

[6] Hosemann R., Bagchi R.N., Direct analysis of diffraction by matter, North-Holland Publs., Amsterdam – New York, 1962

[7] Bessel functions and diffraction by helical structures http://planetphysics.org/encyclopedia/BesselFunctionsAndTheirApplicationsToDiffractionByHelicalStructures.html

[8] X-Ray Diffraction Patterns of Double-Helical Deoxyribonucleic Acid (DNA) Crystals and Paracrystalline Fibers http://planetphysics.org/encyclopedia/BesselFunctionsApplicationsToDiffractionByHelicalStructures.html

[9] Baianu I.C., X-ray scattering by partially disordered membrane systems, *Acta Cryst.* **A**, **34** (1978), 751–753.

[10] http://commons.wikimedia.org/wiki/File:ABDNAxrgpj.jpg

# Quantum optics

**Quantum optics** is a field of research in physics, dealing with the application of quantum mechanics to phenomena involving light and its interactions with matter.

## History of quantum optics

Light is made up of particles called photons and hence inherently is "grainy" (quantized). Quantum optics is the study of the nature and effects of light as quantized photons. The first indication that light might be quantized came from Max Planck in 1899 when he correctly modeled blackbody radiation. By assuming that, Bohr showed that the atoms were also quantized, in the sense that they could only emit discrete amounts of energy. The understanding of the interaction between light and matter following these developments not only formed the basis of quantum optics but were also crucial for the development of quantum mechanics as a whole. However, the subfields of quantum mechanics dealing with matter-light interaction were principally regarded as research into matter rather than into light; hence one rather spoke of atom physics and quantum electronics in 1960. Laser science—i.e., research into principles, design and application of these devices—became an important field, and the quantum mechanics underlying the laser's principles was studied now with more emphasis on the properties of light, and the name *quantum optics* became customary.

As laser science needed good theoretical foundations, and also because research into these soon proved very fruitful, interest in quantum optics rose. Following the work of Dirac in quantum field theory, George Sudarshan, Roy J. Glauber, and Leonard Mandel applied quantum theory to the electromagnetic field in the 1950s and 1960s to gain a more detailed understanding of photodetection and the statistics of light (see degree of coherence). This led to the introduction of the coherent state as a quantum description of laser light and the realization that some states of light could not be described with classical waves. In 1977, Kimble et al. demonstrated the first source of light which required a quantum description: a single atom that emitted one photon at a time. This was the first conclusive evidence that light was made up of photons. Another quantum state of light with certain advantages over any classical state, squeezed light, was soon proposed. At the same time, development of short and ultrashort laser pulses—created by Q switching and modelocking techniques—opened the way to the study of unimaginably fast ("ultrafast") processes. Applications for solid state research (e.g. Raman spectroscopy) were found, and mechanical forces of light on matter were studied. The latter led to levitating and positioning clouds of atoms or even small biological samples in an optical trap or optical tweezers by laser beam. This, along with Doppler cooling was the crucial technology needed to achieve the celebrated Bose-Einstein condensation.

Other remarkable results are the demonstration of quantum entanglement, quantum teleportation, and (recently, in 1995) quantum logic gates. The latter are of much interest in quantum information theory, a subject which partly emerged from quantum optics, partly from theoretical computer science.

Today's fields of interest among quantum optics researchers include parametric down-conversion, parametric oscillation, even shorter (attosecond) light pulses, use of quantum optics for quantum information, manipulation of single atoms, Bose-Einstein condensates, their application, and how to manipulate them (a sub-field often called atom optics), coherent perfect absorbers, and much more.

Research into quantum optics that aims to bring photons into use for information transfer and computation is now often called photonics to emphasize the claim that photons and photonics will take the role that electrons and electronics now have.

## Concepts of quantum optics

| Quantum optics operators |
| --- |
| Ladder operators |
| Creation and annihilation operators |
| Displacement operator |
| Rotation operator (quantum mechanics) |
| Squeeze operator |
| Anti-symmetric operator |
| [1] |

According to quantum theory, light may be considered not only as an electro-magnetic wave but also as a "stream" of particles called photons which travel with *c*, the vacuum speed of light. These particles should not be considered to be classical billiard balls, but as quantum mechanical particles described by a wavefunction spread over a finite region. Each particle carries one quantum of energy equal to *hf*, where h is Planck's constant and f is the frequency of the light. The postulation of the quantization of light by Max Planck in 1899 and the discovery of the general validity of this idea in Albert Einstein's 1905 explanation of the photoelectric effect soon led physicists to realize the possibility of population inversion and the possibility of the laser.

This kind of use of statistical mechanics is the fundament of most concepts of quantum optics: Light is described in terms of field operators for creation and annihilation of photons—i.e. in the language of quantum electrodynamics.

A frequently encountered state of the light field is the coherent state as introduced by George Sudarshan in 1963. This state, which can be used to approximately describe the output of a single-frequency laser well above the laser threshold, exhibits Poissonian photon number statistics. Via certain nonlinear interactions, a coherent state can be transformed into a squeezed coherent state, which can exhibit super- or sub- Poissonean photon statistics. Such light is called squeezed light. Other important quantum aspects are related to correlations of photon statistics between different beams. For example, parametric nonlinear processes can generate so-called twin beams, where ideally each photon of one beam is associated with a photon in the other beam.

Atoms are considered as quantum mechanical oscillators with a discrete energy spectrum with the transitions between the energy eigenstates being driven by the absorption or emission of light according to Einstein's theory with the oscillator strength depending on the quantum numbers of the states.

For solid state matter one uses the energy band models of solid state physics. This is important as understanding how light is detected (typically by a solid-state device that absorbs it) is crucial for understanding experiments.

## See also

- Optics
- Optical phase space
- Optical physics
- Nonclassical light

## References


- L. Mandel, E. Wolf *Optical Coherence and Quantum Optics* (Cambridge 1995)
- D. F. Walls and G. J. Milburn *Quantum Optics* (Springer 1994)
- C. W. Gardiner and Peter Zoller, *Quantum Noise*, (Springer 2004).
- M. O. Scully and M. S. Zubairy *Quantum Optics* (Cambridge 1997)

- W. P. Schleich *Quantum Optics in Phase Space* (Wiley 2001)

## External links

- An introduction to quantum optics of the light field [2]
- Encyclopedia of laser physics and technology [3], with content on quantum optics (particularly quantum noise in lasers), by Rüdiger Paschotta.
- Qwiki [4] - A quantum physics wiki devoted to providing technical resources for practicing quantum physicists.
- Quantiki [5] - a free-content WWW resource in quantum information science that anyone can edit.
- Various Quantum Optics Reports [6]

## References

[1] http://en.wikipedia.org/wiki/Template:Quantum
[2] http://gerdbreitenbach.de/gallery
[3] http://www.rp-photonics.com/encyclopedia.html
[4] http://qwiki.stanford.edu/wiki/Quantum_Optics
[5] http://www.quantiki.org/
[6] http://www.physics.drexel.edu/~tim/Decoherence/index.html

# X-rays

**X-radiation** (composed of **X-rays**) is a form of electromagnetic radiation. X-rays have a wavelength in the range of 0.01 to 10 nanometers, corresponding to frequencies in the range 30 petahertz to 30 exahertz ($3 \times 10^{16}$ Hz to $3 \times 10^{19}$ Hz) and energies in the range 120 eV to 120 keV. They are shorter in wavelength than UV rays and longer than gamma rays. In many languages, X-radiation is called **Röntgen radiation**, after Wilhelm Conrad Röntgen, who is generally credited as its discoverer, and who had named it X-radiation to signify an unknown type of radiation.[1] Correct spelling of X-ray(s) in the English language includes the variants x-ray(s) and X ray(s).[2] XRAY is used as the phonetic pronunciation for the letter x.

X-rays from about 0.12 to 12 keV (10 to 0.10 nm wavelength) are classified as "soft" X-rays, and from about 12 to 120 keV (0.10 to 0.01 nm wavelength) as "hard" X-rays, due to their penetrating abilities.

Hard X-rays can penetrate solid objects, and their most common use is to take images of the inside of objects in diagnostic radiography and crystallography. As a result, the term *X-ray* is metonymically used to refer to a radiographic image produced using this method, in addition to the method itself. By contrast, soft X-rays can

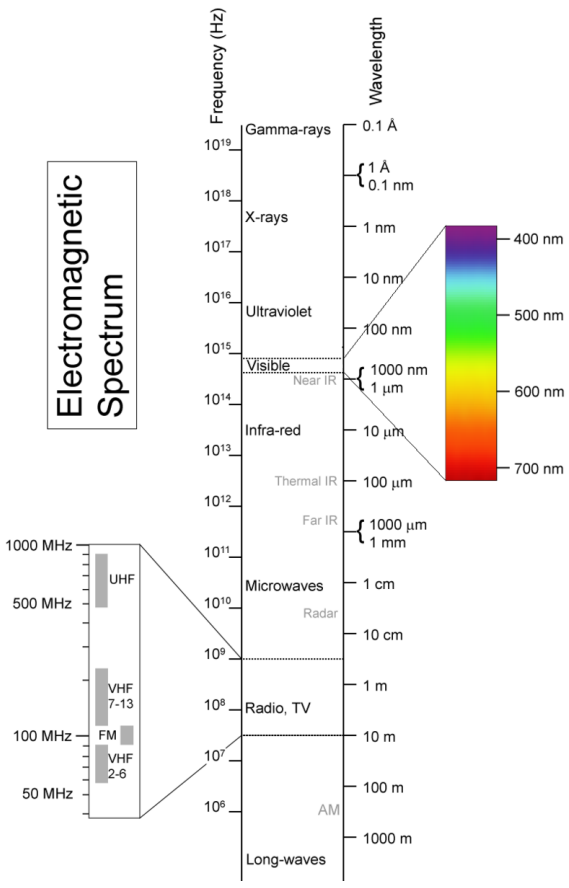

X-rays are part of the electromagnetic spectrum.

hardly be said to penetrate matter at all; for instance, the attenuation length of 600 eV (~ 2 nm) x-rays in water is less than 1 micrometer.[3] X-rays are a form of ionizing radiation, and exposure to them can be a health hazard.

The distinction between X-rays and gamma rays has changed in recent decades. Originally, the electromagnetic radiation emitted by X-ray tubes had a longer wavelength than the radiation emitted by radioactive nuclei (gamma rays).[4] Older literature distinguished between X- and gamma radiation on the basis of wavelength, with radiation shorter than some arbitrary wavelength, such as $10^{-11}$ m, defined as gamma rays.[5] However, as shorter wavelength continuous spectrum "X-ray" sources such as linear accelerators and longer wavelength "gamma ray" emitters were discovered, the wavelength bands largely overlapped. The two types of radiation are now usually distinguished by their origin: X-rays are emitted by electrons outside the nucleus, while gamma rays are emitted by the nucleus.[4] [6] [7] [8]

## Units of measure and exposure

The measure of X-rays ionizing ability is called the exposure:

- The coulomb per kilogram (C/kg) is the SI unit of ionizing radiation exposure, and it is the amount of radiation required to create one coulomb of charge of each polarity in one kilogram of matter.
- The roentgen (R) is an obsolete traditional unit of exposure, which represented the amount of radiation required to create one electrostatic unit of charge of each polarity in one cubic centimeter of dry air. 1.00 roentgen = $2.58\times10^{-4}$ C/kg

However, the effect of ionizing radiation on matter (especially living tissue) is more closely related to the amount of energy deposited into them rather than the charge generated. This measure of energy absorbed is called the absorbed dose:

- The gray (Gy), which has units of (Joules/kilogram), is the SI unit of absorbed dose, and it is the amount of radiation required to deposit one joule of energy in one kilogram of any kind of matter.
- The rad is the (obsolete) corresponding traditional unit, equal to 10 millijoules of energy deposited per kilogram. 100 rad = 1.00 gray.

The equivalent dose is the measure of the biological effect of radiation on human tissue. For X-rays it is equal to the absorbed dose.

- The sievert (Sv) is the SI unit of equivalent dose, which for X-rays is numerically equal to the gray (Gy).
- The Roentgen equivalent man (rem) is the traditional unit of equivalent dose. For X-rays it is equal to the rad or 10 millijoules of energy deposited per kilogram. 1.00 Sv = 100 rem.

Medical X-rays are a significant source of man-made radiation exposure, accounting for 58% in the United States in 1987, but since most radiation exposure is natural (82%), medical X-rays only account for 10% of total American radiation exposure.[9]

Reported dosage due to dental X-rays seems to vary significantly. Depending on the source, a typical dental X-ray of a human results in an exposure of perhaps, 3,[10] 40,[11] 300,[12] or as many as 900[13] mrems (30 to 9,000 μSv).

## Sources

**X-ray K-series spectral line wavelengths (nm) for some common target materials.[14]**

| Target | $K\beta_1$ | $K\beta_2$ | $K\alpha_1$ | $K\alpha_2$ |
|---|---|---|---|---|
| **Fe** | 0.17566 | 0.17442 | 0.193604 | 0.193998 |
| **Co** | 0.162079 | 0.160891 | 0.178897 | 0.179285 |
| **Ni** | 0.15001 | 0.14886 | 0.165791 | 0.166175 |
| **Cu** | 0.139222 | 0.138109 | 0.154056 | 0.154439 |
| **Zr** | 0.070173 | 0.068993 | 0.078593 | 0.079015 |
| **Mo** | 0.063229 | 0.062099 | 0.070930 | 0.071359 |

The main source of x-ray radiation is from outer space (e.g. the sun, black holes, and supernovae). Man-made X-rays are generated by an X-ray tube, a vacuum tube that uses a high voltage to accelerate the electrons released by a hot cathode to a high velocity. The high velocity electrons collide with a metal target, the anode, creating the X-rays.[17] In medical X-ray tubes the target is usually tungsten or a more crack-resistant alloy of rhenium (5%) and tungsten (95%), but sometimes molybdenum for more specialized applications, such as when soft X-rays are needed as in mammography. In crystallography, a copper target is most common, with cobalt often being used when fluorescence from iron content in the sample might otherwise present a problem.

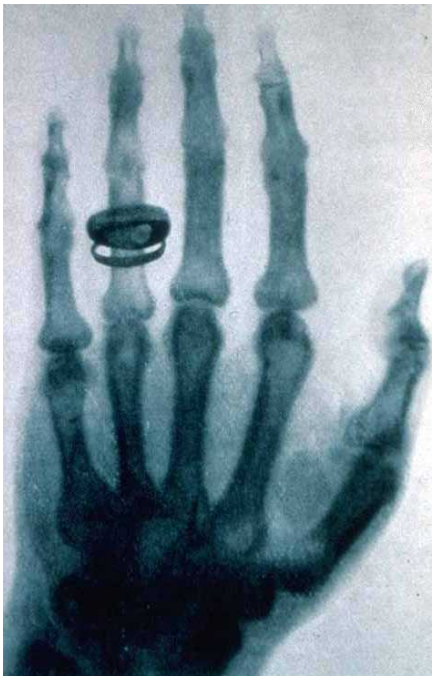

*Hand mit Ringen* (Hand with Rings): print of Wilhelm Röntgen's first "medical" X-ray, of his wife's hand, taken on 22 December 1895 and presented to Professor Ludwig Zehnder of the Physik Institut, University of Freiburg, on 1 January 1896[15] [16]

The maximum energy of the produced X-ray photon is limited by the energy of the incident electron, which is equal to the voltage on the tube, so an 80 kV tube cannot create X-rays with an energy greater than 80 keV. When the electrons hit the target, X-rays are created by two different atomic processes:

1. X-ray fluorescence: If the electron has enough energy it can knock an orbital electron out of the inner electron shell of a metal atom, and as a result electrons from higher energy levels then fill up the vacancy and X-ray photons are emitted. This process produces an emission spectrum of X-rays at a few discrete frequencies, sometimes referred to as the spectral lines. The spectral lines generated depend on the target (anode) element used and thus are called characteristic lines. Usually these are transitions from upper shells into K shell (called K lines), into L shell (called L lines) and so on.
2. *Bremsstrahlung*: This is radiation given off by the electrons as they are scattered by the strong electric field near the high-*Z* (proton number) nuclei. These X-rays have a continuous spectrum. The intensity of the X-rays increases linearly with decreasing frequency, from zero at the energy of the incident electrons, the voltage on the X-ray tube.

So the resulting output of a tube consists of a continuous bremsstrahlung spectrum falling off to zero at the tube voltage, plus several spikes at the characteristic lines. The voltages used in diagnostic X-ray tubes, and thus the highest energies of the X-rays, range from roughly 20 to 150 kV.[18]

Both of these X-ray production processes are very inefficient, with a production efficiency of only about one percent, and hence, to produce a usable flux of X-rays, most of the electric power consumed by the tube is released as waste heat. The X-ray tube must be designed to dissipate this excess heat.

In medical diagnostic applications, the low energy (soft) X-rays are unwanted, since they are totally absorbed by the body, increasing the dose. Hence, a thin metal sheet, often of aluminum, called an X-ray filter, is usually placed over the window of the X-ray tube, filtering out the low energy components in the spectrum. This is called *hardening* the beam.

Radiographs obtained using X-rays can be used to identify a wide spectrum of pathologies. Because the body structures being imaged in medical applications are large compared to the wavelength of the X-rays, the X-rays can be analyzed as particles rather than waves. (This is in contrast to X-ray crystallography, where their wave-like nature is more important because the wavelength is comparable to the sizes of the structures being imaged.)

To make an X-ray image of human or animal bones, short X-ray pulses illuminate the body or limb, with radiographic film placed behind it. Any bones that are present absorb most of the X-ray photons by photoelectric processes. This is because bones have a higher electron density than soft tissues. Note that bones contain a high percentage of calcium (20 electrons per atom), potassium (19 electrons per atom) magnesium (12 electrons per atom), and phosphorus (15 electrons per atom). The X-rays that pass through the flesh leave a latent image in the photographic film. When the film is developed, the parts of the image corresponding to higher X-ray exposure are dark, leaving a white shadow of bones on the film.

To generate an image of the cardiovascular system, including the arteries and veins (angiography) an initial image is taken of the anatomical region of interest. A second image is then taken of the same region after iodinated contrast material has been injected into the blood vessels within this area. These two images are then digitally subtracted, leaving an image of only the iodinated contrast outlining the blood vessels. The radiologist or surgeon then compares the image obtained to normal anatomical images to determine if there is any damage or blockage of the vessel.

A specialized source of X-rays which is becoming widely used in research is synchrotron radiation, which is generated by particle accelerators. Its unique features are X-ray outputs many orders of magnitude greater than those of X-ray tubes, wide X-ray spectra, excellent collimation, and linear polarization.[19]

# Detectors

## Photographic plate

The detection of X-rays is based on various methods. The most commonly known methods are photographic plates, photographic film in cassettes, and rare earth screens. Regardless of what is "catching" the image, they are all categorized as "Image Receptors" (IR).

Before the advent of the digital computer and before the invention of digital imaging, photographic plates were used to produce most radiographic images. The images were produced right on the glass plates. Photographic film largely replaced these plates, and it was used in X-ray laboratories to produce medical images. In more recent years, computerized and digital radiography has been replacing photographic film in medical and dental applications, though film technology remains in widespread use in industrial radiography processes (e.g. to inspect welded seams). Photographic plates are mostly things of history, and their replacement, the "intensifying screen", is also fading into history. The metal silver (formerly necessary to the radiographic & photographic industries) is a non-renewable resource. Thus it is beneficial that this is now being replaced by digital (DR) and computed (CR) technology. Where photographic films required wet processing facilities, these new technologies do not. The digital archiving of images utilizing these new technologies also saves storage space.

Since photographic plates are sensitive to X-rays, they provide a means of recording the image, but they also required much X-ray exposure (to the patient), hence intensifying screens were devised. They allow a lower dose to the patient, because the screens take the X-ray information and intensify it so that it can be recorded on film positioned next to the intensifying screen.

The part of the patient to be X-rayed is placed between the X-ray source and the image receptor to produce a shadow of the internal structure of that particular part of the body. X-rays are partially blocked ("attenuated") by dense tissues such as bone, and pass more easily through soft tissues. Areas where the X-rays strike darken when developed, causing bones to appear lighter than the surrounding soft tissue.

Contrast compounds containing barium or iodine, which are radiopaque, can be ingested in the gastrointestinal tract (barium) or injected in the artery or veins to highlight these vessels. The contrast compounds have high atomic numbered elements in them that (like bone) essentially block the X-rays and hence the once hollow organ or vessel can be more readily seen. In the pursuit of a non-toxic contrast material, many types of high atomic number elements were evaluated. For example, the first time the forefathers used contrast it was chalk, and was used on a cadaver's vessels. Unfortunately, some elements chosen proved to be harmful – for example, thorium was once used as a contrast medium (Thorotrast) – which turned out to be toxic in some cases (causing injury and occasionally death from the effects of thorium poisoning). Modern contrast material has improved, and while there is no way to determine who may have a sensitivity to the contrast, the incidence of "allergic-type reactions" are low. (The risk is comparable to that associated with penicillin.)

## Photostimulable phosphors (PSPs)

An increasingly common method is the use of photostimulated luminescence (PSL), pioneered by Fuji in the 1980s. In modern hospitals a photostimulable phosphor plate (PSP plate) is used in place of the photographic plate. After the plate is X-rayed, excited electrons in the phosphor material remain "trapped" in "colour centres" in the crystal lattice until stimulated by a laser beam passed over the plate surface. The light given off during laser stimulation is collected by a photomultiplier tube and the resulting signal is converted into a digital image by computer technology, which gives this process its common name, computed radiography (also referred to as **digital radiography**). The PSP plate can be reused, and existing X-ray equipment requires no modification to use them.

## Geiger counter

Initially, most common detection methods were based on the ionization of gases, as in the Geiger-Müller counter: a sealed volume, usually a cylinder, with a mica, polymer or thin metal window contains a gas, a cylindrical cathode and a wire anode; a high voltage is applied between the cathode and the anode. When an X-ray photon enters the cylinder, it ionizes the gas and forms ions and electrons. Electrons accelerate toward the anode, in the process causing further ionization along their trajectory. This process, known as a Townsend avalanche, is detected as a sudden current, called a "count" or "event".

In order to gain energy spectrum information, a diffracting crystal may be used to first separate the different photons. The method is called wavelength dispersive X-ray spectroscopy (WDX or WDS). Position-sensitive detectors are often used in conjunction with dispersive elements. Other detection equipment that is inherently energy-resolving may be used, such as the aforementioned proportional counters. In either case, use of suitable pulse-processing (MCA) equipment allows digital spectra to be created for later analysis.

For many applications, counters are not sealed but are constantly fed with purified gas, thus reducing problems of contamination or gas aging. These are called "flow counters".

## Scintillators

Some materials such as sodium iodide (NaI) can "convert" an X-ray photon to a visible photon; an electronic detector can be built by adding a photomultiplier. These detectors are called "scintillators", filmscreens or "scintillation counters". The main advantage of using these is that an adequate image can be obtained while subjecting the patient to a much lower dose of X-rays.

## Image intensification

X-rays are also used in "real-time" procedures such as angiography or contrast studies of the hollow organs (e.g. barium enema of the small or large intestine) using fluoroscopy acquired using an X-ray image intensifier. Angioplasty, medical interventions of the arterial system, rely heavily on X-ray-sensitive contrast to identify potentially treatable lesions.

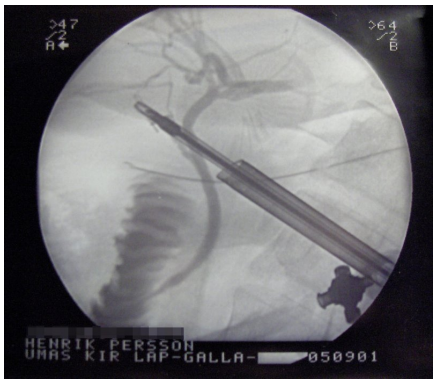

X-ray during cholecystectomy

## Direct semiconductor detectors

Since the 1970s, new semiconductor detectors have been developed (silicon or germanium doped with lithium, Si(Li) or Ge(Li)). X-ray photons are converted to electron-hole pairs in the semiconductor and are collected to detect the X-rays. When the temperature is low enough (the detector is cooled by Peltier effect or even cooler liquid nitrogen), it is possible to directly determine the X-ray energy spectrum; this method is called energy dispersive X-ray spectroscopy (EDX or EDS); it is often used in small X-ray fluorescence spectrometers. These detectors are sometimes called "solid state detectors". Detectors based on cadmium telluride (CdTe) and its alloy with zinc, cadmium zinc telluride, have an increased sensitivity, which allows lower doses of X-rays to be used.

Practical application in medical imaging started in the 1990s. Currently amorphous selenium is used in commercial large area flat panel X-ray detectors for mammography and chest radiography. Current research and development is focused around pixel detectors, such as CERN's energy resolving Medipix detector.

Note: A standard semiconductor diode, such as a 1N4007, will produce a small amount of current when placed in an X-ray beam. A test device once used by Medical Imaging Service personnel was a small project box that contained several diodes of this type in series, which could be connected to an oscilloscope as a quick diagnostic.

Silicon drift detectors (SDDs), produced by conventional semiconductor fabrication, now provide a cost-effective and high resolving power radiation measurement. Unlike conventional X-ray detectors, such as Si(Li)s, they do not need to be cooled with liquid nitrogen.

## Scintillator plus semiconductor detectors (indirect detection)

With the advent of large semiconductor array detectors it has become possible to design detector systems using a scintillator screen to convert from X-rays to visible light which is then converted to electrical signals in an array detector. Indirect Flat Panel Detectors (FPDs) are in widespread use today in medical, dental, veterinary and industrial applications.

The array technology is a variant on the amorphous silicon TFT arrays used in many flat panel displays, like the ones in computer laptops. The array consists of a sheet of glass covered with a thin layer of silicon that is in an amorphous or disordered state. At a microscopic scale, the silicon has been imprinted with millions of transistors arranged in a highly ordered array, like the grid on a sheet of graph paper. Each of these thin film transistors (TFTs) is attached to a light-absorbing photodiode making up an individual pixel (picture element). Photons striking the photodiode are converted into two carriers of electrical charge, called electron-hole pairs. Since the number of charge carriers

produced will vary with the intensity of incoming light photons, an electrical pattern is created that can be swiftly converted to a voltage and then a digital signal, which is interpreted by a computer to produce a digital image. Although silicon has outstanding electronic properties, it is not a particularly good absorber of X-ray photons. For this reason, X-rays first impinge upon scintillators made from e.g. gadolinium oxysulfide or caesium iodide. The scintillator absorbs the X-rays and converts them into visible light photons that then pass onto the photodiode array.

### Visibility to the human eye

While generally considered invisible to the human eye, in special circumstances X-rays can be visible.[20] Brandes, in an experiment a short time after Röntgen's landmark 1895 paper, reported after dark adaptation and placing his eye close to an X-ray tube, seeing a faint "blue-gray" glow which seemed to originate within the eye itself.[21] Upon hearing this, Röntgen reviewed his record books and found he too had seen the effect. When placing an X-ray tube on the opposite side of a wooden door Röntgen had noted the same blue glow, seeming to emanate from the eye itself, but thought his observations to be spurious because he only saw the effect when he used one type of tube. Later he realized that the tube which had created the effect was the only one powerful enough to make the glow plainly visible and the experiment was thereafter readily repeatable. The knowledge that X-rays are actually faintly visible to the dark-adapted naked eye has largely been forgotten today; this is probably due to the desire not to repeat what would now be seen as a recklessly dangerous and potentially harmful experiment with ionizing radiation. It is not known what exact mechanism in the eye produces the visibility: it could be due to conventional detection (excitation of rhodopsin molecules in the retina), direct excitation of retinal nerve cells, or secondary detection via, for instance, X-ray induction of phosphorescence in the eyeball with conventional retinal detection of the secondarily produced visible light.

Though X-rays are otherwise invisible it is possible to see the ionization of the air molecules if the intensity of the X-ray beam is high enough. The beamline from the wiggler at the ID11 [22] at ESRF is one example of such high intensity.[23]

## Medical uses

Since Röntgen's discovery that X-rays can identify bone structures, X-rays have been developed for their use in medical imaging, the first use was less than a month after his seminal paper on the subject.[24] Radiology is a specialized field of medicine. Radiologists employ radiography and other techniques for diagnostic imaging. This is probably the most common use of X-ray technology.

Head CT scan (transverse plane) slice – a modern application of X-rays

X-rays are especially useful in the detection of pathology of the skeletal system, but are also useful for detecting some disease processes in soft tissue. Some notable examples are the very common chest X-ray, which can be used to identify lung diseases such as pneumonia, lung cancer or pulmonary edema, and the abdominal X-ray, which can detect intestinal obstruction, free air (from visceral perforations) and free fluid (in ascites). X-rays may also be used to detect pathology such as gallstones (which are rarely radiopaque) or kidney stones which are often (but not always) visible. Traditional plain X-rays are less useful in the imaging of soft tissues such as the brain or muscle. Imaging alternatives for soft tissues are computed axial tomography (CAT or CT scanning),[25] magnetic resonance imaging (MRI) or ultrasound. The latter two do not

subject the individual to ionizing radiation. In addition to plain X-rays and CT scans, physicians use fluoroscopy as an X-ray test methodology. This method often uses administration of a medical contrast material (intravenously, orally or via enema). Examples include cardiac catheterization (to examine for coronary artery blockages) and Barium swallow (to examine for esophageal disorders.

Since 2005, X-rays are listed as a carcinogen by the U.S. government.[26] The use of X-rays as a treatment is known as radiotherapy and is largely used for the management (including palliation) of cancer; it requires higher radiation energies than for imaging alone.

### Health risks

X-Ray of a pregnant woman

X-rays are a relatively safe method of investigation and the radiation exposure is relatively low, depending upon the study. Experimental and epidemiological data, currently do not support the proposition that there is a threshold dose of radiation below which there is no increased risk of cancer.[27] However, this is under increasing doubt.[28] Diagnostic X-rays account for 14% of the total annual radiation exposure from man-made and natural sources worldwide.[29] It is estimated that the additional radiation will increase a person's cumulative risk of getting cancer by age 75 by 0.6–1.8%.[30] The amount of absorbed radiation depends upon the type of X-ray test and the body part involved.[31] CT and fluoroscopy entail higher doses of radiation than do plain X-rays.

To place the increased risk in perspective, a plain chest X-ray or dental X-ray will expose a person to the same amount from background radiation that we are exposed to (depending upon location) everyday over 10 days.[32] Each such X-ray would add less than 1 per 1,000,000 to the lifetime cancer risk. An abdominal or chest CT would be the equivalent to 2–3 years of background radiation, increasing the lifetime cancer risk between 1 per 10,000 and 1 per 1,000.[32] For instance, the effective dose to the torso from a CT scan of the chest of a 14 year old girl is about 5mSv.[33] These numbers are very small compared to the roughly 40% chance of developing any cancer during our lifetime.[34] It should be noted that the accurate estimation of effective doses due to CT is difficult. For instance, the estimation uncertainty range is about ±19% to ±32% for adult head scans depending upon the method used.[35]

Fathers exposed to diagnostic x-rays are more likely to have infants who contract leukemia, especially if exposure is closer to conception or includes two or more X-rays of the lower gastrointestinal (GI) tract or lower abdomen.[36] The risk of radiation is greater to unborn babies, so in pregnant patients, the benefits of the investigation (X-ray) should be balanced with the potential hazards to the unborn fetus.[37] [38] In the US, there are an estimated 62,000,000 CT scans performed annually, including more than 4,000,000 on children.[31] Avoiding unnecessary X-rays (especially CT scans) will reduce radiation dose and any associated cancer risk.[39]

## Shielding

Lead is the most common shield against X-rays because of its high density (11340 kg/m$^3$), stopping power, ease of installation and low cost. The maximum range of a high-energy photon such as an X-ray in matter is infinite; at every point in the matter traversed by the photon, there is a probability of interaction. Thus there is a very small probability of no interaction over very large distances. The shielding of photon beam is therefore exponential (with an attenuation length being close to the radiation length of the material); doubling the thickness of shielding will square the shielding effect.

The following table shows the recommended thickness of lead shielding in function of X-ray energy, from the Recommendations by the Second International Congress of Radiology.[40]

| X-Rays generated by peak voltages not exceeding | Minimum thickness of Lead |
|---|---|
| 75 kV | 1.0 mm |
| 100 kV | 1.5 mm |
| 125 kV | 2.0 mm |
| 150 kV | 2.5 mm |
| 175 kV | 3.0 mm |
| 200 kV | 4.0 mm |
| 225 kV | 5.0 mm |
| 300 kV | 9.0 mm |
| 400 kV | 15.0 mm |
| 500 kV | 22.0 mm |
| 600 kV | 34.0 mm |
| 900 kV | 51.0 mm |

## Other uses

Other notable uses of X-rays include

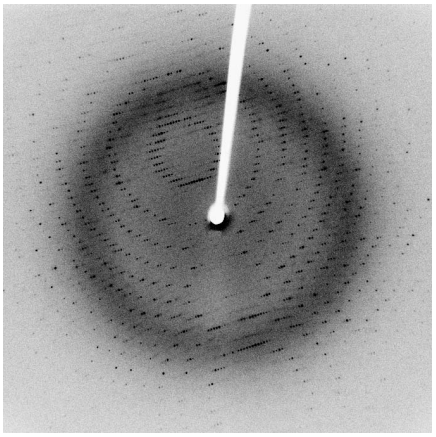

Each dot, called a reflection, in this diffraction pattern forms from the constructive interference of scattered X-rays passing through a crystal. The data can be used to determine the crystalline structure.

- X-ray crystallography in which the pattern produced by the diffraction of X-rays through the closely spaced lattice of atoms in a crystal is recorded and then analysed to reveal the nature of that lattice. A related technique, fiber diffraction, was used by Rosalind Franklin to discover the double helical structure of DNA.[41]
- X-ray astronomy, which is an observational branch of astronomy, which deals with the study of X-ray emission from celestial objects.
- X-ray microscopic analysis, which uses electromagnetic radiation in the soft X-ray band to produce images of very small objects.
- X-ray fluorescence, a technique in which X-rays are generated within a specimen and detected. The outgoing energy of the X-ray can be used to identify the composition of the sample.
- Industrial radiography uses X-rays for inspection of industrial parts, particularly welds.
- Paintings are often X-rayed to reveal the underdrawing and pentimenti or alterations in the course of painting, or by later restorers. Many pigments such as lead white show well in X-ray photographs.
- Airport security luggage scanners use X-rays for inspecting the interior of luggage for security threats before loading on aircraft.
- Border security truck scanners use X-rays for inspecting the interior of trucks for at country borders.
- X-ray fine art photography
- Roentgen Stereophotogrammetry is used to track movement of bones based on the implantation of markers

- X-ray photoelectron spectroscopy is a chemical analysis technique relying on the photoelectric effect, usually employed in surface science.

# History

## Discovery

X-ray fine art photography of needlefish by Peter Dazeley

German physicist Wilhelm Röntgen is usually credited as the discoverer of X-rays because he was the first to systematically study them, though he is not the first to have observed their effects. He is also the one who gave them the name "X-rays", though many referred to these as "Röntgen rays" for several decades after their discovery and to this day in some languages, including Röntgen's native German, and Swedish.

X-rays were found emanating from Crookes tubes, experimental discharge tubes invented around 1875, by scientists investigating the cathode rays, that is energetic electron beams, that were first created in the tubes. Crookes tubes created free electrons by ionization of the residual air in the tube by a high DC voltage of anywhere between a few kilovolts and 100 kV. This voltage accelerated the electrons coming from the cathode to a high enough velocity that they created X-rays when they struck the anode or the glass wall of the tube. Many of the early Crookes tubes undoubtedly radiated X-rays, because early researchers noticed effects that were attributable to them, as detailed below. Wilhelm Röntgen was the first to systematically study them, in 1895.[42]

The important early researchers in X-rays were Ivan Pulyui, William Crookes, Johann Wilhelm Hittorf, Eugen Goldstein, Heinrich Hertz, Philipp Lenard, Hermann von Helmholtz, Nikola Tesla, Thomas Edison, Charles Glover Barkla, Max von Laue, and Wilhelm Conrad Röntgen.

### Johann Hittorf

German physicist Johann Hittorf (1824–1914), a co-inventor and early researcher of the Crookes tube, found when he placed unexposed photographic plates near the tube, that some of them were flawed by shadows, though he did not investigate this effect.

### Ivan Pulyui

In 1877 Ukrainian-born Pulyui, a lecturer in experimental physics at the University of Vienna, constructed various designs of vacuum discharge tube to investigate their properties.[43] He continued his investigations when appointed professor at the Prague Polytechnic and in 1886 he found that sealed photographic plates became dark when exposed to the emanations from the tubes. Early in 1896, just a few weeks after Röntgen published his first X-ray photograph, Pulyui published high-quality X-ray images in journals in Paris and London.[43] Although Pulyui had studied with Röntgen at the University of Strasbourg in the years 1873–75, his biographer Gaida (1997) asserts that his subsequent research was conducted independently.[43]

### Nikola Tesla

In April 1887, Nikola Tesla began to investigate X-rays using high voltages and tubes of his own design, as well as Crookes tubes. From his technical publications, it is indicated that he invented and developed a special single-electrode X-ray tube,[44] [45] which differed from other X-ray tubes in having no target electrode. The principle behind Tesla's device is called the Bremsstrahlung process, in which a high-energy secondary X-ray emission is produced when charged particles (such as electrons) pass through matter. By 1892, Tesla performed several such experiments, but he did not categorize the emissions as what were later called X-rays. Tesla generalized

the phenomenon as radiant energy of "invisible" kinds.[46] [47] Tesla stated the facts of his methods concerning various experiments in his 1897 X-ray lecture before the New York Academy of Sciences.[48] Also in this lecture, Tesla stated the method of construction and safe operation of X-ray equipment. His X-ray experimentation by vacuum high field emissions also led him to alert the scientific community to the biological hazards associated with X-ray exposure.[49]

**Fernando Sanford**

X-rays were generated and detected by Fernando Sanford (1854–1948), the foundation Professor of Physics at Stanford University, in 1891. From 1886 to 1888 he had studied in the Hermann Helmholtz laboratory in Berlin, where he became familiar with the cathode rays generated in vacuum tubes when a voltage was applied across separate electrodes, as previously studied by Heinrich Hertz and Philipp Lenard. His letter of January 6, 1893 (describing his discovery as "electric photography") to The Physical Review was duly published and an article entitled *Without Lens or Light, Photographs Taken With Plate and Object in Darkness* appeared in the San Francisco Examiner.[50]

**Philipp Lenard**

Philipp Lenard, a student of Heinrich Hertz, wanted to see whether cathode rays could pass out of the Crookes tube into the air. He built a Crookes tube (later called a "Lenard tube") with a "window" in the end made of thin aluminum, facing the cathode so the cathode rays would strike it.[51] He found that something came through, that would expose photographic plates and cause fluorescence. He measured the penetrating power of these rays through various materials. It has been suggested that at least some of these "Lenard rays" were actually X-rays.[52] Hermann von Helmholtz formulated mathematical equations for X-rays. He postulated a dispersion theory before Röntgen made his discovery and announcement. It was formed on the basis of the electromagnetic theory of light.[53] However, he did not work with actual X-rays.

**Wilhelm Röntgen**

On November 8, 1895, German physics professor Wilhelm Röntgen stumbled on X-rays while experimenting with Lenard and Crookes tubes and began studying them. He wrote an initial report "*On a new kind of ray: A preliminary communication*" and on December 28, 1895 submitted it to the Würzburg's Physical-Medical Society journal.[54] This was the first paper written on X-rays. Röntgen referred to the radiation as "X", to indicate that it was an unknown type of radiation. The name stuck, although (over Röntgen's great objections) many of his colleagues suggested calling them **Röntgen rays**. They are still referred to as such in many languages, including German and Russian. Röntgen received the first Nobel Prize in Physics for his discovery.

There are conflicting accounts of his discovery because Röntgen had his lab notes burned after his death, but this is a likely reconstruction by his biographers:[55] Röntgen was investigating cathode rays with a fluorescent screen painted with barium platinocyanide and a Crookes tube which he had wrapped in black cardboard so the visible light from the tube wouldn't interfere. He noticed a faint green glow from the screen, about 1 meter away. He realized some invisible rays coming from the tube were passing through the cardboard to make the screen glow. He found they could also pass through books and papers on his desk. Röntgen threw himself into investigating these unknown rays systematically. Two months after his initial discovery, he published his paper.

Röntgen discovered its medical use when he saw a picture of his wife's hand on a photographic plate formed due to X-rays. His wife's hand's photograph was the first ever photograph of a human body part using X-rays. When she saw the picture, she said "I have seen my own death."

### Thomas Edison

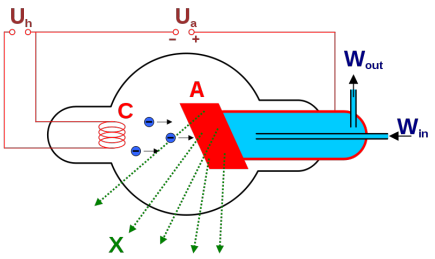

Diagram of a water cooled X-ray tube (simplified/outdated)

In 1895, Thomas Edison investigated materials' ability to fluoresce when exposed to X-rays, and found that calcium tungstate was the most effective substance. Around March 1896, the fluoroscope he developed became the standard for medical X-ray examinations. Nevertheless, Edison dropped X-ray research around 1903 after the death of Clarence Madison Dally, one of his glassblowers. Dally had a habit of testing X-ray tubes on his hands, and acquired a cancer in them so tenacious that both arms were amputated in a futile attempt to save his life. At the 1901 Pan-American Exposition in Buffalo, New York, an assassin shot President William McKinley twice at close range with a .32 caliber revolver. The first bullet was removed but the second remained lodged somewhere in his stomach. McKinley survived for some time and requested that Thomas Edison "rush an X-ray machine to Buffalo to find the stray bullet. It arrived, but was not used as McKinley died of septic shock due to bacterial infection."[56]

### Frank Austin and the Frost brothers

The first medical X-ray made in the United States was obtained using a discharge tube of Pulyui's design. In January 1896, on reading of Röntgen's discovery, Frank Austin of Dartmouth College tested all of the discharge tubes in the physics laboratory and found that only the Pulyui tube produced X-rays. This was a result of Pulyui's inclusion of an oblique "target" of mica, used for holding samples of fluorescent material, within the tube. On 3 February 1896 Gilman Frost, professor of medicine at the college, and his brother Edwin Frost, professor of physics, exposed the wrist of Eddie McCarthy, whom Edwin had treated some weeks earlier for a fracture, to the X-rays and collected the resulting image of the broken bone on gelatin photographic plates obtained from Howard Langill, a local photographer also interested in Röntgen's work.[24]

## 20th century and beyond


A male technician taking an x-ray of a female patient in 1940. This image was used to argue that exposure to radiation during the x-ray procedure would be a myth.

The many applications of X-rays immediately generated enormous interest. Workshops began making specialized versions of Crookes tubes for generating X-rays, and these first generation cold cathode or Crookes X-ray tubes were used until about 1920.

Crookes tubes were unreliable. They had to contain a small quantity of gas (invariably air) as a current will not flow in such a tube if they are fully evacuated. However as time passed the X-rays caused the glass to absorb the gas, causing the tube to generate "harder" X-rays until it soon stopped operating. Larger and more frequently used tubes were provided with devices for restoring the air, known as "softeners". These often took the form of a small side tube which contained a small piece of mica: a substance that traps comparatively large quantities of air within its structure. A small electrical heater heated the mica and caused it to release a small amount of air, thus restoring the tube's efficiency. However the mica had a limited life and the restore process was consequently difficult to control.

In 1904, John Ambrose Fleming invented the thermionic diode valve (vacuum tube). This used a hot cathode which permitted current to flow in a vacuum. This idea was quickly applied to X-ray tubes, and heated cathode X-ray tubes, called Coolidge tubes, replaced the troublesome cold cathode tubes by about 1920.

Two years later, physicist Charles Barkla discovered that X-rays could be scattered by gases, and that each element had a characteristic X-ray. He won the 1917 Nobel Prize in Physics for this discovery. Max von Laue, Paul Knipping and Walter Friedrich observed for the first time the diffraction of X-rays by crystals in 1912. This discovery, along with the early works of Paul Peter Ewald, William Henry Bragg and William Lawrence Bragg gave birth to the field of X-ray crystallography. The Coolidge tube was invented the following year by William D. Coolidge which permitted continuous production of X-rays; this type of tube is still in use today.

The use of X-rays for medical purposes (to develop into the field of radiation therapy) was pioneered by Major John Hall-Edwards in Birmingham, England. In 1908, he had to have his left arm amputated owing to the spread of X-ray dermatitis.[57] The X-ray microscope was invented in the 1950s.

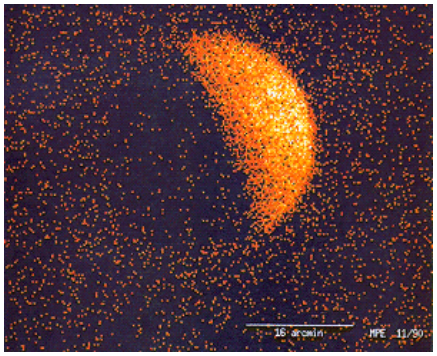

ROSAT image of X-ray fluorescence of, and occultation of the X-ray background by, the Moon

The Chandra X-ray Observatory, launched on July 23, 1999, has been allowing the exploration of the very violent processes in the universe which produce X-rays. Unlike visible light, which is a relatively stable view of the universe, the X-ray universe is unstable, it features stars being torn apart by black holes, galactic collisions, and novas, neutron stars that build up layers of plasma that then explode into space.

An X-ray laser device was proposed as part of the Reagan Administration's Strategic Defense Initiative in the 1980s, but the first and only test of the device (a sort of laser "blaster", or death ray, powered by a thermonuclear explosion) gave inconclusive results. For technical and political reasons, the overall project (including the X-ray laser) was de-funded (though was later revived by the second Bush Administration as National Missile Defense using different technologies).

## See also

- Backscatter X-ray
- detective quantum efficiency
- High energy X-rays
- N ray
- Neutron radiation
- Radiologic technologist
- Resonant inelastic X-ray scattering (RIXS)
- Small angle X-ray scattering (SAXS)
- X-ray absorption spectroscopy
- X-ray generation
- X-ray marker
- X-ray nanoprobe
- X-ray optics
- X-ray vision
- X-ray welding
- X-ray reflectivity

# Notes


[1] Novelline, Robert. *Squire's Fundamentals of Radiology*. Harvard University Press. 5th edition. 1997. ISBN 0674833392.

[2] *Oxford English Dictionary* http://www.oed.com

[3] http://physics.nist.gov/cgi-bin/ffast/ffast.pl?Formula=H2O&gtype=5&range=S&lower=0.300&upper=2.00&density=1.00

[4] Dendy, P. P.; B. Heaton (1999). *Physics for Diagnostic Radiology* (http://books.google.com/?id=1BTQvsQIs4wC&pg=PA12). USA: CRC Press. p. 12. ISBN 0750305916. .

[5] Charles Hodgman, Ed. (1961). *CRC Handbook of Chemistry and Physics, 44th Ed.*. USA: Chemical Rubber Co.. p. 2850.

[6] Feynman, Richard; Robert Leighton, Matthew Sands (1963). *The Feynman Lectures on Physics, Vol.1*. USA: Addison-Wesley. pp. 2–5. ISBN 0201021161.

[7] L'Annunziata, Michael; Mohammad Baradei (2003). *Handbook of Radioactivity Analysis* (http://books.google.com/?id=b519e10OPT0C&pg=PA58&dq=gamma+x-ray). Academic Press. p. 58. ISBN 0124366031. .

[8] Grupen, Claus; G. Cowan, S. D. Eidelman, T. Stroh (2005). *Astroparticle Physics*. Springer. p. 109. ISBN 3540253122.

[9] US National Research Council (2006). *Health Risks from Low Levels of Ionizing Radiation, BEIR 7 phase 2* (http://books.google.com/?id=Uqj4OzBKlHwC&pg=PA5). National Academies Press. pp. 5, fig.PS–2. ISBN 030909156X. ., data credited to NCRP (US National Committee on Radiation Protection) 1987

[10] http://www.doctorspiller.com/Dental%20_X-Rays.htm and http://www.dentalgentlecare.com/x-ray_safety.htm

[11] (http://hss.energy.gov/NuclearSafety/NSEA/fire/trainingdocs/radem3.pdf)

[12] (http://www.hawkhill.com/114s.html)

[13] http://www.solarstorms.org/SWChapter8.html and http://www.powerattunements.com/x-ray.html

[14] David R. Lide, ed (1994). *CRC Handbook of Chemistry and Physics 75th edition*. CRC Press. pp. 10–227. ISBN 0-8493-0475-X.

[15] Kevles, Bettyann Holtzmann (1996). *Naked to the Bone Medical Imaging in the Twentieth Century*. Camden, NJ: Rutgers University Press. pp. 19–22. ISBN 0813523583.

[16] Sample, Sharron (2007-03-27). "X-Rays" (http://science.hq.nasa.gov/kids/imagers/ems/xrays.html). *The Electromagnetic Spectrum*. NASA. . Retrieved 2007-12-03.

[17] Whaites, Eric; Roderick Cawson (2002). *Essentials of Dental Radiography and Radiology* (http://books.google.com/?id=x6ThiifBPcsC&dq=radiography+kilovolt+x-ray+machine). Elsevier Health Sciences. pp. 15–20. ISBN 044307027X. .

[18] Bushburg, Jerrold; Anthony Seibert, Edwin Leidholdt, John Boone (2002). *The Essential Physics of Medical Imaging* (http://books.google.com/?id=VZvqqaQ5DvoC&pg=PT33&dq=radiography+kerma+rem+Sievert). USA: Lippincott Williams & Wilkins. p. 116. ISBN 0683301187. .

[19] Emilio, Burattini; Antonella Ballerna (1994). "Preface" (http://books.google.com/books?id=VEld4080nekC&pg=PA129&dq="synchrotron+radiation"+x-ray+advantages&as_brr=3). . IOS Press. pp. xv. ISBN 9051992483. . Retrieved 2008-11-11.

[20] Martin, Dylan (2005). "X-Ray Detection" (http://www.u.arizona.edu/~dwmartin/). University of Arizona Optical Sciences Center. . Retrieved 2008-05-19.

[21] Frame, Paul. "Wilhelm Röntgen and the Invisible Light" (http://www.orau.org/ptp/articlesstories/invisiblelight.htm). *Tales from the Atomic Age*. Oak Ridge Associated Universities. . Retrieved 2008-05-19.

[22] http://www.esrf.eu/UsersAndScience/Experiments/MaterialsScience/faisceau

[23] *Eæements of Modern X-Ray Physics*. John Wiley & Sons Ltd,. 2001. pp. 40–41. ISBN 0-471-49858-0.

[24] Spiegel, Peter K (1995). "The first clinical X-ray made in America—100 years" (http://www.ajronline.org/cgi/reprint/164/1/241.pdf). *American Journal of Roentgenology* (Leesburg, VA: American Roentgen Ray Society) **164** (1): 241–243. ISSN: 1546-3141. PMID 7998549. .

[25] Herman, Gabor T. (2009). *Fundamentals of Computerized Tomography: Image Reconstruction from Projections* (2nd ed.). Springer. ISBN 978-1-85233-617-2

[26] "11th Report on Carcinogens" (http://ntp.niehs.nih.gov/ntp/roc/toc11.html). Ntp.niehs.nih.gov. . Retrieved 2010-11-08.

[27] Upton, AC (2003). "The state of the art in the 1990s: NCRP report No. 136 on the scientific bases for linearity in the dose-response relationship for ionizing radiation". *Health Physics* **85**: 15–22.

[28] Calabrese and Baldwin, Toxicology rethinks its central belief, *Nature*, **421**, pp.691-2, 13 February 2003.

[29] United Nations Scientific Committee on the Effects of Atomic Radiation. New York. United Nations, 2000

[30] Berrington; de Gonzalez, A; Darby, S (2004). "Risk of cancer from diagnostic X-rays: estimates for the UK and 14 other countries". *Lancet* **363**: 345–351.

[31] Brenner DJ and Hall EJ (2007). "Computed tomography- an increasing source of radiation exposure." (http://www.nejm.org/doi/full/10.1056/NEJMra072149). *New England Journal of Medicine* **357**: 2277–2284. .

[32] (http://www.radiologyinfo.org/en/safety/index.cfm?pg=sfty_xray)|Radiological Society of North America and American College of Radiology

[33] Caon, M., Bibbo, G. & Pattison, J. (2000) Monte Carlo calculated effective dose to teenage girls from computed tomography examinations, *Radiation Protection Dosimetry* **90**(4):445-448.

[34] (http://seer.cancer.gov/csr/1975_2006/browse_csr.php?section=2&page=sect_02_table.11.html#table1)|National Cancer Institute: Surveillance Epidemiology and End Results (SEER) data

[35] Gregory KG, Bibbo G and Pattison JE (2008) On the uncertanties in effective dose estimates of adult CT head scans, *Medical Physics* **35**(8):3501-3510.

[36] Xiao-Ou, Shu; et al (December 1994). "Association of paternal diagnostic X-ray exposure with risk of infant leukemia" (http://www.ncbi.nlm.nih.gov/pubmed/7881337). *Cancer Epidemiology, Biomarkers & Prevention* (American Association for Cancer Research) **3** (8): 645. ISSN 1538-7755. PMID 7881337. .

[37] Stewart, Alice M; Webb, J.W.; Giles, B.D.; Hewitt, D. (1956). "Preliminary Communication: Malignant Disease in Childhood and Diagnostic Irradiation In-Utero". *Lancet* **271** (6940): 447. PMID 13358242.

[38] "Pregnant Women and Radiation Exposure" (http://emedicinelive.com/index.php/Women-s-Health/pregnant-women-and-radiation-exposure.html). *eMedicine Live online medical consultation*. Medscape. 28 December 2008. . Retrieved 2009-01-16.

[39] Donnelly, CF (2005). "Reducing radiation dose associated with pediatric CT by decreasing unnecessary examinations". *American Journal Roentgenology* **32**: 242–244.

[40] Alchemy Art Lead Products – Lead Shielding Sheet Lead For Shielding Applications (http://www.alchemycastings.com/pdf/SheetLead.pdf). Retrieved 2008-12-07.

[41] Kasai, Nobutami; Masao Kakudo (2005). *X-ray diffraction by macromolecules*. Tokyo: Kodansha. pp. 291–2. ISBN 3540253173.

[42] The history, development, and impact of computed imaging in neurological diagnosis and neurosurgery: CT, MRI, DTI: Nature Precedings DOI: 10.1038/npre.2009.3267.5 (http://precedings.nature.com/documents/3267/version/5).

[43] Gaida, Roman; et al. (1997). "Ukrainian Physicist Contributes to the Discovery of X-Rays" (http://web.archive.org/web/20080528172938/http://www.meduniv.lviv.ua/oldsite/puluj.html). Mayo Foundation for Medical Education and Research. Archived from the original (http://www.meduniv.lviv.ua/oldsite/puluj.html) on 2008-05-28. . Retrieved 2008-04-06.

[44] Morton, William James, and Edwin W. Hammer, American Technical Book Co., 1896. Page 68.

[45] U.S. Patent 514170 (http://www.google.com/patents?vid=514170), *Incandescent Electric Light*, and U.S. Patent 454622 (http://www.google.com/patents?vid=454622), *System of Electric Lighting*.

[46] Cheney, Margaret, " Tesla: Man Out of Time (http://books.google.com/books?vid=ISBN0743215362)". Simon and Schuster, 2001. Page 77.

[47] Thomas Commerford Martin (ed.), " The Inventions, Researches and Writings of Nikola Tesla (http://books.google.com/books?vid=OCLC04049568)". Page 252 "When it forms a drop, it will emit visible and invisible waves. [...]". (ed., this material originally appeared in an article by Nikola Tesla in The Electrical Engineer of 1894.)

[48] Nikola Tesla, "The stream of Lenard and Roentgen and novel apparatus for their production", Apr. 6, 1897.

[49] Cheney, Margaret, Robert Uth, and Jim Glenn, " Tesla, master of lightning (http://books.google.com/books?vid=ISBN0760710058)". Barnes & Noble Publishing, 1999. Page 76. ISBN 0760710058

[50] Wyman, Thomas (Spring 2005). "Fernando Sanford and the Discovery of X-rays". *"Imprint", from the Associates of the Stanford University Libraries*: 5–15.

[51] Thomson, Joseph J. (1903). *The Discharge of Electricity through Gasses* (http://books.google.com/?id=Ryw4AAAAMAAJ&pg=PA138). USA: Charles Scribner's Sons. pp. 182–186. .

[52] Thomson, 1903, p.185

[53] *Wiedmann's Annalen*, Vol. XLVIII

[54] Stanton, Arthur (1896-01-23). "Wilhelm Conrad Röntgen On a New Kind of Rays: translation of a paper read before the Würzburg Physical and Medical Society, 1895" (http://www.nature.com/nature/journal/v53/n1369/pdf/053274b0.pdf) (Subscription-only access – Scholar search (http://scholar.google.co.uk/scholar?hl=en&lr=&q=author:Stanton+intitle:Wilhelm+Conrad+RÃ¶ntgen+On+a+New+Kind+of+Rays:+translation+of+a+paper+read+before+the+WÃ¼rzburg+Physical+and+Medical+Society,+1895&as_publication=[[Nature+(journal)|Nature]]&as_ylo=1896&as_yhi=1896&btnG=Search)). *Nature* **53** (1369): 274–6. doi:10.1038/053274b0. see also pp. 268 and 276 of the same issue.

[55] Peters, Peter (1995). "W. C. Roentgen and the discovery of x-rays" (http://www.medcyclopaedia.com/library/radiology/chapter01.aspx). *Ch.1 Textbook of Radiology*. Medcyclopedia.com, GE Healthcare. . Retrieved 2008-05-05.

[56] National Library of Medicine. " Could X-rays Have Saved President William McKinley? (http://www.nlm.nih.gov/visibleproofs/galleries/cases/mckinley.html)" *Visible Proofs: Forensic Views of the Body*.

[57] (http://www.birmingham.gov.uk/xray|Birmingham.gov.uk)

## References


- NASA (http://imagers.gsfc.nasa.gov/ems/xrays.html) Goddard Space Flight centre introduction to X-rays.


## External links

- Example Radiograph: Fractured Humerus (http://www.rtstudents.com/x-rays/broken-humerus-xray.htm)
- A Photograph of an X-ray Machine (http://www.iuk.edu/~koalhe/img/Equipment/xray.jpg)
- X-ray Safety (http://www.x-raysafety.com/)
- An X-ray tube demonstration (Animation) (http://www.ionactive.co.uk/multi-media_video.html?m=4)
- 1896 Article: "On a New Kind of Rays" (http://web.archive.org/web/20070710033139/http://deutsche.nature.com/physics/7.pdf)
- "Digital X-Ray Technologies Project" (http://docs.google.com/fileview?id=0B89CZuXbiY7mNmQxYmVlNDktNjBiZS00NjcwLTg0ODgtZjc3NWUwOWUxZDg5&hl=tr)
- A video of a medical X-ray procedure example (http://nursing-resource.com/?p=198#videolink)
- What is Radiology? (http://rad.usuhs.mil/rad/home/whatis.html) a simple tutorial
- 50,000 X-ray, MRI, and CT pictures (http://rad.usuhs.edu/medpix) MedPix medical image database
- Index of Early Bremsstrahlung Articles (http://www.datasync.com/~rsf1/bremindx.htm)
- Extraordinary X-Rays (http://www.life.com/image/first/in-gallery/44881/extraordinary-x-rays) – slideshow by *Life magazine*

# Electron

| *Electron* | |
|---|---|
| 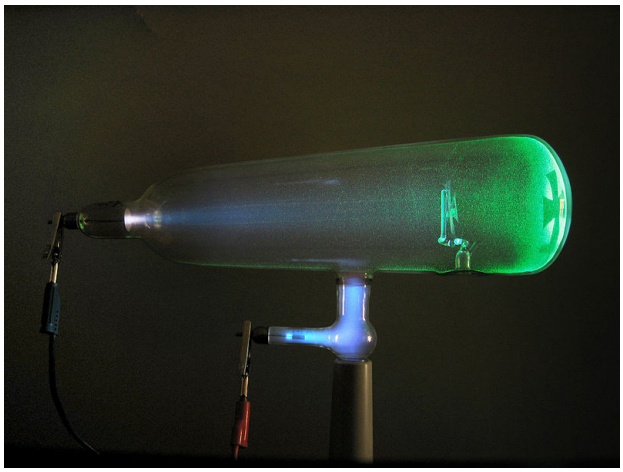 | |
| Experiments with a Crookes tube first demonstrated the particle nature of electrons. In this illustration, the profile of the cross-shaped target is projected against the tube face at right by a beam of electrons.[1] | |
| **Composition:** | Elementary particle[2] |
| **Particle statistics:** | Fermionic |
| **Group:** | Lepton |
| **Generation:** | First |
| **Interaction:** | Gravity, Electromagnetic, Weak |
| **Symbol(s):** | $e^-$, $\beta^-$ |
| **Antiparticle:** | Positron (also called antielectron) |
| **Theorized:** | Richard Laming (1838–1851),[3]<br>G. Johnstone Stoney (1874) and others.[4] [5] |
| **Discovered:** | J. J. Thomson (1897)[6] |
| **Mass:** | $9.10938215(45) \times 10^{-31}$ kg[7] $5.4857990943(23) \times 10^{-4}$ u[7]<br>$[1822.88850204(77)]^{-1}$ u[8]<br>0.510998910(13) MeV/$c^2$[7] |
| **Electric charge:** | −1 e[9]<br>$-1.602176487(40) \times 10^{-19}$ C[7] $-4.803 \times 10^{-10}$ esu [10] |
| **Magnetic moment:** | $-1.00115965218111\ \mu_B$ [7] |
| **Spin:** | $^1/_2$ |

The **electron** is a subatomic particle carrying a negative electric charge. It has no known components or substructure. Therefore, the electron is generally believed to be an elementary particle.[2] An electron has a mass that is approximately 1/1836 that of the proton.[11] The intrinsic angular momentum (spin) of the electron is a half-integer value in units of $\hbar$, which means that it is a fermion. The antiparticle of the electron is called the positron. The positron is identical to the electron except that it carries electrical and other charges of the opposite sign. When an electron collides with a positron, both particles may either scatter off each other or be totally annihilated, producing a pair (or more) of gamma ray photons. Electrons, which belong to the first generation of the lepton particle family,[12]

participate in gravitational, electromagnetic and weak interactions.[13] Electrons, like all matter, have quantum mechanical properties of both particles and waves, so they can collide with other particles and be diffracted like light. However, this duality is best demonstrated in experiments with electrons, due to their tiny mass. Since an electron is a fermion, no two electrons can occupy the same quantum state, in accordance with the Pauli exclusion principle.[12]

The concept of an indivisible amount of electric charge was theorized to explain the chemical properties of atoms, beginning in 1838 by British natural philosopher Richard Laming;[4] the name *electron* was introduced for this charge in 1894 by Irish physicist George Johnstone Stoney. The electron was identified as a particle in 1897 by J. J. Thomson and his team of British physicists.[6] [14] [15]

In many physical phenomena, such as electricity, magnetism, and thermal conductivity, electrons play an essential role. An electron in motion relative to an observer generates a magnetic field, and will be deflected by external magnetic fields. When an electron is accelerated, it can absorb or radiate energy in the form of photons. Electrons, together with atomic nuclei made of protons and neutrons, make up atoms. However, electrons contribute less than 0.06% to an atom's total mass. The attractive Coulomb force between an electron and a proton causes electrons to be bound into atoms. The exchange or sharing of the electrons between two or more atoms is the main cause of chemical bonding.[16]

According to theory, most electrons in the universe were created in the big bang, but they may also be created through beta decay of radioactive isotopes and in high-energy collisions, for instance when cosmic rays enter the atmosphere. Electrons may be destroyed through annihilation with positrons, and may be absorbed during nucleosynthesis in stars. Laboratory instruments are capable of containing and observing individual electrons as well as electron plasma, whereas dedicated telescopes can detect electron plasma in outer space. Electrons have many applications, including welding, cathode ray tubes, electron microscopes, radiation therapy, lasers and particle accelerators.

## History

The ancient Greeks noticed that amber attracted small objects when rubbed with fur. Apart from lightning, this phenomenon is humanity's earliest recorded experience with electricity.[17] In his 1600 treatise *De Magnete*, the English scientist William Gilbert coined the New Latin term *electricus*, to refer to this property of attracting small objects after being rubbed.[18] Both *electric* and *electricity* are derived from the Latin *ēlectrum* (also the root of the alloy of the same name), which came from the Greek word ήλεκτρον (*ēlektron*) for amber.

In 1737 C. F. du Fay and Hawksbee independently discovered what they believed to be two kinds of frictional electricity; one generated from rubbing glass, the other from rubbing resin. From this, Du Fay theorized that electricity consists of two electrical fluids, "vitreous" and "resinous", that are separated by friction and that neutralize each other when combined.[19] A decade later Benjamin Franklin proposed that electricity was not from different types of electrical fluid, but the same electrical fluid under different pressures. He gave them the modern charge nomenclature of positive and negative respectively.[20] [21] Franklin thought that the charge carrier was positive.[22]

Between 1838 and 1851, British natural philosopher Richard Laming developed the idea that an atom is composed of a core of matter surrounded by subatomic particles that had unit electric charges.[3] Beginning in 1846, German physicist William Weber theorized that electricity was composed of positively and negatively charged fluids, and their interaction was governed by the inverse square law. After studying the phenomenon of electrolysis in 1874, Irish physicist George Johnstone Stoney suggested that there existed a "single definite quantity of electricity", the charge of a monovalent ion. He was able to estimate the value of this elementary charge *e* by means of Faraday's laws of electrolysis.[23] However, Stoney believed these charges were permanently attached to atoms and could not be removed. In 1881, German physicist Hermann von Helmholtz argued that both positive and negative charges were divided into elementary parts, each of which "behaves like atoms of electricity".[4]

In 1894, Stoney coined the term *electron* to describe these elementary charges, saying, "... an estimate was made of the actual amount of this most remarkable fundamental unit of electricity, for which I have since ventured to suggest the name *electron*".[24] The word *electron* is a combination of the word *electric* and the suffix *-on*, with the latter now used to designate a subatomic particle, such as a proton or neutron.[25] [26]

## Discovery

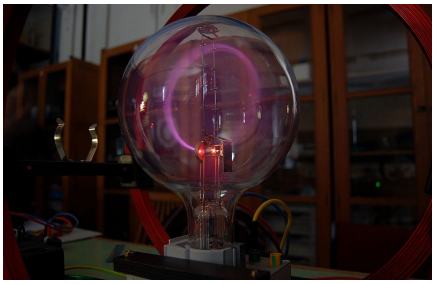

A beam of electrons deflected in a circle by a magnetic field[27]

The German physicist Johann Wilhelm Hittorf undertook the study of electrical conductivity in rarefied gases. In 1869, he discovered a glow emitted from the cathode that increased in size with decrease in gas pressure. In 1876, the German physicist Eugen Goldstein showed that the rays from this glow cast a shadow, and he dubbed them cathode rays.[28] During the 1870s, the English chemist and physicist Sir William Crookes developed the first cathode ray tube to have a high vacuum inside.[29] He then showed that the luminescence rays appearing within the tube carried energy and moved from the cathode to the anode. Furthermore, by applying a magnetic field, he was able to deflect the rays, thereby demonstrating that the beam behaved as though it were negatively charged.[30] [31] In 1879, he proposed that these properties could be explained by what he termed 'radiant matter'. He suggested that this was a fourth state of matter, consisting of negatively charged molecules that were being projected with high velocity from the cathode.[32]

The German-born British physicist Arthur Schuster expanded upon Crookes' experiments by placing metal plates in parallel to the cathode rays and applying an electric potential between the plates. The field deflected the rays toward the positively charged plate, providing further evidence that the rays carried negative charge. By measuring the amount of deflection for a given level of current, in 1890 Schuster was able to estimate the charge-to-mass ratio of the ray components. However, this produced a value that was more than a thousand times greater than what was expected, so little credence was given to his calculations at the time.[30] [33]

In 1896, the British physicist J. J. Thomson, with his colleagues John S. Townsend and H. A. Wilson,[14] performed experiments indicating that cathode rays really were unique particles, rather than waves, atoms or molecules as was believed earlier.[6] Thomson made good estimates of both the charge *e* and the mass *m*, finding that cathode ray particles, which he called "corpuscles," had perhaps one thousandth of the mass of the least massive ion known: hydrogen.[6] [15] He showed that their charge to mass ratio, *e*/*m*, was independent of cathode material. He further showed that the negatively charged particles produced by radioactive materials, by heated materials and by illuminated materials were universal.[6] [34] The name electron was again proposed for these particles by the Irish physicist George F. Fitzgerald, and the name has since gained universal acceptance.[30]

While studying naturally fluorescing minerals in 1896, the French physicist Henri Becquerel discovered that they emitted radiation without any exposure to an external energy source. These radioactive materials became the subject of much interest by scientists, including the New Zealand physicist Ernest Rutherford who discovered they emitted particles. He designated these particles alpha and beta, on the basis of their ability to penetrate matter.[35] In 1900, Becquerel showed that the beta rays emitted by radium could be deflected by an electric field, and that their mass-to-charge ratio was the same as for cathode rays.[36] This evidence strengthened the view that electrons existed as components of atoms.[37] [38]

The electron's charge was more carefully measured by the American physicist Robert Millikan in his oil-drop experiment of 1909, the results of which he published in 1911. This experiment used an electric field to prevent a charged droplet of oil from falling as a result of gravity. This device could measure the electric charge from as few as 1−150 ions with an error margin of less than 0.3%. Comparable experiments had been done earlier by Thomson's team,[6] using clouds of charged water droplets generated by electrolysis,[14] and in 1911 by Abram Ioffe, who

independently obtained the same result as Millikan using charged microparticles of metals, then published his results in 1913.[39] However, oil drops were more stable than water drops because of their slower evaporation rate, and thus more suited to precise experimentation over longer periods of time.[40]

Around the beginning of the twentieth century, it was found that under certain conditions a fast moving charged particle caused a condensation of supersaturated water vapor along its path. In 1911, Charles Wilson used this principle to devise his cloud chamber, allowing the tracks of charged particles, such as fast-moving electrons, to be photographed.[41]

## Atomic theory

By 1914, experiments by physicists Ernest Rutherford, Henry Moseley, James Franck and Gustav Hertz had largely established the structure of an atom as a dense nucleus of positive charge surrounded by lower-mass electrons.[42] In 1913, Danish physicist Niels Bohr postulated that electrons resided in quantized energy states, with the energy determined by the angular momentum of the electron's orbits about the nucleus. The electrons could move between these states, or orbits, by the emission or absorption of photons at specific frequencies. By means of these quantized orbits, he accurately explained the spectral lines of the hydrogen atom.[43] However, Bohr's model failed to account for the relative intensities of the spectral lines and it was unsuccessful in explaining the spectra of more complex atoms.[42]

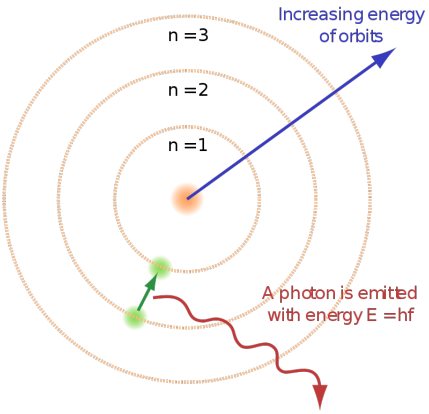


The Bohr model of the atom, showing states of electron with energy quantized by the number n. An electron dropping to a lower orbit emits a photon equal to the energy difference between the orbits.

Chemical bonds between atoms were explained by Gilbert Newton Lewis, who in 1916 proposed that a covalent bond between two atoms is maintained by a pair of electrons shared between them.[44] Later, in 1923, Walter Heitler and Fritz London gave the full explanation of the electron-pair formation and chemical bonding in terms of quantum mechanics.[45] In 1919, the American chemist Irving Langmuir elaborated on the Lewis' static model of the atom and suggested that all electrons were distributed in successive "concentric (nearly) spherical shells, all of equal thickness".[46] The shells were, in turn, divided by him in a number of cells each containing one pair of electrons. With this model Langmuir was able to qualitatively explain the chemical properties of all elements in the periodic table,[45] which were known to largely repeat themselves according to the periodic law.[47]

In 1924, Austrian physicist Wolfgang Pauli observed that the shell-like structure of the atom could be explained by a set of four parameters that defined every quantum energy state, as long as each state was inhabited by no more than a single electron. (This prohibition against more than one electron occupying the same quantum energy state became known as the Pauli exclusion principle.)[48] The physical mechanism to explain the fourth parameter, which had two distinct possible values, was provided by the Dutch physicists Abraham Goudsmith and George Uhlenbeck when they suggested that an electron, in addition to the angular momentum of its orbit, could possess an intrinsic angular momentum.[42] [49] This property became known as spin, and explained the previously mysterious splitting of spectral lines observed with a high-resolution spectrograph; this phenomenon is known as fine structure splitting.[50]

## Quantum mechanics

In his 1924 dissertation *Recherches sur la théorie des quanta* (Research on Quantum Theory), French physicist Louis de Broglie hypothesized that all matter possesses a De Broglie wave similar to light.[51] That is, under the appropriate conditions, electrons and other matter would show properties of either particles or waves. The corpuscular properties of a particle are demonstrated when it is shown to have a localized position in space along its trajectory at any given moment.[52] Wave-like nature is observed, for example, when a beam of light is passed through parallel slits and creates interference patterns. In 1927, the interference effect was demonstrated with a beam of electrons by English physicist George Paget Thomson with a thin metal film and by American physicists Clinton Davisson and Lester Germer using a crystal of nickel.[53]

The success of de Broglie's prediction led to the publication, by Erwin Schrödinger in 1926, of the Schrödinger equation that successfully describes how electron waves propagated.[54] Rather than yielding a solution that determines the location of an electron over time, this wave equation can be used to predict the probability of finding an electron near a position. This approach was later called quantum mechanics, which provided an extremely close derivation to the energy states of an electron in a hydrogen atom.[55] Once spin and the interaction between multiple electrons were considered, quantum mechanics allowed the configuration of electrons in atoms with higher atomic numbers than hydrogen to be successfully predicted.[56]

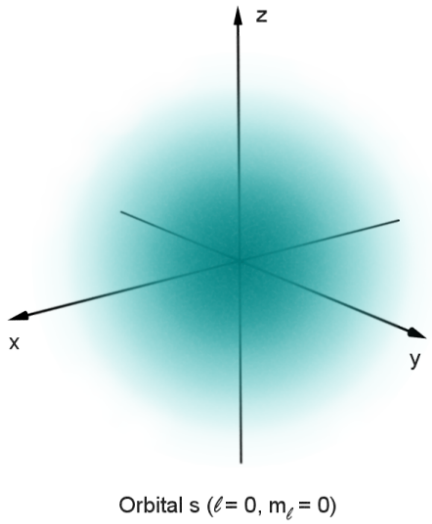


In quantum mechanics, the behavior of an electron in an atom is described by an orbital, which is a probability distribution rather than an orbit. In the figure, the shading indicates the relative probability to "find" the electron, having the energy corresponding to the given quantum numbers, at that point.

In 1928, building on Wolfgang Pauli's work, Paul Dirac produced a model of the electron - the Dirac equation, consistent with relativity theory, by applying relativistic and symmetry considerations to the hamiltonian formulation of the quantum mechanics of the electro-magnetic field.[57] In order to resolve some problems within his relativistic equation, in 1930 Dirac developed a model of the vacuum as an infinite sea of particles having negative energy, which was dubbed the Dirac sea. This led him to predict the existence of a positron, the antimatter counterpart of the electron.[58] This particle was discovered in 1932 by Carl D. Anderson, who proposed calling standard electrons *negatrons*, and using *electron* as a generic term to describe both the positively and negatively charged variants. This usage of the term 'negatron' is still occasionally encountered today, and it may be shortened to 'negaton'.[59] [60]

In 1947 Willis Lamb, working in collaboration with graduate student Robert Rutherford, found that certain quantum states of hydrogen atom, which should have the same energy, were shifted in relation to each other, the difference being the Lamb shift. About the same time, Polykarp Kusch, working with Henry M. Foley, discovered the magnetic moment of the electron is slightly larger than predicted by Dirac's theory. This small difference was later called anomalous magnetic dipole moment of the electron. To resolve these issues, a refined theory called quantum electrodynamics was developed by Sin-Itiro Tomonaga, Julian Schwinger and Richard P. Feynman in the late 1940s.[61]

### Particle accelerators

With the development of the particle accelerator during the first half of the twentieth century, physicists began to delve deeper into the properties of subatomic particles.[62] The first successful attempt to accelerate electrons using Electromagnetic induction was made in 1942 by Donald Kerst. His initial betatron reached energies of 2.3 MeV, while subsequent betatrons achieved 300 MeV. In 1947, synchrotron radiation was discovered with a 70 MeV electron synchrotron at General Electric. This radiation was caused by the acceleration of electrons, moving near the speed of light, through a magnetic field.[63]

With a beam energy of 1.5 GeV, the first high-energy particle collider was ADONE, which began operations in 1968.[64] This device accelerated electrons and positrons in opposite directions, effectively doubling the energy of their collision when compared to striking a static target with an electron.[65] The Large Electron-Positron Collider (LEP) at CERN, which was operational from 1989 to 2000, achieved collision energies of 209 GeV and made important measurements for the Standard Model of particle physics.[66] [67]

## Characteristics

### Classification

In the Standard Model of particle physics, electrons belong to the group of subatomic particles called leptons, which are believed to be fundamental or elementary particles. Electrons have the lowest mass of any charged lepton (or electrically charged particle of any type) and belong to the first-generation of fundamental particles.[68] The second and third generation contain charged leptons, the muon and the tau, which are identical to the electron in charge, spin and interactions, but are more massive. Leptons differ from the other basic constituent of matter, the quarks, by their lack of strong interaction. All members of the lepton group are fermions, because they all have half-odd integer spin; the electron has spin $1/2$.[69]

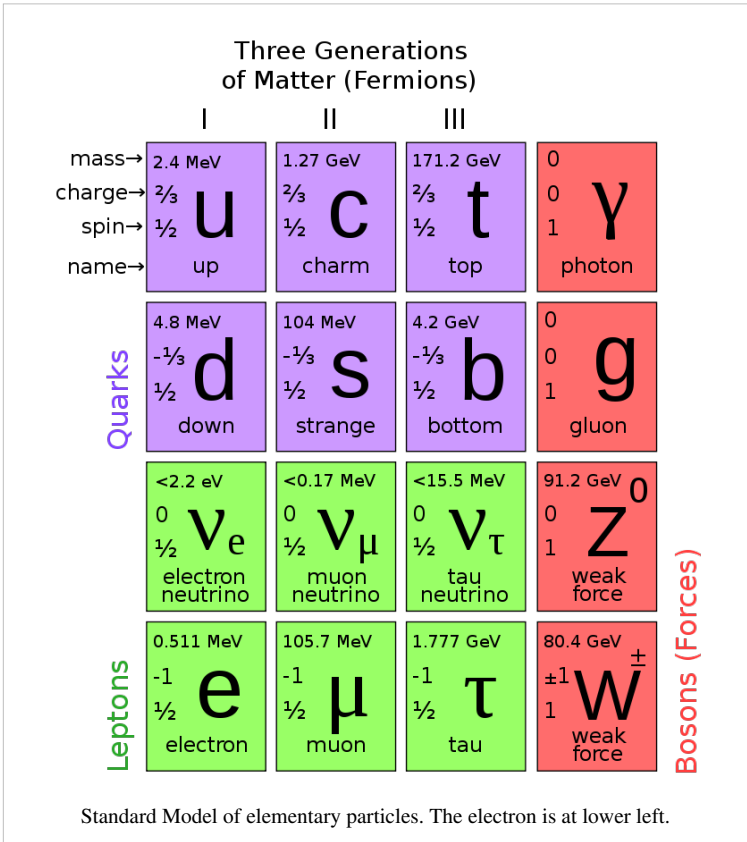


Standard Model of elementary particles. The electron is at lower left.

### Fundamental properties

The invariant mass of an electron is approximately $9.109 \times 10^{-31}$ kilogram,[7] or $5.489 \times 10^{-4}$ atomic mass unit. On the basis of Einstein's principle of mass–energy equivalence, this mass corresponds to a rest energy of 0.511 MeV. The ratio between the mass of a proton and that of an electron is about 1836.[11] [70] Astronomical measurements show that the proton-to-electron mass ratio has held the same value for at least half the age of the universe, as is predicted by the Standard Model.[71]

Electrons have an electric charge of $-1.602 \times 10^{-19}$ coulomb,[7] which is used as a standard unit of charge for subatomic particles. Within the limits of experimental accuracy, the electron charge is identical to the charge of a proton, but with the opposite sign.[72] As the symbol $e$ is used for the elementary charge, the electron is commonly symbolized by $e^-$, where the minus sign indicates the negative charge. The positron is symbolized by $e^+$ because it

has the same properties as the electron but with a positive rather than negative charge.[7] [69]

The electron has an intrinsic angular momentum or spin of $^1/_2$.[7] This property is usually stated by referring to the electron as a spin-$^1/_2$ particle.[69] For such particles the spin magnitude is $^{\sqrt{3}}/_2\,\hbar$.[73] while the result of the measurement of a projection of the spin on any axis can only be $\pm^{\hbar}/_2$. In addition to spin, the electron has an intrinsic magnetic moment along its spin axis.[7] It is approximately equal to one Bohr magneton,[74] [75] which is a physical constant equal to 9.274 009 15(23) × $10^{-24}$ joules per tesla.[7] The orientation of the spin with respect to the momentum of the electron defines the property of elementary particles known as helicity.[76]

The electron has no known substructure.[2] [77] Hence, it is defined or assumed to be a point particle with a point charge and no spatial extent.[12] Observation of a single electron in a Penning trap shows the upper limit of the particle's radius is $10^{-22}$ meters.[78] There *is* a physical constant called the "classical electron radius", with the much larger value of $2.8179 \times 10^{-15}$ m. However, the terminology comes from a simplistic calculation that ignores the effects of quantum mechanics; in reality, the so-called classical electron radius has little to do with the true fundamental structure of the electron.[79] [80]

There are elementary particles that spontaneously decay into less massive particles. An example is the muon, which decays into an electron, a neutrino and an antineutrino, with a mean lifetime of $2.2 \times 10^{-6}$ seconds. However, the electron is thought to be stable on theoretical grounds: the electron is the least massive particle with non-zero electric charge, so its decay would violate charge conservation.[81] The experimental lower bound for the electron's mean lifetime is $4.6 \times 10^{26}$ years, at a 90% confidence level.[82]

## Quantum properties

As with all particles, electrons can act as waves. This is called the wave–particle duality and can be demonstrated using the double-slit experiment. The wave-like nature of the electron allows it to pass through two parallel slits simultaneously, rather than just one slit as would be the case for a classical particle. In quantum mechanics, the wave-like property of one particle can be described mathematically as a complex-valued function, the wave function, commonly denoted by the Greek letter psi ($\psi$). When the absolute value of this function is squared, it gives the probability that a particle will be observed near a location—a probability density.[83]

Electrons are identical particles because they cannot be distinguished from each other by their intrinsic physical properties. In quantum mechanics, this means that a pair of interacting electrons must be able to swap positions without an observable change to the state of the system. The wave function of fermions, including electrons, is antisymmetric, meaning that it changes sign when two electrons are swapped; that is, $\psi(r_1, r_2) = -\psi(r_2, r_1)$, where the variables $r_1$ and $r_2$ correspond to the first and second electrons, respectively. Since the absolute value is not changed by a sign swap, this corresponds to equal probabilities. Bosons, such as the photon, have symmetric wave functions instead.[83]

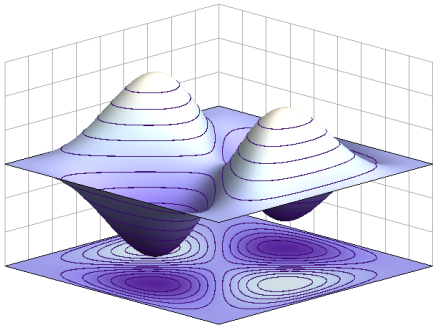

Example of an antisymmetric wave function for a quantum state of two identical fermions in a 2-dimensional box. If the particles swap position, the wave function inverts its sign.

In the case of antisymmetry, solutions of the wave equation for interacting electrons result in a zero probability that each pair will occupy the same location or state. This is responsible for the Pauli exclusion principle, which precludes any two electrons from occupying the same quantum state. This principle explains many of the properties of electrons. For example, it causes groups of bound electrons to occupy different orbitals in an atom, rather than all overlapping each other in the same orbit.[83]

## Virtual particles

Physicists believe that empty space may be continually creating pairs of virtual particles, such as a positron and electron, which rapidly annihilate each other shortly thereafter.[84] The combination of the energy variation needed to create these particles, and the time during which they exist, fall under the threshold of detectability expressed by the Heisenberg uncertainty relation, $\Delta E \cdot \Delta t \geq \hbar$. In effect, the energy needed to create these virtual particles, $\Delta E$, can be "borrowed" from the vacuum for a period of time, $\Delta t$, so that their product is no more than the reduced Planck constant, $\hbar \approx 6.6 \times 10^{-16}$ eV•s. Thus, for a virtual electron, $\Delta t$ is at most $1.3 \times 10^{-21}$ s.[85]

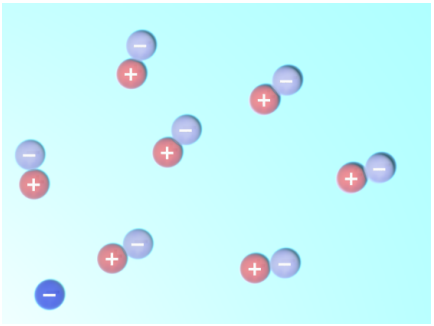

A schematic depiction of virtual electron–positron pairs appearing at random near an electron (at lower left)

While an electron–positron virtual pair is in existence, the coulomb force from the ambient electric field surrounding an electron causes a created positron to be attracted to the original electron, while a created electron experiences a repulsion. This causes what is called vacuum polarization. In effect, the vacuum behaves like a medium having a dielectric permittivity more than unity. Thus the effective charge of an electron is actually smaller than its true value, and the charge decreases with increasing distance from the electron.[86] [87] This polarization was confirmed experimentally in 1997 using the Japanese TRISTAN particle accelerator.[88] Virtual particles cause a comparable shielding effect for the mass of the electron.[89]

The interaction with virtual particles also explains the small (about 0.1%) deviation of the intrinsic magnetic moment of the electron from the Bohr magneton (the anomalous magnetic moment).[74] [90] The extraordinarily precise agreement of this predicted difference with the experimentally determined value is viewed as one of the great achievements of quantum electrodynamics.[91]

In classical physics, the angular momentum and magnetic moment of an object depend upon its physical dimensions. Hence, the concept of a dimensionless electron possessing these properties might seem inconsistent. The apparent paradox can be explained by the formation of virtual photons in the electric field generated by the electron. These photons cause the electron to shift about in a jittery fashion (known as zitterbewegung),[92] which results in a net circular motion with precession. This motion produces both the spin and the magnetic moment of the electron.[12] [93] In atoms, this creation of virtual photons explains the Lamb shift observed in spectral lines.[86]

## Interaction

An electron generates an electric field that exerts an attractive force on a particle with a positive charge, such as the proton, and a repulsive force on a particle with a negative charge. The strength of this force is determined by Coulomb's inverse square law.[94] When an electron is in motion, it generates a magnetic field.[95] The Ampère-Maxwell law relates the magnetic field to the mass motion of electrons (the current) with respect to an observer. It is this property of induction which supplies the magnetic field that drives an electric motor.[96] The electromagnetic field of an arbitrary moving charged particle is expressed by the Liénard–Wiechert potentials, which are valid even when the particle's speed is close to that of light (relativistic).

When an electron is moving through a magnetic field, it is subject to the Lorentz force that exerts an influence in a direction perpendicular to the plane defined by the magnetic field and the electron velocity. This centripetal force causes the electron to follow a helical trajectory through the field at a radius called the gyroradius. The acceleration from this curving motion induces the electron to radiate energy in the form of synchrotron radiation.[97] [98] [99] The energy emission in turn causes a recoil of the electron, known as the Abraham-Lorentz-Dirac force, which creates a friction that slows the electron. This force is caused by a back-reaction of the electron's own field upon itself.[100]

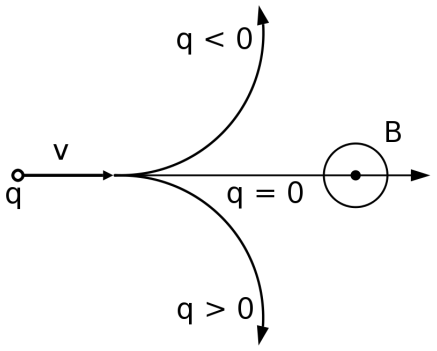


A particle with charge $q$ (at left) is moving with velocity $v$ through a magnetic field $B$ that is oriented toward the viewer. For an electron, $q$ is negative so it follows a curved trajectory toward the top.

In quantum electrodynamics the electromagnetic interaction between particles is mediated by photons. An isolated electron that is not undergoing acceleration is unable to emit or absorb a real photon; doing so would violate conservation of energy and momentum. Instead, virtual photons can transfer momentum between two charged particles. It is this exchange of virtual photons that, for example, generates the Coulomb force.[101] Energy emission can occur when a moving electron is deflected by a charged particle, such as a proton. The acceleration of the electron results in the emission of Bremsstrahlung radiation.[102]

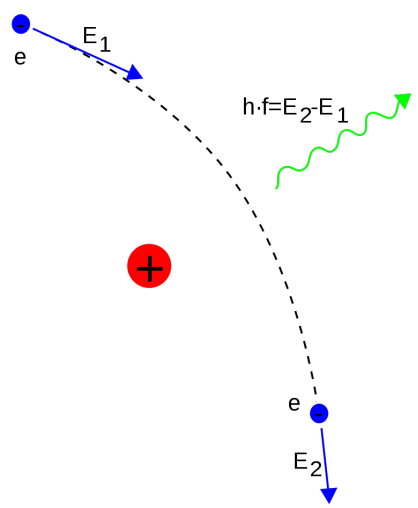


Here, Bremsstrahlung is produced by an electron $e$ deflected by the electric field of an atomic nucleus. The energy change $E_2 - E_1$ determines the frequency $f$ of the emitted photon.

An inelastic collision between a photon (light) and a solitary (free) electron is called Compton scattering. This collision results in a transfer of momentum and energy between the particles, which modifies the wavelength of the photon by an amount called the Compton shift.[103] The maximum magnitude of this wavelength shift is $h/m_e c$, which is known as the Compton wavelength.[104] For an electron, it has a value of $2.43 \times 10^{-12}$ m.[7] When the wavelength of the light is long (for instance, the wavelength of the visible light is 0.4–0.7 μm) the wavelength shift becomes negligible. Such interaction between the light and free electrons is called Thomson scattering or Linear Thomson scattering.[105]

The relative strength of the electromagnetic interaction between two charged particles, such as an electron and a proton, is given by the fine-structure constant. This value is a dimensionless quantity formed by the ratio of two energies: the electrostatic energy of attraction (or repulsion) at a separation of one Compton wavelength, and the rest

energy of the charge. It is given by $\alpha \approx 7.297353 \times 10^{-3}$, which is approximately equal to $^1/_{137}$.[7]

When electrons and positrons collide, they annihilate each other, giving rise to two or more gamma ray photons. If the electron and positron have negligible momentum, a positronium atom can form before annihilation results in two or three gamma ray photons totalling 1.022 MeV.[106] [107] On the other hand, high-energy photons may transform into an electron and a positron by a process called pair production, but only in the presence of a nearby charged particle, such as a nucleus.[108] [109]

In the theory of electroweak interaction, the left-handed component of electron's wavefunction forms a weak isospin doublet with the electron neutrino. This means that during weak interactions, electron neutrinos behave like electrons. Either member of this doublet can undergo a charged current interaction by emitting or absorbing a W and be converted into the other member. Charge is conserved during this reaction because the W boson also carries a charge, canceling out any net change during the transmutation. Charged current interactions are responsible for the phenomenon of beta decay in a radioactive atom. Both the electron and electron neutrino can undergo a neutral current interaction via a $Z^0$ exchange, and this is responsible for neutrino-electron elastic scattering.[110]

## Atoms and molecules

An electron can be *bound* to the nucleus of an atom by the attractive Coulomb force. A system of several electrons bound to a nucleus is called an atom. If the number of electrons is different from the nucleus' electrical charge, such an atom is called an ion. The wave-like behavior of a bound electron is described by a function called an atomic orbital. Each orbital has its own set of quantum numbers such as energy, angular momentum and projection of angular momentum, and only a discrete set of these orbitals exist around the nucleus. According to the Pauli exclusion principal each orbital can be occupied by up to two electrons, which must differ in their spin quantum number.

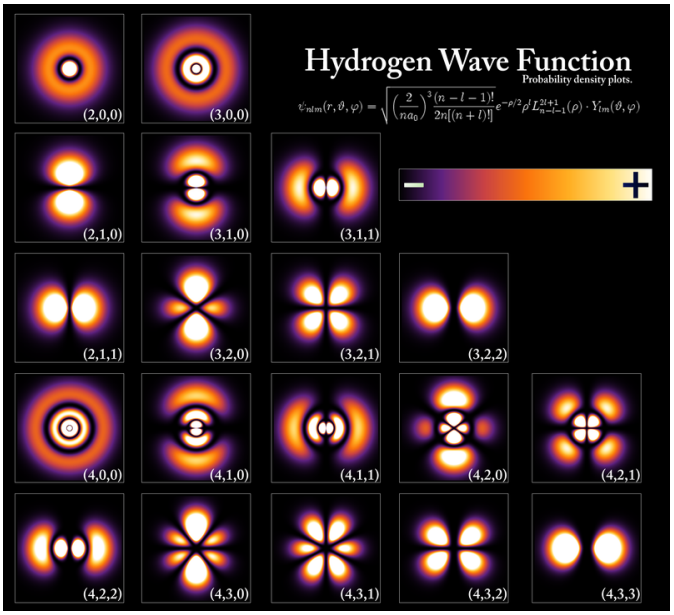


Probability densities for the first few hydrogen atom orbitals, seen in cross-section. The energy level of a bound electron determines the orbital it occupies, and the color reflects the probability to find the electron at a given position.

Electrons can transfer between different orbitals by the emission or absorption of photons with an energy that matches the difference in potential.[111] Other methods of orbital transfer include collisions with particles, such as electrons, and the Auger effect.[112] In order to escape the atom, the energy of the electron must be increased above its binding energy to the atom. This occurs, for example, with the photoelectric effect, where an incident photon exceeding the atom's ionization energy is absorbed by the electron.[113]

The orbital angular momentum of electrons is quantized. Because the electron is charged, it produces an orbital magnetic moment that is proportional to the angular momentum. The net magnetic moment of an atom is equal to the vector sum of orbital and spin magnetic moments of all electrons and the nucleus. The nuclear magnetic moment is, however, negligible in comparison to the effect from the electrons. The magnetic moments of the electrons that occupy the same orbital (so called, paired electrons) cancel each other out.[114]

The chemical bond between atoms occurs as a result of electromagnetic interactions, as described by the laws of quantum mechanics.[115] The strongest bonds are formed by the sharing or transfer of electrons between atoms,

allowing the formation of molecules.[16] Within a molecule, electrons move under the influence of several nuclei, and occupy molecular orbitals; much as they can occupy atomic orbitals in isolated atoms.[116] A fundamental factor in these molecular structures is the existence of electron pairs. These are electrons with opposed spins, allowing them to occupy the same molecular orbital without violating the Pauli exclusion principle (much like in atoms). Different molecular orbitals have different spatial distribution of the electron density. For instance, in bonded pairs (i.e. in the pairs that actually bind atoms together) electrons can be found with the maximal probability in a relatively small volume between the nuclei. On the contrary, in non-bonded pairs electrons are distributed in a large volume around nuclei.[117]

## Conductivity

If a body has more or fewer electrons than are required to balance the positive charge of the nuclei, then that object has a net electric charge. When there is an excess of electrons, the object is said to be negatively charged. When there are fewer electrons than the number of protons in nuclei, the object is said to be positively charged. When the number of electrons and the number of protons are equal, their charges cancel each other and the object is said to be electrically neutral. A macroscopic body can develop an electric charge through rubbing, by the triboelectric effect.[121]

A lightning discharge consists primarily of a flow of electrons.[118] The electric potential needed for lightning may be generated by a triboelectric effect.[119] [120]

Independent electrons moving in vacuum are termed *free* electrons. Electrons in metals also behave as if they were free. In reality the particles that are commonly termed electrons in metals and other solids are quasi-electrons—quasi-particles, which have the same electrical charge, spin and magnetic moment as real electrons but may have a different mass.[122] When free electrons—both in vacuum and metals—move, they produce a net flow of charge called an electric current, which generates a magnetic field. Likewise a current can be created by a changing magnetic field. These interactions are described mathematically by Maxwell's equations.[123]

At a given temperature, each material has an electrical conductivity that determines the value of electric current when an electric potential is applied. Examples of good conductors include metals such as copper and gold, whereas glass and Teflon are poor conductors. In any dielectric material, the electrons remain bound to their respective atoms and the material behaves as an insulator. Most semiconductors have a variable level of conductivity that lies between the extremes of conduction and insulation.[124] On the other hand, metals have an electronic band structure containing partially filled electronic bands. The presence of such bands allows electrons in metals to behave as if they were free or delocalized electrons. These electrons are not associated with specific atoms, so when an electric field is applied, they are free to move like a gas (called Fermi gas)[125] through the material much like free electrons.

Because of collisions between electrons and atoms, the drift velocity of electrons in a conductor is on the order of millimeters per second. However, the speed at which a change of current at one point in the material causes changes in currents in other parts of the material, the velocity of propagation, is typically about 75% of light speed.[126] This occurs because electrical signals propagate as a wave, with the velocity dependent on the dielectric constant of the material.[127]

Metals make relatively good conductors of heat, primarily because the delocalized electrons are free to transport thermal energy between atoms. However, unlike electrical conductivity, the thermal conductivity of a metal is nearly independent of temperature. This is expressed mathematically by the Wiedemann-Franz law,[125] which states that the ratio of thermal conductivity to the electrical conductivity is proportional to the temperature. The thermal

disorder in the metallic lattice increases the electrical resistivity of the material, producing a temperature dependence for electrical current.[128]

When cooled below a point called the critical temperature, materials can undergo a phase transition in which they lose all resistivity to electrical current, in a process known as superconductivity. In BCS theory, this behavior is modeled by pairs of electrons entering a quantum state known as a Bose–Einstein condensate. These Cooper pairs have their motion coupled to nearby matter via lattice vibrations called phonons, thereby avoiding the collisions with atoms that normally create electrical resistance.[129] (Cooper pairs have a radius of roughly 100 nm, so they can overlap each other.)[130] However, the mechanism by which higher temperature superconductors operate remains uncertain.

Electrons inside conducting solids, which are quasi-particles themselves, when tightly confined at temperatures close to absolute zero, behave as though they had split into two other quasiparticles: spinons and holons.[131] [132] The former carries spin and magnetic moment, while the latter electrical charge.

## Motion and energy

According to Einstein's theory of special relativity, as an electron's speed approaches the speed of light, from an observer's point of view its relativistic mass increases, thereby making it more and more difficult to accelerate it from within the observer's frame of reference. The speed of an electron can approach, but never reach, the speed of light in a vacuum, *c*. However, when relativistic electrons—that is, electrons moving at a speed close to *c*—are injected into a dielectric medium such as water, where the local speed of light is significantly less than *c*, the electrons temporarily travel faster than light in the medium. As they interact with the medium, they generate a faint light called Cherenkov radiation.[133]

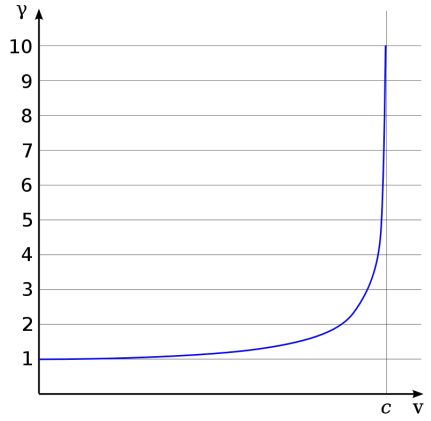


Lorentz factor as a function of velocity. It starts at value 1 and goes to infinity as *v* approaches *c*.

The effects of special relativity are based on a quantity known as the Lorentz factor, defined as $\gamma = 1/\sqrt{1 - v^2/c^2}$ where *v* is the speed of the particle. The kinetic energy $K_e$ of an electron moving with velocity *v* is:

$$K_e = (\gamma - 1)m_e c^2,$$

where $m_e$ is the mass of electron. For example, the Stanford linear accelerator can accelerate an electron to roughly 51 GeV.[134] This gives a value of nearly 100,000 for $\gamma$, since the mass of an electron is 0.51 MeV/$c^2$. The relativistic momentum of this electron is 100,000 times the momentum that classical mechanics would predict for an electron at the same speed.[135]

Since an electron behaves as a wave, at a given velocity it has a characteristic de Broglie wavelength. This is given by $\lambda_e = h/p$ where *h* is the Planck constant and *p* is the momentum.[51] For the 51 GeV electron above, the wavelength is about $2.4 \times 10^{-17}$ m, small enough to explore structures well below the size of an atomic nucleus.[136]

## Formation

The Big Bang theory is the most widely accepted scientific theory to explain the early stages in the evolution of the Universe.[137] For the first millisecond of the Big Bang, the temperatures were over 10 billion kelvins and photons had mean energies over a million electronvolts. These photons were sufficiently energetic that they could react with each other to form pairs of electrons and positrons,

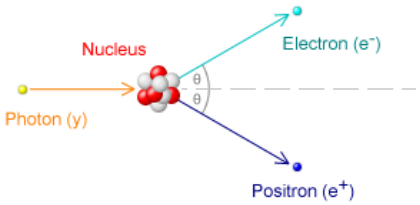


Pair production caused by the collision of a photon with an atomic nucleus

$$\gamma + \gamma \rightleftharpoons \mathrm{e}^+ + \mathrm{e}^-,$$

where $\gamma$ is a photon, $e^+$ is a positron and $e^-$ is an electron. Likewise, positron-electron pairs annihilated each other and emitted energetic photons. An equilibrium between electrons, positrons and photons was maintained during this phase of the evolution of the Universe. After 15 seconds had passed, however, the temperature of the universe dropped below the threshold where electron-positron formation could occur. Most of the surviving electrons and positrons annihilated each other, releasing gamma radiation that briefly reheated the universe.[138]

For reasons that remain uncertain, during the process of leptogenesis there was an excess in the number of electrons over positrons.[139] Hence, about one electron in every billion survived the annihilation process. This excess matched the excess of protons over anti-protons, in a condition known as baryon asymmetry, resulting in a net charge of zero for the universe.[140] [141] The surviving protons and neutrons began to participate in reactions with each other—in the process known as nucleosynthesis, forming isotopes of hydrogen and helium, with trace amounts of lithium. This process peaked after about five minutes.[142] Any leftover neutrons underwent negative beta decay with a half-life of about a thousand seconds, releasing a proton and electron in the process,

$$\mathrm{n} \Rightarrow \mathrm{p} + \mathrm{e}^- + \bar{\nu}_\mathrm{e},$$

where n is a neutron, p is a proton and $\nu_e$ is an electron antineutrino. For about the next 300,000–400,000 years, the excess electrons remained too energetic to bind with atomic nuclei.[143] What followed is a period known as recombination, when neutral atoms were formed and the expanding universe became transparent to radiation.[144]

Roughly one million years after the big bang, the first generation of stars began to form.[144] Within a star, stellar nucleosynthesis results in the production of positrons from the fusion of atomic nuclei. These antimatter particles immediately annihilate with electrons, releasing gamma rays. The net result is a steady reduction in the number of electrons, and a matching increase in the number of neutrons. However, the process of stellar evolution can result in the synthesis of radioactive isotopes. Selected isotopes can subsequently undergo negative beta decay, emitting an electron and antineutrino from the nucleus.[145] An example is the cobalt-60 ($^{60}$Co) isotope, which decays to form nickel-60 ($^{60}$Ni).[146]

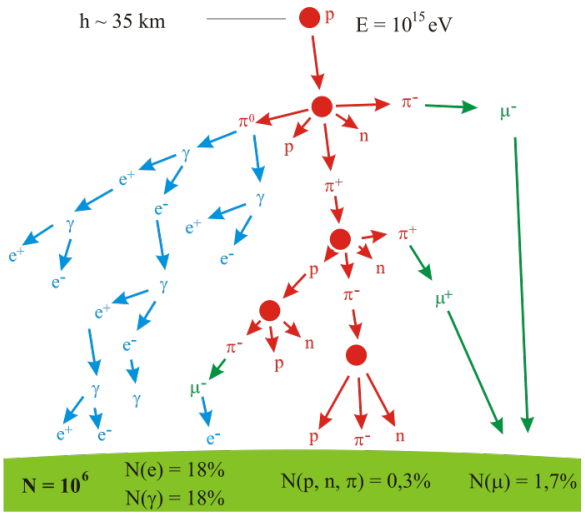


An extended air shower generated by an energetic cosmic ray striking the Earth's atmosphere

At the end of its lifetime, a star with more than about 20 solar masses can undergo gravitational collapse to form a black hole.[147] According to classical physics, these massive stellar objects exert a gravitational attraction that is strong enough to prevent anything, even electromagnetic radiation, from escaping past the Schwarzschild radius. However, it is believed that quantum mechanical effects may allow Hawking radiation to be emitted at this distance. Electrons (and positrons) are thought to be created at the event horizon of these stellar remnants.

When pairs of virtual particles (such as an electron and positron) are created in the vicinity of the event horizon, the random spatial distribution of these particles may permit one of them to appear on the exterior; this process is called quantum tunneling. The gravitational potential of the black hole can then supply the energy that transforms this virtual particle into a real particle, allowing it to radiate away into space.[148] In exchange, the other member of the pair is given negative energy, which results in a net loss of mass-energy by the black hole. The rate of Hawking radiation increases with decreasing mass, eventually causing the black hole to evaporate away until, finally, it explodes.[149]

Cosmic rays are particles traveling through space with high energies. Energy events as high as $3.0 \times 10^{20}$ eV have been recorded.[150] When these particles collide with nucleons in the Earth's atmosphere, a shower of particles is generated, including pions.[151] More than half of the cosmic radiation observed from the Earth's surface consists of muons. The particle called a muon is a lepton which is produced in the upper atmosphere by the decay of a pion. A muon, in turn, can decay to form an electron or positron. Thus, for the negatively charged pion $\pi^-$,[152]

$$\pi^- \rightarrow \mu^- + \bar{\nu_\mu},$$
$$\mu^- \rightarrow \mathrm{e}^- + \bar{\nu}_\mathrm{e} + \nu_\mu,$$

where $\mu^-$ is a muon and $\nu_\mu$ is a muon neutrino.

## Observation

Remote observation of electrons requires detection of their radiated energy. For example, in high-energy environments such as the corona of a star, free electrons form a plasma that radiates energy due to Bremsstrahlung. Electron gas can undergo plasma oscillation, which is waves caused by synchronized variations in electron density, and these produce energy emissions that can be detected by using radio telescopes.[154]

Aurorae are mostly caused by energetic electrons precipitating into the atmosphere.[153]

The frequency of a photon is proportional to its energy. As a bound electron transitions between different energy levels of an atom, it will absorb or emit photons at characteristic frequencies. For instance, when atoms are irradiated by a source with a broad spectrum, distinct absorption lines will appear in the spectrum of transmitted radiation. Each element or molecule displays a characteristic set of spectral lines, such as the hydrogen spectral series. Spectroscopic measurements of the strength and width of these lines allow the composition and

physical properties of a substance to be determined.[155] [156]

In laboratory conditions, the interactions of individual electrons can be observed by means of particle detectors, which allow measurement of specific properties such as energy, spin and charge.[113] The development of the Paul trap and Penning trap allows charged particles to be contained within a small region for long durations. This enables precise measurements of the particle properties. For example, in one instance a Penning trap was used to contain a single electron for a period of 10 months.[157] The magnetic moment of the electron was measured to a precision of eleven digits, which, in 1980, was a greater accuracy than for any other physical constant.[158]

The first video images of an electron's energy distribution were captured by a team at Lund University in Sweden, February 2008. The scientists used extremely short flashes of light, called attosecond pulses, which allowed an electron's motion to be observed for the first time.[159] [160]

The distribution of the electrons in solid materials can be visualized by angle resolved photoemission spectroscopy (ARPES). This technique employs the photoelectric effect to measure the reciprocal space—a mathematical representation of periodic structures that is used to infer the original structure. ARPES can be used to determine the direction, speed and scattering of electrons within the material.[161]

# Plasma applications

## Particle beams

Electron beams are used in welding,[163] which allows energy densities up to $10^7$ W•cm$^{-2}$ across a narrow focus diameter of 0.1–1.3 mm and usually does not require a filler material. This welding technique must be performed in a vacuum, so that the electron beam does not interact with the gas prior to reaching the target, and it can be used to join conductive materials that would otherwise be considered unsuitable for welding.[164] [165]

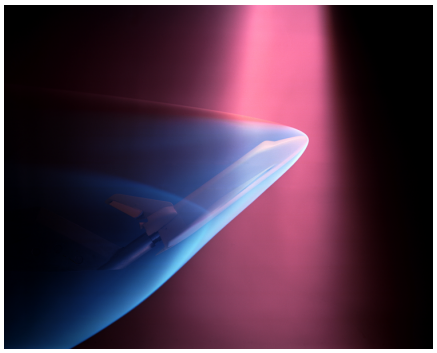

During a NASA wind tunnel test, a model of the Space Shuttle is targeted by a beam of electrons, simulating the effect of ionizing gases during re-entry.[162]

Electron beam lithography (EBL) is a method of etching semiconductors at resolutions smaller than a micron.[166] This technique is limited by high costs, slow performance, the need to operate the beam in the vacuum and the tendency of the electrons to scatter in solids. The last problem limits the resolution to about 10 nm. For this reason, EBL is primarily used for the production of small numbers of specialized integrated circuits.[167]

Electron beam processing is used to irradiate materials in order to change their physical properties or sterilize medical and food products.[168] In radiation therapy, electron beams are generated by linear accelerators for treatment of superficial tumors. Because an electron beam only penetrates to a limited depth before being absorbed, typically up to 5 cm for electron energies in the range 5–20 MeV, electron therapy is useful for treating skin lesions such as basal cell carcinomas. An electron beam can be used to supplement the treatment of areas that have been irradiated by X-rays.[169] [170]

Particle accelerators use electric fields to propel electrons and their antiparticles to high energies. As these particles pass through magnetic fields, they emit synchrotron radiation. The intensity of this radiation is spin dependent, which causes polarization of the electron beam—a process known as the Sokolov–Ternov effect.[171] The polarized electron beams can be useful for various experiments. Synchrotron radiation can also be used for cooling the electron beams, which reduces the momentum spread of the particles. Once the particles have accelerated to the required energies, separate electron and positron beams are brought into collision. The resulting energy emissions are observed with particle detectors and are studied in particle physics.[172]

### Imaging

Low-energy electron diffraction (LEED) is a method of bombarding a crystalline material with a collimated beam of electrons, then observing the resulting diffraction patterns to determine the structure of the material. The required energy of the electrons is typically in the range 20–200 eV.[173] The reflection high energy electron diffraction (RHEED) technique uses the reflection of a beam of electrons fired at various low angles to characterize the surface of crystalline materials. The beam energy is typically in the range 8–20 keV and the angle of incidence is 1–4°.[174] [175]

The electron microscope directs a focused beam of electrons at a specimen. As the beam interacts with the material, some electrons change their properties, such as movement direction, angle, relative phase and energy. By recording these changes in the electron beam, microscopists can produce atomically resolved image of the material.[176] In blue light, conventional optical microscopes have a diffraction-limited resolution of about 200 nm.[177] By comparison, electron microscopes are limited by the de Broglie wavelength of the electron. This wavelength, for example, is equal to 0.0037 nm for electrons accelerated across a 100,000-volt potential.[178] The Transmission Electron Aberration-corrected Microscope is capable of sub-0.05 nm resolution, which is more than enough to resolve individual atoms.[179] This capability makes the electron microscope a useful laboratory instrument for high resolution imaging. However, electron microscopes are expensive instruments that are costly to maintain.

There are two main types of electron microscopes: transmission and scanning. Transmission electron microscopes function in a manner similar to overhead projector, with a beam of electrons passing through a slice of material then being projected by lenses on a photographic slide or a charge-coupled device. In scanning electron microscopes, the image is produced by rastering a finely focused electron beam, as in a TV set, across the studied sample. The magnifications range from 100× to 1,000,000× or higher for both microscope types. The scanning tunneling microscope uses quantum tunneling of electrons from a sharp metal tip into the studied material and can produce atomically resolved images of its surface.[180] [181] [182]

### Other

In the free electron laser (FEL), a relativistic electron beam is passed through a pair of undulators containing arrays of dipole magnets, whose fields are oriented in alternating directions. The electrons emit synchrotron radiation, which, in turn, coherently interacts with the same electrons. This leads to the strong amplification of the radiation field at the resonance frequency. FEL can emit a coherent high-brilliance electromagnetic radiation with a wide range of frequencies, from microwaves to soft X-rays. These devices can be used in the future for manufacturing, communication and various medical applications, such as soft tissue surgery.[183]

Electrons are at the heart of cathode ray tubes, which are used extensively as display devices in laboratory instruments, computer monitors and television sets.[184] In a photomultiplier tube, every photon striking the photocathode initiates an avalanche of electrons that produces a detectable current pulse.[185] Vacuum tubes use the flow of electrons to manipulate electrical signals, and they played a critical role in the development of electronics technology. However, they have been largely supplanted by solid-state devices such as the transistor.[186]

## See also

- Anyon
- Covalent bonding
- Electride
- Electron bubble
- Exoelectron emission
- *g*-factor
- Spintronics
- Stern–Gerlach experiment
- Zeeman effect

# Notes


[1] Dahl, Per F. (1997). *Flash of the Cathode Rays: A History of J J Thomson's Electron* (http://books.google.com/?id=xUzaWGocMdMC&printsec=frontcover). CRC Press. p. 72. ISBN 0750304537. .

[2] Eichten, Estia J.; Peskin, Michael E.; Peskin, Michael (1983). "New Tests for Quark and Lepton Substructure". *Physical Review Letters* **50** (11): 811–814. doi:10.1103/PhysRevLett.50.811.

[3] Farrar, Wilfred V. (1969). "Richard Laming and the Coal-Gas Industry, with His Views on the Structure of Matter". *Annals of Science* **25**: 243–254. doi:10.1080/00033796900200141.

[4] Arabatzis, Theodore (2006). *Representing Electrons: A Biographical Approach to Theoretical Entities* (http://books.google.com/?id=rZHT-chpLmAC&pg=PA70). University of Chicago Press. pp. 70–74. ISBN 0226024210. .

[5] Buchwald, Jed Z.; Warwick, Andrew (2001). *Histories of the Electron: The Birth of Microphysics* (http://books.google.com/?id=1yqqhlIdCOoC&pg=PA195). MIT Press. pp. 195–203. ISBN 0262524244. .

[6] Thomson, Joseph John (1897). "Cathode Rays" (http://web.lemoyne.edu/~GIUNTA/thomson1897.html). *Philosophical Magazine* **44**: 293. .

[7] The original source for CODATA is:

> Mohr, Peter J.; Taylor, Barry N.; Newell, David B. (2006-06-06). "CODATA recommended values of the fundamental physical constants". *Reviews of Modern Physics* **80**: 633–730. doi:10.1103/RevModPhys.80.633.

Individual physical constants from the CODATA are available at:

> "The NIST Reference on Constants, Units and Uncertainty" (http:// / physics. nist. gov/ cuu/ ). National Institute of Standards and Technology. . Retrieved 2009-01-15.

[8] The fractional version's denominator is the inverse of the decimal value (along with its relative standard uncertainty of $4.2 \times 10^{-10}$ u).

[9] The electron's charge is the negative of elementary charge, which has a positive value for the proton.

[10] Purcell, Edward M. (1985). *Electricity and Magnetism*. Berkeley Physics Course Volume 2. McGraw-Hill. ISBN 0-07-004908-4.

[11] "CODATA value: proton-electron mass ratio" (http://physics.nist.gov/cgi-bin/cuu/Value?mpsme). National Institute of Standards and Technology. . Retrieved 2009-07-18.

[12] Curtis, Lorenzo J. (2003). *Atomic Structure and Lifetimes: A Conceptual Approach* (http://books.google.com/?id=KmwCsuvxClAC&pg=PA74). Cambridge University Press. p. 74. ISBN 0521536359. .

[13] Anastopoulos, Charis (2008). *Particle Or Wave: The Evolution of the Concept of Matter in Modern Physics* (http://books.google.com/?id=rDEvQZhpltEC&pg=PA236). Princeton University Press. pp. 236–237. ISBN 0691135126. .

[14] Dahl (1997:122–185).

[15] Wilson, Robert (1997). *Astronomy Through the Ages: The Story of the Human Attempt to Understand the Universe* (http://books.google.com/?id=AoiJ3hA8bQ8C&pg=PA138). CRC Press. p. 138. ISBN 0748407480. .

[16] Pauling, Linus C. (1960). *The Nature of the Chemical Bond and the Structure of Molecules and Crystals: an introduction to modern structural chemistry* (http://books.google.com/?id=L-1K9HmKmUUC) (3rd ed.). Cornell University Press. pp. 4–10. ISBN 0801403332. .

[17] Shipley, Joseph T. (1945). *Dictionary of Word Origins*. The Philosophical Library. p. 133.

[18] Baigrie, Brian (2006). *Electricity and Magnetism: A Historical Perspective* (http://books.google.com/?id=3XEc5xkWxi4C&pg=PA7). Greenwood Press. pp. 7–8. ISBN 0-3133-3358-0. .

[19] Keithley, Joseph F. (1999). *The Story of Electrical and Magnetic Measurements: From 500 B.C. to the 1940s* (http://books.google.com/?id=uwgNAtqSHuQC&pg=PA207). Wiley. ISBN 0-780-31193-0. .

[20] *Benjamin Franklin (1706–1790).* (http://scienceworld.wolfram.com/biography/FranklinBenjamin.html) Science World, from Eric Weisstein's World of Scientific Biography.

[21] The Encyclopedia Americana; a library of universal knowledge. (1918). New York: Encyclopedia Americana Corp.

[22] Myers, Rusty L. (2006). *The basics of physics* (http://books.google.com/books?id=KnynjL44pI4C). Greenwood Publishing Group. p. 242. ISBN 0-313-32857-9. ., Chapter 13, page 242 (http://books.google.com/books?id=KnynjL44pI4C&pg=PA242)

[23] Barrow, John D. (1983). "Natural Units Before Planck". *Royal Astronomical Society Quarterly Journal* **24**: 24–26. Bibcode: 1983QJRAS..24...24B.

[24] Stoney, George Johnstone (1894). "Of the "Electron," or Atom of Electricity". *Philosophical Magazine* **38** (5): 418–420.

[25] Soukhanov, Anne H. ed. (1986). *Word Mysteries & Histories*. Houghton Mifflin Company. p. 73. ISBN 0-395-40265-4.

[26] Guralnik, David B. ed. (1970). *Webster's New World Dictionary*. Prentice-Hall. p. 450.

[27] Born, Max; Blin-Stoyle, Roger John; Radcliffe, J. M. (1989). *Atomic Physics* (http://books.google.com/?id=NmM-KujxMtoC&pg=PA26). Courier Dover. p. 26. ISBN 0486659844. .

[28] Dahl (1997:55–58).

[29] DeKosky, Robert (1983). "William Crookes and the quest for absolute vacuum in the 1870s". *Annals of Science* **40** (1): 1–18. doi:10.1080/00033798300200101.

[30] Leicester, Henry M. (1971). *The Historical Background of Chemistry* (http://books.google.com/?id=aJZVQnqcwv4C&pg=PA221). Courier Dover Publications. pp. 221–222. ISBN 0486610535. .

[31] Dahl (1997:64–78).

[32] Zeeman, Pieter (1907). "Sir William Crookes, F.R.S." (http://books.google.com/?id=UtYRAAAAYAAJ). *Nature* **77** (1984): 1–3. doi:10.1038/077001a0. .

[33] Dahl (1997:99).

[34] Thomson, J. J. (1906). "Nobel Lecture: Carriers of Negative Electricity" (http://nobelprize.org/nobel_prizes/physics/laureates/1906/thomson-lecture.pdf). The Nobel Foundation. . Retrieved 2008-08-25.

[35] Trenn, Thaddeus J. (1976). "Rutherford on the Alpha-Beta-Gamma Classification of Radioactive Rays". *Isis* **67** (1): 61–75. doi:10.1086/351545. JSTOR 231134.

[36] Becquerel, Henri (1900). "Déviation du Rayonnement du Radium dans un Champ Électrique". *Comptes Rendus de l'Académie des Sciences* **130**: 809–815. **(French)**

[37] Buchwald and Warwick (2001:90–91).

[38] Myers, William G. (1976). "Becquerel's Discovery of Radioactivity in 1896" (http://jnm.snmjournals.org/cgi/content/abstract/17/7/579). *Journal of Nuclear Medicine* **17** (7): 579–582. PMID 775027. .

[39] Kikoin, Isaak K.; Sominskiĭ, Isaak S. (1961). "Abram Fedorovich Ioffe (on his eightieth birthday)". *Soviet Physics Uspekhi* **3**: 798–809. doi:10.1070/PU1961v003n05ABEH005812. Original publication in Russian: Кикоин, И.К.; Соминский, М.С. (1960). "Академик А.Ф. Иоффе" (http://ufn.ru/ufn60/ufn60_10/Russian/r6010e.pdf). *Успехи Физических Наук* **72** (10): 303–321. .

[40] Millikan, Robert A. (1911). "The Isolation of an Ion, a Precision Measurement of its Charge, and the Correction of Stokes' Law". *Physical Review* **32** (2): 349–397. doi:10.1103/PhysRevSeriesI.32.349.

[41] Das Gupta, N. N.; Ghosh, Sanjay K. (1999). "A Report on the Wilson Cloud Chamber and Its Applications in Physics". *Reviews of Modern Physics* **18**: 225–290. doi:10.1103/RevModPhys.18.225.

[42] Smirnov, Boris M. (2003). *Physics of Atoms and Ions* (http://books.google.com/?id=I1O8WYOcUscC&pg=PA14). Springer. pp. 14–21. ISBN 038795550X. .

[43] Bohr, Niels (1922). "Nobel Lecture: The Structure of the Atom" (http://nobelprize.org/nobel_prizes/physics/laureates/1922/bohr-lecture.pdf). The Nobel Foundation. . Retrieved 2008-12-03.

[44] Lewis, Gilbert N. (1916). "The Atom and the Molecule". *Journal of the American Chemical Society* **38** (4): 762–786. doi:10.1021/ja02261a002.

[45] Arabatzis, Theodore; Gavroglu, Kostas (1997). "The chemists' electron". *European Journal of Physics* **18**: 150–163. doi:10.1088/0143-0807/18/3/005.

[46] Langmuir, Irving (1919). "The Arrangement of Electrons in Atoms and Molecules". *Journal of the American Chemical Society* **41** (6): 868–934. doi:10.1021/ja02227a002.

[47] Scerri, Eric R. (2007). *The Periodic Table* (http://books.google.com/?id=SNRdGWCGt1UC&pg=PA205). Oxford University Press. pp. 205–226. ISBN 0195305736. .

[48] Massimi, Michela (2005). *Pauli's Exclusion Principle, The Origin and Validation of a Scientific Principle* (http://books.google.com/?id=YS91Gsbd13cC&pg=PA7). Cambridge University Press. pp. 7–8. ISBN 0521839114. .

[49] Uhlenbeck, G. E.; Goudsmith, S. (1925). "Ersetzung der Hypothese vom unmechanischen Zwang durch eine Forderung bezüglich des inneren Verhaltens jedes einzelnen Elektrons". *Die Naturwissenschaften* **13** (47). Bibcode: 1925NW.....13..953E. **(German)**

[50] Pauli, Wolfgang (1923). "Über die Gesetzmäßigkeiten des anomalen Zeemaneffektes". *Zeitschrift für Physik* **16** (1): 155–164. doi:10.1007/BF01327386. Bibcode: 1923ZPhy...16..155P. **(German)**

[51] de Broglie, Louis (1929). "Nobel Lecture: The Wave Nature of the Electron" (http://nobelprize.org/nobel_prizes/physics/laureates/1929/broglie-lecture.pdf). The Nobel Foundation. . Retrieved 2008-08-30.

[52] Falkenburg, Brigitte (2007). *Particle Metaphysics: A Critical Account of Subatomic Reality* (http://books.google.com/?id=EbOz5I9RNrYC&pg=PA85). Springer. p. 85. ISBN 3540337318. .

[53] Davisson, Clinton (1937). "Nobel Lecture: The Discovery of Electron Waves" (http://nobelprize.org/nobel_prizes/physics/laureates/1937/davisson-lecture.pdf). The Nobel Foundation. . Retrieved 2008-08-30.

[54] Schrödinger, Erwin (1926). "Quantisierung als Eigenwertproblem". *Annalen der Physik* **385** (13): 437–490. doi:10.1002/andp.19263851302. Bibcode: 1926AnP...385..437S. **(German)**

[55] Rigden, John S. (2003). *Hydrogen* (http://books.google.com/?id=FhFxn_lUvz0C&pg=PT66). Harvard University Press. pp. 59–86. ISBN 0674012526. .

[56] Reed, Bruce Cameron (2007). *Quantum Mechanics* (http://books.google.com/?id=4sluccbpwjsC&pg=PA275). Jones & Bartlett Publishers. pp. 275–350. ISBN 0763744514. .

[57] Dirac, Paul A. M. (1928). "The Quantum Theory of the Electron". *Proceedings of the Royal Society of London A* **117** (778): 610–624. doi:10.1098/rspa.1928.0023.

[58] Dirac, Paul A. M. (1933). "Nobel Lecture: Theory of Electrons and Positrons" (http://nobelprize.org/nobel_prizes/physics/laureates/1933/dirac-lecture.pdf). The Nobel Foundation. . Retrieved 2008-11-01.

[59] Kragh, Helge (2002). *Quantum Generations: A History of Physics in the Twentieth Century* (http://books.google.com/?id=ELrFDIldlawC&pg=PA132). Princeton University Press. p. 132. ISBN 0691095523. .

[60] Gaynor, Frank (1950). *Concise Encyclopedia of Atomic Energy*. The Philosophical Library. p. 117.

[61] "The Nobel Prize in Physics 1965" (http://nobelprize.org/nobel_prizes/physics/laureates/1965/). The Nobel Foundation. . Retrieved 2008-11-04.

[62] Panofsky, Wolfgang K. H. (1997). "The Evolution of Particle Accelerators & Colliders" (http://www.slac.stanford.edu/pubs/beamline/27/1/27-1-panofsky.pdf). Stanford University. . Retrieved 2008-09-15.

[63] Elder, F. R.; Gurewitsch, A. M.; Langmuir, R. V.; Pollock, H. C. (1947). "Radiation from Electrons in a Synchrotron". *Physical Review* **71** (11): 829–830. doi:10.1103/PhysRev.71.829.5.

[64] Hoddeson, Lillian; Brown, Laurie; Riordan, Michael; Dresden, Max (1997). *The Rise of the Standard Model: Particle Physics in the 1960s and 1970s* (http://books.google.com/?id=klLUs2XUmOkC&pg=PA25). Cambridge University Press. pp. 25–26. ISBN 0521578167. .

[65] Bernardini, Carlo (2004). "AdA: The First Electron–Positron Collider". *Physics in Perspective* **6** (2): 156–183. doi:10.1007/s00016-003-0202-y. Bibcode: 2004PhP.....6..156B.

[66] "Testing the Standard Model: The LEP experiments" (http://public.web.cern.ch/PUBLIC/en/Research/LEPExp-en.html). CERN. 2008. . Retrieved 2008-09-15.

[67] "LEP reaps a final harvest" (http://cerncourier.com/cws/article/cern/28335). *CERN Courier*. 2000. . Retrieved 2008-11-01.

[68] Frampton, Paul H. (2000). "Quarks and Leptons Beyond the Third Generation". *Physics Reports* **330**: 263–348. doi:10.1016/S0370-1573(99)00095-2.

[69] Raith, Wilhelm; Mulvey, Thomas (2001). *Constituents of Matter: Atoms, Molecules, Nuclei and Particles*. CRC Press. pp. 777–781. ISBN 0849312027.

[70] Zombeck, Martin V. (2007). *Handbook of Space Astronomy and Astrophysics* (http://books.google.com/?id=tp_G85jm6IAC&pg=PA14) (3rd ed.). Cambridge University Press. p. 14. ISBN 0521782422. .

[71] Murphy, Michael T.; Flambaum, VV; Muller, S; Henkel, C (2008-06-20). "Strong Limit on a Variable Proton-to-Electron Mass Ratio from Molecules in the Distant Universe" (http://www.sciencemag.org/cgi/content/abstract/320/5883/1611). *Science* **320** (5883): 1611–1613. doi:10.1126/science.1156352. PMID 18566280. . Retrieved 2008-09-03.

[72] Zorn, Jens C.; Chamberlain, George E.; Hughes, Vernon W. (1963). "Experimental Limits for the Electron-Proton Charge Difference and for the Charge of the Neutron". *Physical Review* **129** (6): 2566–2576. doi:10.1103/PhysRev.129.2566.

[73] This magnitude is obtained from the spin quantum number as

$$S = \sqrt{s(s+1)} \cdot \frac{h}{2\pi} = \frac{\sqrt{3}}{2}\hbar$$

for quantum number $s = {}^1/_2$.
See: Gupta, M. C. (2001). *Atomic and Molecular Spectroscopy* (http://books.google.com/?id=0tIA1M6DiQIC&pg=PA81). New Age Publishers. p. 81. ISBN 8122413005. .

[74] Odom, B.; Hanneke, D.; D'urso, B.; Gabrielse, G. (2006). "New Measurement of the Electron Magnetic Moment Using a One-Electron Quantum Cyclotron". *Physical Review Letters* **97**: 030801(1–4). doi:10.1103/PhysRevLett.97.030801.

[75] Bohr magneton:

$$\mu_B = \tfrac{e\hbar}{2m_e}.$$

[76] Anastopoulos, Charis (2008). *Particle Or Wave: The Evolution of the Concept of Matter in Modern Physics* (http://books.google.com/?id=rDEvQZhpltEC&pg=PA261). Princeton University Press. pp. 261–262. ISBN 0691135126. .

[77] Gabrielse, G.; Hanneke, D.; Kinoshita, T.; Nio, M.; Odom, B. (2006). "New Determination of the Fine Structure Constant from the Electron *g* Value and QED". *Physical Review Letters* **97**: 030802(1–4). doi:10.1103/PhysRevLett.97.030802.

[78] Dehmelt, Hans (1988). "A Single Atomic Particle Forever Floating at Rest in Free Space: New Value for Electron Radius". *Physica Scripta* **T22**: 102–110. doi:10.1088/0031-8949/1988/T22/016.

[79] Meschede, Dieter (2004). *Optics, light and lasers: The Practical Approach to Modern Aspects of Photonics and Laser Physics* (http://books.google.com/?id=PLISLfBLcmgC&pg=PA168). Wiley-VCH. p. 168. ISBN 3527403647. .

[80] The classical electron radius is derived as follows. Assume that the electron's charge is spread uniformly throughout a spherical volume. Since one part of the sphere would repel the other parts, the sphere contains electrostatic potential energy. This energy is assumed to equal the electron's rest energy, defined by special relativity ($E=mc^2$).
From electrostatics theory, the potential energy of a sphere with radius *r* and charge *e* is given by:

$$E_\mathrm{p} = \frac{e^2}{8\pi\varepsilon_0 r},$$

where $\varepsilon_0$ is the vacuum permittivity. For an electron with rest mass $m_0$, the rest energy is equal to:

$$E_\mathrm{p} = m_0 c^2,$$

where *c* is the speed of light in a vacuum. Setting them equal and solving for *r* gives the classical electron radius.
See: Haken, Hermann; Wolf, Hans Christoph; Brewer, W. D. (2005). *The Physics of Atoms and Quanta: Introduction to Experiments and Theory* (http://books.google.com/?id=SPrAMy8glocC&pg=PA70). Springer. p. 70. ISBN 3540672745. .

[81] Steinberg, R. I.; Kwiatkowski, K.; Maenhaut, W.; Wall, N. S. (1999). "Experimental test of charge conservation and the stability of the electron". *Physical Review D* **61** (2): 2582–2586. doi:10.1103/PhysRevD.12.2582.

[82] Yao, W.-M. (2006). "Review of Particle Physics". *Journal of Physics G: Nuclear and Particle Physics* **33** (1): 77–115. doi:10.1088/0954-3899/33/1/001.

[83] Munowitz, Michael (2005). *Knowing, The Nature of Physical Law* (http://books.google.com/?id=IjVtDc85CYwC&pg=PA162). Oxford University Press. pp. 162–218. ISBN 0195167376. .

[84] Kane, Gordon (2006-10-09). "Are virtual particles really constantly popping in and out of existence? Or are they merely a mathematical bookkeeping device for quantum mechanics?" (http://www.sciam.com/article.cfm?id=are-virtual-particles-rea&topicID=13). Scientific American. . Retrieved 2008-09-19.

[85] Taylor, John (1989). Davies, Paul. ed. *The New Physics* (http://books.google.com/?id=akb2FpZSGnMC&pg=PA464). Cambridge University Press. p. 464. ISBN 0521438314. Gauge Theories in Particle Physics.

[86] Genz, Henning (2001). *Nothingness: The Science of Empty Space*. Da Capo Press. pp. 241–243, 245–247. ISBN 0738206105.

[87] Gribbin, John (1997-01-25). "More to electrons than meets the eye" (http://www.newscientist.com/article/mg15320662.300-science--more-to-electrons-than-meets-the-eye.html). *New Scientist*. . Retrieved 2008-09-17.

[88] Levine, I.; Koltick, D.; Howell, B.; Shibata, E.; Fujimoto, J.; Tauchi, T.; Abe, K.; Abe, T. *et al*. (1997). "Measurement of the Electromagnetic Coupling at Large Momentum Transfer". *Physical Review Letters* **78**: 424–427. doi:10.1103/PhysRevLett.78.424.

[89] Murayama, Hitoshi (March 10–17, 2006). "Supersymmetry Breaking Made Easy, Viable and Generic". *Proceedings of the XLIInd Rencontres de Moriond on Electroweak Interactions and Unified Theories*. La Thuile, Italy. arXiv:0709.3041.—lists a 9% mass difference for an electron that is the size of the Planck distance.

[90] Schwinger, Julian (1948). "On Quantum-Electrodynamics and the Magnetic Moment of the Electron". *Physical Review* **73** (4): 416–417. doi:10.1103/PhysRev.73.416.

[91] Huang, Kerson (2007). *Fundamental Forces of Nature: The Story of Gauge Fields* (http://books.google.com/?id=q-CIFHpHxfEC&pg=PA123). World Scientific. pp. 123–125. ISBN 9812706453. .

[92] Foldy, Leslie L.; Wouthuysen, Siegfried (1950). "On the Dirac Theory of Spin 1/2 Particles and Its Non-Relativistic Limit". *Physical Review* **78**: 29–36. doi:10.1103/PhysRev.78.29.

[93] Sidharth, Burra G. (2008). "Revisiting Zitterbewegung". *International Journal of Theoretical Physics* **48**: 497–506. doi:10.1007/s10773-008-9825-8. arXiv:0806.0985.

[94] Elliott, Robert S. (1978). "The history of electromagnetics as Hertz would have known it" (http://ieeexplore.ieee.org/xpls/abs_all.jsp?arnumber=3600). *IEEE Transactions on Microwave Theory and Techniques* **36** (5): 806–823. doi:10.1109/22.3600. . Retrieved 2008-09-22. A subscription required for access.

[95] Munowitz (2005:140).

[96] Crowell, Benjamin (2000). *Electricity and Magnetism* (http://books.google.com/?id=s9QWZNfnz1oC&pg=PT129). Light and Matter. pp. 129–152. ISBN 0970467044. .

[97] Munowitz (2005:160).

[98] Mahadevan, Rohan; Narayan, Ramesh; Yi, Insu (1996). "Harmony in Electrons: Cyclotron and Synchrotron Emission by Thermal Electrons in a Magnetic Field". *Astrophysical Journal* **465**: 327–337. doi:10.1086/177422. arXiv:astro-ph/9601073v1.

[99] Radiation from non-relativistic electrons is sometimes termed cyclotron radiation.

[100] Rohrlich, Fritz (1999). "The self-force and radiation reaction". *American Journal of Physics* **68** (12): 1109–1112. doi:10.1119/1.1286430.

[101] Georgi, Howard (1989). Davies, Paul. ed. *The New Physics* (http://books.google.com/?id=akb2FpZSGnMC&pg=PA427). Cambridge University Press. p. 427. ISBN 0521438314. Grand Unified Theories.

[102] Blumenthal, George J.; Gould, Robert (1970). "Bremsstrahlung, Synchrotron Radiation, and Compton Scattering of High-Energy Electrons Traversing Dilute Gases". *Reviews of Modern Physics* **42**: 237–270. doi:10.1103/RevModPhys.42.237.

[103] The change in wavelength, $\Delta\lambda$, depends on the angle of the recoil, $\theta$, as follows,

$$\Delta\lambda = \frac{h}{m_e c}(1 - \cos\theta),$$

where $c$ is the speed of light in a vacuum and $m_e$ is the electron mass. See Zombeck (2007:393,396).

[104] Staff (2008). "The Nobel Prize in Physics 1927" (http://nobelprize.org/nobel_prizes/physics/laureates/1927/). The Nobel Foundation. . Retrieved 2008-09-28.

[105] Chen, Szu-yuan; Chen, Szu-Yuan; Maksimchuk, Anatoly (1998). "Experimental observation of relativistic nonlinear Thomson scattering". *Nature* **396**: 653–655. doi:10.1038/25303.

[106] Beringer, Robert; Montgomery, C. G. (1942). "The Angular Distribution of Positron Annihilation Radiation". *Physical Review* **61** (5–6): 222–224. doi:10.1103/PhysRev.61.222.

[107] Wilson, Jerry; Buffa, Anthony (2000). *College Physics* (4th ed.). Prentice Hall. p. 888. ISBN 0130824445.

[108] Eichler, Jörg (2005-11-14). "Electron–positron pair production in relativistic ion–atom collisions". *Physics Letters A* **347** (1–3): 67–72. doi:10.1016/j.physleta.2005.06.105.

[109] Hubbell, J. H. (2006). "Electron positron pair production by photons: A historical overview". *Radiation Physics and Chemistry* **75** (6): 614–623. doi:10.1016/j.radphyschem.2005.10.008. Bibcode: 2006RaPC...75..614H.

[110] Quigg, Chris (June 4–30, 2000). "The Electroweak Theory". *TASI 2000: Flavor Physics for the Millennium*. Boulder, Colorado: arXiv. p. 80. arXiv:hep-ph/0204104v1.

[111] Mulliken, Robert S. (1967). "Spectroscopy, Molecular Orbitals, and Chemical Bonding". *Science* **157** (3784): 13–24. doi:10.1126/science.157.3784.13. PMID 5338306.

[112] Burhop, Eric H. S. (1952). *The Auger Effect and Other Radiationless Transitions*. New York: Cambridge University Press. pp. 2–3.

[113] Grupen, Claus (June 28 – July 10, 1999). "Physics of Particle Detection". *AIP Conference Proceedings, Instrumentation in Elementary Particle Physics, VIII*. **536**. Istanbul: Dordrecht, D. Reidel Publishing Company. pp. 3–34. doi:10.1063/1.1361756.

[114] Jiles, David (1998). *Introduction to Magnetism and Magnetic Materials* (http://books.google.com/?id=axyWXjsdorMC&pg=PA280). CRC Press. pp. 280–287. ISBN 0412798603. .

[115] Löwdin, Per Olov; Erkki Brändas, Erkki; Kryachko, Eugene S. (2003). *Fundamental World of Quantum Chemistry: A Tribute to the Memory of Per- Olov Löwdin* (http://books.google.com/?id=8QiR8lCX_qcC&pg=PA393). Springer. pp. 393–394. ISBN 140201290X. .

[116] McQuarrie, Donald Allan; Simon, John Douglas (1997). *Physical Chemistry: A Molecular Approach* (http://books.google.com/?id=f-bje0-DEYUC&pg=PA325). University Science Books. pp. 325–361. ISBN 0935702997. .

[117] Daudel, R.; Bader, R.F.W.; Stephens, M.E.; Borrett, D.S. (1973-10-11). "The Electron Pair in Chemistry" (http://article.pubs.nrc-cnrc.gc.ca/ppv/RPViewDoc?issn=1480-3291&volume=52&issue=8&startPage=1310). *Canadian Journal of Chemistry* **52**: 1310–1320. doi:10.1139/v74-201. . Retrieved 2008-10-12.

[118] Rakov, Vladimir A.; Uman, Martin A. (2007). *Lightning: Physics and Effects* (http://books.google.com/?id=TuMa5lAa3RAC&pg=PA4). Cambridge University Press. p. 4. ISBN 0521035414. .

[119] Freeman, Gordon R. (1999). "Triboelectricity and some associated phenomena". *Materials science and technology* **15** (12): 1454–1458.

[120] Forward, Keith M.; Lacks, Daniel J.; Sankaran, R. Mohan (2009). "Methodology for studying particle–particle triboelectrification in granular materials". *Journal of Electrostatics* **67** (2–3): 178–183. doi:10.1016/j.elstat.2008.12.002.

[121] Weinberg, Steven (2003). *The Discovery of Subatomic Particles* (http://books.google.com/?id=tDpwhp2lOKMC&pg=PA15). Cambridge University Press. pp. 15–16. ISBN 052182351X. .

[122] Lou, Liang-fu (2003). *Introduction to phonons and electrons* (http://books.google.com/?id=XMv-vfsoRF8C&pg=PA162). World Scientific. pp. 162, 164. ISBN 9789812384614. .

[123] Guru, Bhag S.; Hızıroğlu, Hüseyin R. (2004). *Electromagnetic Field Theory* (http://books.google.com/?id=b2f8rCngSuAC&pg=PA138). Cambridge University Press. pp. 138, 276. ISBN 0521830168. .

[124] Achuthan, M. K.; Bhat, K. N. (2007). *Fundamentals of Semiconductor Devices* (http://books.google.com/?id=REQkwBF4cVoC&pg=PA49). Tata McGraw-Hill. pp. 49–67. ISBN 007061220X. .

[125] Ziman, J. M. (2001). *Electrons and Phonons: The Theory of Transport Phenomena in Solids* (http://books.google.com/?id=UtEy63pjngsC&pg=PA260). Oxford University Press. p. 260. ISBN 0198507798. .

[126] Main, Peter (1993-06-12). "When electrons go with the flow: Remove the obstacles that create electrical resistance, and you get ballistic electrons and a quantum surprise" (http://www.newscientist.com/article/mg13818774.500-when-electrons-go-with-the-flow-remove-the-obstacles-thatcreate-electrical-resistance-and-you-get-ballistic-electrons-and-a-quantumsurprise.html). *New Scientist* **1887**: 30. . Retrieved 2008-10-09.

[127] Blackwell, Glenn R. (2000). *The Electronic Packaging Handbook* (http://books.google.com/?id=D0PBG53PQlUC&pg=SA6-PA39). CRC Press. pp. 6.39–6.40. ISBN 0849385911. .

[128] Durrant, Alan (2000). *Quantum Physics of Matter: The Physical World*. CRC Press. p. http://books.google.com/books?id=F0JmHRkJHiUC&pg=PA43. ISBN 0750307218.

[129] Staff (2008). "The Nobel Prize in Physics 1972" (http://nobelprize.org/nobel_prizes/physics/laureates/1972/). The Nobel Foundation. . Retrieved 2008-10-13.

[130] Kadin, Alan M. (2007). "Spatial Structure of the Cooper Pair". *Journal of Superconductivity and Novel Magnetism* **20** (4): 285–292. doi:10.1007/s10948-006-0198-z. arXiv:cond-mat/0510279.

[131] "Discovery About Behavior Of Building Block Of Nature Could Lead To Computer Revolution" (http://www.sciencedaily.com/releases/2009/07/090730141607.htm). *ScienceDaily.com*. 2009-07-31. . Retrieved 2009-08-01.

[132] Jompol, Yodchay; Ford, CJ; Griffiths, JP; Farrer, I; Jones, GA; Anderson, D; Ritchie, DA; Silk, TW *et al*. (2009-07-31). "Probing Spin-Charge Separation in a Tomonaga-Luttinger Liquid" (http://www.sciencemag.org/cgi/content/abstract/325/5940/597). *Science* **325** (5940): 597–601. doi:10.1126/science.1171769. PMID 19644117. . Retrieved 2009-08-01.

[133] Staff (2008). "The Nobel Prize in Physics 1958, for the discovery and the interpretation of the Cherenkov effect" (http://nobelprize.org/nobel_prizes/physics/laureates/1958/). The Nobel Foundation. . Retrieved 2008-09-25.

[134] Staff (2008-08-26). "Special Relativity" (http://www2.slac.stanford.edu/vvc/theory/relativity.html). Stanford Linear Accelerator Center. . Retrieved 2008-09-25.

[135] Solving for the velocity of the electron, and using an approximation for large $\gamma$, one obtains:

$$\begin{aligned} v &= c\sqrt{1 \ - \gamma^{-2}} \\ &= 0.999\,999\,999\,95\,c. \end{aligned}$$

[136] Adams, Steve (2000). *Frontiers: Twentieth Century Physics* (http://books.google.com/?id=yIsMaQblCisC&pg=PA215). CRC Press. p. 215. ISBN 0748408401. .

[137] Lurquin, Paul F. (2003). *The Origins of Life and the Universe*. Columbia University Press. p. 2. ISBN 0231126557.

[138] Silk, Joseph (2000). *The Big Bang: The Creation and Evolution of the Universe* (3rd ed.). Macmillan. pp. 110–112, 134–137. ISBN 080507256X.

[139] Christianto, Vic (2007). "Thirty Unsolved Problems in the Physics of Elementary Particles" (http://www.ptep-online.com/index_files/2007/PP-11-16.PDF) (PDF). *Progress in Physics* **4**: 112–114. . Retrieved 2008-09-04.

[140] Kolb, Edward W. (1980-04-07). "The Development of Baryon Asymmetry in the Early Universe". *Physics Letters B* **91** (2): 217–221. doi:10.1016/0370-2693(80)90435-9.

[141] Sather, Eric (Spring/Summer 1996). "The Mystery of Matter Asymmetry" (http://www.slac.stanford.edu/pubs/beamline/26/1/26-1-sather.pdf) (PDF). *Beam Line*. University of Stanford. . Retrieved 2008-11-01.

[142] Burles, Scott; Nollett, Kenneth M.; Turner, Michael S. (1999-03-19). "Big-Bang Nucleosynthesis: Linking Inner Space and Outer Space". arXiv, University of Chicago.

[143] Boesgaard, A. M.; Steigman, G (1985). "Big bang nucleosynthesis – Theories and observations" (http://adsabs.harvard.edu/cgi-bin/bib_query?1985ARA&A..23..319B). *Annual review of astronomy and astrophysics* **23** (2): 319–378. doi:10.1146/annurev.aa.23.090185.001535. . Retrieved 2008-08-28.

[144] Barkana, Rennan (2006-08-18). "The First Stars in the Universe and Cosmic Reionization" (http://www.sciencemag.org/cgi/content/full/313/5789/931). *Science* **313** (5789): 931–934. doi:10.1126/science.1125644. PMID 16917052. . Retrieved 2008-11-01.

[145] Burbidge, E. Margaret; Burbidge, G. R.; Fowler, William A.; Hoyle, F. (1957). "Synthesis of Elements in Stars". *Reviews of Modern Physics* **29** (4): 548–647. doi:10.1103/RevModPhys.29.547.

[146] Rodberg, L. S.; Weisskopf, VF (1957). "Fall of Parity: Recent Discoveries Related to Symmetry of Laws of Nature". *Science* **125** (3249): 627–633. doi:10.1126/science.125.3249.627. PMID 17810563.

[147] Fryer, Chris L. (1999). "Mass Limits For Black Hole Formation". *The Astrophysical Journal* **522** (1): 413–418. doi:10.1086/307647. Bibcode: 1999ApJ...522..413F.

[148] Parikh, Maulik K.; Wilczek, F (2000). "Hawking Radiation As Tunneling". *Physical Review Letters* **85** (24): 5042–5045. doi:10.1103/PhysRevLett.85.5042. PMID 11102182.

[149] Hawking, S. W. (1974-03-01). "Black hole explosions?". *Nature* **248**: 30–31. doi:10.1038/248030a0.

[150] Halzen, F.; Hooper, Dan (2002). "High-energy neutrino astronomy: the cosmic ray connection" (http://adsabs.harvard.edu/abs/2002astro.ph..4527H). *Reports on Progress in Physics* **66**: 1025–1078. doi:10.1088/0034-4885/65/7/201++++++++++++++0034-4885/65/7/201++++++++++++++++++++0034-4885/65/7/201. . Retrieved 2008-08-28.

[151] Ziegler, James F (1998). "Terrestrial cosmic ray intensities". *IBM Journal of Research and Development* **42** (1): 117–139. doi:10.1147/rd.421.0117.

[152] Sutton, Christine (1990-08-04). "Muons, pions and other strange particles" (http://www.newscientist.com/article/mg12717284.700-muons-pions-and-other-strange-particles-.html). *New Scientist*. . Retrieved 2008-08-28.

[153] Wolpert, Stuart (2008-07-24). "Scientists solve 30-year-old aurora borealis mystery" (http://www.universityofcalifornia.edu/news/article/18277). University of California. . Retrieved 2008-10-11.

[154] Gurnett, Donald A.; Anderson, RR (1976-12-10). "Electron Plasma Oscillations Associated with Type III Radio Bursts". *Science* **194** (4270): 1159–1162. doi:10.1126/science.194.4270.1159. PMID 17790910.

[155] Martin, W. C.; Wiese, W. L. (2007). "Atomic Spectroscopy: A Compendium of Basic Ideas, Notation, Data, and Formulas" (http://physics.nist.gov/Pubs/AtSpec/). National Institute of Standards and Technology. . Retrieved 2007-01-08.

[156] Fowles, Grant R. (1989). *Introduction to Modern Optics* (http://books.google.com/?id=SL1n9TuJ5YMC&pg=PA227). Courier Dover Publications. pp. 227–233. ISBN 0486659577. .

[157] Staff (2008). "The Nobel Prize in Physics 1989" (http://nobelprize.org/nobel_prizes/physics/laureates/1989/illpres/). The Nobel Foundation. . Retrieved 2008-09-24.

[158] Ekstrom, Philip (1980). "The isolated Electron" (http://tf.nist.gov/general/pdf/166.pdf) (PDF). *Scientific American* **243** (2): 91–101. . Retrieved 2008-09-24.

[159] Mauritsson, Johan. "Electron filmed for the first time ever" (http://www.atto.fysik.lth.se/video/pressrelen.pdf) (PDF). Lunds Universitet. . Retrieved 2008-09-17.

[160] Mauritsson, J.; Johnsson, P.; Mansten, E.; Swoboda, M.; Ruchon, T.; L'huillier, A.; Schafer, K. J. (2008). "Coherent Electron Scattering Captured by an Attosecond Quantum Stroboscope" (http://www.atto.fysik.lth.se/publications/papers/MauritssonPRL2008.pdf) (PDF). *Physical Review Letters* **100**: 073003. doi:10.1103/PhysRevLett.100.073003. .

[161] Damascelli, Andrea (2004). "Probing the Electronic Structure of Complex Systems by ARPES". *Physica Scripta* **T109**: 61–74. doi:10.1238/Physica.Topical.109a00061.

[162] Staff (1975-04-14). "Image # L-1975-02972" (http://grin.hq.nasa.gov/ABSTRACTS/GPN-2000-003012.html). Langley Research Center, NASA. . Retrieved 2008-09-20.

[163] Elmer, John (2008-03-03). "Standardizing the Art of Electron-Beam Welding" (https://www.llnl.gov/str/MarApr08/elmer.html). Lawrence Livermore National Laboratory. . Retrieved 2008-10-16.

[164] Schultz, Helmut (1993). *Electron Beam Welding* (http://books.google.com/?id=I0xMo28DwcIC&pg=PA2). Woodhead Publishing. pp. 2–3. ISBN 1855730502. .

[165] Benedict, Gary F. (1987). *Nontraditional Manufacturing Processes* (http://books.google.com/?id=xdmNVSio8jUC&pg=PA273). Manufacturing engineering and materials processing. **19**. CRC Press. p. 273. ISBN 0824773527. .

[166] Ozdemir, Faik S. (June 25–27, 1979). "Electron beam lithography" (http://portal.acm.org/citation.cfm?id=800292.811744). . San Diego, CA, USA: IEEE Press. pp. 383–391. . Retrieved 2008-10-16.

[167] Madou, Marc J. (2002). *Fundamentals of Microfabrication: the Science of Miniaturization* (http://books.google.com/?id=9bk3gJeQKBYC&pg=PA53) (2nd ed.). CRC Press. pp. 53–54. ISBN 0849308267. .

[168] Jongen, Yves; Herer, Arnold (May 2–5, 1996). "Electron Beam Scanning in Industrial Applications" (http://adsabs.harvard.edu/abs/1996APS..MAY.H9902J). . American Physical Society. . Retrieved 2008-10-16.
[169] Beddar, A. S. (2001). "Mobile linear accelerators for intraoperative radiation therapy" (http://findarticles.com/p/articles/mi_m0FSL/is_/ai_81161386). *AORN Journal* **74**: 700. doi:10.1016/S0001-2092(06)61769-9. . Retrieved 2008-10-26.
[170] Gazda, Michael J.; Coia, Lawrence R. (2007-06-01). "Principles of Radiation Therapy" (http://www.cancernetwork.com/cancer-management/chapter02/article/10165/1165822). Cancer Network. . Retrieved 2008-10-26.
[171] The polarization of an electron beam means that the spins of all electrons point into one direction. In other words, the projections of the spins of all electrons onto their momentum vector have the same sign.
[172] Chao, Alexander W.; Tigner, Maury (1999). *Handbook of Accelerator Physics and Engineering* (http://books.google.com/?id=Z3J4SjftF1YC&pg=PA155). World Scientific Publishing Company. pp. 155, 188. ISBN 9810235003. .
[173] Oura, K.; Lifshifts, V. G.; Saranin, A. A.; Zotov, A. V.; Katayama, M. (2003). *Surface Science: An Introduction*. Springer-Verlag. pp. 1–45. ISBN 3540005455.
[174] Ichimiya, Ayahiko; Cohen, Philip I. (2004). *Reflection High-energy Electron Diffraction* (http://books.google.com/?id=AUVbPerNxTcC&pg=PA1). Cambridge University Press. p. 1. ISBN 0521453739. .
[175] Heppell, T. A. (1967). "A combined low energy and reflection high energy electron diffraction apparatus". *Journal of Scientific Instruments* **44**: 686–688. doi:10.1088/0950-7671/44/9/311.
[176] McMullan, D. (1993). "Scanning Electron Microscopy: 1928–1965" (http://www-g.eng.cam.ac.uk/125/achievements/mcmullan/mcm.htm). University of Cambridge. . Retrieved 2009-03-23.
[177] Slayter, Henry S. (1992). *Light and electron microscopy* (http://books.google.com/?id=LlePVS9oq7MC&pg=PA1). Cambridge University Press. p. 1. ISBN 0521339480. .
[178] Cember, Herman (1996). *Introduction to Health Physics* (http://books.google.com/?id=obcmBZe9es4C&pg=PA42). McGraw-Hill Professional. pp. 42–43. ISBN 0071054618. .
[179] Erni, Rolf; Rossell, MD; Kisielowski, C; Dahmen, U (2009). "Atomic-Resolution Imaging with a Sub-50-pm Electron Probe". *Physical Review Letters* **102** (9): 096101. doi:10.1103/PhysRevLett.102.096101. PMID 19392535.
[180] Bozzola, John J.; Russell, Lonnie D. (1999). *Electron Microscopy: Principles and Techniques for Biologists* (http://books.google.com/?id=RqSMzR-IXk0C&pg=PA12). Jones & Bartlett Publishers. pp. 12, 197–199. ISBN 0763701920. .
[181] Flegler, Stanley L.; Heckman Jr., John W.; Klomparens, Karen L. (1995-10-01). *Scanning and Transmission Electron Microscopy: An Introduction* (Reprint ed.). Oxford University Press. pp. 43–45. ISBN 0195107519.
[182] Bozzola, John J.; Russell, Lonnie Dee (1999). *Electron Microscopy: Principles and Techniques for Biologists* (http://books.google.com/?id=RqSMzR-IXk0C&pg=PA9) (2nd ed.). Jones & Bartlett Publishers. p. 9. ISBN 0763701920. .
[183] Freund, Henry P.; Antonsen, Thomas (1996). *Principles of Free-Electron Lasers* (http://books.google.com/?id=73w9tqTgbiIC&pg=PA1). Springer. pp. 1–30. ISBN 0412725401. .
[184] Kitzmiller, John W. (1995). *Television Picture Tubes and Other Cathode-Ray Tubes: Industry and Trade Summary*. DIANE Publishing. pp. 3–5. ISBN 0788121006.
[185] Sclater, Neil (1999). *Electronic Technology Handbook*. McGraw-Hill Professional. pp. 227–228. ISBN 0070580480.
[186] Staff (2008). "The History of the Integrated Circuit" (http://nobelprize.org/educational_games/physics/integrated_circuit/history/). The Nobel Foundation. . Retrieved 2008-10-18.

## References

## External links

- "The Discovery of the Electron" (http://www.aip.org/history/electron/). American Institute of Physics, Center for History of Physics. Retrieved 2006-08-10.
- "Particle Data Group" (http://pdg.lbl.gov/). University of California. Retrieved 2008-11-17.
- Bock, Rudolf K.; Vasilescu, Angela (1998). *The Particle Detector BriefBook* (http://physics.web.cern.ch/Physics/ParticleDetector/BriefBook/) (14th ed.). Springer. ISBN 3540641203. Retrieved 2008-10-02.

# Neutron

| *Neutron* | |
|---|---|
| 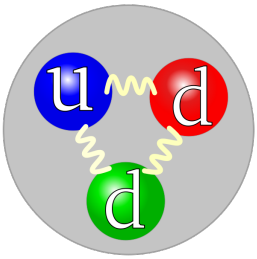 | |
| The quark structure of the neutron. (The color assignment of individual quarks is not important, only that all three colors are present.) | |
| **Classification:** | Baryon |
| **Composition:** | 1 up quark, 2 down quarks |
| **Particle statistics:** | Fermionic |
| **Group:** | Hadron |
| **Interaction:** | Gravity, Weak, Strong |
| **Symbol(s):** | n, $n^0$, $N^0$ |
| **Antiparticle:** | Antineutron |
| **Theorized:** | Ernest Rutherford[1] (1920) |
| **Discovered:** | James Chadwick[1] (1932) |
| **Mass:** | $1.67492729(28) \times 10^{-27}$ kg<br>939.565560(81) MeV/$c^2$<br>1.0086649156(6) u[2] |
| **Mean lifetime:** | 885.7(8) s (free) |
| **Electric charge:** | 0 e<br>0 C |
| **Electric dipole moment:** | $<2.9 \times 10^{-26}$ e·cm |
| **Electric polarizability:** | $1.16(15) \times 10^{-3}$ $fm^3$ |
| **Magnetic moment:** | $-1.9130427(5)$ $\mu_N$ |
| **Magnetic polarizability:** | $3.7(20) \times 10^{-4}$ $fm^3$ |
| **Spin:** | $\frac{1}{2}$ |
| **Isospin:** | $\frac{1}{2}$ |
| **Parity:** | +1 |
| **Condensed:** | $I(J^P) = \frac{1}{2}(\frac{1}{2}^+)$ |

The **neutron** is a subatomic particle with no net electric charge and a mass slightly larger than that of a proton. With the exception of hydrogen, nuclei of atoms consist of protons and neutrons, which are therefore collectively referred

to as nucleons. The number of protons in a nucleus is the atomic number and defines the type of element the atom forms. The number of neutrons is the neutron number and determines the isotope of an element. For example, the abundant carbon-12 isotope has 6 protons and 6 neutrons, while the very rare radioactive carbon-14 isotope has 6 protons and 8 neutrons.

While bound neutrons in stable nuclei are stable, free neutrons are unstable; they undergo beta decay with a mean lifetime of just under 15 minutes ($885.7 \pm 0.8$ s).[2] Free neutrons are produced in nuclear fission and fusion. Dedicated neutron sources like research reactors and spallation sources produce free neutrons for use in irradiation and in neutron scattering experiments. Even though it is not a chemical element, the free neutron is sometimes included in tables of nuclides.[3] It is then considered to have an atomic number of zero and a mass number of one, and is sometimes referred to as neutronium.

The neutron has been the key to nuclear power production. After the neutron was discovered in 1932, it was realized in 1933 that it might mediate a nuclear chain reaction. In the 1930's, neutrons were used to produce many different types of nuclear transmutations. When nuclear fission was discovered in 1938, it was soon realized that this might be the mechanism to produce the neutrons for the chain reaction, if the process also produced neutrons, and this was proven in 1939, making the path to nuclear power production evident. These events and findings led directly to the first nuclear chain reaction which was self-sustaining (1942) and to the first nuclear weapons in 1945.

## Discovery

In 1920, Ernest Rutherford conceptualised the possible existence of the neutron. In particular, Rutherford considered that the disparity found between the atomic number of an atom and its atomic mass could be explained by the existence of a neutrally charged particle within the atomic nucleus.[]

In 1931 Walther Bothe and Herbert Becker in Germany found that if the very energetic alpha particles emitted from polonium fell on certain light elements, specifically beryllium, boron, or lithium, an unusually penetrating radiation was produced. At first this radiation was thought to be gamma radiation, although it was more penetrating than any gamma rays known, and the details of experimental results were very difficult to interpret on this basis. The next important contribution was reported in 1932 by Irène Joliot-Curie and Frédéric Joliot in Paris. They showed that if this unknown radiation fell on paraffin, or any other hydrogen-containing compound, it ejected protons of very high energy. This was not in itself inconsistent with the assumed gamma ray nature of the new radiation, but detailed quantitative analysis of the data became increasingly difficult to reconcile with such a hypothesis.

In 1930 Viktor Ambartsumian and Dmitri Ivanenko in USSR found that contrary to the prevailing opinion of the time nucleus can not consist of protons and electrons. They proved that some neutral particles must be present besides the protons. [4]

In 1932, James Chadwick performed a series of experiments at the University of Cambridge, showing that the gamma ray hypothesis was untenable. He suggested that the new radiation consisted of uncharged particles of approximately the mass of the proton, and he performed a series of experiments verifying his suggestion.[5] These uncharged particles were called *neutrons*, apparently from the Latin root for *neutral* and the Greek ending *-on* (by imitation of *electron* and *proton*).

The discovery of the neutron explained a puzzle involving the spin of the nitrogen-14 nucleus, which had been experimentally measured to be 1 ħ. It was known that atomic nuclei usually had about half as many positive charges as if they were composed completely of protons, and in existing models this was often explained by proposing that nuclei also contained some "nuclear electrons" to neutralize the excess charge. Thus, nitrogen-14 would be composed of 14 protons and 7 electrons to give it a charge of +7 but a mass of 14 atomic mass units. However, it was also known that both protons and electrons carried an intrinsic spin of $^1/_2$ ħ, and there was no way to arrange an odd number (21) of spins $\pm^1/_2$ ħ to give a spin of 1 ħ. Instead, when nitrogen-14 was proposed to consist of 3 pairs of protons and neutrons, with an additional unpaired neutron and proton each contributing a spin of $^1/_2$ ħ in the same direction for a total spin of 1 ħ, the model became viable. Soon, nuclear neutrons were used to naturally explain spin

differences in many different nuclides in the same way, and the neutron as a basic structural unit of atomic nuclei was accepted.

# Intrinsic properties

## Stability and beta decay

Under the Standard Model of particle physics, because the neutron consists of three quarks, the only possible decay mode without a change of baryon number is for one of the quarks to change flavour via the weak interaction. The neutron consists of two down quarks with charge $-{}^{1}\!/_{3}$ e and one up quark with charge $+{}^{2}\!/_{3}$ e, and the decay of one of the down quarks into a lighter up quark can be achieved by the emission of a W boson. By this means the neutron decays into a proton (which contains one down and two up quarks), an electron, and an electron antineutrino.

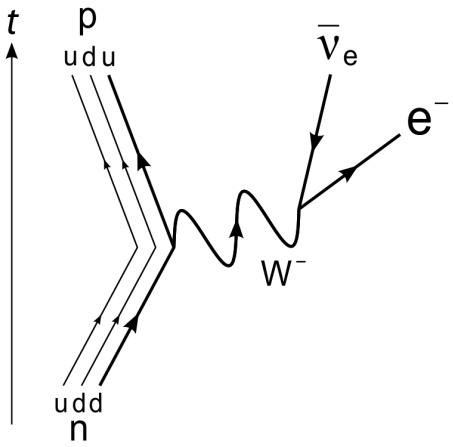


The Feynman diagram for beta decay of a neutron into a proton, electron, and electron antineutrino via an intermediate heavy W boson

Outside the nucleus, free neutrons are unstable and have a mean lifetime of 885.7 ± 0.8 s (about 14 minutes, 46 seconds); therefore the half-life for this process (which differs from the mean lifetime by a factor of ln(2) = 0.693) is 613.9 ± 0.8 s (about 10 minutes, 14 seconds).[2] Free neutrons decay by emission of an electron and an electron antineutrino to become a proton, a process known as beta decay:[6]

$$n^0 \rightarrow p^+ + e^- + \nu_e$$

Neutrons in unstable nuclei can also decay in this manner. However, inside a nucleus, protons can also transform into a neutron via inverse beta decay. This transformation occurs by emission of a antielectron (also called positron) and a neutrino:

$$p^+ \rightarrow n^0 + e^+ + \nu_e$$

The transformation of a proton to a neutron inside of a nucleus is also possible through electron capture:

$$p^+ + e^- \rightarrow n^0 + \nu_e$$

Positron capture by neutrons in nuclei that contain an excess of neutrons is also possible, but is hindered because positrons are repelled by the nucleus, and quickly annihilate when they encounter electrons.

When bound inside of a nucleus, the instability of a single neutron to beta decay is balanced against the instability that would be acquired by the nucleus as a whole if an additional proton were to participate in repulsive interactions with the other protons that are already present in the nucleus. As such, although free neutrons are unstable, bound neutrons are not necessarily so. The same reasoning explains why protons, which are stable in empty space, may transform into neutrons when bound inside of a nucleus.

## Electric dipole moment

The Standard Model of particle physics predicts a tiny separation of positive and negative charge within the neutron leading to a permanent electric dipole moment.[7] The predicted value is, however, well below the current sensitivity of experiments. From several unsolved puzzles in particle physics, it is clear that the Standard Model is not the final and full description of all particles and their interactions. New theories going beyond the Standard Model generally lead to much larger predictions for the electric dipole moment of the neutron. Currently, there are at least four experiments trying to measure for the first time a finite neutron electric dipole moment, including:

- [8] Cryogenic neutron EDM experiment being set up at the Institut Laue-Langevin
- [9] nEDM experiment under construction at the new UCN source at the Paul Scherrer Institute
- [10] nEDM experiment being envisaged at the Spallation Neutron Source
- [11] nEDM experiment being built at the Institut Laue-Langevin

### Magnetic moment

Magnetic moment of a neutron is nonzero, unexpected from an electrically neutral particle. This indicates that neutron is a composite particle.

### Anti-neutron

The antineutron is the antiparticle of the neutron. It was discovered by Bruce Cork in the year 1956, a year after the antiproton was discovered. CPT-symmetry puts strong constraints on the relative properties of particles and antiparticles, so studying antineutrons yields provide stringent tests on CPT-symmetry. The fractional difference in the masses of the neutron and antineutron is $9 \pm 5 \times 10^{-5}$. Since the difference is only about 2 standard deviations away from zero, this does not give any convincing evidence of CPT-violation.[2]

### Structure and geometry of charge distribution within the neutron

An article published in 2007 featuring a model-independent analysis concluded that the neutron has a negatively charged exterior, a positively charged middle, and a negative core.[12] In a simplified classical view, the negative "skin" of the neutron assists it to be attracted to the protons with which it interacts in the nucleus. However, the main attraction between neutrons and protons is via the nuclear force, which does not involve charge.

## Neutron compounds

### Dineutrons and tetraneutrons

The existence of stable clusters of 4 neutrons, or tetraneutrons, has been hypothesised by a team led by Francisco-Miguel Marqués at the CNRS Laboratory for Nuclear Physics based on observations of the disintegration of beryllium-14 nuclei. This is particularly interesting because current theory suggests that these clusters should not be stable.

The dineutron is another hypothetical particle.

### Neutronium and neutron stars

At extremely high pressures and temperatures, nucleons and electrons are believed to collapse into bulk neutronic matter, called neutronium. This is presumed to happen in neutron stars.

## Detection

The common means of detecting a charged particle by looking for a track of ionization (such as in a cloud chamber) does not work for neutrons directly. Neutrons that elastically scatter off atoms can create an ionization track that is detectable, but the experiments are not as simple to carry out; other means for detecting neutrons, consisting of allowing them to interact with atomic nuclei, are more commonly used. The commonly used methods to detect neutrons can therefore be categorized according to the nuclear processes relied upon, mainly neutron capture or elastic scattering. A good discussion on neutron detection is found in chapter 14 of the book *Radiation Detection and Measurement* by Glenn F. Knoll (John Wiley & Sons, 1979).

### Neutron detection by neutron capture

A common method for detecting neutrons involves converting the energy released from such reactions into electrical signals. Certain nuclides have neutron deficit and therefore a high probability to absorb a neutron. Upon neutron capture, the compound nucleus emits more easily detectable radiation, for example an alpha particle, which is then detected. The nuclides $^{3}$He, $^{6}$Li, $^{10}$B, $^{233}$U, $^{235}$U, $^{237}$Np and $^{239}$Pu are useful for this purpose. These nuclides are rarely found in nature, but can be accumulated through processes such as isotopic enrichment.

The cross section for the process of neutron capture is much lower at high energies than at low energies. Therefore, the detection of neutrons by neutron capture requires a preceding slowing down of neutrons. For this purpose, a so-called moderator is used, typically a thick slab of polyethylene. Neutron detection according to the moderate-and-capture approach is not capable of measuring neutron energy, precise time of arrival, or direction of incidence, since this information is lost during moderation.

### Neutron detection by elastic scattering

Neutrons can elastically scatter off nuclei, causing the struck nucleus to recoil. Kinematically, a neutron can transfer more energy to light nuclei such as hydrogen or helium than to heavier nuclei. Detectors relying on elastic scattering are called fast neutron detectors. Recoiling nuclei can ionize and excite further atoms through collisions. Charge and/or scintillation light produced in this way can be collected to produce a detected signal. A major challenge in fast neutron detection is discerning such signals from erroneous signals produced by gamma radiation in the same detector.

Fast neutron detectors have the advantage of not requiring a moderator, and therefore being capable of measuring the neutron's energy, time of arrival, and in certain cases direction of incidence.

## Uses

The neutron plays an important role in many nuclear reactions. For example, neutron capture often results in neutron activation, inducing radioactivity. In particular, knowledge of neutrons and their behavior has been important in the development of nuclear reactors and nuclear weapons. The fissioning of elements like uranium-235 and plutonium-239 is caused by their absorption of neutrons.

*Cold*, *thermal* and *hot* neutron radiation is commonly employed in neutron scattering facilities, where the radiation is used in a similar way one uses X-rays for the analysis of condensed matter. Neutrons are complementary to the latter in terms of atomic contrasts by different scattering cross sections; sensitivity to magnetism; energy range for inelastic neutron spectroscopy; and deep penetration into matter.

The development of "neutron lenses" based on total internal reflection within hollow glass capillary tubes or by reflection from dimpled aluminum plates has driven ongoing research into neutron microscopy and neutron/gamma ray tomography.[13] [14] [15]

A major use of neutrons is to excite delayed and prompt gamma rays from elements in materials. This forms the basis of neutron activation analysis (NAA) and prompt gamma neutron activation analysis (PGNAA). NAA is most often used to analyze small samples of materials in a nuclear reactor whilst PGNAA is most often used to analyze subterranean rocks around bore holes and industrial bulk materials on conveyor belts.

Another use of neutron emitters is the detection of light nuclei, particularly the hydrogen found in water molecules. When a fast neutron collides with a light nucleus, it loses a large fraction of its energy. By measuring the rate at which slow neutrons return to the probe after reflecting off of hydrogen nuclei, a neutron probe may determine the water content in soil.

## Sources

Because free neutrons are unstable, they can be obtained only from nuclear disintegrations, nuclear reactions, and high-energy reactions (such as in cosmic radiation showers or accelerator collisions). Free neutron beams are obtained from neutron sources by neutron transport. For access to intense neutron sources, researchers must go to specialist facilities, such as the ISIS facility in the United Kingdom, which is currently the world's most intense pulsed neutron and muon source.

The neutron's lack of total electric charge makes it difficult to steer or accelerate them. Charged particles can be accelerated, decelerated, or deflected by electric or magnetic fields. These methods have little effect on neutrons beyond a small effect of an inhomogeneous magnetic field because of the neutron's magnetic moment. Neutrons can be controlled by methods that include moderation, reflection and velocity selection.

## Protection

Exposure to free neutrons can be hazardous, since the interaction of neutrons with molecules in the body can cause disruption to molecules and atoms, and can also cause reactions which give rise to other forms of radiation (such as protons). The normal precautions of radiation protection apply: avoid exposure, stay as far from the source as possible, and keep exposure time to a minimum. Some particular thought must be given to how to protect from neutron exposure, however. For other types of radiation, e.g. alpha particles, beta particles, or gamma rays, material of a high atomic number and with high density make for good shielding; frequently lead is used. However, this approach will not work with neutrons, since the absorption of neutrons does not increase straightforwardly with atomic number, as it does with alpha, beta, and gamma radiation. Instead one needs to look at the particular interactions neutrons have with matter (see the section on detection above). For example, hydrogen rich materials are often used to shield against neutrons, since ordinary hydrogen both scatters and slows neutrons. This often means that simple concrete blocks or even paraffin-loaded plastic blocks afford better protection from neutrons than do far more dense materials. After slowing, neutrons may then be absorbed with an isotope which has high affinity for slow neutrons without causing secondary capture-radiation, such as lithium-6.

Hydrogen-rich ordinary water affects neutron absorption in nuclear fission reactors: usually neutrons are so strongly absorbed by normal water that fuel-enrichment with fissionable isotope is required. The deuterium in heavy water has a very much lower absorption affinity for neutrons than does protium (normal light hydrogen). Deuterium is therefore used in CANDU-type reactors, in order to slow (moderate) neutron velocity, to increase the probability of nuclear fission compared to neutron capture.

## Production

Various nuclides become more stable by expelling neutrons as a decay mode; this is known as neutron emission, and happens commonly during spontaneous fission.

Institut Laue–Langevin (ILL) in Grenoble, France - one of the most important neutron research facilities worldwide

Cosmic radiation interacting with the Earth's atmosphere continuously generates neutrons that can be detected at the surface. Even stronger neutron radiation is produced at the surface of Mars where the atmosphere is thick enough to generate neutrons from cosmic ray spallation, but not thick enough to provide significant protection from the neutrons produced. These neutrons not only produce a Martian surface neutron radiation hazard from direct downward-going neutron radiation, but also a significant hazard from reflection of neutrons from the Martian surface, which will produce reflected neutron radiation penetrating upward into a Martian craft or habitat from the floor.[16]

Nuclear fission reactors naturally produce free neutrons; their role is to sustain the energy-producing chain reaction. The intense neutron radiation can also be used to produce various radioisotopes through the process of neutron activation, which is a type of neutron capture.

Experimental nuclear fusion reactors produce free neutrons as a waste product. However, it is these neutrons that possess most of the energy, and converting that energy to a useful form has proved a difficult engineering challenge. Fusion reactors which generate neutrons are likely to create around twice the amount of radioactive waste of a fission reactor, but the waste is composed of neutron-activated lighter isotopes, which have relatively short (50–100 years) decay periods as compared to typical half lives of 10,000 years for fission waste, which is long primarily due to the long half life of alpha-emitting transuranic actinides. [17] Nuclear power#Solid waste

# Neutron temperature

## Thermal neutron

A **thermal neutron** is a free neutron that is Boltzmann distributed with kT = 0.0253 eV ($4.0\times10^{-21}$ J) at room temperature. This gives characteristic (not average, or median) speed of 2.2 km/s. The name 'thermal' comes from their energy being that of the room temperature gas or material they are permeating. (see *kinetic theory* for energies and speeds of molecules). After a number of collisions (often in the range of 10–20) with nuclei, neutrons arrive at this energy level, provided that they are not absorbed.

In many substances, thermal neutrons have a much larger effective cross-section than faster neutrons, and can therefore be absorbed more easily by any atomic nuclei that they collide with, creating a heavier — and often unstable — isotope of the chemical element as a result.

Most fission reactors use a neutron moderator to slow down, or *thermalize* the neutrons that are emitted by nuclear fission so that they are more easily captured, causing further fission. Others, called fast breeder reactors, use fission energy neutrons directly.

## Cold neutrons

These neutrons are thermal neutrons that have been equilibrated in a very cold substance such as liquid deuterium. These are produced in neutron scattering research facilities.

## Ultracold neutrons

Ultracold neutrons are produced by inelastically scattering cold neutrons in substances with a temperature of a few kelvins, such as solid deuterium or superfluid helium. An alternative production method is the mechanical deceleration of cold neutrons.

## Fission energy neutron

A **fast neutron** is a free neutron with a kinetic energy level close to 2 MeV (20 TJ/kg), hence a speed of 28,000 km/s. They are named *fission energy* or *fast* neutrons to distinguish them from lower-energy thermal neutrons, and high-energy neutrons produced in cosmic showers or accelerators. Fast neutrons are produced by nuclear processes such as nuclear fission.

Fast neutrons can be made into thermal neutrons via a process called moderation. This is done with a neutron moderator. In reactors, typically heavy water, light water, or graphite are used to moderate neutrons.

## Fusion neutron

D-T (deuterium-tritium) fusion is the fusion reaction that produces the most energetic neutrons, with 14.1 MeV of kinetic energy and traveling at 17% of the speed of light. D-T fusion is also the easiest fusion reaction to ignite, reaching near-peak rates even when the deuterium and tritium nuclei have only a thousandth as much kinetic energy as the 14.1 MeV that will be produced.

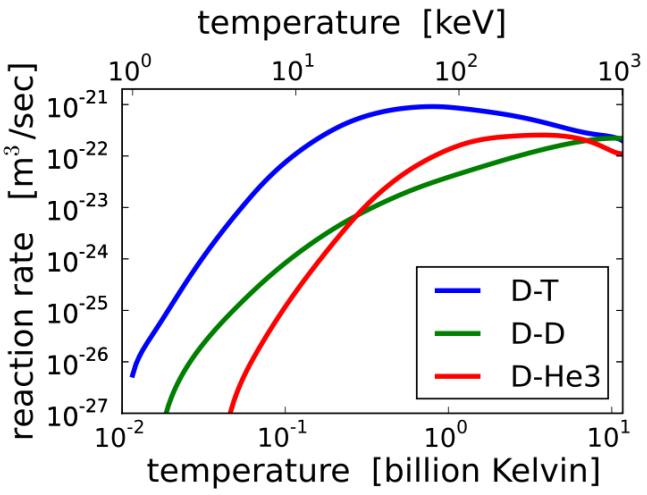


The fusion reaction rate increases rapidly with temperature until it maximizes and then gradually drops off. The DT rate peaks at a lower temperature (about 70 keV, or 800 million kelvins) and at a higher value than other reactions commonly considered for fusion energy.

14.1 MeV neutrons have about 10 times as much energy as fission neutrons, and are very effective at fissioning even non-fissile heavy nuclei, and these high-energy fissions produce more neutrons on average than fissions by lower-energy neutrons. This makes D-T fusion neutron sources such as proposed tokamak power reactors useful for transmutation of transuranic waste. 14.1 MeV neutrons can also produce neutrons by knocking them loose from nuclei.

On the other hand, these very high energy neutrons are less likely to simply be captured without causing fission or spallation. For these reasons, nuclear weapon design extensively utilizes D-T fusion 14.1 MeV neutrons to cause more fission. Fusion neutrons are able to cause fission in ordinarily non-fissile materials, such as depleted uranium (uranium-238), and these materials have used in the jackets of thermonuclear weapons. Fusion neutrons also can cause fission in substances that are unsuitable or difficult to make into primary fission bombs, such as reactor grade plutonium. This physical fact thus causes ordinary non-weapons grade materials to become of concern in certain nuclear proliferation discussions and treaties.

Other fusion reactions produce much less energetic neutrons. D-D fusion produces a 2.45 MeV neutron and helium-3 half of the time, and produces tritium and a proton but no neutron the other half of the time. D-$^3$He fusion produces no neutron.

### Intermediate-energy neutrons

A fission energy neutron that has slowed down but not yet reached thermal energies is called an epithermal neutron.

Cross sections for both capture and fission reactions often have multiple resonance peaks at specific energies in the epithermal energy range. These are of less significance in a fast neutron reactor where most neutrons are absorbed before slowing down to this range, or in a well-moderated thermal reactor where epithermal neutrons mostly interact with moderator nuclei, not with either fissile or fertile actinide nuclides. However, in a partially moderated reactor with more interactions of epithermal neutrons with heavy metal nuclei, there are greater possibilities for transient changes in reactivity which might make reactor control more difficult.

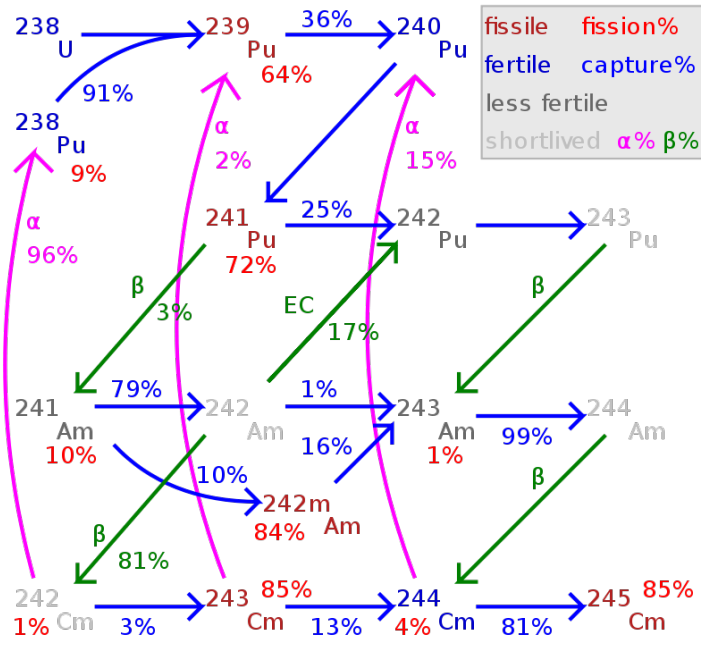


Transmutation flow in LWR which is a thermal-spectrum reactor

Ratios of capture reactions to fission reactions are also worse (more captures without fission) in most nuclear fuels such as plutonium-239, making epithermal-spectrum reactors using these fuels less desirable, as captures not only waste the one neutron captured but also usually result in a nuclide which is not fissile with thermal or epithermal neutrons, though still fissionable with fast neutrons. The exception is uranium-233 of the thorium cycle which has good capture-fission ratios at all neutron energies.

### High-energy neutrons

These neutrons have more energy than fission energy neutrons and are generated as secondary particles by particle accelerators or in the atmosphere from cosmic rays. They can have energies as high as tens of joules per neutron.

## See also

- Neutron radiation
- List of particles
- Nuclear reaction
- Thermal reactor
- Fast neutron
- Ionizing radiation
- Isotope
- Neutron flux
- Neutron generator
- Neutron magnetic moment
- Neutron capture nucleosynthesis
  - R-process
  - S-process

- Neutron radiation and the Sievert radiation scale

### Neutron sources

- Astronomical neutron sources
- Neutron sources
- Neutron generator

### Processes involving neutrons

- Neutron bomb
- Neutron diffraction
- Neutron flux
- Neutron transport

## References

[1] 1935 Nobel Prize in Physics (http://nobelprize.org/nobel_prizes/physics/laureates/1935/)
[2] Particle Data Group's Review of Particle Physics 2006 (http://pdg.lbl.gov/2006/tables/bxxx.pdf)
[3] http://www.nndc.bnl.gov/nudat2
[4] http://www.springerlink.com/content/ek2q156624661848/fulltext.pdf
[5] Chadwick, James (1932). "Possible Existence of a Neutron". *Nature* **129**: 312. doi:10.1038/129312a0.
[6] Particle Data Group Summary Data Table on Baryons (http://pdg.lbl.gov/2007/tables/bxxx.pdf)
[7] University of Sussex (20 February 2006). "Pear-shaped particles probe big-bang mystery" (http://www.sussex.ac.uk/press_office/media/media537.shtml). Press release. . Retrieved 2009-12-14.
[8] http://hepwww.rl.ac.uk/EDM/index_files/CryoEDM.htm
[9] http://nedm.web.psi.ch/
[10] http://p25ext.lanl.gov/edm/edm.html
[11] http://nrd.pnpi.spb.ru/LabSereb/neutronedm.htm
[12] G.A. Miller (2007). "Charge Densities of the Neutron and Proton". *Physical Review Letters* **99**: 112001. doi:10.1103/PhysRevLett.99.112001.
[13] Kumakhov, M. A.; Sharov, V. A. (1992). "A neutron lens". *Nature* **357**: 390–391. doi:10.1038/357390a0.
[14] Physorg.com, "New Way of 'Seeing': A 'Neutron Microscope'" (http://www.physorg.com/news599.html)
[15] NASA.gov: "NASA Develops a Nugget to Search for Life in Space" (http://www.nasa.gov/vision/earth/technologies/nuggets.html)
[16] http://www.physicamedica.com/VOLXVII_S1/20-CLOWDSLEY%20et%20alii.pdf
[17] http://news.bbc.co.uk/1/hi/sci/tech/4627237.stm

- Annotated bibliography for neutrons from the Alsos Digital Library for Nuclear Issues (http://alsos.wlu.edu/qsearch.aspx?browse=science/Neutrons)

## Further reading

- Knoll, G. F. (2000) *Radiation Detection and Measurement*
- Krane, K. S. (1998) *Introductory Nuclear Physics*
- Squires, G. L. (1997) *Introduction to the Theory of Thermal Neutron Scattering*
- Dewey, M. S., Gilliam, D. M., Nico, J. S., Snow, M. S., Wietfeldt, F. E. *NIST Neutron Lifetime Experiment*

# Muon

| *Muon* | |
|---|---|
| 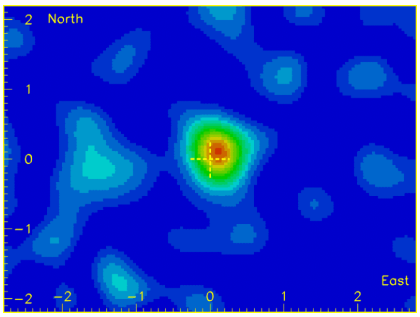 | |
| The Moon's cosmic ray shadow, as seen in secondary muons generated by cosmic rays in the atmosphere, and detected 700 meters below ground, at the Soudan II detector. | |
| **Composition:** | Elementary particle |
| **Particle statistics:** | Fermionic |
| **Group:** | Lepton |
| **Generation:** | Second |
| **Interaction:** | Gravity, Electromagnetic, Weak |
| **Symbol(s):** | $\mu^-$ |
| **Antiparticle:** | Antimuon ($\mu^+$) |
| **Theorized:** | — |
| **Discovered:** | Carl D. Anderson (1936) |
| **Mass:** | 105.65836668(38) MeV/$c^2$ |
| **Mean lifetime:** | 2.197034(21) × $10^{-6}$ s[1] |
| **Electric charge:** | −1 e |
| **Color charge:** | None |
| **Spin:** | $^1/_2$ |

The **muon** (from the Greek letter mu (μ) used to represent it) is an elementary particle similar to the electron, with a negative electric charge and a spin of ½. Together with the electron, the tau, and the three neutrinos, it is classified as a lepton. It is an unstable subatomic particle with the second longest mean lifetime (2.2 μs), exceeded only by that of the free neutron (~15 min). Like all elementary particles, the muon has a corresponding antiparticle of opposite charge but equal mass and spin: the **antimuon** (also called a *positive muon*). Muons are denoted by $\mu^-$ and antimuons by $\mu^+$. Muons were previously called **mu mesons**, but are not classified as mesons by modern particle physicists (see *History*).

Muons have a mass of 105.7 MeV/$c^2$, which is about 200 times the mass of an electron. Since the muon's interactions are very similar to those of the electron, a muon can be thought of as a much heavier version of the electron. Due to their greater mass, muons are not as sharply accelerated when they encounter electromagnetic fields, and do not emit as much bremsstrahlung radiation. Thus muons of a given energy penetrate matter far more deeply than electrons, since the deceleration of electrons and muons is primarily due to energy loss by this mechanism. So-called "secondary muons", generated by cosmic rays hitting the atmosphere, can penetrate to the Earth's surface

and into deep mines.

As with the case of the other charged leptons, the muon has an associated muon neutrino. Muon neutrinos are denoted by $\nu_\mu$.

## History

Muons were discovered by Carl D. Anderson and Seth Neddermeyer at Caltech in 1936 while studying cosmic radiation. Anderson had noticed particles that curved differently from electrons and other known particles when passed through a magnetic field. They were negatively charged but curved less sharply than electrons, but more sharply than protons, for particles of the same velocity. It was assumed that the magnitude of their negative electric charge was equal to that of the electron, and so to account for the difference in curvature, it was supposed that their mass was greater than an electron but smaller than a proton. Thus Anderson initially called the new particle a *mesotron*, adopting the prefix *meso-* from the Greek word for "mid-". Shortly thereafter, additional particles of intermediate mass were discovered, and the more general term *meson* was adopted to refer to any such particle. To differentiate between different types of mesons, the mesotron was in 1947 renamed the *mu meson* (the Greek letter $\mu$ (*mu*) corresponds to *m*).

It was soon found that the mu meson significantly differed from other mesons: for example, its decay products included a neutrino and an antineutrino, rather than just one or the other, as was observed with other mesons. Other mesons were eventually understood to be hadrons—that is, particles made of quarks—and thus subject to the residual strong force. In the quark model, a *meson* is composed of exactly two quarks (a quark and antiquark) unlike baryons, which are composed of three quarks. Mu mesons, however, were found to be fundamental particles (leptons) like electrons, with no quark structure. Thus, mu mesons were not mesons at all (in the new sense and use of the term *meson*), and so the term *mu meson* was abandoned, and replaced with the modern term *muon*.

Another particle (the pion, with which the muon was initially confused) had been predicted by theorist Hideki Yukawa:[2]

> "It seems natural to modify the theory of Heisenberg and Fermi in the following way. The transition of a heavy particle from neutron state to proton state is not always accompanied by the mission of light particles. The transition is sometimes taken up by another heavy particle."

The existence of the muon was confirmed in 1937 by J. C. Street and E. C. Stevenson's cloud chamber experiment.[3] The discovery of the muon seemed so incongruous and surprising at the time that Nobel laureate I. I. Rabi famously quipped, "Who ordered that?"

In a 1941 experiment on Mount Washington in New Hampshire, muons were used to observe the time dilation predicted by special relativity for the first time.[4]

## Muon sources

Since the production of muons requires an available center of momentum frame energy of 105.7 MeV, neither ordinary radioactive decay events nor nuclear fission and fusion events (such as those occurring in nuclear reactors and nuclear weapons) are energetic enough to produce muons. Only nuclear fission produces single-nuclear-event energies in this range, but do not produce muons as the production of a single muon would violate the conservation of quantum numbers (see under "muon decay" below).

On Earth, most naturally occurring muons are created by cosmic rays, which consist mostly of protons, many arriving from deep space at very high energy[5]

> About 10,000 muons reach every square meter of the earth's surface a minute; these charged particles form as by-products of cosmic rays colliding with molecules in the upper atmosphere. Travelling at relativistic speeds, muons can penetrate tens of meters into rocks and other matter before attenuating as a result of absorption or deflection by other atoms.

— Mark Wolverton (September 2007). "Muons for Peace: New Way to Spot Hidden Nukes Gets Ready to Debut" [6]. *Scientific American* **297** (3): 26–28.

When a cosmic ray proton impacts atomic nuclei of air atoms in the upper atmosphere, pions are created. These decay within a relatively short distance (meters) into muons (the pion's preferred decay product), and neutrinos. The muons from these high energy cosmic rays generally continue in about the same direction as the original proton, at a very high velocity. Although their lifetime *without* relativistic effects would allow a half-survival distance of only about 0.66 km (660 meters) at most (as seen from Earth) the time dilation effect of special relativity (from the viewpoint of the Earth) allows cosmic ray secondary muons to survive the flight to the Earth's surface, since in the Earth frame, the muons have a longer half-life due to their velocity. From the viewpoint (inertial frame) of the muon, on the other hand, it is the length contraction effect of special relativity which allows this penetration, since in the muon frame, its life time is unaffected, but the distance through the atmosphere and earth appears far shorter than these distances in the Earth rest-frame. Both are equally valid ways of explaining the fast muon's unusual survival over distances.

Since muons are unusually penetrative of ordinary matter, like neutrinos, they are also detectable deep underground (700 meters at the Soudan II detector, pictured above) and underwater, where they form a major part of the natural background ionizing radiation. Like cosmic rays, as noted, this secondary muon radiation is also directional.

The same nuclear reaction described above (i.e. hadron-hadron impacts to produce pion beams, which then quickly decay to muon beams over short distances) is used by particle physicists to produce muon beams, such as the beam used for the muon $g - 2$ experiment.[7]

## Muon decay

Muons are unstable elementary particles and are heavier than electrons and neutrinos but lighter than all other matter particles. They decay via the weak interaction. Because lepton numbers must be conserved, one of the product neutrinos of muon decay must be a muon-type neutrino and the other an electron-type antineutrino (antimuon decay produces the corresponding antiparticles, as detailed below). Because charge must be conserved, one of the products of muon decay is always an electron of the same charge as the muon (a positron if it is a positive muon). Thus all muons decay to at least an electron, and two neutrinos. Sometimes, besides these necessary products, additional other particles that have a net charge and spin of zero (i.e. a pair of photons, or an electron-positron pair), are produced.

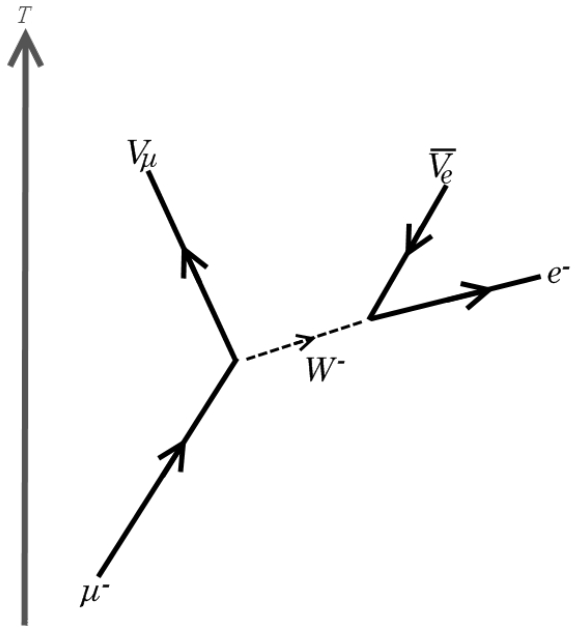

The most common decay of the muon

The dominant muon decay mode (sometimes called the Michel decay after Louis Michel) is the simplest possible: the muon decays to an electron, an electron-antineutrino, and a muon-neutrino. Antimuons, in mirror fashion, most often decay to the corresponding antiparticles: a positron, an electron-neutrino, and a muon-antineutrino. In formulaic terms, these two decays are:

$$\mu^- \rightarrow e^- + \bar{\nu}_e + \nu_\mu, \quad \mu^+ \rightarrow e^+ + \nu_e + \bar{\nu}_\mu\,.$$

The mean lifetime of the (positive) muon is 2.197 019 ± 0.000 021 μs[8] . The equality of the muon and anti-muon lifetimes has been established to better than one part in $10^4$.

The tree-level muon decay width is

$$\Gamma = \frac{G_F^2 m_\mu^5}{192\pi^3} I\left(\frac{m_e^2}{m_\mu^2}\right),$$

where $I(x) = 1 - 8x - 12x^2 \ln x + 8x^3 - x^4$; $G_F^2$ is the Fermi coupling constant.

The decay distributions of the electron in muon decays have been parameterised using the so-called Michel parameters. The values of these four parameters are predicted unambiguously in the Standard Model of particle physics, thus muon decays represent a good test of the space-time structure of the weak interaction. No deviation from the Standard Model predictions has yet been found.

Certain neutrino-less decay modes are kinematically allowed but forbidden in the Standard Model. Examples forbidden by lepton flavour conservation are

$$\mu^- \to e^- + \gamma \text{ and } \mu^- \to e^- + e^+ + e^-.$$

Observation of such decay modes would constitute clear evidence for physics beyond the Standard Model (BSM). Current experimental upper limits for the branching fractions of such decay modes are in the range $10^{-11}$ to $10^{-12}$.

## Muonic atoms

The muon was the first elementary particle discovered that does not appear in ordinary atoms. Negative muons can, however, form muonic atoms (also called mu-mesic atoms), by replacing an electron in ordinary atoms. Muonic *hydrogen* atoms are much smaller than typical hydrogen atoms because the much larger mass of the muon gives it a much smaller ground-state wavefunction than is observed for the electron. In multi-electron atoms, when only one of the electrons is replaced by a muon, the size of the atom continues to be determined by the other electrons, and the atomic size is nearly unchanged. However, in such cases the orbital of the muon continues to be smaller and far closer to the nucleus than the atomic orbitals of the electrons.

A positive muon, when stopped in ordinary matter, can also bind an electron and form an exotic atom known as muonium (Mu) atom, in which the muon acts as the nucleus. The positive muon, in this context, can be considered a pseudo-isotope of hydrogen with one ninth of the mass of the proton. Because the reduced mass of muonium, and hence its Bohr radius, is very close to that of hydrogen, this short-lived "atom" behaves chemically — to a first approximation — like hydrogen, deuterium and tritium.

## Use in measurement of the proton charge radius

The recent culmination of a twelve year experiment [9] investigating the proton's charge radius involved the use of muonic hydrogen. This form of hydrogen is composed of a muon orbiting a proton[10] . The Lamb shift in muonic hydrogen was measured by driving the muon from the from its 2s state up to an excited 2p state using a laser [11]. The frequency of the photon required to induce this transition was revealed to be 50 terahertz which, according to present theories of quantum electrodynamics, yields a value of 0.84184 ± 0.00067 femtometres for the charge radius of the proton.[12]

## Anomalous magnetic dipole moment

The anomalous magnetic dipole moment is the difference between the experimentally observed value of the magnetic dipole moment and the theoretical value predicted by the Dirac equation. The measurement and prediction of this value is very important in the precision tests of QED (quantum electrodynamics). The E821 experiment [13] at Brookhaven National Laboratory (BNL) studied the precession of muon and anti-muon in a constant external magnetic field as they circulated in a confining storage ring. The E821 Experiment reported the following average value (from the July 2007 review by Particle Data Group) [14]

$$a = \frac{g-2}{2} = 0.00116592080(54)(33)$$

where the first errors are statistical and the second systematic.

The difference between the g-factors of the muon and the electron is due to their difference in mass. Because of the muon's larger mass, contributions to the theoretical calculation of its anomalous magnetic dipole moment from Standard Model weak interactions and from contributions involving hadrons are important at the current level of precision, whereas these effects are not important for the electron. The muon's anomalous magnetic dipole moment is also sensitive to contributions from new physics beyond the Standard Model, such as supersymmetry. For this reason, the muon's anomalous magnetic moment is normally used as a probe for new physics beyond the Standard Model rather than as a test of QED (Phys.Lett. B649, 173 (2007) [15]).

## See also

- Mumesic atom
- Muonium
- Muon spin spectroscopy
- Muon-catalyzed fusion
- List of particles

## References

[1] K. Nakamura et al. (Particle Data Group), J. Phys. G 37, 075021 (2010), URL: http://pdg.lbl.gov
[2] Yukaya Hideka, On the Interaction of Elementary Particles 1, Proceedings of the Physico-Mathematical Society of Japan (3) 17, 48, pp 139-148 (1935). (Read 17 November 1934)
[3] New Evidence for the Existence of a Particle Intermediate Between the Proton and Electron", Phys. Rev. 52, 1003 (1937).
[4] David H. Frisch and James A. Smith, "Measurement of the Relativistic Time Dilation Using Muons", American Journal of Physics, 31, 342, 1963, cited by Michael Fowler, " Special Relativity: What Time is it? (http://galileoandeinstein.physics.virginia.edu/lectures/srelwhat.html)"
[5] S. Carroll (2004). Spacetime and Geometry: An Introduction to General Relativity. Addison Wesly. p. 204
[6] http://www.sciam.com/article.cfm?id=muons-for-peace
[7] Brookhaven National Laboratory (30 July 2002). "Physicists Announce Latest Muon g-2 Measurement" (http://www.bnl.gov/bnlweb/pubaf/pr/2002/bnlpr073002.htm). Press release. . Retrieved 2009-11-14.
[8] (http://arxiv.org/abs/0704.1981v1)
[9] https://muhy.web.psi.ch/wiki/
[10] TRIUMF Muonic Hydrogen collaboration. "A brief description of Muonic Hydrogen research". Retrieved 2010-11-7
[11] https://muhy.web.psi.ch/wiki/index.php/Main/Gallery
[12] Pohl, Randolf et al. "*The Size of the Proton*" *Nature* 466, 213-216 (8 July 2010)
[13] http://www.g-2.bnl.gov/
[14] http://pdg.lbl.gov/2007/reviews/g-2_s004219.pdf
[15] http://arxiv.org/abs/hep-ph/0611102

- S.H. Neddermeyer, C.D. Anderson (1937). "Note on the Nature of Cosmic-Ray Particles". *Physical Review* **51**: 884–886. doi:10.1103/PhysRev.51.884.
- J.C. Street, E.C. Stevenson (1937). "New Evidence for the Existence of a Particle of Mass Intermediate Between the Proton and Electron". *Physical Review* **52**: 1003–1004. doi:10.1103/PhysRev.52.1003.
- G. Feinberg, S. Weinberg (1961). "Law of Conservation of Muons.". *Physical Review Letters* **6**: 381–383. doi:10.1103/PhysRevLett.6.381.
- Serway & Faughn (1995). *College Physics* (4th ed.). Saunders. p. 841.
- M. Knecht (2003). "The Anomalous Magnetic Moments of the Electron and the Muon" (http://books.google.com/?id=me6ftonVM_EC&pg=PA265&lpg=PA265&dq="The+Anomalous+Magnetic+Moments+of+the+Electron+and+the+Muon"&q="The Anomalous Magnetic Moments of the Electron and the Muon"). In B. Duplantier, V. Rivasseau. *Poincaré Seminar 2002: Vacuum Energy − Renormalization*. Progress in Mathematical Physics. **30**. Birkhäuser. p. 265. ISBN 3-7643-0579-7.

- E. Derman (2004). *My Life As A Quant*. Wiley. pp. 58–62.


## External links

- Muon anomalous magnetic moment and supersymmetry (http://antwrp.gsfc.nasa.gov/apod/ap050828.html)
- g-2 (muon anomalous magnetic moment) experiment (http://www.g-2.bnl.gov/)
- muLan (Measurement of the Positive Muon Lifetime) experiment (http://www.npl.uiuc.edu/exp/mulan/)
- The Review of Particle Physics (http://pdg.lbl.gov/)
- The TRIUMF Weak Interaction Symmetry Test (http://twist.triumf.ca/)

# X-ray diffraction

**X-ray scattering techniques** are a family of non-destructive analytical techniques which reveal information about the crystallographic structure, chemical composition, and physical properties of materials and thin films. These techniques are based on observing the scattered intensity of an X-ray beam hitting a sample as a function of incident and scattered angle, polarization, and wavelength or energy.

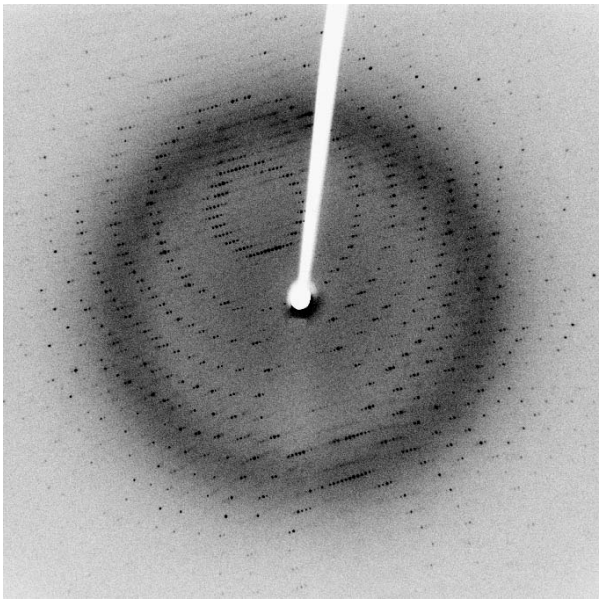

This is an X-ray diffraction pattern formed when X-rays are focused on a crystalline material, in this case a protein. Each dot, called a reflection, forms from the coherent interference of scattered X-rays passing through the crystal.

## X-ray diffraction techniques

X-ray diffraction yields the atomic structure of materials and is based on the elastic scattering of X-rays from the electron clouds of the individual atoms in the system. The most comprehensive description of scattering from crystals is given by the dynamical theory of diffraction.[1]

- Single-crystal X-ray diffraction is a technique used to solve the complete structure of crystalline materials, ranging from simple inorganic solids to complex macromolecules, such as proteins.
- Powder diffraction (XRD) is a technique used to characterise the crystallographic structure, crystallite size (grain size), and preferred orientation in polycrystalline or powdered solid samples. Powder diffraction is commonly used to identify unknown substances, by comparing diffraction data against a database maintained by the International Centre for Diffraction Data. It may also be used to characterize heterogeneous solid mixtures to determine relative abundance of crystalline compounds and, when coupled with lattice refinement techniques, such as Rietveld refinement, can provide structural information on unknown materials. Powder diffraction is also a common method for determining strains in crystalline materials. An effect of the finite crystallite sizes is seen as a broadening of the peaks in an X-ray diffraction as is explained by the Scherrer Equation.
- Thin film diffraction and grazing incidence X-ray diffraction may be used to characterize the crystallographic structure and preferred orientation of substrate-anchored thin films.
- High-resolution X-ray diffraction is used to characterize thickness, crystallographic structure, and strain in thin epitaxial films. It employs parallel-beam optics.

- X-ray pole figure analysis enables one to analyze and determine the distribution of crystalline orientations within a crystalline thin-film sample.
- X-ray rocking curve analysis is used to quantify grain size and mosaic spread in crystalline materials.

## Scattering techniques

### Elastic scattering

Materials that do not have long range order may also be studied by scattering methods that rely on elastic scattering of monochromatic X-rays.

- Small angle X-ray scattering (SAXS) probes structure in the nanometer to micrometer range by measuring scattering intensity at scattering angles $2\theta$ close to $0°$.[2]
- X-ray reflectivity is an analytical technique for determining thickness, roughness, and density of single layer and multilayer thin films.
- Wide angle X-ray scattering (WAXS), a technique concentrating on scattering angles $2\theta$ larger than $5°$.

### Inelastic scattering

When the energy and angle of the inelastically scattered X-rays are monitored scattering techniques can be used to probe the electronic band structure of materials.

- Compton scattering
- Resonant inelastic X-ray scattering (RIXS)
- X-ray Raman scattering
- X-ray diffraction pattern

## See also

- Structure determination
- Materials Science
- Metallurgy
- Mineralogy
- X-ray crystallography
- X-ray generator

## References

[1] Azároff, L. V.; R. Kaplow, N. Kato, R. J. Weiss, A. J. C. Wilson, R. A. Young (1974). *X-ray diffraction*. McGraw-Hill.

[2] Glatter, O.; O. Kratky (1982). *Small Angle X-ray Scattering* (http://physchem.kfunigraz.ac.at/sm/Software.htm). Academic Press. .

## External links

- International Union of Crystallography (http://www.iucr.ac.uk/)
- IUCr Crystallography Online (http://www.iucr.org/cww-top/crystal.index.html)
- The International Centre for Diffraction Data (ICDD) (http://www.icdd.com/)
- The British Crystallographic Association (http://crystallography.org.uk/)
- Introduction to X-ray Diffraction (http://www.mrl.ucsb.edu/mrl/centralfacilities/xray/xray-basics/index.html) at University of California, Santa Barbara

# Electron diffraction

**Electron diffraction** refers to the wave nature of electrons. However, from a technical or practical point of view, it may be regarded as a technique used to study matter by firing electrons at a sample and observing the resulting interference pattern. This phenomenon is commonly known as the wave-particle duality, which states that the *behavior* of a particle of matter (in this case the incident electron) can be described by a wave. For this reason, an electron can be regarded as a wave much like sound or water waves. This technique is similar to X-ray and neutron diffraction.

Electron diffraction is most frequently used in solid state physics and chemistry to study the crystal structure of solids. Experiments are usually performed in a transmission electron microscope (TEM), or a scanning electron microscope (SEM) as electron backscatter diffraction. In these instruments, electrons are accelerated by an electrostatic potential in order to gain the desired energy and determine their wavelength before they interact with the sample to be studied.

The periodic structure of a crystalline solid acts as a diffraction grating, scattering the electrons in a predictable manner. Working back from the observed diffraction pattern, it may be possible to deduce the structure of the crystal producing the diffraction pattern. However, the technique is limited by the phase problem.

Apart from the study of crystals i.e. electron crystallography, electron diffraction is also a useful technique to study the short range order of amorphous solids, and the geometry of gaseous molecules.

## History

The de Broglie hypothesis, formulated in 1926, predicts that particles should also behave as waves. De Broglie's formula was confirmed three years later for electrons (which have a rest-mass) with the observation of electron diffraction in two independent experiments. At the University of Aberdeen George Paget Thomson passed a beam of electrons through a thin metal film and observed the predicted interference patterns. At Bell Labs Clinton Joseph Davisson and Lester Halbert Germer guided their beam through a crystalline grid. Thomson and Davisson shared the Nobel Prize for Physics in 1937 for their work.

## Theory

### Electron interaction with matter

Unlike other types of radiation used in diffraction studies of materials, such as X-rays and neutrons, electrons are charged particles and interact with matter through the Coulomb forces. This means that the incident electrons feel the influence of both the positively charged atomic nuclei and the surrounding electrons. In comparison, X-rays interact with the spatial distribution of the valence electrons, while neutrons are scattered by the atomic nuclei through the strong nuclear forces. In addition, the magnetic moment of neutrons is non-zero, and they are therefore also scattered by magnetic fields. Because of these different forms of interaction, the three types of radiation are suitable for different studies.

## Intensity of diffracted beams

In the kinematical approximation for electron diffraction, the intensity of a diffracted beam is given by:

$$I_{\mathbf{g}} = |\psi_{\mathbf{g}}|^2 \propto |F_{\mathbf{g}}|^2$$

Here $\psi_{\mathbf{g}}$is the wavefunction of the diffracted beam and $F_{\mathbf{g}}$is the so called structure factor which is given by:

$$F_{\mathbf{g}} = \sum_i f_i e^{-2\pi i \mathbf{g}\cdot\mathbf{r}_i}$$

where $\mathbf{g}$is the scattering vector of the diffracted beam, $\mathbf{r}_i$ is the position of an atom $i$ in the unit cell, and $f_i$ is the scattering power of the atom, also called the atomic form factor. The sum is over all atoms in the unit cell.

The structure factor describes the way in which an incident beam of electrons is scattered by the atoms of a crystal unit cell, taking into account the different scattering power of the elements through the term $f_i$ . Since the atoms are spatially distributed in the unit cell, there will be a difference in phase when considering the scattered amplitude from two atoms. This phase shift is taken into account by the exponential term in the equation.

The atomic form factor, or scattering power, of an element depends on the type of radiation considered. Because electrons interact with matter though different processes than for example X-rays, the atomic form factors for the two cases are not the same.

## Wavelength of electrons

The wavelength of an electron is given by the de Broglie equation

$$\lambda = \frac{h}{p}$$

Here $h$ is Planck's constant and $p$the relativistic momentum of the electron. $\lambda$ is called the de Broglie wavelength. The electrons are accelerated in an electric potential $U$ to the desired velocity:

$$v = \sqrt{\frac{2eU}{m_0}}$$

$m_0$is the mass of the electron, and $e$ is the elementary charge.The electron wavelength is then given by:

$$\lambda = \frac{h}{p} = \frac{h}{m_0 v} = \frac{h}{\sqrt{2m_0 eU}}$$

However, in an electron microscope, the accelerating potential is usually several thousand volts causing the electron to travel at an appreciable fraction of the speed of light. An SEM may typically operate at an accelerating potential of 10,000 volts (10 kV) giving an electron velocity approximately 20% of the speed of light, while a typical TEM can operate at 200 kV raising the electron velocity to 70% the speed of light. We therefore need to take relativistic effects into account. It can be shown that the electron wavelength is then modified according to:

$$\lambda = \frac{h}{\sqrt{2m_0 eU}} \frac{1}{\sqrt{1 + \frac{eU}{2m_0 c^2}}}$$

$c$ is the speed of light. We recognize the first term in this final expression as the non-relativistic expression derived above, while the last term is a relativistic correction factor. The wavelength of the electrons in a 10 kV SEM is then 12.3 x $10^{-12}$ m (12.3 pm) while in a 200 kV TEM the wavelength is 2.5 pm. In comparison the wavelength of X-rays usually used in X-ray diffraction is in the order of 100 pm (Cu kα: λ=154 pm).

# Electron diffraction in a TEM

Electron diffraction of solids is usually performed in a Transmission Electron Microscope (TEM) where the electrons pass through a thin film of the material to be studied. The resulting diffraction pattern is then observed on a fluorescent screen, recorded on photographic film, on imaging plates or using a CCD camera.

## Benefits

As mentioned above, the wavelength of electron accelerated in a TEM is much smaller than that of the radiation usually used for X-ray diffraction experiments. A consequence of this is that the radius of the Ewald sphere is much larger in electron diffraction experiments than in X-ray diffraction. This allows the diffraction experiment to reveal more of the two dimensional distribution of reciprocal lattice points.

Furthermore, electron lenses allows the geometry of the diffraction experiment to be varied. The conceptually simplest geometry is that of a parallel beam of electrons incident on the specimen. However, by converging the electrons in a cone onto the specimen, one can in effect perform a diffraction experiment over several incident angles simultaneously. This technique is called Convergent Beam Electron Diffraction (CBED) and can reveal the full three dimensional symmetry of the crystal.

In a TEM, a single crystal grain or particle may be selected for the diffraction experiments. This means that the diffraction experiments can be performed on single crystals of nanometer size, whereas other diffraction techniques would be limited to studying the diffraction from a multicrystalline or powder sample. Furthermore, electron diffraction in TEM can be combined with direct imaging of the sample, including high resolution imaging of the crystal lattice, and a range of other techniques. These include solving and refining crystal structures by electron crystallography, chemical analysis of the sample composition through energy-dispersive X-ray spectroscopy, investigations of electronic structure and bonding through electron energy loss spectroscopy, and studies of the mean inner potential through electron holography.

## Practical aspects

Figure 1 to the right is a simple sketch of the path of a parallel beam of electrons in a TEM from just above the sample and down the column to the fluorescent screen. As the electrons pass through the sample, they are scattered by the electrostatic potential set up by the constituent elements. After the electrons have left the sample they pass through the electromagnetic objective lens. This lens acts to collect all electrons scattered from one point of the sample in one point on the fluorescent screen, causing an image of the sample to be formed. We note that at the dashed line in the figure, electrons scattered in the same direction by the sample are collected into a single point. This is the back focal plane of the microscope, and is where the diffraction pattern is formed. By manipulating the magnetic lenses of the microscope, the diffraction pattern may be observed by projecting it onto the screen instead of the image. An example of what a diffraction pattern obtained in this way may look like is shown in figure 2.

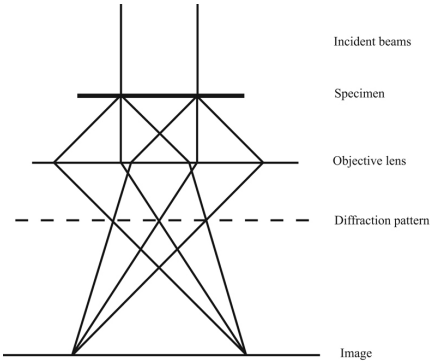

1: Sketch of the electron beam-path in a TEM.

If the sample is tilted with respect to the incident electron beam, one can obtain diffraction patterns from several crystal orientations. In this way, the reciprocal lattice of the crystal can be mapped in three

dimensions. By studying the systematic absence of diffraction spots the Bravais lattice and any screw axes and glide planes present in the crystal structure may be determined.

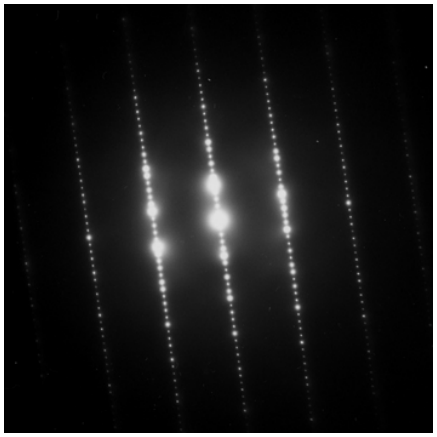

2: Typical electron diffraction pattern obtained in a TEM with a parallel electron beam

## Limitations

Electron diffraction in TEM is subject to several important limitations. First, the sample to be studied must be electron transparent, meaning the sample thickness must be of the order of 100 nm or less. Careful and time consuming sample preparation may therefore be needed. Furthermore, many samples are vulnerable to radiation damage caused by the incident electrons.

The study of magnetic materials is complicated by the fact that electrons are deflected in magnetic fields by the Lorentz force. Although this phenomenon may be exploited to study the magnetic domains of materials by *Lorentz force microscopy*, it may make crystal structure determination virtually impossible.

Furthermore, electron diffraction is often regarded as a *qualitative* technique suitable for symmetry determination, but too inaccurate for determination of lattice parameters and atomic positions. But there are also several examples where unknown crystal structures (both inorganic, organic and biological) have been solved by electron crystallography. Lattice parameters of high accuracy can in fact be obtained from electron diffraction, relative errors less than 0.1% have been demonstrated. However, the right experimental conditions may be difficult to obtain, and these procedures are often viewed as too time consuming and the data too difficult to interpret. X-ray or neutron diffraction are therefore often the preferred methods for determining lattice parameters and atomic positions.

However, the main limitation of electron diffraction in TEM remains the comparatively high level of user interaction needed. Whereas both the execution of powder X-ray (and neutron) diffraction experiments and the data analysis are highly automated and routinely performed, electron diffraction requires a much higher level of user input.

# See also

- Electron microscope
- Transmission electron microscopy
- Selected area diffraction
- Gas electron diffraction
- RHEED
- Low-energy electron diffraction
- Stereographic projection
- Kikuchi line
- Electron backscatter diffraction

## References


- Leonid A. Bendersky and Frank W. Gayle, "Electron Diffraction Using Transmission Electron Microscopy [1]", *Journal of Research of the National Institute of Standards and Technology*, **106** (2001) pp. 997–1012.
- Gareth Thomas and Michael J. Goringe (1979). *Transmission Electron Microscopy of Materials*. John Wiley. ISBN 0-471-12244-0.


## External links

- Remote experiment on electron diffraction [2] (choose English and then "Labs")
- Jmol-mediated image/diffraction analysis of an unknown [3]

## References


[1] http://nvl.nist.gov/pub/nistpubs/jres/106/6/j66ben.pdf
[2] http://rcl.physik.uni-kl.de
[3] http://newton.umsl.edu/run//nano/unknown173.html


# Neutron diffraction

**Neutron diffraction** is a method by which neutrons are used to determine the atomic and/or magnetic structure of a material. It can be applied to study the structure of crystalline solids (see crystallography), gasses, liquids or amorphous materials. Neutron diffraction is a form of elastic scattering where the neutrons scattered from the sample have comparable energy to the incident neutrons. The technique is similar to X-ray diffraction but due to the different scattering properties of neutrons versus x-rays complementary information can be obtained. A sample to be examined is placed in a beam of thermal or cold neutrons and the diffraction pattern intensity from the sample provides information of the structure of the material.

## Description

### Principle

Neutrons are particles found in the atomic nucleus of almost all atoms, but they are bound. The technique requires free neutrons and these normally do not occur in nature, because they have limited life-time. In a nuclear reactor, however, neutrons can be set free through nuclei decay particularly when fission occurs. All quantum particles can exhibit wave phenomena we typically associate with light or sound. Diffraction is one of these phenomena; it occurs when waves encounter obstacles whose size is comparable with the wavelength. If the wavelength of a quantum particle is short enough, atoms or their nuclei can serve as diffraction obstacles. When a beam of neutrons emanating from a reactor is slowed down and selected properly by their speed, their wavelength lies near one Ångström (0.1 nanometer), the typical separation between atoms in a solid material. Such a beam can then be used to perform a diffraction experiment. Impinging on a crystalline sample it will scatter under a limited number of well-defined angles according to the same Bragg's law that describes X-ray diffraction.

### Instrumental requirements

A neutron diffraction measurement requires a neutron source (e.g. a nuclear reactor or spallation source), a sample (the material to be studied), and a detector. Samples sizes are large compared to those used in X-ray diffraction. The technique is therefore mostly performed as powder diffraction. At a research reactor other components such as crystal monochromators or filters may be needed to select the desired neutron wavelength. Some parts of the setup may also be movable. At a spallation source the time of flight technique is used to sort the energies of the incident

neutrons (Higher energy neutrons are faster), so no monochromator is needed, but rather a series of aperture elements synchronized to filter neutron pulses with the desired wavelength.

### Nuclear scattering

Neutrons interact with matter differently than x-rays. X-rays interact primarily with the electron cloud surrounding each atom. The contribution to the diffracted x-ray intensity is therefore larger for atoms with a large atomic number (Z) than it is for atoms with a small Z. On the other hand, neutrons interact directly with the *nucleus* of the atom, and the contribution to the diffracted intensity is different for each isotope; for example, regular hydrogen and deuterium contribute differently. It is also often the case that light (low Z) atoms contribute strongly to the diffracted intensity even in the presence of large Z atoms. The scattering length varies from isotope to isotope rather than linearly with the atomic number. An element like Vanadium is a strong scatterer of X-rays, but its nuclei hardly scatter neutrons, which is why it often used as a container material. Non-magnetic neutron diffraction is directly sensitive to the positions of the nuclei of the atoms.

A major difference with X-rays is that the scattering is mostly due to the tiny nuclei of the atoms. That means that there is no need for an atomic form factor to describe the shape of the electron cloud of the atom and the scattering power of an atom does not fall off with the scattering angle as it does for X-rays. Diffractograms therefore can show strong well defined diffraction peaks even at high angles, particularly if the experiment is done at low temperatures. Many neutron sources are equipped with liquid helium cooling systems that allow to collect data at temperatures down to 4.2 K. The superb high angle (i.e. high *resolution*) information means that the data can give very precise values for the atomic positions in the structure. On the other hand, Fourier maps (and to a lesser extent difference Fourier maps) derived from neutron data suffer from series termination errors, sometimes so much that the results are meaningless.

### Magnetic scattering

Although neutrons are uncharged, they carry a spin, and therefore interact with magnetic moments, including those arising from the electron cloud around an atom. Neutron diffraction can therefore reveal the microscopic magnetic structure of a material[1] .

Magnetic scattering does require an atomic form factor as it is caused by the much larger electron cloud around the tiny nucleus. The intensity of the magnetic contribution to the diffraction peaks will therefore dwindle towards higher angles.

## History

The first neutron diffraction experiments were carried out in 1945 by Ernest O. Wollan using the Graphite Reactor at Oak Ridge. He was joined shortly thereafter (June 1946)[2] by Clifford Shull, and together they established the basic principles of the technique, and applied it successfully to many different materials, addressing problems like the structure of ice and the microscopic arrangements of magnetic moments in materials. For this achievement Shull was awarded one half of the 1994 Nobel Prize in Physics. Wollan had died in the 1990s. (The other half of the 1994 Nobel Prize for Physics went to Bert Brockhouse for development of the inelastic scattering technique at the Chalk River facility of AECL. This also involved the invention of the triple axis spectrometer). Brockhouse and Shull jointly take the somewhat dubious distinction of the longest gap between the work being done (1946) and the Nobel Prize being awarded (1994).

## Uses

Neutron diffraction is closely related to X-ray powder diffraction[3] . In fact the single crystal version of the technique is less commonly used because currently available neutron sources require relatively large samples and large single crystals are hard or impossible to come by for most materials. Future developments, however, may well change this picture. Because the data is typically a 1D powder diffractogram they are usually processed using Rietveld refinement. In fact the latter found its origin in neutron diffraction (at Petten in the Netherlands) and was later extended for use in X-ray diffraction.

One practical application of elastic neutron scattering/diffraction is that the lattice constant of metals and other crystalline materials can be very accurately measured. Together with an accurately aligned micropositioner a map of the lattice constant through the metal can be derived. This can easily be converted to the stress field experienced by the material. This has been used to analyse stresses in aerospace and automotive components to give just two examples. This technique has led to the development of dedicated stress diffractometers, such as the ENGIN-X instrument at the ISIS neutron source.

### Hydrogen, null-scattering and contrast variation

Neutron diffraction can be used to establish the structure of low atomic number materials like proteins and surfactants much more easily with lower flux than at a synchrotron radiation source. This is because some low atomic number materials have a higher cross section for neutron interaction than higher atomic weight materials.

One major advantage of neutron diffraction over X-ray diffraction is that the latter is rather insensitive to the presence of hydrogen (H) in a structure, whereas the nuclei $^{1}$H and $^{2}$H (i.e. Deuterium, D) are strong scatterers for neutrons. This means that the position of hydrogen in a crystal structure and its thermal motions can be determined far more precisely with neutrons. In addition the neutron scattering lengths $b_{H}$ = -3.7406(11) fm [4] and $b_{D}$ = 6.671(4) fm [4] , for H and D respectively, have opposite sign allowing for contrast variation. In fact there is a particular isotope ratio for which the contribution of the element would cancel, this is called null-scattering. In practice however it is not desirable to work with the relatively high concentration of H in such a sample. The scattering intensity by H-nuclei has a large ineleastic component and this creates a large continuous background that is more or less independent of scattering angle. The elastic pattern typically consists of sharp Bragg reflections if the sample is crystalline. They tend to drown in the inelastic background. This is even more serious when the technique is used for the study of liquid structure. Nevertheless, by preparing samples with different isotope ratios it is possible to vary the scattering contrast enough to highlight one element in an otherwise complicated structure. The variation of other elements is possible but usually rather expensive. Hydrogen is inexpensive and particularly interesting because it plays an exceptionally large role in biochemical structures and is difficult to study structurally in other ways.

## Further reading


- Lovesey, S. W. (1984). *Theory of Neutron Scattering from Condensed Matter; Volume 1: Neutron Scattering*. Oxford: Clarendon Press. ISBN 0-19-852015-8.
- Lovesey, S. W. (1984). *Theory of Neutron Scattering from Condensed Matter; Volume 2: Condensed Matter*. Oxford: Clarendon Press. ISBN 0-19-852017-4.
- Squires, G.L. (1996). *Introduction to the Theory of Thermal Neutron Scattering* (2nd ed.). Mineola, New York: Dover Publications Inc. ISBN 0-486-69447-X.

**Applied Computational Powder Diffraction Data Analysis**

- Young, R.A., ed (1993). *The Rietveld Method*. Oxford: Oxford University Press & International Union of Crystallography. ISBN 0-19-855577-6.

## See also

- Bragg diffraction
- Crystallography
- Crystallographic database
- Diffraction
- Electron crystallography
- Electron diffraction
- Neutron crystallography
- Neutron Diffraction at OPAL
- X-ray crystallography
- X-ray diffraction
- X-ray scattering techniques

## References

[1] Neutron diffraction of magnetic materials / Yu. A. Izyumov, V.E. Naish, and R.P. Ozerov ; translated from Russian by Joachim Büchner. New York : Consultants Bureau, c1991.ISBN 0-306-11030-X

[2] Clifford Shull: Early development of neutron scattering. Rev. Mod. Phys. 67 (1995) 753–757

[3] *Neutron powder diffraction* by Richard M. Ibberson and William I.F. David, Chapter 5 of Structure determination form powder diffraction data IUCr monographphs on crystallography, Oxford scientific publications 2002, ISBN 0-19-850091-2

[4] Sears, V. F. (1992), "Neutron scattering lengths and cross sections", *Neutron News* **3**: 26–37

## External links

- National Institute of Standards and Technology Center for Neutron Research (http://www.ncnr.nist.gov/)

# Neutron scattering

**Neutron scattering** encompasses all scientific techniques whereby the deflection of neutron radiation is used as a scientific probe. Neutrons readily interact with atomic nuclei and magnetic fields from unpaired electrons, making a useful probe of both structure and magnetic order. Neutron Scattering falls into two basic categories, elastic and inelastic. Elastic scattering is when a neutron interacts with a nucleus or electronic magnetic field but does not leave it in an excited state, meaning the emitted neutron has the same energy as the injected neutron. Scattering processes that involve an energetic excitation or relaxation by the neutron are inelastic: the injected neutron's energy is used or increased to create an excitation or by absorbing the excess energy from a relaxation, and consequently the emitted neutron's energy is reduced or increased respectively.

For several good reasons, moderated neutrons provide an ideal tool for the study of almost all forms of condensed matter. Firstly, they are readily produced at a nuclear research reactor or a spallation source. Normally in such processes neutrons are however produced with much higher energies than are needed. Therefore moderators are generally used which slow the neutrons down and therefore produce wavelengths that are comparable to the atomic spacing in solids and liquids, and kinetic energies that are comparable to those of dynamic processes in materials. Moderators can be made from aluminium and filled with liquid hydrogen (for very long wavelength neutrons) or liquid methane (for shorter wavelength neutrons). Fluxes of $10^7$/s - $10^8$/s are not atypical in most neutron sources from any given moderator.

The neutrons cause pronounced interference and energy transfer effects in scattering experiments. Unlike an x-ray photon with a similar wavelength, which interacts with the electron cloud surrounding the nucleus, neutrons interact with the nucleus itself. Because the neutron is an electrically neutral particle, it is deeply penetrating, and is therefore more able to probe the bulk material. Consequently, it enables the use of a wide range of sample environments that are difficult to use with synchrotron x-ray sources. It also has the advantage that the cross sections for interaction do not increase with atomic number as they do with radiation from a synchrotron x-ray source. Thus neutrons can be used to analyse materials with low atomic numbers like proteins and surfactants. This can be done at synchrotron sources but very high intensities are needed which may cause the structures to change. Moreover, the nucleus provides a very short range, isotropic potential varying randomly from isotope to isotope, making it possible to tune the nuclear scattering contrast to suit the experiment.

The neutron has an additional advantage over the x-ray photon in the study of condensed matter. It readily interacts with internal magnetic fields in the sample. In fact, the strength of the magnetic scattering signal is often very similar to that of the nuclear scattering signal in many materials, which allows the simultaneous exploration of both nuclear and magnetic structure. Because the neutron scattering amplitude can be measured in absolute units, both the structural and magnetic properties as measured by neutrons can be compared quantitatively with the results of other characterisation techniques.

## See also

- Neutron diffraction
  - Small angle neutron scattering
  - Neutron Reflectometry
- Inelastic neutron scattering
  - neutron triple-axis spectrometry
  - neutron time-of-flight scattering
  - neutron backscattering
  - neutron spin echo
  - neutron resonance spin echo

- Neutron scattering facilities

## Applications

Neutron scattering has been used to study various vibration modes, [1] including low-frequency collective motion in proteins and DNA, [2] [3] [4] [5] [6] as reviewed by Dr. P. Martel in 1992.[1]

## References

[1] Martel, P. (1992) Biophysical aspects of neutron scattering from vibrational modes of proteins. Prog Biophys Mol Biol, 57, 129-179.
[2] Chou, K.C. (1983) Low-frequency vibrations of helical structures in protein molecules. Biochemical Journal, 209, 573-580.
[3] Chou, K.C. (1985) Low-frequency motions in protein molecules: beta-sheet and beta-barrel. Biophysical Journal, 48, 289-297.
[4] Chou, K.C., Maggiora, G.M. and Mao, B. (1989) Quasi-continuum models of twist-like and accordion-like low-frequency motions in DNA. Biophysical Journal, 56, 295-305.
[5] Kuo-Chen Chou (1988) Review: Low-frequency collective motion in biomacromolecules and its biological functions. Biophysical Chemistry, 30, 3-48.
[6] Chou, K.C. (1989) Low-frequency resonance and cooperativity of hemoglobin. Trends in Biochemical Sciences, 14, 212.

## External links

- Neutron Scattering - A primer (http://knocknick.files.wordpress.com/2008/04/neutrons-a-primer-by-rogen-pynn.pdf) ( LANL-hosted black and white version (http://library.lanl.gov/cgi-bin/getfile?00326651.pdf)) - An introductory article written by Roger Pynn (Los Alamos National Laboratory)
- Podcast Interview with two ILL scientists about neutron science/scattering at the ILL (http://omegataupodcast.net/2010/03/28-neutron-science-at-the-ill/)

# Inelastic neutron scattering

**Inelastic neutron scattering** is an experimental technique commonly used in condensed matter research to study atomic and molecular motion as well as magnetic and crystal field excitations. It distinguishes itself from other neutron scattering techniques by resolving the change in kinetic energy that occurs when the collision between neutrons and the sample is an inelastic one. Results are generally communicated as the dynamic structure factor (also called inelastic scattering law) $S(q,\omega)$, sometimes also as the dynamic susceptibility $\chi(q,\omega)$ where the scattering vector $q$ is the difference between incoming and outgoing wave vector, and $\hbar\omega$ is the energy change experienced by the sample (negative that of the scattered neutron). When results are plotted as function of $\omega$, they can often be interpreted in the same way as spectra obtained by conventional spectroscopic techniques; insofar as inelastic neutron scattering can be seen as a special spectroscopy.

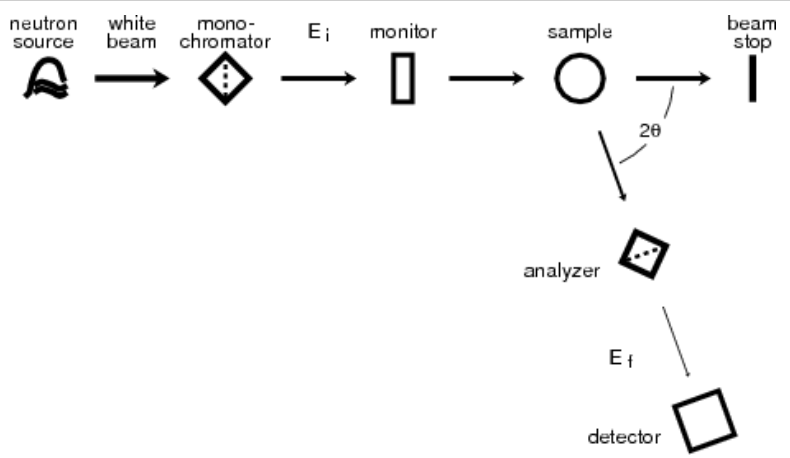

Generic layout of an inelastic neutron scattering experiment

Inelastic scattering experiments normally require a monochromatization of the incident or outgoing beam and an energy analysis of the scattered neutrons. This can be done either through time-of-flight techniques (neutron time-of-flight scattering) or through Bragg reflection from single crystals (neutron triple-axis spectroscopy, neutron backscattering). Monochromatization is not needed in echo techniques (neutron spin echo, neutron resonance spin echo), which use the quantum mechanical phase of the neutrons in addition to their amplitudes.

## Types of Inelastic Neutron Scattering

- neutron triple-axis scattering
- neutron time-of-flight scattering
- neutron backscattering
- neutron spin echo

## Further Information

Literature:

- G L Squires *Introduction to the Theory of Thermal Neutron Scattering* Dover 1997 (reprint?)

## External links

- Joachim Wuttke: Introduction to Inelastic Crystal Spectrometers [1]

## References

[1] http://iffwww.iff.kfa-juelich.de/~wuttke/doku/lib/exe/fetch.php?id=spheres%3Aprinciple&cache=cache&media=spheres:np9v05.pdf

# Ionization cooling

## Physical Principle

**Ionization cooling** is a process by which the beam emittance of a beam of particles may be reduced [1] . In ionization cooling, particles are passed through some material. The momentum of the particles is reduced as they ionize atomic electrons in the material. Thus the normalised beam emittance is reduced. By re-accelerating the beam, for example in an RF cavity, the longitudinal momentum may be restored without replacing transverse momentum. Thus overall the angular spread and hence the geometric emittance in the beam will be reduced.

Ionization cooling can be spoiled by stochastic physical processes. Multiple Coulomb scattering in muons as well as nuclear scattering in protons and ions can reduce the cooling or even lead to net heating transverse to the direction of beam motion. In addition, energy straggling can cause heating parallel to the direction of beam motion.

## Muon Cooling

The primary use of ionization cooling is envisaged to be for cooling of muon beams. This is because ionization cooling is the only technique that works on the timescale of the muon lifetime. Ionization cooling channels have been designed for use in a Neutrino Factory and a Muon Collider. Muon ionization cooling is expected to be demonstrated for the first time by the Proof of Principle International Muon Ionization Cooling Experiment. Other PoP muon ionization cooling experiments have been devised.

## Other Particles

Ionization cooling has also been proposed for use in low energy ion beams and proton beams.

## References

[1] G.I. Budker, in: Proceedings of 15th International Conference on High Energy Physics, Kiev, 1970 A.N. Skrinsky, Intersecting storage rings at Novosibirsk, in: Proceedings of Morges Seminar, 1971 Report CERN/D.PH II/YGC/mng

# Deep inelastic scattering

**Deep inelastic scattering** is the name given to a process used to probe the insides of hadrons (particularly the baryons, such as protons and neutrons), using electrons, muons and neutrinos. It provided the first convincing evidence of the reality of quarks, which up until that point had been considered by many to be a purely mathematical phenomenon. It is a relatively new process, first attempted in the 1960s and 1970s. It is conceptually similar to Rutherford Scattering, but with important differences. The reason why this type of scattering is described as "deep" and "inelastic" is discussed at the Oxford University page.[1]

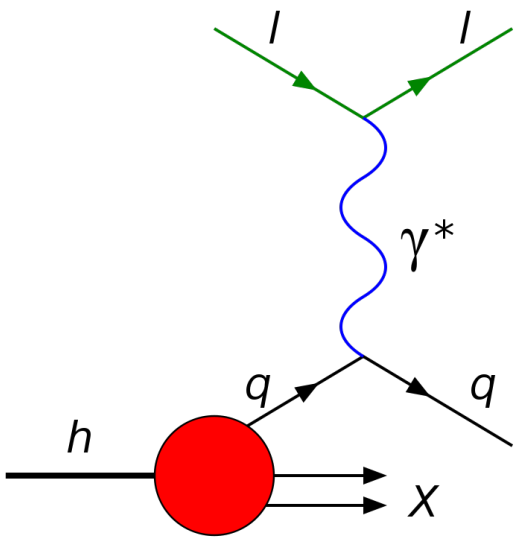


Deep inelastic scattering of a lepton on a hadron, at leading order in perturbative expansion.

## Quarks

The Standard Model of physics, particularly given the work of Murray Gell-Mann in the 1960s, had been successful in uniting much of the previously disparate concepts in particle physics into one, relatively straightforward, scheme. In essence, there were three types of particles.

- The leptons, which were light (as in not particularly massive) particles such as electrons, neutrinos and their antiparticles. They have integer charge
- The bosons, which were particles that exchange forces. These ranged from the massless, easy-to-detect photon (the carrier of the electro-magnetic force) to the exotic (though still massless) gluons that carry the strong nuclear force
- The quarks, which were massive particles that carried fractional charges. They are the "building blocks" of the hadrons. They are also the only particles to be affected by the strong interaction

The leptons had been detected since 1897, when J. J. Thomson had shown that electric current is a flow of electrons. Some bosons were being routinely detected, although the $W^+$, $W^-$ and $Z^0$ particles of the electroweak force were only categorically seen in the early 1980s, and gluons were only firmly pinned down at DESY in Hamburg at about the same time. Quarks, however, were still elusive.

## The experiments

Drawing on Rutherford's groundbreaking experiments in the early years of the Twentieth century, ideas for detecting quarks were formulated. Rutherford had proven that atoms had a small, massive, charged nucleus at their centre by firing alpha particles at atoms in gold. Most had gone through with little or no deviation, but a few were deflected through large angles or came right back. This suggested that atoms had internal structure, and a lot of empty space.

In order to enter baryons (where quarks were theoretically to be found), a small, penetrating (ie easily accelerated; in reality this meant charged) and easily produced particle needed to be found. Electrons were considered ideal for the role, and in a series of remarkable technological and engineering leaps, electrons were fired at protons and neutrons in atomic nuclei. As an added bonus, the electrostatic attraction of the positively charged nucleus and the negatively charged electron increased the speed. Later experiments were conducted with muons, but the same principles apply.

The collision absorbs some kinetic energy, and as such it is inelastic (this compares to Rutherford scattering which is elastic, with no loss of kinetic energy, taking into account recoils of the nuclei). The electron emerges from the nucleus, and its trajectory and velocity can be detected.

Analysis of the results led to the following conclusions:

- The hadrons do have internal structure
- In baryons, there are three points of deflection (i.e. baryons consist of three quarks)
- In mesons, there are two points of deflection (i.e. mesons consist of a quark and an anti-quark. The reason they do not consist of two quarks is to do with their colour; see the quark article for more explanation)
- Quarks appear to be point charges, as electrons appear to be, with the fractional charges suggested by the Standard Model

The experiments were important because, not only did they confirm the physical reality of quarks but also proved again that the Standard Model was the correct avenue of research for particle physicists to pursue.

## References

[1] Deep inelastic scattering (http://www.physics.ox.ac.uk/documents/PUS/dis/DIS.htm). *Oxford University Physics Department*, 2003.

# Timeline of microphysics

**Timeline of atomic and subatomic physics**

## Early beginnings

- 585 BC Buddha states that there were indivisible particles of mind and matter which vibrated 3 trillion times in the blink of an eye which he calls "kalapas"
- 440 BC Democritus speculates about fundamental indivisible particles—calls them "atoms"

## The beginning of chemistry

- 1766 Henry Cavendish discovers and studies hydrogen
- 1778 Carl Scheele and Antoine Lavoisier discover that air is composed mostly of nitrogen and oxygen
- 1781 Joseph Priestley creates water by igniting hydrogen and oxygen
- 1800 William Nicholson and Anthony Carlisle use electrolysis to separate water into hydrogen and oxygen
- 1803 John Dalton introduces atomic ideas into chemistry and states that matter is composed of atoms of different weights
- 1805 Thomas Young conducts Double-slit experiment (approximate time)
- 1811 Amedeo Avogadro claims that equal volumes of gases should contain equal numbers of molecules
- 1832 Michael Faraday states his laws of electrolysis
- 1871 Dmitri Ivanovich Mendeleev systematically examines the periodic table and predicts the existence of gallium, scandium, and germanium
- 1873 Johannes van der Waals introduces the idea of weak attractive forces between molecules
- 1885 Johann Balmer finds a mathematical expression for observed hydrogen line wavelengths
- 1887 Heinrich Hertz discovers the photoelectric effect
- 1894 Lord Rayleigh and William Ramsay discover argon by spectroscopically analyzing the gas left over after nitrogen and oxygen are removed from air
- 1895 William Ramsay discovers terrestrial helium by spectroscopically analyzing gas produced by decaying uranium

- 1896 Antoine Becquerel discovers the radioactivity of uranium
- 1896 Pieter Zeeman studies the splitting of sodium D lines when sodium is held in a flame between strong magnetic poles
- 1897 J.J. Thomson discovers the electron
- 1898 William Ramsay and Morris Travers discover neon, and negatively charged beta particles

## The age of quantum mechanics

- 1900 Paul Villard discovers gamma-rays while studying uranium decay
- 1900 Johannes Rydberg refines the expression for observed hydrogen line wavelengths
- 1900 Max Planck states his quantum hypothesis and blackbody radiation law
- 1902 Philipp Lenard observes that maximum photoelectron energies are independent of illuminating intensity but depend on frequency
- 1902 Theodor Svedberg suggests that fluctuations in molecular bombardment cause the Brownian motion
- 1905 Albert Einstein explains the photoelectric effect
- 1906 Charles Barkla discovers that each element has a characteristic X-ray and that the degree of penetration of these X-rays is related to the atomic weight of the element
- 1909 Hans Geiger and Ernest Marsden discover large angle deflections of alpha particles by thin metal foils
- 1909 Ernest Rutherford and Thomas Royds demonstrate that alpha particles are doubly ionized helium atoms
- 1911 Ernest Rutherford explains the Geiger-Marsden experiment by invoking a nuclear atom model and derives the Rutherford cross section
- 1911 Jean Perrin proves the existence of atoms and molecules
- 1912 Max von Laue suggests using crystal lattices to diffract X-rays
- 1912 Walter Friedrich and Paul Knipping diffract X-rays in zinc blende
- 1913 William Henry Bragg and William Lawrence Bragg work out the Bragg condition for strong X-ray reflection
- 1913 Henry Moseley shows that nuclear charge is the real basis for numbering the elements
- 1913 Niels Bohr presents his quantum model of the atom
- 1913 Robert Millikan measures the fundamental unit of electric charge
- 1913 Johannes Stark demonstrates that strong electric fields will split the Balmer spectral line series of hydrogen
- 1914 James Franck and Gustav Hertz observe atomic excitation
- 1914 Ernest Rutherford suggests that the positively charged atomic nucleus contains protons
- 1915 Arnold Sommerfeld develops a modified Bohr atomic model with elliptic orbits to explain relativistic fine structure
- 1916 Gilbert N. Lewis and Irving Langmuir formulate an electron shell model of chemical bonding
- 1917 Albert Einstein introduces the idea of stimulated radiation emission
- 1921 Alfred Landé introduces the Landé g-factor
- 1922 Arthur Compton studies X-ray photon scattering by electrons
- 1922 Otto Stern and Walther Gerlach show "space quantization"
- 1923 Louis de Broglie suggests that electrons may have wavelike properties
- 1923 Lise Meitner discovers the Auger process
- 1924 John Lennard-Jones proposes a semiempirical interatomic force law
- 1924 Satyendra Bose and Albert Einstein introduce Bose-Einstein statistics
- 1925 Wolfgang Pauli states the quantum exclusion principle
- 1925 George Uhlenbeck and Samuel Goudsmit postulate electron spin
- 1925 Pierre Auger discovers the Auger process (2 years after Lise Meitner)
- 1925 Werner Heisenberg, Max Born, and Pascual Jordan formulate quantum matrix mechanics

- 1926 Erwin Schrödinger states his nonrelativistic quantum wave equation and formulates quantum wave mechanics
- 1926 Erwin Schrödinger proves that the wave and matrix formulations of quantum theory are mathematically equivalent
- 1926 Oskar Klein and Walter Gordon state their relativistic quantum wave equation, now the Klein-Gordon equation
- 1926 Enrico Fermi discovers the spin-statistics connection
- 1926 Paul Dirac introduces Fermi-Dirac statistics
- 1927 Clinton Davisson, Lester Germer, and George Paget Thomson confirm the wavelike nature of electrons
- 1927 Werner Heisenberg states the quantum uncertainty principle
- 1927 Max Born interprets the probabilistic nature of wavefunctions
- 1927 Walter Heitler and Fritz London introduce the concepts of valence bond theory and apply it to the hydrogen molecule.
- 1927 Thomas and Fermi develop the Thomas-Fermi model
- 1927 Max Born and Robert Oppenheimer introduce the Born-Oppenheimer approximation
- 1928 Chandrasekhara Raman studies optical photon scattering by electrons
- 1928 Paul Dirac states his relativistic electron quantum wave equation
- 1928 Charles G. Darwin and Walter Gordon solve the Dirac equation for a Coulomb potential
- 1928 Friedrich Hund and Robert S. Mulliken introduce the concept of molecular orbital
- 1929 Oskar Klein discovers the Klein paradox
- 1929 Oskar Klein and Yoshio Nishina derive the Klein-Nishina cross section for high energy photon scattering by electrons
- 1929 Nevill Mott derives the Mott cross section for the Coulomb scattering of relativistic electrons
- 1930 Paul Dirac introduces electron hole theory
- 1930 Erwin Schrödinger predicts the zitterbewegung motion
- 1930 Fritz London explains van der Waals forces as due to the interacting fluctuating dipole moments between molecules
- 1931 John Lennard-Jones proposes the Lennard-Jones interatomic potential
- 1931 Irène Joliot-Curie and Frédéric Joliot observe but misinterpret neutron scattering in paraffin
- 1931 Wolfgang Pauli puts forth the neutrino hypothesis to explain the apparent violation of energy conservation in beta decay
- 1931 Linus Pauling discovers resonance bonding and uses it to explain the high stability of symmetric planar molecules
- 1931 Paul Dirac shows that charge quantization can be explained if magnetic monopoles exist
- 1931 Harold Urey discovers deuterium using evaporation concentration techniques and spectroscopy
- 1932 John Cockcroft and Ernest Walton split lithium and boron nuclei using proton bombardment
- 1932 James Chadwick discovers the neutron
- 1932 Werner Heisenberg presents the proton-neutron model of the nucleus and uses it to explain isotopes
- 1932 Carl D. Anderson discovers the positron
- 1933 Ernst Stueckelberg (1932), Lev Davidovich Landau (1932), and Clarence Zener discover the Landau-Zener transition
- 1933 Max Delbruck suggests that quantum effects will cause photons to be scattered by an external electric field
- 1934 Irène Joliot-Curie and Frédéric Joliot bombard aluminum atoms with alpha particles to create artificially radioactive phosphorus-30
- 1934 Leó Szilárd realizes that nuclear chain reactions may be possible
- 1934 Enrico Fermi formulates his theory of beta decay

- 1934 Lev Davidovich Landau tells Edward Teller that nonlinear molecules may have vibrational modes which remove the degeneracy of an orbitally degenerate state (Jahn-Teller effect)
- 1934 Enrico Fermi suggests bombarding uranium atoms with neutrons to make a 93 proton element
- 1934 Pavel Alekseyevich Cherenkov reports that light is emitted by relativistic particles traveling in a nonscintillating liquid
- 1935 Hideki Yukawa presents a theory of strong interactions and predicts mesons
- 1935 Albert Einstein, Boris Podolsky, and Nathan Rosen put forth the EPR paradox
- 1935 Henry Eyring develop the transition state theory
- 1935 Niels Bohr presents his analysis of the EPR paradox
- 1936 Eugene Wigner develops the theory of neutron absorption by atomic nuclei
- 1936 Hermann Arthur Jahn and Edward Teller present their systematic study of the symmetry types for which the Jahn-Teller effect is expected
- 1937 Hans Hellmann finds the Hellmann-Feynman theorem
- 1937 Seth Neddermeyer, Carl Anderson, J.C. Street, and E.C. Stevenson discover muons using cloud chamber measurements of cosmic rays
- 1939 Richard Feynman finds the Hellmann-Feynman theorem
- 1939 Otto Hahn and Fritz Strassmann bombard uranium salts with thermal neutrons and discover barium among the reaction products
- 1939 Lise Meitner and Otto Robert Frisch determine that nuclear fission is taking place in the Hahn-Strassmann experiments
- 1942 Enrico Fermi makes the first controlled nuclear chain reaction
- 1942 Ernst Stueckelberg introduces the propagator to positron theory and interprets positrons as negative energy electrons moving backwards through spacetime
- 1943 Sin-Itiro Tomonaga publishes his paper on the basic physical principles of quantum electrodynamics
- 1947 Willis Lamb and Robert Retheford measure the Lamb-Retheford shift
- 1947 Cecil Powell, César Lattes, and Giuseppe Occhialini discover the pi-meson by studying cosmic ray tracks
- 1947 Richard Feynman presents his propagator approach to quantum electrodynamics
- 1948 Hendrik Casimir predicts a rudimentary attractive Casimir force on a parallel plate capacitor
- 1951 Martin Deutsch discovers positronium
- 1952 David Bohm propose his interpretation of quantum mechanics
- 1953 Robert Wilson observes Delbruck scattering of 1.33 MeV gamma-rays by the electric fields of lead nuclei
- 1954 Chen Ning Yang and Robert Mills investigate a theory of hadronic isospin by demanding local gauge invariance under isotopic spin space rotations---first non-Abelian gauge theory
- 1955 Owen Chamberlain, Emilio Segrè, Clyde Wiegand, and Thomas Ypsilantis discover the antiproton
- 1956 Frederick Reines and Clyde Cowan detect antineutrino
- 1956 Chen Ning Yang and Tsung Lee propose parity violation by the weak nuclear force
- 1956 Chien Shiung Wu discovers parity violation by the weak force in decaying cobalt
- 1957 Gerhart Luders proves the CPT theorem
- 1957 Richard Feynman, Murray Gell-Mann, Robert Marshak, and E.C.G. Sudarshan propose a vector/axial vector (VA) Lagrangian for weak interactions
- 1958 Marcus Sparnaay experimentally confirms the Casimir effect
- 1959 Yakir Aharonov and David Bohm predict the Aharonov-Bohm effect
- 1960 R.G. Chambers experimentally confirms the Aharonov-Bohm effect
- 1961 Murray Gell-Mann and Yuval Ne'eman discover the Eightfold Way patterns---SU(3) group
- 1961 Jeffrey Goldstone considers the breaking of global phase symmetry
- 1962 Leon Lederman shows that the electron neutrino is distinct from the muon neutrino

## The formation and successes of the Standard Model

- 1963 Murray Gell-Mann and George Zweig propose the quark/aces model
- 1964 Peter Higgs considers the breaking of local phase symmetry
- 1964 John Stewart Bell shows that all local hidden variable theories must satisfy Bell's inequality
- 1964 Val Fitch and James Cronin observe CP violation by the weak force in the decay of K mesons
- 1967 Steven Weinberg puts forth his electroweak model of leptons
- 1969 John Clauser, Michael Horne, Abner Shimony and Richard Holt propose a polarization correlation test of Bell's inequality
- 1970 Sheldon Glashow, John Iliopoulos, and Luciano Maiani propose the charm quark
- 1971 Gerard 't Hooft shows that the Glashow-Salam-Weinberg electroweak model can be renormalized
- 1972 Stuart Freedman and John Clauser perform the first polarization correlation test of Bell's inequality
- 1973 David Politzer proposes the asymptotic freedom of quarks
- 1974 Burton Richter and Samuel Ting discover the psi meson implying the existence of the charm quark
- 1974 Robert J. Buenker and Sigrid D. Peyerimhoff introduce the multireference configuration interaction method.
- 1975 Martin Perl discovers the tau lepton
- 1977 Steve Herb finds the upsilon resonance implying the existence of the beauty/bottom quark
- 1982 Alain Aspect, J. Dalibard, and G. Roger perform a polarization correlation test of Bell's inequality that rules out conspiratorial polarizer communication
- 1983 Carlo Rubbia, Simon van der Meer, and the CERN UA-1 collaboration find the W and Z intermediate vector bosons
- 1989 The Z intermediate vector boson resonance width indicates three quark-lepton generations
- 1994 The CERN LEAR Crystal Barrel Experiment justifies the existence of glueballs (exotic meson).
- 1995 after 18 years searching at Fermilab was discovered the top quark, it had very big mass
- 1998 Super-Kamiokande (Japan) observes evidence for neutrino oscillations, implying that at least one neutrino has mass.
- 2001 The Sudbury Neutrino Observatory (Canada) confirms the existence of neutrino oscillations.
- 2005 At the RHIC accelerator of Brookhaven National Laboratory they have created a quark-gluon liquid of very low viscosity, perhaps the quark-gluon plasma
- 2008 The Large Hadron Collider at CERN is scheduled to begin operation in this year. Its primary goal is to search for the Higgs boson, which has not yet been found.

# Automatic calculation of particle interaction or decay

The **automatic calculation of particle interaction or decay** is part of the computational particle physics branch. It refers to computing tools that help calculating the complex particle interactions as studied in high-energy physics, astroparticle physics and cosmology. The goal of the automation is to handle the full sequence of calculations in an automatic (programmed) way: from the Lagrangian expression describing the physics model up to the cross-sections values and to the event generator software.

Particle accelerator or colliders produce collisions (interactions) of particle (like the electron or the proton). The colliding particles form the *Initial State*. In the collision, particles can be annihilated or/and exchanged producing possibly different sets of particles, the *Final States*. The Initial and Final States of the interaction relate through the so-called scattering matrix (S-matrix).

For example at LEP, $e^+ + e^- \rightarrow e^+ + e^-$, or $e^+ + e^- \rightarrow \mu^+ + \mu^-$ are processes where the *initial state* is an electron and a positron colliding to produce an electron and a positron or two muons of opposite charge: the *final states*. In these simple cases, no automatic packages are needed and cross-section analytical expression can be easily derived at least for the lowest approximation: the Born approximation also called the leading order or the tree level (as Feynman diagrams have only trunk and branches, no loops).

But particle physics is now requiring much more complex calculations like at LHC $pp \rightarrow n_{\mathrm{jets}}$ where $p$ are protons and $n_{\mathrm{jets}}$ is the number of jets of particles initiated by proton constituents (quarks and gluons). The number of subprocesses describing a given process is so large that automatic tools have been developed to mitigate the burden of hand calculations.

Interactions at higher energies open a large spectrum of possible final states and consequently increase the number of processes to compute.

High precision experiments impose the calculation of higher order calculation, namely the inclusion of subprocesses where more than one virtual particle can be created and annihilated during the interaction lapse creating so-called *loops* which induce much more involved calculations.

Finally new theoretical models like the supersymmetry model (MSSM in its minimal version) predict a flurry of new processes.

The automatic packages, once seen as mere teaching support, have become, this last 10 years an essential component of the data simulation and analysis suite for all experiments. They help constructing event generators and are sometime viewed as *generators of event generators* or *Meta-generators*.

A particle physics model is essentially described by its Lagrangian. To simulate the production of events through event generators, 3 steps have to be taken. The Automatic Calculation project is to create the tools to make those steps as automatic (or programmed) as possible:

**I** Feynman rules, coupling and mass generation

LanHEP is an example of Feynman rules generation. Some model needs an additional step to compute, based on some parameters, the mass and coupling of new predicted particles.

**II** Matrix element code generation: Various methods are used to automatically produce the Matrix element expression in a computer language (Fortran, C/C++). They use values (i.e. for the masses) or expressions (i.e. for the couplings) produced by step **I** or model specific libraries constructed *by hands* (usually heavily relying on Computer algebra languages). When this expression is integrated (usually numerically) over the internal degrees of freedom it will provide the total and differential cross-sections for a given set of initial parameters like the *initial state* particle energies and polarization.

**III** Event generator code generation: This code must them be interfaced to other packages to fully provide the actual *final state*. The various effects or phenomenon that need to be implemeted are:

Initial state radiation and beamstrahlung for e+e− initial states. Parton distribution functions describing the actual content in terms of gluons and quarks of the p or p-bar initial state particles Parton showering describing the way final state quarks or gluons due to the QCD confinement generate additional quark/gluon pairs generating a so-called shower of partons before transforming into hadrons. Hadronization describing how the final quark pairs/triplets form the visible and detectable hadrons. Underlying event takes care of the way the rest, in term of constituent, of the initial protons also contribute to any given event.

The interplay or *matching* of the precise matrix element calculation and the approximations resulting from the simulation of the *parton shower* gives rise to further complications, either within a given level of precision like at leading order (LO) for the production of n jets or between two levels of precision when tempting to connect matrix element computed at next-to-leading (NLO) (1-loop) or next-to-next-leading order (NNLO) (2-loops) with LO partons shower package.

Several methods have been developed for this matching:

- Subtraction methods
- ...

But the only correct way is to match packages at the same level theoretical accuracy like the NLO matrix element calculation with NLO parton shower packages. This is currently in development.

# History

The idea of automation of the calculations in high-energy physics is not new. It dates back to the 1960s when packages such as SCHOONSCHIP and then REDUCE had been developed.

These are symbolic manipulation codes that automatize the algebraic parts of a matrix element evaluation, like traces on Dirac matrices and contraction of Lorentz indices. Such codes have evolved quite a lot with applications not only optimized for high-energy physics like FORM but also more general purpose programs like Mathematica and Maple.

Generation of QED Feynman graphs at any order in the coupling constant was automatized in the late 70's[15]. One of the first major application of these early developments in this field was the calculation of the anomalous magnetic moments of the electron and the muon[16]. The first automatic system incorporating all the steps for the calculation of a cross section, from Feynman graph generation, amplitude generation through a REDUCE source code that produces a FORTRAN code, phase space integration and event generation with BASES/SPRING[17] is GRAND[18]. It was limited to tree-level processes in QED. In the early nineties, a few groups started to develop packages aiming at the automation in the SM[19].[1] [2] [3] [4] [5] [6] [7] [8] [9] [10]

# Matrix element calculation methods

## Helicity amplitude

Feynman amplitudes are written in terms of spinor products of wave functions for massless fermions, and then evaluated numerically before the amplitudes are squared. Taking into account fermion masses implies that Feynman amplitudes are decomposed into vertex amplitudes by splitting the internal lines into wave function of fermions and polarization vectors of gauge bosons.

All helicity configuration can be computed independently.

### Helicity amplitude squared

The method is similar to the previous one, but the numerical calculation is performed after squaring the Feynman Amplitude. The final expression is shorter and therefore faster to compute, but independent helicity information are not anymore available.

### Dyson-Schwinger recursive equations

The scattering amplitude is evaluated recursively through a set of Dyson-Schwinger equations. The computational cost of this algorithm grows asymptotically as $3^n$, where n is the number of particles involved in the process, compared to n! in the traditional Feynman graphs approach. Unitary gauge is used and mass effects are available as well. Additionally, the color and helicity structures are appropriately transformed so the usual summation is replaced by the Monte Carlo techniques.[11]

## Higher order calculations

[12]

## Additional package for Event generation

The integration of the "matrix element" over the multidimensional internal parameters phase space provides the total and differential cross-sections. Each point of this phase space is associated to an event probability. This is used to randomly generate events closely mimicking experimental data. This is called event generation, the first step in the complete chain of event simulation. The initial and final state particles can be elementary particles like electrons, muons, or photons but also partons (protons and neutrons).

More effects must then be implemented to reproduce real life events as those detected at the colliders.

The initial electron or positron may undergo radiation before they actually interact: initial state radiation and beamstrahlung.

The bare partons that do not exist in nature (they are confined inside the hadrons) must be so to say dressed so that they form the known hadrons or mesons. They are made in two steps: parton shower and hadronization.

When the initial state particles are protons at high energy, it is only their constituents which interact. Therefore the specific parton that will experience the "hard interaction" has to be selected. Structure functions must therefore be implemented. The other parton may interact "softly" must be also be simulated as they contribute to the complexity of the event: Underlying event

### Initial state radiation and beamstrahlung

(*to be written*)

### Parton shower and Hadronization

(*to be written*)

#### At leading Order (LO)

(*to be written*)

#### At Next-to-Leading order (NLO)

(*to be written*)

### Structure and Fragmentation Functions

(*to be written*)

### Underlying event

(*to be written*)

## Model specific packages

(*to be written*)

## Related computational issues

(*to be written*)

### Multi-dimensional integrators

(*to be written*)

### Ultra-High Precision Numerical computation

(*to be written*)

## Existing Packages

### Feynman rules generators

- FeynRules [13]
- LanHEP

### Tree Level Packages

| Name | Model | Max FS | Tested FS | Short description | Publication | Method | Output | Status |
|---|---|---|---|---|---|---|---|---|
| MadGraph5 [14] | Any Model | 1/2->n | 2->8 | complete, massive, helicity, color, decay chain | what is MG5 [15] | HA (automatic generation) | Output | PD [14] |
| Grace | SM/MSSM | 2->n | 2->6 | complete,massive,helicity,color | Manual v2.0 [16] | HA | Output | PD [17] |
| CompHEP | Model | Max FS | Tested FS | Short description | Publication | method | Output | Status |
| CalcHEP | Model | Max FS | Tested FS | Short description | Publication | Method | Output | Status |
| Sherpa | SM/MSSM | 2->n | 2->8 | massive | publication [18] | HA/DS | Output | PD [19] |
| GenEva | Model | Max FS | Tested FS | Short description | Publication | Method | Output | Status |
| HELAC | Model | Max FS | Tested FS | Short description | Publication | Method | Output | Status |
| Name | Model | Max FS | Tested FS | Short description | Publication | Method | Output | Status |

**Status**: *PD*: Public Domain,

**Model**: *SM*: Standard Model, *MSSM*: Minimal Supersymmetric Standard Model

**Method**: *HA*: Helicity Amplitude, *DS*: Dyson Schwinger

**Output**: *ME*: Matrix Element, *CS*: Cross-Sections, *PEG*: Parton level Event Generation, *FEG*: Full particle level Event Generation

### Higher-order Packages

| Name | Model | Order tested | Max FS | Tested FS | Short description | Publication | Method | Status |
|---|---|---|---|---|---|---|---|---|
| Grace L-1 | SM/MSSM | 1-loop | 2->n | 2->4 | complete,massive,helicity,color | NA | Method | NA |
| Name | Order | Model | Max FS | Tested FS | Short description | Publication | Method | Status |

## References


[1] Kaneko, T. (1990). "Automatic calculation of Feynman amplitudes" (http://www.slac.stanford.edu/spires/find/hep?key=5471150). . pp. 555. .

[2] Boos, E.E; *et al.* (1994). "Automatic calculation in high-energy physics by Grace/Chanel and CompHEP.". *International Journal of Modern Physics C* **5** (4): 615. doi:10.1142/S0129183194000787.

[3] Wang, J.-X. (1993). "Automatic calculation of Feynman loop-diagrams I. Generation of a simplified form of the amplitude". *Computer Physics Communications* **77** (2): 263. doi:10.1016/0010-4655(93)90010-A.

[4] Kaneko, T.; Nakazawa, N. (1995). "Automatic calculation of two loop weak corrections to muon anomalous magnetic moment" (http://www.slac.stanford.edu/spires/find/hep?key=3147525). . pp. 173. arXiv:hep-ph/9505278. .

[5] Jimbo, M.; *et al.* (Minami-Tateya Collaboration) (1995). "Automatic calculation of SUSY particle production" (http://www.slac.stanford.edu/spires/find/hep?key=3360695). . p. 155. arXiv:hep-ph/9605414. .

[6] Franzkowski, J. (1997). "Automatic calculation of massive two-loop self-energies with XLOOPS". *Nuclear Instruments and Methods in Physics Research A* **389** (1–2): 333. doi:10.1016/S0168-9002(97)00121-6. arXiv:hep-ph/9611378.

[7] Brucher, L. (2000). "Automatic Feynman diagram calculation with xloops: A Short overview" (http://www.slac.stanford.edu/spires/find/hep?key=4306120). *arXiv:hep-ph/0002028* [hep-ph]. .

[8] Perret-Gallix, D. (1999). "Automatic amplitude calculation and event generation for collider physics: GRACE and CompHEP" (http://www.slac.stanford.edu/spires/find/hep?key=4515617). . pp. 270. .

[9] Belanger, G.; *et al.* (2006). "Automatic calculations in high energy physics and GRACE at one-loop". *Physics Reports* **430** (3): 117. doi:10.1016/j.physrep.2006.02.001. arXiv:hep-ph/0308080.
[10] Fujimoto, J.; *et al.* (2004). "Automatic one-loop calculation of MSSM processes with GRACE". *Nuclear Instruments and Methods in Physics Research A* **534** (1–2): 246. doi:10.1016/j.nima.2004.07.095. arXiv:hep-ph/0402145.
[11] Kanaki, A.; Papadopoulos, C.G. (2000). "HELAC: A Package to compute electroweak helicity amplitudes". *Computer Physics Communications* **132**: 306. doi:10.1016/S0010-4655(00)00151-X. arXiv:hep-ph/0002082.
[12] Belanger, G.; *et al.* (2006). "Automatic calculations in high energy physics and Grace at one-loop". *Physics Reports* **430**: 117. doi:10.1016/j.physrep.2006.02.001. arXiv:hep-ph/0308080.
[13] https://server06.fynu.ucl.ac.be/projects/feynrules
[14] https://launchpad.net/madgraph5
[15] https://server06.fynu.ucl.ac.be/projects/madgraph
[16] http://minami-home.kek.jp/grace/gracedoc.ps
[17] http://minami-home.kek.jp
[18] http://www.slac.stanford.edu/spires/find/hep/www?rawcmd=FIND+EPRINT+HEP-PH%2F0311263
[19] http://www.sherpa-mc.de

# S-matrix

***Scattering matrix*** *redirects here. For the meaning in linear electrical networks, see scattering parameters.*

For the 1960's approach to particle physics, see *S-matrix theory*.

In physics, the **scattering matrix** (or **S-matrix**) relates the initial state and the final state of a physical system undergoing a scattering process. It is used in quantum mechanics, scattering theory and quantum field theory.

More formally, the S-matrix is defined as the unitary matrix connecting asymptotic particle states in the Hilbert space of physical states (scattering channels). While the S-matrix may be defined for any background (spacetime) that is asymptotically solvable and has no horizons, it has a simple form in the case of the Minkowski space. In this special case, the Hilbert space is a space of irreducible unitary representations of the inhomogeneous Lorentz group; the S-matrix is the evolution operator between time equal to minus infinity, and time equal to plus infinity. It is defined only in the limit of zero energy density (or infinite particle separation distance). It can be shown that if a quantum field theory in Minkowski space has a mass gap, the state in the asymptotic past and in the asymptotic future are both described by Fock spaces.

## History

The S-matrix was first introduced by John Archibald Wheeler in the 1937 paper "'On the Mathematical Description of Light Nuclei by the Method of Resonating Group Structure'".[1] In this paper Wheeler introduced a *scattering matrix* - a unitary matrix of coefficients connecting "the asymptotic behaviour of an arbitrary particular solution [of the integral equations] with that of solutions of a standard form".[2]

In the 1940s Werner Heisenberg developed, independently, the idea of the S-matrix. Due to the problematic divergences present in quantum field theory at that time Heisenberg was motivated to isolate the essential features of the theory that would not be affected by future changes as the theory developed. In doing so he was led to introduce a unitary "characteristic" S-matrix.[2]

# Motivation

In high-energy particle physics we are interested in computing the probability for different outcomes in scattering experiments. These experiments can be broken down into three stages:

1. Collide together a collection of incoming particles (usually *two* particles with high energies).

2. Allowing the incoming particles to interact. These interactions may change the types of particles present (e.g. if an electron and a positron annihilate they may produce two photons).

3. Measuring the resulting outgoing particles.

The process by which the incoming particles are transformed (through their interaction) into the outgoing particles is called scattering. For particle physics a physical theory of these processes must be able to compute the probability for different outgoing particles when we collide different incoming particles with different energies. The S-matrix in quantum field theory is used to do exactly this. It is assumed that the small-energy-density approximation is valid in these cases.

## Use of S-matrices

The S-matrix is closely related to the transition probability amplitude in quantum mechanics and to cross sections of various interactions; the elements (individual numerical entries) in the S-matrix are known as **scattering amplitudes**. Poles of the S-matrix in the complex-energy plane are identified with bound states, virtual states or resonances. Branch cuts of the S-matrix in the complex-energy plane are associated to the opening of a scattering channel.

In the Hamiltonian approach to quantum field theory, the S-matrix may be calculated as a time-ordered exponential of the integrated Hamiltonian in the interaction picture; it may be also expressed using Feynman's path integrals. In both cases, the perturbative calculation of the S-matrix leads to Feynman diagrams.

In scattering theory, the **S-matrix** is an operator mapping free particle *in-states* to free particle *out-states* (scattering channels) in the Heisenberg picture. This is very useful because we cannot describe exactly the interaction (at least, the most interesting ones).

## Mathematical definition

In Dirac notation, we define $|0\rangle$ as the vacuum quantum state. If $a^\dagger(k)$is a creation operator, its hermitian conjugate (destruction or annihilation operator) acts on the vacuum as follows:

$$a(k)\,|0\rangle = 0.$$

Now, we define two kinds of creation/destruction operators, acting on different Hilbert spaces (IN space *i*, OUT space *f*), $a_i^\dagger(k)$and $a_f^\dagger(k)$.

So now

$$\mathcal{H}_{\mathrm{IN}} = \mathrm{span}\{|I, k_1 \dots k_n\rangle = a_i^\dagger(k_1)\cdots a_i^\dagger(k_n)\,|I,0\rangle\},$$
$$\mathcal{H}_{\mathrm{OUT}} = \mathrm{span}\{|F, p_1 \dots p_n\rangle = a_f^\dagger(p_1)\cdots a_f^\dagger(p_n)\,|F,0\rangle\}.$$

It is possible to play the trick assuming that $|I,0\rangle$ and $|F,0\rangle$ are both invariant under translation and that the states $|I, k_1 \dots k_n\rangle$ and $|F, p_1 \dots p_n\rangle$ are eigenstates of the momentum operator $\mathcal{P}^\mu$, by adiabatically turning on and off the interaction.
In the Heisenberg picture the states are time-independent, so we can expand initial states on a basis of final states (or vice versa) as follows:

Where $|C_m|^2$is the probability that the interaction transforms $|I, k_1 \dots k_n\rangle$ into $|F, p_1 \dots p_m\rangle$
According to Wigner's theorem, $S$ must be a unitary operator such that $\langle I,\beta|\,S\,|I,\alpha\rangle = S_{\alpha\beta} = \langle F,\beta|I,\alpha\rangle$ .
Moreover, $S$ leaves the vacuum state invariant and transforms IN-space fields in OUT-space fields:

$$S\left|0\right\rangle = \left|0\right\rangle$$
$$\phi_f = S^{-1}\phi_i S$$

If $S$ describes an interaction correctly, these properties must be also true:

If the system is made up with a single particle in momentum eigenstate $\left|k\right\rangle$ , then $S\left|k\right\rangle = \left|k\right\rangle$

The S-matrix element must be nonzero if and only if momentum is conserved.

### S-matrix and evolution operator *U*

$$a\left(k,t\right) = U^{-1}(t)a_i\left(k\right)U\left(t\right)$$
$$\phi_f = U^{-1}(\infty)\phi_i U(\infty) = S^{-1}\phi_i S.$$

Therefore $S = e^{i\alpha}U(\infty)$where

$$e^{i\alpha} = \langle 0|U(\infty)|0\rangle^{-1}$$

because

$$S\left|0\right\rangle = \left|0\right\rangle.$$

Substituting the explicit expression for *U* we obtain:

$$S = \frac{1}{\langle 0|U(\infty)|0\rangle}\mathcal{T}e^{-i\int d\tau V_i(\tau)}.$$

By inspection it can be seen that this formula is not explicitly covariant.

## Dyson series

The most widely used expression for the S-matrix is the Dyson series. This expresses the S-matrix operator as the series:

where:

- $T[\cdots]$denotes time-ordering,
- $H_{int}(x)$denotes the interaction Hamiltonian which describes the interactions in the theory.

## See also

- Feynman diagram
- LSZ reduction formula
- Wick's theorem

## Notes

[1] John A. Wheeler, ' On the Mathematical Description of Light Nuclei by the Method. of Resonating Group Structure (http://link.aps.org/abstract/PR/v52/p1107)' Phys. Rev. 52, 1107 - 1122 (1937)

[2] Jagdish Mehra, Helmut Rechenberg, *The Historical Development of Quantum Theory* (Pages 990 and 1031) Springer, 2001 ISBN 0387950869, 9780387950860

## References

- Barut, A.O. (1967). *The Theory of the Scattering Matrix.*
- Tony Philips (11 2001). "Finite-dimensional Feynman Diagrams" (http://www.math.sunysb.edu/~tony/whatsnew/column/feynman-1101/feynman1.html). *What's New In Math*. American Mathematical Society. Retrieved 2007-10-23.

# List of materials analysis methods

List of materials analysis methods:



- **μSR** - see Muon spin spectroscopy
- **χ** - see Magnetic susceptibility

## A

- **Analytical ultracentrifugation** - Analytical ultracentrifugation
- **AAS** - Atomic absorption spectroscopy
- **AED** - Auger electron diffraction
- **AES** - Auger electron spectroscopy
- **AFM** - Atomic force microscopy
- **AFS** - Atomic fluorescence spectroscopy
- **APFIM** - Atom probe field ion microscopy
- **APS** - Appearance potential spectroscopy
- **ARPES** - Angle resolved photoemission spectroscopy
- **ARUPS** - Angle resolved ultraviolet photoemission spectroscopy
- **ATR** - Attenuated total reflectance

## B

- **BET** - BET surface area measurement (BET from Brunauer, Emmett, Teller)
- **BiFC** - Bimolecular fluorescence complementation
- **BKD** - Backscatter Kikuchi diffraction, see **EBSD**
- **BRET** - Bioluminescence resonance energy transfer
- **BSED** - Back scattered electron diffraction, see **EBSD**

## C

- **CAICISS** - Coaxial impact collision ion scattering spectroscopy
- **CARS** - Coherent anti-Stokes Raman spectroscopy
- **CBED** - Convergent beam electron diffraction
- **CCM** - Charge collection microscopy
- **CDI** - Coherent diffraction imaging
- **CE** - Capillary electrophoresis
- **CET** - Cryo-electron tomography
- **CL** - Cathodoluminescence
- **CLSM** - Confocal laser scanning microscopy
- **COSY** - Correlation spectroscopy
- **Cryo-EM** - Cryo-electron microscopy
- **CV** - Cyclic voltammetry

## D

- **DE(T)A** - Dielectric thermal analysis
- **dHvA** - De Haas-van Alphen effect
- **DIC** - Differential interference contrast microscopy
- **Dielectric spectroscopy** - Dielectric spectroscopy
- **DLS** - Dynamic light scattering
- **DLTS** - Deep-level transient spectroscopy
- **DMA** - Dynamic mechanical analysis
- **DPI** - Dual polarisation interferometry
- **DRS** - Differential reflectance spectroscopy
- **DSC** - Differential scanning calorimetry
- **DTA** - Differential thermal analysis
- **DVS** - Dynamic vapour sorption

## E

- **EBIC** - Electron beam induced current (and see IBIC: ion beam induced charge)
- **EBS** - Elastic (non-Rutherford) backscattering spectrometry (see RBS)
- **EBSD** - Electron backscatter diffraction
- **ECOSY** - Exclusive correlation spectroscopy
- **ECT** - Electrical capacitance tomography
- **EDAX** - Energy-dispersive analysis of x-rays
- **EDMR** - Electrically Detected Magnetic Resonance, see ESR or EPR
- **EDS** - Energy Dispersive Spectroscopy
- **EDX** - Energy dispersive X-ray spectroscopy
- **EELS** - Electron energy loss spectroscopy
- **EFTEM** - Energy filtered transmission electron microscopy
- **EID** - Electron induced desorption
- **EIT** and **ERT** - Electrical impedance tomography and Electrical resistivity tomography
- **EL** - Electroluminescence
- **Electron crystallography** - Electron crystallography
- **ELS** - Electrophoretic light scattering
- **ENDOR** - Electron nuclear double resonance, see ESR or EPR
- **EPMA** - Electron probe microanalysis
- **EPR** - Electron paramagnetic resonance spectroscopy
- **ERD** or **ERDA** - Elastic recoil detection or Elastic recoil detection analysis
- **ESCA** - Electron spectroscopy for chemical analysis* **see XPS**
- **ESD** - Electron stimulated desorption
- **ESEM** - Environmental scanning electron microscopy
- **ESI-MS** or **ES-MS** - Electrospray ionization mass spectrometry or Electrospray mass spectrometry
- **ESR** - Electron spin resonance spectroscopy
- **ESTM** - Electrochemical scanning tunneling microscopy
- **EXAFS** - Extended X-ray absorption fine structure
- **EXSY** - Exchange spectroscopy

## F

- **FCS** - Fluorescence correlation spectroscopy
- **FCCS** - Fluorescence cross-correlation spectroscopy
- **FEM** - Field emission microscopy
- **FIB** - Focused ion beam microscopy
- **FIM-AP** - Field ion microscopy–atom probe
- **Flow birefringence** - Flow birefringence
- **Fluorescence anisotropy** - Fluorescence anisotropy
- **FLIM** - Fluorescence lifetime imaging
- **Fluorescence microscopy** - Fluorescence microscopy
- **FRET** - Fluorescence resonance energy transfer
- **FRS** - Forward Recoil Spectrometry, a synonym of ERD
- **FTICR** or **FT-MS** - Fourier transform ion cyclotron resonance or Fourier transform mass spectrometry
- **FTIR** - Fourier transform infrared spectroscopy

## G

- **GC-MS** - Gas chromatography-mass spectrometry
- **GDMS** - Glow discharge mass spectrometry
- **GDOS** - Glow discharge optical spectroscopy
- **GISAXS** - Grazing incidence small angle X-ray scattering
- **GIXD** - Grazing incidence X-ray diffraction
- **GIXR** - Grazing incidence X-ray reflectivity
- **GLC** - Gas-liquid chromatography

## H

- **HAADF** - high angle annular dark-field imaging
- **HAS** - Helium atom scattering
- **HPLC** - High performance liquid chromatography
- **HREELS** - High resolution electron energy loss spectroscopy
- **HREM** - High-resolution electron microscopy
- **HRTEM** - High-resolution transmission electron microscopy

## I

- **IAES** - Ion induced Auger electron spectroscopy
- **IBA** - Ion beam analysis
- **IBIC** - Ion beam induced charge microscopy
- **ICP-AES** - Inductively_coupled_plasma_atomic_emission_spectroscopy
- **ICP-MS** - Inductively coupled plasma mass spectrometry
- **Immunofluorescence** - Immunofluorescence
- **ICR** - Ion cyclotron resonance
- **IETS** - Inelastic electron tunneling spectroscopy
- **IGA** - Intelligent gravimetric analysis
- **IIX** - Ion induced X-ray analysis: See Particle induced X-ray emission
- **INS** - Ion neutralization spectroscopy
  Inelastic neutron scattering

- **IRS** - Infrared spectroscopy
- **ISS** - Ion scattering spectroscopy
- **ITC** - Isothermal titration calorimetry
- **IVEM** - Intermediate voltage electron microscopy

## L

- List of materials analysis methods (deliberate self-link)
- **LALLS** - Low-angle laser light scattering
- **LC-MS** - Liquid chromatography-mass spectrometry
- **LEED** - Low-energy electron diffraction
- **LEEM** - Low-energy electron microscopy
- **LEIS** - Low-energy ion scattering
- **LIBS** - Laser induced breakdown spectroscopy
- **LOES** - Laser optical emission spectroscopy
- **LS** - Light (Raman) scattering

## M

- **MALDI** - Matrix-assisted laser desorption/ionization
- **MBE** - Molecular beam epitaxy
- **MEIS** - Medium energy ion scattering
- **MFM** - Magnetic force microscopy
- **MIT** - Magnetic induction tomography
- **MPM** - Multiphoton fluorescence microscopy
- **MRFM** - Magnetic resonance force microscopy
- **MRI** - Magnetic resonance imaging
- **MS** - Mass spectrometry
- **MS/MS** - Tandem mass spectrometry
- **Mössbauer spectroscopy** - Mössbauer spectroscopy
- **MTA** - Microthermal analysis

## N

- **NAA** - Neutron activation analysis
- **Nanovid microscopy** - Nanovid microscopy
- **ND** - Neutron diffraction
- **NDP** - Neutron depth profiling
- **NEXAFS** - Near edge X-ray absorption fine structure
- **NIS** - Nuclear inelastic scattering/absorption
- **NMR** - Nuclear magnetic resonance spectroscopy
- **NOESY** - Nuclear Overhauser effect spectroscopy
- **NRA** - Nuclear reaction analysis
- **NSOM** - Near-field optical microscopy

## O

- **OBIC** - Optical beam induced current
- **ODNMR** - Optically detected magnetic resonance, see ESR or EPR
- **OES** - Optical emission spectroscopy
- **Osmometry** - Osmometry

## P

- **PAS** - Positron annihilation spectroscopy
- **Photoacoustic spectroscopy** - Photoacoustic spectroscopy
- **PAT** or **PACT** - Photoacoustic tomography or photoacoustic computed tomography
- **PAX** - Photoemission of adsorbed xenon
- **PC or PCS** - Photocurrent spectroscopy
- **Phase contrast microscopy** - Phase contrast microscopy
- **PhD** - Photoelectron diffraction
- **PD** - Photodesorption
- **PDEIS** - Potentiodynamic electrochemical impedance spectroscopy
- **PDS** - Photothermal deflection spectroscopy
- **PED** - Photoelectron diffraction
- **PEELS** - parallel electron energy loss spectroscopy
- **PES** - Photoelectron spectroscopy
- **PINEM** - photon-induced near-field electron microscopy
- **PIGE** - Particle (or proton) induced gamma-ray spectroscopy, see Nuclear reaction analysis
- **PIXE** - Particle (or proton) induced X-ray spectroscopy
- **PL** - Photoluminescence
- **Porosimetry** - Porosimetry
- **Powder diffraction** - Powder diffraction
- **PTMS** - Photothermal microspectroscopy
- **PTS** - Photothermal spectroscopy

## Q

- **QENS** - Quasi-elastic neutron scattering

## R

- **Raman** - Raman spectroscopy
- **RAXRS** - Resonant anomalous X-ray scattering
- **RBS** - Rutherford backscattering spectrometry
- **REM** - Reflection electron microscopy
- **RDS** - Reflectance Difference Spectroscopy
- **RHEED** - Reflection high energy electron diffraction
- **RIXS** - Resonant inelastic X-ray scattering
- **RR spectroscopy** - Resonance Raman spectroscopy

## S

- **SAD** - Selected area diffraction
- **SAED** - Selected area electron diffraction
- **SAM** - Scanning Auger microscopy
- **SANS** - Small angle neutron scattering
- **SAXS** - Small angle X-ray scattering
- **SCANIIR** - Surface composition by analysis of neutral species and ion-impact radiation
- **SCEM** - Scanning confocal electron microscopy
- **SE** - Spectroscopic ellipsometry
- **SEC** - Size exclusion chromatography
- **SEIRA** - Surface enhanced infrared absorption spectroscopy
- **SEM** - Scanning electron microscopy
- **SERS** - Surface enhanced Raman spectroscopy
- **SERRS** - Surface enhanced resonance Raman spectroscopy
- **SEXAFS** - Surface extended X-ray absorption fine structure
- **SICM** - Scanning ion-conductance microscopy
- **SIL** - Solid immersion lens
- **SIM** - Solid immersion mirror
- **SIMS** - Secondary ion mass spectrometry
- **SNMS** - Sputtered neutral species mass spectroscopy
- **SNOM** - Scanning near-field optical microscopy
- **SPECT** - Single photon emission computed tomography
- **SPM** - Scanning probe microscopy
- **SRM-CE/MS** - Selected-reaction-monitoring capillary-electrophoresis mass-spectrometry
- **SSNMR** - Solid-state nuclear magnetic resonance
- **Stark spectroscopy** - Stark spectroscopy
- **STED** - Stimulated Emission Depletion microscopy
- **STEM** - Scanning transmission electron microscopy
- **STM** - Scanning tunneling microscopy
- **STS** - Scanning tunneling spectroscopy
- **SXRD** - Surface X-ray Diffraction (SXRD)

## T

- **TAT** or **TACT** - Thermoacoustic tomography or thermoacoustic computed tomography (see also photoacoustic tomography - PAT)
- **TEM** - transmission electron microscope/microscopy
- **TGA** - Thermogravimetric analysis
- **TIKA** - Transmitting ion kinetic analysis
- **TIRFM** - Total internal reflection fluorescence microscopy
- **TLS** - Photothermal lens spectroscopy, a type of Photothermal spectroscopy
- **TMA** - Thermomechanical analysis
- **TOF-MS** - Time-of-flight mass spectrometry
- **Two-photon excitation microscopy** - Two-photon excitation microscopy
- **TXRF** - Total reflection X-ray fluorescence analysis

## U

- **Ultrasound attenuation spectroscopy** - Ultrasound attenuation spectroscopy
- **Ultrasonic testing** - Ultrasonic testing
- **UPS** - UV-photoelectron spectroscopy

## V

- **VEDIC** - Video-enhanced differential interference contrast microscopy
- **Voltammetry** - Voltammetry

## W

- **WAXS** - Wide angle X-ray scattering
- **WDX or WDS** - Wavelength dispersive X-ray spectroscopy

## X

- **XAES** - X-ray induced Auger electron spectroscopy
- **XANES** - XANES, synonymous with NEXAFS (Near edge X-ray absorption fine structure)
- **XAS** - X-ray absorption spectroscopy
- **X-CTR** - X-ray crystal truncation rod scattering
- **X-ray crystallography** - X-ray crystallography
- **XDS** - X-ray diffuse scattering
- **XPEEM** - X-ray photoelectron emission microscopy
- **XPS** - X-ray photoelectron spectroscopy
- **XRD** - X-ray diffraction
- **XRES** - X-ray resonant exchange scattering
- **XRF** - X-ray fluorescence analysis
- **XRR** - X-ray reflectivity
- **XRS** - X-ray Raman scattering
- **XSW** - X-ray standing wave technique

## References


- Callister, WD (2000). *Materials Science and Engineering - An Introduction*. *John Wiley and Sons* : London. ISBN 0-471-32013-7.
- Yao, N, ed (2007). *Focused Ion Beam Systems: Basics and Applications*. *Cambridge University Press* : Cambridge, UK. ISBN 978-052183-1994.

# List of neutrino experiments

This is a list of neutrino experiments, neutrino detectors, and neutrino telescopes.

| Abbreviation | Full name | Sensitivity[a] | Type | Induced reaction | Type of reaction[b] | Detector | Type of detector | Threshold energy | Location | Operation | Home page |
|---|---|---|---|---|---|---|---|---|---|---|---|
| ANTARES | Astronomy with a Neutrino Telescope and Abyss Environmental RESearch | ATM, CR, AGN, PUL | $\nu_e$, $\nu_\mu$, $\nu_\tau$ | | | | | | Mediterranean Sea, France | 2006– | [1] |
| BOREXINO | BORon EXperiment | LS | $\nu_e$ | $\nu_x + e^- \rightarrow \nu_x + e^-$ | ES | LOS shielded by water | Scintillation | 250–665 keV | Gran Sasso, Italy | May 2007– | [2] [3] |
| CLEAN | Cryogenic Low-Energy Astrophysics with Neon | LS, SN, WIMP | $\nu_e$ | $\nu_x + e^- \rightarrow \nu_x + e^-$ $\nu_e + {}^{20}Ne \rightarrow \nu_e + {}^{20}Ne$ | ES ES | Liquid Ne (10 t) | Scintillation | | | *future* | [4] |
| Daya Bay | Daya Bay Reactor Neutrino Experiment | R | $\nu_e$ | $\nu_e + p \rightarrow e^+ + n$ | CC | Gd-doped LOS | Scintillation | 1.8 MeV | Daya Bay, China | 2009– | [5] |
| Double CHOOZ | Double Chooz Reactor Neutrino Experiment | R | $\nu_e$ | $\nu_e + p \rightarrow e^+ + n$ | CC | Gd-doped LOS | Scintillation | 1.8 MeV | Chooz, France | 2008– | [6] |
| EXO-200 | Enriched Xenon Observatory | | | | BB | LXe | | | WIPP, New Mexico | 2009- | [7] |
| GALLEX | GALLium EXperiment | LS | $\nu_e$ | $\nu_e + {}^{71}Ga \rightarrow {}^{71}Ge + e^-$ | CC | $GaCl_3$ (30 t) | Radiochemical | 233.2 keV | Gran Sasso, Italy | 1991–1997 | [8] |
| GNO | Gallium Neutrino Observatory | LS | $\nu_e$ | $\nu_e + {}^{71}Ga \rightarrow {}^{71}Ge + e^-$ | CC | $GaCl_3$ (30 t) | Radiochemical | 233.2 keV | Gran Sasso, Italy | May 1998–Jan 2002 | [9] |
| HERON | Helium Roton Observation of Neutrinos | LS | $\nu_e$ (mainly) | $\nu_e + e^- \rightarrow \nu_e + e^-$ | NC | Superfluid He | Rotational excitation | 1 MeV | | *future* | [10] |
| HOMESTAKE–CHLORINE | Homestake chlorine experiment | S | $\nu_e$ | ${}^{37}Cl + \nu_e \rightarrow {}^{37}Ar^* + e^-$ ${}^{37}Ar^* \rightarrow {}^{37}Cl + e^+ + \nu_e$ | CC | $C_2Cl_4$ (615 t) | Radiochemical | 814 keV | Homestake Mine, South Dakota | 1967–1998 | [11] |

| | | | | | | | | | | | |
|---|---|---|---|---|---|---|---|---|---|---|---|
| HOMESTAKE–IODINE | Homestake iodine experiment | S | $\nu_e$ | $\nu + e^- \rightarrow \nu + e^-$ $\nu_e + {}^{127}I \rightarrow {}^{127}Xe + e^-$ | ES CC | NaI in water | Radiochemical | 789 keV | Homestake Mine, South Dakota | *future* | [11] |
| ICARUS | Imaging Cosmic And Rare Underground Signal | S, ATM, GSN | $\nu_e$, $\nu_\mu$, $\nu_\tau$ | $\nu + e^- \rightarrow \nu + e^-$ | ES | Liquid Ar | Cherenkov | 5.9 MeV | Gran Sasso, Italy | | [12] |
| IceCube | IceCube Neutrino Detector | S, ATM, CR, ? | $\nu_e$, $\nu_\mu$, $\nu_\tau$ | $\nu + e^- \rightarrow \nu + e^-$ | ES | Water ice (1 $km^3$) | Cherenkov | ~10 MeV | South Pole, Antarctica | 2006– | [13] |
| Kamiokande | Kamioka Nucleon Decay Experiment | S, ATM | $\nu_e$ | $\nu + e^- \rightarrow \nu + e^-$ | ES | Water ($H_2O$) | Cherenkov | 7.5 MeV | Kamioka, Japan | 1986–1995 | [14] |
| KamLAND | Kamioka Liquid Scintillator Antineutrino Detector | | | | | | | | Kamioka, Japan | 2002– | [15] |
| KM3NeT | KM3 Neutrino Telescope | | | | | | | | Mediterranean Sea, ? | 2009– | [16] |
| LENS | Low Energy Neutrino Spectroscopy | LS | $\nu_e$ | $\nu_e + {}^{115}In \rightarrow {}^{115}Sn + \nu_e + 2\gamma$ | CC | In-doped LOS | Scintillation | 120 keV | | | [17] [18] |
| Majorana | Neutrinoless Double Beta Decay in $^{76}Ge$ to measure lepton number violation and neutrino mass scale | BB | $\nu_e$ | ${}^{76}Ga \rightarrow {}^{76}As + e^- + e^-$ | BB | HPGe | Semiconductor | 2039 keV | Homestake Mine, South Dakota | *construction start* 2010 | [19] |
| MOON | Molybdenum Observatory Of Neutrinos | LS, LSN | $\nu_e$ | $\nu_e + {}^{100}Mo \rightarrow {}^{100}Tc + e^-$ | CC | $^{100}Mo$ (1 kt) + MoF6 (gas) | Scintillation | 168 keV | Washington, USA | | [20] |
| MiniBooNE | Mini Booster Neutrino Experiment | AC | $\nu_e$, $\nu_\mu$ | $\nu_e + {}^{12}C \rightarrow e^- + X$ | CC | Mineral oil (1 kton) | Cherenkov | ~100 keV | Illinois, USA | 2002– | [21] |
| NEMO Experiment | Neutrino Ettore Majorana Observatory | | | | | | | | Fréjus Road Tunnel, Italy/France | 2003– | [22] |
| NEMO Telescope | NEutrino Mediterranean Observatory | | | | | | | | Mediterranean Sea, Italy | 2007– | [23] |

| | | | | | | | | | | | |
|---|---|---|---|---|---|---|---|---|---|---|---|
| NEVOD | Cherenkov water detector NEVOD | ATM, CR | $\nu_\mu$ | $\nu_\mu + n \rightarrow \mu^- + p$ $\nu_\mu + p \rightarrow \mu^+ + n$ | CC | Water ($H_2O$) | Cherenkov | ~2 GeV | Moscow, Russia | 1993– | [24] |
| NOvA | NuMI Off-Axis $\nu_e$ Appearance | | | | | | | | Illinois and Minnesota, United States | 2011– | [25] |
| OPERA | Oscillation Project with Emulsion-tRacking Apparatus | | $\nu_\tau$ | | | | | | LNGS (Italy) and CERN | 2008– | [26] |
| SAGE | Soviet–American Gallium Experiment | LS | $\nu_e$ | $\nu_e + {}^{71}Ga \rightarrow {}^{71}Ge + e^-$ | CC | $GaCl_3$ | Radiochemical | 233.2 keV | Baksan Valley, Russia | 1990–2006 | [27] |
| SciBooNE | SciBar (Scintillator Bar) Booster Neutrino Experiment | AC | $\nu_\mu$ | $\nu_\mu + {}^{12}C \rightarrow \mu^- + X$ | CC, NC | Plastic (CH,10 ton) | Scintillation | ~100 keV | Illinois, USA | 2007–2008 | [28] |
| SNO | Sudbury Neutrino Observatory | S, ATM, GSN | $\nu_e$, $\nu_\mu$, $\nu_\tau$ | $\nu_e + {}^2D \rightarrow 2p + e^-$ $\nu_x + {}^2D \rightarrow \nu_x + n + p$ $\nu_e + e^- \rightarrow \nu_e + e^-$ | CC NC ES | Heavy water (1 kt $D_2O$) | Cherenkov | 3.5 MeV | Creighton Mine, Ontario | 1999–2006 | [29] |
| SNO+ | SNO with liquid scintillator | | | | | | | | Creighton Mine, Ontario | 2009– | [29] |
| SK | Super-Kamiokande | S, ATM, GSN | $\nu_e$, $\nu_\mu$, $\nu_\tau$ | $\nu_e + e^- \rightarrow \nu_e + e^-$ $\nu_e + n \rightarrow e^- + p$ $\nu_e + p \rightarrow e^+ + n$ | ES CC CC | Water ($H_2O$) | Cherenkov | | Kamioka, Japan | 1996– | [30] [31] |
| UNO | Underground Nucleon decay and neutrino Observatory | S, ATM, GSN, RSN | $\nu_e$, $\nu_\mu$, $\nu_\tau$ | $\nu_e + e^- \rightarrow \nu_e + e^-$ | ES | Water (440 kt $H_2O$) | Cherenkov | | Henderson Mine, Colorado | *future* | [32] |

**[a]** Solar neutrino (S), Low-energy solar neutrino (LS), Reactor neutrino (R), Terrestrial neutrino (T), Atmospheric neutrino (ATM), Accelerator neutrino (AC), Cosmic ray neutrino (CR), Supernova neutrino (SN), Low-energy supernova neutrino (LSN), Active galactic nuclei neutrino (AGN), Pulsar neutrino (PUL)

**[b]** Elastic scattering (ES), Neutral current (NC), Charged current (CC), Double beta decay (BB)

# References


[1] http://antares.in2p3.fr/index.html
[2] http://www.ge.infn.it/borexino/
[3] http://borex.lngs.infn.it/
[4] http://mckinseygroup.physics.yale.edu/publications/CLEAN.pdf
[5] http://dayawane.ihep.ac.cn/
[6] http://doublechooz.in2p3.fr/
[7] http://www-project.slac.stanford.edu/exo/
[8] http://www.mpi-hd.mpg.de/nuastro/gallex.html
[9] http://www.lngs.infn.it/lngs_infn/contents/lngs_en/research/experiments_scientific_info/experiments/past/gno/
[10] http://www.physics.brown.edu/physics/researchpages/cme/heron/LTD_home.html
[11] http://www-spires.dur.ac.uk/cgi-bin/spiface/find/experiments/www2?rawcmd=fin+expt+homestake
[12] http://www.aquila.infn.it/icarus/
[13] http://icecube.wisc.edu/
[14] http://www-sk.icrr.u-tokyo.ac.jp/doc/kam/index.html
[15] http://www.awa.tohoku.ac.jp/KamLAND/
[16] http://www.km3net.org/
[17] http://www.phys.vt.edu/~lens/
[18] http://lens.in2p3.fr/
[19] http://majorana.npl.washington.edu/
[20] http://ewi.npl.washington.edu/moon/
[21] http://www-boone.fnal.gov
[22] http://nemo.in2p3.fr/nemow3/
[23] http://nemoweb.lns.infn.it
[24] http://www.nevod.mephi.ru/English/index.htm
[25] http://www-nova.fnal.gov
[26] http://operaweb.lngs.infn.it/
[27] http://ewi.npl.washington.edu/SAGE/sage.html
[28] http://www-sciboone.fnal.gov
[29] http://www.sno.phy.queensu.ca/
[30] http://neutrino.phys.washington.edu/~superk/
[31] http://www-sk.icrr.u-tokyo.ac.jp/sk/index_e.html
[32] http://ale.physics.sunysb.edu/uno/

# Instruments

## Optical microscope


| | |
|---|---|
| **Uses** | Small sample observation |
| **Notable experiments** | Discovery of cells |
| **Inventor** | Hans Lippershey<br>Zacharias Janssen |
| **Related items** | Microscope<br>Electron microscope |

The **optical microscope**, often referred to as the "**light microscope**", is a type of microscope which uses visible light and a system of lenses to magnify images of small samples. Optical microscopes are the oldest design of microscope and were designed around 1600. Basic optical microscopes can be very simple, although there are many complex designs which aim to improve resolution and sample contrast. Historically optical microscopes were easy to develop and are popular because they use visible light so the sample can be directly observed by eye.

A modern microscope with a mercury bulb for fluorescence microscopy. The microscope has a digital camera, and is attached to a computer.

The image from an optical microscope can be captured by normal light-sensitive cameras to generate a micrograph. Originally images were captured by photographic film but modern developments in CMOS and later charge-coupled device (CCD) cameras allow the capture of digital images. Purely Digital microscopes are now available which just use a CCD camera to examine a sample, and the image is shown directly on a computer screen without the need for eye-pieces.

Alternatives to optical microscopy which do not use visible light include scanning electron microscopy and transmission electron microscopy.

## Optical configurations

There are two basic configurations of the conventional optical microscope, the simple (one lens) and compound (many lenses). The vast majority of modern research microscopes are compound microscopes while some cheaper commercial digital microscopes are simple single lens microscopes. A magnifying glass is, in essence, a basic single lens microscope. In general microscope optics are static; to focus at different focal depths the lens to sample distance is adjusted and to get a wider or narrower field of view a different magnification objective lens must be used. Most modern research microscopes also have a separate set of optics for illuminating the sample.

### Single lens (simple) microscope

A *simple microscope* is a microscope that uses only one lens for magnification, and is the original design of light microscope. Van Leeuwenhoek's microscopes consisted of a small, single converging lens mounted on a brass plate, with a screw mechanism to hold the sample or specimen to be examined. Demonstrations [1] by British microscopist have images from such basic instruments. Though now considered primitive, the use of a single, convex lens for viewing is still found in simple magnification devices, such as the magnifying glass, and the loupe.

### Compound microscope

A **compound microscope** is a microscope which uses multiple lenses to collect light from the sample and then a separate set of lenses to focus the light into the eye or camera. Compound microscopes are heavier, larger and more expensive than simple microscopes due to the increased number of lenses used in construction. The main advantages of multiple lenses are improved numerical aperture (see resolution limit below), reduced chromatic aberration and exchangeable objective lenses to adjust the magnification. A compound microscope also makes more advanced illumination setups, such as phase contrast.

# History

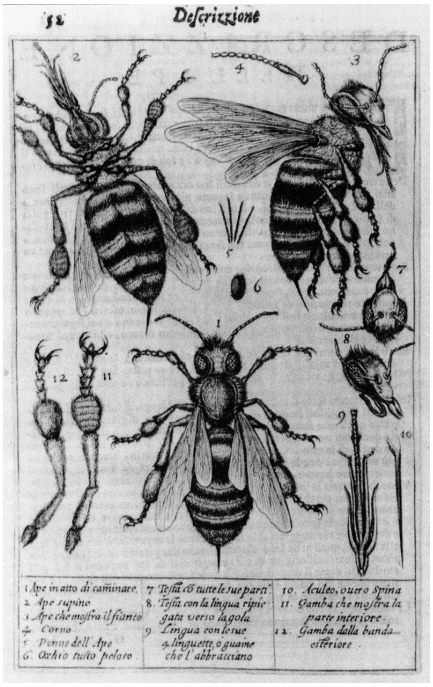


The oldest published image known to have been made with a microscope: bees by Francesco Stelluti, 1630[2]

## Invention

It is difficult to say who invented the compound microscope. Dutch spectacle-makers Hans Janssen and his son Zacharias Janssen are often said to have invented the first compound microscope in 1590, but this was a declaration made by Zacharias Janssen himself during the mid 17th century. The date is unlikely, as it has been shown that Zacharias Janssen actually was born around 1590. Another favorite for the title of 'inventor of the microscope' was Galileo Galilei. He developed an *occhiolino* or compound microscope with a convex and a concave lens in 1609. Galileo's microscope was celebrated in the Accademia dei Lincei in 1624 and was the first such device to be given the name "microscope" a year later by fellow Lincean Giovanni Faber. Faber coined the name from the Greek words *μικρόν* (micron) meaning "small", and *σκοπεῖν* (skopein) meaning "to look at", a name meant to be analogous with "telescope", another word coined by the Linceans.[3]

Christiaan Huygens, another Dutchman, developed a simple 2-lens ocular system in the late 17th century that was achromatically corrected, and therefore a huge step forward in microscope development. The Huygens ocular is still being produced to this day, but suffers from a small field size, and other minor problems.

## Popularisation

Anton van Leeuwenhoek (1632–1723) is credited with bringing the microscope to the attention of biologists, even though simple magnifying lenses were already being produced in the 16th century. Van Leeuwenhoek's home-made microscopes were very small simple instruments, with a single, yet strong lens. They were awkward in use, but enabled van Leeuwenhoek to see detailed images. It took about 150 years of optical development before the compound microscope was able to provide the same quality image as van Leeuwenhoek's simple microscopes, due to difficulties in configuring multiple lenses. Still, despite widespread claims, van Leeuwenhoek is not the inventor of the microscope.

## Lighting techniques

While basic microscope technology and optics have been available for over 400 years it is much more recently that techniques in sample illumination were developed to generate the high quality images seen today.

In August 1893 August Köhler developed Köhler illumination. This method of sample illumination gives rise to extremely even lighting and overcomes many limitations of older techniques of sample illumination. Before development of Köhler illumination the image of the light source, for example a lightbulb filament, was always visible in the image of the sample.

The Nobel Prize in physics was awarded to Fritz Zernike in 1953 for his development of phase contrast illumination which allows imaging of transparent samples. By using interference rather than absorption of light, extremely transparent samples, such as live mammalian cells, can be imaged without having to use staining techniques. Just two years later, in 1955, George Nomarski published the theory for differential interference contrast microscopy, another interference-based technique for imaging transparent samples.

### Fluorescence microscopy

Modern biological microscopy depends heavily on the development of fluorescent probes for specific structures within a cell. In contrast to normal transilluminated light microscopy in fluorescence microscopy the sample is illuminated through the objective lens with a narrow set of wavelengths of light. This light interacts with fluorophores in the sample which then emit light of a longer wavelength. It is this emitted light which makes up the image.

Since the mid 20th century chemical fluorescent stains, such as DAPI which binds to DNA, have been used to label specific structures within the cell. More recent developments include immunofluorescence, which uses fluorescently labelled antibodies to recognise specific proteins within a sample, and fluorescent proteins like GFP which a live cell can express making it fluorescent.

## Components

All modern optical microscopes designed for viewing samples by transmitted light share the same basic components of the light path, listed here in the order the light travels through them:

- Light source, a light or a mirror (7)
- Diaphragm and condenser lens (8)
- *Objective* (3)
- Ocular lens (eyepiece) (1)

In addition the vast majority of microscopes have the same 'structural' components:

- Objective turret (to hold multiple objective lenses) (2)
- Stage (to hold the sample) (9)
- Focus wheel to move the stage (4 - coarse adjustment, 5 - fine adjustment)

These entries are numbered according to the image on the right.

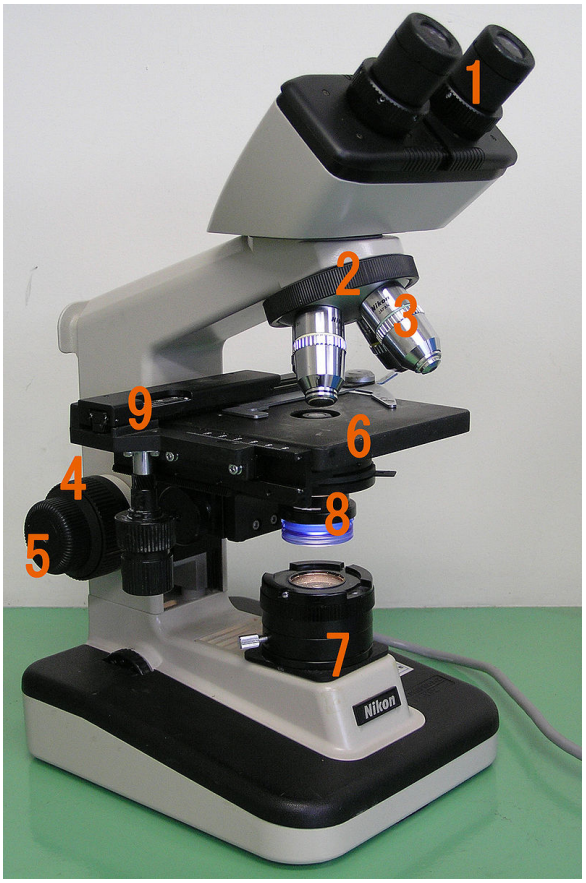

Basic optical transmission microscope elements(1990's)

### Ocular (eyepiece)

The ocular, or eyepiece, is a cylinder containing two or more lenses; its function is to bring the image into focus for the eye. The eyepiece is inserted into the top end of the body tube. Eyepieces are interchangeable and many different eyepieces can be inserted with different degrees of magnification. Typical magnification values for eyepieces include 2×, 5× and 10×. In some high performance microscopes, the optical configuration of the

objective lens and eyepiece are matched to give the best possible optical performance. This occurs most commonly with apochromatic objectives.

Two Leica oil immersion microscope objective lenses; left 100x, right 40x.

## Objective

The objective is a cylinder containing one or more lenses that are typically made of glass; its function is to collect light from the sample. At the lower end of the microscope tube one or more objective lenses are screwed into a circular nose piece which may be rotated to select the required objective lens. Typical magnification values of objective lenses are 4×, 5×, 10×, 20×, 40×, 50×, 60× and 100×. Some high performance objective lenses may require matched eyepieces to deliver the best optical performance.

## Stage

The stage is a platform below the objective which supports the specimen being viewed. In the center of the stage is a hole through which light passes to illuminate the specimen. The stage usually has arms to hold slides (rectangular glass plates with typical dimensions of 25 mm by 75 mm, on which the specimen is mounted).

## Light source

Many sources of light can be used. At its simplest, daylight is directed via a mirror. Most microscopes, however, have their own controllable light source - normally a halogen lamp.

## Condenser

The condenser is a lens designed to focus light from the illumination source onto the sample. The condenser may also include other features, such as a diaphragm and/or filters, to manage the quality and intensity of the illumination. For illumination techniques like dark field, phase contrast and differential interference contrast microscopy additional optical components must be precisely aligned in the light path.

## Frame

The whole of the optical assembly is traditionally attached to a rigid arm which in turn is attached to a robust U shaped foot to provide the necessary rigidity. The arm angle may be adjustable to allow the viewing angle to be adjusted.

The frame provides a mounting point for various microscope controls. Normally this will include controls for focusing, typically a large knurled wheel to adjust coarse focus, together with a smaller knurled wheel to control fine focus. Other features may be lamp controls and/or controls for adjusting the condenser.

## Objective lenses

On a typical compound optical microscope there are a selection of lenses available for different applications. Many different objective lenses with different properties and magnification are available.

Typically there will be around three objective lenses: a low power lens for scanning the sample, a medium power lens for normal observation and a high power lens for detailed observation. The typical magnification of objective lenses depends on the intended application, normal groups of lens magnificaitons may be [4×, 10×, 20×] for low magnification work and [10×, 40×, 100×] for high magnification work.

Objective lenses with higher magnifications normally have a higher numerical aperture and a shorter depth of field in the resulting image.

### Oil immersion objective

Some microscopes make use of oil immersion lens. These objectives must be used with oil (immersion oil) between the objective lens and the sample. The refractive index of the immersion oil is higher than air and this allows the objective lens to have a larger numerical aperture. The larger numerical aperture allows collection of more light making detailed observation of faint details possible.

Immersion lenses are designed so that the refractive index of the oil and of the cover slip are closely matched so that the light is transmitted from the specimen to the outer face of the objective lens with minimal refraction. An oil immersion lens usually has a magnification of 40 to 100×.

## Magnification

The actual power or magnification of a compound optical microscope is the product of the powers of the ocular (eyepiece) and the objective lens. The maximum normal magnifications of the occular and objective are 10× and 100× respectively giving a final magnification of 1000×.

### Magnification and micrographs

When using a camera to capture a micrograph the effective magnification of the image must take into account the size of the image. This is independent of whether it is on a print from a film negative or displayed digitally on a computer screen.

In the case of photographic film cameras the calculation is simple; the final magnification is the product of: the objective lens magnification, the camera optics magnification and the enlargement factor of the film print relative to the negative. A typical value of the enlargement factor is around 5× (for the case of 35mm film and a 6×4 inch print).

In the case of digital cameras the size of the pixels in the CMOS or CCD detector and the size of the pixels on the screen have to be known. The enlargement factor from the detector to the pixels on screen can then be calculated. As with a film camera the final magnification is the product of: the objective lens magnification, the camera optics magnification and the enlargement factor.

## Operation

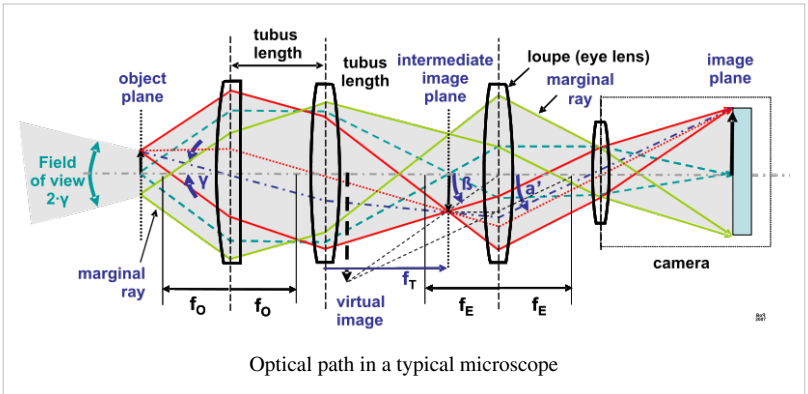


Optical path in a typical microscope

The optical components of a modern microscope are very complex and for a microscope to work well, the whole optical path has to be very accurately set up and controlled. Despite this, the basic operating principles of a microscope are quite simple.

The objective lens is, at its simplest, a very high powered magnifying glass *i.e.* a lens with a very short focal length. This is brought very close to the specimen being examined so that the light from the specimen comes to a focus about 160 mm inside the microscope tube. This creates an enlarged image of the subject. This image is inverted and can be seen by removing the eyepiece and placing a piece of tracing paper over the end of the tube. By carefully focusing a brightly lit specimen, a highly enlarged image can be seen. It is this real image that is viewed by the eyepiece lens that provides further enlargement.

In most microscopes, the eyepiece is a compound lens, with one component lens near the front and one near the back of the eyepiece tube. This forms an air-separated couplet. In many designs, the virtual image comes to a focus between the two lenses of the eyepiece, the first lens bringing the real image to a focus and the second lens enabling the eye to focus on the virtual image.

In all microscopes the image is intended to be viewed with the eyes focused at infinity (mind that the position of the eye in the above figure is determined by the eye's focus). Headaches and tired eyes after using a microscope are usually signs that the eye is being forced to focus at a close distance rather than at infinity.

The essential principle of the microscope is that an objective lens with very short focal length (often a few mm) is used to form a highly magnified real image of the object. Here, the quantity of interest is linear magnification, and this number is generally inscribed on the objective lens casing. In practice, today, this magnification is carried out by means of two lenses: the objective lens which creates an image at infinity, and a second weak tube lens which then forms a real image in its focal plane.[4]

## Illumination techniques

Many techniques are available which modify the light path to generate an improved contrast image from a sample. Major techniques for generating increased contrast from the sample include cross-polarized light, dark field, phase contrast and differential interference contrast illumination. A recent technique (Sarfus) combines cross-polarized light and specific contrast-enhanced slides for the visualization of nanometric samples.

Four examples of transilumination techniques used to generate contrast in a sample of [[tissue paper]]. 1.559 μm/pixel.

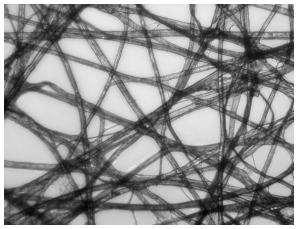

Bright field illumination, sample contrast comes from absorbance of light in the sample.

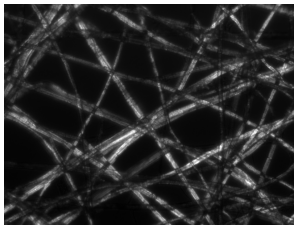

Cross-polarized light illumination, sample contrast comes from rotation of polarized light through the sample.

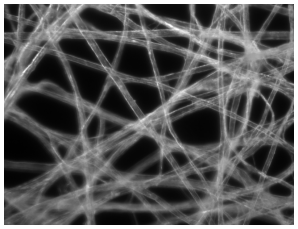

Dark field illumination, sample contrast comes from light scattered by the sample.

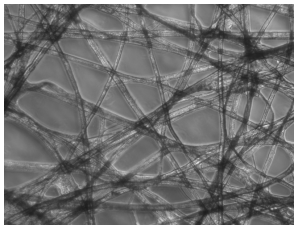

Phase contrast illumination, sample contrast comes from interference of different path lengths of light through the sample.

## Other techniques

Modern microscopes allow more than just observation of transmitted light image of a sample; there are many techniques which can be used to extract other kinds of data. Most of these require additional equipment in addition to a basic compound microscope.

- Reflected light, or incident, illumnation (for analysis of surface structures)
- Fluorescence microscopy, both:
  - Epifluorescence microscopy
  - Confocal microscopy
- Sample spectroscopy
- Automation (for automatic scanning of a large sample or image capture)

## Applications

Optical microscopy is used extensively in microelectronics, nanophysics, biotechnology, pharmaceutic research and microbiology.[5]

Optical microscopy is used for medical diagnosis, the field being termed histopathology when dealing with tissues, or in smear tests on free cells or tissue fragments.

## Optical microscope variants

There are many variants of the basic compound optical microscope design for specialized purposes. Some of these are physical design differences allowing specialization for certain purposes:

- Stereo microscope, a low powered microscope which provides a stereoscopic view of the sample, commonly used for dissection.
- Comparison microscope, which has two separate light paths allowing direct comparison of two samples via one image in each eye.
- Inverted microscope, for studying samples from below; useful for cell cultures in liquid.
- Student microscope, designed for low cost, durability, and ease of use.

A miniature USB microscope.

Other microscope variants are designed for different illumination techniques:

- Petrographic microscope, whose design usually includes a polarizing filter, rotating stage and gypsum plate to facilitate the study of minerals or other crystalline materials whose optical properties can vary with orientation.
- Polarizing microscope, similar to the petrographic microscope.
- Phase contrast microscope, which applies the phase contrast illumination method.
- Epifluorescence microscope, designed for analysis of samples which include fluorophores.
- Confocal microscope, a widely used variant of epifluorescent illumination which uses a scanning laser to illuminate a sample for fluorescence.

### Digital microscope

A digital microscope is a microscope equipped with a digital camera allowing observation of a sample via a computer. Microscopes can also be partly or wholly computer-controlled with various levels of automation. Digital microscopy allows greater analysis of a microscope image, for example measurements of distances and areas and quantitaton of a fluorescent or histological stain. Low-powered digital microscopes, USB microscopes, are also commercially available. These are essentially webcams with a high-powered macro lens and generally do not use transillumination. The camera attached directly to the USB port of a computer, so that the images are shown directly on the monitor. They offer modest magnifications (up to about 200×) without the need to use eyepieces, and at very low cost. The lack of illumination optics limits their use in a similar manner to stereo microscopes.

)

# Limitations

At very high magnifications with transmitted light, point objects are seen as fuzzy discs surrounded by diffraction rings. These are called Airy disks. The *resolving power* of a microscope is taken as the ability to distinguish between two closely spaced Airy disks (or, in other words the ability of the microscope to reveal adjacent structural detail as distinct and separate). It is these impacts of diffraction that limit the ability to resolve fine details. The extent and magnitude of the diffraction patterns are affected by both the wavelength of light ( $\lambda$ ), the refractive materials used to manufacture the objective lens and the numerical aperture (NA) of the objective lens. There is therefore a finite limit beyond which it is impossible to resolve separate points in the objective field, known as the diffraction limit. Assuming that optical aberrations in the whole optical set-up are negligible, the resolution *d*, can be stated as:

$$d = \frac{\lambda}{2NA}$$

Usually a wavelength of 550 nm is assumed, which corresponds to green light. With air as the external medium, the highest practical *NA* is 0.95, and with oil, up to 1.5. In practice the lowest value of *d* obtainable is about 200 nm.

## Surpassing the resolution limit

Multiple techniques are available for reaching resolutions higher than the transmitted light limit described above. Techniques for surpassing the resolution limit for bright field microscopy include ultraviolet microscopes, which use shorter wavelengths of light so the diffraction limit is lower. Holographic techniques, as described by Courjon and Bulabois in 1979, are also capable of breaking this resolution limit, although resolution was restricted in their experimental analysis.[6]

Using fluorescent samples more techniques are available. Examples include Vertico SMI, near field scanning optical microscopy which uses evanescent waves, and stimulated emission depletion. In 2005, a microscope capable of detecting a single molecule was described as a teaching tool.[7]

While most techniques focus on increases in lateral resolution there are also some techniques which aim to allow analysis of extremely thin samples. For example sarfus methods place the thin sample on a contrast-enhancing surface and thereby allows to directly visualize films as thin as 0.3 nanometers.

### STED

Stimulated emission depletion is a simple example of how higher resolution surpassing the diffraction limit is possible, but it has major limitations. STED is a fluorescence microscopy technique which uses a combination of light pulses to induce fluorescence in a small sub-population of fluorescent molecules in a sample. Each molecule produces a diffraction-limited spot of light in the image, and the centre of each of these spots corresponds to the location of the molecule. As the number of fluorescing molecules is low the spots of light are unlikely to overlap and therefore can be placed accurately. This process is then repeated many times to generate the image. Stefan Hell of the Max Planck Institute for Biophysical Chemistry was awarded the 10th German Future Prize in 2006 for his development of the STED microscope.[8]

## Alternatives

In order to overcome the limitations set by the diffraction limit of visible light other microscopes have been designed which use other waves.

- Atomic Force Microscope (AFM)
- Scanning Electron Microscope (SEM)
- Scanning Ion-Conductance Microscope (SICM)
- Scanning Tunneling Microscope (STM)
- Transmission Electron Microscope (TEM)
- X-ray microscope

The use of electrons and x-rays in place of light allows much higher resolution - the wavelength of the radiation is shorter so the diffraction limit is lower. To make the short-wavelength probe non-destructive, the atomic beam imaging system (atomic nanoscope) has been proposed and widely discussed in the literature, but it is not yet competitive with conventional imaging systems.

STM and AFM are scanning probe techniques using a small probe which is scanned over the sample surface. Resolution in these cases is limited by the size of the probe; micromachining techniques can produce probes with tip radii of 5-10 nm.

Additionally, methods such as electron or X-ray microscopy use a vacuum or partial vacuum, which limits their use for live and biological samples (with the exception of ESEM). The specimen chambers needed for all such instruments also limits sample size, and sample manipulation is more difficult. Color cannot be seen in images made by these methods, so some information is lost. They are however, essential when investigating molecular or atomic effects, such as age hardening in aluminium alloys, or the microstructure of polymers.

## See also

- Digital microscope
- Köhler illumination
- Microscope slide
- Objective

## References

[1] http://www.brianjford.com/wavrbcs.htm

[2] "*The Lying stones of Marrakech*", by Stephen Jay Gould, 2000

[3] Fi.it (http://brunelleschi.imss.fi.it/esplora/microscopio/dswmedia/risorse/testi_completi.pdf), "Il microscopio di Galileo"

[4] Stephen G. Lipson, Ariel Lipson, Henry Lipson, *Optical Physics 4th Edition*, Cambridge University Press, ISBN 9780521493451

[5] O1 Optical Microscopy (http://www.fy.chalmers.se/microscopy/students/imagecourse/O1.pdf) By Katarina Logg. Chalmers Dept. Applied Physics. 2006-01-20

[6] D. Courjon and J. Bulabois (1979). "Real Time Holographic Microscopy Using a Peculiar Holographic Illuminating System and a Rotary Shearing Interferometer". +*Journal of Optic* **10** (3).

[7] "Demonstration of a Low-Cost, Single-Molecule Capable, Multimode Optical Microscope" (http://chemeducator.org/bibs/0010004/1040269mk.htm). . Retrieved February 25, 2009.

[8] "German Future Prize for crossing Abbe's Limit" (http://www.heise.de/english/newsticker/news/81528). . Retrieved Feb 24, 2009.

## Further reading

- "Metallographic and Materialographic Specimen Preparation, Light Microscopy, Image Analysis and Hardness Testing", Kay Geels in collaboration with Struers A/S, ASTM International 2006.

## External links

- Antique Microscopes.com (http://www.antique-microscopes.com) A collection of early microscopes
- Historical microscopes (http://www.musoptin.com/mikro1.html), an illustrated collection with more than 3000 photos of scientific microscopes by European makers **(German)**
- The Golub Collection (http://golubcollection.berkeley.edu), A collection of 17th through 19th Century microscopes, including extensive descriptions
- *Molecular Expressions* (http://micro.magnet.fsu.edu/primer/anatomy/anatomy.html), concepts in optical microscopy
- Online tutorial of practical optical microscopy (http://www.doitpoms.ac.uk/tlplib/optical-microscopy/index.php)
- OpenWetWare (http://openwetware.org/wiki/Microscopy)
- Cell Centered Database (http://ccdb.ucsd.edu/sand/main?stype=lite&keyword=light microscopy&Submit=Go&event=display&start=1)
- Antonie van Leeuwenhoek: Father of Microscopy and Microbiology (http://www.juliantrubin.com/bigten/leeuwenhoek_microscope.html)

# Confocal microscope

**Confocal microscopy** is an optical imaging technique used to increase optical resolution and contrast of a micrograph by using point illumination and a spatial pinhole to eliminate out-of-focus light in specimens that are thicker than the focal plane.[1] It enables the reconstruction of three-dimensional structures from the obtained images. This technique has gained popularity in the scientific and industrial communities and typical applications are in life sciences, semiconductor inspection and material science.

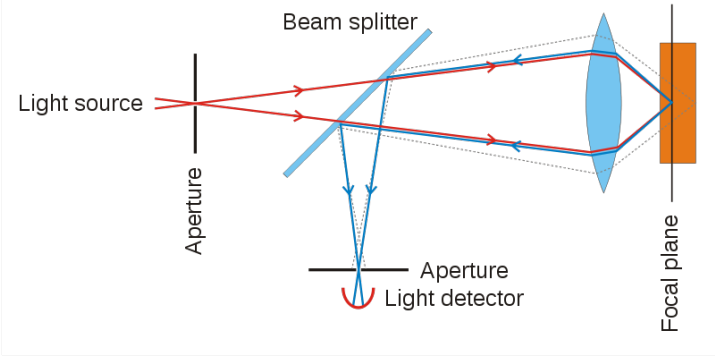


Principle of confocal microscopy

## Basic concept

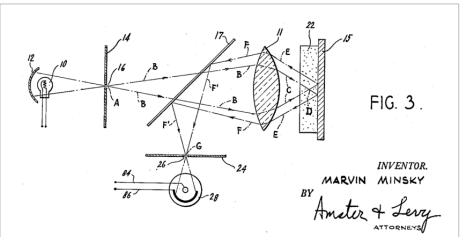

Confocal point sensor principle from Minsky's patent

The principle of confocal imaging was patented by Marvin Minsky[2] and aims to overcome some limitations of traditional wide-field fluorescence microscopes. In a conventional (i.e., wide-field) fluorescence microscope, the entire specimen is flooded evenly in light from a light source. All parts of the specimen in the optical path are excited at the same time and the resulting fluorescence is detected by the microscope's photodetector or camera including a large unfocused background part. In contrast, a confocal microscope uses point illumination (see Point Spread Function) and a pinhole in an optically conjugate plane in front of the detector to eliminate out-of-focus signal - the name "confocal" stems from this configuration. As only light produced by fluorescence very close to the focal plane can be detected the image optical resolution, particularly in the sample depth direction, is much better than that of wide-field microscopes. However, as much of the light from sample fluorescence is blocked at the pinhole, this increased resolution is at the cost of decreased signal intensity so long exposures are often required.

As only one point in the sample is illuminated at a time, 2D or 3D imaging requires scanning over a regular raster (i.e. a rectangular pattern of parallel scanning lines) in the specimen. The achievable thickness of the focal plane is defined mostly by the wavelength of the used light divided by the numerical aperture of the objective lens, but also by the optical properties of the specimen. The thin optical sectioning possible make these types of microscopes particularly good at 3D imaging and surface profiling of samples.

## Types

Three types of confocal microscopes are commercially available:

- **Confocal laser scanning microscopes**
- **Spinning-disk (Nipkow disk) confocal microscopes**
- **Programmable Array Microscopes (PAM)**

Each of these classes of confocal microscope have particular advantages and disadvantages, most systems are either optimised for resolution or high recording speed (i.e. video capture). Confocal laser scanning microscopes can have a programmable sampling density while Nipkow and PAM use a fixed sampling density defined by the camera resolution. Imaging frame rates are typically very slow for laser scanning systems (e.g. less than 3 frames/second). Commercial spinning-disk confocal microscopes achieve frame rates of over 50 per second[3] - a desirable feature for dynamic observations such as live cell imaging. So the spinning-disk as well as the programmble array microscopes [4] - can be seen as parallel versions of the confocal scanning principle. Cutting edge development of confocal laser scanning microscopy now allows better than video rate (60 frames/second) imaging by using multiple microelectromechanical systems based scanning mirrors.

Confocal x-ray fluorescence imaging is a newer technique that allows control over depth, in addition to horizontal and vertical aiming, for example, when analyzing buried layers in a painting.[5]

## Images

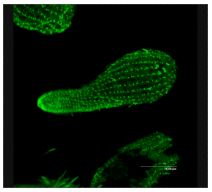

β-tubulin in *Tetrahymena* (a ciliated protozoan).

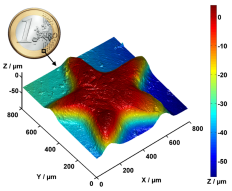

Partial surface profile of a 1-Euro coin, measured with a Nipkow Disk Confocal Microscope.

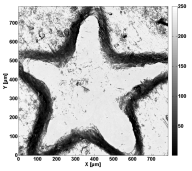

Reflection data for 1-Euro coin.

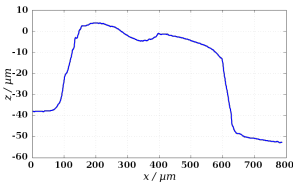

Cross section at y=200 through profile of 1-Euro coin.

## References


[1] Pawley JB (editor) (2006). *Handbook of Biological Confocal Microscopy* (3rd ed.). Berlin: Springer. ISBN 038725921X.

[2] Filed in 1957 and granted 1961. US 3013467 (http://v3.espacenet.com/textdoc?DB=EPODOC&IDX=US3013467)

[3] "Data Sheet of NanoFocus *µsurf* spinning disk confocal white light microscope" (http://www.nanofocus-us.com/fileadmin/user_upload/download/Produkte/NanoFocus-usurf_explore_.pdf) (pdf). .

[4] "Data Sheet of Sensofar 'PLu neox *Dual Technology sensor head combining Confocal and Interferometry techniques, as well as Spectroscopic Reflectometry"* (http://www.sensofar.com/products/products_neox.html). .

[5] Vincze L (2005). "Confocal X-ray Fluorescence Imaging and XRF Tomography for Three Dimensional Trace Element Microanalysis" (http://journals.cambridge.org/action/displayFulltext?type=1&fid=326128&jid=MAM&volumeId=11&issueId=S02&aid=326127). *Microscopy and Microanalysis* **11** (Supplement 2). doi:10.1017/S1431927605503167. .


## External links

- *Molecular Expressions*: (http://micro.magnet.fsu.edu) Laser Scanning Confocal Microscopy (http://micro.magnet.fsu.edu/primer/techniques/confocal/index.html)
- Nikon's MicroscopyU (http://www.microscopyu.com/articles/confocal/confocalintrobasics.html). Comprehensive introduction to confocal microscopy.
- Emory's Physics Department (http://www.physics.emory.edu/~weeks/confocal/). Introduction to confocal microscopy and fluorescence.
- The Science Creative Quarterly's overview of confocal microscopy (http://www.scq.ubc.ca/?p=278) - high res images also available.
- Programmable Array Microscope (http://spiedl.aip.org/getabs/servlet/GetabsServlet?prog=normal&id=PSISDG006441000001644 10S000001&idtype=cvips&gifs=yes) - Confocal Microscope Capabilities.

# Atomic force microscope

**Atomic force microscopy** (AFM) or scanning force microscopy (SFM) is a very high-resolution type of scanning probe microscopy, with demonstrated resolution on the order of fractions of a nanometer, more than 1000 times better than the optical diffraction limit. The precursor to the AFM, the scanning tunneling microscope, was developed by Gerd Binnig and Heinrich Rohrer in the early 1980s at IBM Research - Zurich, a development that earned them the Nobel Prize for Physics in 1986. Binnig, Quate and Gerber invented the first atomic force microscope (also abbreviated as AFM) in 1986. The first commercially available atomic force microscope was introduced in 1989. The AFM is one of the foremost tools for imaging, measuring, and manipulating matter at the nanoscale. The information is gathered by "feeling" the surface with a mechanical probe. Piezoelectric elements that facilitate tiny but accurate and precise movements on (electronic) command enable the very precise scanning. In some variations, electric potentials can also be scanned using conducting cantilevers. In newer more advanced versions, currents can even be passed through the tip to probe the electrical conductivity or transport of the underlying surface, but this is much more challenging with very few groups reporting reliable data.

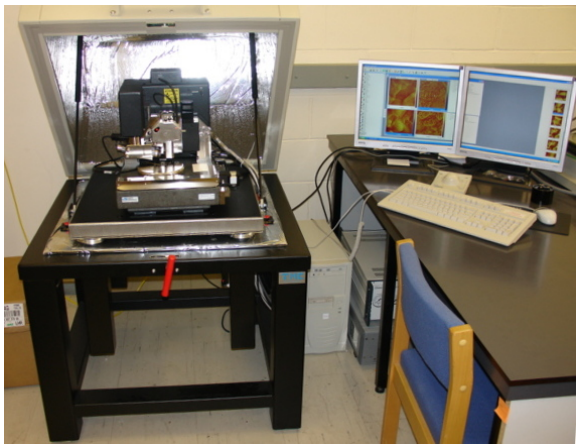

A commercial AFM setup

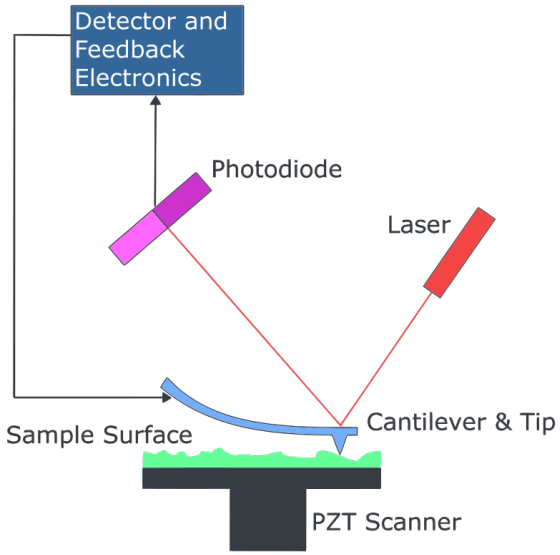


Block diagram of atomic force microscope

## Basic principles

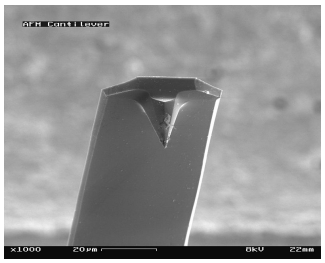

Electron micrograph of a used AFM cantilever image width ~100 micrometers...

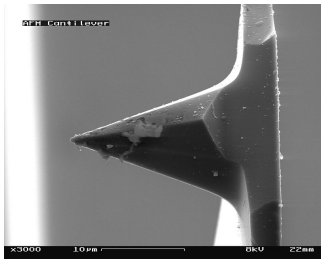

and ~30 micrometers

The AFM consists of a cantilever with a sharp tip (probe) at its end that is used to scan the specimen surface. The cantilever is typically silicon or silicon nitride with a tip radius of curvature on the order of nanometers. When the tip is brought into proximity of a sample surface, forces between the tip and the sample lead to a deflection of the cantilever according to Hooke's law. Depending on the situation, forces that are measured in AFM include mechanical contact force, van der Waals forces, capillary forces, chemical bonding, electrostatic forces, magnetic forces (see magnetic force microscope, MFM), Casimir forces, solvation forces, etc. Along with force, additional quantities may simultaneously be measured through the use of specialized types of probe (see scanning thermal microscopy, scanning joule expansion microscopy, photothermal microspectroscopy, etc.). Typically, the deflection is measured using a laser spot reflected from the top surface of the cantilever into an array of photodiodes. Other methods that are used include optical interferometry, capacitive sensing or piezoresistive AFM cantilevers. These cantilevers are fabricated with piezoresistive elements that act as a strain gauge. Using a Wheatstone bridge, strain in the AFM cantilever due to deflection can be measured, but this method is not as sensitive as laser deflection or interferometry.

If the tip was scanned at a constant height, a risk would exist that the tip collides with the surface, causing damage. Hence, in most cases a feedback mechanism is employed to adjust the tip-to-sample distance to maintain a constant force between the tip and the sample. Traditionally, the sample is mounted on a piezoelectric tube, that can move the sample in the $z$ direction for maintaining a constant force, and the $x$ and $y$ directions for scanning the sample. Alternatively a 'tripod' configuration of three piezo crystals may be employed, with each responsible for scanning in the x,y and z directions. This eliminates some of the distortion effects seen with a tube scanner. In newer designs, the tip is mounted on a vertical piezo scanner while the sample is being scanned in X and Y using another piezo block. The resulting map of the area $s = f(x,y)$ represents the topography of the sample.

The AFM can be operated in a number of modes, depending on the application. In general, possible imaging modes are divided into static (also called *contact*) modes and a variety of dynamic (or non-contact) modes where the cantilever is vibrated.

## Imaging modes

The primary modes of operation for an AFM are static mode and dynamic mode. In static mode, the cantilever is "dragged" across the surface of the sample and the contours of the surface are measured directly using the deflection of the cantilever. In the dynamic mode, the cantilever is externally oscillated at or close to its fundamental resonance frequency or a harmonic. The oscillation amplitude, phase and resonance frequency are modified by tip-sample interaction forces. These changes in oscillation with respect to the external reference oscillation provide information about the sample's characteristics.

### Contact mode

In the static mode operation, the static tip deflection is used as a feedback signal. Because the measurement of a static signal is prone to noise and drift, low stiffness cantilevers are used to boost the deflection signal. However, close to the surface of the sample, attractive forces can be quite strong, causing the tip to "snap-in" to the surface. Thus static mode AFM is almost always done in contact where the overall force is repulsive. Consequently, this technique is typically called "contact mode". In contact mode, the force between the tip and the surface is kept constant during scanning by maintaining a constant deflection.

## Non-contact mode

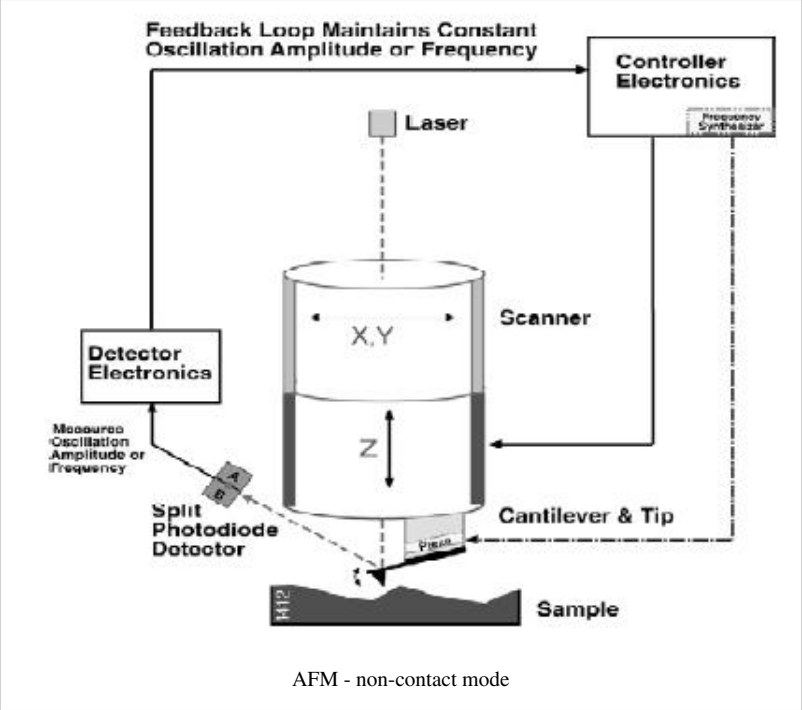


AFM - non-contact mode

In this mode, the tip of the cantilever does not contact the sample surface. The cantilever is instead oscillated at a frequency slightly above its resonance frequency where the amplitude of oscillation is typically a few nanometers (<10 nm). The van der Waals forces, which are strongest from 1 nm to 10 nm above the surface, or any other long range force which extends above the surface acts to decrease the resonance frequency of the cantilever. This decrease in resonance frequency combined with the feedback loop system maintains a constant oscillation amplitude or frequency by adjusting the average tip-to-sample distance. Measuring the tip-to-sample distance at each (x,y) data point allows the scanning software to construct a topographic image of the sample surface.

Non-contact mode AFM does not suffer from tip or sample degradation effects that are sometimes observed after taking numerous scans with contact AFM. This makes non-contact AFM preferable to contact AFM for measuring soft samples. In the case of rigid samples, contact and non-contact images may look the same. However, if a few monolayers of adsorbed fluid are lying on the surface of a rigid sample, the images may look quite different. An AFM operating in contact mode will penetrate the liquid layer to image the underlying surface, whereas in non-contact mode an AFM will oscillate above the adsorbed fluid layer to image both the liquid and surface.

Schemes for dynamic mode operation include frequency modulation and the more common amplitude modulation. In frequency modulation, changes in the oscillation frequency provide information about tip-sample interactions. Frequency can be measured with very high sensitivity and thus the frequency modulation mode allows for the use of very stiff cantilevers. Stiff cantilevers provide stability very close to the surface and, as a result, this technique was the first AFM technique to provide true atomic resolution in ultra-high vacuum conditions.[1]

In amplitude modulation, changes in the oscillation amplitude or phase provide the feedback signal for imaging. In amplitude modulation, changes in the phase of oscillation can be used to discriminate between different types of materials on the surface. Amplitude modulation can be operated either in the non-contact or in the intermittent contact regime. In dynamic contact mode, the cantilever is oscillated such that the separation distance between the cantilever tip and the sample surface is modulated.

Amplitude modulation has also been used in the non-contact regime to image with atomic resolution by using very stiff cantilevers and small amplitudes in an ultra-high vacuum environment.

### Tapping mode

In ambient conditions, most samples develop a liquid meniscus layer. Because of this, keeping the probe tip close enough to the sample for short-range forces to become detectable while preventing the tip from sticking to the surface presents a major problem for non-contact dynamic mode in ambient conditions. Dynamic contact mode (also called intermittent contact or tapping mode) was developed to bypass this problem.[3]

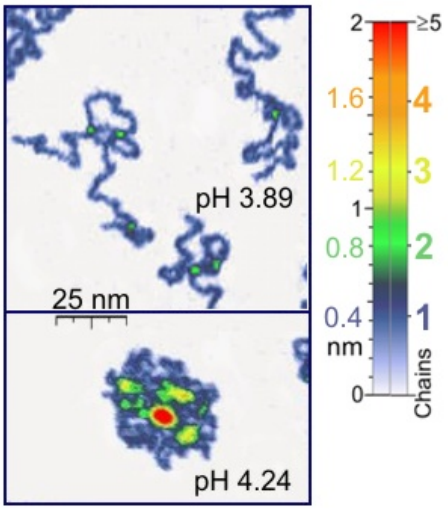


Single polymer chains (0.4 nm thick) recorded in a tapping mode under aqueous media with different pH.[2]

In *tapping mode*, the cantilever is driven to oscillate up and down at near its resonance frequency by a small piezoelectric element mounted in the AFM tip holder similar to non-contact mode. However, the amplitude of this oscillation is greater than 10 nm, typically 100 to 200 nm. Due to the interaction of forces acting on the cantilever when the tip comes close to the surface, Van der Waals force, dipole-dipole interaction, electrostatic forces, etc. cause the amplitude of this oscillation to decrease as the tip gets closer to the sample. An electronic servo uses the piezoelectric actuator to control the height of the cantilever above the sample. The servo adjusts the height to maintain a set cantilever oscillation amplitude as the cantilever is scanned over the sample. A *tapping AFM* image is therefore produced by imaging the force of the intermittent contacts of the tip with the sample surface.

This method of "tapping" lessens the damage done to the surface and the tip compared to the amount done in contact mode. Tapping mode is gentle enough even for the visualization of supported lipid bilayers or adsorbed single polymer molecules (for instance, 0.4 nm thick chains of synthetic polyelectrolytes) under liquid medium. With proper scanning parameters, the conformation of single molecules can remain unchanged for hours.[2]

## AFM cantilever deflection measurement

Laser light from a solid state diode is reflected off the back of the cantilever and collected by a position sensitive detector (PSD) consisting of two closely spaced photodiodes whose output signal is collected by a differential amplifier. Angular displacement of cantilever results in one photodiode collecting more light than the other photodiode, producing an output signal (the difference between the photodiode signals normalized by their sum) which is proportional to the deflection of the cantilever. It detects cantilever deflections <10 nm (thermal noise limited). A long beam path (several centimeters) amplifies changes in beam angle.

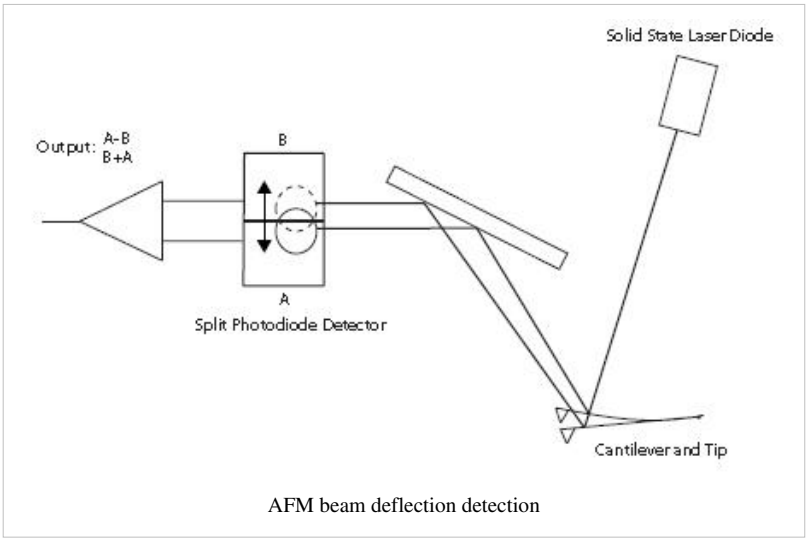


AFM beam deflection detection

## Force spectroscopy

Another major application of AFM (besides imaging) is force spectroscopy, the direct measurement of tip-sample interaction forces as a function of the gap between the tip and sample (the result of this measurement is called a force-distance curve). For this method, the AFM tip is extended towards and retracted from the surface as the deflection of the cantilever is monitored as a function of piezoelectric displacement. These measurements have been used to measure nanoscale contacts, atomic bonding, Van der Waals forces, and Casimir forces, dissolution forces in liquids and single molecule stretching and rupture forces.[4] Furthermore, AFM was used to measure in aqueous environment dispersion force due to polymer adsorbed on the substrate.[5] Forces of the order of a few piconewtons can now be routinely measured with a vertical distance resolution of better than 0.1 nanometers. Force spectroscopy can be performed with either static or dynamic modes. In dynamic modes, information about the cantilever vibration is monitored in addition to the static deflection.[6]

Problems with the technique include no direct measurement of the tip-sample separation and the common need for low stiffness cantilevers which tend to 'snap' to the surface. The snap-in can be reduced by measuring in liquids or by using stiffer cantilevers, but in the latter case a more sensitive deflection sensor is needed. By applying a small dither to the tip, the stiffness (force gradient) of the bond can be measured as well.[7]

## Identification of individual surface atoms

The AFM can be used to image and manipulate atoms and structures on a variety of surfaces. The atom at the apex of the tip "senses" individual atoms on the underlying surface when it forms incipient chemical bonds with each atom. Because these chemical interactions subtly alter the tip's vibration frequency, they can be detected and mapped. This principle was used to distinguish between atoms of silicon, tin and lead on an alloy surface, by comparing these 'atomic fingerprints' to values obtained from large-scale density functional theory (DFT) simulations.[8]

The trick is to first measure these forces precisely for each type of atom expected in the sample, and then to compare with forces given by DFT simulations. The team found that the tip interacted most strongly with silicon atoms, and interacted 23% and 41% less strongly with tin and lead atoms, respectively. Thus, each different type of atom can be identified in the matrix as the tip is moved across the surface.

Such a technique has been used now in biology and extended recently to cell biology. Forces corresponding to (i) the unbinding of receptor ligand couples (ii) unfolding of proteins (iii) cell adhesion at single cell scale have been gathered.

## Advantages and disadvantages

Just like any other tool, an AFM's usefulness has limitations. When determining whether or not analyzing a sample with an AFM is appropriate, there are various advantages and disadvantages that must be considered.

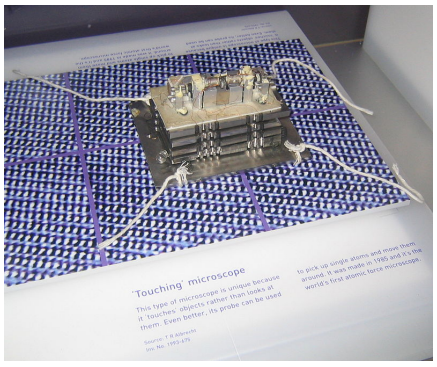

The first atomic force microscope

### Advantages

AFM has several advantages over the scanning electron microscope (SEM). Unlike the electron microscope which provides a two-dimensional projection or a two-dimensional image of a sample, the AFM provides a three-dimensional surface profile. Additionally,

samples viewed by AFM do not require any special treatments (such as metal/carbon coatings) that would irreversibly change or damage the sample. While an electron microscope needs an expensive vacuum environment for proper operation, most AFM modes can work perfectly well in ambient air or even a liquid environment. This makes it possible to study biological macromolecules and even living organisms. In principle, AFM can provide higher resolution than SEM. It has been shown to give true atomic resolution in ultra-high vacuum (UHV) and, more recently, in liquid environments. High resolution AFM is comparable in resolution to scanning tunneling microscopy and transmission electron microscopy.

### Disadvantages

A disadvantage of AFM compared with the scanning electron microscope (SEM) is the single scan image size. In one pass, the SEM can image an area on the order of square millimeters with a depth of field on the order of millimeters. Whereas the AFM can only image a maximum height on the order of 10-20 micrometers and a maximum scanning area of about 150×150 micrometers. One method of improving the scanned area size for AFM is by using parallel probes in a fashion similar to that of millipede data storage.

The scanning speed of an AFM is also a limitation. Traditionally, an AFM cannot scan images as fast as a SEM, requiring several minutes for a typical scan, while a SEM is capable of scanning at near real-time, although at relatively low quality. The relatively slow rate of scanning during AFM imaging often leads to thermal drift in the image[9] [10] making the AFM microscope less suited for measuring accurate distances between topographical features on the image. However, several fast-acting designs [11] [12] were suggested to increase microscope scanning productivity including what is being termed videoAFM (reasonable quality images are being obtained with videoAFM at video rate: faster than the average SEM). To eliminate image distortions induced by thermal drift, several methods have been introduced.[9] [10]

AFM images can also be affected by hysteresis of the piezoelectric material[13] and cross-talk between the *x*, *y*, *z* axes that may require software enhancement and filtering. Such filtering could "flatten" out real topographical features. However, newer AFMs utilize closed-loop scanners which practically eliminate these problems. Some AFMs also use separated orthogonal scanners (as opposed to a single tube) which also serve to eliminate part of the cross-talk problems.

As with any other imaging technique, there is the possibility of image artifacts, which could be induced by an unsuitable tip, a poor operating environment, or even by the sample itself. These image artifacts are unavoidable however, their occurrence and effect on results can be reduced through various methods.

Due to the nature of AFM probes, they cannot normally measure steep walls or overhangs. Specially made cantilevers and AFMs can be used to modulate the probe sideways as well as up and down (as with dynamic contact and non-contact modes) to measure sidewalls, at the cost of more expensive cantilevers, lower lateral resolution and additional artifacts.

## Piezoelectric scanners

AFM scanners are made from piezoelectric material, which expands and contracts proportionally to an applied voltage. Whether they elongate or contract depends upon the polarity of the voltage applied. The scanner is constructed by combining independently operated piezo electrodes for X, Y, and Z into a single tube, forming a scanner which can manipulate samples and probes with extreme precision in 3 dimensions.

Scanners are characterized by their sensitivity which is the ratio of piezo movement to piezo voltage, i.e., by how much the piezo material extends or contracts per applied volt. Because of differences in material or size, the sensitivity varies from scanner to scanner. Sensitivity varies non-linearly with respect to scan size. Piezo scanners exhibit more sensitivity at the end than at the beginning of a scan. This causes the forward and reverse scans to behave differently and display hysteresis[13] between the two scan directions. This can be corrected by applying a

non-linear voltage to the piezo electrodes to cause linear scanner movement and calibrating the scanner accordingly.[13]

The sensitivity of piezoelectric materials decreases exponentially with time. This causes most of the change in sensitivity to occur in the initial stages of the scanner's life. Piezoelectric scanners are run for approximately 48 hours before they are shipped from the factory so that they are past the point where they may have large changes in sensitivity. As the scanner ages, the sensitivity will change less with time and the scanner would seldom require recalibration.[14]

## See also

- Frictional force mapping
- Scanning tunneling microscope
- Scanning probe microscopy
- Scanning voltage microscopy
- Surface force apparatus

## References


[1] Giessibl, Franz J. (2003). "Advances in atomic force microscopy". *Reviews of Modern Physics* **75**: 949. doi:10.1103/RevModPhys.75.949.

[2] Roiter, Y; Minko, S (Nov 2005). "AFM single molecule experiments at the solid-liquid interface: in situ conformation of adsorbed flexible polyelectrolyte chains". *Journal of the American Chemical Society* **127** (45): 15688–9. doi:10.1021/ja0558239. ISSN 0002-7863. PMID 16277495.

[3] Zhong, Q; Inniss, D; Kjoller, K; Elings, V (1993). "Fractured polymer/silica fiber surface studied by tapping mode atomic force microscopy". *Surface Science Letters* **290**: L688. doi:10.1016/0167-2584(93)90906-Y.

[4] Hinterdorfer, P; Dufrêne, Yf (May 2006). "Detection and localization of single molecular recognition events using atomic force microscopy". *Nature methods* **3** (5): 347–55. doi:10.1038/nmeth871. ISSN 1548-7091. PMID 16628204.

[5] J Colloid Interface Sci. 2010 Jul 1;347(1):15-24. Epub 2010 Mar 7. Interaction of cement model systems with superplasticizers investigated by atomic force microscopy, zeta potential, and adsorption measurements. Ferrari L., Kaufmann J., Winnefeld F., Plank J.,

[6] Butt, H; Cappella, B; Kappl, M (2005). "Force measurements with the atomic force microscope: Technique, interpretation and applications". *Surface Science Reports* **59**: 1–152. doi:10.1016/j.surfrep.2005.08.003.

[7] M. Hoffmann, Ahmet Oral, Ralph A. G, Peter (2001). "Direct measurement of interatomic force gradients using an ultra-low-amplitude atomic force microscope". *Proceedings of the Royal Society a Mathematical Physical and Engineering Sciences* **457**: 1161. doi:10.1098/rspa.2000.0713.

[8] Sugimoto, Y; Pou, P; Abe, M; Jelinek, P; Pérez, R; Morita, S; Custance, O (Mar 2007). "Chemical identification of individual surface atoms by atomic force microscopy". *Nature* **446** (7131): 64–7. doi:10.1038/nature05530. ISSN 0028-0836. PMID 17330040.

[9] R. V. Lapshin (2004). "Feature-oriented scanning methodology for probe microscopy and nanotechnology" (http://www.nanoworld.org/homepages/lapshin/publications.htm#feature2004) (PDF). *Nanotechnology* (UK: IOP) **15** (9): 1135–1151. doi:10.1088/0957-4484/15/9/006. ISSN 0957-4484. .

[10] R. V. Lapshin (2007). "Automatic drift elimination in probe microscope images based on techniques of counter-scanning and topography feature recognition" (http://www.nanoworld.org/homepages/lapshin/publications.htm#automatic2007) (PDF). *Measurement Science and Technology* (UK: IOP) **18** (3): 907–927. doi:10.1088/0957-0233/18/3/046. ISSN 0957-0233. .

[11] G. Schitter, M. J. Rost (2008). "Scanning probe microscopy at video-rate" (http://www.materialstoday.com/view/2194/scanning-probe-microscopy-at-videorate/) (PDF). *Materials Today* (UK: Elsevier) **11** (special issue): 40–48. doi:10.1016/S1369-7021(09)70006-9. ISSN 1369-7021. .

[12] R. V. Lapshin, O. V. Obyedkov (1993). "Fast-acting piezoactuator and digital feedback loop for scanning tunneling microscopes" (http://www.nanoworld.org/homepages/lapshin/publications.htm#fast1993) (PDF). *Review of Scientific Instruments* (USA: AIP) **64** (10): 2883–2887. doi:10.1063/1.1144377. ISSN 0034-6748. .

[13] R. V. Lapshin (1995). "Analytical model for the approximation of hysteresis loop and its application to the scanning tunneling microscope" (http://www.nanoworld.org/homepages/lapshin/publications.htm#analytical1995) (PDF). *Review of Scientific Instruments* (USA: AIP) **66** (9): 4718–4730. doi:10.1063/1.1145314. ISSN 0034-6748. . ( is available).

[14] R. V. Lapshin (1998). "Automatic lateral calibration of tunneling microscope scanners" (http://www.nanoworld.org/homepages/lapshin/publications.htm#automatic1998) (PDF). *Review of Scientific Instruments* (USA: AIP) **69** (9): 3268–3276. doi:10.1063/1.1149091. ISSN 0034-6748. .

## External links

- ME 597/PHYS 570: Fundamentals of Atomic Force Microscopy (http://nanohub.org/resources/7320)
- DoITPoMS Teaching and Learning Package - Atomic Force Microscopy (http://www.doitpoms.ac.uk/tlplib/afm/index.php)
- SPM gallery: surface scans, collages, artworks, desktop wallpapers (http://www.nanoworld.org/homepages/lapshin/gallery.htm)

## Further reading

- SPM - Scanning Probe Microscopy Website (http://www.mobot.org/jwcross/spm/)
- Atomic Force Microscopy resource library (http://www.afmuniversity.org)
- R. W. Carpick and M. Salmeron, Scratching the surface: Fundamental investigations of tribology with atomic force microscopy (http://dx.doi.org/10.1021/cr960068q), Chemical Reviews, vol. 97, iss. 4, pp. 1163–1194 (2007).

# Electron microscope

An **electron microscope** is a type of microscope that produces an electronically-magnified image of a specimen for detailed observation. The electron microscope (EM) uses a particle beam of electrons to illuminate the specimen and create a magnified image of it. The microscope has a greater resolving power than a light-powered optical microscope, because it uses electrons that have wavelengths about 100,000 times shorter than visible light (photons), and can achieve magnifications of up to 2,000,000x, whereas ordinary, non-confocal light microscopes are limited to 2000x magnification.

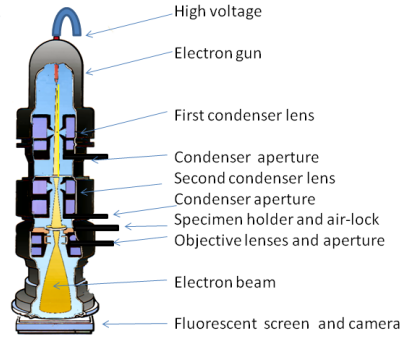

Diagram of a transmission electron microscope

The electron microscope uses electrostatic and electromagnetic "lenses" to control the electron beam and focus it to form an image. These lenses are analogous to, but different from the glass lenses of an optical microscope that form a magnified image by focusing light on or through the specimen. In transmission, the electron beam is first diffracted by the specimen, and then, the electron microscope “lenses" re-focus the beam into a Fourier-transformed image of the diffraction pattern for the selected area of investigation. The real image thus formed is a highly `magnified' image by a factor of several million, and can be then recorded on a special photographic plate, or viewed on a detecting screen. Electron microscopes are used to observe a wide range of biological and inorganic specimens including microorganisms, cells, large molecules, biopsy samples, metals, and crystals. Industrially, the electron microscope is primarily used for quality control and failure analysis in semiconductor device fabrication.

An electron microscope's advantages over X-ray crystallography are that the specimen need not be a single crystal or even a polycrystalline powder, and also that the Fourier transform reconstruction of the object's magnified structure occurs physically and thus avoids the need for solving the phase problem faced by the X-ray crystalographers after obatining their X-ray diffraction patterns of a single crystal or polycrystalline powder. The transmission electron microscope's major `disadvantage' is the need for extremely thin sections of the specimens, typically less than 10 nanometers. For biological specimens it also requires biological sample special `staining' with heavy atom labels in order to achieve the required contrast, and then chemical fixation as well as encasing with a polymer resin to stabilize the biological specimen which is thin sectioned.

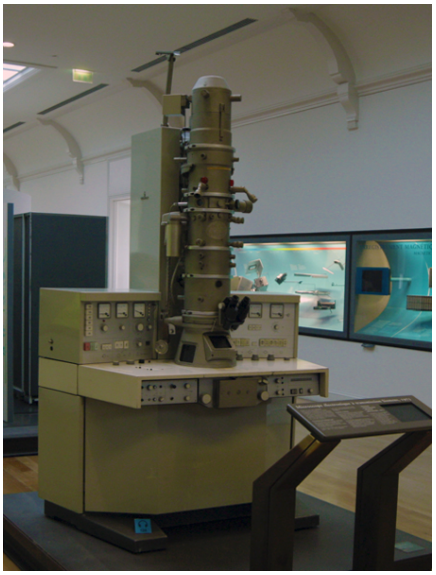

A 1973 Siemens electron microscope, Musée des Arts et Métiers, Paris

## History

In 1931, the German physicist Ernst Ruska and German electrical engineer Max Knoll constructed the prototype electron microscope, capable of four-hundred-power magnification; the apparatus was a practical application of the principles of electron microscopy.[1] Two years later, in 1933, Ruska built an electron microscope that exceeded the resolution attainable with an optical (lens) microscope.[1] Moreover, Reinhold Rudenberg, the scientific director of Siemens-Schuckertwerke, obtained the patent for the electron microscope in May 1931. Family illness compelled the electrical engineer to devise an electrostatic microscope, because he wanted to make visible the poliomyelitis virus.

In 1937, the Siemens company financed the development work of Ernst Ruska and Bodo von Borries, and employed Helmut Ruska (Ernst's brother) to develop applications for the microscope, especially with biologic specimens.[1] [2] Also in 1937, Manfred von Ardenne pioneered the scanning electron microscope.[3] The first *practical* electron microscope was constructed in 1938, at the University of Toronto, by Eli Franklin Burton and students Cecil Hall, James Hillier, and Albert Prebus; and Siemens produced the first *commercial* Transmission Electron Microscope (TEM) in 1939.[4] Although contemporary electron microscopes are capable of two million-power magnification, as scientific instruments, they remain based upon Ruska's prototype.

Electron microscope constructed by Ernst Ruska in 1933

# Types

### Transmission electron microscope (TEM)

The original form of electron microscope, the transmission electron microscope (TEM) uses a high voltage electron beam to create an image. The electrons are emitted by an electron gun, commonly fitted with a tungsten filament cathode as the electron source. The electron beam is accelerated by an anode typically at +100 keV (40 to 400 keV) with respect to the cathode, focused by electrostatic and electromagnetic lenses, and transmitted through the specimen that is in part transparent to electrons and in part scatters them out of the beam. When it emerges from the specimen, the electron beam carries information about the structure of the specimen that is magnified by the objective lens system of the microscope. The spatial variation in this information (the "image") is viewed by projecting the magnified electron image onto a fluorescent viewing screen coated with a phosphor or scintillator material such as zinc sulfide. The image can be photographically recorded by exposing a photographic film or plate directly to the electron beam, or a high-resolution phosphor may be coupled by means of a lens optical system or a fibre optic light-guide to the sensor of a CCD (charge-coupled device) camera. The image detected by the CCD may be displayed on a monitor or computer.

Resolution of the TEM is limited primarily by spherical aberration, but a new generation of aberration correctors have been able to partially overcome spherical aberration to increase resolution. Hardware correction of spherical aberration for the High Resolution TEM (HRTEM) has allowed the production of images with resolution below 0.5 Ångström (50 picometres)[5] at magnifications above 50 million times.[6] The ability to determine the positions of atoms within materials has made the HRTEM an important tool for nano-technologies research and development.[7]

### Scanning electron microscope (SEM)

Unlike the TEM, where electrons of the high voltage beam carry the image of the specimen, the electron beam of the Scanning Electron Microscope (SEM)[8] does not at any time carry a complete image of the specimen. The SEM produces images by probing the specimen with a focused electron beam that is scanned across a rectangular area of the specimen (raster scanning). At each point on the specimen the incident electron beam loses some energy, and that lost energy is converted into other forms, such as heat, emission of low-energy secondary electrons, light emission (cathodoluminescence) or x-ray emission. The display of the SEM maps the varying intensity of any of these signals into the image in a position corresponding to the position of the beam on the specimen when the signal was generated. In the SEM image of an ant shown at right, the image was constructed from signals produced by a secondary electron detector, the normal or conventional imaging mode in most SEMs.

An image of an ant in a scanning electron microscope

Generally, the image resolution of an SEM is about an order of magnitude poorer than that of a TEM. However, because the SEM image relies on surface processes rather than transmission, it is able to image bulk samples up to many centimetres in size and (depending on instrument design and settings) has a great depth of field, and so can produce images that are good representations of the three-dimensional shape of the sample.

### Reflection electron microscope (REM)

In the **Reflection Electron Microscope** (REM) as in the TEM, an electron beam is incident on a surface, but instead of using the transmission (TEM) or secondary electrons (SEM), the reflected beam of elastically scattered electrons is detected. This technique is typically coupled with Reflection High Energy Electron Diffraction (RHEED) and *Reflection high-energy loss spectrum (RHELS)*. Another variation is Spin-Polarized Low-Energy Electron Microscopy (SPLEEM), which is used for looking at the microstructure of magnetic domains.[9]

### Scanning transmission electron microscope (STEM)

The STEM rasters a focused incident probe across a specimen that (as with the TEM) has been thinned to facilitate detection of electrons scattered *through* the specimen. The high resolution of the TEM is thus possible in STEM. The focusing action (and aberrations) occur before the electrons hit the specimen in the STEM, but afterward in the TEM. The STEMs use of SEM-like beam rastering simplifies annular dark-field imaging, and other analytical techniques, but also means that image data is acquired in serial rather than in parallel fashion.

### Low voltage electron microscope (LVEM)

The low voltage electron microscope (LVEM) is a combination of SEM, TEM and STEM in one instrument, which operates at relatively low electron accelerating voltage of 5 kV. Low voltage increases image contrast which is especially important for biological specimens. This increase in contrast significantly reduces, or even eliminates the need to stain. Sectioned samples generally need to be thinner than they would be for conventional TEM (20-65 nm). Resolutions of a few nm are possible in TEM, SEM and STEM modes.[10] [11]

## Sample preparation

Materials to be viewed under an electron microscope may require processing to produce a suitable sample. The technique required varies depending on the specimen and the analysis required:

An insect coated in gold for viewing with a scanning electron microscope.

- *Chemical fixation* for biological specimens aims to stabilize the specimen's mobile macromolecular structure by chemical crosslinking of proteins with aldehydes such as formaldehyde and glutaraldehyde, and lipids with osmium tetroxide.
- *Cryofixation* – freezing a specimen so rapidly, to liquid nitrogen or even liquid helium temperatures, that the water forms vitreous (non-crystalline) ice. This preserves the specimen in a snapshot of its solution state. An entire field called cryo-electron microscopy has branched from this technique. With the development of cryo-electron microscopy of vitreous sections (CEMOVIS), it is now possible to observe samples from virtually any biological specimen close to its native state.
- *Dehydration* – freeze drying, or replacement of water with organic solvents such as ethanol or acetone, followed by critical point drying or infiltration with embedding resins.
- *Embedding, biological specimens* – after dehydration, tissue for observation in the transmission electron microscope is embedded so it can be sectioned ready for viewing. To do this the tissue is passed through a 'transition solvent' such as epoxy propane and then infiltrated with a resin such as Araldite epoxy resin; tissues may also be embedded directly in water-miscible acrylic resin. After the resin has been polymerised (hardened) the sample is thin sectioned (ultrathin sections) and stained - it is then ready for viewing.
- *Embedding, materials* - after embedding in resin, the specimen is usually ground and polished to a mirror-like finish using ultra-fine abrasives. The polishing process must be performed carefully to minimize scratches and

other polishing artifacts that reduce image quality.

- *Sectioning* – produces thin slices of specimen, semitransparent to electrons. These can be cut on an ultramicrotome with a diamond knife to produce ultrathin slices about 60-90 nm thick. Disposable glass knives are also used because they can be made in the lab and are much cheaper.
- *Staining* – uses heavy metals such as lead, uranium or tungsten to scatter imaging electrons and thus give contrast between different structures, since many (especially biological) materials are nearly "transparent" to electrons (weak phase objects). In biology, specimens are can be stained "en bloc" before embedding and also later after sectioning. Typically thin sections are stained for several minutes with an aqueous or alcoholic solution of uranyl acetate followed by aqueous lead citrate.
- *Freeze-fracture or freeze-etch* – a preparation method particularly useful for examining lipid membranes and their incorporated proteins in "face on" view. The fresh tissue or cell suspension is frozen rapidly (cryofixed), then fractured by simply breaking or by using a microtome while maintained at liquid nitrogen temperature. The cold fractured surface (sometimes "etched" by increasing the temperature to about −100 °C for several minutes to let some ice sublime) is then shadowed with evaporated platinum or gold at an average angle of 45° in a high vacuum evaporator. A second coat of carbon, evaporated perpendicular to the average surface plane is often performed to improve stability of the replica coating. The specimen is returned to room temperature and pressure, then the extremely fragile "pre-shadowed" metal replica of the fracture surface is released from the underlying biological material by careful chemical digestion with acids, hypochlorite solution or SDS detergent. The still-floating replica is thoroughly washed from residual chemicals, carefully fished up on fine grids, dried then viewed in the TEM.
- *Ion Beam Milling* – thins samples until they are transparent to electrons by firing ions (typically argon) at the surface from an angle and sputtering material from the surface. A subclass of this is Focused ion beam milling, where gallium ions are used to produce an electron transparent membrane in a specific region of the sample, for example through a device within a microprocessor. Ion beam milling may also be used for cross-section polishing prior to SEM analysis of materials that are difficult to prepare using mechanical polishing.
- *Conductive Coating* – an ultrathin coating of electrically-conducting material, deposited either by high vacuum evaporation or by low vacuum sputter coating of the sample. This is done to prevent the accumulation of static electric fields at the specimen due to the electron irradiation required during imaging. Such coatings include gold, gold/palladium, platinum, tungsten, graphite etc. and are especially important for the study of specimens with the scanning electron microscope. Another reason for coating, even when there is more than enough conductivity, is to improve contrast, a situation more common with the operation of a FESEM (field emission SEM).

## Disadvantages

Electron microscopes are expensive to build and maintain, but the capital and running costs of confocal light microscope systems now overlaps with those of basic electron microscopes. They are dynamic rather than static in their operation, requiring extremely stable high-voltage supplies, extremely stable currents to each electromagnetic coil/lens, continuously-pumped high- or ultra-high-vacuum systems, and a cooling water supply circulation through the lenses and pumps. As they are very sensitive to vibration and external magnetic fields, microscopes designed to achieve high resolutions must be housed in stable buildings (sometimes underground) with special services such as magnetic field cancelling systems. Some desktop low voltage electron microscopes have TEM capabilities at very low voltages (around 5 kV) without stringent voltage supply, lens coil current, cooling water or vibration isolation requirements and as such are much less expensive to buy and far easier to install and maintain, but do not have the same ultra-high (atomic scale) resolution capabilities as the larger instruments.

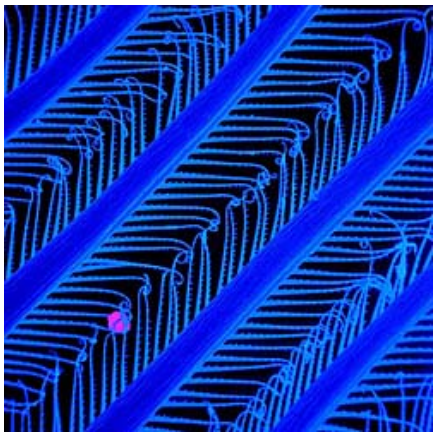

False-color SEM image of the filter setae of an Antarctic krill. (Raw electron microscope images carry no color information.)
**Pictured:** First degree filter setae with V-shaped second degree setae pointing towards the inside of the feeding basket. The purple ball is 1 μm in diameter.

The samples largely have to be viewed in vacuum, as the molecules that make up air would scatter the electrons. One exception is the environmental scanning electron microscope, which allows hydrated samples to be viewed in a low-pressure (up to 20 Torr/2.7 kPa), wet environment.

Scanning electron microscopes usually image conductive or semi-conductive materials best. Non-conductive materials can be imaged by an environmental scanning electron microscope. A common preparation technique is to coat the sample with a several-nanometer layer of conductive material, such as gold, from a sputtering machine; however, this process has the potential to disturb delicate samples.

Small, stable specimens such as carbon nanotubes, diatom frustules and small mineral crystals (asbestos fibres, for example) require no special treatment before being examined in the electron microscope. Samples of hydrated materials, including almost all biological specimens have to be prepared in various ways to stabilize them, reduce their thickness (ultrathin sectioning) and increase their electron optical contrast (staining). These processes may result in *artifacts*, but these can usually be identified by comparing the results obtained by using radically different specimen preparation methods. It is generally believed by scientists working in the field that as results from various preparation techniques have been compared and that there is no reason that they should all produce similar artifacts, it is reasonable to believe that electron microscopy features correspond with those of living cells. In addition, higher-resolution work has been directly compared to results from X-ray crystallography, providing independent confirmation of the validity of this technique. Since the 1980s, analysis of cryofixed, vitrified specimens has also become increasingly used by scientists, further confirming the validity of this technique.[12] [13] [14]

## Applications

Semiconductor and data storage

- Circuit edit
- Defect analysis
- Failure analysis

**Biology and life sciences**

- Diagnostic electron microscopy
- Cryobiology
- Protein localization
- Electron tomography
- Cellular tomography
- Cryo-electron microscopy
- Toxicology
- Biological production and viral load monitoring
- Particle analysis
- Pharmaceutical QC
- Structural biology
- 3D tissue imaging
- Virology
- Vitrification

Research

- Electron beam-induced deposition
- Materials qualification
- Materials and sample preparation
- Nanoprototyping
- Nanometrology
- Device testing and characterization

Industry

- High-resolution imaging
- 2D & 3D micro-characterization
- Macro sample to nanometer metrology
- Particle detection and characterization
- Direct beam-writing fabrication
- Dynamic materials experiments
- Sample preparation
- Forensics
- Mining (mineral liberation analysis)
- Chemical/Petrochemical

## See also

- Category:Electron microscope images
- Electron energy loss spectroscopy (EELS)
- Energy filtered transmission electron microscopy (EFTEM)
- Field emission microscope
- HiRISE
- High-resolution transmission electron microscopy (HRTEM)
- Scanning tunneling microscope
- Scanning confocal electron microscopy
- Scanning electron microscope (SEM)
- Scanning transmission electron microscope (STEM)
- Transmission Electron Aberration-corrected Microscope
- Electron diffraction
- X-ray diffraction
- X-ray microscope
- X-ray crystallography
- X-ray photoelectron spectroscopy (XPS)
- Microscope image processing
- Microscopy
- Acronyms in microscopy
- Nanoscience
- Nanotechnology
- Surface science
- *Ultramicroscopy* (journal)

## References


[1] Ernst Ruska (1986). "Ernst Ruska Autobiography" (http://nobelprize.org/nobel_prizes/physics/laureates/1986/ruska-autobio.html). Nobel Foundation. . Retrieved 2010-01-31.

[2] Kruger DH, Schneck P, Gelderblom HR (May 2000). "Helmut Ruska and the visualisation of viruses" (http://linkinghub.elsevier.com/retrieve/pii/S0140673600022509). *Lancet* **355** (9216): 1713–7. doi:10.1016/S0140-6736(00)02250-9. PMID 10905259. .

[3] M von Ardenne and D Beischer (1940). "Untersuchung von metalloxyd-rauchen mit dem universal-elektronenmikroskop" (in German). *Zeitschrift Electrochemie* **46**: 270–277.

[4] "James Hillier" (http://web.mit.edu/Invent/iow/hillier.html). *Inventor of the Week: Archive*. 2003-05-01. . Retrieved 2010-01-31.

[5] Erni, Rolf; Rossell, MD; Kisielowski, C; Dahmen, U (2009). "Atomic-Resolution Imaging with a Sub-50-pm Electron Probe". *Physical Review Letters* **102** (9): 096101. doi:10.1103/PhysRevLett.102.096101. PMID 19392535.

[6] "The Scale of Things" (http://www.sc.doe.gov/bes/scale_of_things.html). Office of Basic Energy Sciences, U.S. Department of Energy. 2006-05-26. . Retrieved 2010-01-31.

[7] O'Keefe MA, Allard LF (pdf). *Sub-Ångstrom Electron Microscopy for Sub-Ångstrom Nano-Metrology* (http://www.osti.gov/bridge/servlets/purl/821768-E3YVgN/native/821768.pdf). Information Bridge: DOE Scientific and Technical Information - Sponsored by OSTI. . Retrieved 2010-01-31.

[8] McMullan D (1993). "Scanning Electron Microscopy, 1928 - 1965" (http://www-g.eng.cam.ac.uk/125/achievements/mcmullan/mcm.htm). . Cincinnati, OH. . Retrieved 2010-01-31.

[9] "SPLEEM" (http://ncem.lbl.gov/frames/spleem.html). National Center for Electron Microscopy (NCEM). . Retrieved 2010-01-31.

[10] Nebesářová1, Jana; Vancová, Marie (2007). "How to Observe Small Biological Objects in Low Voltage Electron Microscope" (http://journals.cambridge.org/abstract_S143192760708124X). *Microscopy and Microanalysis* **13** (3): 248–249. .

[11] Drummy, Lawrence, F.; Yang, Junyan; Martin, David C. (2004). "Low-voltage electron microscopy of polymer and organic molecular thin films". *Ultramicroscopy* **99** (4): 247–256. doi:10.1016/j.ultramic.2004.01.011. PMID 15149719.

[12] Adrian, Marc; Dubochet, Jacques; Lepault, Jean; McDowall, Alasdair W. (1984). "Cryo-electron microscopy of viruses". *Nature* **308** (5954): 32–36. doi:10.1038/308032a0. PMID 6322001.

[13] Sabanay, I.; Arad, T.; Weiner, S.; Geiger, B. (1991). "Study of vitrified, unstained frozen tissue sections by cryoimmunoelectron microscopy" (http://jcs.biologists.org/cgi/content/abstract/100/1/227). *Journal of Cell Science* **100** (1): 227–236. PMID 1795028. .

[14] Kasas, S.; Dumas, G.; Dietler, G.; Catsicas, S.; Adrian, M. (2003). "Vitrification of cryoelectron microscopy specimens revealed by high-speed photographic imaging". *Journal of Microscopy* **211** (1): 48–53. doi:10.1046/j.1365-2818.2003.01193.x.


## External links

- Science Aid: Electron Microscopy (http://scienceaid.co.uk/biology/cell/analysingcells.html) High School (GCSE, A Level) resource
- Cell Centered Database - Electron microscopy data (http://ccdb.ucsd.edu/sand/main?typeid=4&event=showMPByType&start=1)

### General

- Nanohedron.com|Nano image gallery (http://www.nanohedron.com/) beautiful images generated with electron microscopes.
- electron microscopy (http://www.microscopy.ethz.ch) Website of the ETH Zurich: Very good graphics and images, which illustrate various procedures.
- Environmental Scanning Electron Microscope (ESEM) (http://www.danilatos.com)
- X-ray element analysis in electron microscope (http://www.microanalyst.net/index_e.phtml) – Information portal with X-ray microanalysis and EDX contents

### History

- John H.L. Watson: Very early Electron Microscopy in the Department of Physics, the University of Toronto – A personal recollection (http://www.physics.utoronto.ca/overview/history/microsco)
- Rubin Borasky Electron Microscopy Collection, 1930-1988 (http://americanhistory.si.edu/archives/d8452.htm) Archives Center, National Museum of American History, Smithsonian Institution.

### Other

- The Royal Microscopical Society, Electron Microscopy Section (UK) (http://www.rms.org.uk/em.shtml)
- Albert Lleal micrograph. Scanning Electron Micrograph Coloured SEM (http://www.albertlleal.com/microphotography.html)

# Synchrotron

A **synchrotron** is a particular type of cyclic particle accelerator in which the magnetic field (to turn the particles so they circulate) and the electric field (to accelerate the particles) are carefully synchronised with the travelling particle beam. The proton synchrotron was originally conceived by Sir Marcus Oliphant[1] . The honour of being the first to publish the idea went to Vladimir Veksler, and the first electron synchrotron was constructed by Edwin McMillan.

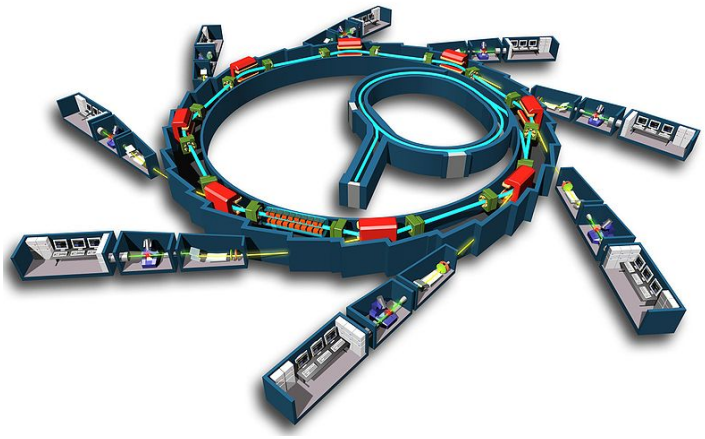

Here, the synchrotron is the circular track, off which the beamlines branch.

## Characteristics

While a cyclotron uses a constant magnetic field and a constant-frequency applied electric field (one of these is varied in the synchrocyclotron), both of these fields are varied in the synchrotron. By increasing these parameters appropriately as the particles gain energy, their path can be held constant as they are accelerated. This allows the vacuum chamber for the particles to be a large thin torus. In reality it is easier to use some straight sections between the bending magnets and some bent sections within the magnets giving the torus the shape of a round-cornered polygon. A path of large effective radius may thus be constructed using simple straight and curved pipe segments, unlike the disc-shaped chamber of the cyclotron type devices. The shape also allows and requires the use of multiple magnets to bend the particle beams. Straight sections are required at spacings around a ring for both radiofrequency cavities, and in third generation setups space is allowed for insertion of energy extraction devices such as wigglers and undulators.

The maximum energy that a cyclic accelerator can impart is typically limited by the strength of the magnetic field(s) and the minimum radius (maximum curvature) of the particle path.

The interior of the Australian Synchrotron facility. Dominating the image is the storage ring, showing the optical diagnostic beamline at front right. In the middle of the storage ring is the booster synchrotron and linac

In a cyclotron the maximum radius is quite limited as the particles start at the center and spiral outward, thus the entire path must be a self-supporting disc-shaped evacuated chamber. Since the radius is limited, the power of the machine becomes limited by the strength of the magnetic field. In the case of an ordinary electromagnet the field strength is limited by the saturation of the core (when all magnetic domains are aligned the field may not be further increased to any practical extent). The arrangement of the single pair of magnets the full width of the device also limits the economic size of the device.

Synchrotrons overcome these limitations, using a narrow beam pipe which can be surrounded by much smaller and more tightly focusing magnets. The ability of this device to accelerate particles is limited by the fact that the particles must be charged to be accelerated at all, but charged particles under acceleration emit photons (light), thereby losing energy. The limiting beam energy is reached when the energy lost to the lateral acceleration required to maintain the beam path in a circle equals the energy added each cycle. More powerful accelerators are built by using large radius paths and by using more numerous and more powerful microwave cavities to accelerate the particle beam between corners. Lighter particles (such as electrons) lose a larger fraction of their energy when turning. Practically speaking, the energy of electron/positron accelerators is limited by this radiation loss, while it does not play a significant role in the dynamics of proton or ion accelerators. The energy of those is limited strictly by the strength of magnets and by the cost.

## Design and operation

Particles are injected into the main ring at substantial energies by either a linear accelerator or by an intermediate synchrotron which is in turn fed by a linear accelerator. The "linac" is in turn fed by particles accelerated to intermediate energy by a simple high voltage power supply, typically a Cockcroft-Walton generator.

Starting from an appropriate initial value determined by the injection velocity the magnetic field is then increased. The particles pass through an electrostatic accelerator driven by a high alternating voltage. At particle speeds not close to the speed of light the frequency of the accelerating voltage can be made roughly proportional to the current in the bending magnets. A finer control of the frequency is performed by a servo loop which responds to the detection of the passing of the traveling group of particles. At particle speeds approaching light speed the frequency becomes more nearly constant, while the current in the bending magnets continues to increase. The maximum energy that can be applied to the particles (for a given ring size and magnet count) is determined by the saturation of the cores of the bending magnets (the point at which increasing current does not produce additional magnetic field). One way to obtain additional power is to make the torus larger and add additional bending magnets. This allows the amount of particle redirection at saturation to be less and so the particles can be more energetic. Another means of obtaining higher power is to use superconducting magnets, these not being limited by core saturation.

## Large synchrotrons

One of the early large synchrotrons, now retired, is the Bevatron, constructed in 1950 at the Lawrence Berkeley Laboratory. The name of this proton accelerator comes from its power, in the range of 6.3 GeV (then called BeV for billion electron volts; the name predates the adoption of the SI prefix giga-). A number of heavy elements, unseen in the natural world, were first created with this machine. This site is also the location of one of the first large bubble chambers used to examine the results of the atomic collisions produced here.

Modern industrial-scale synchrotrons can be very large (here, Soleil near Paris)

Another early large synchrotron is the Cosmotron built at Brookhaven National Laboratory which reached 3.3 GeV in 1953.[2]

Until August 2008, the highest energy synchrotron in the world was the Tevatron, at the Fermi National Accelerator Laboratory, in the United States. It accelerates protons and antiprotons to slightly less than 1 TeV of kinetic energy and collides them together. The Large Hadron Collider (LHC), which has been built at the European Laboratory for High Energy Physics (CERN), has roughly seven times this energy (so proton-proton collisions occur at roughly 14 TeV). It is housed in the 27 km tunnel which formerly housed the Large Electron Positron (LEP) collider, so it will maintain the claim as the largest scientific device ever built. The LHC will also accelerate heavy ions (such as lead) up to an energy of 1.15 PeV.

The largest device of this type seriously proposed was the Superconducting Super Collider (SSC), which was to be built in the United States. This design, like others, used superconducting magnets which allow more intense magnetic fields to be created without the limitations of core saturation. While construction was begun, the project was cancelled in 1994, citing excessive budget overruns — this was due to naïve cost estimation and economic management issues rather than any basic engineering flaws. It can also be argued that the end of the Cold War resulted in a change of scientific funding priorities that contributed to its ultimate cancellation. While there is still potential for yet more powerful proton and heavy particle cyclic accelerators, it appears that the next step up in electron beam energy must avoid losses due to synchrotron radiation. This will require a return to the linear accelerator, but with devices significantly longer than those currently in use. There is at present a major effort to design and build the International Linear Collider (ILC), which will consist of two opposing linear accelerators, one for electrons and one for positrons. These will collide at a total center of mass energy of 0.5 TeV.

However, synchrotron radiation also has a wide range of applications (see synchrotron light) and many 2nd and 3rd generation synchrotrons have been built especially to harness it. The largest of those 3rd generation synchrotron light sources are the European Synchrotron Radiation Facility (ESRF) in Grenoble, France, the Advanced Photon Source (APS) near Chicago, USA, and SPring-8 in Japan, accelerating electrons up to 6, 7 and 8 GeV, respectively.

Synchrotrons which are useful for cutting edge research are large machines, costing tens or hundreds of millions of dollars to construct, and each beamline (there may be 20 to 50 at a large synchrotron) costs another two or three million dollars on average. These installations are mostly built by the science funding agencies of governments of developed countries, or by collaborations between several countries in a region, and operated as infrastructure facilities available to scientists from universities and research organisations throughout the country, region, or world. More compact models, however, have been developed, such as the Compact Light Source.

## List of installations

| Synchrotron | Location & Country | Energy (GeV) | Circumference (m) | Commissioned | Decommissioned |
|---|---|---|---|---|---|
| Advanced Photon Source (APS) | Argonne National Laboratory, USA | 7.0 | 1104 | 1995 | |
| ALBA | Cerdanyola del Vallès near Barcelona, Spain | 3 | 270 | 2010 | |
| ISIS | Rutherford Appleton Laboratory, UK | 0.8 | 163 | 1985 | |
| Australian Synchrotron | Melbourne, Australia | 3 | 216 | 2006 | |
| ANKA | Karlsruhe Institute of Technology, Germany | 2.5 | 110.4 | 2000 | |
| LNLS | Campinas, Brazil | 1.37 | 93.2 | 1997 | |
| SESAME | Allaan, Jordan | 2.5 | 125 | Under Design | |
| Bevatron | Lawrence Berkeley Laboratory, USA | 6 | 114 | 1954 | 1993 |
| Advanced Light Source | Lawrence Berkeley Laboratory, USA | 1.9 | 196.8 | 1993 | |
| Cosmotron | Brookhaven National Laboratory, USA | 3 | 72 | 1953 | 1968 |
| National Synchrotron Light Source | Brookhaven National Laboratory, USA | 2.8 | 170 | 1982 | |
| Nimrod | Rutherford Appleton Laboratory, UK | 7 | | 1957 | 1978 |
| Alternating Gradient Synchrotron (AGS) | Brookhaven National Laboratory, USA | 33 | 800 | 1960 | |
| Stanford Synchrotron Radiation Lightsource | SLAC National Accelerator Laboratory, USA | 3 | 234 | 1973 | |
| Synchrotron Radiation Center (SRC) | Madison, USA | 1 | 121 | 1968 | |
| Cornell High Energy Synchrotron Source (CHESS) | Cornell University, USA | 5.5 | 768 | 1979 | |
| Soleil | Paris, France | 3 | 354 | 2006 | |
| Shanghai Synchrotron Radiation Facility (SSRF) | Shanghai, China | 3.5 | 432 | 2007 | |
| Proton Synchrotron | CERN, Switzerland | 28 | 628.3 | 1959 | |
| Tevatron | Fermi National Accelerator Laboratory, USA | 1000 | 6300 | 1983 | |
| Swiss Light Source | Paul Scherrer Institute, Switzerland | 2.8 | 288 | 2001 | |
| Large Hadron Collider (LHC) | CERN, Switzerland | 7000 | 26659 | 2008 | |
| BESSY II | Helmholtz-Zentrum Berlin in Berlin, Germany | 1.7 | 240 | 1998 | |
| European Synchrotron Radiation Facility (ESRF) | Grenoble, France | 6 | 844 | 1992 | |
| MAX-I | MAX-lab, Sweden | 0.55 | 30 | 1986 | |
| MAX-II | MAX-lab, Sweden | 1.5 | 90 | 1997 | |
| MAX-III | MAX-lab, Sweden | 0.7 | 36 | 2008 | |
| ELETTRA | Trieste, Italy | 2-2.4 | 260 | 1993 | |
| Synchrotron Radiation Source | Daresbury Laboratory, UK | 2 | 96 | 1980 | 2008 |

| | | | | | |
|---|---|---|---|---|---|
| ASTRID | Aarhus University, Denmark | 0.58 | 40 | 1991 | |
| Diamond Light Source | Oxfordshire, UK | 3 | 561.6 | 2006 | |
| DORIS III | DESY, Germany | 4.5 | 289 | 1980 | |
| PETRA II | DESY, Germany | 12 | 2304 | 1995 | 2007 |
| PETRA III | DESY, Germany | 6.5 | 2304 | 2009 | |
| Canadian Light Source | University of Saskatchewan, Canada | 2.9 | 171 | 2002 | |
| SPring-8 | RIKEN, Japan | 8 | 1436 | 1997 | |
| KEK | Tsukuba, Japan | 12 | | | |
| National Synchrotron Radiation Research Center | Hsinchu Science Park, Taiwan | 3.3 | 518.4 | 2008 | |
| Synchrotron Light Research Institute (SLRI) | Nakhon Ratchasima, Thailand | 1.2 | 81.4 | 2004 | |
| Indus 1 | Raja Ramanna Centre for Advanced Technology, Indore, India | 0.45 | 18.96 | 1999 | |
| Indus 2 | Raja Ramanna Centre for Advanced Technology, Indore, India | 2.5 | 36 | 2005 | |
| Synchrophasotron | JINR, Dubna, Russia | 10 | 180 | 1957 | 2005 |
| U-70 synchrotron | IHEP, Protvino, Russia | 70 | | 1967 | |
| CAMD | LSU, Louisiana, US | 1.5 | - | - | |
| PLS | PAL, Pohang, Korea | 2.5 | 280.56 | 1994 | |

- Note: in the case of colliders, the quoted energy is often double what is shown here. The above table shows the energy of one beam but if two opposing beams collide head on, the centre of mass energy is double the beam energy shown.

## Applications

- Life sciences: protein and large molecule crystallography
- LIGA based microfabrication
- Drug discovery and research
- "Burning" computer chip designs into metal wafers
- Studying molecule shapes and protein crystals
- Analysing chemicals to determine their composition
- Observing the reaction of living cells to drugs
- Inorganic material crystallography and microanalysis
- Fluorescence studies
- Semiconductor material analysis and structural studies
- Geological material analysis
- Medical imaging
- Proton therapy to treat some forms of cancer

## See also

- List of synchrotron radiation facilities
- Synchrotron X-ray tomographic microscopy
- Energy amplifier
- Superconducting Radio Frequency

## References

[1] Nature 407, 468 (28 September 2000) (http://www.nature.com/nature/journal/v407/n6803/full/407468a0.html).
[2] The Cosmotron (http://www.bnl.gov/bnlweb/history/cosmotron.asp)

## External links

- Canadian Light Source (http://www.lightsource.ca)
- Australian Synchrotron (http://www.synchrotron.org.au)
- Diamond UK Synchrotron (http://www.diamond.ac.uk)
- Lightsources.org (http://www.lightsources.org/cms/)
- CERN Large Hadron Collider (http://lhc-new-homepage.web.cern.ch/lhc-new-homepage)
- Synchrotron Light Sources of the World (http://www-als.lbl.gov/als/synchrotron_sources.html)
- A Miniature Synchrotron: (http://www.technologyreview.com/Biotech/20149/) room-size synchrotron offers scientists a new way to perform high-quality x-ray experiments in their own labs, *Technology Review*, February 04, 2008
- Brazilian Synchrotron Light Laboratory (http://www.lnls.br/lnls/cgi/cgilua.exe/sys/start.htm?UserActiveTemplate=lnls_2007_english&tpl=home)
- Podcast interview (http://omegataupodcast.net/2009/03/28/11-synchrotron-radiation-science-at-esrf/) with a scientist at the European Synchrotron Radiation Facility
- Indian SRS (http://www.cat.gov.in/index.html)

# X-ray microscope

An **X-ray microscope** uses electromagnetic radiation in the soft X-ray band to produce images of very small objects.

Unlike visible light, X-rays do not reflect or refract easily, and they are invisible to the human eye. Therefore the basic process of an X-ray microscope is to expose film or use a charge-coupled device (CCD) detector to detect X-rays that pass through the specimen. It is a contrast imaging technology using the difference in absorption of soft x-ray in the water window region (wavelength region: 2.3 - 4.4 nm, photon energy region: 0.28 - 0.53 keV) by the carbon atom (main element composing the living cell) and the oxygen atom (main element for water).

Early X-ray microscopes by Paul Kirkpatrick and Albert Baez used grazing-incidence reflective optics to focus the X-rays, which grazed X-rays off parabolic curved mirrors at a very high angle of incidence. An alternative method of focusing X-rays is to use a tiny fresnel zone plate of concentric gold or nickel rings on a silicon dioxide substrate. Sir Lawrence Bragg produced some of the first usable X-ray images with his apparatus in the late 1940's.

In the 1950's Newberry produced a shadow X-ray microscope which placed the specimen between the source and a target plate, this became the basis for the first commercial X-ray microscopes from the General Electric Company.

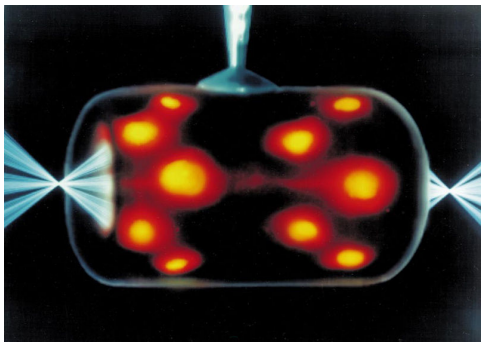

Indirect drive laser inertial confinement fusion uses a "hohlraum" which is irradiated with laser beam cones from either side on it its inner surface to bathe a fusion microcapsule inside with smooth high intensity X-rays. The highest energy X-rays which penetrate the hohlraum can be visualized using an X-ray microscope such as here, where X-radiation is represented in orange/red.

The Advanced Light Source (ALS)[1] in Berkeley CA is home to XM-1 (http://www.cxro.lbl.gov/BL612/), a full field soft X-ray microscope operated by the Center for X-ray Optics [2] and dedicated to various applications in modern nanoscience, such as nanomagnetic materials, environmental and materials sciences and biology. XM-1 uses an X-ray lens to focus X-rays on a CCD, in a manner similar to an optical microscope. XM-1 still holds the world record in spatial resolution with Fresnel zone plates down to 15nm and is able to combine high spatial resolution with a sub-100ps time resolution to study e.g. ultrafast spin dynamics.

The ALS is also home to the world's first soft x-ray microscope designed for biological and biomedical research. This new instrument, XM-2 was designed and built by scientists from the National Center for X-ray Tomography (http://ncxt.lbl.gov).XM-2 is capable of producing 3-Dimensional tomograms of cells.

Sources of soft X-rays suitable for microscopy, such as synchrotron radiation sources, have fairly low brightness of the required wavelengths, so an alternative method of image formation is scanning transmission soft X-ray microscopy. Here the X-rays are focused to a point and the sample is mechanically scanned through the produced focal spot. At each point the transmitted X-rays are recorded with a detector such as a proportional counter or an avalanche photodiode. This type of Scanning Transmission X-ray Microscope (STXM) was first developed by researchers at Stony Brook University and was employed at the National Synchrotron Light Source at Brookhaven National Laboratory.

The resolution of X-ray microscopy lies between that of the optical microscope and the electron microscope. It has an advantage over conventional electron microscopy in that it can view biological samples in their natural state. Electron microscopy is widely used to obtain images with nanometer level resolution but the relatively thick living cell cannot be observed as the sample has to be chemically fixed, dehydrated, embedded in resin, then sliced ultra thin. However, it should be mentioned that cryo-electron microscopy allows the observation of biological specimens in their hydrated natural state, albeit embedded in water ice. Until now, resolutions of 30 nanometer are possible using the Fresnel zone plate lens which forms the image using the soft x-rays emitted from a synchrotron. Recently, the use of soft x-rays emitted from laser-produced plasmas rather than synchrotron radiation is becoming more

popular.

Additionally, X-rays cause fluorescence in most materials, and these emissions can be analyzed to determine the chemical elements of an imaged object. Another use is to generate diffraction patterns, a process used in X-ray crystallography. By analyzing the internal reflections of a diffraction pattern (usually with a computer program), the three-dimensional structure of a crystal can be determined down to the placement of individual atoms within its molecules. X-ray microscopes are sometimes used for these analyses because the samples are too small to be analyzed in any other way.

## See also

- Synchrotron X-ray tomographic microscopy
- Electron microscope

## External links

- Application of X-ray microscopy in analysis of living hydrated cells [3]
- Hard X-ray microbeam experiments with a sputtered-sliced Fresnel zone plate and its applications [4]
- Scientific applications of soft x-ray microscopy [5]

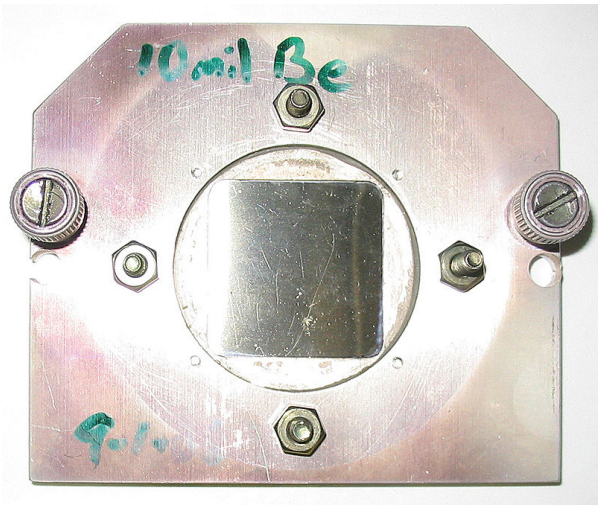


A square beryllium foil mounted in a steel case to be used as a window between a vacuum chamber and an X-ray microscope. Beryllium, due to its low Z number is highly transparent to X-rays.

## References

[1] http://www-als.lbl.gov
[2] http://www.cxro.lbl.gov
[3] http://www.ncbi.nlm.nih.gov/entrez/query.fcgi?cmd=Retrieve&db=pubmed&dopt=Abstract&list_uids=12379938
[4] http://www.ncbi.nlm.nih.gov/entrez/query.fcgi?cmd=Retrieve&db=pubmed&dopt=Abstract&list_uids=11972376
[5] http://www.cxro.lbl.gov/BL612/index.php?content=research.html

# Field emission microscope

**Field emission microscopy** (FEM) is an analytical technique used in materials science to investigate molecular surface structures and their electronic properties.[1] Invented by Erwin Wilhelm Müller in 1936, the FEM was one of the first surface analysis instruments that approached near-atomic resolution.

## Introduction

Microscopy techniques are used to produce real space magnified images of a surface showing what it looks like. In general microscopy information concerns surface crystallography (i.e. how the atoms are arranged at the surface, surface morphology (i.e. the shape and size of topographic features making the surface), and surface composition (the elements and compounds the surface is composed of).

Field emission microscopy (FEM) was invented by Erwin Müller in 1936. In FEM, the phenomenon of field electron emission was used to obtain an image on the detector on the basis of the difference in work function of the various crystallographic planes on the surface.

## Design

A Field Emission Microscope consists of a metallic sample in the form of a sharp tip and a conducting fluorescent screen enclosed in ultrahigh vacuum. The tip radius used is typically of the order of 100 nm. The sample is held at a large negative potential (1-10 kV) relative to the fluorescent screen. This gives the electric field near the tip apex to be the order of $10^{10}$ V/m which is high enough for field emission of electrons to take place. Fig.1 shows the experimental set up for FEM.

The field emitted electrons travel along the field lines and produce bright and dark patches on the fluorescent screen giving a one-to-one correspondence with the crystal planes of the hemispherical emitter. The emission current varies strongly with the local work function in accordance with the Fowler-Nordheim equation; hence, the FEM image displays the projected work function map of the emitter surface. The closely packed faces have higher work functions than atomically rough regions and thus they show up in the image as dark spots on the brighter background. In short, the work function anisotropy of the crystal planes is mapped onto the screen as intensity variations.

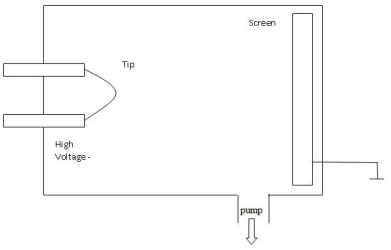

Fig.1:FEM experimental set-up

The magnification is given by the ratio $M = L/R$, where $R$ is the tip apex radius and $L$ is the tip-screen distance. Linear magnifications of about $10^5$ to $10^6$ are attained. The spatial resolution of this technique is of the order of 2 nm and is limited by the momentum of the emitted electrons parallel to the tip surface, which is of the order of the Fermi velocity of the electron in metal.

It is possible to set up an FEM with a probe hole in the phosphor screen and a Faraday cup collector behind it to collect the current emitted from a single plane. This technique allows the measurement of the variation of work function with orientation for a wide variety of orientations on a single sample. The FEM has also been used to study adsorption and surface diffusion processes, making use of the work function change associated with the adsorption process.

Field emission requires a very good vacuum, and often, even in ultra high vacuum (UHV), emission is not due to the clean surface. A typical field emitter needs to be 'flashed' to clean it, usually by passing a current through a loop on which it is mounted. After flashing the emission current is high but unstable. The current decays with time and in the process becomes more stable due to the contamination of the tip, either from the vacuum, or more often from

diffusion of adsorbed surface species to the tip. Thus the real nature of the FEM tips during use is somewhat unknown.

Application of FEM is limited by the materials which can be fabricated in the shape of a sharp tip, can be used in a UHV environment, and can tolerate the high electrostatic fields. For these reasons, refractory metals with high melting temperature (for e.g. W, Mo, Pt, Ir) are conventional objects for FEM experiments.

## See also

- Atom Probe
- Electron microscope
- Field ion microscope
- List of surface analysis methods

## References

[1] "Intro to Field Emission" (http://physics.unipune.ernet.in/~fem/intro-fem.htm). Field Emission / Ion Microscopy Laboratory, Purdue University, Dept. of Physics. . Retrieved 2007-05-10.

- 2. K.Oura, V.G.Lifshits, A.ASaranin, A.V.Zotov and M.Katayama, Surface Science – An Introduction, (Springer-Verlag Berlin Heidelberg 2003).
- 3. John B. Hudson, Surface Science – An Introduction, (BUTTERWORTH-Heinemann 1992).

# Scanning tunneling microscope

A **scanning tunneling microscope** (STM) is an instrument for imaging surfaces at the atomic level. Its development in 1981 earned its inventors, Gerd Binnig and Heinrich Rohrer (at IBM Zürich), the Nobel Prize in Physics in 1986.[1] [2] For an STM, good resolution is considered to be 0.1 nm lateral resolution and 0.01 nm depth resolution.[3] With this resolution, individual atoms within materials are routinely imaged and manipulated. The STM can be used not only in ultra high vacuum but also in air, water, and various other liquid or gas ambients, and at temperatures ranging from near zero kelvin to a few hundred degrees Celsius.[4]

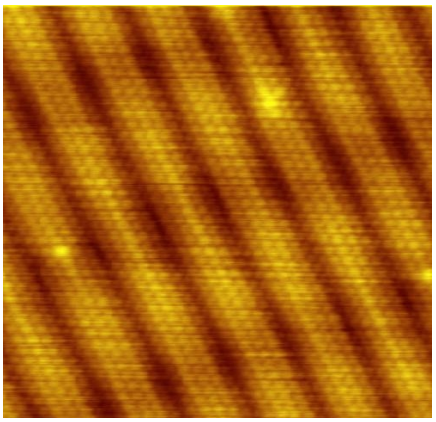

Image of reconstruction on a clean Gold(100) surface

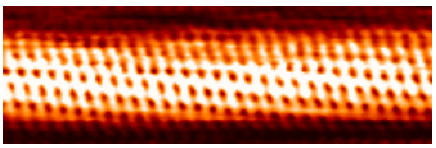

An STM image of single-walled carbon nanotube

The STM is based on the concept of quantum tunneling. When a conducting tip is brought very near to the surface to be examined, a bias (voltage difference) applied between the two can allow electrons to tunnel through the vacuum between them. The resulting *tunneling current* is a function of tip position, applied voltage, and the local density of states (LDOS) of the sample.[4] Information is acquired by monitoring the current as the tip's position scans across the surface, and is usually displayed in image form. STM can be a challenging technique, as it requires extremely clean and stable surfaces, sharp tips, excellent vibration control, and sophisticated electronics.

## Procedure

First, a voltage bias is applied and the tip is brought close to the sample by some coarse sample-to-tip control, which is turned off when the tip and sample are sufficiently close. At close range, fine control of the tip in all three dimensions when near the sample is typically piezoelectric, maintaining tip-sample separation W typically in the 4-7 Å range, which is the equilibrium position between attractive (3<W<10Å) and repulsive (W<3Å) interactions[4] . In this situation, the voltage bias will cause electrons to tunnel between the tip and sample, creating a current that can be measured. Once tunneling is established, the tip's bias and position with respect to the sample can be varied (with the details of this variation depending on the experiment) and data is obtained from the resulting changes in current.

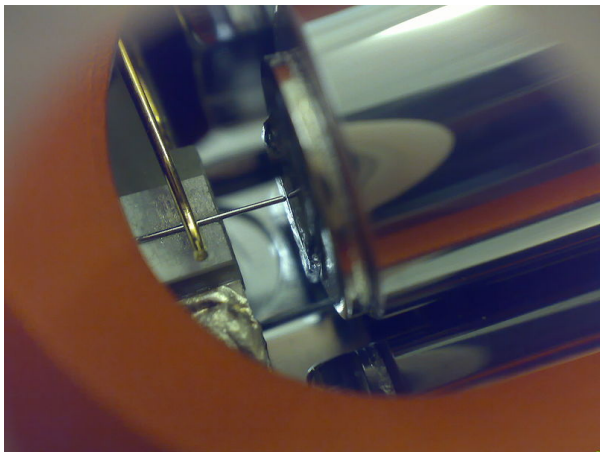

A close-up of a simple scanning tunneling microscope head using a platinum-iridium stylus.

If the tip is moved across the sample in the x-y plane, the changes in surface height and density of states cause changes in current. These changes are mapped in images. This change in current with respect to position can be measured itself, or the height, z, of the tip corresponding to a constant current can be measured[4] . These two modes are called constant height mode and constant current mode, respectively. In constant current mode, feedback electronics adjust the height by a voltage to the piezoelectric height control mechanism[5] . This leads to a height variation and thus the image comes from the tip topography across the sample and gives a constant charge density surface; this means contrast on the image is due to variations in charge density[6] . In constant height mode, the voltage and height are both held constant while the current changes to keep the voltage from changing; this leads to an image made of current changes over the surface, which can be related to charge density[6] . The benefit to using a constant height mode is that it is faster, as the piezoelectric movements require more time to register the change in constant current mode than the voltage response in constant height mode[6] . All images produced by STM are grayscale, with color optionally added in post-processing in order to visually emphasize important features.

In addition to scanning across the sample, information on the electronic structure at a given location in the sample can be obtained by sweeping voltage and measuring current at a specific location[3] . This type of measurement is called scanning tunneling spectroscopy (STS) and typically results in a plot of the local density of states as a function of energy within the sample. The advantage of STM over other measurements of the density of states lies in its ability to make extremely local measurements: for example, the density of states at an impurity site can be compared to the density of states far from impurities.[7]

Framerates of at least 1 Hz enable so called Video-STM (up to 50 Hz is possible).[8] [9] This can be used to scan surface diffusion.[10]

## Instrumentation

The components of an STM include scanning tip, piezoelectric controlled height and x,y scanner, coarse sample-to-tip control, vibration isolation system, and computer[5] .

The resolution of an image is limited by the radius of curvature of the scanning tip of the STM. Additionally, image artifacts can occur if the tip has two tips at the end rather than a single atom; this leads to "double-tip imaging," a situation in which both tips contribute to the tunneling[3] . Therefore it has been essential to develop processes for consistently obtaining sharp, usable tips. Recently, carbon nanotubes have been used in this instance.[11]

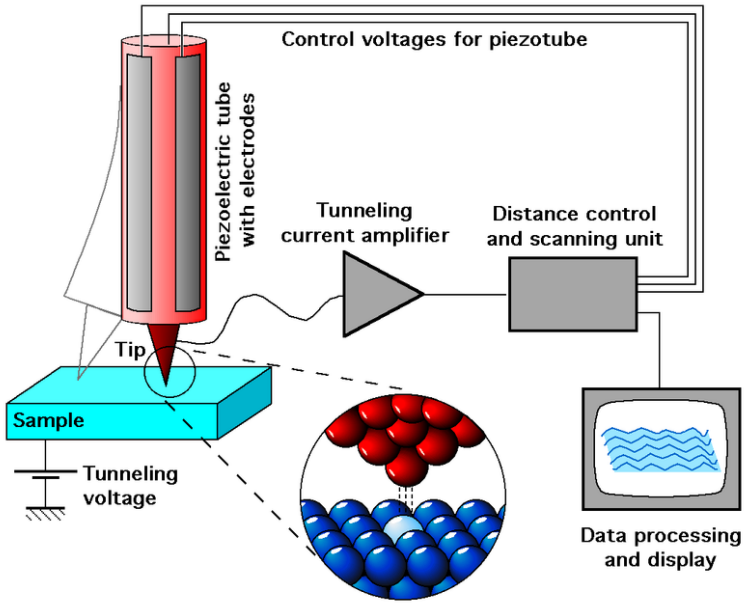


Schematic view of an STM

The tip is often made of tungsten or platinum-iridium, though gold is also used[3] . Tungsten tips are usually made by electrochemical etching, and platinum-iridium tips by mechanical shearing[3] .

Due to the extreme sensitivity of tunnel current to height, proper vibration isolation or an extremely rigid STM body is imperative for obtaining usable results. In the first STM by Binnig and Rohrer, magnetic levitation was used to keep the STM free from vibrations; now mechanical spring or gas spring systems are often used[4] . Additionally, mechanisms for reducing eddy currents are sometimes implemented.

Maintaining the tip position with respect to the sample, scanning the sample and acquiring the data is computer controlled[5] . The computer may also be used for enhancing the image with the help of image processing[12] [13] as well as performing quantitative measurements.[14]

## Other STM related studies

Many other microscopy techniques have been developed based upon STM. These include photon scanning microscopy (PSTM), which uses an optical tip to tunnel photons[3] ; scanning tunneling potentiometry (STP), which measures electric potential across a surface[3] ; spin polarized scanning tunneling microscopy (SPSTM), which uses a ferromagnetic tip to tunnel spin-polarized electrons into a magnetic sample,[15] and atomic force microscopy (AFM), in which the force caused by interaction between the tip and sample is measured.

Other STM methods involve manipulating the tip in order to change the topography of the sample. This is attractive for several reasons. Firstly the STM has an atomically precise positioning system which allows very accurate atomic scale manipulation. Furthermore, after the

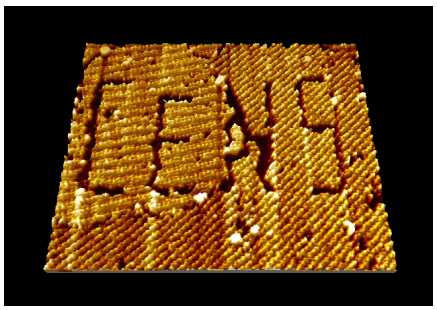

Nanomanipulation via STM of a self-assembled organic semiconductor monolayer (here: PTCDA molecules) on graphite, in which the logo of the Center for NanoScience (CeNS), LMU has been written.

surface is modified by the tip, it is a simple matter to then image with the same tip, without changing the instrument. IBM researchers developed a way to manipulate Xenon atoms absorbed on a nickel surface[3] This technique has been used to create electron "corrals" with a small number of adsorbed atoms, which allows the STM to be used to observe electron Friedel oscillations on the surface of the material. Aside from modifying the actual sample surface, one can also use the STM to tunnel electrons into a layer of E-Beam photoresist on a sample, in order to do lithography. This has the advantage of offering more control of the exposure than traditional Electron beam lithography. Another practical application of STM is atomic deposition of metals (Au, Ag, W, etc.) with any desired (pre-programmed) pattern, which can be used as contacts to nanodevices or as nanodevices themselves.

Recently groups have found they can use the STM tip to rotate individual bonds within single molecules. The electrical resistance of the molecule depends on the orientation of the bond, so the molecule effectively becomes a molecular switch.

## Principle of operation

Tunneling is a functioning concept that arises from quantum mechanics. Classically, an object hitting an impenetrable barrier will not pass through. In contrast, objects with a very small mass, such as the electron, have wavelike characteristics which permit such an event, referred to as tunneling.

Electrons behave as beams of energy, and in the presence of a potential $U(z)$, assuming 1-dimensional case, the energy levels $\psi_n(z)$ of the electrons are given by solutions to Schrödinger's equation,

$$-\frac{\hbar^2}{2m}\frac{\partial^2\psi_n(z)}{\partial z^2} + U(z)\psi_n(z) = E\psi_n(z),$$

where $\hbar$ is the reduced Planck's constant, $z$ is the position, and $m$ is the mass of an electron[4] . If an electron of energy $E$ is incident upon an energy barrier of height $U(z)$, the electron wave function is a traveling wave solution,

$$\psi_n(z) = \psi_n(0)e^{\pm ikz},$$

where

$$k = \frac{\sqrt{2m(E-U(z))}}{\hbar}$$

if $E > U(z)$, which is true for a wave function inside the tip or inside the sample[4] . Inside a barrier, $E < U(z)$ so the wave functions which satisfy this are decaying waves,

$$\psi_n(z) = \psi_n(0)e^{\pm\kappa z},$$

where

$$\kappa = \frac{\sqrt{2m(U-E)}}{\hbar}$$

quantifies the decay of the wave inside the barrier, with the barrier in the $+z$ direction for $-\kappa$ [4] .

Knowing the wave function allows one to calculate the probability density for that electron to be found at some location. In the case of tunneling, the tip and sample wave functions overlap such that when under a bias, there is some finite probability to find the electron in the barrier region and even on the other side of the barrier[4] . Let us assume the bias is $V$ and the barrier width is $W$. This probability, $P$, that an electron at $z$=0 (left edge of barrier) can be found at $z$=$W$ (right edge of barrier) is proportional to the wave function squared,

$$P \propto |\psi_n(0)|^2 e^{-2\kappa W}$$ [4].

If the bias is small, we can let $U - E \approx \varphi M$ in the expression for $\kappa$, where $\varphi M$, the work function, gives the minimum energy needed to bring an electron from an occupied level, the highest of which is at the Fermi level (for metals at $T$=0 kelvins), to vacuum level. When a small bias $V$ is applied to the system, only electronic states very near the Fermi level, within $eV$ (a product of electron charge and voltage, not to be confused here with electronvolt unit), are

excited[4] . These excited electrons can tunnel across the barrier. In other words, tunneling occurs mainly with electrons of energies near the Fermi level.

However, tunneling does require that there is an empty level of the same energy as the electron for the electron to tunnel into on the other side of the barrier. It is because of this restriction that the tunneling current can be related to the density of available or filled states in the sample. The current due to an applied voltage $V$ (assume tunneling occurs sample to tip) depends on two factors: 1) the number of electrons between $E_f$ and $eV$ in the sample, and 2) the number among them which have corresponding free states to tunnel into on the other side of the barrier at the tip[4] . The higher density of available states the greater the tunneling current. When $V$ is positive, electrons in the tip tunnel into empty states in the sample; for a negative bias, electrons tunnel out of occupied states in the sample into the tip[4] .

Mathematically, this tunneling current is given by

$$I \propto \sum_{E_f - eV}^{E_f} |\psi_n(0)|^2 e^{-2\kappa W}.$$

One can sum the probability over energies between $E_f - eV$ and $eV$ to get the number of states available in this energy range per unit volume, thereby finding the local density of states (LDOS) near the Fermi level[4] . The LDOS near some energy $E$ in an interval $\varepsilon$ is given by

$$\rho_s(z, E) = \frac{1}{\epsilon} \sum_{E-\epsilon}^{E} |\psi_n(z)|^2,$$

and the tunnel current at a small bias V is proportional to the LDOS near the Fermi level, which gives important information about the sample[4] . It is desirable to use LDOS to express the current because this value does not change as the volume changes, while probability density does[4] . Thus the tunneling current is given by

$$I \propto V \rho_s(0, E_f) e^{-2\kappa W}$$

where $\rho_s(0,E_f)$ is the LDOS near the Fermi level of the sample at the sample surface[4] . This current can also be expressed in terms of the LDOS near the Fermi level of the sample at the tip surface,

$$I \propto V \rho_s(W, E_f) V$$

The exponential term in the above equations means that small variations in W greatly influence the tunnel current. If the separation is decreased by 1 Å, the current increases by an order of magnitude, and vice versa.[6]

This approach fails to account for the *rate* at which electrons can pass the barrier. This rate should affect the tunnel current, so it can be treated using the Fermi's golden rule with the appropriate tunneling matrix element. John Bardeen solved this problem in his study of the metal-insulator-metal junction.[16] He found that if he solved Schrödinger's equation for each side of the junction separately to obtain the wave functions $\psi$ and $\chi$ for each electrode, he could obtain the tunnel matrix, M, from the overlap of these two wave functions[4] . This can be applied to STM by making the electrodes the tip and sample, assigning $\psi$ and $\chi$ as sample and tip wave functions, respectively, and evaluating M at some surface S between the metal electrodes, where z=0 at the sample surface and z=W at the tip surface[4] .

Now, Fermi's Golden Rule gives the rate for electron transfer across the barrier, and is written

$$w = \frac{2\pi}{\hbar} |M|^2 \delta(E_\psi - E_\chi),$$

where $\delta(E_\psi - E_\chi)$ restricts tunneling to occur only between electron levels with the same energy[4] . The tunnel matrix element, given by

$$M = \frac{\hbar}{2\pi} \int_{z=z_0} (\chi * \frac{\partial \psi}{\partial z} - \psi \frac{\partial \chi *}{\partial z}) dS\,,$$

is a description of the lower energy associated with the interaction of wave functions at the overlap, also called the resonance energy[4] .

Summing over all the states gives the tunneling current as

,

where *f* is the Fermi function, $\rho_s$ and $\rho_T$ are the density of states in the sample and tip, respectively[4] . The Fermi distribution function describes the filling of electron levels at a given temperature T.

## Early invention

An earlier, similar invention, the *Topografiner* of R. Young, J. Ward, and F. Scire from the NIST [17] , relied on field emission. However, Young is credited by the Nobel Committee as the person who realized that it should be possible to achieve better resolution by using the tunnel effect.[18]

## See also

- Microscopy
- Scanning probe microscopy
- Scanning tunneling spectroscopy
- Electrochemical scanning tunneling microscope
- Atomic force microscope
- Electron microscope
- Spin polarized scanning tunneling microscopy

## References


[1] G. Binnig, H. Rohrer (1986). "Scanning tunneling microscopy". *IBM Journal of Research and Development* **30**: 4.

[2] Press release for the 1986 Nobel Prize in physics (http://nobelprize.org/nobel_prizes/physics/laureates/1986/press.html)

[3] C. Bai (2000). *Scanning tunneling microscopy and its applications* (http://books.google.com/?id=3Q08jRmmtrkC&pg=PA345). New York: Springer Verlag. ISBN 3540657150. .

[4] C. Julian Chen (1993). *Introduction to Scanning Tunneling Microscopy* (http://www.columbia.edu/~jcc2161/documents/stm_R.pdf). Oxford University Press. ISBN 0195071506. .

[5] K. Oura, V. G. Lifshits, A. A. Saranin, A. V. Zotov, and M. Katayama (2003). *Surface science: an introduction* (http://books.google.com/?id=TTPMbOGqF-YC&pg=PP1). Berlin: Springer-Verlag. ISBN 3540005455. .

[6] D. A. Bonnell and B. D. Huey (2001). "Basic principles of scanning probe microscopy". In D. A. Bonnell. *Scanning probe microscopy and spectroscopy: Theory, techniques, and applications* (2 ed.). New York: Wiley-VCH. ISBN 047124824X.

[7] Pan, S. H.; Hudson, EW; Lang, KM; Eisaki, H; Uchida, S; Davis, JC (2000). "Imaging the effects of individual zinc impurity atoms on superconductivity in Bi2Sr2CaCu2O8+delta". *Nature* **403** (6771): 746–750. doi:10.1038/35001534. PMID 10693798.

[8] G. Schitter, M. J. Rost (2008). "Scanning probe microscopy at video-rate" (http://www.materialstoday.com/view/2194/scanning-probe-microscopy-at-videorate/) (PDF). *Materials Today* (UK: Elsevier) **11** (special issue): 40–48. doi:10.1016/S1369-7021(09)70006-9. ISSN 1369-7021. .

[9] R. V. Lapshin, O. V. Obyedkov (1993). "Fast-acting piezoactuator and digital feedback loop for scanning tunneling microscopes" (http://www.nanoworld.org/homepages/lapshin/publications.htm#fast1993) (PDF). *Review of Scientific Instruments* **64** (10): 2883–2887. doi:10.1063/1.1144377. .

[10] B. S. Swartzentruber (1996). "Direct measurement of surface diffusion using atom-tracking scanning tunneling microscopy". *Physical Review Letters* **76** (3): 459–462. doi:10.1103/PhysRevLett.76.459. PMID 10061462.

[11] "STM carbon nanotube tips fabrication for critical dimension measurements". *Sensors and Actuators A* **123-124**: 655. 2005. doi:10.1016/j.sna.2005.02.036.

[12] R. V. Lapshin (1995). "Analytical model for the approximation of hysteresis loop and its application to the scanning tunneling microscope" (http://www.nanoworld.org/homepages/lapshin/publications.htm#analytical1995) (PDF). *Review of Scientific Instruments* **66** (9): 4718–4730. doi:10.1063/1.1145314. . ( is available).

[13] R. V. Lapshin (2007). "Automatic drift elimination in probe microscope images based on techniques of counter-scanning and topography feature recognition" (http://www.nanoworld.org/homepages/lapshin/publications.htm#automatic2007) (PDF). *Measurement Science and Technology* **18** (3): 907–927. doi:10.1088/0957-0233/18/3/046. .

[14] R. V. Lapshin (2004). "Feature-oriented scanning methodology for probe microscopy and nanotechnology" (http://www.nanoworld.org/homepages/lapshin/publications.htm#feature2004) (PDF). *Nanotechnology* **15** (9): 1135–1151. doi:10.1088/0957-4484/15/9/006. .

[15] R. Wiesendanger, I. V. Shvets, D. Bürgler, G. Tarrach, H.-J. Güntherodt, and J.M.D. Coey (1992). "Recent advances in spin-polarized scanning tunneling microscopy". *Ultramicroscopy* **42-44**: 338. doi:10.1016/0304-3991(92)90289-V.

[16] J. Bardeen (1961). "Tunneling from a many particle point of view". *Phys. Rev. Lett.* **6** (2): 57–59. doi:10.1103/PhysRevLett.6.57.
[17] R. Young, J. Ward, F. Scire (1972). "The Topografiner: An Instrument for Measuring Surface Topography" (http://www.nanoworld.org/museum/young2.pdf). *Rev. Sci. Instrum.* **43**: 999. doi:10.1063/1.1685846. .
[18] "The Topografiner: An Instrument for Measuring Surface Microtopography" (http://nvl.nist.gov/pub/nistpubs/sp958-lide/214-218.pdf). NIST. .

## Further reading

- Tersoff, J.: Hamann, D. R.: Theory of the scanning tunneling microscope, Physical Review B 31, 1985, p. 805 - 813 (http://dx.doi.org/10.1103/PhysRevB.31.805).
- Bardeen, J.: Tunnelling from a many-particle point of view, Physical Review Letters 6 (2), 1961, p. 57-59 (http://dx.doi.org/10.1103/PhysRevLett.6.57).
- Chen, C. J.: Origin of Atomic Resolution on Metal Surfaces in Scanning Tunneling Microscopy, Physical Review Letters 65 (4), 1990, p. 448-451 (http://dx.doi.org/10.1103/PhysRevLett.65.448)
- G. Binnig, H. Rohrer, Ch. Gerber, and E. Weibel, Phys. Rev. Lett. 50, 120 - 123 (1983) (http://dx.doi.org/10.1103/PhysRevLett.50.120)
- G. Binnig, H. Rohrer, Ch. Gerber, and E. Weibel, Phys. Rev. Lett. 49, 57 - 61 (1982) (http://dx.doi.org/10.1103/PhysRevLett.49.57)
- G. Binnig, H. Rohrer, Ch. Gerber, and E. Weibel, Appl. Phys. Lett., Vol. 40, Issue 2, pp. 178-180 (1982) (http://dx.doi.org/10.1063/1.92999)
- R. V. Lapshin, Feature-oriented scanning methodology for probe microscopy and nanotechnology, Nanotechnology, volume 15, issue 9, pages 1135-1151, 2004 (http://stacks.iop.org/Nano/15/1135)
- D. Fujita and K. Sagisaka, Topical review: Active nanocharacterization of nanofunctional materials by scanning tunneling microscopy Sci. Technol. Adv. Mater. 9, 013003(9pp) (2008) (http://dx.doi.org/10.1088/1468-6996/9/1/013003) (free download).
- Roland Wiesendanger (1994). *Scanning probe microscopy and spectroscopy: methods and applications* (http://books.google.com/?id=EXae0pjS2vwC&printsec=frontcover). Cambridge University Press. ISBN 0521428475.
- *Theory of STM and Related Scanning Probe Methods.* Springer Series in Surface Sciences, Band 3. Springer, Berlin 1998

## External links

- A microscope is filming a microscope (http://www.fz-juelich.de/ibn/microscope_e) (Mpeg, AVI movies)
- Zooming into the NanoWorld (http://www.nano.geo.uni-muenchen.de/SW/images/zoom.html) (Animation with measured STM images)
- NobelPrize.org website about STM (http://nobelprize.org/educational_games/physics/microscopes/scanning/index.html), including an interactive STM simulator.
- SPM - Scanning Probe Microscopy Website (http://www.mobot.org/jwcross/spm/)
- STM Image Gallery at IBM Almaden Research Center (http://www.almaden.ibm.com/vis/stm/gallery.html)
- STM Gallery at Vienna University of technology (http://www.iap.tuwien.ac.at/www/surface/STM_Gallery/)
- Build a simple STM with a cost of materials less than $100.00 excluding oscilloscope (http://www.geocities.com/spm_stm/Project.html)
- Nanotimes Simulation engine download page (http://www.nanotimes-corp.com/content/view/22/38/)
- Structure and Dynamics of Organic Nanostructures discovered by STM (http://www.uni-ulm.de/~hhoster/personal/self_assembly.htm)
- Metal organic coordination networks of oligopyridines and Cu on graphite investigated by STM (http://www.uni-ulm.de/~hhoster/personal/metal_organic.htm)

- Surface Alloys discovered by STM (http://www.uni-ulm.de/~hhoster/personal/surface_alloys.html)
- Animated illustration of tunneling and STM (http://molecularmodelingbasics.blogspot.com/2009/09/tunneling-and-stm.html)
- 60 second movie clip with an introduction to Scanning Tunneling Microscopy(STM) (http://nanohub.org/resources/2620)

# Transmission Electron Aberration-corrected Microscope

**Transmission Electron Aberration-corrected Microscope** or **TEAM** is a collaborative research project between four US laboratories and two companies. It is based at the Lawrence Berkeley National Laboratory in Berkeley, California and involves Argonne National Laboratory, Oak Ridge National Laboratory and Frederick Seitz Materials Research Laboratory at the University of Illinois at Urbana-Champaign, as well as FEI and CEOS companies, and is supported by the U.S. Department of Energy. The project's main activity is design and application of a transmission electron microscope (TEM) with a spatial resolution below 0.05 nanometers, which is roughly half the size of an atom of hydrogen. [1] The project was started in 2004; the operational microscope was built in 2008 and achieved the 0.05 nm resolution target in 2009. The microscope is a shared facility available to external users.[2]

## Scientific background

It has long been known that the best achievable spatial resolution of an optical microscope, that is the smallest feature it can observe, is of the order of the wavelength of the light λ, which is about 550 nm for green light. One route to improve this resolution is to use particles with smaller λ, such as high-energy electrons. Practical limitations set a convenient electron energy to 100-300 keV that corresponds to λ = 3.7-2.0 pm. Unfortunately, the resolution of electron microscopes is limited not by the electron wavelength, but by intrinsic imperfections of electron lenses. These are referred to as spherical and chromatic aberrations because of their similarity to aberrations in optical lenses. Those aberrations are reduced by installing in a microscope a set of specially designed auxiliary "lenses" which are called aberration correctors.[3] [4]

## Hardware

The TEAM is based on a commercial FEI Titan 80-300 electron microscope, which can be operated at voltages between 80 and 300 keV, both in TEM and STEM (that is scanning TEM) modes. To minimize the mechanical vibrations, the microscope is located in a separate room within a sound-proof enclosure and is operated remotely. The electron source is a Schottky type field emission gun with a relatively low energy spread of 0.8 eV at 300 keV. In order to reduce chromatic aberrations, this spread is further lowered to 0.13 eV at 300 keV and 0.08 eV at 80 kV using a Wien-filter type monochromator.[3] Both the illumination lens, which is located above the sample and is conventionally called the condenser lens, and the collection lens (called the objective lens) are equipped with fifth-order spherical aberration correctors. The electrons are further energy filtered by a GIF filter and detected by a CCD camera. The filter makes it possible to select electrons scattered by specific chemical elements and so identify individual atoms in the sample being studied.[5]

## Applications

The TEAM has been tested on various crystalline solids, resolving individual atoms in GaN ([211] orientation), germanium ([114]), gold ([111]) and others, and reaching the spatial resolution below 0.05 nm (about 0.045 nm). In the images of graphene—a single sheet of graphite—not only the atoms, but also the chemical bonds could be observed (see top picture). A movie has been recorded inside the microscope showing hopping of individual carbon atoms around a hole punched in a graphene sheet.[1] [6] [7] [8] Similar pictures, resolving carbon atoms and bonds between them, have been independently produced for pentacene—a planar organic molecule consisting of five carbon rings—using a very different microscopy technique, atomic force microscopy (AFM).[9] [10] In AFM, the atoms are probed not by electrons, but by a sharp vibrating tip.

## References


[1] "Berkeley Scientists Produce First Live Action Movie of Individual Carbon Atoms in Action" (http://newscenter.lbl.gov/press-releases/2009/03/26/atoms-in-action/). March 26, 2009. .

[2] "The TEM project timeline" (http://ncem.lbl.gov/TEAM-project/files/when_where.html). .

[3] H. H. Rose (2008). "Optics of high-performance electron Microscopes" (free download review on electron optics). *Science and Technology of Advanced Materials* **9**: 014107. doi:10.1088/0031-8949/9/1/014107.

[4] N. Tanaka (2008). "Present status and future prospects of spherical aberration corrected TEM/STEM for study of nanomaterials" (free download review). *Sci. Technol. Adv. Mater.* **9**: 014111. doi:10.1088/1468-6996/9/1/014111.

[5] C. Kisielowski *et al.* (2008). "Detection of Single Atoms and Buried Defects in Three Dimensions by Aberration-Corrected Electron Microscope with 0.5-Å Information Limit" (http://ncem.lbl.gov/team/TEAM pubs/MAM14-5_Kisielowski_et_al-Author.pdf) (free-download pdf). *Microscopy Microanalysis* **14**: 469–477. doi:10.1017/S1431927608080902. .

[6] R. Erni *et al.* (2009). "Atomic-Resolution Imaging with a Sub-50-pm Electron Probe". *Physical Review Letters* **102**: 096101. doi:10.1103/PhysRevLett.102.096101.

[7] C. O. Girit *et al.* (27 March 2009). "Graphene at the Edge: Stability and Dynamics". *Science* **323**: 1705. doi:10.1126/science.1166999.

[8] J. C. Meyer *et al.* (2008). "Direct Imaging of Lattice Atoms and Topological Defects in Graphene Membranes". *Nano Lett.* **8**: 3582. doi:10.1021/nl801386m.

[9] "Single molecule's stunning image" (http://news.bbc.co.uk/2/hi/science/nature/8225491.stm). 2009-08-28. . Retrieved 2009-08-28.

[10] L. Gross (2009). "The Chemical Structure of a Molecule Resolved by Atomic Force Microscopy". *Science* **325**: 1110. doi:10.1126/science.1176210.


## External links

- TEAM Project main site (http://ncem.lbl.gov/team/TEAMpage/TEAMpage.html)

# ISIS

**Isis** was a goddess in Egyptian mythology.

**Isis** may also refer to:

## Aircraft

- Integrated Standby Instrument System, used on the Airbus A320 family of airliners
- Integrated Sensor is Structure, project to develop an airship for intelligence uses

## Automobiles

- Morris Isis
- Toyota Isis

## Comics

- Isis (Bluewater Comics)
- Isis (DC Comics)
- Isis (Marvel Comics)

## Computing

- Image and Scanner Interface Specification, interface for image scanning technologies
- IS-IS, network routing protocol
- ISIS/Draw, chemistry modeling program
- Integrated Software for Imagers and Spectrometers, software used by the United States Geological Survey
- ISIS Modelling Software, river modelling software
- ISIS (operating system), operating system used on the Intel 8085 processor
- ISIS programming language, variant of JOSS
- Integrated Scientific Information System, software program including the MDL *Chime* plug-in
- Infinitely Scalable Information Storage, Avid Technology storage method known as Avid Unity ISIS, used for broadcasting
- ISIS, a networking tool, part of Proteus (design software)
- ISIS Papyrus, Swiss-based commercial enterprise software vendor
- International Species Information System, non-profit software developer for zoos and aquariums
- CDS/ISIS, non-numerical information storage and retrieval software developed by UNESCO

## Geography

- The Isis, segment of the River Thames
- Isis Highway, Australian highway
- Shire of Isis, Queensland, Australia

## Music

- Isis (band), American post-metal band
- Isis (Brisbane band), rock band
- Isis (horn-rock band), 1970s all-female band
- Isis (Lully), opera by Jean-Baptiste Lully and Philippe Quinault
- "Isis" (song), by Bob Dylan
- "Isis," song from the album *Voyage to Isis* by Delta-S
- "Isis," song from the EP *Is Is* by The Yeah Yeah Yeahs
- Isyss, R&B group

## Organizations

- Isis Innovation, British technology transfer company
- ISIS neutron source
- Institute for Science and International Security
- Institute for the Scientific Investigation of Sexuality, former name of the Family Research Institute
- Institute for the Study of Interdisciplinary Sciences
- International Species Information System, an organization which maintains a database on zoo animal populations
- The Institute of Science in Society, an organization providing scientific information on ecological sustainability
- ISIS (mobile payment system), a joint venture between AT&T, Verizon Wireless and T-Mobile, in the mobile payments industry

## Outer space

- Isis (lunar crater)
- ISIS (satellite)
- 42 Isis, an asteroid

## Publications

- *Isis* (journal), academic journal
- *Isis* magazine, student magazine at Oxford University

## Ships

- HMS *Isis*, several British Royal Navy ships
- USC&GS *Isis*, a survey ship in service in the United States Coast and Geodetic Survey from 1915 to 1917 and from 1919 to 1920
- USS *Isis* (1901), a United States Navy patrol vessel in commission from 1917 to 1919

## Television

- *The Secrets of Isis*, 1970s television series
- Isis (*Stargate*)
- Isis (*Battlestar Galactica*)
- Isis Tsunami, contestant on *America's Next Top Model*
- International Secret Intelligence Service, fictional spy agency in *Archer* (TV series)
- Isis Eaglet, fictional character in Magical Chronicle Lyrical Nanoha Force
- Isis (*Smallville*)
- Project Isis (*Chuck*)

## Other uses

- Maria Isis (Maria-Jesus), daughter of Agustin de Iturbide.
- Hurricane Isis (disambiguation), the name of several tropical cyclones
- International Studies of Infarct Survival, a set of clinical trials
- Isis Adventure, puzzle game
- *Isis (coral)*, a soft coral genus
- ISIS Drive, a bicycle bottom bracket interface

# ISIS neutron source

**ISIS** is a pulsed neutron and muon source. It is situated at the Rutherford Appleton Laboratory on the Harwell Science and Innovation Campus in Oxfordshire, United Kingdom and is part of the Science and Technology Facilities Council. It uses the techniques muon spectroscopy and neutron scattering to probe the structure and dynamics of condensed matter on a microscopic scale ranging from the subatomic to the macromolecular.

ISIS Logo

Hundreds of experiments are performed annually at ISIS by visiting researchers from around the world, in diverse science areas including physics, chemistry, materials engineering, earth sciences, biology and archaeology.


ISIS experimental hall for Target Station 1

## Neutrons and muons

Neutrons are uncharged constituents of atoms and penetrate materials well, deflecting only from the nuclei of atoms. The statistical accumulation of deflected neutrons at different positions beyond the sample can be used to find the structure of a material, and the loss or gain of energy by neutrons can reveal the dynamic behaviour of parts of a sample, for example diffusive processes in solids. At ISIS the neutrons are created by accelerating 'bunches' of protons in a synchrotron, then colliding these with a heavy tantalum metal target, under a constant cooling load to dissipate the heat from the 160 kW proton beam. The impacts cause neutrons to spall off the tantalum atoms, and the neutrons are channelled through guides, or beamlines, to about 20 instruments, individually optimised for the study of different types of matter. The target station and most of the instruments are set in a large hall. Neutrons are a dangerous form of radiation, so the target and beamlines are heavily shielded with concrete.

ISIS produces muons by colliding a fraction of the proton beam with a graphite target, producing pions which decay rapidly into muons, delivered in a spin-polarised beam to sample stations.

## Science at ISIS

Another view of the ISIS experimental hall for Target Station 1

ISIS is administered and operated by the Science and Technology Facilities Council (previously CCLRC). Experimental time is open to academic users from funding countries and is applied for through a twice-yearly 'call for proposals'. Research allocation, or 'beam-time', is allotted to applicants via a peer-review process. Users and their parent institutions do not pay for the running costs of the facility, which are as much as £11,000 per instrument per day. Their transport and living costs are also refunded whilst carrying out the experiment. Most users stay in Ridgeway House, a hotel near the site, or at Cosener's House, an STFC-run conference centre in Abingdon. Over 600 experiments by 1600 users are completed every year.

A large number of support staff operate the facility, aid users, and carry out research, the control room is staffed 24 hours a day, every day of the year. Instrument scientists oversee the running of each instrument and liaise with users, and other divisions provide sample environment, data analysis and computing expertise, maintain the accelerator, and run education programmes.

Among the important and pioneering work carried out was the discovery of the structure of high-temperature superconductors and the solid phase of buckminster-fullerene.

Construction for a second target station started in 2003, and the first neutrons were delivered to the target on December 14, 2007[1] . It will use low-energy neutrons to study soft condensed matter, biological systems, advanced composites and nanomaterials. To supply the extra protons for this, the accelerator is being upgraded.

## History and background of ISIS

The source was approved in 1977 for the RAL site on the Harwell campus and recycled components from earlier UK science programmes including the accelerator hall which had previously been occupied by the Nimrod accelerator. The first beam was produced in 1984, and the facility was formally opened by the then Prime Minister Margaret Thatcher in October 1985.[2]

The name ISIS is not an acronym: it refers to the Ancient Egyptian goddess and the local name for the River Thames. The name was selected for the official opening of the facility in 1985, prior to this it was known as the SNS, or Spallation Neutron Source. The name was considered appropriate as Isis was a goddess who could restore life to the dead, and ISIS made use of equipment previously constructed for the Nimrod and Nina accelerators[3] .

## External links

- ISIS facility [4]
- ISIS Second Target Station [5]
- The Science and Technology Facilities Council [6]

## References

[1] ISIS Second Target Station Project (http://ts-2.isis.rl.ac.uk/)
[2] Linacs at the Rutherford Appleton Laboratory (http://epubs.cclrc.ac.uk/bitstream/692/linacplahistory.pdf)
[3] Explanation of the name of ISIS (http://www.isis.rl.ac.uk/aboutIsis/index.htm)
[4] http://www.isis.stfc.ac.uk/
[5] http://www.isis.stfc.ac.uk/about-isis/target-station-2/
[6] http://www.stfc.ac.uk

Geographical coordinates: 51°34′18″N 1°19′12″W

# Sudbury Neutrino Observatory

The **Sudbury Neutrino Observatory** (**SNO**) is a neutrino observatory located 6,800 feet (about 2 km) underground in Vale Inco's Creighton Mine in Sudbury, Ontario, Canada. The detector was designed to detect solar neutrinos through their interactions with a large tank of heavy water. The detector turned on in May 1999, and was turned off on 28 November 2006. While new data is no longer being taken the SNO collaboration will continue to analyze the data taken during that period for the next several years. The underground laboratory has been enlarged and continues to operate other experiments at SNOLAB. The SNO equipment itself is currently being refurbished for use in the SNO+ experiment.

Artist's concept of SNO's detector. (Courtesy of SNO)

## Experimental motivation

The first measurements of the number of solar neutrinos reaching the earth were taken in the 1960s, and all experiments prior to SNO observed a third to a half fewer neutrinos than were predicted by the Standard Solar Model. As several experiments confirmed this deficit the effect became known as the solar neutrino problem. Over several decades many ideas were put forward to try to explain the effect, one of which was the hypothesis of neutrino oscillations. All of the solar neutrino detectors prior to SNO had been sensitive primarily or exclusively to electron neutrinos and yielded little to no information on muon neutrinos and tau neutrinos.

In 1984, Herb Chen of the University of California at Irvine first pointed out the advantages of using heavy water as a detector for solar neutrinos. Unlike previous detectors, using heavy water would make the detector sensitive to two reactions, one sensitive to all neutrino flavours, which would allow a detector to measure neutrino oscillations directly. The Creighton Mine in Sudbury, among the deepest in the world and accordingly low background radiation, was quickly identified as an ideal place for Chen's proposed experiment to be built.

The SNO collaboration held its first meeting in 1984. At the time it competed with TRIUMF's KAON Factory proposal for federal funding, and the wide variety of universities backing SNO quickly led to it being selected for development. The official go-ahead was given in 1990.

The experiment observed the light produced by relativistic electrons in the water created by neutrino interactions. As relativistic electrons travel through a medium, they lose energy producing a cone of blue light through the Cerenkov effect, and it is this light that is directly detected.

## Detector description

The SNO detector target consisted of 1000 tonnes (1102 short tons) of heavy water contained in a 6-metre (20 ft) radius acrylic vessel. The detector cavity outside the vessel was filled with normal water to provide both buoyancy for the vessel and radioactive shielding. The heavy water was viewed by approximately 9,600 photomultiplier tubes (PMTs) mounted on a geodesic sphere at a radius of about 850 centimetres (335 in). The cavity housing the detector is the largest man-made underground cavity in the world, requiring a variety of high-performance rock bolting techniques to prevent rock bursts.

The observatory is located at the end of a 1.5-kilometre (0.9 mi) long drift, whimsically named the "SNO drift", isolating it from other mining operations. Along the drift are a number of operations and equipment rooms, all held in a clean room setting. Most of the facility is Class 3000 (fewer than 3,000 particles of 1 μm or larger per 1 $m^3$ of air) but the final cavity containing the detector is Class 1000.[1]

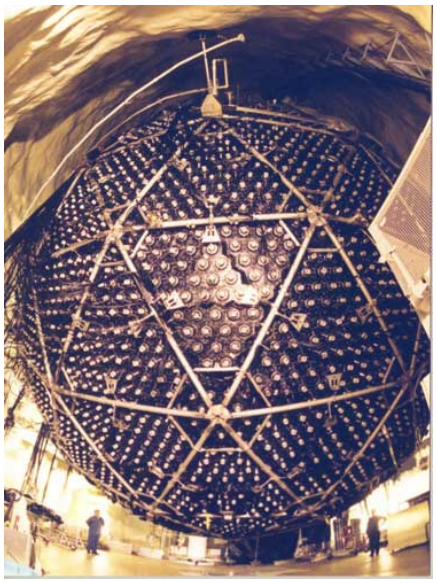

The Sudbury Neutrino Detector

### Charged current interaction

In the charged current interaction, a neutrino converts the neutron in a deuteron to a proton. The neutrino is absorbed in the reaction and an electron is produced. Solar neutrinos have energies smaller than the mass of muons and tau leptons, so only electron neutrinos can participate in this reaction. The emitted electron carries off most of the neutrino's energy, on the order of 5–15 MeV, and is detectable. The proton which is produced does not have enough energy to be detected easily. The electrons produced in this reaction are emitted in all directions, but there is a slight tendency for them to point back in the direction from which the neutrino came.

### Neutral current interaction

In the neutral current interaction, a neutrino dissociates the deuteron, breaking it into its constituent neutron and proton. The neutrino continues on with slightly less energy, and all three neutrino flavours are equally likely to participate in this interaction. Heavy water has a small cross section for neutrons, and when neutrons capture on a deuterium nucleus a gamma ray (photon) with roughly 6 MeV of energy is produced. The direction of the gamma ray is completely uncorrelated with the direction of the neutrino. Some of the neutrons wander past the acrylic vessel into the light water, and since light water has a very large cross section for neutron capture these neutrons are captured very quickly. A gamma ray with roughly 2 MeV of energy is produced in this reaction, but because this is below the detector's energy threshold they are not observable.

### Electron elastic scattering

In the elastic scattering interaction, a neutrino collides with an atomic electron and imparts some of its energy to the electron. All three neutrinos can participate in this interaction through the exchange of the neutral Z boson, and electron neutrinos can also participate with the exchange of a charged W boson. For this reason this interaction is dominated by electron neutrinos, and this is the channel through which the Super-Kamiokande (Super-K) detector can observe solar neutrinos. This interaction is the relativistic equivalent of billiards, and for this reason the electrons produced usually point in the direction that the neutrino was travelling (away from the sun). Because this interaction takes place on atomic electrons it occurs with the same rate in both the heavy and light water.

## Experimental results and impact

On 18 June 2001, the first scientific results of SNO were published,[2] [3] bringing the first clear evidence that neutrinos oscillate (i.e. that they can transmute into one another), as they travel in the sun. This oscillation in turn implies that neutrinos have non-zero masses. The total flux of all neutrino flavours measured by SNO agrees well with the theoretical prediction. Further measurements carried out by SNO have since confirmed and improved the precision of the original result.

Although Super-K had beaten SNO to the punch, having published evidence for neutrino oscillation as early as 1998, the Super-K results were not conclusive and did not specifically deal with solar neutrinos. SNO's results were the first to directly demonstrate oscillations in solar neutrinos. The results of the experiment had a major impact on the field, as evidenced by the fact that two of the SNO papers have been cited over 1,500 times, and two others have been cited over 750 times.[4] In 2007, the Franklin Institute awarded the director of SNO Art McDonald with the Benjamin Franklin Medal in Physics.[5]

## Other possible analyses

The SNO detector would have been capable of detecting a supernova within our galaxy if one had occurred while the detector was online. As neutrinos emitted by a supernova are released earlier than the photons, it is possible to alert the astronomical community before the supernova is visible. SNO was a founding member of the Supernova Early Warning System (SNEWS) with Super-Kamiokande and the Large Volume Detector. No such supernovas have yet been detected.

The SNO experiment was also able to observe atmospheric neutrinos produced by cosmic ray interactions in the atmosphere. Due to the limited size of the SNO detector in comparison with Super-K the low cosmic ray neutrino signal is not statistically significant at neutrino energies below 1 GeV.

## Participating institutions

Large particle physics experiments require large collaborations. With approximately 100 collaborators, SNO was a rather small group compared to collider experiments. The participating institutions have included:

### Canada

- Carleton University
- Laurentian University
- Queen's University – designed and built many calibration sources and the device for deploying sources
- TRIUMF
- University of British Columbia
- University of Guelph

Although no longer a collaborating institution, Chalk River Laboratories led the construction of the acrylic vessel that holds the heavy water, and Atomic Energy of Canada Limited was the source of the heavy water.

### United Kingdom

- University of Oxford – developed much of the experiment's Monte Carlo analysis program (SNOMAN), and maintained the program

### United States of America

- LBNL – Led the construction of the geodesic structure that holds the PMTs
- LANL
- University of Pennsylvania – designed and built the front end electronics and trigger
- University of Washington – designed and built proportional counter tubes for detection of neutrons in the third phase of the experiment
- Brookhaven National Laboratory
- University of Texas at Austin
- Massachusetts Institute of Technology

## Honours and awards

- Asteroid 14724 SNO is named in honour of SNO.
- In November 2006, the entire SNO team was awarded the inaugural John C. Polanyi Award for "a recent outstanding advance in any field of the natural sciences or engineering" conducted in Canada.[6]

## See also

- SNOLAB – A permanent underground physics laboratory being built around SNO
- SNO+ – The successor of SNO

## References

[1] "The Sudbury Neutrino Observatory – Canada's eye on the universe" (http://cerncourier.com/cws/article/cern/28553). *CERN Courier*. CERN. 4 December 2001. . Retrieved 2008-06-04.

[2] Ahmad, QR; *et al.* (2001). "Measurement of the Rate of $\nu_e + d \rightarrow p + p + e^-$ Interactions Produced by $^8$B Solar Neutrinos at the Sudbury Neutrino Observatory". *Physical Review Letters* **87** (7): 071301. doi:10.1103/PhysRevLett.87.071301.

[3] "Sudbury Neutrino Observatory First Scientific Results" (http://www.sno.phy.queensu.ca/sno/first_results/). 3 July 2001. . Retrieved 2008-06-04.

[4] "SPIRES HEP Results" (http://www-library.desy.de/cgi-bin/spiface/find/blu/hep/wwwcite?rawcmd=FIND+COLLABORATION+SNO+and+topcite+500+). *SPIRES*. SLAC. . Retrieved 2009-10-06.

[5] "Arthur B. McDonald, Ph.D." (http://www.fi.edu/winners/2007/mcdonald_arthur.faw?winner_id=4411). *Franklin Laureate Database*. Franklin Institute. . Retrieved 2008-06-04.

[6] "Past Winners – The Sudbury Neutrino Observatory" (http://www.nserc.gc.ca/award_e.asp?nav=polanyi&lbi=past). NSERC. 3 March 2008. . Retrieved 2008-06-04.

## External links

- SNO's official site (http://www.sno.phy.queensu.ca/)
- Joshua Klein's *Introduction to SNO, Solar Neutrinos, and Penn at SNO* (http://www.hep.upenn.edu/SNO/intro.html)
- " Experiment Cave (http://www.pbs.org/kcet/wiredscience/story/49-experiment_cave.html)". *WIRED Science*. PBS. 2007-10-24. No. 104.
- " The Ghost Particle (http://www.pbs.org/wgbh/nova/neutrino/)". Written and Directed by David Sington. *Nova*. PBS. 2006-02-21. No. 3306 (607), season 34.

Geographical coordinates: 46°28′00″N 81°10′22″W

# ATLAS experiment

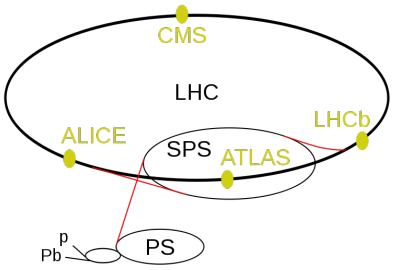


| LHC experiments | |
|---|---|
| **ATLAS** | A Toroidal LHC Apparatus |
| **CMS** | Compact Muon Solenoid |
| **LHCb** | LHC-beauty |
| **ALICE** | A Large Ion Collider Experiment |
| **TOTEM** | Total Cross Section, Elastic Scattering and Diffraction Dissociation |
| **LHCf** | LHC-forward |
| **MoEDAL** | Monopole and Exotics Detector At the LHC |
| **LHC preaccelerators** | |
| **p and Pb** | Linear accelerators for protons (Linac 2) and Lead (Linac 3) |
| **(not marked)** | Proton Synchrotron Booster |
| **PS** | Proton Synchrotron |
| **SPS** | Super Proton Synchrotron |

Geographical coordinates: 46°14′8″N 6°3′19″E


ATLAS logo.

**ATLAS** (**A** **T**oroidal **L**HC **A**pparatu**S**) is one of the six particle detector experiments (ALICE, ATLAS, CMS, TOTEM, LHCb, and LHCf) constructed at the Large Hadron Collider (LHC), a new particle accelerator at the European Organization for Nuclear Research (CERN) in Switzerland. ATLAS is 44 metres long and 25 metres in diameter, weighing about 7,000 tonnes. The project is led by Fabiola Gianotti and involves roughly 2,000 scientists and engineers at 165 institutions in 35 countries.[1] The construction was originally scheduled to be completed in June 2007, but was ready and detected its first beam events on 10 September 2008.[2] The experiment is designed to observe phenomena that involve highly massive particles which were not observable using earlier lower-energy accelerators and might shed light on new theories of particle physics beyond the Standard Model.

The *ATLAS collaboration*, the group of physicists building the detector, was formed in 1992 when the proposed EAGLE (**E**xperiment for **A**ccurate **G**amma, **L**epton and **E**nergy Measurements) and ASCOT (**A**pparatus with **S**uper **CO**nducting **T**oroids) collaborations merged their efforts into building a single, general-purpose particle detector for the Large Hadron Collider.[3] The design was a combination of those two previous designs, as well as the detector research and development that had been done for the Superconducting Supercollider. The ATLAS experiment was

proposed in its current form in 1994, and officially funded by the CERN member countries beginning in 1995. Additional countries, universities, and laboratories joined in subsequent years, and further institutions and physicists continue to join the collaboration even today. The work of construction began at individual institutions, with detector components shipped to CERN and assembled in the ATLAS experimental pit beginning in 2003.

ATLAS is designed as a general-purpose detector. When the proton beams produced by the Large Hadron Collider interact in the center of the detector, a variety of different particles with a broad range of energies may be produced. Rather than focusing on a particular physical process, ATLAS is designed to measure the broadest possible range of signals. This is intended to ensure that, whatever form any new physical processes or particles might take, ATLAS will be able to detect them and measure their properties. Experiments at earlier colliders, such as the Tevatron and Large Electron-Positron Collider, were designed based on a similar philosophy. However, the unique challenges of the Large Hadron Collider—its unprecedented energy and extremely high rate of collisions—require ATLAS to be larger and more complex than any detector ever built.

## Background

ATLAS experiment detector under construction in October 2004 in its experimental pit; the current status of construction can be seen on the CERN website.[4] Note the people in the background, for comparison.

The first cyclotron, an early type of particle accelerator, was built by Ernest O. Lawrence in 1931, with a radius of just a few centimetres and a particle energy of 1 megaelectronvolt (MeV). Since then, accelerators have grown enormously in the quest to produce new particles of greater and greater mass. As accelerators have grown, so too has the list of known particles that they might be used to investigate. The most comprehensive model of particle interactions available today is known as the Standard Model of Particle Physics. With the important exception of the Higgs boson, all of the particles predicted by the model have been observed. While the standard model predicts that quarks, electrons, and neutrinos should exist, it does not explain why the masses of the particles are so very different. Due to this violation of "naturalness" most particle physicists believe it is possible that the Standard Model will break down at energies beyond the current energy frontier of about one teraelectronvolt (TeV) (set at the Tevatron). If such beyond-the-Standard-Model physics is observed it is hoped that a new model, which is identical to the Standard Model at energies thus far probed, can be developed to describe particle physics at higher energies. Most of the currently proposed theories predict new higher-mass particles, some of which are hoped to be light enough to be observed by ATLAS. At 27 kilometres in circumference, the Large Hadron Collider (LHC) will collide two beams of protons together, each proton carrying about 7 TeV of energy — enough energy to produce particles with masses up to roughly ten times more massive than any particles currently known — assuming of course that such particles exist. With an energy seven million times that of the first accelerator the LHC represents a "new generation" of particle accelerators.

Particles that are produced in accelerators must also be observed, and this is the task of particle detectors. While interesting phenomena may occur when protons collide it is not enough to just produce them. Particle detectors must be built to detect particles, their masses, momentum, energies, charges, and nuclear spins. In order to identify all particles produced at the interaction point where the particle beams collide, particle detectors are usually designed with a similarity to an onion. The layers are made up of detectors of different types, each of which is adept at observing specific types of particles. The different features that particles leave in each layer of the detector allow for effective particle identification and accurate measurements of energy and momentum. (The role of each layer in the detector is discussed below.) As the energy of the particles produced by the accelerator increases, the detectors attached to it must grow to effectively measure and stop higher-energy particles. ATLAS is the largest detector ever

built at a particle collider as of 2008.[1]

## Physics Program

ATLAS is intended to investigate many different types of physics that might become detectable in the energetic collisions of the LHC. Some of these are confirmations or improved measurements of the Standard Model, while many others are searches for new physical theories.

One of the most important goals of ATLAS is to investigate a missing piece of the Standard Model, the Higgs boson.[5] The Higgs mechanism, which includes the Higgs boson, is invoked to give masses to elementary particles, giving rise to the differences between the weak force and electromagnetism by giving the W and Z bosons masses while leaving the photon massless. If the Higgs boson is not discovered by ATLAS, it is expected that another mechanism of electroweak symmetry breaking that explains the same phenomena, such as technicolour, will be discovered. The Standard Model is simply not mathematically consistent at the energies of the LHC without such a mechanism. The Higgs boson would be detected by the particles it decays into; the easiest to observe are two photons, two bottom quarks, or four leptons. Sometimes these decays can only be definitively identified as originating with the Higgs boson when they are associated with additional particles; for an example of this, see the diagram at right.

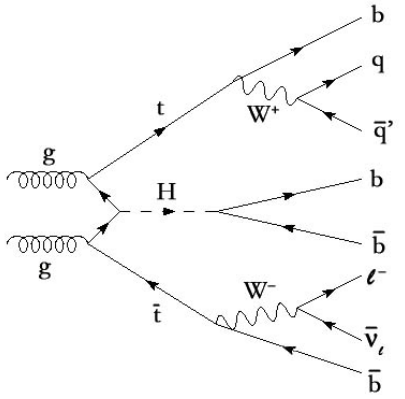


A schematic, called a Feynman diagram, of two virtual gluons from colliding LHC protons interacting to produce a hypothetical Higgs boson, a top quark, and an antitop quark. These in turn decay into a specific combination of quarks and leptons that is very unlikely to be duplicated by other processes. Collecting sufficient evidence of signals like this one may eventually allow ATLAS collaboration members to discover the Higgs boson.

The asymmetry between the behavior of matter and antimatter, known as CP violation, will also be investigated.[5] Current CP-violation experiments, such as BaBar and Belle, have not yet detected sufficient CP violation in the Standard Model to explain the lack of detectable antimatter in the universe. It is possible that new models of physics will introduce additional CP violation, shedding light on this problem; these models might either be detected directly by the production of new particles, or indirectly by measurements made of the properties of B-mesons. (LHCb, an LHC experiment dedicated to B-mesons, is likely to be better suited to the latter).[6]

The top quark, discovered at Fermilab in 1995, has thus far had its properties measured only approximately. With much greater energy and greater collision rates, LHC will produce a tremendous number of top quarks, allowing ATLAS to make much more precise measurements of its mass and interactions with other particles.[7] These measurements will provide indirect information on the details of the Standard Model, perhaps revealing inconsistencies that point to new physics. Similar precision measurements will be made of other known particles; for example, ATLAS may eventually measure the mass of the W boson twice as accurately as has previously been achieved.

Perhaps the most exciting lines of investigation are those searching directly for new models of physics. One theory that is the subject of much current research is broken supersymmetry. The theory is popular because it could potentially solve a number of problems in theoretical physics and is present in almost all models of string theory. Models of supersymmetry involve new, highly massive particles; in many cases these decay into high-energy quarks and stable heavy particles that are very unlikely to interact with ordinary matter. The stable particles would escape the detector, leaving as a signal one or more high-energy quark jets and a large amount of "missing" momentum. Other hypothetical massive particles, like those in Kaluza-Klein theory, might leave a similar signature, but its discovery would certainly indicate that there was some kind of physics beyond the Standard Model.

One remote possibility (if the universe contains large extra dimensions) is that microscopic black holes might be produced by the LHC.[8] These would decay immediately by means of Hawking radiation, producing all particles in the Standard Model in equal numbers and leaving an unequivocal signature in the ATLAS detector.[9] In fact, if this occurs, the primary studies of Higgs bosons and top quarks would be conducted on those produced by the black holes.

## Components

The ATLAS detector consists of a series of ever-larger concentric cylinders around the interaction point where the proton beams from the LHC collide. It can be divided into four major parts: the Inner Detector, the calorimeters, the muon spectrometer and the magnet systems.[10] Each of these is in turn made of multiple layers. The detectors are complementary: the Inner Detector tracks particles precisely, the calorimeters measure the energy of easily stopped particles, and the muon system makes additional measurements of highly penetrating muons. The two magnet systems bend charged particles in the Inner Detector and the muon spectrometer, allowing their momenta to be measured.

The only established stable particles that cannot be detected directly are neutrinos; their presence is inferred by noticing a momentum imbalance among detected particles. For this to work, the detector must be "hermetic", and detect all non-neutrinos produced, with no blind spots. Maintaining detector performance in the high radiation areas immediately surrounding the proton beams is a significant engineering challenge.

### Inner detector

The Inner Detector begins a few centimetres from the proton beam axis, extends to a radius of 1.2 metres, and is seven metres in length along the beam pipe. Its basic function is to track charged particles by detecting their interaction with material at discrete points, revealing detailed information about the type of particle and its momentum.[11] The magnetic field surrounding the entire inner detector causes charged particles to curve; the direction of the curve reveals a particle's charge and the degree of curvature reveals its momentum. The starting points of the tracks yield useful information for identifying particles; for example, if a group of tracks seem to originate from a point other than the original proton–proton collision, this may be a sign that the particles came from the decay of a bottom quark (see B-tagging). The Inner Detector has three parts, which are explained below.

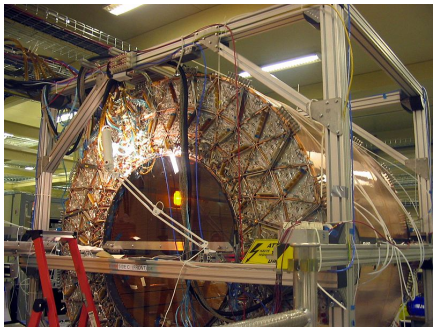

The **ATLAS TRT** central section, the outermost part of the Inner Detector, as of September 2005, assembled on the surface and taking data from cosmic rays.

The Pixel Detector, the innermost part of the detector, contains three layers and three disks on each end-cap, with a total of 1744 *modules*, each measuring two centimetres by six centimetres. The detecting material is 250 µm thick silicon. Each module contains 16 readout chips and other electronic components. The smallest unit that can be read out is a pixel (each 50 by 400 micrometres); there are roughly 47,000 pixels per module. The minute pixel size is designed for extremely precise tracking very close to the interaction point. In total, the Pixel Detector will have over 80 million readout channels, which is about 50% of the total readout channels; such a large count created a design and engineering challenge. Another challenge was the radiation the Pixel Detector will be exposed to because of its proximity to the interaction point, requiring that all components be radiation hardened in order to continue operating after significant exposures.

The Semi-Conductor Tracker (SCT) is the middle component of the inner detector. It is similar in concept and function to the Pixel Detector but with long, narrow strips rather than small pixels, making coverage of a larger area practical. Each strip measures 80 micrometres by 12.6 centimetres. The SCT is the most critical part of the inner

detector for basic tracking in the plane perpendicular to the beam, since it measures particles over a much larger area than the Pixel Detector, with more sampled points and roughly equal (albeit one dimensional) accuracy. It is composed of four double layers of silicon strips, and has 6.2 million readout channels and a total area of 61 square meters.

The Transition radiation tracker (TRT), the outermost component of the inner detector, is a combination of a straw tracker and a transition radiation detector. The detecting elements are drift tubes (straws), each four millimetres in diameter and up to 144 centimetres long. The uncertainty of track position measurements (position resolution) is about 200 micrometres, not as precise as those for the other two detectors, a necessary sacrifice for reducing the cost of covering a larger volume and having transition radiation detection capability. Each straw is filled with gas that becomes ionized when a charged particle passes through. The straws are held at about -1500V, driving the negative ions to a fine wire down the centre of each straw, producing a current pulse (signal) in the wire. The wires with signals create a pattern of 'hit' straws that allow the path of the particle to be determined. Between the straws, materials with widely varying indices of refraction cause ultra-relativistic charged particles to produce transition radiation and leave much stronger signals in some straws. Xenon gas is used to increase the number of straws with strong signals. Since the amount of transition radiation is greatest for highly relativistic particles (those with a speed very near the speed of light), and particles of a particular energy have a higher speed the lighter they are, particle paths with many very strong signals can be identified as the lightest charged particles, electrons. The TRT has about 298,000 straws in total.

## Calorimeters

The calorimeters are situated outside the solenoidal magnet that surrounds the inner detector. Their purpose is to measure the energy from particles by absorbing it. There are two basic calorimeter systems: an inner electromagnetic calorimeter and an outer hadronic calorimeter.[12] Both are *sampling calorimeters*; that is, they absorb energy in high-density metal and periodically sample the shape of the resulting particle shower, inferring the energy of the original particle from this measurement.

September 2005: the main barrel section of the ATLAS hadronic calorimeter, waiting to be moved inside the toroid magnets.

The electromagnetic (EM) calorimeter absorbs energy from particles that interact electromagnetically, which include charged particles and photons. It has high precision, both in the amount of energy absorbed and in the precise location of the energy deposited. The angle between the particle's trajectory and the detector's beam axis (or more precisely the pseudorapidity) and its angle within the perpendicular plane are both measured to within roughly 0.025 radians. The energy-absorbing materials are lead and stainless steel, with liquid argon as the sampling material, and a cryostat is required around the EM calorimeter to keep it sufficiently cool.

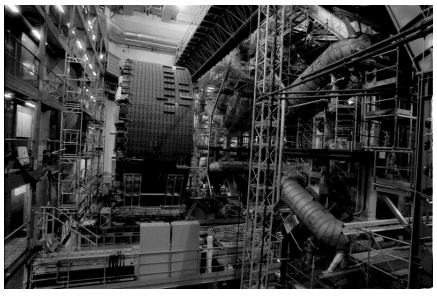

One of the sections of the extensions of the hadronic calorimeter, waiting to be inserted in late February 2006

The hadron calorimeter absorbs energy from particles that pass through the EM calorimeter, but do interact via the strong force; these particles are primarily hadrons. It is less precise, both in energy magnitude and in the localization (within about 0.1 radians only).[6] The energy-absorbing material is steel, with scintillating tiles that sample the energy deposited. Many of the features of the calorimeter are chosen for their cost-effectiveness; the instrument

is large and comprises a huge amount of construction material: the main part of the calorimeter—the tile calorimeter—is eight metres in diameter and covers 12 metres along the beam axis. The far-forward sections of the hadronic calorimeter are contained within the EM calorimeter's cryostat, and use liquid argon as it does.

## Muon spectrometer

The muon spectrometer is an extremely large tracking system, extending from a radius of 4.25 m around the calorimeters out to the full radius of the detector (11 m).[10] Its tremendous size is required to accurately measure the momentum of muons, which penetrate other elements of the detector; the effort is vital because one or more muons are a key element of a number of interesting physical processes, and because the total energy of particles in an event could not be measured accurately if they were ignored. It functions similarly to the inner detector, with muons curving so that their momentum can be measured, albeit with a different magnetic field configuration, lower spatial precision, and a much larger volume. It also serves the function of simply identifying muons—very few particles of other types are expected to pass through the calorimeters and subsequently leave signals in the muon spectrometer. It has roughly one million readout channels, and its layers of detectors have a total area of 12,000 square meters.

## Magnet system

The ATLAS detector uses two large superconducting magnet systems to bend charged particles so that their momenta can be measured. This bending is due to the Lorentz force, which is proportional to velocity. Since all particles produced in the LHC's proton collisions will be traveling at very close to the speed of light, the force on particles of different momenta is equal. (In the theory of relativity, momentum is *not* proportional to velocity at such speeds.) Thus high-momentum particles will curve very little, while low-momentum particles will curve significantly; the amount of curvature can be quantified and the particle momentum can be determined from this value.

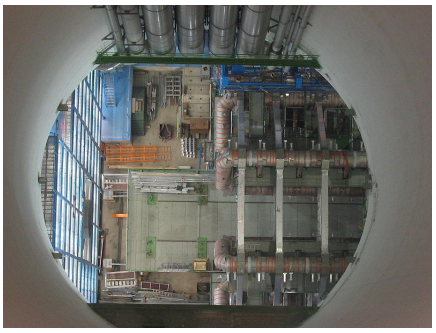

The ends of four of eight ATLAS toroid magnets, seen from the surface, about 90 metres above, in September 2005.

The inner solenoid produces a two tesla magnetic field surrounding the Inner Detector.[13] This high magnetic field allows even very energetic particles to curve enough for their momentum to be determined, and its nearly uniform direction and strength allow measurements to be made very precisely. Particles with momenta below roughly 400 MeV will be curved so strongly that they will loop repeatedly in the field and most likely not be measured; however, this energy is very small compared to the several TeV of energy released in each proton collision.

The outer toroidal magnetic field is produced by eight very large air-core superconducting barrel loops and two end-caps, all situated outside the calorimeters and within the muon system.[13] This magnetic field is 26 metres long and 20 metres in diameter, and it stores 1.6 gigajoules of energy. Its magnetic field is not uniform, because a solenoid magnet of sufficient size would be prohibitively expensive to build. Fortunately, measurements need to be much less precise to measure momentum accurately in the large volume of the muon system.

### Forward detectors

The ATLAS detector will be complemented with a set of detectors in the very forward region. These detectors will be located in the LHC tunnel far away from the interaction point. The basic idea is to measure elastic scattering at very small angles in order to get a handle on the absolute luminosity at the interaction point of ATLAS.

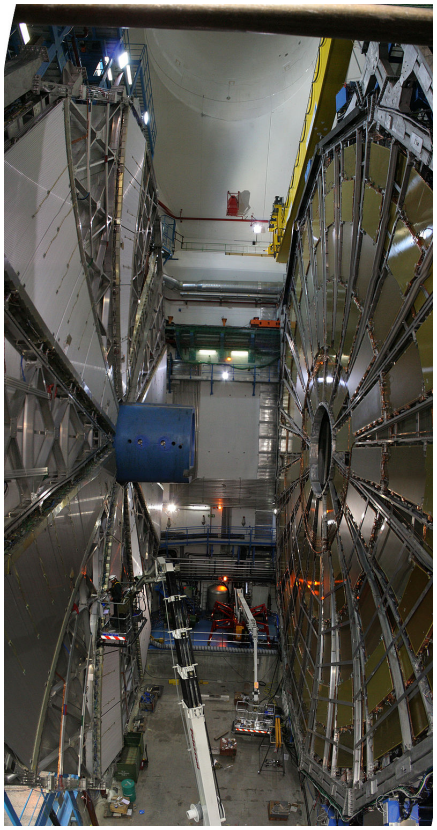

Part of the ATLAS, as it looked February 2007.

## Data systems and analysis

The detector generates unmanageably large amounts of raw data, about 25 megabytes per event (raw; zero suppression reduces this to 1.6 MB)times 23 events per beam crossing, times 40 million beam crossings per second in the center of the detector, for a total of 23 petabyte/second of raw data.[14] The trigger system uses simple information to identify, in real time, the most interesting events to retain for detailed analysis. There are three trigger levels, the first based in electronics on the detector and the other two primarily run on a large computer cluster near the detector. After the first-level trigger, about 100,000 events per second have been selected. After the third-level trigger, a few hundred events remain to be stored for further analysis. This amount of data will require over 100 megabytes of disk space per second — at least a petabyte each year.[15]

Offline event reconstruction will be performed on all permanently stored events, turning the pattern of signals from the detector into physics objects, such as jets, photons, and leptons. Grid computing will be extensively used for event reconstruction, allowing the parallel use of university and laboratory computer networks throughout the world for the CPU-intensive task of reducing large quantities of raw data into a form suitable for physics analysis. The software for these tasks has been under development for many years, and will continue to be refined once the experiment is running.

Individuals and groups within the collaboration will write their own code to perform further analysis of these objects, searching in the pattern of detected particles for particular physical models or hypothetical particles. These studies are already being developed and tested on detailed simulations of particles and their interactions with the detector. Such simulations give physicists a good sense of which new particles can be detected and how long it will take to confirm them with sufficient statistical certainty.

## See also

LHC

## Notes

[1] CERN (2006-11-20). "World's largest superconducting magnet switches on" (http://press.web.cern.ch/Press/PressReleases/Releases2006/PR17.06E.html). Press release. . Retrieved 2007-03-03.
[2] "First beam and first events in ATLAS" (http://www.atlas.ch/news/2008/first-beam-and-event.html). Atlas.ch. . Retrieved 2008-09-13.
[3] "ATLAS Collaboration records" (http://library.cern.ch/archives/isad/isaatlas.html). CERN Archive. . Retrieved 2007-02-25.
[4] "UX15 Installation; WEB cameras" (http://atlaseye-webpub.web.cern.ch/atlaseye-webpub/web-sites/pages/UX15_webcams.htm). *ATLAS Control Room*. cern.ch. . Retrieved September 15, 2010.
[5] "Introduction and Overview" (http://atlas.web.cern.ch/Atlas/TP/NEW/HTML/tp9new/node4.html#SECTION00400000000000000000). *ATLAS Technical Proposal*. CERN. 1994. .
[6] N. V. Krasnikov, V. A. Matveev (September 1997). "Physics at LHC" (http://arxiv.org/abs/hep-ph/9703204). *Physics of Particles and Nuclei* **28** (5): 441–470. doi:10.1134/1.953049. .
[7] "Top-Quark Physics" (http://atlas.web.cern.ch/Atlas/TP/NEW/HTML/tp9new/node416.html#SECTION00241000000000000000). *ATLAS Technical Proposal*. CERN. 1994. .
[8] C.M. Harris, M.J. Palmer, M.A. Parker, P. Richardson, A. Sabetfakhri and B.R. Webber (2005). "Exploring higher dimensional black holes at the Large Hadron Collider". *Journal of High Energy Physics* **5**: 053. doi:10.1088/1126-6708/2005/05/053.
[9] J. Tanaka, T. Yamamura, S. Asai, J. Kanzaki (2005). "Study of Black Holes with the ATLAS detector at the LHC" (http://www.springerlink.com/content/x067g845688470r4/). *The European Physical Journal C* **41** (s2): 19–33. doi:10.1140/epjcd/s2005-02-008-x. .
[10] "Overall detector concept" (http://atlas.web.cern.ch/Atlas/TP/NEW/HTML/tp9new/node6.html#SECTION00420000000000000000). *ATLAS Technical Proposal*. CERN. 1994. .
[11] "Inner detector" (http://atlas.web.cern.ch/Atlas/TP/NEW/HTML/tp9new/node10.html#SECTION00433000000000000000). *ATLAS Technical Proposal*. CERN. 1994. .
[12] "Calorimetry" (http://atlas.web.cern.ch/Atlas/TP/NEW/HTML/tp9new/node9.html#SECTION00432000000000000000). *ATLAS Technical Proposal*. CERN. 1994. .
[13] "Magnet system" (http://atlas.web.cern.ch/Atlas/TP/NEW/HTML/tp9new/node8.html#SECTION00431000000000000000). *ATLAS Technical Proposal*. CERN. 1994. .
[14] . http://atlas.ch/detector.html.See also 32:30 for information on the various trigger levels.
[15] "The sensitive giant" (http://www.eurekalert.org/features/doe/2004-03/dnal-tsg032604.php). *United States Department of Energy Research News*. March 2004. .

## References

- ATLAS Technical Proposal. (http://atlas.web.cern.ch/Atlas/TP/tp.html) CERN: The Atlas Experiment. Retrieved on 2007-04-10
- ATLAS Detector and Physics Performance Technical Design Report. (http://atlas.web.cern.ch/Atlas/GROUPS/PHYSICS/TDR/access.html) CERN: The Atlas Experiment. Retrieved on 2007-04-10
- N. V. Krasnikov, V. A. Matveev (September 1997). "Physics at LHC" (http://arxiv.org/abs/hep-ph/9703204). *Physics of Particles and Nuclei* **28** (5): 441–470. doi:10.1134/1.953049.

## External links

- Official ATLAS Public Webpage (http://atlas.ch) at CERN *(The "award winning ATLAS movie" is a very good general introduction!)*
- Official ATLAS Collaboration Webpage (http://atlas.web.cern.ch/Atlas/internal/Welcome.html) at CERN *(Lots of technical and logistical information)*
- ATLAS Cavern Webcams (http://atlaseye-webpub.web.cern.ch/atlaseye-webpub/web-sites/pages/UX15_webcams.htm)
- Time lapse video of the assembly (http://www.youtube.com/watch?v=kVrUR_SOykk)
- ATLAS section from US/LHC Website (http://www.uslhc.us/What_is_the_LHC/Experiments/ATLAS)
- PhysicsWorld article on LHC and experiments (http://physicsweb.org/articles/world/13/5/9/1)

- New York Times article on LHC and experiments (http://www.nytimes.com/2000/11/21/science/21HIGG.html?ex=1130040000&en=5282f51cf019f1b7&ei=5070&ex=1082001600&en=39ccf65ca6047eb2&ei=5070)
- United States Department of Energy article on ATLAS (http://www.eurekalert.org/features/doe/2004-03/dnal-tsg032604.php)
- The Large Hadron Collider ATLAS Experiment Virtual Reality (VR) photography panoramas (http://www.petermccready.com/portfolio/05091901.html)
- Large Hadron Collider Project Director Dr Lyn Evans CBE on the engineering behind the ATLAS experiment, *Ingenia* magazine, June 2008 (http://www.ingenia.org.uk/ingenia/articles.aspx?Index=489)
- Atlas Experiment News and social networking (http://www.AtlasExperiment.net)
- The ATLAS Collaboration, G Aad *et al.* (2008-08-14). "The ATLAS Experiment at the CERN Large Hadron Collider" (http://www.iop.org/EJ/journal/-page=extra.lhc/jinst). *Journal of Instrumentation* **3** (S08003): S08003. doi:10.1088/1748-0221/3/08/S08003. Retrieved 2008-08-26. (Full design documentation)
- Press release from October 2008 by EB Industries regarding the ATLAS project (http://ebindustries.com/ATLAS article.pdf)

# Techniques

## Microscopy

**Microscopy** is the technical field of using microscopes to view samples and objects that cannot be seen with the unaided eye (objects that are not within the resolution range of the normal eye). There are three well-known branches of microscopy, optical, electron, and scanning probe microscopy.

Optical and electron microscopy involve the diffraction, reflection, or refraction of electromagnetic radiation/electron beams interacting with the specimen, and the subsequent collection of this scattered radiation or another signal in order to create an image. This process may be carried out by wide-field irradiation of the sample (for example standard light microscopy and transmission electron microscopy) or by scanning of a fine beam over the sample (for example confocal laser scanning microscopy and scanning electron microscopy). Scanning probe microscopy involves the interaction of a scanning probe with the surface of the object of interest. The development of microscopy revolutionized biology and remains an essential technique in the life and physical sciences.

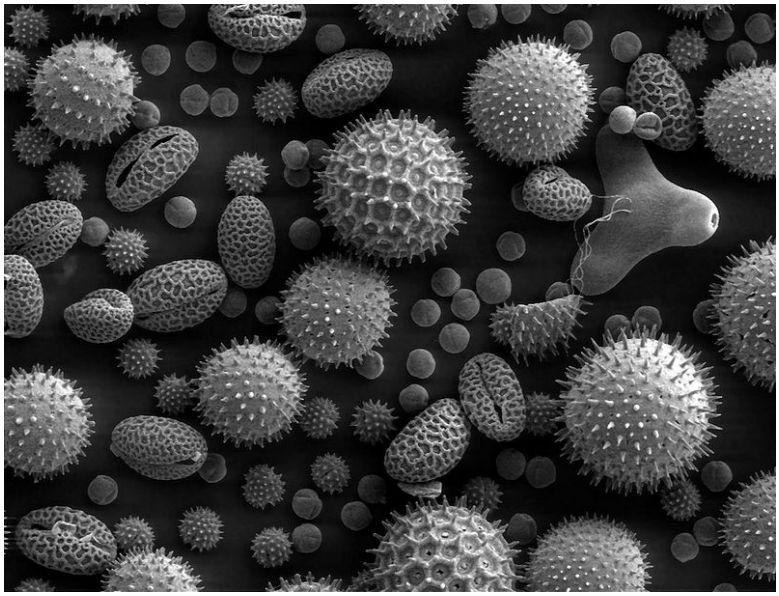

Scanning electron microscope image of pollen.

# Optical microscopy

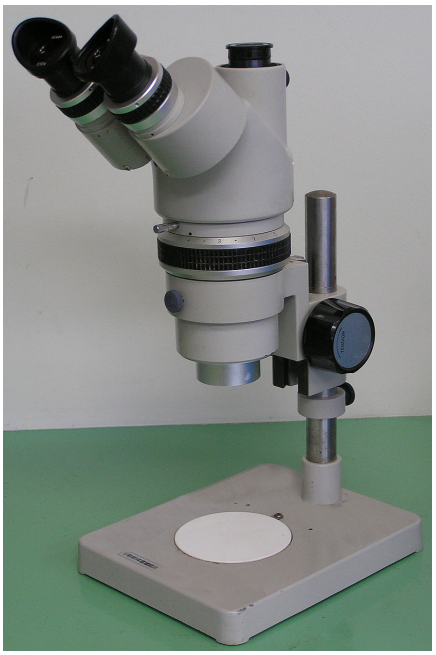

Stereo microscope

Optical or light microscopy involves passing visible light transmitted through or reflected from the sample through a single or multiple lenses to allow a magnified view of the sample.[1] The resulting image can be detected directly by the eye, imaged on a photographic plate or captured digitally. The single lens with its attachments, or the system of lenses and imaging equipment, along with the appropriate lighting equipment, sample stage and support, makes up the basic light microscope. The most recent development is the digital microscope, which uses a CCD camera to focus on the exhibit of interest. The image is shown on a computer screen since the camera is attached to it via a USB port, so eye-pieces are unnecessary.

## Limitations

Limitations of standard optical microscopy (bright field microscopy) lie in three areas;

- The technique can only image dark or strongly refracting objects effectively.
- Diffraction limits resolution to approximately 0.2 micrometre (*see: microscope*).
- Out of focus light from points outside the focal plane reduces image clarity.

Live cells in particular generally lack sufficient contrast to be studied successfully, internal structures of the cell are colourless and transparent. The most common way to increase contrast is to stain the different structures with selective dyes, but this involves killing and fixing the sample. Staining may also introduce artifacts, apparent structural details that are caused by the processing of the specimen and are thus not a legitimate feature of the specimen.

These limitations have all been overcome to some extent by specific microscopy techniques that can non-invasively increase the contrast of the image. In general, these techniques make use of differences in the refractive index of cell structures. It is comparable to looking through a glass window: you (bright field microscopy) don't see the glass but merely the dirt on the glass. There is however a difference as glass is a denser material, and this creates a difference in phase of the light passing through. The human eye is not sensitive to this difference in phase but clever optical solutions have been thought out to change this difference in phase into a difference in amplitude (light intensity).

## Techniques

In order to improve specimen contrast or highlight certain structures in a sample special techniques must be used. A huge selection of microscopy techniques are available to increase contrast or label a sample.

Four examples of transilumination techniques used to generate contrast in a sample of [[tissue paper]]. 1.559 μm/pixel.

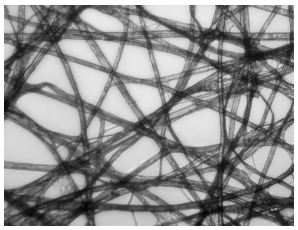

Bright field illumination, sample contrast comes from absorbance of light in the sample.

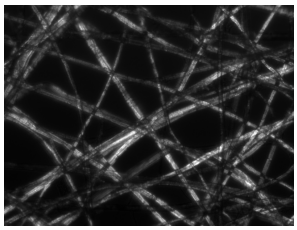

Cross-polarized light illumination, sample contrast comes from rotation of polarized light through the sample.

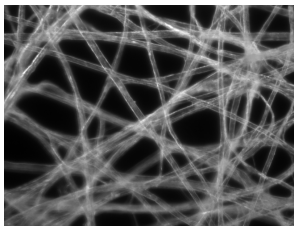

Dark field illumination, sample contrast comes from light scattered by the sample.

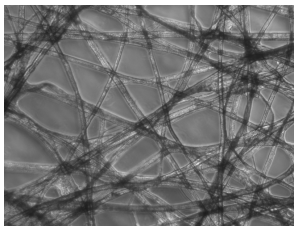

Phase contrast illumination, sample contrast comes from interference of different path lengths of light through the sample.

### Bright field

Bright field microscopy is the simplest of all the light microscopy techniques. Sample illumination is via transmitted white light, i.e. illuminated from below and observed from above. Limitations include low contrast of most biological samples and low apparent resolution due to the blur of out of focus material. The simplicity of the technique and the minimal sample preparation required are significant advantages.

### Oblique illumination

The use of oblique (from the side) illumination gives the image a 3-dimensional appearance and can highlight otherwise invisible features. A more recent technique based on this method is *Hoffmann's modulation contrast*, a system found on inverted microscopes for use in cell culture. Oblique illumination suffers from the same limitations as bright field microscopy (low contrast of many biological samples; low apparent resolution due to out of focus objects), but may highlight otherwise invisible structures.

### Dark field

Dark field microscopy is a technique for improving the contrast of unstained, transparent specimens.[2] Dark field illumination uses a carefully aligned light source to minimize the quantity of directly-transmitted (unscattered) light entering the image plane, collecting only the light scattered by the sample. Darkfield can dramatically improve image contrast—especially of transparent objects – while requiring little equipment setup or sample preparation. However, the technique does suffer from low light intensity in final image of many biological samples, and continues to be affected by low apparent resolution.

*Rheinberg illumination* is a special variant of dark field illumination in which transparent, colored filters are inserted just before the condenser so that light rays at high aperture are differently colored than those at low aperture (i.e. the background to the specimen may be blue while the object appears self-luminous yellow). Other color combinations are possible but their effectiveness is quite variable.[3]

### Dispersion staining

Dispersion staining is an optical technique that results in a colored image of a colorless object. This is an optical staining technique and requires no stains or dyes to produce a color effect. There are five different microscope configurations used in the broader technique of dispersion staining. They include brightfield Becke` line, oblique, darkfield, phase contrast, and objective stop dispersion staining.

### Phase contrast

> *In electron microscopy: Phase-contrast imaging*

More sophisticated techniques will show proportional differences in optical density . **Phase contrast** is a widely used technique that shows differences in refractive index as difference in contrast. It was developed by the Dutch physicist Frits Zernike in the 1930s (for which he was awarded the Nobel Prize in 1953). The nucleus in a cell for example will show up darkly against the surrounding cytoplasm. Contrast is excellent; however it is not for use with thick objects. Frequently, a halo is formed even around small objects, which obscures detail. The system consists of a circular annulus in the condenser, which produces a cone of light. This cone is superimposed on a similar sized ring within the phase-objective. Every objective has a different size ring, so for every objective another condenser setting has to be chosen. The ring in the objective has special optical properties: it first of all reduces the direct light in intensity, but more importantly, it creates an artificial phase difference of about a quarter wavelength. As the physical properties of this direct light have changed, interference with the diffracted light occurs, resulting in the phase contrast image.

Phase-contrast image of uncalcified matrix (top) and calcified matrix (bottom).

### Differential interference contrast

Superior and much more expensive is the use of **interference contrast**. Differences in optical density will show up as differences in relief. A nucleus within a cell will actually show up as a globule in the most often used **differential interference contrast** system according to Georges Nomarski. However, it has to be kept in mind that this is an *optical effect*, and the relief does not necessarily resemble the true shape! Contrast is very good and the condenser aperture can be used fully open, thereby reducing the depth of field and maximizing resolution.

The system consists of a special prism (Nomarski prism, Wollaston prism) in the condenser that splits light in an ordinary and an extraordinary beam. The spatial difference between the two beams is minimal (less than the maximum resolution of the objective). After passage through the specimen, the beams are reunited by a similar prism in the objective.

In a homogeneous specimen, there is no difference between the two beams, and no contrast is being generated. However, near a refractive boundary (say a nucleus within the cytoplasm), the difference between the ordinary and the extraordinary beam will generate a relief in the image. Differential interference contrast requires a polarized light source to function; two polarizing filters have to be fitted in the light path, one below the condenser (the polarizer), and the other above the objective (the analyzer).

Note: In cases where the optical design of a microscope produces an appreciable lateral separation of the two beams we have the case of classical interference microscopy, which does not result in relief images, but can nevertheless be used for the quantitative determination of mass-thicknesses of microscopic objects.

**Interference reflection microscopy**

An additional technique using interference is **interference reflection microscopy** (also known as reflected interference contrast, or RIC). It is used to examine the adhesion of cells to a glass surface, using polarized light of a narrow range of wavelengths to be reflected whenever there is an interface between two substances with different refractive indices. Whenever a cell is attached to the glass surface, reflected light from the glass and from the attached cell will interfere, while if there is no cell attached to the glass, there will be no interference.

Interference reflection microscopy can be obtained by using the same elements used by DIC, but without the prisms. Also, the light that is being detected is reflected and not transmitted as it is when DIC is employed.

**Fluorescence**

When certain compounds are illuminated with high energy light, they then emit light of a different, lower frequency. This effect is known as fluorescence. Often specimens show their own characteristic autofluorescence image, based on their chemical makeup.

This method is of critical importance in the modern life sciences, as it can be extremely sensitive, allowing the detection of single molecules. Many different fluorescent dyes can be used to stain different structures or chemical compounds. One particularly powerful method is the combination of antibodies coupled to a fluorochrome as in immunostaining. Examples of commonly used fluorochromes are fluorescein or rhodamine. The antibodies can be made tailored specifically for a chemical compound. For example, one strategy often in use is the artificial production of proteins, based on the genetic code (DNA). These proteins can then be used to immunize rabbits, which then form antibodies which bind to the protein. The antibodies are then coupled chemically to a fluorochrome and then used to trace the proteins in the cells under study.

Highly-efficient fluorescent proteins such as the green fluorescent protein (GFP) have been developed using the molecular biology technique of gene fusion, a process that links the expression of the fluorescent compound to that of the target protein. Piston DW, Patterson GH, Lippincott-Schwartz J, Claxton NS, Davidson MW (2007). "Nikon MicroscopyU: Introduction to Fluorescent Proteins" [4]. *Nikon MicroscopyU*. Retrieved 2007-08-22. This combined fluorescent protein is, in general, non-toxic to the organism and rarely interferes with the function of the protein under study. Genetically modified cells or organisms directly express the fluorescently-tagged proteins, which enables the study of the function of the original protein in vivo.

Since fluorescence emission differs in wavelength (color) from the excitation light, an ideal fluorescent image shows only the structure of interest that was labeled with the fluorescent dye. This high specificity led to the widespread use of fluorescence light microscopy in biomedical research. Different fluorescent dyes can be used to stain different biological structures, which can then be detected simultaneously, while still being specific due to the individual color of the dye.

To block the excitation light from reaching the observer or the detector, filter sets of high quality are needed. These typically consist of an excitation filter selecting the range of excitation wavelengths, a dichroic mirror, and an emission filter blocking the excitation light. Most fluorescence microscopes are operated in the Epi-illumination mode (illumination and detection from one side of the sample) to further decrease the amount of excitation light

entering the detector.

See also total internal reflection fluorescence microscope.

### Confocal

Confocal microscopy generates the image in a completely different way to normal "wide-field" microscopes. Using a scanning point of light instead of full sample illumination confocal microscopy gives slightly higher resolution, and significant improvements in optical sectioning by blocking the influence of out-of-focus light that would otherwise degrade the image. Confocal microscopy is, therefore, commonly used where 3D structure is important.

### Deconvolution

Fluorescence microscopy is extremely powerful due to its ability to show specifically labeled structures within a complex environment and also because of its inherent ability to provide three-dimensional information of biological structures. However, this information is blurred by the fact that, upon illumination, all fluorescently labeled structures emit light no matter whether they are in focus or not. This means that an image of a certain structure is always blurred by the contribution of light from structures that are out of focus. This phenomenon becomes apparent as a loss of contrast especially when using objectives with a high resolving power, typically oil immersion objectives with a high numerical aperture.

However, this phenomenon is not caused by random processes such as light scattering but can be relatively well defined by the optical properties of the image formation in the microscope imaging system. If one considers a small fluorescent light source (essentially a bright spot), light coming from this spot spreads out the further out of focus one is. Under ideal conditions, this produces a sort of "hourglass" shape of this point source in the third (axial) dimension. This shape is called the point spread function (PSF) of the microscope imaging system. Since any fluorescence image is made up of a large number of such small fluorescent light sources, the image is said to be "convolved by the point spread function".

Knowing this point spread function[5] means that it is possible to reverse this process to a certain extent by computer-based methods commonly known as deconvolution microscopy.[6] There are various algorithms available for 2D or 3D deconvolution. They can be roughly classified in *nonrestorative* and *restorative* methods. While the nonrestorative methods can improve contrast by removing out-of-focus light from focal planes, only the restorative methods can actually reassign light to its proper place of origin. This can be an advantage over other types of 3D microscopy such as confocal microscopy, because light is not thrown away but reused. For 3D deconvolution, one typically provides a series of images derived from different focal planes (called a Z-stack) plus the knowledge of the PSF, which can be derived either experimentally or theoretically from knowing all contributing parameters of the microscope.

## Sub-diffraction techniques

It is well known that there is a spatial limit to which light can focus: approximately half of the wavelength of the light one is using. But this is not a true barrier, because this diffraction limit is only true in the far-field and localization precision can be increased with many photons and careful analysis; and like the sound barrier, the diffraction barrier is breakable. This section explores some approaches to imaging objects smaller than ~250 nm. In 1978, the first theoretical ideas had been developed to break this barrier using a 4Pi microscope as a confocal laser scanning fluorescence microscope where the light is focused ideally from all sides to a common focus that is used to scan the object by 'point-by-point' excitation combined with 'point-by-point' detection [7] . Most of the following information was gathered (with permission) from a chemistry blog's review of sub-diffraction microscopy techniques Part I [8] and Part II [9]. For a review, see also reference [10] .

### Vertico SMI - SPDMphymod Superresolution Microscopy

#### Localization Microscopy/Spatially Structured Illumination

Around 1995, Christoph Cremer commenced with the development of a light microscopic process, which achieved a substantially improved size resolution of cellular nanostructures stained with a fluorescent marker. This time he employed the principle of wide field microscopy combined with structured laser illumination (spatially modulated illumination, SMI[11] . In addition, this technology is no longer subjected to the speed limitations of the focusing microscopy so that it becomes possible to undertake 3D analyses of whole cells within short observation times (at the moment around a few seconds).

Also since around 1995, Christoph Cremer developed and realized new fluorescence-based wide-field microscopy approaches that had as their goal the improvement of the effective optical resolution (in terms of the smallest detectable distance between two localized objects) down to a fraction of the conventional resolution (spectral precision distance/position determination microscopy, SPDM).

Combining SPDM and SMI, known as Vertico-SMI microscopy[12] Christoph Cremer can currently achieve a resolution of approx. 10 nm in 2D and 40 nm in 3D in wide field images of whole living cells[13] . The Vertico SMI is currently the fastest optical 3D nanoscope for the three-dimensional structural analysis of whole cells world-wide.

The Vertico SMI works with high recording speed and processes a complete 3D stack in 40 seconds (2000 frames: 50 frames/s), the very fast image processing based on specific proprietary algorithms makes the image available after 2min/3min (1-/2-color). The specific wide-field technique captures very large areas up to 5000 µm2.

SPDMphymod: Super Resolution Microscopy Images of standard GFP, RFP, YFP fluorescent dyes

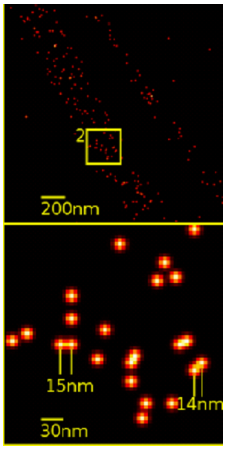


Single YFP molecule detection in a human cancer cell. Typical distance measurements in the 15 nm range (5 nm standard deviation)

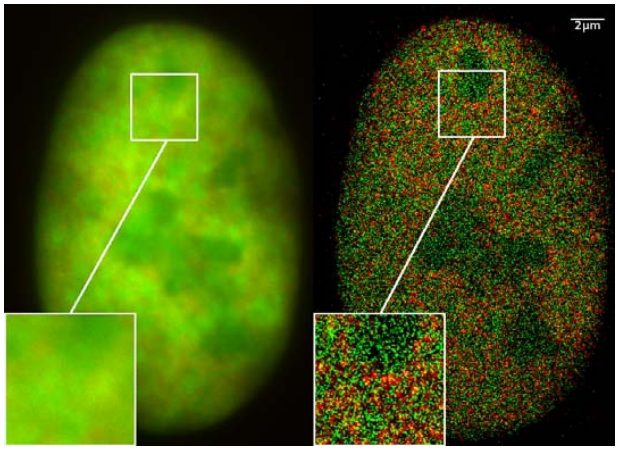


Co-localisation microscopy (2CLM) with GFP and RFP fusion proteins (nucleus of a bone cancer cell) 120.000 localized molecules in a widefield area(470 µm2)

### Use of standard dyes like normal GFP

In 2008, Cremer´s lab discovered that super resolution microscopy was also possible for many standard fluorescent dyes like GFP, Alexa dyes and fluorescein molecules, provided certain photo-physical conditions are present. Using his specific localization microscopy called SPDMPhymod, it is possible to detect and count two different fluorescent molecule types (this technology is referred to as 2CLM, 2 Color Localization Microscopy)[14]

### Near-field scanning

Near-field scanning is also called NSOM. Probably the most conceptual way to break the diffraction barrier is to use a light source and/or a detector that is itself nanometer in scale. Diffraction as we know it is truly a far-field effect: The light from an aperture is the Fourier transform of the aperture in the far-field.[15] But, in the near-field, all of this is not necessarily the case. Near-field scanning optical microscopy (NSOM) forces light through the tiny tip of a pulled fiber — and the aperture can be on the order of tens of nanometers.[16] When the tip is brought to nanometers away from a molecule, the resolution is limited not by diffraction but by the size of the tip aperture (because only that one molecule will see the light coming out of the tip). An image can be built by a raster scan of the tip over the surface to create an image.

The main down-side to NSOM is the limited number of photons you can force out a tiny tip, and the minuscule collection efficiency (if one is trying to collect fluorescence in the near-field). Other techniques such as ANSOM (see below) try to avoid this drawback.

### Local enhancement / ANSOM / optical nano-antennas

Instead of forcing photons down a tiny tip, some techniques create a local bright spot in an otherwise diffraction-limited spot. ANSOM is apertureless NSOM: it uses a tip very close to a fluorophore to enhance the local electric field the fluorophore sees.[17] Basically, the ANSOM tip is like a lightning rod which creates a hot spot of light.

Bowtie nanoantennas have been used to greatly and reproducibly enhance the electric field in the nanometer gap between the tips two gold triangles. Again, the point is to enhance a very small region of a diffraction-limited spot, thus improving the mismatch between light and nanoscale objects—and breaking the diffraction barrier.[18] [19]

### Stimulated emission depletion

Stefan Hell at the Max Planck Institute for Biophysical Chemistry - Göttingen (Germany) developed STED microscopy (stimulated emission depletion), which uses two laser pulses. The first pulse is a diffraction-limited spot that is tuned to the absorption wavelength, so excites any fluorophores in that region; an immediate second pulse is red-shifted to the emission wavelength and stimulates emission back to the ground state before, thereby depleting the excited state of any fluorophores in this depletion pulse. The trick is that the depletion pulse goes through a phase modulator that makes the pulse illuminate the sample in the shape of a donut, *so the outer part of the diffraction limited spot is depleted and the small center can still fluoresce*. By saturating the depletion pulse, the center of the donut gets smaller and smaller until they can get resolution of tens of nanometers.[20]

This technique also requires a raster scan like NSOM and standard confocal laser scanning microscopy.

### Fitting the point-spread function

Fitting the point-spread function (also called PSF). The methods above (and below) use experimental techniques to circumvent the diffraction barrier, but one can also use crafty analysis to increase the ability to know where a nanoscale object is located. The image of a point source on a charge-coupled device camera is called a point-spread function (PSF), which is limited by diffraction to be no less than approximately half the wavelength of the light. But it is possible to simply fit that PSF with a Gaussian to locate the center of the PSF — and thus the location of the fluorophore. The precision by which this technique can locate the center depends on the number of photons collected

(as well as the CCD pixel size and other factors).[21] This concept was first used to achieve resolution beyond the diffraction limit with single molecules by Van Oijen et al. in 1998 (Chem. Phys. Lett. V.292, p183). Subsequently at room temperature, groups like the Selvin lab [22] and many others have employed this analysis to localize single fluorophores to a few nanometers. This, of course, requires careful measurements and collecting *many* photons.

### PALM, STORM

What fitting a PSF is to localization, photo-activated localization microscopy (PALM) is to "resolution"—this term is here used loosely to mean measuring the distance between objects, not true optical resolution. Eric Betzig [23] and colleagues developed PALM;[24] Xiaowei Zhuang [25] at Harvard used a similar technique and calls it STORM: stochastic optical reconstruction microscopy.[26] Sam Hess at University of Maine developed the technique simultaneously [27]. The basic premise of both techniques is to fill the imaging area with many dark fluorophores that can be photoactivated into a fluorescing state by a flash of light. Because photoactivation is stochastic, only a few, well-separated molecules "turn on." Then Gaussians are fit to their PSFs to high precision (see section above). After the few bright dots photobleach, another flash of the photoactivating light activates random fluorophores again and the PSFs are fit of these different well-spaced objects. This process is repeated many times, building up an image molecule-by-molecule; and, because the molecules were localized at different times, the "resolution" of the final image can be much higher than that limited by diffraction.

The major problem with these techniques is that to get these beautiful pictures, it takes on the order of hours to collect the data. This is not the technique to study dynamics (fitting the PSF is better for that).

### Structured illumination

There is also the wide-field structured-illumination (SI) approach to breaking the diffraction limit of light [28] [29] . SI—or patterned illumination—relies on both specific microscopy protocols and extensive software analysis post-exposure. But, because SI is a wide-field technique, it is usually able to capture images at a higher rate than confocal-based schemes like STED (This is only a generalization, because SI is not actually superfast). The main concept of SI is to illuminate a sample with patterned light and increase the resolution by measuring the fringes in the Moiré pattern (from the interference of the illumination pattern and the sample). "Otherwise-unobservable sample information can be deduced from the fringes and computationally restored."[30]

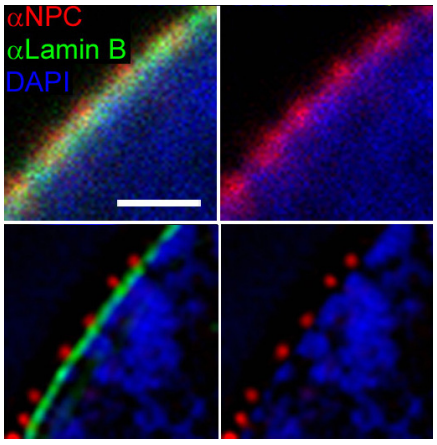


Comparison of the resolution obtained by confocal laser scanning microscopy (top) and 3D structured illumination microscopy (3D-SIM-Microscopy, bottom). Shown are details of a nuclear envelope. Nuclear pores (anti-NPC) red, nuclear envelope (anti-Lamin) green, chromatin (DAPI-staining) blue. Scale bars: 1µm.

SI enhances spatial resolution by collecting information from frequency space outside the observable region. This process is done in reciprocal space: The Fourier transform (FT) of an SI image contains superimposed additional information from different areas of reciprocal space; with several frames with the illumination shifted by some phase, it is possible to computationally separate and reconstruct the FT image, which has much more resolution information. The reverse FT returns the reconstructed image to a super-resolution image.

But this enhances the resolution only by a factor of 2 (because the SI pattern cannot be focused to anything smaller than half the wavelength of the excitation light). To further increase the resolution, one can introduce *nonlinearities*, which show up as higher-order harmonics in the FT. In reference [30] , Gustafsson uses saturation of the fluorescent sample as the nonlinear effect. A sinusoidal saturating excitation beam produces the distorted fluorescence intensity pattern in the emission. This nonpolynomial nonlinearity yields a series of higher-order harmonics in the FT.

Each higher-order harmonic in the FT allows another set of images that can be used to reconstruct a larger area in reciprocal space, and thus a higher resolution. In this case, Gustafsson achieves less than 50-nm resolving power, more than five times that of the microscope in its normal configuration.

The main problems with SI are that, in this incarnation, saturating excitation powers cause more photodamage and lower fluorophore photostability, and sample drift must be kept to below the resolving distance. The former limitation might be solved by using a different nonlinearity (such as stimulated emission depletion or reversible photoactivation, both of which are used in other sub-diffraction imaging schemes); the latter limits live-cell imaging and may require faster frame rates or the use of some fiduciary markers for drift subtraction. Nevertheless, SI is certainly a strong contender for further application in the field of super-resolution microscopy.

Images of [[cell nucleus|cell nuclei]] and [[Mitosis|mitotic]] stages recorded with 3D-SIM Microscopy.

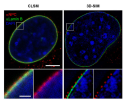

Comparison confocal microscopy - 3D-SIM

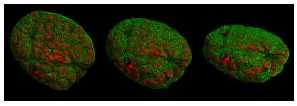

Cell nucleus in prophase from various angles

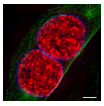

Two mouse cell nuclei in prophase.

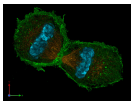

mouse cell in telophase

## Extensions

Most modern instruments provide simple solutions for micro-photography and image recording electronically. However such capabilities are not always present and the more experienced microscopist will, in many cases, still prefer a hand drawn image rather than a photograph. This is because a microscopist with knowledge of the subject can accurately convert a three dimensional image into a precise two dimensional drawing . In a photograph or other image capture system however, only one thin plane is ever in good focus.

The creation of careful and accurate micrographs requires a microscopical technique using a monocular eyepiece. It is essential that both eyes are open and that the eye that is not observing down the microscope is instead concentrated on a sheet of paper on the bench besides the microscope. With practice, and without moving the head or eyes, it is possible to accurately record the observed details by tracing round the observed shapes by simultaneously "seeing" the pencil point in the microscopical image.

Practicing this technique also establishes good general microscopical technique. It is always less tiring to observe with the microscope focused so that the image is seen at infinity and with both eyes open at all times.

### X-ray

As resolution depends on the wavelength of the light. Electron microscopy has been developed since the 1930s that use electron beams instead of light. Because of the much smaller wavelength of the electron beam, resolution is far higher.

Though less common, X-ray microscopy has also been developed since the late 1940s. The resolution of X-ray microscopy lies between that of light microscopy and electron microscopy.

## Electron microscopy

For light microscopy, the wavelength of the light limits the resolution to around 0.2 micrometers. In order to gain higher resolution, the use of an electron beam with a far smaller wavelength is used in electron microscopes.

- Transmission electron microscopy (TEM) is quite similar to the compound light microscope, by sending an electron beam through a very thin slice of the specimen. The resolution limit in 2005 was around 0.05 nanometer and has not increased appreciably since that time.
- Scanning electron microscopy (SEM) visualizes details on the surfaces of cells and particles and gives a very nice 3D view. It gives results much like those of the stereo light microscope, and, akin to that, its most useful magnification is in the lower range than that of the transmission electron microscope.

### Atomic de Broglie

The *atomic de Broglie microscope* is an imaging system which is expected to provide resolution at the nanometer scale using neutral He atoms as probe particles. [31] [32] . Such a device could provide the resolution at nanometer scale and be absolutely non-destructive, but it is not developed as well as optical or electron microscopes.

## Scanning probe microscopy

This is a sub-diffraction technique. Examples of scanning probe microscopes are the atomic force microscope (AFM), the Scanning tunneling microscope and the photonic force microscope. All such methods imply a solid probe tip in the vicinity (near field) of an object, which is supposed to be almost flat.

### Ultrasonic force

Ultrasonic Force Microscopy (UFM) has been developed in order to improve the details and image contrast on "flat" areas of interest where the AFM images are limited in contrast. The combination of AFM-UFM allows a near field acoustic microscopic image to be generated. The AFM tip is used to detect the ultrasonic waves and overcomes the limitation of wavelength that occurs in acoustic microscopy. By using the elastic changes under the AFM tip, an image of much greater detail than the AFM topography can be generated.

Ultrasonic force microscopy allows the local mapping of elasticity in atomic force microscopy by the application of ultrasonic vibration to the cantilever or sample. In an attempt to analyze the results of ultrasonic force microscopy in a quantitative fashion, a force-distance curve measurement is done with ultrasonic vibration applied to the cantilever base, and the results are compared with a model of the cantilever dynamics and tip-sample interaction based on the finite-difference technique.

## Infrared microscopy

The term *infrared microscope* covers two main types of diffraction-limited microscopy. The first provides optical visualization plus IR spectroscopic data collection. The second (more recent and more advanced) technique employs *focal plane array detection* for infrared chemical imaging, where the image contrast is determined by the response of individual sample regions to particular IR wavelengths selected by the user.

IR versions of sub-diffraction microscopy (see above) exist also. These include IR NSOM [33] and photothermal microspectroscopy.

## Digital holographic microscopy

In digital holographic microscopy (DHM), interfering wave fronts from a coherent (monochromatic) light-source are recorded on a sensor. The image is digitally reconstructed by a computer from the recorded hologram. Besides the ordinary bright field image, a phase shift image is created as well.

DHM can operate both in reflection and transmission mode. In reflection mode, the phase shift image provides a relative distance measurement and thus represents a topography map of the reflecting surface. In transmission mode, the phase shift image provides a label-free quantitative measurement of the optical thickness of the specimen. Phase shift images of biological cells are very similar to images of stained cells and have successfully been analyzed by high content analysis software.

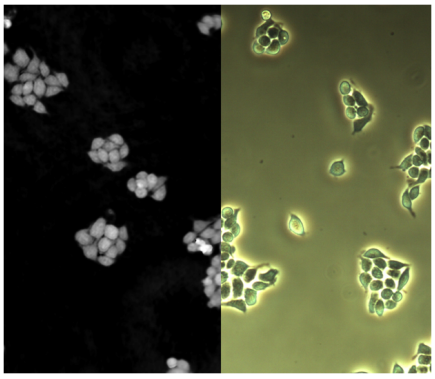

Human cells imaged by DHM phase shift (left) and phase contrast microscopy (right).

A unique feature of DHM is the ability to adjust focus after the image is recorded, since all focus planes are recorded simultaneously by the hologram. This feature makes it possible to image moving particles in a volume or to rapidly scan a surface. Another attractive feature is DHM's ability to use low cost optics by correcting optical aberrations by software.

## Digital Pathology (virtual microscopy)

Digital Pathology is an image-based information environment enabled by computer technology that allows for the management of information generated from a digital slide. Digital pathology is enabled in part by virtual microscopy, which is the practice of converting glass slides into digital slides that can be viewed, managed, and analyzed.

## Amateur microscopy

*Amateur Microscopy* is the investigation and observation of biological and non-biological specimens for recreational purposes. Collectors of minerals, insects, seashells, and plants may use microscopes as tools to uncover features that help them classify their collected items. Other amateurs may be interested in observing the life found in pond water and of other samples. Microscopes may also prove useful for the water quality assessment for people that keep a home aquarium. Photographic documentation and drawing of the microscopic images are additional tasks that augment the spectrum of tasks of the amateur. There are even competitions for photomicrograph art. Participants of this pastime either may use commercially prepared microscopic slides or may engage in the task of specimen preparation.

While microscopy is a central tool in the documentation of biological specimens, it is, in general, insufficient to justify the description of a new species based on microscopic investigations alone. Often genetic and biochemical

tests are necessary to confirm the discovery of a new species. A laboratory and access to academic literature is a necessity, which is specialized and, in general, not available to amateurs. There is, however, one huge advantage that amateurs have above professionals: time to explore their surroundings. Often, advanced amateurs team up with professionals to validate their findings and (possibly) describe new species.

In the late 1800s, amateur microscopy became a popular hobby in the United States and Europe. Several 'professional amateurs' were being paid for their sampling trips and microscopic explorations by philanthropists, to keep them amused on the Sunday afternoon (e.g., the diatom specialist A. Grunow, being paid by (among others) a Belgian industrialist). Professor John Phin published "Practical Hints on the Selection and Use of the Microscope (Second Edition, 1878)," and was also the editor of the “American Journal of Microscopy.”

In 1995, a loose group of amateur microscopists, drawn from several organizations in the UK and USA, founded a site for microscopy based on the knowledge and input of amateur (perhaps better referred to as 'enthusiast') microscopists. This was the first attempt to establish 'amateur' microscopy as a serious subject in the then-emerging new media of the Internet. Today, it remains as a powerful established international resource for all ages, to input their findings and share information. It is a nonprofit-making web presence dedicated to the pursuit of science and understanding of the small-scale world: [34]

**Examples of amateur microscopy images:**

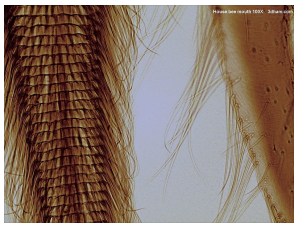

"house bee" Mouth 100X

Rice Stem cs 400X

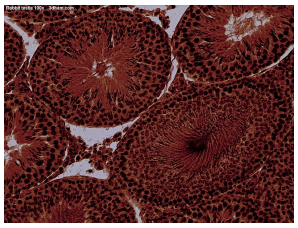

Rabbit Testis 100X

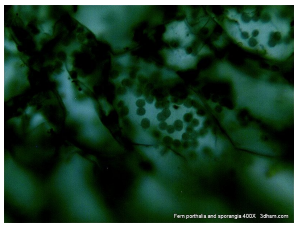

Fern Porothallium 400X

## See also

- Acronyms in microscopy
- Digital microscope
- Digital Pathology
- Interferometric microscopy
- Köhler illumination
- Timeline of microscope technology
- Two-photon excitation microscopy

## References

[1] Abramowitz M, Davidson MW (2007). "Introduction to Microscopy" (http://micro.magnet.fsu.edu/primer/anatomy/introduction.html). *Molecular Expressions*. . Retrieved 2007-08-22.

[2] Abramowitz M, Davidson MW (2003-08-01). "Darkfield Illumination" (http://micro.magnet.fsu.edu/primer/techniques/darkfield.html). . Retrieved 2008-10-21.

[3] Abramowitz M, Davidson MW (2003-08-01). "Rheinberg Illumination" (http://micro.magnet.fsu.edu/primer/techniques/rheinberg.html). . Retrieved 2008-10-21.

[4] http://www.microscopyu.com/articles/livecellimaging/fpintro.html

[5] Nasse M. J., Woehl J. C. (2010). "Realistic modeling of the illumination point spread function in confocal scanning optical microscopy". *J. Opt. Soc. Am. A* **27** (2): 295–302. doi:10.1364/JOSAA.27.000295.

[6] Wallace W, Schaefer LH, Swedlow JR (2001). "A workingperson's guide to deconvolution in light microscopy". *BioTechniques* **31** (5): 1076–8, 1080, 1082 passim. PMID 11730015.

[7] Considerations on a laser-scanning-microscope with high resolution and depth of field: C. Cremer and T. Cremer in M1CROSCOPICA ACTA VOL. 81 NUMBER 1 September,pp. 31—44 (1978)

[8] http://blog.everydayscientist.com/?p=184
[9] http://blog.everydayscientist.com/?p=354
[10] WEM News and Views (http://dx.doi.org/10.1038/nmeth1006-781)
[11] Nano-structure analysis using Spatially Modulated Illumination microscopy: D. Baddeley, C. Batram, Y. Weiland, C. Cremer, U.J. Birk in NATURE PROTOCOLS, Vol 2, pp. 2640–2646 (2007)
[12] High-precision structural analysis of subnuclear complexes in fixed and live cells via Spatially Modulated Illumination (SMI) microscopy: J. Reymann, D. Baddeley, P. Lemmer, W. Stadter, T. Jegou, K. Rippe, C. Cremer, U. Birk in CHROMOSOME RESEARCH, Vol. 16, pp. 367–382 (2008)
[13] SPDM – Light Microscopy with Single Molecule Resolution at the Nanoscale: P. Lemmer, M.Gunkel, D.Baddeley, R. Kaufmann, A. Urich, Y. Weiland, J.Reymann, P. Müller, M. Hausmann, C. Cremer in APPLIED PHYSICS B, Vol 93, pp. 1-12 (2008).
[14] Manuel Gunkel, Fabian Erdel, Karsten Rippe, Paul Lemmer, Rainer Kaufmann, Christoph Hörmann, Roman Amberger and Christoph Cremer: *Dual color localization microscopy of cellular nanostructures*. In: Biotechnology Journal, 2009, 4, 927-938. ISSN 1860-6768
[15] "Fresnel Diffraction Applet" (http://www.falstad.com/diffraction/) (Java applet). . Retrieved 2007-08-22.
[16] Cummings JR, Fellers TJ, Davidson MW (2007). "Specialized Microscopy Techniques - Near-Field Scanning Optical Microscopy" (http://www.olympusmicro.com/primer/techniques/nearfield/nearfieldintro.html). *Olympus Microscopy Resource Center*. . Retrieved 2007-08-22.
[17] Sánchez EJ, Novotny L, Xie XS (1999). "Near-Field Fluorescence Microscopy Based on Two-Photon Excitation with Metal Tips" (http://link.aps.org/abstract/PRL/v82/p4014). *Phys Rev Lett* **82**: 4014–7. doi:10.1103/PhysRevLett.82.4014. .
[18] Schuck PJ, Fromm DP, Sundaramurthy A, Kino GS, Moerner WE (2005). "Improving the Mismatch between Light and Nanoscale Objects with Gold Bowtie Nanoantennas" (http://link.aps.org/abstract/PRL/v94/e017402). *Phys Rev Lett* **94** (1): 017402. doi:10.1103/PhysRevLett.94.017402. PMID 15698131. .
[19] Muhlschlegel P, Eisler H-J, Martin OJF, Hecht B, Pohl DW (2005). "Resonant optical antennas" (http://www.sciencemag.org/cgi/content/abstract/308/5728/1607). *Science* **308**: 1607. doi:10.1126/science.1111886. .
[20] STED (http://dx.doi.org/10.1038/nbt895)
[21] Webb paper (http://www.biophysj.org/cgi/content/abstract/82/5/2775)
[22] http://www.physics.uiuc.edu/people/Selvin/index.htm
[23] http://www.hhmi.org/news/betzig.html
[24] PALM (http://dx.doi.org/10.1126/science.1127344)
[25] http://zhuang.harvard.edu/
[26] STORM (http://dx.doi.org/10.1038/nmeth929)
[27] http://dx.doi.org/10.1529/biophysj.106.091116
[28] Bailey, B.; Farkas, D. L.; Taylor, D. L.; Lanni, F. Enhancement of axial resolution in fluorescence microscopy by standing-wave excitation (http://dx.doi.org/10.1038/366044a0). *Nature* **1993**, *366*, 44–48.
[29] Gustafsson, M. G. L. Surpassing the lateral resolution limit by a factor of two using structured illumination microscopy (http://dx.doi.org/10.1046/j.1365-2818.2000.00710.x). *J. of Microsc.* **2000**, *198*(2), 82–87.
[30] Gustafsson, M. G. L. Nonlinear structured-illumination microscopy: Wide-field fluorescence imaging with theoretically unlimited resolution (http://dx.doi.org/10.1073/pnas.0406877102). *PNAS* **2005**, *102*(37), 13081–13086.
[31] D.Kouznetsov; H. Oberst, K. Shimizu, A. Neumann, Y. Kuznetsova, J.-F. Bisson, K. Ueda, S. R. J. Brueck (2006). "Ridged atomic mirrors and atomic nanoscope" (http://stacks.iop.org/0953-4075/39/1605). *JOPB* **39**: 1605–1623. doi:10.1088/0953-4075/39/7/005. .
[32] Atom Optics and Helium Atom Microscopy. Cambridge University, http://www-sp.phy.cam.ac.uk/research/mirror.php3
[33] H M Pollock and D A Smith, The use of near-field probes for vibrational spectroscopy and photothermal imaging, in Handbook of vibrational spectroscopy, J.M. Chalmers and P.R. Griffiths (eds), John Wiley & Sons Ltd, Vol. 2, pp. 1472 - 1492 (2002)
[34] http://www.microscopy-uk.org.uk

## Further reading

- *Advanced Light Microscopy vol. 1 Principles and Basic Properties* by Maksymilian Pluta, Elsevier (1988)
- *Advanced Light Microscopy vol. 2 Specialised Methods* by Maksymilian Pluta, Elsevier (1989)
- *Introduction to Light Microscopy* by S. Bradbury, B. Bracegirdle, BIOS Scientific Publishers (1998)
- *Video Microscopy* by Shinya Inoue, Plenum Press (1986)
- (http://www.kip.uni-heidelberg.de/AG_Cremer/pdf-files/Cremer_Micros_Acta_1978.pdf) 1978: Theoretical basis of super resolution 4Pi microscopy & design of a confocal laser scanning fluorescence microscope
- Portraits of life, one molecule at a time (http://pubs.acs.org/subscribe/journals/ancham/79/i05/pdf/0307feature_willis.pdf), a feature article on sub-diffraction microscopy from the March 1, 2007 issue of *Analytical Chemistry* (http://pubs3.acs.org/acs/journals/toc.page?incoden=ancham&indecade=0&involume=79&inissue=5)

# External links

## General

- (http://www.imaging-git.com/news/world-s-fastest-optical-microscope-chosen-best-business-idea) Bwcon award: world´s fastest superresolution microscope as best business idea
- GFP Superresolution (PDF file; 330 kB) (http://www.tlb.de/uploads/media/GFP_Superresolution_01.pdf)
- Olympus Microscopy Resource Center (http://www.olympusmicro.com/) ( website critique (http://www.genengnews.com/bestofweb/list.aspx?iid=93))
- Nikon MicroscopyU (http://www.microscopyu.com)
- Andor Microscopy Techniques (http://www.andor.com/microscopy_systems/techniques/) - Various techniques used in microscopy.
- Carl Zeiss "Microscopy from the very beginning" (http://www.zeiss.de/C1256B5E0047FF3F?Open), a step by step tutorial into the basics of microscopy.
- Microscopy in Detail (http://www.biologie.uni-hamburg.de/b-online/e03/03.htm) - A resource with many illustrations elaborating the most common microscopy techniques
- Microscopy Information (http://www.microbehunter.com) - Microscopy information and techniques for teachers, educators and enthusiasts.
- WITec SNOM System (http://witec.de/en/products/snom/alpha300s/) - NSOM/SNOM and Hybrid Microscopy techniques in combination with AFM, RAMAN, Confocal, Dark-field, DIC & Fluorescence Microscopy techniques.
- Manawatu Microscopy (http://confocal-manawatu.pbworks.com/) - first known collaboration environment for Microscopy and Image Analysis.
- Audio microscope glossary (http://www.histology-world.com/microscope/audiomicroscope/audiomicroscope.htm)
- PSF Lab (http://onemolecule.chem.uwm.edu/software), freeware (for academic use) permitting the calculation of the Point Spread Function in stratified media including polarization effects based on a rigorous vector-based model.

## Techniques

- Ratio-metric Imaging Applications For Microscopes (http://www.pti-nj.com/EasyRatio/EasyRatioPro-Applications.html) Examples of Ratiometric Imaging Work on a Microscope
- Interactive Fluorescence Dye and Filter Database (https://www.micro-shop.zeiss.com/?s=2525647761b33&l=en&p=us&f=f) Carl Zeiss Interactive Fluorescence Dye and Filter Database.
- Images formed by simple microscopes (http://www.brianjford.com/wav-spf.htm) - examples of observations with single-lens microscopes.

## Organizations

- Royal Microscopical Society (http://www.rms.org.uk/) (RMS)
- Microscopy Society of America (http://www.microscopy.org/) (MSA)
- European Microscopy Society (http://www.eurmicsoc.org/) (EMS)
- Non-membership International online organisation (http://www.microscopy-uk.org.uk/) (Mic-UK)

# X-ray crystallography

**X-ray crystallography** is a method of determining the arrangement of atoms within a crystal, in which a beam of X-rays strikes a crystal and diffracts into many specific directions. From the angles and intensities of these diffracted beams, a crystallographer can produce a three-dimensional picture of the density of electrons within the crystal. From this electron density, the mean positions of the atoms in the crystal can be determined, as well as their chemical bonds, their disorder and various other information.

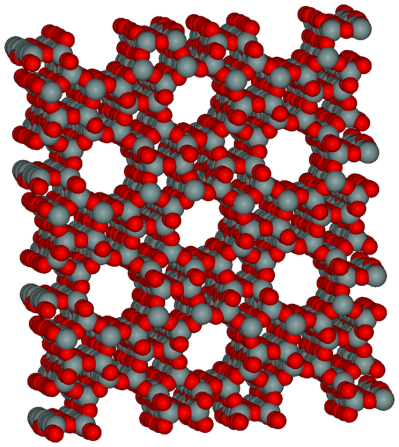

X-ray crystallography can locate every atom in a zeolite, an aluminosilicate with many important applications, such as water purification.

Since many materials can form crystals — such as salts, metals, minerals, semiconductors, as well as various inorganic, organic and biological molecules — X-ray crystallography has been fundamental in the development of many scientific fields. In its first decades of use, this method determined the size of atoms, the lengths and types of chemical bonds, and the atomic-scale differences among various materials, especially minerals and alloys. The method also revealed the structure and functioning of many biological molecules, including vitamins, drugs, proteins and nucleic acids such as DNA. X-ray crystallography is still the chief method for characterizing the atomic structure of new materials and in discerning materials that appear similar by other experiments. X-ray crystal structures can also account for unusual electronic or elastic properties of a material, shed light on chemical interactions and processes, or serve as the basis for designing pharmaceuticals against diseases.

In an X-ray diffraction measurement, a crystal is mounted on a goniometer and gradually rotated while being bombarded with X-rays, producing a diffraction pattern of regularly spaced spots known as *reflections*. The two-dimensional images taken at different rotations are converted into a three-dimensional model of the density of electrons within the crystal using the mathematical method of Fourier transforms, combined with chemical data known for the sample. Poor resolution (fuzziness) or even errors may result if the crystals are too small, or not uniform enough in their internal makeup.

X-ray crystallography is related to several other methods for determining atomic structures. Similar diffraction patterns can be produced by scattering electrons or neutrons, which are likewise interpreted as a Fourier transform. If single crystals of sufficient size cannot be obtained, various other X-ray methods can be applied to obtain less detailed information; such methods include fiber diffraction, powder diffraction and small-angle X-ray scattering (SAXS). If the material under investigation is only available in the form of nanocrystalline powders or suffers from poor crystallinity, the methods of electron crystallography can be applied for determining the atomic structure.

For all above mentioned X-ray diffraction methods, the scattering is elastic; the scattered X-rays have the same wavelength as the incoming X-ray. By contrast, *inelastic* X-ray scattering methods are useful in studying excitations of the sample, rather than the distribution of its atoms.

# History

## Early scientific history of crystals and X-rays

Crystals have long been admired for their regularity and symmetry, but they were not investigated scientifically until the 17th century. Johannes Kepler hypothesized in his work *Strena seu de Nive Sexangula* (1611) that the hexagonal symmetry of snowflake crystals was due to a regular packing of spherical water particles.[1]

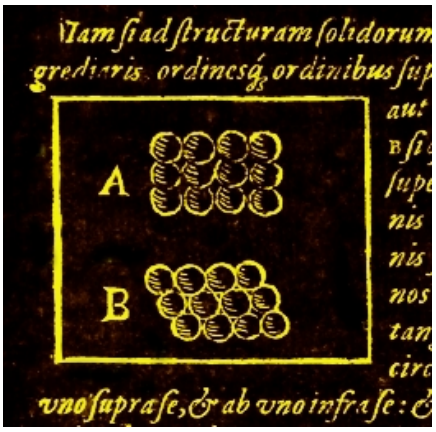


Drawing of square (Figure A, above) and hexagonal (Figure B, below) packing from Kepler's work, *Strena seu de Nive Sexangula*.

As shown by X-ray crystallography, the hexagonal symmetry of snowflakes results from the tetrahedral arrangement of hydrogen bonds about each water molecule. The water molecules are arranged similarly to the silicon atoms in the tridymite polymorph of $SiO_2$. The resulting crystal structure has hexagonal symmetry when viewed along a principal axis.

Crystal symmetry was first investigated experimentally by Nicolas Steno (1669), who showed that the angles between the faces are the same in every exemplar of a particular type of crystal,[2] and by René Just Haüy (1784), who discovered that every face of a crystal can be described by simple stacking patterns of blocks of the same shape and size. Hence, William Hallowes Miller in 1839 was able to give each face a unique label of three small integers, the Miller indices which are still used today for identifying crystal faces. Haüy's study led to the correct idea that crystals are a regular three-dimensional array (a Bravais lattice) of atoms and molecules; a single unit cell is repeated indefinitely along three principal directions that are not necessarily perpendicular. In the 19th century, a complete catalog of the possible symmetries of a crystal was worked out by Johann Hessel,[3] Auguste Bravais,[4] Yevgraf Fyodorov,[5] Arthur Schönflies[6] and (belatedly) William Barlow. From the available data and physical reasoning, Barlow proposed several crystal structures in the 1880s that were validated later by X-ray crystallography;[7] however, the available data were too scarce in the 1880s to accept his models as conclusive.

X-rays were discovered by Wilhelm Conrad Röntgen in 1895, just as the studies of crystal symmetry were being concluded. Physicists were initially uncertain of the nature of X-rays, although it was soon suspected (correctly) that they were waves of electromagnetic radiation, in other words, another form of light. At that time, the wave model of light — specifically, the Maxwell theory of electromagnetic radiation — was well accepted among scientists, and experiments by Charles Glover Barkla showed that X-rays exhibited phenomena associated with electromagnetic waves, including transverse polarization and spectral lines akin to those observed in the visible wavelengths. Single-slit experiments in the laboratory of Arnold Sommerfeld suggested the wavelength of X-rays was about 1 Angström. However, X-rays are composed of photons, and thus are not only waves of electromagnetic radiation but also exhibit particle-like properties. The photon concept was introduced by Albert Einstein in 1905,[8] but it was not broadly accepted until 1922,[9] [10] when Arthur Compton confirmed it by the scattering of X-rays from electrons.[11] Therefore, these particle-like properties of X-rays, such as their ionization of gases, caused William Henry Bragg to argue in 1907 that X-rays were *not* electromagnetic radiation.[12] [13] [14] [15] Nevertheless, Bragg's view was not broadly accepted and the observation of X-ray diffraction in 1912[16] confirmed for most scientists that X-rays were a form of electromagnetic radiation.

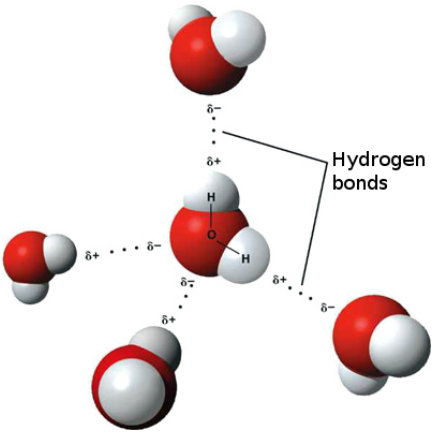


X-ray crystallography shows the arrangement of water molecules in ice, revealing the hydrogen bonds that hold the solid together. Few other methods can determine the structure of matter with such sub-atomic precision (*resolution*).

## X-ray analysis of crystals

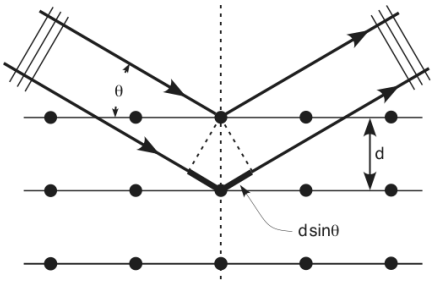


The incoming beam (coming from upper left) causes each scatterer to re-radiate a small portion of its intensity as a spherical wave. If scatterers are arranged symmetrically with a separation *d*, these spherical waves will be in sync (add constructively) only in directions where their path-length difference 2*d* sin θ equals an integer multiple of the wavelength λ. In that case, part of the incoming beam is deflected by an angle 2θ, producing a *reflection* spot in the diffraction pattern.

Crystals are regular arrays of atoms, and X-rays can be considered waves of electromagnetic radiation. Atoms scatter X-ray waves, primarily through the atoms' electrons. Just as an ocean wave striking a lighthouse produces secondary circular waves emanating from the lighthouse, so an X-ray striking an electron produces secondary spherical waves emanating from the electron. This phenomenon is known as elastic scattering, and the electron (or lighthouse) is known as the *scatterer*. A regular array of scatterers produces a regular array of spherical waves. Although these waves cancel one another out in most directions through destructive interference, they add constructively in a few specific directions, determined by Bragg's law:

$$2d \sin\theta = n\lambda$$

Here *d* is the spacing between diffracting planes, $\theta$ is the incident angle, *n* is any integer, and λ is the wavelength of the beam. These specific directions appear as spots on the diffraction pattern called *reflections*. Thus, X-ray diffraction results from an electromagnetic wave (the X-ray) impinging on a regular array of scatterers (the repeating arrangement of atoms within the crystal).

X-rays are used to produce the diffraction pattern because their wavelength λ is typically the same order of magnitude (1-100 Ångströms) as the spacing *d* between planes in the crystal. In principle, any wave impinging on a regular array of scatterers produces diffraction, as predicted first by Francesco Maria Grimaldi in 1665. To produce significant diffraction, the spacing between the scatterers and the wavelength of the impinging wave should be similar in size. For illustration, the diffraction of sunlight through a bird's feather was first reported by James Gregory in the later 17th century. The first artificial diffraction gratings for visible light were constructed by David Rittenhouse in 1787, and Joseph von Fraunhofer in 1821. However, visible light has too long a wavelength (typically, 5500 Ångströms) to observe diffraction from crystals. Prior to the first X-ray diffraction experiments, the spacings between lattice planes in a crystal were not known with certainty.

The idea that crystals could be used as a diffraction grating for X-rays arose in 1912 in a conversation between Paul Peter Ewald and Max von Laue in the English Garden in Munich. Ewald had proposed a resonator model of crystals for his thesis, but this model could not be validated using visible light, since the wavelength was much larger than the spacing between the resonators. Von Laue realized that electromagnetic radiation of a shorter wavelength was needed to observe such small spacings, and suggested that X-rays might have a wavelength comparable to the unit-cell spacing in crystals. Von Laue worked with two technicians, Walter Friedrich and his assistant Paul Knipping, to shine a beam of X-rays through a copper sulfate crystal and record its diffraction on a photographic plate. After being developed, the plate showed a large number of well-defined spots arranged in a pattern of intersecting circles around the spot produced by the central beam.[16] [17] Von Laue developed a law that connects the scattering angles and the size and orientation of the unit-cell spacings in the crystal, for which he was awarded the Nobel Prize in Physics in 1914.[18]

As described in the mathematical derivation below, the X-ray scattering is determined by the density of electrons within the crystal. Since the energy of an X-ray is much greater than that of a valence electron, the scattering may be modeled as Thomson scattering, the interaction of an electromagnetic ray with a free electron. This model is generally adopted to describe the polarization of the scattered radiation. The intensity of Thomson scattering declines as $1/m^2$ with the mass $m$ of the charged particle that is scattering the radiation; hence, the atomic nuclei, which are thousands of times heavier than an electron, contribute negligibly to the scattered X-rays.

### Development from 1912 to 1920

After Von Laue's pioneering research, the field developed rapidly, most notably by physicists William Lawrence Bragg and his father William Henry Bragg. In 1912-1913, the younger Bragg developed Bragg's law, which connects the observed scattering with reflections from evenly spaced planes within the crystal.[19] [20] [21] The Braggs, father and son, shared the 1915 Nobel Prize in Physics for their work in crystallography. The earliest structures were generally simple and marked by one-dimensional symmetry. However, as computational and experimental methods improved over the next decades, it became feasible to deduce reliable atomic positions for more complicated two- and three-dimensional arrangements of atoms in the unit-cell.

The potential of X-ray crystallography for determining the structure of molecules and minerals — then only known vaguely from chemical and hydrodynamic experiments — was realized immediately. The earliest structures were simple inorganic crystals and minerals, but even these revealed fundamental laws of physics and chemistry. The first atomic-resolution structure to be "solved" (i.e. determined) in 1914 was that of table salt.[22] [23] [24] The distribution of electrons in the table-salt structure showed that crystals are not necessarily composed of covalently bonded molecules, and proved the existence of ionic compounds.[25] The structure of diamond was solved in the same year,[26] [27] proving the tetrahedral arrangement of its chemical bonds and showing that the length of C–C single bond was 1.52 Ångströms. Other early structures included copper,[28] calcium fluoride ($CaF_2$, also known as *fluorite*), calcite ($CaCO_3$) and pyrite ($FeS_2$)[29] in 1914; spinel ($MgAl_2O_4$) in 1915;[30] [31] the rutile and anatase forms of titanium dioxide ($TiO_2$) in 1916;[32] pyrochroite $Mn(OH)_2$ and, by extension, brucite $Mg(OH)_2$ in 1919;.[33] [34] Also in 1919 sodium nitrate ($NaNO_3$) and cesium dichloroiodide ($CsICl_2$) were determined by Ralph Walter Graystone Wyckoff, and the wurtzite (hexagonal ZnS) structure became known in 1920.[35]

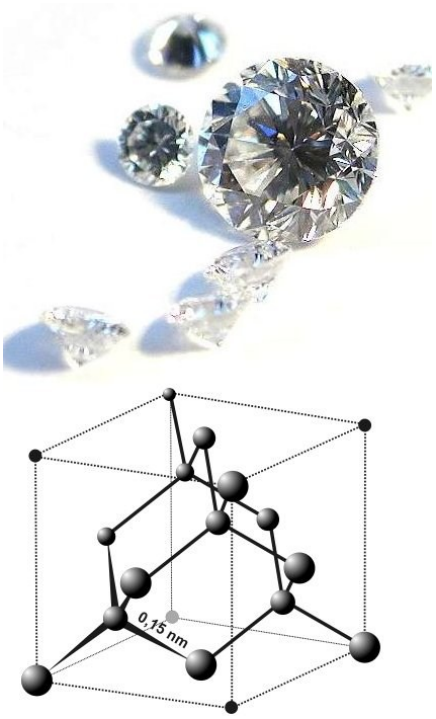


Although diamonds (top left) and graphite (top right) are identical in chemical composition — being both pure carbon — X-ray crystallography revealed the arrangement of their atoms (bottom) accounts for their different properties. In diamond, the carbon atoms are arranged tetrahedrally and held together by single covalent bonds, making it strong in all directions. By contrast, graphite is composed of stacked sheets. Within the sheet, the bonding is covalent and has hexagonal symmetry, but there are no covalent bonds between the sheets, making graphite easy to cleave into flakes.

The structure of graphite was solved in 1916[36] by the related method of powder diffraction,[37] which was developed by Peter Debye and Paul Scherrer and, independently, by Albert Hull in 1917.[38] The structure of graphite was determined from single-crystal diffraction in 1924 by two groups independently.[39] [40] Hull also used the powder method to determine the structures of various metals, such as iron[41] and magnesium.[42]

## Contributions to chemistry and material science

X-ray crystallography has led to a better understanding of chemical bonds and non-covalent interactions. The initial studies revealed the typical radii of atoms, and confirmed many theoretical models of chemical bonding, such as the tetrahedral bonding of carbon in the diamond structure,[26] the octahedral bonding of metals observed in ammonium hexachloroplatinate (IV),[43] and the resonance observed in the planar carbonate group[29] and in aromatic molecules.[44] Kathleen Lonsdale's 1928 structure of hexamethylbenzene[45] established the hexagonal symmetry of

benzene and showed a clear difference in bond length between the aliphatic C–C bonds and aromatic C–C bonds; this finding led to the idea of resonance between chemical bonds, which had profound consequences for the development of chemistry.[46] Her conclusions were anticipated by William Henry Bragg, who published models of naphthalene and anthracene in 1921 based on other molecules, an early form of molecular replacement.[44] [47]

Also in the 1920s, Victor Moritz Goldschmidt and later Linus Pauling developed rules for eliminating chemically unlikely structures and for determining the relative sizes of atoms. These rules led to the structure of brookite (1928) and an understanding of the relative stability of the rutile, brookite and anatase forms of titanium dioxide.

The distance between two bonded atoms is a sensitive measure of the bond strength and its bond order; thus, X-ray crystallographic studies have led to the discovery of even more exotic types of bonding in inorganic chemistry, such as metal-metal double bonds,[48] [49] [50] metal-metal quadruple bonds,[51] [52] [53] and three-center, two-electron bonds.[54] X-ray crystallography — or, strictly speaking, an inelastic Compton scattering experiment — has also provided evidence for the partly covalent character of hydrogen bonds.[55] In the field of organometallic chemistry, the X-ray structure of ferrocene initiated scientific studies of sandwich compounds,[56] [57] while that of Zeise's salt stimulated research into "back bonding" and metal-pi complexes.[58] [59] [60] [61] Finally, X-ray crystallography had a pioneering role in the development of supramolecular chemistry, particularly in clarifying the structures of the crown ethers and the principles of host-guest chemistry.

In material sciences, many complicated inorganic and organometallic systems have been analyzed using single-crystal methods, such as fullerenes, metalloporphyrins, and other complicated compounds. Single-crystal diffraction is also used in the pharmaceutical industry, due to recent problems with polymorphs. The major factors affecting the quality of single-crystal structures are the crystal's size and regularity; recrystallization is a commonly used technique to improve these factors in small-molecule crystals. The Cambridge Structural Database contains over 500,000 structures; over 99% of these structures were determined by X-ray diffraction.

## Mineralogy and metallurgy

Since the 1920s, X-ray diffraction has been the principal method for determining the arrangement of atoms in minerals and metals. The application of X-ray crystallography to mineralogy began with the structure of garnet, which was determined in 1924 by Menzer. A systematic X-ray crystallographic study of the silicates was undertaken in the 1920s. This study showed that, as the Si/O ratio is altered, the silicate crystals exhibit significant changes in their atomic arrangements. Machatschki extended these insights to minerals in which aluminium substitutes for the silicon atoms of the silicates. The first application of X-ray crystallography to metallurgy likewise occurred in the mid-1920s.[62] [63] [64] [65] [66] [67] Most notably, Linus Pauling's structure of the alloy $Mg_2Sn$[68] led to his theory of the stability and structure of complex ionic crystals.[69]

### Early organic and small biological molecules

The first structure of an organic compound, hexamethylenetetramine, was solved in 1923.[70] This was followed by several studies of long-chain fatty acids, which are an important component of biological membranes.[71] [72] [73] [74] [75] [76] [77] [78] [79] In the 1930s, the structures of much larger molecules with two-dimensional complexity began to be solved. A significant advance was the structure of phthalocyanine,[80] a large planar molecule that is closely related to porphyrin molecules important in biology, such as heme, corrin and chlorophyll.

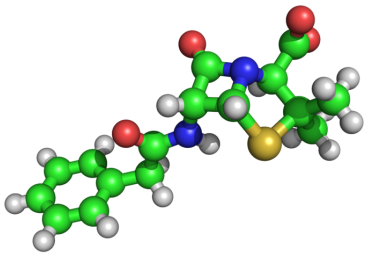

The three-dimensional structure of penicillin, for which Dorothy Crowfoot Hodgkin was awarded the Nobel Prize in Chemistry in 1964. The green, white, red, yellow and blue spheres represent atoms of carbon, hydrogen, oxygen, sulfur and nitrogen, respectively.

X-ray crystallography of biological molecules took off with Dorothy Crowfoot Hodgkin, who solved the structures of cholesterol (1937), vitamin B12 (1945) and penicillin (1954), for which she was awarded the Nobel Prize in Chemistry in 1964. In 1969, she succeeded in solving the structure of insulin, on which she worked for over thirty years.[81]

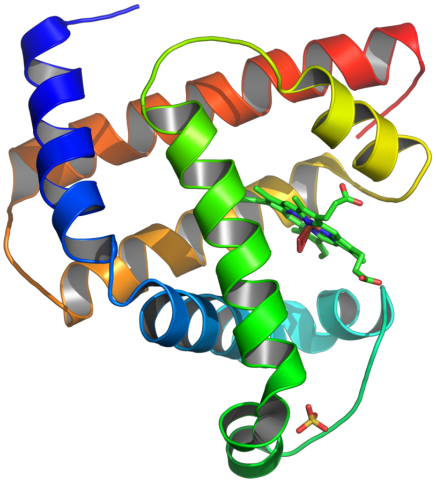

Ribbon diagram of the structure of myoglobin, showing colored alpha helices. Such proteins are long, linear molecules with thousands of atoms; yet the relative position of each atom has been determined with sub-atomic resolution by X-ray crystallography. Since it is difficult to visualize all the atoms at once, the ribbon shows the rough path of the protein polymer from its N-terminus (blue) to its C-terminus (red).

### Biological macromolecular crystallography

Crystal structures of proteins (which are irregular and hundreds of times larger than cholesterol) began to be solved in the late 1950s, beginning with the structure of sperm whale myoglobin by Max Perutz and Sir John Cowdery Kendrew, for which they were awarded the Nobel Prize in Chemistry in 1962.[82] Since that success, over 48970 X-ray crystal structures of proteins, nucleic acids and other biological molecules have been determined.[83] For comparison, the nearest competing method in terms of structures analyzed is nuclear magnetic resonance (NMR) spectroscopy, which has resolved 7806 chemical structures.[84] Moreover, crystallography can solve structures of arbitrarily large molecules, whereas solution-state NMR is restricted to relatively small ones (less than 70 kDa). X-ray crystallography is now used routinely by scientists to determine how a pharmaceutical drug interacts with its protein target and what changes might improve it.[85] However, intrinsic membrane proteins remain challenging to crystallize because they require detergents or other means to solubilize them in isolation, and such detergents often interfere with crystallization. Such membrane proteins are a large component of the genome and include many proteins of great physiological importance, such as ion channels and receptors.[86] [87]

## Relationship to other scattering techniques

### Elastic vs. inelastic scattering

X-ray crystallography is a form of elastic scattering; the outgoing X-rays have the same energy, and thus same wavelength, as the incoming X-rays, only with altered direction. By contrast, *inelastic scattering* occurs when energy is transferred from the incoming X-ray to the crystal, e.g., by exciting an inner-shell electron to a higher energy

level. Such inelastic scattering reduces the energy (or increases the wavelength) of the outgoing beam. Inelastic scattering is useful for probing such excitations of matter, but not in determining the distribution of scatterers within the matter, which is the goal of X-ray crystallography.

X-rays range in wavelength from 10 to 0.01 nanometers; a typical wavelength used for crystallography is 1 Å (0.1 nm), which is on the scale of covalent chemical bonds and the radius of a single atom. Longer-wavelength photons (such as ultraviolet radiation) would not have sufficient resolution to determine the atomic positions. At the other extreme, shorter-wavelength photons such as gamma rays are difficult to produce in large numbers, difficult to focus, and interact too strongly with matter, producing particle-antiparticle pairs. Therefore, X-rays are the "sweetspot" for wavelength when determining atomic-resolution structures from the scattering of electromagnetic radiation.

## Other X-ray techniques

Other forms of elastic X-ray scattering include powder diffraction, SAXS and several types of X-ray fiber diffraction, which was used by Rosalind Franklin in determining the double-helix structure of DNA. In general, single-crystal X-ray diffraction offers more structural information than these other techniques; however, it requires a sufficiently large and regular crystal, which is not always available.

These scattering methods generally use *monochromatic* X-rays, which are restricted to a single wavelength with minor deviations. A broad spectrum of X-rays (that is, a blend of X-rays with different wavelengths) can also be used to carry out X-ray diffraction, a technique known as the Laue method. This is the method used in the original discovery of X-ray diffraction. Laue scattering provides much structural information with only a short exposure to the X-ray beam, and is therefore used in structural studies of very rapid events (Time resolved crystallography). However, it is not as well-suited as monochromatic scattering for determining the full atomic structure of a crystal and therefore works better with crystals with relatively simple atomic arrangements.

The Laue back reflection mode records X-rays scattered backwards from a broad spectrum source. This is useful if the sample is too thick for X-rays to transmit through it. The diffracting planes in the crystal are determined by knowing that the normal to the diffracting plane bisects the angle between the incident beam and the diffracted beam. A Greninger chart can be used [88] to interpret the back reflection Laue photograph.

## Electron and neutron diffraction

Other particles, such as electrons and neutrons, may be used to produce a diffraction pattern. Although electron, neutron, and X-ray scattering are based on different physical processes, the resulting diffraction patterns are analyzed using the same coherent diffraction imaging techniques.

As derived below, the electron density within the crystal and the diffraction patterns are related by a simple mathematical method, the Fourier transform, which allows the density to be calculated relatively easily from the patterns. However, this works only if the scattering is *weak*, i.e., if the scattered beams are much less intense than the incoming beam. Weakly scattered beams pass through the remainder of the crystal without undergoing a second scattering event. Such re-scattered waves are called "secondary scattering" and hinder the analysis. Any sufficiently thick crystal will produce secondary scattering, but since X-rays interact relatively weakly with the electrons, this is generally not a significant concern. By contrast, electron beams may produce strong secondary scattering even for relatively thin crystals (>100 nm). Since this thickness corresponds to the diameter of many viruses, a promising direction is the electron diffraction of isolated macromolecular assemblies, such as viral capsids and molecular machines, which may be carried out with a cryo-electron microscope. Moreover the strong interaction of electrons with matter (about 1000 times stronger than for X-rays) allows determination of the atomic structure of extremely small volumes. The field of applications for electron crystallography ranges from bio molecules like membrane proteins over organic thin films to the complex structures of (nanocrystalline) intermetallic compounds and zeolites.

Neutron diffraction is an excellent method for structure determination, although it has been difficult to obtain intense, monochromatic beams of neutrons in sufficient quantities. Traditionally, nuclear reactors have been used, although the new Spallation Neutron Source holds much promise in the near future. Being uncharged, neutrons scatter much more readily from the atomic nuclei rather than from the electrons. Therefore, neutron scattering is very useful for observing the positions of light atoms with few electrons, especially hydrogen, which is essentially invisible in the X-ray diffraction. Neutron scattering also has the remarkable property that the solvent can be made invisible by adjusting the ratio of normal water, $H_2O$, and heavy water, $D_2O$.

# Methods

## Overview of single-crystal X-ray diffraction

The oldest and most precise method of X-ray crystallography is *single-crystal X-ray diffraction*, in which a beam of X-rays strikes a single crystal, producing scattered beams. When they land on a piece of film or other detector, these beams make a *diffraction pattern* of spots; the strengths and angles of these beams are recorded as the crystal is gradually rotated.[89] Each spot is called a *reflection*, since it corresponds to the reflection of the X-rays from one set of evenly spaced planes within the crystal. For single crystals of sufficient purity and regularity, X-ray diffraction data can determine the mean chemical bond lengths and angles to within a few thousandths of an Ångström and to within a few tenths of a degree, respectively. The atoms in a crystal are not static, but oscillate about their mean positions, usually by less than a few tenths of an Ångström. X-ray crystallography allows measuring the size of these oscillations.

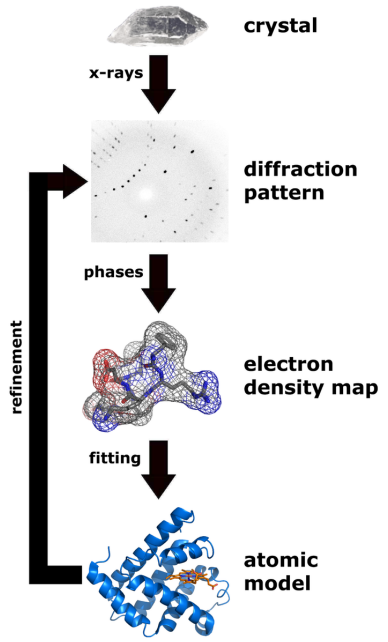


Workflow for solving the structure of a molecule by X-ray crystallography.

### Procedure

The technique of single-crystal X-ray crystallography has three basic steps. The first — and often most difficult — step is to obtain an adequate crystal of the material under study. The crystal should be sufficiently large (typically larger than 0.1 mm in all dimensions), pure in composition and regular in structure, with no significant internal imperfections such as cracks or twinning.

In the second step, the crystal is placed in an intense beam of X-rays, usually of a single wavelength (*monochromatic X-rays*), producing the regular pattern of reflections. As the crystal is gradually rotated, previous reflections disappear and new ones appear; the intensity of every spot is recorded at every orientation of the crystal. Multiple data sets may have to be collected, with each set covering slightly more than half a full rotation of the crystal and typically containing tens of thousands of reflections.

In the third step, these data are combined computationally with complementary chemical information to produce and refine a model of the arrangement of atoms within the crystal. The final, refined model of the atomic arrangement — now called a *crystal structure* — is usually stored in a public database.

### Limitations

As the crystal's repeating unit, its unit cell, becomes larger and more complex, the atomic-level picture provided by X-ray crystallography becomes less well-resolved (more "fuzzy") for a given number of observed reflections. Two limiting cases of X-ray crystallography—"small-molecule" and "macromolecular" crystallography—are often discerned. *Small-molecule crystallography* typically involves crystals with fewer than 100 atoms in their asymmetric unit; such crystal structures are usually so well resolved that the atoms can be discerned as isolated "blobs" of electron density. By contrast, *macromolecular crystallography* often involves tens of thousands of atoms in the unit cell. Such crystal structures are generally less well-resolved (more "smeared out"); the atoms and chemical bonds appear as tubes of electron density, rather than as isolated atoms. In general, small molecules are also easier to crystallize than macromolecules; however, X-ray crystallography has proven possible even for viruses with hundreds of thousands of atoms.

## Crystallization

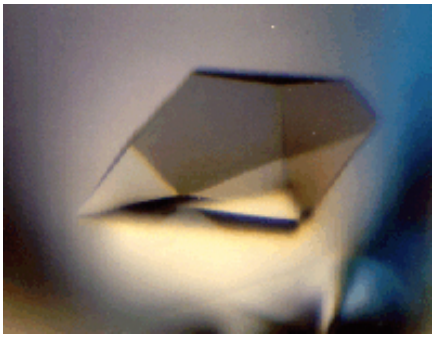

A protein crystal seen under a microscope. Crystals used in X-ray crystallography may be smaller than a millimeter across.

Although crystallography can be used to characterize the disorder in an impure or irregular crystal, crystallography generally requires a pure crystal of high regularity to solve the structure of a complicated arrangement of atoms. Pure, regular crystals can sometimes be obtained from natural or synthetic materials, such as samples of metals, minerals or other macroscopic materials. The regularity of such crystals can sometimes be improved with macromolecular crystal annealing [90] [91] [92] and other methods. However, in many cases, obtaining a diffraction-quality crystal is the chief barrier to solving its atomic-resolution structure.[93]

Small-molecule and macromolecular crystallography differ in the range of possible techniques used to produce diffraction-quality crystals. Small molecules generally have few degrees of conformational freedom, and may be crystallized by a wide range of methods, such as chemical vapor deposition and recrystallization. By contrast, macromolecules generally have many degrees of freedom and their crystallization must be carried out to maintain a stable structure. For example, proteins and larger RNA molecules cannot be crystallized if their tertiary structure has been unfolded; therefore, the range of crystallization conditions is restricted to solution conditions in which such molecules remain folded.

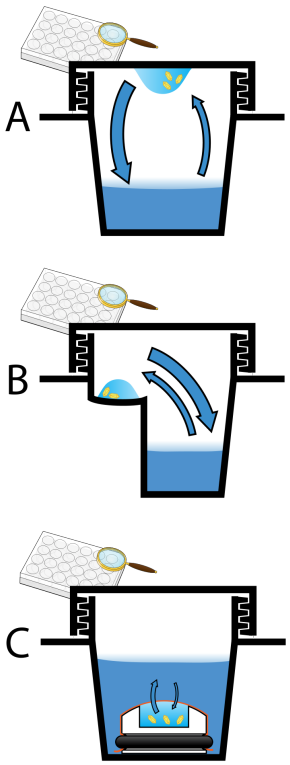


Three methods of preparing crystals, A: Hanging drop. B: Sitting drop. C: Microdialysis

Protein crystals are almost always grown in solution. The most common approach is to lower the solubility of its component molecules very gradually; if this is done too quickly, the molecules will precipitate from solution, forming a useless dust or amorphous gel on the bottom of the container. Crystal growth in solution is characterized by two steps: *nucleation* of a microscopic crystallite (possibly having only 100 molecules), followed by *growth* of that crystallite, ideally to a diffraction-quality crystal.[94] The solution conditions that favor the first step (nucleation) are not always the same conditions that favor the second step (subsequent growth). The crystallographer's goal is to identify solution conditions that favor the development of a single, large crystal, since larger crystals offer improved resolution of the molecule. Consequently, the solution conditions should *disfavor* the first step (nucleation) but *favor* the second (growth), so that only one large crystal forms per droplet. If nucleation is favored too much, a shower of small crystallites will form in the droplet, rather than one large crystal; if favored too little, no crystal will form whatsoever.

It is extremely difficult to predict good conditions for nucleation or growth of well-ordered crystals.[95] In practice, favorable conditions are identified by *screening*; a very large batch of the molecules is prepared, and a wide variety of crystallization solutions are tested.[96] Hundreds, even thousands, of solution conditions are generally tried before finding the successful one. The various conditions can use one or more physical mechanisms to lower the solubility of the molecule; for example, some may change the pH, some contain salts of the Hofmeister series or chemicals that lower the dielectric constant of the solution, and still others contain large polymers such as polyethylene glycol that drive the molecule out of solution by entropic effects. It is also common to try several temperatures for encouraging crystallization, or to gradually lower the temperature so that the solution becomes supersaturated. These methods require large amounts of the target molecule, as they use high concentration of the molecule(s) to be crystallized. Due to the difficulty in obtaining such large quantities (milligrams) of crystallization grade protein, robots have been developed that are capable of accurately dispensing crystallization trial drops that are in the order of 100 nanoliters in volume. This means that 10-fold less protein is used per-experiment when compared to crystallization trials setup by hand (in the order of 1 microliter).[97]

Several factors are known to inhibit or mar crystallization. The growing crystals are generally held at a constant temperature and protected from shocks or vibrations that might disturb their crystallization. Impurities in the molecules or in the crystallization solutions are often inimical to crystallization. Conformational flexibility in the molecule also tends to make crystallization less likely, due to entropy. Ironically, molecules that tend to self-assemble into regular helices are often unwilling to assemble into crystals. Crystals can be marred by twinning, which can occur when a unit cell can pack equally favorably in multiple orientations; although recent advances in computational methods may allow solving the structure of some twinned crystals. Having failed to crystallize a target molecule, a crystallographer may try again with a slightly modified version of the molecule; even small changes in molecular properties can lead to large differences in crystallization behavior.

## Data collection

### Mounting the crystal

The crystal is mounted for measurements so that it may be held in the X-ray beam and rotated. There are several methods of mounting. Although crystals were once loaded into glass capillaries with the crystallization solution (the mother liquor), a modern approach is to scoop the crystal up in a tiny loop, made of nylon or plastic and attached to a solid rod, that is then flash-frozen with liquid nitrogen.[98] This freezing reduces the radiation damage of the X-rays, as well as the noise in the Bragg peaks due to thermal motion (the Debye-Waller effect). However, untreated crystals often crack if flash-frozen; therefore, they are generally pre-soaked in a cryoprotectant solution before freezing.[99] Unfortunately, this pre-soak may itself cause the crystal to crack, ruining it for crystallography. Generally, successful cryo-conditions are identified by trial and error.

The capillary or loop is mounted on a goniometer, which allows it to be positioned accurately within the X-ray beam and rotated. Since both the crystal and the beam are often very small, the crystal must be centered within the beam to within ~25 micrometers accuracy, which is aided by a camera focused on the crystal. The most common type of goniometer is the "kappa goniometer", which offers three angles of rotation: the ω angle, which rotates about an axis perpendicular to the beam; the κ angle, about an axis at ~50° to the ω axis; and, finally, the φ angle about the loop/capillary axis. When the κ angle is zero, the ω and φ axes are aligned. The κ rotation allows for convenient mounting of the crystal, since the arm in which the crystal is mounted may be swung out towards the crystallographer. The oscillations carried out during data collection (mentioned below) involve the ω axis only. An older type of goniometer is the four-circle goniometer, and its relatives such as the six-circle goniometer.

### X-ray sources

The mounted crystal is then irradiated with a beam of monochromatic X-rays. The brightest and most useful X-ray sources are synchrotrons; their much higher luminosity allows for better resolution. They also make it convenient to tune the wavelength of the radiation, which is useful for multi-wavelength anomalous dispersion (MAD) phasing, described below. Synchrotrons are generally national facilities, each with several dedicated beamlines where data is collected around the clock, seven days a week.

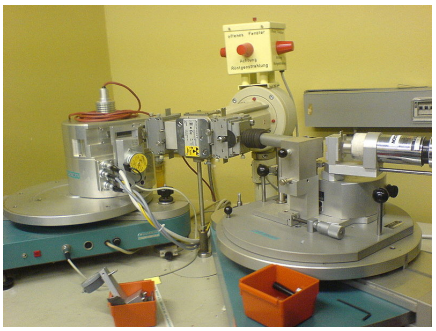

A diffractometer

Smaller, X-ray generators are often used in laboratories to check the quality of crystals before bringing them to a synchrotron and sometimes to solve a crystal structure. In such systems, electrons are boiled off of a cathode and accelerated through a strong electric potential of ~50 kV; having reached a high speed, the electrons collide with a metal plate, emitting *bremsstrahlung* and some strong spectral lines corresponding to the excitation of inner-shell electrons of the metal. The most common metal used is copper, which can be kept cool easily, due to its high thermal conductivity, and which produces strong $K_\alpha$ and $K_\beta$ lines. The $K_\beta$ line is sometimes suppressed with a thin (~10 μm) nickel foil. The simplest and cheapest variety of sealed X-ray tube has a stationary anode (the Crookes tube) and produces ~2 kW of X-ray radiation. The more expensive variety has a rotating-anode type source that produces ~14 kW of X-ray radiation.

X-rays are generally filtered (by use of X-Ray Filters) to a single wavelength (made monochromatic) and collimated to a single direction before they are allowed to strike the crystal. The filtering not only simplifies the data analysis, but also removes radiation that degrades the crystal without contributing useful information. Collimation is done either with a collimator (basically, a long tube) or with a clever arrangement of gently curved mirrors. Mirror systems are preferred for small crystals (under 0.3 mm) or with large unit cells (over 150 Å)

### Recording the reflections

When a crystal is mounted and exposed to an intense beam of X-rays, it scatters the X-rays into a pattern of spots or *reflections* that can be observed on a screen behind the crystal. A similar pattern may be seen by shining a laser pointer at a compact disc. The relative intensities of these spots provide the information to determine the arrangement of molecules within the crystal in atomic detail. The intensities of these reflections may be recorded with photographic film, an area detector or with a charge-coupled device (CCD) image sensor. The peaks at small angles correspond to low-resolution data, whereas those at high angles represent high-resolution data; thus, an upper limit on the eventual resolution of the structure can be determined from the first few images. Some measures of diffraction quality can be determined at this point, such as the mosaicity of the crystal and its overall disorder, as observed in the peak widths. Some pathologies of the crystal that would render it unfit for solving the structure can also be diagnosed quickly at this point.

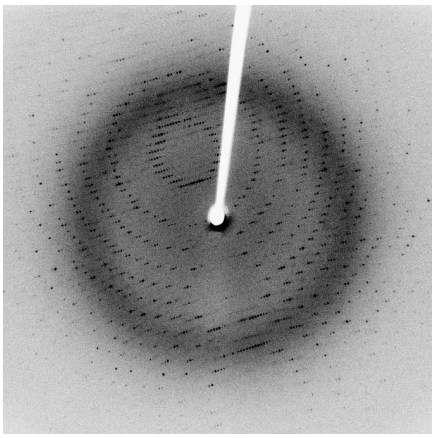

An X-ray diffraction pattern of a crystallized enzyme. The pattern of spots (called *reflections*) can be used to determine the structure of the enzyme.

One image of spots is insufficient to reconstruct the whole crystal; it represents only a small slice of the full Fourier transform. To collect all the necessary information, the crystal must be rotated step-by-step through 180°, with an image recorded at every step; actually, slightly more than 180° is required to cover reciprocal space, due to the curvature of the Ewald sphere. However, if the crystal has a higher symmetry, a smaller angular range such as 90° or 45° may be recorded. The rotation axis should be changed at least once, to avoid developing a "blind spot" in reciprocal space close to the rotation axis. It is customary to rock the crystal slightly (by 0.5-2°) to catch a broader region of reciprocal space.

Multiple data sets may be necessary for certain phasing methods. For example, MAD phasing requires that the scattering be recorded at least three (and usually four, for redundancy) wavelengths of the incoming X-ray radiation. A single crystal may degrade too much during the collection of one data set, owing to radiation damage; in such cases, data sets on multiple crystals must be taken.[100]

## Data analysis

### Crystal symmetry, unit cell, and image scaling

The recorded series of two-dimensional diffraction patterns, each corresponding to a different crystal orientation, is converted into a three-dimensional model of the electron density; the conversion uses the mathematical technique of Fourier transforms, which is explained below. Each spot corresponds to a different type of variation in the electron density; the crystallographer must determine *which* variation corresponds to *which* spot (*indexing*), the relative strengths of the spots in different images (*merging and scaling*) and how the variations should be combined to yield the total electron density (*phasing*).

Data processing begins with *indexing* the reflections. This means identifying the dimensions of the unit cell and which image peak corresponds to which position in reciprocal space. A byproduct of indexing is to determine the symmetry of the crystal, i.e., its *space group*. Some space groups can be eliminated from the beginning. For example, reflection symmetries cannot be observed in chiral molecules; thus, only 65 space groups of 243 possible are allowed for protein molecules which are almost always chiral. Indexing is generally accomplished using an *autoindexing* routine.[101] Having assigned symmetry, the data is then *integrated*. This converts the hundreds of images containing the thousands of reflections into a single file, consisting of (at the very least) records of the Miller index of each reflection, and an intensity for each reflection (at this state the file often also includes error estimates

and measures of partiality (what part of a given reflection was recorded on that image)).

A full data set may consist of hundreds of separate images taken at different orientations of the crystal. The first step is to merge and scale these various images, that is, to identify which peaks appear in two or more images (*merging*) and to scale the relative images so that they have a consistent intensity scale. Optimizing the intensity scale is critical because the relative intensity of the peaks is the key information from which the structure is determined. The repetitive technique of crystallographic data collection and the often high symmetry of crystalline materials cause the diffractometer to record many symmetry-equivalent reflections multiple times. This allows calculating the symmetry-related R-factor, a reliability index based upon how similar are the measured intensities of symmetry-equivalent reflections, thus assessing the quality of the data.

**Initial phasing**

The data collected from a diffraction experiment is a reciprocal space representation of the crystal lattice. The position of each diffraction 'spot' is governed by the size and shape of the unit cell, and the inherent symmetry within the crystal. The intensity of each diffraction 'spot' is recorded, and this intensity is proportional to the square of the *structure factor* amplitude. The structure factor is a complex number containing information relating to both the amplitude and phase of a wave. In order to obtain an interpretable *electron density map*, both amplitude and phase must be known (an electron density map allows a crystallographer to build a starting model of the molecule). The phase cannot be directly recorded during a diffraction experiment: this is known as the phase problem. Initial phase estimates can be obtained in a variety of ways:

- ***Ab initio*** **phasing** or **direct methods** - This is usually the method of choice for small molecules (<1000 non-hydrogen atoms), and has been used successfully to solve the phase problems for small proteins. If the resolution of the data is better than 1.4 Å (140 pm), direct methods can be used to obtain phase information, by exploiting known phase relationships between certain groups of reflections.[102] [103]
- **Molecular replacement** - if a related structure is known, it can be used as a search model in molecular replacement to determine the orientation and position of the molecules within the unit cell. The phases obtained this way can be used to generate *electron density maps*.[104]
- **Anomalous X-ray scattering** (*MAD or SAD phasing*) - the X-ray wavelength may be scanned past an absorption edge of an atom, which changes the scattering in a known way. By recording full sets of reflections at three different wavelengths (far below, far above and in the middle of the absorption edge) one can solve for the substructure of the anomalously diffracting atoms and thence the structure of the whole molecule. The most popular method of incorporating anomalous scattering atoms into proteins is to express the protein in a methionine auxotroph (a host incapable of synthesizing methionine) in a media rich in seleno-methionine, which contains selenium atoms. A MAD experiment can then be conducted around the absorption edge, which should then yield the position of any methionine residues within the protein, providing initial phases.[105]
- **Heavy atom methods** (multiple isomorphous replacement) - If electron-dense metal atoms can be introduced into the crystal, direct methods or Patterson-space methods can be used to determine their location and to obtain initial phases. Such heavy atoms can be introduced either by soaking the crystal in a heavy atom-containing solution, or by co-crystallization (growing the crystals in the presence of a heavy atom). As in MAD phasing, the changes in the scattering amplitudes can be interpreted to yield the phases. Although this is the original method by which protein crystal structures were solved, it has largely been superseded by MAD phasing with selenomethionine.[104]

### Model building and phase refinement

Having obtained initial phases, an initial model can be built. This model can be used to refine the phases, leading to an improved model, and so on. Given a model of some atomic positions, these positions and their respective Debye-Waller factors (or **B**-factors, accounting for the thermal motion of the atom) can be refined to fit the observed diffraction data, ideally yielding a better set of phases. A new model can then be fit to the new electron density map and a further round of refinement is carried out. This continues until the correlation between the diffraction data and the model is maximized. The agreement is measured by an *R*-factor defined as

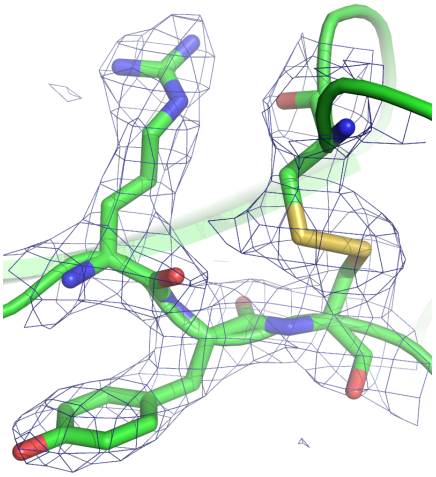

A protein crystal structure at 2.7 Å resolution. The mesh encloses the region in which the electron density exceeds a given threshold. The straight segments represent chemical bonds between the non-hydrogen atoms of an arginine (upper left), a tyrosine (lower left), a disulfide bond (upper right, in yellow), and some peptide groups (running left-right in the middle). The two curved green tubes represent spline fits to the polypeptide backbone.

$$R = \frac{\sum_{\text{all reflections}} |F_o - F_c|}{\sum_{\text{all reflections}} |F_o|}$$

A similar quality criterion is $R_{\text{free}}$, which is calculated from a subset (~10%) of reflections that were not included in the structure refinement. Both *R* factors depend on the resolution of the data. As a rule of thumb, $R_{\text{free}}$ should be approximately the resolution in Ångströms divided by 10; thus, a data-set with 2 Å resolution should yield a final $R_{\text{free}}$ ~ 0.2. Chemical bonding features such as stereochemistry, hydrogen bonding and distribution of bond lengths and angles are complementary measures of the model quality. Phase bias is a serious problem in such iterative model building. *Omit maps* are a common technique used to check for this.

It may not be possible to observe every atom of the crystallized molecule - it must be remembered that the resulting electron density is an average of all the molecules within the crystal. In some cases, there is too much residual disorder in those atoms, and the resulting electron density for atoms existing in many conformations is smeared to such an extent that it is no longer detectable in the electron density map. Weakly scattering atoms such as hydrogen are routinely invisible. It is also possible for a single atom to appear multiple times in an electron density map, e.g., if a protein sidechain has multiple (<4) allowed conformations. In still other cases, the crystallographer may detect that the covalent structure deduced for the molecule was incorrect, or changed. For example, proteins may be cleaved or undergo post-translational modifications that were not detected prior to the crystallization.

### Deposition of the structure

Once the model of a molecule's structure has been finalized, it is often deposited in a crystallographic database such as the Cambridge Structural Database (for small molecules), the Inorganic Crystal Structure Database (ICSD) (for inorganic compounds) or the Protein Data Bank (for protein structures). Many structures obtained in private commercial ventures to crystallize medicinally relevant proteins, are not deposited in public crystallographic databases.

## Diffraction theory

The main goal of X-ray crystallography is to determine the density of electrons $f(\mathbf{r})$ throughout the crystal, where $\mathbf{r}$ represents the three-dimensional position vector within the crystal. To do this, X-ray scattering is used to collect data about its Fourier transform $F(\mathbf{q})$, which is inverted mathematically to obtain the density defined in real space, using the formula

$$f(\mathbf{r}) = \int \frac{d\mathbf{q}}{(2\pi)^3} F(\mathbf{q}) e^{i\mathbf{q}\cdot\mathbf{r}}$$

where the integral is taken over all values of $\mathbf{q}$. The three-dimensional real vector $\mathbf{q}$ represents a point in reciprocal space, that is, to a particular oscillation in the electron density as one moves in the direction in which $\mathbf{q}$ points. The length of $\mathbf{q}$ corresponds to $2\ \pi$ divided by the wavelength of the oscillation. The corresponding formula for a Fourier transform will be used below

$$F(\mathbf{q}) = \int d\mathbf{r} f(\mathbf{r}) e^{-i\mathbf{q}\cdot\mathbf{r}}$$

where the integral is summed over all possible values of the position vector $\mathbf{r}$ within the crystal.

The Fourier transform $F(\mathbf{q})$ is generally a complex number, and therefore has a magnitude $|F(\mathbf{q})|$ and a phase $\varphi(\mathbf{q})$ related by the equation

$$F(\mathbf{q}) = |F(\mathbf{q})| e^{i\phi(\mathbf{q})}$$

The intensities of the reflections observed in X-ray diffraction give us the magnitudes $|F(\mathbf{q})|$ but not the phases $\varphi(\mathbf{q})$. To obtain the phases, full sets of reflections are collected with known alterations to the scattering, either by modulating the wavelength past a certain absorption edge or by adding strongly scattering (i.e., electron-dense) metal atoms such as mercury. Combining the magnitudes and phases yields the full Fourier transform $F(\mathbf{q})$, which may be inverted to obtain the electron density $f(\mathbf{r})$.

Crystals are often idealized as being *perfectly* periodic. In that ideal case, the atoms are positioned on a perfect lattice, the electron density is perfectly periodic, and the Fourier transform $F(\mathbf{q})$ is zero except when $\mathbf{q}$ belongs to the reciprocal lattice (the so-called *Bragg peaks*). In reality, however, crystals are not perfectly periodic; atoms vibrate about their mean position, and there may be disorder of various types, such as mosaicity, dislocations, various point defects, and heterogeneity in the conformation of crystallized molecules. Therefore, the Bragg peaks have a finite width and there may be significant *diffuse scattering*, a continuum of scattered X-rays that fall between the Bragg peaks.

### Intuitive understanding by Bragg's law

An intuitive understanding of X-ray diffraction can be obtained from the Bragg model of diffraction. In this model, a given reflection is associated with a set of evenly spaced sheets running through the crystal, usually passing through the centers of the atoms of the crystal lattice. The orientation of a particular set of sheets is identified by its three Miller indices ($h$, $k$, $l$), and let their spacing be noted by $d$. William Lawrence Bragg proposed a model in which the incoming X-rays are scattered specularly (mirror-like) from each plane; from that assumption, X-rays scattered from adjacent planes will combine constructively (constructive interference) when the angle $\theta$ between the plane and the X-ray results in a path-length difference that is an integer multiple $n$ of the X-ray wavelength $\lambda$.

$$2d \sin\theta = n\lambda$$

A reflection is said to be *indexed* when its Miller indices (or, more correctly, its reciprocal lattice vector components) have been identified from the known wavelength and the scattering angle 2θ. Such indexing gives the unit-cell parameters, the lengths and angles of the unit-cell, as well as its space group. Since Bragg's law does not interpret the relative intensities of the reflections, however, it is generally inadequate to solve for the arrangement of atoms within the unit-cell; for that, a Fourier transform method must be carried out.

## Scattering as a Fourier transform

The incoming X-ray beam has a polarization and should be represented as a vector wave; however, for simplicity, let it be represented here as a scalar wave. We also ignore the complication of the time dependence of the wave and just focus on the wave's spatial dependence. Plane waves can be represented by a wave vector $\mathbf{k}_{in}$, and so the strength of the incoming wave at time *t=0* is given by

$$Ae^{i\mathbf{k}_{in}\cdot\mathbf{r}}$$

At position **r** within the sample, let there be a density of scatterers *f*(**r**); these scatterers should produce a scattered spherical wave of amplitude proportional to the local amplitude of the incoming wave times the number of scatterers in a small volume *dV* about **r**

$$\text{amplitude of scattered wave} = Ae^{i\mathbf{k}\cdot\mathbf{r}}Sf(\mathbf{r})dV$$

where *S* is the proportionality constant.

Let's consider the fraction of scattered waves that leave with an outgoing wave-vector of $\mathbf{k}_{out}$ and strike the screen at $\mathbf{r}_{screen}$. Since no energy is lost (elastic, not inelastic scattering), the wavelengths are the same as are the magnitudes of the wave-vectors $|\mathbf{k}_{in}|=|\mathbf{k}_{out}|$. From the time that the photon is scattered at **r** until it is absorbed at $\mathbf{r}_{screen}$, the photon undergoes a change in phase

$$e^{i\mathbf{k}_{out}\cdot(\mathbf{r}_{\text{screen}}-\mathbf{r})}$$

The net radiation arriving at $\mathbf{r}_{screen}$ is the sum of all the scattered waves throughout the crystal

which may be written as a Fourier transform

$$ASe^{i\mathbf{k}_{out}\cdot\mathbf{r}_{\text{screen}}}\int d\mathbf{r}\, f(\mathbf{r})e^{-i\mathbf{q}\cdot\mathbf{r}} = ASe^{i\mathbf{k}_{out}\cdot\mathbf{r}_{\text{screen}}}F(\mathbf{q})$$

where $\mathbf{q} = \mathbf{k}_{out} - \mathbf{k}_{in}$. The measured intensity of the reflection will be square of this amplitude

$$A^2S^2\,|F(\mathbf{q})|^2$$

## Friedel and Bijvoet mates

For every reflection corresponding to a point **q** in the reciprocal space, there is another reflection of the same intensity at the opposite point -**q**. This opposite reflection is known as the *Friedel mate* of the original reflection. This symmetry results from the mathematical fact that the density of electrons *f*(**r**) at a position **r** is always a real number. As noted above, *f*(**r**) is the inverse transform of its Fourier transform *F*(**q**); however, such an inverse transform is a complex number in general. To ensure that *f*(**r**) is real, the Fourier transform *F*(**q**) must be such that the Friedel mates *F*(**−q**) and *F*(**q**) are complex conjugates of one another. Thus, *F*(**−q**) has the same magnitude as *F*(**q**) but they have the opposite phase, i.e., $\varphi(\mathbf{q}) = -\varphi(\mathbf{q})$

$$F(-\mathbf{q}) = |F(-\mathbf{q})|\,e^{i\phi(-\mathbf{q})} = F^*(\mathbf{q}) = |F(\mathbf{q})|\,e^{-i\phi(\mathbf{q})}$$

The equality of their magnitudes ensures that the Friedel mates have the same intensity $|F|^2$. This symmetry allows one to measure the full Fourier transform from only half the reciprocal space, e.g., by rotating the crystal slightly more than a 180°, instead of a full turn. In crystals with significant symmetry, even more reflections may have the same intensity (Bijvoet mates); in such cases, even less of the reciprocal space may need to be measured, e.g., slightly more than 90°.

The Friedel-mate constraint can be derived from the definition of the inverse Fourier transform

$$f(\mathbf{r}) = \int \frac{d\mathbf{q}}{(2\pi)^3} F(\mathbf{q}) e^{i\mathbf{q}\cdot\mathbf{r}} = \int \frac{d\mathbf{q}}{(2\pi)^3} \left|F(\mathbf{q})\right| e^{i\phi(\mathbf{q})} e^{i\mathbf{q}\cdot\mathbf{r}}$$

Since Euler's formula states that $e^{ix} = \cos(x) + i\sin(x)$, the inverse Fourier transform can be separated into a sum of a purely real part and a purely imaginary part

The function $f(\mathbf{r})$ is real if and only if the second integral $I_{\text{sin}}$ is zero for all values of $\mathbf{r}$. In turn, this is true if and only if the above constraint is satisfied

since $I_{\text{sin}} = -I_{\text{sin}}$ implies that $I_{\text{sin}}=0$.

## Ewald's sphere

Each X-ray diffraction image represents only a slice, a spherical slice of reciprocal space, as may be seen by the Ewald sphere construction. Both $\mathbf{k}_{\text{out}}$ and $\mathbf{k}_{\text{in}}$ have the same length, due to the elastic scattering, since the wavelength has not changed. Therefore, they may be represented as two radial vectors in a sphere in reciprocal space, which shows the values of $\mathbf{q}$ that are sampled in a given diffraction image. Since there is a slight spread in the incoming wavelengths of the incoming X-ray beam, the values of$|F(\mathbf{q})|$can be measured only for $\mathbf{q}$ vectors located between the two spheres corresponding to those radii. Therefore, to obtain a full set of Fourier transform data, it is necessary to rotate the crystal through slightly more than 180°, or sometimes less if sufficient symmetry is present. A full 360° rotation is not needed because of a symmetry intrinsic to the Fourier transforms of real functions (such as the electron density), but "slightly more" than 180° is needed to cover all of reciprocal space within a given resolution because of the curvature of the Ewald sphere. In practice, the crystal is rocked by a small amount (0.25-1°) to incorporate reflections near the boundaries of the spherical Ewald shells.

## Patterson function

A well-known result of Fourier transforms is the autocorrelation theorem, which states that the autocorrelation $c(\mathbf{r})$ of a function $f(\mathbf{r})$

$$c(\mathbf{r}) = \int d\mathbf{x} f(\mathbf{x}) f(\mathbf{x}+\mathbf{r}) = \int \frac{d\mathbf{q}}{(2\pi)^3} C(\mathbf{q}) e^{i\mathbf{q}\cdot\mathbf{r}}$$

has a Fourier transform $C(\mathbf{q})$ that is the squared magnitude of $F(\mathbf{q})$

$$C(\mathbf{q}) = \left|F(\mathbf{q})\right|^2$$

Therefore, the autocorrelation function $c(\mathbf{r})$ of the electron density (also known as the *Patterson function*[106] ) can be computed directly from the reflection intensities, without computing the phases. In principle, this could be used to determine the crystal structure directly; however, it is difficult to realize in practice. The autocorrelation function corresponds to the distribution of vectors between atoms in the crystal; thus, a crystal of $N$ atoms in its unit cell may have $N(N-1)$ peaks in its Patterson function. Given the inevitable errors in measuring the intensities, and the mathematical difficulties of reconstructing atomic positions from the interatomic vectors, this technique is rarely used to solve structures, except for the simplest crystals.

## Advantages of a crystal

In principle, an atomic structure could be determined from applying X-ray scattering to non-crystalline samples, even to a single molecule. However, crystals offer a much stronger signal due to their periodicity. A crystalline sample is by definition periodic; a crystal is composed of many unit cells repeated indefinitely in three independent directions. Such periodic systems have a Fourier transform that is concentrated at periodically repeating points in reciprocal space known as *Bragg peaks*; the Bragg peaks correspond to the reflection spots observed in the diffraction image. Since the amplitude at these reflections grows linearly with the number $N$ of scatterers, the observed *intensity* of these spots should grow quadratically, like $N^2$. In other words, using a crystal concentrates the

weak scattering of the individual unit cells into a much more powerful, coherent reflection that can be observed above the noise. This is an example of constructive interference.

In a liquid, powder or amorphous sample, molecules within that sample are in random orientations. Such samples have a continuous Fourier spectrum that uniformly spreads its amplitude thereby reducing the measured signal intensity, as is observed in SAXS. More importantly, the orientational information is lost. Although theoretically possible, it is experimentally difficult to obtain atomic-resolution structures of complicated, asymmetric molecules from such rotationally averaged data. An intermediate case is fiber diffraction in which the subunits are arranged periodically in at least one dimension.

## See also

- Bragg diffraction
- Bravais lattice
- Crystallographic database
- Crystallographic point groups
- Difference density map
- Electron crystallography
- Electron diffraction
- Neutron diffraction
- Ptychography
- Powder diffraction
- Scherrer Equation
- Small angle X-ray scattering (SAXS)
- Structure determination
- Wide angle X-ray scattering (WAXS)

## References


[1] Kepler J (1611). *Strena seu de Nive Sexangula* (http://www.thelatinlibrary.com/kepler/strena.html). Frankfurt: G. Tampach. ISBN 3321000210. .

[2] Steno N (1669). *De solido intra solidum naturaliter contento dissertationis prodromus*. Florentiae.

[3] Hessel JFC (1831). *Kristallometrie oder Kristallonomie und Kristallographie*. Leipzig.

[4] Bravais A (1850). "Mémoire sur les systèmes formés par des points distribués regulièrement sur un plan ou dans l'espace". *J. L'Ecole Polytech.* **19**: 1.

[5] Shafranovskii I I and Belov N V (1962). "E. S. Fedorov" (http://www.iucr.org/iucr-top/publ/50YearsOfXrayDiffraction/fedorov.pdf). *50 Years of X-Ray Diffraction, ed. Paul Ewald (Springer)*: 351. ISBN 9027790299. .

[6] Schönflies A (1891). *Kristallsysteme und Kristallstruktur*. Leipzig.

[7] Barlow W (1883). "Probable nature of the internal symmetry of crystals". *Nature* **29**: 186. doi:10.1038/029186a0. See also Barlow, William (1883). "Probable Nature of the Internal Symmetry of Crystals". *Nature* **29**: 205. doi:10.1038/029205a0. Sohncke, L. (1884). ""Probable Nature of the Internal Symmetry of Crystals"". *Nature* **29**: 383. doi:10.1038/029383a0. Barlow, WM. (1884). ""Probable Nature of the Internal Symmetry of Crystals"". *Nature* **29**: 404. doi:10.1038/029404b0.

[8] Einstein A (1905). "Über einen die Erzeugung und Verwandlung des Lichtes betreffenden heuristischen Gesichtspunkt (trans. A Heuristic Model of the Creation and Transformation of Light)". *Annalen der Physik* **17**: 132. **(German)**. An English translation is available from Wikisource.

[9] Einstein A (1909). "Über die Entwicklung unserer Anschauungen über das Wesen und die Konstitution der Strahlung (trans. The Development of Our Views on the Composition and Essence of Radiation)". *Physikalische Zeitschrift* **10**: 817. **(German)**. An English translation is available from Wikisource.

[10] Pais A (1982). *Subtle is the Lord: The Science and the Life of Albert Einstein*. Oxford University Press. ISBN 019853907X.

[11] Compton A (1923). "A Quantum Theory of the Scattering of X-rays by Light Elements" (http://www.aip.org/history/gap/Compton/01_Compton.html). *Phys. Rev.* **21**: 483. doi:10.1103/PhysRev.21.483. .

[12] Bragg WH (1907). "The nature of Röntgen rays". *Transactions of the Royal Society of Science of Australia* **31**: 94.

[13] Bragg WH (1908). "The nature of γ- and X-rays". *Nature* **77**: 270. doi:10.1038/077270a0. See also Bragg, W. H. (1908). "The Nature of the γ and X-Rays". *Nature* **78**: 271. doi:10.1038/078271a0. Bragg, W. H. (1908). "The Nature of the γ and X-Rays". *Nature* **78**: 293.

doi:10.1038/078293d0. Bragg, W. H. (1908). "The Nature of X-Rays". *Nature* **78**: 665. doi:10.1038/078665b0.

[14] Bragg WH (1910). "The consequences of the corpuscular hypothesis of the γ- and X-rays, and the range of β-rays". *Phil. Mag.* **20**: 385. doi:10.1080/14786441008636917.

[15] Bragg WH (1912). "On the direct or indirect nature of the ionization by X-rays". *Phil. Mag.* **23**: 647. doi:10.1080/14786440408637253.

[16] Friedrich W, Knipping P, von Laue M (1912). "Interferenz-Erscheinungen bei Röntgenstrahlen". *Sitzungsberichte der Mathematisch-Physikalischen Classe der Königlich-Bayerischen Akademie der Wissenschaften zu München* **1912**: 303.

[17] von Laue M (1914). "Concerning the detection of x-ray interferences" (http://nobelprize.org/nobel_prizes/physics/laureates/1914/laue-lecture.pdf) (PDF). *Nobel Lectures, Physics* **1901-1921**. . Retrieved 2009-02-18.

[18] Dana ES, Ford WE (1932). *A Textbook of Mineralogy, fourth edition*. New York: John Wiley & Sons. p. 28.

[19] Bragg WL (1912). "The Specular Reflexion of X-rays". *Nature* **90**: 410. doi:10.1038/090410b0.

[20] Bragg WL (1913). "The Diffraction of Short Electromagnetic Waves by a Crystal". *Proceedings of the Cambridge Philosophical Society* **17**: 43.

[21] Bragg (1914). "Die Reflexion der Röntgenstrahlen". *Jahrbuch der Radioaktivität und Elektronik* **11**: 350.

[22] Bragg (1913). "The Structure of Some Crystals as Indicated by their Diffraction of X-rays" (http://www.jstor.org/pss/93488). *Proc. R. Soc. Lond.* **A89** (610): 248. .

[23] Bragg WL, James RW, Bosanquet CH (1921). "The Intensity of Reflexion of X-rays by Rock-Salt". *Phil. Mag.* **41**: 309. doi:10.1080/14786442108636225.

[24] Bragg WL, James RW, Bosanquet CH (1921). "The Intensity of Reflexion of X-rays by Rock-Salt. Part II". *Phil. Mag.* **42**: 1. doi:10.1080/14786442108633730.

[25] Bragg WL, James RW, Bosanquet CH (1922). "The Distribution of Electrons around the Nucleus in the Sodium and Chlorine Atoms". *Phil. Mag.* **44**: 433. doi:10.1080/14786440908565188.

[26] Bragg WH, Bragg WL (1913). "The structure of the diamond". *Nature* **91**: 557. doi:10.1038/091557a0.

[27] Bragg WH, Bragg WL (1913). "The structure of the diamond". *Proc. R. Soc. Lond.* **A89**: 277. doi:10.1098/rspa.1913.0084.

[28] Bragg WL (1914). "The Crystalline Structure of Copper". *Phil. Mag.* **28**: 355. doi:10.1080/14786440908635219.

[29] Bragg WL (1914). "The analysis of crystals by the X-ray spectrometer". *Proc. R. Soc. Lond.* **A89**: 468. doi:10.1098/rspa.1914.0015.

[30] Bragg WH (1915). "The structure of the spinel group of crystals". *Phil. Mag.* **30**: 305. doi:10.1080/14786440808635400.

[31] Nishikawa S (1915). "Structure of some crystals of spinel group". *Proc. Tokyo Math. Phys. Soc.* **8**: 199.

[32] Vegard L (1916). "Results of Crystal Analysis". *Phil. Mag.* **32**: 65. doi:10.1080/14786441608635544.

[33] Aminoff G (1919). "Crystal Structure of Pyrochroite". *Stockholm Geol. Fören. Förh.* **41**: 407.

[34] Aminoff G (1921). "Über die Struktur des Magnesiumhydroxids". *Z. Kristallogr.* **56**: 505.

[35] Bragg WL (1920). "The crystalline structure of zinc oxide". *Phil. Mag.* **39**: 647. doi:10.1080/14786440608636079.

[36] Debije P, Scherrer P (1916). "Interferenz an regellos orientierten Teilchen im Röntgenlicht I". *Physikalische Zeitschrift* **17**: 277.

[37] Friedrich W (1913). "Eine neue Interferenzerscheinung bei Röntgenstrahlen". *Physikalische Zeitschrift* **14**: 317.

[38] Hull AW (1917). "A New Method of X-ray Crystal Analysis". *Phys. Rev.* **10**: 661. doi:10.1103/PhysRev.10.661.

[39] Bernal JD (1924). "The Structure of Graphite" (http://www.jstor.org/pss/94336). *Proc. R. Soc. Lond.* **A106** (740): 749. .

[40] Hassel O, Mack H (1924). "Über die Kristallstruktur des Graphits". *Zeitschrift für Physik* **25**: 317. doi:10.1007/BF01327534.

[41] Hull AW (1917). "The Crystal Structure of Iron". *Phys. Rev.* **9**: 84.

[42] Hull AW (1917). "The Crystal Structure of Magnesium". *PNAS* **3**: 470. doi:10.1073/pnas.3.7.470.

[43] Wyckoff RWG, Posnjak E (1921). "The Crystal Structure of Ammonium Chloroplatinate". *J. Amer. Chem. Soc.* **43**: 2292. doi:10.1021/ja01444a002.

[44] Bragg WH (1921). "The structure of organic crystals". *Proc. R. Soc. Lond.* **34**: 33. doi:10.1088/1478-7814/34/1/306.

[45] Lonsdale K (1928). "The structure of the benzene ring". *Nature* **122**: 810. doi:10.1038/122810c0.

[46] Pauling L. *The Nature of the Chemical Bond* (3rd ed.). Ithaca, NY: Cornell University Press. ISBN 0801403332.

[47] Bragg WH (1922). "The crystalline structure of anthracene". *Proc. R. Soc. Lond.* **35**: 167. doi:10.1088/1478-7814/35/1/320.

[48] Powell HM, Ewens RVG (1939). "The crystal structure of iron enneacarbonyl". *J. Chem. Soc.*: 286. doi:10.1039/jr9390000286.

[49] Bertrand JA, Cotton FA, Dollase WA (1963). "The Metal-Metal Bonded, Polynuclear Complex Anion in $CsReCl_4$". *J. Amer. Chem. Soc.* **85**: 1349. doi:10.1021/ja00892a029.

[50] Robinson WT, Fergusson JE, Penfold BR (1963). "Configuration of Anion in $CsReCl_4$". *Proceedings of the Chemical Society of London*: 116.

[51] Cotton FA, Curtis NF, Harris CB, Johnson BFG, Lippard SJ, Mague JT, Robinson WR, Wood JS (1964). "Mononuclear and Polynuclear Chemistry of Rhenium (III): Its Pronounced Homophilicity". *Science* **145** (3638): 1305. doi:10.1126/science.145.3638.1305. PMID 17802015.

[52] Cotton FA, Harris CB (1965). "The Crystal and Molecular Structure of Dipotassium Octachlorodirhenate(III) Dihydrate". *Inorganic Chemistry* **4**: 330. doi:10.1021/ic50025a015.

[53] Cotton FA (1965). "Metal-Metal Bonding in $[Re_2X_8]^{2-}$ Ions and Other Metal Atom Clusters". *Inorganic Chemistry* **4**: 334. doi:10.1021/ic50025a016.

[54] Eberhardt WH, Crawford W, Jr., Lipscomb WN (1954). "The valence structure of the boron hydrides". *J. Chem. Phys.* **22**: 989. doi:10.1063/1.1740320.

[55] Martin TW, Derewenda ZS (1999). "The name is Bond — H bond". *Nature Structural Biology* **6** (5): 403. doi:10.1038/8195. PMID 10331860.

[56] Dunitz JD, Orgel LE, Rich A (1956). "The crystal structure of ferrocene". *Acta Crystallographica* **9**: 373. doi:10.1107/S0365110X56001091.

[57] Seiler P, Dunitz JD (1979). "A new interpretation of the disordered crystal structure of ferrocene". *Acta Crystallographica* **B35**: 1068. doi:10.1107/S0567740879005598.

[58] Wunderlich JA, Mellor DP (1954). "A note on the crystal structure of Zeise's salt". *Acta Crystallographica* **7**: 130. doi:10.1107/S0365110X5400028X.

[59] Jarvis JAJ, Kilbourn BT, Owston PG (1970). "A re-determination of the crystal and molecular structure of Zeise's salt, $KPtCl_3.C_2H_4.H_2O$. A correction". *Acta Crystallographica* **B26**: 876. doi:10.1107/S056774087000328X.

[60] Jarvis JAJ, Kilbourn BT, Owston PG (1971). "A re-determination of the crystal and molecular structure of Zeise's salt, $KPtCl_3.C_2H_4.H_2O$". *Acta Crystallographica* **B27**: 366. doi:10.1107/S0567740871002231.

[61] Love RA, Koetzle TF, Williams GJB, Andrews LC, Bau R (1975). "Neutron diffraction study of the structure of Zeise's salt, $KPtCl_3(C_2H_4).H_2O$". *Inorganic Chemistry* **14**: 2653. doi:10.1021/ic50153a012.

[62] Westgren A, Phragmén G (1925). "X-ray Analysis of the Cu-Zn, Ag-Zn and Au-Zn Alloys". *Phil. Mag.* **50**: 311.

[63] Bradley AJ, Thewlis J (1926). "The structure of γ-Brass". *Proc. R. Soc. Lond.* **112**: 678. doi:10.1098/rspa.1926.0134.

[64] Hume-Rothery W (1926). "Researches on the Nature, Properties and Conditions of Formation of Intermetallic Compounds (with special Reference to certain Compounds of Tin)". *Journal of the Institute of Metals* **35**: 295.

[65] Bradley AJ, Gregory CH (1927). "The Structure of certain Ternary Alloys". *Nature* **120**: 678. doi:10.1038/120678a0.

[66] Westgren A (1932). "Zur Chemie der Legierungen". *Angewandte Chemie* **45**: 33. doi:10.1002/ange.19320450202.

[67] Bernal JD (1935). "The Electron Theory of Metals". *Annual Reports on the Progress of Chemistry* **32**: 181.

[68] Pauling L (1923). "The Crystal Structure of Magnesium Stannide". *J. Amer. Chem. Soc.* **45**: 2777. doi:10.1021/ja01665a001.

[69] Pauling L (1929). "The Principles Determining the Structure of Complex Ionic Crystals". *J. Amer. Chem. Soc.* **51**: 1010. doi:10.1021/ja01379a006.

[70] Dickinson RG, Raymond AL (1923). "The Crystal Structure of Hexamethylene-Tetramine". *J. Amer. Chem. Soc.* **45**: 22. doi:10.1021/ja01654a003.

[71] Müller A (1923). "The X-ray Investigation of Fatty Acids". *Journal of the Chemical Society (London)* **123**: 2043.

[72] Saville WB, Shearer G (1925). "An X-ray Investigation of Saturated Aliphatic Ketones". *Journal of the Chemical Society (London)* **127**: 591.

[73] Bragg WH (1925). "The Investigation of thin Films by Means of X-rays". *Nature* **115**: 266. doi:10.1038/115266a0.

[74] de Broglie M, Trillat JJ (1925). "Sur l'interprétation physique des spectres X d'acides gras". *Comptes rendus hebdomadaires des séances de l'Académie des sciences* **180**: 1485.

[75] Trillat JJ (1926). "Rayons X et Composeés organiques à longe chaine. Recherches spectrographiques sue leurs structures et leurs orientations". *Annales de physique* **6**: 5.

[76] Caspari WA (1928). "Crystallography of the Aliphatic Dicarboxylic Acids". *Journal of the Chemical Society (London)* **?**: 3235.

[77] Müller A (1928). "X-ray Investigation of Long Chain Compounds (n. Hydrocarbons)". *Proc. R. Soc. Lond.* **120**: 437. doi:10.1098/rspa.1928.0158.

[78] Piper SH (1929). "Some Examples of Information Obtainable from the long Spacings of Fatty Acids". *Transactions of the Faraday Society* **25**: 348. doi:10.1039/tf9292500348.

[79] Müller A (1929). "The Connection between the Zig-Zag Structure of the Hydrocarbon Chain and the Alternation in the Properties of Odd and Even Numbered Chain Compounds". *Proc. R. Soc. Lond.* **124**: 317. doi:10.1098/rspa.1929.0117.

[80] Robertson JM (1936). "An X-ray Study of the Phthalocyanines, Part II". *Journal of the Chemical Society*: 1195.

[81] Crowfoot Hodgkin D (1935). "X-ray Single Crystal Photographs of Insulin". *Nature* **135**: 591. doi:10.1038/135591a0.

[82] Kendrew J. C. *et al.* (1958-03-08). "A Three-Dimensional Model of the Myoglobin Molecule Obtained by X-Ray Analysis". *Nature* **181**: 662. doi:10.1038/181662a0.

[83] "Table of entries in the PDB, arranged by experimental method" (http://www.rcsb.org/pdb/statistics/holdings.do). .

[84] "PDB Statistics" (http://pdbbeta.rcsb.org/pdb/static.do?p=general_information/pdb_statistics/index.html). RCSB Protein Data Bank. . Retrieved 2007-05-03.

[85] Scapin G (2006). "Structural biology and drug discovery". *Curr. Pharm. Des.* **12** (17): 2087. doi:10.2174/138161206777585201. PMID 16796557.

[86] Lundstrom K (2006). "Structural genomics for membrane proteins". *Cell. Mol. Life Sci.* **63** (22): 2597. doi:10.1007/s00018-006-6252-y. PMID 17013556.

[87] Lundstrom K (2004). "Structural genomics on membrane proteins: mini review". *Comb. Chem. High Throughput Screen.* **7** (5): 431. PMID 15320710.

[88] Greninger AB (1935). *Zeitschrift fur Kristallographie* **91**: 424.

[89] An analogous diffraction pattern may be observed by shining a laser pointer on a compact disc or DVD; the periodic spacing of the CD tracks corresponds to the periodic arrangement of atoms in a crystal.

[90] Harp, JM; Timm, DE; Bunick, GJ (1998). "Macromolecular crystal annealing: overcoming increased mosaicity associated with cryocrystallography.". *Acta crystallographica. Section D, Biological crystallography* **54** (Pt 4): 622–8. doi:10.1107/S0907444997019008. PMID 9761858.

[91] Harp, JM; Hanson, BL; Timm, DE; Bunick, GJ (1999). "Macromolecular crystal annealing: evaluation of techniques and variables.". *Acta crystallographica. Section D, Biological crystallography* **55** (Pt 7): 1329–34. doi:10.1107/S0907444999005442. PMID 10393299.

[92] Hanson, BL; Harp, JM; Bunick, GJ (2003). "The well-tempered protein crystal: annealing macromolecular crystals.". *Methods in enzymology* **368**: 217–35. doi:10.1016/S0076-6879(03)68012-2. PMID 14674276.

[93] Geerlof A *et al.* (2006). "The impact of protein characterization in structural proteomics". *Acta Crystallogr. D* **62** (Pt 10): 1125. doi:10.1107/S0907444906030307. PMID 17001090.

[94] Chernov AA (2003). "Protein crystals and their growth". *J. Struct. Biol.* **142** (1): 3. doi:10.1016/S1047-8477(03)00034-0. PMID 12718915.

[95] Rupp B, Wang J (2004). "Predictive models for protein crystallization". *Methods* **34** (3): 390. doi:10.1016/j.ymeth.2004.03.031. PMID 15325656.

[96] Chayen NE (2005). "Methods for separating nucleation and growth in protein crystallization". *Prog. Biophys. Mol. Biol.* **88** (3): 329. doi:10.1016/j.pbiomolbio.2004.07.007. PMID 15652248.

[97] Stock D, Perisic O, Lowe J (2005). "Robotic nanolitre protein crystallisation at the MRC Laboratory of Molecular Biology.". *Prog Biophys Mol Biol* **88** (3): 311. doi:10.1016/j.pbiomolbio.2004.07.009. PMID 15652247.

[98] Jeruzalmi D (2006). "First analysis of macromolecular crystals: biochemistry and x-ray diffraction". *Methods Mol. Biol.* **364**: 43. doi:10.1385/1-59745-266-1:43. PMID 17172760.

[99] Helliwell JR (2005). "Protein crystal perfection and its application". *Acta Crystallogr. D Biol. Crystallogr.* **61** (Pt 6): 793. doi:10.1107/S0907444905001368. PMID 15930642.

[100] Ravelli RB, Garman EF (2006). "Radiation damage in macromolecular cryocrystallography". *Curr. Opin. Struct. Biol.* **16** (5): 624. doi:10.1016/j.sbi.2006.08.001. PMID 16938450.

[101] Powell HR (1999). "The Rossmann Fourier autoindexing algorithm in MOSFLM.". *Acta Crystallogr. D* **55** (Pt 10): 1690. doi:10.1107/S0907444999009506. PMID 10531518.

[102] Hauptman H (1997). "Phasing methods for protein crystallography". *Curr. Opin. Struct. Biol.* **7** (5): 672. doi:10.1016/S0959-440X(97)80077-2. PMID 9345626.

[103] Usón I, Sheldrick GM (1999). "Advances in direct methods for protein crystallography". *Curr. Opin. Struct. Biol.* **9** (5): 643. doi:10.1016/S0959-440X(99)00020-2. PMID 10508770.

[104] Taylor G (2003). "The phase problem". *Acta Crystallogr. D* **59**: 1881. doi:10.1107/S0907444903017815.

[105] Ealick SE (2000). "Advances in multiple wavelength anomalous diffraction crystallography". *Current opinion in chemical biology* **4** (5): 495. doi:10.1016/S1367-5931(00)00122-8. PMID 11006535.

[106] Patterson AL (1935). "A Direct Method for the Determination of the Components of Interatomic Distances in Crystals". *Zeitschrift für Kristallographie* **90**: 517.

# Further reading

## *International Tables for Crystallography*

- Theo Hahn, ed (2002). *International Tables for Crystallography. Volume A, Space-group Symmetry* (5 ed.). Dordrecht: Kluwer Academic Publishers, for the International Union of Crystallography. ISBN 0792365909.
- Michael G. Rossmann and Eddy Arnold, ed (2001). *International Tables for Crystallography. Volume F, Crystallography of biological molecules*. Dordrecht: Kluwer Academic Publishers, for the International Union of Crystallography. ISBN 0792368576.
- Theo Hahn, ed (1996). *International Tables for Crystallography. Brief Teaching Edition of Volume A, Space-group Symmetry* (4 ed.). Dordrecht: Kluwer Academic Publishers, for the International Union of Crystallography. ISBN 0792342526.

## Bound collections of articles


- Charles W. Carter and Robert M. Sweet., ed (1997). *Macromolecular Crystallography, Part A (Methods in Enzymology, v. 276)*. San Diego: Academic Press. ISBN 0121821773.
- Charles W. Carter Jr., Robert M. Sweet., ed (1997). *Macromolecular Crystallography, Part B (Methods in Enzymology, v. 277)*. San Diego: Academic Press. ISBN 0121821781.
- A. Ducruix and R. Giegé, ed (1999). *Crystallization of Nucleic Acids and Proteins: A Practical Approach* (2 ed.). Oxford: Oxford University Press. ISBN 0199636788.


## Textbooks


- Blow D (2002). *Outline of Crystallography for Biologists*. Oxford: Oxford University Press. ISBN 0198510519.
- Burns G., Glazer A M (1990). *Space Groups for Scientists and Engineers* (2nd ed.). Boston: Academic Press, Inc. ISBN 0121457613.
- Clegg W (1998). *Crystal Structure Determination (Oxford Chemistry Primer)*. Oxford: Oxford University Press. ISBN 0198559011.
- Cullity B.D. (1978). *Elements of X-Ray Diffraction* (2nd ed.). Reading, Massachusetts: Addison-Wesley Publishing Company. ISBN 0534553966.
- Drenth J (1999). *Principles of Protein X-Ray Crystallography*. New York: Springer-Verlag. ISBN 0387985875.
- Giacovazzo C *et al.* (1992). *Fundamentals of Crystallography*. Oxford: Oxford University Press. ISBN 0198555784.
- Glusker JP, Lewis M, Rossi M (1994). *Crystal Structure Analysis for Chemists and Biologists*. New York: VCH Publishers. ISBN 0471185434.
- Massa W (2004). *Crystal Structure Determination*. Berlin: Springer. ISBN 3540206442.
- McPherson A (1999). *Crystallization of Biological Macromolecules*. Cold Spring Harbor, NY: Cold Spring Harbor Laboratory Press. ISBN 0879696176.
- McPherson A (2003). *Introduction to Macromolecular Crystallography*. John Wiley & Sons. ISBN 0471251224.
- McRee DE (1993). *Practical Protein Crystallography*. San Diego: Academic Press. ISBN 0124860508.
- O'Keeffe M, Hyde B G (1996). *Crystal Structures; I. Patterns and Symmetry*. Washington, DC: Mineralogical Society of America, *Monograph Series*. ISBN 0939950405.
- Rhodes G (2000). *Crystallography Made Crystal Clear*. San Diego: Academic Press. ISBN 0125870728., PDF copy of select chapters (http://www.chem.uwec.edu/Chem406_F06/Pages/lecture_notes/lect07/Crystallography_Rhodes.pdf)
- Rupp B (2009). *Biomolecular Crystallography: Principles, Practice and Application to Structural Biology*. New York: Garland Science. ISBN 0815340818.
- Zachariasen WH (1945). *Theory of X-ray Diffraction in Crystals*. New York: Dover Publications. LCCN 67-26967.

### Applied computational data analysis


- Young, R.A., ed (1993). *The Rietveld Method*. Oxford: Oxford University Press & International Union of Crystallography. ISBN 0198555776.


### Historical


- Bijvoet JM, Burgers WG, Hägg G, eds. (1969). *Early Papers on Diffraction of X-rays by Crystals (Volume I)*. Utrecht: published for the International Union of Crystallography by A. Oosthoek's Uitgeversmaatschappij N.V..
- Bijvoet JM, Burgers WG, Hägg G, eds. (1972). *Early Papers on Diffraction of X-rays by Crystals (Volume II)*. Utrecht: published for the International Union of Crystallography by A. Oosthoek's Uitgeversmaatschappij N.V..
- Bragg W L, Phillips D C and Lipson H (1992). *The Development of X-ray Analysis*. New York: Dover. ISBN 0486673162.
- Ewald PP, editor, and numerous crystallographers (1962). *Fifty Years of X-ray Diffraction*. Utrecht: published for the International Union of Crystallography by A. Oosthoek's Uitgeversmaatschappij N.V..
- Ewald, P. P., editor *50 Years of X-Ray Diffraction* (http://www.iucr.org/iucr-top/publ/50YearsOfXrayDiffraction/) (Reprinted in pdf format for the IUCr XVIII Congress, Glasgow, Scotland, International Union of Crystallography).
- Friedrich W (1922). "Die Geschichte der Auffindung der Röntgenstrahlinterferenzen". *Die Naturwissenschaften* **10**: 363. doi:10.1007/BF01565289.
- Lonsdale K (1949). *Crystals and X-rays*. New York: D. van Nostrand.


## External links

### Tutorials

- Crystallography for beginners (http://www.xtal.iqfr.csic.es/Cristalografia/index-en.html)
- Simple, non technical introduction (http://stein.bioch.dundee.ac.uk/~charlie/index.php?section=1)
- "Small Molecule Crystalization" (http://acaschool.iit.edu/lectures04/JLiangXtal.pdf) (PDF) at Illinois Institute of Technology website
- International Union of Crystallography (http://iucr.org)
- Crystallography 101 (http://www.ruppweb.org/Xray/101index.html)
- Interactive structure factor tutorial (http://www.ysbl.york.ac.uk/~cowtan/sfapplet/sfintro.html), demonstrating properties of the diffraction pattern of a 2D crystal.
- Picturebook of Fourier Transforms (http://www.ysbl.york.ac.uk/~cowtan/fourier/fourier.html), illustrating the relationship between crystal and diffraction pattern in 2D.
- Lecture notes on X-ray crystallography and structure determination (http://www.chem.uwec.edu/Chem406_F06/Pages/lectnotes.html#lecture7)
- Online lecture on Modern X-ray Scattering Methods for Nanoscale Materials Analysis (http://nanohub.org/resources/5580) by Richard J. Matyi

### Primary databases

- Crystallography Open Database (http://www.crystallography.net/) (COD)
- Protein Data Bank (http://www.rcsb.org/pdb/home/home.do) (PDB)
- Nucleic Acid Databank (http://ndbserver.rutgers.edu/) (NDB)
- Cambridge Structural Database (http://www.ccdc.cam.ac.uk/products/csd/) (CSD)
- Inorganic Crystal Structure Database (http://www.fiz-karlsruhe.de/icsd.html) (ICSD)
- Biological Macromolecule Crystallization Database (http://xpdb.nist.gov:8060/BMCD4/) (BMCD)

### Derivative databases

- PDBsum (http://www.ebi.ac.uk/thornton-srv/databases/pdbsum/)
- Proteopeida - the collaborative, 3D encyclopedia of proteins and other molecules (http://www.proteopedia.org)
- RNABase (http://www.rnabase.org/)
- HIC-Up database of PDB ligands (http://xray.bmc.uu.se/hicup/)
- Structural Classification of Proteins database
- CATH Protein Structure Classification
- List of transmembrane proteins with known 3D structure (http://blanco.biomol.uci.edu/Membrane_Proteins_xtal.html)
- Orientations of Proteins in Membranes database

### Structural validation

- WHAT-IF structural validation suite (http://swift.cmbi.kun.nl/WIWWWI//)
- Biotech structural validation suite (http://biotech.ebi.ac.uk/) (formerly ProCheck)
- MolProbity structural validation suite (http://molprobity.biochem.duke.edu/)
- ProSA-web (https://prosa.services.came.sbg.ac.at/prosa.php)
- NQ-Flipper (https://flipper.services.came.sbg.ac.at/) (check for unfavorable rotamers of Asn and Gln residues)
- DALI server (http://www.ebi.ac.uk/dali/) (identifies proteins similar to a given protein)

# X-ray scattering techniques

**X-ray scattering techniques** are a family of non-destructive analytical techniques which reveal information about the crystallographic structure, chemical composition, and physical properties of materials and thin films. These techniques are based on observing the scattered intensity of an X-ray beam hitting a sample as a function of incident and scattered angle, polarization, and wavelength or energy.

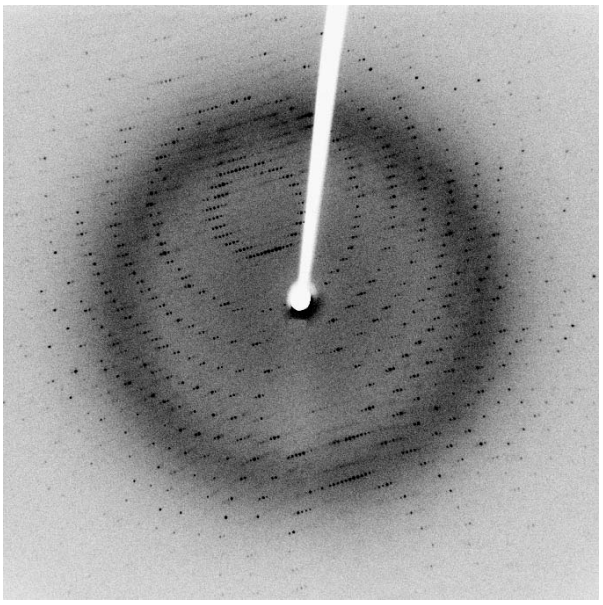

This is an X-ray diffraction pattern formed when X-rays are focused on a crystalline material, in this case a protein. Each dot, called a reflection, forms from the coherent interference of scattered X-rays passing through the crystal.

## X-ray diffraction techniques

X-ray diffraction yields the atomic structure of materials and is based on the elastic scattering of X-rays from the electron clouds of the individual atoms in the system. The most comprehensive description of scattering from crystals is given by the dynamical theory of diffraction.[1]

- Single-crystal X-ray diffraction is a technique used to solve the complete structure of crystalline materials, ranging from simple inorganic solids to complex macromolecules, such as proteins.
- Powder diffraction (XRD) is a technique used to characterise the crystallographic structure, crystallite size (grain size), and preferred orientation in polycrystalline or powdered solid samples. Powder diffraction is commonly used to identify unknown substances, by comparing diffraction data against a database maintained by the International Centre for Diffraction Data. It may also be used to characterize heterogeneous solid mixtures to determine relative abundance of crystalline compounds and, when coupled with lattice refinement techniques, such as Rietveld refinement, can provide structural information on unknown materials. Powder diffraction is also a common method for determining strains in crystalline materials. An effect of the finite crystallite sizes is seen as a broadening of the peaks in an X-ray diffraction as is explained by the Scherrer Equation.
- Thin film diffraction and grazing incidence X-ray diffraction may be used to characterize the crystallographic structure and preferred orientation of substrate-anchored thin films.
- High-resolution X-ray diffraction is used to characterize thickness, crystallographic structure, and strain in thin epitaxial films. It employs parallel-beam optics.
- X-ray pole figure analysis enables one to analyze and determine the distribution of crystalline orientations within a crystalline thin-film sample.
- X-ray rocking curve analysis is used to quantify grain size and mosaic spread in crystalline materials.

# Scattering techniques

## Elastic scattering

Materials that do not have long range order may also be studied by scattering methods that rely on elastic scattering of monochromatic X-rays.

- Small angle X-ray scattering (SAXS) probes structure in the nanometer to micrometer range by measuring scattering intensity at scattering angles 2θ close to 0°.[2]
- X-ray reflectivity is an analytical technique for determining thickness, roughness, and density of single layer and multilayer thin films.
- Wide angle X-ray scattering (WAXS), a technique concentrating on scattering angles 2θ larger than 5°.

## Inelastic scattering

When the energy and angle of the inelastically scattered X-rays are monitored scattering techniques can be used to probe the electronic band structure of materials.

- Compton scattering
- Resonant inelastic X-ray scattering (RIXS)
- X-ray Raman scattering
- X-ray diffraction pattern

# See also

- Structure determination
- Materials Science
- Metallurgy
- Mineralogy
- X-ray crystallography
- X-ray generator

# References

[1] Azároff, L. V.; R. Kaplow, N. Kato, R. J. Weiss, A. J. C. Wilson, R. A. Young (1974). *X-ray diffraction*. McGraw-Hill.

[2] Glatter, O.; O. Kratky (1982). *Small Angle X-ray Scattering* (http://physchem.kfunigraz.ac.at/sm/Software.htm). Academic Press. .

# External links

- International Union of Crystallography (http://www.iucr.ac.uk/)
- IUCr Crystallography Online (http://www.iucr.org/cww-top/crystal.index.html)
- The International Centre for Diffraction Data (ICDD) (http://www.icdd.com/)
- The British Crystallographic Association (http://crystallography.org.uk/)
- Introduction to X-ray Diffraction (http://www.mrl.ucsb.edu/mrl/centralfacilities/xray/xray-basics/index.html) at University of California, Santa Barbara

# Fourier transform spectroscopy

**Fourier transform spectroscopy** is a measurement technique whereby spectra are collected based on measurements of the coherence of a radiative source, using time-domain or space-domain measurements of the electromagnetic radiation or other type of radiation. It can be applied to a variety of types of spectroscopy including optical spectroscopy, infrared spectroscopy (FTIR, FT-NIRS), nuclear magnetic resonance (NMR) and magnetic resonance spectroscopic imaging (MRSI)[1] , mass spectrometry and electron spin resonance spectroscopy. There are several methods for measuring the temporal coherence of the light (see: field-autocorrelation), including the continuous wave *Michelson* or *Fourier transform* spectrometer and the pulsed Fourier transform spectrograph (which is more sensitive and has a much shorter sampling time than conventional spectroscopic techniques, but is only applicable in a laboratory environment).

The term *Fourier transform spectroscopy* reflects the fact that in all these techniques, a Fourier transform is required to turn the raw data into the actual spectrum, and in many of the cases in optics involving interferometers, is based on the Wiener–Khinchin theorem.

## Conceptual introduction

### Measuring an emission spectrum

One of the most basic tasks in spectroscopy is to characterize the spectrum of a light source: How much light is emitted at each different wavelength. The most straightforward way to measure a spectrum is to pass the light through a monochromator, an instrument that blocks all of the light *except* the light at a certain wavelength (the un-blocked wavelength is set by a knob on the monochromator). Then the intensity of this remaining (single-wavelength) light is measured. The measured intensity directly indicates how much light is emitted at that wavelength. By varying the monochromator's wavelength setting, the full spectrum can be measured. This simple scheme in fact describes how *some* spectrometers work.

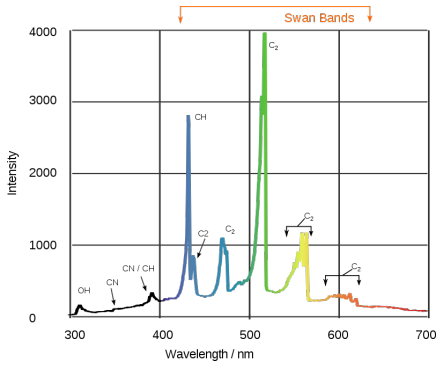


An example of a spectrum: The spectrum of light emitted by the blue flame of a butane torch. The horizontal axis is the wavelength of light, and the vertical axis represents how much light is emitted by the torch at that wavelength.

Fourier transform spectroscopy is a less intuitive way to get the same information. Rather than allowing only one wavelength at a time to pass through to the detector, this technique lets through a beam containing many different wavelengths of light at once, and measures the *total* beam intensity. Next, the beam is modified to contain a *different* combination of wavelengths, giving a second data point. This process is repeated many times. Afterwards, a computer takes all this data and works backwards to infer how much light there is at each wavelength.

To be more specific, between the light source and the detector, there is a certain configuration of mirrors that allows some wavelengths to pass through but blocks others (due to wave interference). The beam is modified for each new data point by moving one of the mirrors; this changes the set of wavelengths that can pass through.

As mentioned, computer processing is required to turn the raw data (light intensity for each mirror position) into the desired result (light intensity for each wavelength). The processing required turns out to be a common algorithm called the Fourier transform (hence the name, "Fourier transform spectroscopy"). The raw data is sometimes called an "interferogram".

### Measuring an absorption spectrum

The method of Fourier transform spectroscopy can also be used for absorption spectroscopy. The primary example is "FTIR Spectroscopy", a common technique in chemistry.

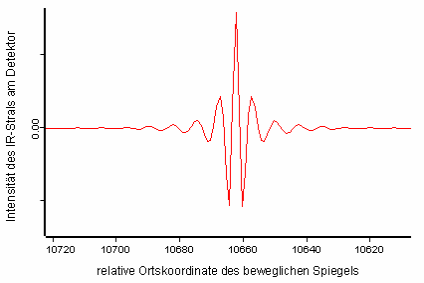


An "interferogram" from a Fourier transform spectrometer. The horizontal axis is the position of the mirror, and the vertical axis is the amount of light detected. This is the "raw data" which can be Fourier transformed into an actual spectrum.

In general, the goal of absorption spectroscopy is to measure how well a sample absorbs or transmits light at each different wavelength. Although absorption spectroscopy and emission spectroscopy are different in principle, they are closely related in practice; any technique for emission spectroscopy can also be used for absorption spectroscopy. First, the emission spectrum of a broadband lamp is measured (this is called the "background spectrum"). Second, the emission spectrum of the same lamp *shining through the sample* is measured (this is called the "sample spectrum"). The sample will absorb some of the light, causing the spectra to be different. The ratio of the "sample spectrum" to the "background spectrum" is directly related to the sample's absorption spectrum.

Accordingly, the technique of "Fourier transform spectroscopy" can be used both for measuring emission spectra (for example, the emission spectrum of a star), *and* absorption spectra (for example, the absorption spectrum of a glass of liquid).

## Continuous wave *Michelson* or *Fourier transform* spectrograph

The Michelson spectrograph is similar to the instrument used in the Michelson-Morley experiment. Light from the source is split into two beams by a half-silvered mirror, one is reflected off a fixed mirror and one off a moving mirror which introduces a time delay—the Fourier transform spectrometer is just a Michelson interferometer with a movable mirror. The beams interfere, allowing the temporal coherence of the light to be measured at each different time delay setting, effectively converting the time domain into a spatial coordinate. By making measurements of the signal at many discrete positions of the moving mirror, the spectrum can be reconstructed using a Fourier transform of the temporal coherence of the light. Michelson spectrographs are capable of very high spectral resolution observations of very bright sources. The Michelson or Fourier transform spectrograph was popular for infra-red applications at a time when infra-red astronomy only had single pixel detectors. Imaging Michelson spectrometers are a possibility, but in general have been supplanted by imaging Fabry–Pérot instruments which are easier to construct.

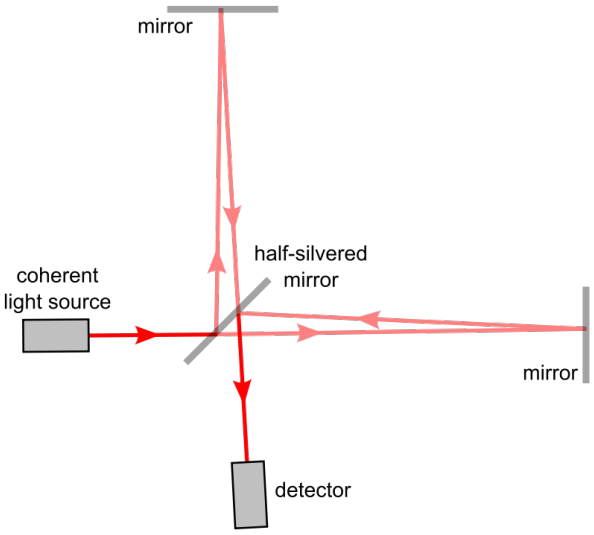


The Fourier transform spectrometer is just a Michelson interferometer but one of the two fully-reflecting mirrors is movable, allowing a variable delay (in the travel-time of the light) to be included in one of the beams.

### Extracting the spectrum

The intensity as a function of the path length difference in the interferometer $p$ and wavenumber $\tilde{\nu} = 1/\lambda$ is [2]

$$I(p, \tilde{\nu}) = I(\tilde{\nu})[1 + \cos(2\pi\tilde{\nu}p)],$$

where $I(\tilde{\nu})$ is the spectrum to be determined. Note that it is not necessary for $I(\tilde{\nu})$ to be modulated by the sample before the interferometer. In fact, most FTIR spectrometers place the sample after the interferometer in the optical path. The total intensity at the detector is

$$I(p) = \int_0^\infty I(p, \tilde{\nu}) d\tilde{\nu} = \int_0^\infty I(\tilde{\nu})[1 + \cos(2\pi\tilde{\nu}p)] d\tilde{\nu}.$$

This is just a Fourier cosine transform. The inverse gives us our desired result in terms of the measured quantity $I(p)$:

$$I(\tilde{\nu}) = 4 \int_0^\infty [I(p) - \tfrac{1}{2} I(p = 0)] \cos(2\pi\tilde{\nu}p) dp.$$

## Pulsed *Fourier transform* spectrometer

A pulsed *Fourier transform* spectrometer does not employ transmittance techniques. In the most general description of pulsed FT spectrometry, a sample is exposed to an energizing event which causes a periodic response. The frequency of the periodic response, as governed by the field conditions in the spectrometer, is indicative of the measured properties of the analyte.

### Examples of pulsed Fourier transform spectrometry

In magnetic spectroscopy (EPR, NMR), an RF pulse in a strong ambient magnetic field is used as the energizing event. This turns the magnetic particles at an angle to the ambient field, resulting in gyration. The gyrating spins then induce a periodic current in a detector coil. Each spin exhibits a characteristic frequency of gyration (relative to the field strength) which reveals information about the analyte.

In Fourier transform mass spectrometry, the energizing event is the injection of the charged sample into the strong electromagnetic field of a cyclotron. These particles travel in circles, inducing a current in a fixed coil on one point in their circle. Each traveling particle exhibits a characteristic cyclotron frequency-field ratio revealing the masses in the sample.

### Free induction decay

Pulsed FT spectrometry gives the advantage of requiring a single, time-dependent measurement which can easily deconvolute a set of similar but distinct signals. The resulting composite signal, is called a *free induction decay,* because typically the signal will decay due to inhomogeneities in sample frequency, or simply unrecoverable loss of signal due to entropic loss of the property being measured.

## Stationary forms of Fourier transform spectrometers

In addition to the scanning forms of Fourier transform spectrometers, there are a number of stationary or self-scanned forms.[3] While the analysis of the interferometric output is similar to that of the typical scanning interferometer, significant differences apply,as shown in the published analyses. Some stationary forms retain the Fellgett multiplex advantage, and their use in the spectral region where detector noise limits apply is similar to the scanning forms of the FTS. In the photon-noise limited region, the application of stationary interferometers is dictated by specific consideration for the spectral region and the application.

## Fellgett advantage

One of the most important advantages of Fourier transform spectroscopy was shown by P.B. Fellgett, an early advocate of the method. The Fellgett advantage, also known as the multiplex principle, states that when obtaining a spectrum when measurement noise is dominated by detector noise, a multiplex spectrometer such as a Fourier transform spectrometer will produce a relative improvement in signal-to-noise ratio, compared to an equivalent scanning monochromator, of the order of the square root of m, where m is the number of sample points comprising the spectrum.

## Converting spectra from time domain to frequency domain

$$S(t) = \int_{-\infty}^{\infty} I(\nu) e^{-i\nu 2\pi t}\, d\nu$$

The sum is performed over all contributing frequencies to give a signal S(t) in the time domain.

$$I(\nu) = \int_{-\infty}^{\infty} S(t) e^{i\nu 2\pi t} dt$$

gives non-zero value when S(t) contains a component that matches the oscillating function.
Remember that

$$e^{ix} = \cos x + i \sin x$$

## See also

- Applied spectroscopy
- Forensic chemistry
- Forensic polymer engineering
- Nuclear Magnetic Resonance
- Infrared spectroscopy

## References

[1] Antoine Abragam. 1968. *Principles of Nuclear Magnetic Resonance.*, Cambridge University Press: Cambridge, UK.
[2] Peter Atkins, Julio De Paula. 2006. *Physical Chemistry*, 8th ed. Oxford University Press: Oxford, UK.
[3] William H. Smith U.S. Patent 4976542 (http://www.google.com/patents?vid=4976542) Digital Array Scanned Interferometer, issued Dec. 11, 1990

## External links

- Description of how a Fourier transform spectrometer works (http://scienceworld.wolfram.com/physics/FourierTransformSpectrometer.html)
- The Michelson or Fourier transform spectrograph (http://www.astro.livjm.ac.uk/courses/phys362/notes/)
- Internet Journal of Vibrational Spectroscopy - How FTIR works (http://www.ijvs.com/volume5/edition5/section1.html#Feature)
- Fourier Transform Spectroscopy Topical Meeting and Tabletop Exhibit (http://www.osa.org/meetings/topicalmeetings/fts/default.aspx)

# Hyperspectral imaging

**Hyperspectral imaging** collects and processes information from across the electromagnetic spectrum. Unlike the human eye, which just sees visible light, hyperspectral imaging is more like the eyes of the mantis shrimp, which can see visible light as well as from the ultraviolet to infrared. Hyperspectral capabilities enable the mantis shrimp to recognize different types of coral, prey, or predators, all of which may appear as the same color to the human eye.

Humans build sensors and processing systems to provide the same type of capability for application in agriculture, mineralogy, physics, and surveillance. Hyperspectral sensors look at objects using a vast portion of the electromagnetic spectrum. Certain objects leave unique 'fingerprints' across the electromagnetic spectrum. These 'fingerprints' are known as spectral signatures and enable identification of the materials that make up a scanned object. For example, having the spectral signature for oil helps mineralogists find new oil fields.

## Acquisition and Analysis

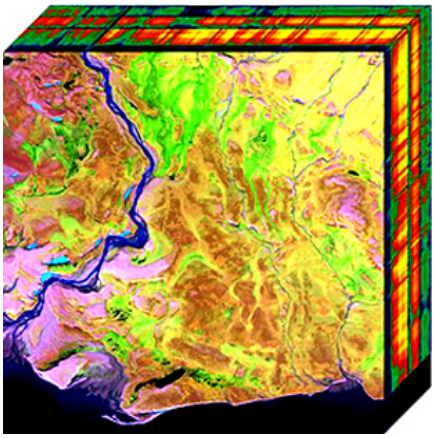

*Example of a hyperspectral cube*

Hyperspectral sensors collect information as a set of 'images'. Each image represents a range of the electromagnetic spectrum and is also known as a spectral band. These 'images' are then combined and form a three dimensional hyperspectral cube for processing and analysis.

Hyperspectral cubes are generated from airborne sensors like the NASA's *Airborne Visible/Infrared Imaging Spectrometer* (AVIRIS), or from satellites like NASA's Hyperion.[1] However, for many development and validation studies handheld sensors are used.[2]

The precision of these sensors is typically measured in spectral resolution, which is the width of each band of the spectrum that is captured. If the scanner picks up on a large number of fairly narrow frequency bands, it is possible to identify objects even if said objects are only captured in a handful of pixels. However, spatial resolution is a factor in addition to spectral resolution. If the pixels are too large, then multiple objects are captured in the same pixel and become difficult to identify. If the pixels are too small, then the energy captured by each sensor-cell is low, and the decreased signal-to-noise ratio reduces the reliability of measured features.

MicroMSI, Opticks and Envi are three remote sensing applications that support the processing and analysis of hyperspectral data. The acquisition and processing of hyperspectral images is also referred to as imaging spectroscopy.

## Differences between hyperspectral and multispectral imaging

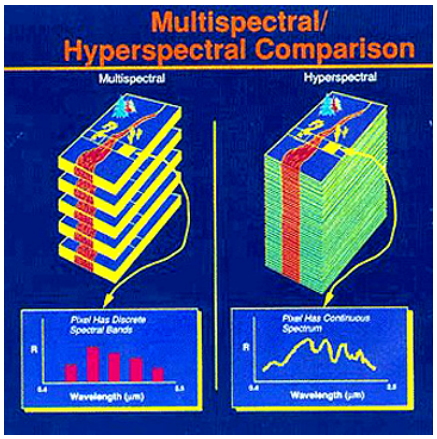


*Hyperspectral and Multispectral Differences.*

Hyperspectral imaging is part of a class of techniques commonly referred to as spectral imaging or spectral analysis. Hyperspectral imaging is related to multispectral imaging. The distinction between hyper- and multi-spectral should not be based on a random or arbitrary "number of bands". A distinction that is based on the type of measurement may be more appropriate.

Multispectral deals with several images at discrete and somewhat narrow bands. The "discrete and somewhat narrow" is what distinguishes multispectral in the visible from color photography. A multispectral sensor may have many bands covering the spectrum from the visible to the longwave infrared. Multispectral images do not produce the "spectrum" of an object. Landsat is an excellent example.

Hyperspectral deals with imaging narrow spectral bands over a contiguous spectral range, and produce the spectra of all pixels in the scene. So a sensor with only 20 bands can also be hyperspectral when it covers the range from 500 to 700 nm with 20 10-nm wide bands. (While a sensor with 20 discrete bands covering the VIS, NIR, SWIR, MWIR, and LWIR would be considered multispectral.)

Ultraspectral could be reserved for interferometer type imaging sensors with a very fine spectral resolution. These sensor often have (but not necessarily) a low spatial resolution of several pixels only, a restriction imposed by the high data rate.

## Applications

Hyperspectral remote sensing is used in a wide array of real-life applications. Although originally developed for mining and geology (the ability of hyperspectral imaging to identify various minerals makes it ideal for the mining and oil industries, where it can be used to look for ore and oil[2] [3] ) it has now spread into fields as widespread as ecology and surveillance, as well as historical manuscript research such as the imaging of the Archimedes Palimpsest. This technology is continually becoming more available to the public, and has been used in a wide variety of ways. Organizations such as NASA and the USGS have catalogues of various minerals and their spectral signatures, and have posted them online to make them readily available for researchers.

### Agriculture

Although the costs of acquiring hyperspectral images is typically high, for specific crops and in specific climates hyperspectral remote sensing is used more and more for monitoring the development and health of crops. In Australia work is under way to use imaging spectrometers to detect grape variety, and develop an early warning system for disease outbreaks.[4] Furthermore work is underway to use hyperspectral data to detect the chemical composition of plants[5] which can be used to detect the nutrient and water status of wheat in irrigated systems[6] .

Another important area in agriculture is the detection of animal proteins in compound feeds in order to avoid the Bovine spongiform encephalopathy (BSE) or mad-cow disease (MCD). For this, different studies have been done in order to propose alternative tools to the reference method (classical microscopy). One of the first alternatives is the use of NIR microscopy (Infrared microscopy), which combines the advantages of microscopy and NIR. In 2004, the first study relating this problematic with Hyperspectral imaging was published [7] . Hyperspectral libraries are constructed, which are representative of the wide diversity of ingredients usually present in the preparation of compound feeds. These libraries can be used together with chemometric tools to investigate the limit of detection, specificity and reproducibility of the NIR hyperspectral imaging method for the detection and quantification of animal ingredient in feed.

## Mineralogy

The original field of development for hyperspectral remote sensing, hyperspectral sensing of minerals is now well developed. Many minerals can be identified from images, and their relation to the presence of valuable minerals such as gold and diamonds is well understood. Currently the move is towards understanding the relation between oil and gas leakages from pipelines and natural wells; their effect on the vegetation and the spectral signatures. Recent work includes the PhD dissertations of Werff[8] and Noomen[9] .

## Physics

Physicists use an electron microscopy technique that involves microanalysis using either Energy dispersive X-ray spectroscopy (EDS), Electron energy loss spectroscopy (EELS), Infrared Spectroscopy(IR), Raman Spectroscopy, or cathodoluminescence (CL) spectroscopy, in which the entire spectrum measured at each point is recorded. EELS hyperspectral imaging is performed in a scanning transmission electron microscope (STEM); EDS and CL mapping can be performed in STEM as well, or in a scanning electron microscope or electron probe microanalyzer (EPMA). Often, multiple techniques (EDS, EELS, CL) are used simultaneously.

In a "normal" mapping experiment, an image of the sample will be made that is simply the intensity of a particular emission mapped in an XY raster. For example, an EDS map could be made of a steel sample, in which iron x-ray intensity is used for the intensity grayscale of the image. Dark areas in the image would indicate not-iron-bearing impurities. This could potentially give misleading results; if the steel contained tungsten inclusions, for example, the high atomic number of tungsten could result in bremsstrahlung radiation that made the iron-free areas *appear* to be rich in iron.

By hyperspectral mapping, instead, the entire spectrum at each mapping point is acquired, and a quantitative analysis can be performed by computer post-processing of the data, and a quantitative map of iron content produced. This would show which areas contained no iron, despite the anomalous x-ray counts caused by bremsstrahlung. Because EELS core-loss edges are small signals on top of a large background, hyperspectral imaging allows large improvements to the quality of EELS chemical maps.

Similarly, in CL mapping, small shifts in the peak emission energy could be mapped, which would give information regarding slight chemical composition changes or changes in the stress state of a sample.

## Surveillance

Hyperspectral surveillance is the implementation of hyperspectral scanning technology for surveillance purposes. Hyperspectral imaging is particularly useful in military surveillance because of measures that military entities now take to avoid airborne surveillance. Airborne surveillance has been in effect since soldiers used tethered balloons to spy on troops during the American Civil War, and since that time we have learned not only to hide from the naked eye, but to mask our heat signature to blend in to the surroundings and avoid infrared scanning, as well. The idea that drives hyperspectral surveillance is that hyperspectral scanning draws information from such a large portion of the light spectrum that any given object should have a unique spectral signature in at least a few of the many bands that get scanned.[1]

## Advantages and disadvantages

The primary advantages to hyperspectral imaging is that, because an entire spectrum is acquired at each point, the operator needs no prior knowledge of the sample, and post-processing allows all available information from the dataset to be mined.

The primary disadvantages are cost and complexity. Fast computers, sensitive detectors, and large data storage capacities are needed for analyzing hyperspectral data. Significant data storage capacity is necessary since hyperspectral cubes are large multi-dimensional datasets, potentially exceeding hundreds of megabytes. All of these factors greatly increase the cost of acquiring and processing hyperspectral data. Also, one of the hurdles that researchers have had to face is finding ways to program hyperspectral satellites to sort through data on their own and transmit only the most important images, as both transmission and storage of that much data could prove difficult and costly.[1] As a relatively new analytical technique, the full potential of hyperspectral imaging has not yet been realized.

## See also

- Airborne Real-time Cueing Hyperspectral Enhanced Reconnaissance
- Full spectral imaging
- Multi-spectral image
- Chemical imaging
- Remote Sensing
- Sensor fusion
- ERDAS IMAGINE
- Liquid Crystal Tunable Filter

## References

[1] Schurmer, J.H., (Dec 2003), Air Force Research Laboratories Technology Horizons

[2] Ellis, J., (Jan 2001) *Searching for oil seeps and oil-impacted soil with hyperspectral imagery* (http://www.eomonline.com/Common/currentissues/Jan01/ellis.htm), Earth Observation Magazine.

[3] Smith, R.B. (July 14, 2006), *Introduction to hyperspectral imaging with TMIPS* (http://www.microimages.com/getstart/pdf/hyprspec.pdf), MicroImages Tutorial Web site

[4] Lacar, F.M., et al., *Use of hyperspectral imagery for mapping grape varieties in the Barossa Valley, South Australia* (http://hdl.handle.net/2440/39292), Geoscience and remote sensing symposium (IGARSS'01) - IEEE 2001 International, vol.6 2875-2877p. doi:10.1109/IGARSS.2001.978191

[5] Ferwerda, J.G. (2005), *Charting the quality of forage: measuring and mapping the variation of chemical components in foliage with hyperspectral remote sensing* (http://www.itc.nl/library/Papers_2005/phd/ferwerda.pdf), Wageningen University , ITC Dissertation 126, 166p. ISBN 90-8504-209-7

[6] Tilling, A.K., et al., (2006) *Remote sensing to detect nitrogen and water stress in wheat* (http://www.regional.org.au/au/asa/2006/plenary/technology/4584_tillingak.htm), The Australian Society of Agronomy

[7] Fernández Pierna, J.A., et al., 'Combination of Support Vector Machines (SVM) and Near Infrared (NIR) imaging spectroscopy for the detection of meat and bone meat (MBM) in compound feeds' Journal of Chemometrics 18 (2004) 341-349

[8] Werff H. (2006), *Knowledge based remote sensing of complex objects: recognition of spectral and spatial patterns resulting from natural hydrocarbon seepages* (http://www.itc.nl/library/papers_2006/phd/vdwerff.pdf), Utrecht University, ITC Dissertation 131, 138p. ISBN 90-6164-238-8

[9] Noomen, M.F. (2007), *Hyperspectral reflectance of vegetation affected by underground hydrocarbon gas seepage* (http://www.itc.nl/library/papers_2007/phd/noomen.pdf), Enschede, ITC 151p. ISBN 978-90-8504-671-4.

## External links

- SpecTIR (http://www.spectir.com/) - Hyperspectral solutions and end to end global data collection & analysis
- Specim, Spectral Imaging Ltd. (http://www.specim.fi/) Hyperspectral Imaging Solutions
- Opticks (http://opticks.org/) - open source, remote sensing application and development framework.
- ITT Visual Information Solutions - ENVI Hyperspectral Image Processing Software (http://www.ittvis.com/ProductServices/ENVI.aspx)
- A Hyperspectral Imaging Prototype (http://www.inrim.it/res/hyperspectral_imaging/) Fourier transform spectroscopy is combined with Fabry-Perot interferometry
- Middleton Research (http://www.middletonresearch.com) Hyperspectral Imaging products, custom engineering solutions
- Photon etc. (http://photonetc.com/index.php?lan=en&sec=300&sub1=3000&sub2=1023) Hyperspectral Imaging Systems
- UmBio - Evince. Hyperspectral image analysis in real-time. Visual information solutions, see industrial demo movies (http://beta.umbio.com/Public files/Products/Evince Image/EvinceImage.aspx)
- A Matlab Hyperspectral Toolbox (http://matlabhyperspec.sourceforge.net/)
- Telops Hyper-Cam (http://www.hyper-cam.com/) Commercial infrared hyperspectral camera

# 2D-FT NMRI and Spectroscopy

**2D-FT Nuclear Magnetic resonance imaging** (**2D-FT NMRI**), or **Two-dimensional Fourier transform** magnetic resonance imaging (**NMRI**), is primarily a non--invasive imaging technique most commonly used in biomedical research and medical radiology/nuclear medicine/MRI to visualize structures and functions of the living systems and single cells. For example it can provides fairly detailed images of a human body in any selected cross-sectional plane, such as longitudinal, transversal, sagital, etc. NMRI provides much greater contrast especially for the different soft tissues of the body than computed tomography (CT) as its most sensitive option observes the nuclear spin distribution and dynamics of highly mobile molecules that contain the naturally abundant, stable hydrogen isotope $^{1}$H as in plasma water molecules, blood, disolved metabolites and fats. This approach makes it most useful in cardiovascular, oncological (cancer), neurological (brain), musculoskeletal, and cartilage imaging. Unlike CT, it uses no ionizing radiation, and also unlike nuclear imaging it does not employ any radioactive isotopes. Some of the first MRI images reported were published in 1973[1] and the first study performed on a human took place on July 3, 1977.[2] Earlier papers were also published by Peter Mansfield[3] in UK (Nobel Laureate in 2003), and R. Damadian in the USA, (together with an approved patent for magnetic imaging). Unpublished `high-resolution' (50 micron resolution) images of other living systems, such as hydrated wheat grains, were obtained and communicated in UK in 1977-1979, and were subsequently confirmed by articles published in *Nature*.

## NMRI Principle

Certain nuclei such as $^{1}H$ nuclei, or `fermions' have spin-1/2, because there are two spin states, referred to as "up" and "down" states. The nuclear magnetic resonance absorption phenomenon occurs when samples containing such nuclear spins are placed in a static magnetic field and a very short radiofrequency pulse is applied with a center, or carrier, frequency matching that of the transition between the up and down states of the spin-1/2 $^{1}H$ nuclei that were polarized by the static magnetic field. [4] Very low field schemes have also been recently reported.[5]

Advanced clinical diagnostics and biomedical research NMR Imaging instrument.

## Chemical Shifts

NMR is a very useful family of techniques for chemical and biochemical research because of the chemical shift; this effect consists in a frequency shift of the nuclear magnetic resonance for specific chemical groups or atoms as a result of the partial shielding of the corresponding nuclei from the applied, static external magnetic field by the electron orbitals (or molecular orbitals) surrounding such nuclei present in the chemical groups. Thus, the higher the electron density surounding a specific nucleus the larger the chemical shift will be. The resulting magnetic field at the nucleus is thus lower than the applied external magnetic field and the resonance frequencies observed as a result of such shielding are lower than the value that would be observed in the absence of any electronic orbital shielding. Furthermore, in order to obtain a chemical shift value independent of the strength of the applied magnetic field and allow for the direct comparison of spectra obtained at different magnetic field values, the chemical shift is defined by the ratio of the strength of the local magnetic field value at the observed (electron orbital-shielded) nucleus by the external magnetic field strength, $H_{loc}/ H_{0}$. The first NMR observations of the chemical shift, with the correct physical chemistry interpretation, were reported for $^{19}F$ containing compounds in the early 1950's by Herbert S. Gutowsky and Charles P. Slichter from the University of Illinois at Urbana (USA).

## NMR Imaging Principles

A number of methods have been devised for combining magnetic field gradients and radiofrequency pulsed excitation to obtain an image. Two major maethods involve either 2D -FT or 3D-FT[6] reconstruction from projections, somewhat similar to Computed Tomography, with the exception of the image interpretation that in the former case must include dynamic and relaxation/contrast enhancement information as well. Other schemes involve building the NMR image either point-by-point or line-by-line. Some schemes use instead gradients in the rf field rather than in the static magnetic field. The majority of NMR images routinely obtained are either by the Two-Dimensional Fourier Transform (2D-FT) technique [7] (with slice selection), or by the Three-Dimensional Fourier Transform (3D--FT) techniques that are however much more time consuming at present. 2D-FT NMRI is sometime called in common parlance a "spin-warp". An NMR image corresponds to a spectrum consisting of a number of `spatial frequencies' at different locations in the sample investigated, or in a patient.[8] A two–dimensional

Fourier transformation of such a "real" image may be considered as a representation of such "real waves" by a matrix of spatial frequencies known as the k–space. We shall see next in some mathematical detail how the 2D-FT computation works to obtain 2D-FT NMR images.

## Two-dimensional Fourier transform imaging and spectroscopy

A two-dimensional Fourier transform (2D-FT) is computed numerically or carried out in two stages, both involving `standard', one-dimensional Fourier transforms. However, the second stage Fourier transform is not the inverse Fourier transform (which would result in the original function that was transformed at the first stage), but a Fourier transform in a second variable-- which is `shifted' in value-- relative to that involved in the result of the first Fourier transform. Such 2D-FT analysis is a very powerful method for both NMRI and two-dimensional nuclear magnetic resonance spectroscopy (2D-FT NMRS)[9] that allows the three-dimensional reconstruction of polymer and biopolymer structures at atomic resolution]].[10] for molecular weights (Mw) of dissolved biopolymers in aqueous solutions (for example) up to about 50,000 Mw. For larger biopolymers or polymers, more complex methods have been developed to obtain limited structural resolution needed for partial 3D-reconstructions of higher molecular structures, e.g. for up 900,000 Mw or even oriented microcrystals in aqueous suspensions or single crystals; such methods have also been reported for *in vivo* 2D-FT NMR spectroscopic studies of algae, bacteria, yeast and certain mammalian cells, including human ones. The 2D-FT method is also widely utilized in optical spectroscopy, such as *2D-FT NIR hyperspectral imaging* (2D-FT NIR-HS), or in MRI imaging for research and clinical, diagnostic applications in Medicine. In the latter case, 2D-FT NIR-HS has recently allowed the identification of single, malignant cancer cells surrounded by healthy human breast tissue at about 1 micron resolution, well-beyond the resolution obtainable 2D-FT NMRI for such systems in the limited time available for such diagnostic investigations (and also in magnetic fields up to the FDA approved magnetic field strength $\mathbf{H}_0$ of 4.7 T, as shown in the top image of the state-of-the-art NMRI instrument). A more precise mathematical definition of the `double' (2D) Fourier transform involved in both 2D NMRI and 2D-FT NMRS is specified next, and a precise example follows this generally accepted definition.

### 2D-FT Definition

A *2D-FT, or two-dimensional Fourier transform*, is a standard Fourier transformation of a function of two variables, $f(x_1, x_2)$, carried first in the first variable $x_1$, followed by the Fourier transform in the second variable $x_2$of the resulting function $F(s_1, x_2)$. Note that in the case of both 2D-FT NMRI and 2D-FT NMRS the two independent variables in this definition are in the time domain, whereas the results of the two successive Fourier transforms have, of course, frequencies as the independent variable in the NMRS, and ultimately spatial coordinates for both 2D NMRI and 2D-FT NMRS following computer structural recontructions based on special algorithms that are different from FT or 2D-FT. Moreover, such structural algorithms are different for 2D NMRI and 2D-FT NMRS: in the former case they involve macroscopic, or anatomical structure detrmination, whereas in the latter case of 2D-FT NMRS the atomic structure reconstruction algorithms are based on the quantum theory of a microphysical (quantum) process such as nuclear Overhauser enhancement NOE, or specific magnetic dipole-dipole interactions[11] between neighbor nuclei.

### Example 1

A 2D Fourier transformation and phase correction is applied to a set of 2D NMR (FID) signals : $s(t_1, t_2)$ yielding a real 2D-FT NMR `spectrum' (collection of 1D FT-NMR spectra) represented by a matrix **S** whose elements are

$$S(\nu_1, \nu_2) = \mathbf{Re} \int \int cos(\nu_1 t_1) exp^{(-i\nu_2 t_2)} s(t_1, t_2) dt_1 dt_2$$

where : $\nu_1$ and : $\nu_2$ denote the discrete indirect double-quantum and single-quantum(detection) axes, respectively, in the 2D NMR experiments. Next, the \emph{covariance matrix} is calculated in the frequency domain according to the following equation

$C(\nu_2', \nu_2) = S^T S = \sum_{\nu^1} [S(\nu_1, \nu_2') S(\nu_1, \nu_2)]$, with : $\nu_2, \nu_2'$ taking all possible single-quantum frequency values and with the summation carried out over all discrete, double quantum frequencies : $\nu_1$.

### Example 2

Atomic Structure from 2D-FT STEM Images [12] of electron distributions in a high-temperature cuprate superconductor `paracrystal' reveal both the domains (or `location') and the local symmetry of the 'pseudo-gap' in the electron-pair correlation band responsible for the high--temperature superconductivity effect (obtained at Cornell University). So far there have been three Nobel prizes awarded for 2D-FT NMR/MRI during 1992-2003, and an additional, earlier Nobel prize for 2D-FT of X-ray data (`CAT scans'); recently the advanced possibilities of 2D-FT techniques in Chemistry, Physiology and Medicine [13] received very significant recognition.[14]

## Brief explanation of NMRI diagnostic uses in Pathology

As an example, a diseased tissue such as a malign tumor, can be detected by 2D-FT NMRI because the hydrogen nuclei of molecules in different tissues return to their equilibrium spin state at different relaxation rates, and also because of the manner in which a malign tumor spreads and grows rapidly along the blood vessels adjacent to the tumor, also inducing further vascularization to occur. By changing the pulse delays in the RF pulse sequence employed, and/or the RF pulse sequence itself, one may obtain a `relaxation--based contrast', or contrast enhancement between different types of body tissue, such as normal vs. diseased tissue cells for example. Excluded from such diagnostic observations by NMRI are all patients with ferromagnetic metal implants, (e.g., cochlear implants), and all cardiac pacemaker patients who cannot undergo any NMRI scan because of the very intense magnetic and RF fields employed in NMRI which would strongly interfere with the correct functioning of such pacemakers. It is, however, conceivable that future developments may also include along with the NMRI diagnostic treatments with special techniques involving applied magnetic fields and very high frequency RF. Already, surgery with special tools is being experimented on in the presence of NMR imaging of subjects.Thus, NMRI is used to image almost every part of the body, and is especially useful for diagnosis in neurological conditions, disorders of the muscles and joints, for evaluating tumors, such as in lung or skin cancers, abnormalities in the heart (especially in children with hereditary disorders), blood vessels, CAD, atherosclerosis and cardiac infarcts [15] (courtesy of Dr. Robert R. Edelman)

## See also

- Nuclear magnetic resonance (NMR)
- Medical imaging
- Protein nuclear magnetic resonance spectroscopy
- Kurt Wüthrich
- Chemical shift
- Computed tomography (CT)
- Fourier transform spectroscopy(FTS)
- Richard R. Ernst
- Magnetic resonance microscopy
- Solid-state NMR
- Herbert S. Gutowsky
- John S. Waugh
- Charles P. Slichter
- FT-NIRS (NIR)
- Magnetic resonance elastography
- Relaxation
- Earth's field NMR (EFNMR)
- Robinson oscillator

## Reference list


[1] Lauterbur, P.C., Nobel Laureate in 2003 (1973). "Image Formation by Induced Local Interactions: Examples of Employing Nuclear Magnetic Resonance". *Nature* **242**: 190–1. doi:10.1038/242190a0.

[2] [http://www.howstuffworks.com/mri.htm/printable Howstuffworks "How MRI Works"

[3] Peter Mansfield. 2003. Nobel Laureate in Physiology and Medicine for (2D and 3D) MRI (http://www.parteqinnovations.com/pdf-doc/fandr-Gaz1006.pdf)

[4] Antoine Abragam. 1968. *Principles of Nuclear Magnetic Resonance.*, 895 pp., Cambridge University Press: Cambridge, UK.

[5] Raftery D (August 2006). "MRI without the magnet" (http://www.pubmedcentral.nih.gov/articlerender.fcgi?tool=pmcentrez&artid=1568902). *Proc Natl Acad Sci USA.* **103** (34): 12657–8. doi:10.1073/pnas.0605625103. PMID 16912110. PMC 1568902.

[6] Wu Y, Chesler DA, Glimcher MJ, *et al* (February 1999). "Multinuclear solid-state three-dimensional MRI of bone and synthetic calcium phosphates" (http://www.pnas.org/cgi/pmidlookup?view=long&pmid=9990066). *Proc. Natl. Acad. Sci. U.S.A.* **96** (4): 1574–8. doi:10.1073/pnas.96.4.1574. PMID 9990066. PMC 15521. .

[7] http://www.math.cuhk.edu.hk/course/mat2071a/lec1_08.ppt

[8] *Haacke, E Mark; Brown, Robert F; Thompson, Michael; Venkatesan, Ramesh (1999). *Magnetic resonance imaging: physical principles and sequence design*. New York: J. Wiley & Sons. ISBN 0-471-35128-8.

[9] Richard R. Ernst. 1992. Nuclear Magnetic Resonance Fourier Transform (2D-FT) Spectroscopy. Nobel Lecture (http://nobelprize.org/nobel_prizes/chemistry/laureates/1991/ernst-lecture.pdf), on December 9, 1992.

[10] http://en.wikipedia.org/wiki/Nuclear_magnetic_resonance#Nuclear_spin_and_magnets Kurt Wutrich in 1982-1986 : 2D-FT NMR of solutions

[11] Charles P. Slichter.1996. *Principles of Magnetic Resonance.* Springer: Berlin and New York, Third Edition., 651pp. ISBN 0-387-50157-6.

[12] http://www.physorg.com/news129395045.html

[13] http://nobelprize.org/nobel_prizes/chemistry/laureates/1991/ernst-lecture.pdf

[14] Protein structure determination in solution by NMR spectroscopy (http://www.ncbi.nlm.nih.gov/entrez/query.fcgi?cmd=Retrieve&db=pubmed&dopt=Abstract&list_uids=2266107&query_hl=33&itool=pubmed_docsum) Wuthrich K. J Biol Chem. 1990 December 25;265(36):22059-62.

[15] http://www.mr-tip.com/serv1.php?type=img&img=Cardiac%20Infarct%20Short%20Axis%20Cine%204


## References


- Antoine Abragam. 1968. *Principles of Nuclear Magnetic Resonance.*, 895 pp., Cambridge University Press: Cambridge, UK.
- Charles P. Slichter.1996. *Principles of Magnetic Resonance.* Springer: Berlin and New York, Third Edition., 651pp. ISBN 0-387-50157-6.
- Kurt Wüthrich. 1986, *NMR of Proteins and Nucleic Acids*., J. Wiley and Sons: New York, Chichester, Brisbane, Toronto, Singapore. ( Nobel Laureate in 2002 for 2D-FT NMR Studies of Structure and Function of Biological Macromolecules (http://nobelprize.org/nobel_prizes/chemistry/laureates/2002/wutrich-lecture.pdf)
- Protein structure determination in solution by NMR spectroscopy (http://www.ncbi.nlm.nih.gov/entrez/query.fcgi?cmd=Retrieve&db=pubmed&dopt=Abstract&list_uids=2266107&query_hl=33&itool=pubmed_docsum) Wuthrich K. J Biol Chem. 1990 December 25;265(36):22059-62
- 2D-FT NMRI Instrument image: A JPG color image of a 2D-FT NMRI `monster' Instrument (http://upload.wikimedia.org/wikipedia/en/b/bf/HWB-NMRv900.jpg).

- Richard R. Ernst. 1992. Nuclear Magnetic Resonance Fourier Transform (2D-FT) Spectroscopy. Nobel Lecture (http://nobelprize.org/nobel_prizes/chemistry/laureates/1991/ernst-lecture.pdf), on December 9, 1992.
- Peter Mansfield. 2003. Nobel Laureate in Physiology and Medicine for (2D and 3D) MRI (http://www.parteqinnovations.com/pdf-doc/fandr-Gaz1006.pdf)
- D. Benett. 2007. PhD Thesis. Worcester Polytechnic Institute. PDF of 2D-FT Imaging Applications to NMRI in Medical Research. (http://www.wpi.edu/Pubs/ETD/Available/etd-081707-080430/unrestricted/dbennett.pdf) Worcester Polytechnic Institute. (Includes many 2D-FT NMR images of human brains.)
- Paul Lauterbur. 2003. Nobel Laureate in Physiology and Medicine for (2D and 3D) MRI. (http://nobelprize.org/nobel_prizes/medicine/laureates/2003/)
- Jean Jeener. 1971. Two-dimensional Fourier Transform NMR, presented at an Ampere International Summer School, Basko Polje, unpublished. A verbatim quote follows from Richard R. Ernst's Nobel Laureate Lecture delivered on December 2, 1992, "A new approach to measure two-dimensional (2D) spectra." has been proposed by Jean Jeener at an Ampere Summer School in Basko Polje, Yugoslavia, 1971 (Jean Jeneer,1971}). He suggested a 2D Fourier transform experiment consisting of two $\pi/2$ pulses with a variable time $t_1$ between the pulses and the time variable $t_2$ measuring the time elapsed after the second pulse as shown in Fig. 6 that expands the principles of Fig. 1. Measuring the response $s(t_1,t_2)$ of the two-pulse sequence and Fourier-transformation with respect to both time variables produces a two-dimensional spectrum $S(O_1,O_2)$ of the desired form. This two-pulse experiment by Jean Jeener is the forefather of a whole class of $2D$ experiments that can also easily be expanded to multidimensional spectroscopy.
- Dudley, Robert, L (1993). "High-Field NMR Instrumentation". *Ch. 10 in Physical Chemistry of Food Processes* (New York: Van Nostrand-Reinhold) **2**: 421-30. ISBN 0-442-00582-2.
- Baianu, I.C.; Kumosinski, Thomas (August 1993). "NMR Principles and Applications to Structure and Hydration,". *Ch.9 in Physical Chemistry of Food Processes* (New York: Van Nostrand-Reinhold) **2**: 338-420. ISBN 0-442-00582-2.
- Haacke, E Mark; Brown, Robert F; Thompson, Michael; Venkatesan, Ramesh (1999). *Magnetic resonance imaging: physical principles and sequence design*. New York: J. Wiley & Sons. ISBN 0-471-35128-8.
- Raftery D (August 2006). "MRI without the magnet" (http://www.pubmedcentral.nih.gov/articlerender.fcgi?tool=pmcentrez&artid=1568902). *Proc Natl Acad Sci USA*. **103** (34): 12657–8. doi:10.1073/pnas.0605625103. PMID 16912110. PMC 1568902.
- Wu Y, Chesler DA, Glimcher MJ, *et al* (February 1999). "Multinuclear solid-state three-dimensional MRI of bone and synthetic calcium phosphates" (http://www.pnas.org/cgi/pmidlookup?view=long&pmid=9990066). *Proc. Natl. Acad. Sci. U.S.A.* **96** (4): 1574–8. doi:10.1073/pnas.96.4.1574. PMID 9990066. PMC 15521.


## External links

- Cardiac Infarct or "heart attack" Imaged in Real Time by 2D-FT NMRI (http://www.mr-tip.com/exam_gifs/cardiac_infarct_short_axis_cine_6.gif)
- 3D Animation Movie about MRI Exam (http://www.patiencys.com/MRI/)
- Interactive Flash Animation on MRI (http://www.e-mri.org) - *Online Magnetic Resonance Imaging physics and technique course*
- International Society for Magnetic Resonance in Medicine (http://www.ismrm.org)
- Danger of objects flying into the scanner (http://www.simplyphysics.com/flying_objects.html)

## Related Wikipedia websites

- Medical imaging
- Computed tomography
- Magnetic resonance microscopy
- Fourier transform spectroscopy
- FT-NIRS
- Magnetic resonance elastography
- Nuclear magnetic resonance (NMR)
- Chemical shift
- Relaxation
- Robinson oscillator
- Earth's field NMR (EFNMR)
- Rabi cycle

*This article incorporates material by the original author from 2D-FT MR- Imaging and related Nobel awards* (http://planetphysics.org/encyclopedia/2DFTImaging.html) on PlanetPhysics (http://planetphysics.org/), which is licensed under the GFDL.

# NMR microscopy

**Magnetic Resonance Microscopy** (MRM, μMRI) is Magnetic Resonance Imaging (MRI) at a microscopic level. A strict definition is MRI having voxel resolutions of better than 100 $\mu m^3$ [1].

## Nomenclature

Many scientist in the field consider the name Magnetic Resonance Microscopy to be a misnomer, since the images produced are much worse than those produced by even a marginal optical or electron microscope. As such, the name High Resolution Magnetic Resonance Imaging is often preferred in scientific literature on the subject. In fact, the term is most widely used by the High Resolution Magnetic Resonance Imaging group from Duke University, headed by Allan Johnson.

## Differences between MRI and MRM

- Resolution: Typical medical MRI resolution is about 1 $mm^3$; the desired resolution of MRM is 100 $\mu m^3$ or smaller.
- Specimen size: Medical MRI machines are designed so that a patient may fit inside. MRM chambers are usually small, typically less than 1 $cm^3$.

## Current status of MRM

Although MRI is very common for medical applications, MRM is still developed in laboratories. The major barriers for practical MRM include:

- Magnetic field gradient: High gradient focus the magnetic resonance in a smaller volume (smaller point spread function), results in a better spatial resolution. The gradients for MRM are typically 50 to 100 times those of clinical systems. However, the construction of radio frequency (RF) coil used in MRM does not allow ultrahigh gradient.
- Sensitivity: Because the voxels for MRM can be 1/100,000 of those in MRI, the signal will be proportionately weaker [2].

## Alternative MRM

Magnetic Resonance Force Microscopy (MRFM) is claimed to have nm³-scale resolutions. It improves the sensitivity issue by introducing microfabricated cantilever to measure tiny signals. The magnetic gradient is generated by a micrometre-scale magnetic tip, yielding a typical gradient 10 million times larger than those of clinical systems. This technique is still in the beginning stage. Because the specimen need to be in high vacuum at cryogenic temperatures, MRFM can be only used for solid state matters.

## References

[1] P. Glover and P. Mansfield, Limits to magnetic resonance microscopy, Rep. Prog. Phys. 65 1489–1511, 2002

[2] R. Maronpot Applications of Magnetic Resonance Microscopy, Toxicologic Pathology, 32(Suppl. 2):42–48, 2004

## External links

- Introduction to Magnetic Resonance Microscopy (http://cbaweb2.med.unc.edu/henson_mrm/pages/mrmfaq.html#MRMAnchor) Auditory Research Laboratory at the Univ. of North Carolina.

# Chemical imaging

**Chemical imaging** (as quantitative - *chemical mapping*) is the analytical capability to create a visual image of components distribution from simultaneous measurement of spectra and spatial, time informations. [1] [2]

The main idea - for chemical imaging, the analyst may choose to take as many data spectrum measured at a particular chemical component in spatial location at time; this is useful for chemical identification and quantification. Alternatively, selecting an image plane at a particular data spectrum (PCA - multivariable data of wavelength, spatial location at time) can mapp the spatial distribution of sample components, provided that their spectral signatures are different at the selected data spectrum.

Software for chemical imaging is most specific and distinguished from chemical methods as the chemometrics.

Imaging technique is most often applied to either solid or gel samples, and has applications in chemistry, biology[3] [4] [5] [6] [7] [8] , medicine[9] [10] , pharmacy[11] (see also for example: Chemical Imaging Without Dyeing [12]), food science, biotechnology[13] [14] , agriculture and industry (see for example:NIR Chemical Imaging in Pharmaceutical Industry [15] and Pharmaceutical Process Analytical Technology: [16]). NIR, IR and Raman chemical imaging is also referred to as hyperspectral, spectroscopic, spectral or multispectral imaging (also see microspectroscopy). However, other ultra-sensitive and selective imaging techniques are also in use that involve either UV-visible or fluorescence microspectroscopy. Many imaging techniques can be used to analyze samples of all sizes, from the single molecule[17] [18] to the cellular level in biology and medicine[19] [20] [21] , and to images of planetary systems in astronomy, but different instrumentation is employed for making observations on such widely different systems.

Imaging instrumentation is composed of three components: a radiation source to illuminate the sample, a spectrally selective element, and usually a detector array (the camera) to collect the images. When many stacked spectral channels (wavelengths) are collected for different locations of the microspectrometer focus on a line or planar array in the focal plane, the data is called hyperspectral; fewer wavelength data sets are called multispectral. The data format is called a hypercube. The data set may be visualized as a three-dimensional block of data spanning two spatial dimensions (x and y), with a series of wavelengths (lambda) making up the third (spectral) axis. The hypercube can be visually and mathematically treated as a series of spectrally resolved images (each image plane corresponding to the image at one wavelength) or a series of spatially resolved spectra.

Many materials, both manufactured and naturally occurring, derive their functionality from the spatial distribution of sample components. For example, extended release pharmaceutical formulations can be achieved by using a coating

that acts as a barrier layer. The release of active ingredient is controlled by the presence of this barrier, and imperfections in the coating, such as discontinuities, may result in altered performance. In the semi-conductor industry, irregularities or contaminants in silicon wafers or printed micro-circuits can lead to failure of these components. The functionality of biological systems is also dependent upon chemical gradients – a single cell, tissue, and even whole organs function because of the very specific arrangement of components. It has been shown that even small changes in chemical composition and distribution may be an early indicator of disease.

Any material that depends on chemical gradients for functionality may be amenable to study by an analytical technique that couples spatial and chemical characterization. To efficiently and effectively design and manufacture such materials, the 'what' and the 'where' must both be measured. The demand for this type of analysis is increasing as manufactured materials become more complex. Chemical imaging techniques is critical to understanding modern manufactured products and in some casses is a non-destructive technique so that samples are preserved for further testing.

## History

Commercially available laboratory-based chemical imaging systems emerged in the early 1990s (ref. 1-5). In addition to economic factors, such as the need for sophisticated electronics and extremely high-end computers, a significant barrier to commercialization of infrared imaging was that the focal plane array (FPA) needed to read IR images were not readily available as commercial items. As high-speed electronics and sophisticated computers became more commonplace, and infrared cameras became readily commercially available, laboratory chemical imaging systems were introduced.

Initially used for novel research in specialized laboratories, chemical imaging became a more commonplace analytical technique used for general R&D, quality assurance (QA) and quality control (QC) in less than a decade. The rapid acceptance of the technology in a variety of industries (pharmaceutical, polymers, semiconductors, security, forensics and agriculture) rests in the wealth of information characterizing both chemical composition and morphology. The parallel nature of chemical imaging data makes it possible to analyze multiple samples simultaneously for applications that require high throughput analysis in addition to characterizing a single sample.

## Principles

Chemical imaging shares the fundamentals of vibrational spectroscopic techniques, but provides additional information by way of the simultaneous acquisition of spatially resolved spectra. It combines the advantages of digital imaging with the attributes of spectroscopic measurements. Briefly, vibrational spectroscopy measures the interaction of light with matter. Photons that interact with a sample are either absorbed or scattered; photons of specific energy are absorbed, and the pattern of absorption provides information, or a fingerprint, on the molecules that are present in the sample.

On the other hand, in terms of the observation setup, chemical imaging can be carried out in one of the following modes: (optical) absorption, emission (fluorescence), (optical) transmission or scattering (Raman). A consensus currently exists that the fluorescence (emission) and Raman scattering modes are the most sensitive and powerful, but also the most expensive.

In a transmission measurement, the radiation goes through a sample and is measured by a detector placed on the far side of the sample. The energy transferred from the incoming radiation to the molecule(s) can be calculated as the difference between the quantity of photons that were emitted by the source and the quantity that is measured by the detector. In a diffuse reflectance measurement, the same energy difference measurement is made, but the source and detector are located on the same side of the sample, and the photons that are measured have re-emerged from the illuminated side of the sample rather than passed through it. The energy may be measured at one or multiple wavelengths; when a series of measurements are made, the response curve is called a spectrum.

A key element in acquiring spectra is that the radiation must somehow be energy selected – either before or after interacting with the sample. Wavelength selection can be accomplished with a fixed filter, tunable filter, spectrograph, an interferometer, or other devices. For a fixed filter approach, it is not efficient to collect a significant number of wavelengths, and multispectral data are usually collected. Interferometer-based chemical imaging requires that entire spectral ranges be collected, and therefore results in hyperspectral data. Tunable filters have the flexibility to provide either multi- or hyperspectral data, depending on analytical requirements.

Spectra may be measured one point at a time using a single element detector (single-point mapping), as a line-image using a linear array detector (typically 16 to 28 pixels) (linear array mapping), or as a two-dimensional image using a Focal Plane Array (FPA)(typically 256 to 16,384 pixels) (FPA imaging). For single-point the sample is moved in the x and y directions point-by-point using a computer-controlled stage. With linear array mapping, the sample is moved line-by-line with a computer-controlled stage. FPA imaging data are collected with a two-dimensional FPA detector, hence capturing the full desired field-of-view at one time for each individual wavelength, without having to move the sample. FPA imaging, with its ability to collected tens of thousands of spectra simultaneously is orders of magnitude faster than linear arrays which are can typically collect 16 to 28 spectra simultaneously, which are in turn much faster than single-point mapping.

## Terminology

Some words common in spectroscopy, optical microscopy and photography have been adapted or their scope modified for their use in chemical imaging. They include: resolution, field of view and magnification. There are two types of resolution in chemical imaging. The spectral resolution refers to the ability to resolve small energy differences; it applies to the spectral axis. The spatial resolution is the minimum distance between two objects that is required for them to be detected as distinct objects. The spatial resolution is influenced by the field of view, a physical measure of the size of the area probed by the analysis. In imaging, the field of view is a product of the magnification and the number of pixels in the detector array. The magnification is a ratio of the physical area of the detector array divided by the area of the sample field of view. Higher magnifications for the same detector image a smaller area of the sample.

## Types of vibrational chemical imaging instruments

Chemical imaging has been implemented for mid-infrared, near-infrared spectroscopy and Raman spectroscopy. As with their bulk spectroscopy counterparts, each imaging technique has particular strengths and weaknesses, and are best suited to fulfill different needs.

### Mid-infrared chemical imaging

Mid-infrared (MIR) spectroscopy probes fundamental molecular vibrations, which arise in the spectral range 2,500-25,000 nm. Commercial imaging implementations in the MIR region typically employ Fourier Transform Infrared (FT-IR) interferometers and the range is more commonly presented in wavenumber, 4,000 – 400 $cm^{-1}$. The MIR absorption bands tend to be relatively narrow and well-resolved; direct spectral interpretation is often possible by an experienced spectroscopist. MIR spectroscopy can distinguish subtle changes in chemistry and structure, and is often used for the identification of unknown materials. The absorptions in this spectral range are relatively strong; for this reason, sample presentation is important to limit the amount of material interacting with the incoming radiation in the MIR region. Most data collected in this range is collected in transmission mode through thin sections (~10 micrometres) of material. Water is a very strong absorber of MIR radiation and wet samples often require advanced sampling procedures (such as attenuated total reflectance). Commercial instruments include point and line mapping, and imaging. All employ an FT-IR interferometer as wavelength selective element and light source.

For types of MIR microscope, see Microscopy#Infrared microscopy.

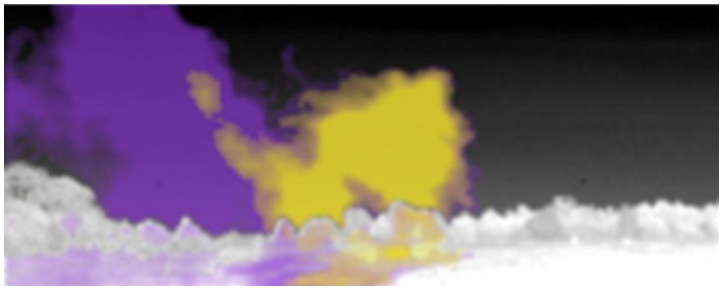

Remote chemical imaging of a simultaneous release of $SF_6$ and $NH_3$ at 1.5km using the FIRST imaging spectrometer[22]

Atmospheric windows in the infrared spectrum are also employed to perform chemical imaging remotely. In these spectral regions the atmospheric gases (mainly water and $CO_2$) present low absorption and allow infrared viewing over kilometer distances. Target molecules can then be viewed using the selective absorption/emission processes described above. An example of the chemical imaging of a simultaneous release of $SF_6$ and $NH_3$ is shown in the image.

**Near-infrared chemical imaging**

The analytical near infrared (NIR) region spans the range from approximately 700-2,500 nm. The absorption bands seen in this spectral range arise from overtones and combination bands of O-H, N-H, C-H and S-H stretching and bending vibrations. Absorption is one to two orders of magnitude smaller in the NIR compared to the MIR; this phenomenon eliminates the need for extensive sample preparation. Thick and thin samples can be analyzed without any sample preparation, it is possible to acquire NIR chemical images through some packaging materials, and the technique can be used to examine hydrated samples, within limits. Intact samples can be imaged in transmittance or diffuse reflectance.

The lineshapes for overtone and combination bands tend to be much broader and more overlapped than for the fundamental bands seen in the MIR. Often, multivariate methods are used to separate spectral signatures of sample components. NIR chemical imaging is particularly useful for performing rapid, reproducible and non-destructive analyses of known materials[23] [24] . NIR imaging instruments are typically based on one of two platforms: imaging using a tunable filter and broad band illumination, and line mapping employing an FT-IR interferometer as the wavelength filter and light source.

**Raman chemical imaging**

The Raman shift chemical imaging spectral range spans from approximately 50 to 4,000 $cm^{-1}$; the actual spectral range over which a particular Raman measurement is made is a function of the laser excitation frequency. The basic principle behind Raman spectroscopy differs from the MIR and NIR in that the x-axis of the Raman spectrum is measured as a function of energy shift (in $cm^{-1}$) relative to the frequency of the laser used as the source of radiation. Briefly, the Raman spectrum arises from inelastic scattering of incident photons, which requires a change in polarizability with vibration, as opposed to infrared absorption, which requires a change in dipole moment with vibration. The end result is spectral information that is similar and in many cases complementary to the MIR. The Raman effect is weak - only about one in $10^7$ photons incident to the sample undergoes Raman scattering. Both organic and inorganic materials possess a Raman spectrum; they generally produce sharp bands that are chemically specific. Fluorescence is a competing phenomenon and, depending on the sample, can overwhelm the Raman signal, for both bulk spectroscopy and imaging implementations.

Raman chemical imaging requires little or no sample preparation. However, physical sample sectioning may be used to expose the surface of interest, with care taken to obtain a surface that is as flat as possible. The conditions required for a particular measurement dictate the level of invasiveness of the technique, and samples that are sensitive to high power laser radiation may be damaged during analysis. It is relatively insensitive to the presence of water in the sample and is therefore useful for imaging samples that contain water such as biological material.

### Fluorescence imaging (visible and NIR)

This emission microspectroscopy mode is the most sensitive in both visible and FT-NIR microspectroscopy, and has therefore numerous biomedical, biotechnological and agricultural applications. There are several powerful, highly specific and sensitive fluorescence techniques that are currently in use, or still being developed; among the former are FLIM, FRAP, FRET and FLIM-FRET; among the latter are NIR fluorescence and probe-sensitivity enhanced NIR fluorescence microspectroscopy and nanospectroscopy techniques (see "Further reading" section).

## Sampling and samples

The value of imaging lies in the ability to resolve spatial heterogeneities in solid-state or gel/gel-like samples. Imaging a liquid or even a suspension has limited use as constant sample motion serves to average spatial information, unless ultra-fast recording techniques are employed as in fluorescence correlation microspectroscopy or FLIM obsevations where a single molecule may be monitored at extremely high (photon) detection speed. High-throughput experiments (such as imaging multi-well plates) of liquid samples can however provide valuable information. In this case, the parallel acquisition of thousands of spectra can be used to compare differences between samples, rather than the more common implementation of exploring spatial heterogeneity within a single sample.

Similarly, there is no benefit in imaging a truly homogeneous sample, as a single point spectrometer will generate the same spectral information. Of course the definition of homogeneity is dependent on the spatial resolution of the imaging system employed. For MIR imaging, where wavelengths span from 3-10 micrometres, objects on the order of 5 micrometres may theoretically be resolved. The sampled areas are limited by current experimental implementations because illumination is provided by the interferometer. Raman imaging may be able to resolve particles less than 1 micrometre in size, but the sample area that can be illuminated is severely limited. With Raman imaging, it is considered impractical to image large areas and, consequently, large samples. FT-NIR chemical/hyperspectral imaging usually resolves only larger objects (>10 micrometres), and is better suited for large samples because illumination sources are readily available. However, FT-NIR microspectroscopy was recently reported to be capable of about 1.2 micron (micrometer) resolution in biological samples[25] Furthermore, two-photon excitation FCS experiments were reported to have attained 15 nanometer resolution on biomembrane thin films with a special coincidence photon-counting setup.

### Detection limit

The concept of the detection limit for chemical imaging is quite different than for bulk spectroscopy, as it depends on the sample itself. Because a bulk spectrum represents an average of the materials present, the spectral signatures of trace components are simply overwhelmed by dilution. In imaging however, each pixel has a corresponding spectrum. If the physical size of the trace contaminant is on the order of the pixel size imaged on the sample, its spectral signature will likely be detectable. If however, the trace component is dispersed homogeneously (relative to pixel image size) throughout a sample, it will not be detectable. Therefore, detection limits of chemical imaging techniques are strongly influenced by particle size, the chemical and spatial heterogeneity of the sample, and the spatial resolution of the image.

### Data analysis

Data analysis methods for chemical imaging data sets typically employ mathematical algorithms common to single point spectroscopy or to image analysis. The reasoning is that the spectrum acquired by each detector is equivalent to a single point spectrum; therefore pre-processing, chemometrics and pattern recognition techniques are utilized with the similar goal to separate chemical and physical effects and perform a qualitative or quantitative characterization of individual sample components. In the spatial dimension, each chemical image is equivalent to a digital image and standard image analysis and robust statistical analysis can be used for feature extraction.

## See also

- Multispectral image
- Microspectroscopy
- Imaging spectroscopy

## References


[1] http://www.imaging.net/chemical-imaging/Chemical imaging

[2] http://www.malvern.com/LabEng/products/sdi/bibliography/sdi_bibliography.htm E. N. Lewis, E. Lee and L. H. Kidder, Combining Imaging and Spectroscopy: Solving Problems with Near-Infrared Chemical Imaging. Microscopy Today, Volume 12, No. 6, 11/2004.

[3] C.L. Evans and X.S. Xie.2008. Coherent Anti-Stokes Raman Scattering Microscopy: Chemical Imaging for Biology and Medicine., doi:10.1146/annurev.anchem.1.031207.112754 *Annual Review of Analytical Chemistry*, **1**: 883-909.

[4] Diaspro, A., and Robello, M. (1999). Multi-photon Excitation Microscopy to Study Biosystems. European Microscopy and Analysis., 5:5-7.

[5] D.S. Mantus and G. H. Morrison. 1991. Chemical imaging in biology and medicine using ion microscopy., *Microchimica Acta*, **104**, (1-6) January 1991, doi: 10.1007/BF01245536

[6] Bagatolli, L.A., and Gratton, E. (2000). Two-photon fluorescence microscopy of coexisting lipid domains in giant unilamellar vesicles of binary phospholipid mixtures. Biophys J., 78:290-305.

[7] Schwille, P., Haupts, U., Maiti, S., and Webb. W.(1999). Molecular dynamics in living cells observed by fluorescence correlation spectroscopy with one- and two-photon excitation. Biophysical Journal, 77(10):2251-2265.

[8] 1.Lee, S. C. et al., (2001). One Micrometer Resolution NMR Microscopy. J. Magn. Res., 150: 207-213.

[9] Near Infrared Microspectroscopy, Fluorescence Microspectroscopy,Infrared Chemical Imaging and High Resolution Nuclear Magnetic Resonance Analysis of Soybean Seeds, Somatic Embryos and Single Cells., Baianu, I.C. et al. 2004., In *Oil Extraction and Analysis.*, D. Luthria, Editor pp.241-273, AOCS Press., Champaign, IL.

[10] Single Cancer Cell Detection by Near Infrared Microspectroscopy, Infrared Chemical Imaging and Fluorescence Microspectroscopy.2004.I. C. Baianu, D. Costescu, N. E. Hofmann and S. S. Korban, q-bio/0407006 (July 2004) (http://arxiv.org/abs/q-bio/0407006)

[11] J. Dubois, G. Sando, E. N. Lewis, Near-Infrared Chemical Imaging, A Valuable Tool for the Pharmaceutical Industry, G.I.T. Laboratory Journal Europe, No. 1-2, 2007.

[12] http://witec.de/en/download/Raman/ImagingMicroscopy04.pdf

[13] Raghavachari, R., Editor. 2001. *Near-Infrared Applications in Biotechnology*, Marcel-Dekker, New York, NY.

[14] Applications of Novel Techniques to Health Foods, Medical and Agricultural Biotechnology.(June 2004) I. C. Baianu, P. R. Lozano, V. I. Prisecaru and H. C. Lin q-bio/0406047 (http://arxiv.org/abs/q-bio/0406047)

[15] http://www.spectroscopyeurope.com/NIR_14_3.pdf

[16] http://www.fda.gov/cder/OPS/PAT.htm

[17] Eigen, M., and Rigler, R. (1994). Sorting single molecules: Applications to diagnostics and evolutionary biotechnology, Proc. Natl. Acad. Sci. USA 91:5740.

[18] Rigler R. and Widengren J. (1990). Ultrasensitive detection of single molecules by fluorescence correlation spectroscopy, *BioScience* (Ed. Klinge & Owman) p.180.

[19] Single Cancer Cell Detection by Near Infrared Microspectroscopy, Infrared Chemical Imaging and Fluorescence Microspectroscopy.2004.I. C. Baianu, D. Costescu, N. E. Hofmann, S. S. Korban and et al., q-bio/0407006 (July 2004) (http://arxiv.org/abs/q-bio/0407006)

[20] Oehlenschläger F., Schwille P. and Eigen M. (1996). Detection of HIV-1 RNA by nucleic acid sequence-based amplification combined with fluorescence correlation spectroscopy, *Proc. Natl. Acad. Sci. USA* **93**:1281.

[21] Near Infrared Microspectroscopy, Fluorescence Microspectroscopy,Infrared Chemical Imaging and High Resolution Nuclear Magnetic Resonance Analysis of Soybean Seeds, Somatic Embryos and Single Cells., Baianu, I.C. et al. 2004., In *Oil Extraction and Analysis.*, D. Luthria, Editor pp.241-273, AOCS Press., Champaign, IL.

[22] M. Chamberland, V. Farley, A. Vallières, L. Belhumeur, A. Villemaire, J. Giroux et J. Legault, High-Performance Field-Portable Imaging Radiometric Spectrometer Technology For Hyperspectral imaging Applications, Proc. SPIE 5994, 59940N, September 2005.

[23] Novel Techniques for Microspectroscopy and Chemical Imaging Analysis of Soybean Seeds and Embryos.(2002). Baianu, I.C., Costescu, D.M., and You, T. *Soy2002 Conference*, Urbana, Illinois.

[24] Near Infrared Microspectroscopy, Chemical Imaging and NMR Analysis of Oil in Developing and Mutagenized Soybean Embryos in Culture. (2003). Baianu, I.C., Costescu, D.M., Hofmann, N., and Korban, S.S. *AOCS Meeting, Analytical Division*.

[25] Near Infrared Microspectroscopy, Fluorescence Microspectroscopy,Infrared Chemical Imaging and High Resolution Nuclear Magnetic Resonance Analysis of Soybean Seeds, Somatic Embryos and Single Cells., Baianu, I.C. et al. 2004., In *Oil Extraction and Analysis.*, D. Luthria, Editor pp.241-273, AOCS Press., Champaign, IL.

## Further reading


1. E. N. Lewis, P. J. Treado, I. W. Levin, Near-Infrared and Raman Spectroscopic Imaging, American Laboratory, 06/1994:16 (1994)
2. E. N. Lewis, P. J. Treado, R. C. Reeder, G. M. Story, A. E. Dowrey, C. Marcott, I. W. Levin, FTIR spectroscopic imaging using an infrared focal-plane array detector, Analytical Chemistry, 67:3377 (1995)
3. P. Colarusso, L. H. Kidder, I. W. Levin, J. C. Fraser, E. N. Lewis Infrared Spectroscopic Imaging: from Planetary to Cellular Systems, Applied Spectroscopy, 52 (3):106A (1998)
4. P. J. Treado I. W. Levin, E. N. Lewis, Near-Infrared Spectroscopic Imaging Microscopy of Biological Materials Using an Infrared Focal-Plane Array and an Acousto-Optic Tunable Filter (AOTF), Applied Spectroscopy, 48:5 (1994)
5. Hammond, S.V., Clarke, F. C., Near-infrared microspectroscopy. In: Handbook of Vibrational Spectroscopy, Vol. 2, J.M. Chalmers and P.R. Griffiths Eds. John Wiley and Sons, West Sussex, UK, 2002, p.1405-1418
6. L.H. Kidder, A.S. Haka, E.N. Lewis, Instrumentation for FT-IR Imaging. In: Handbook of Vibrational Spectroscopy, Vol. 2, J.M. Chalmers and P.R. Griffiths Eds. John Wiley and Sons, West Sussex, UK, 2002, pp.1386-1404
7. J. Zhang; A. O'Connor; J. F. Turner II, Cosine Histogram Analysis for Spectral Image Data Classification,Applied Spectroscopy, Volume 58, Number 11, November 2004, pp. 1318-1324(7)
8. J. F. Turner II; J. Zhang; A. O'Connor, A Spectral Identity Mapper for Chemical Image Analysis, Applied Spectroscopy, Volume 58, Number 11, November 2004, pp. 1308-1317(10)
9. H. R. MORRIS, J. F. TURNER II, B. MUNRO, R. A. RYNTZ, P. J. TREADO, Chemical imaging of thermoplastic olefin (TPO) surface architecture, Langmuir, 1999, vol. 15, no8, pp. 2961-2972
10. J. F. Turner II, Chemical imaging and spectroscopy using tunable filters: Instrumentation, methodology, and multivariate analysis, Thesis (PhD). UNIVERSITY OF PITTSBURGH, Source DAI-B 59/09, p. 4782, Mar 1999, 286 pages.
11. P. Schwille.(2001). in *Fluorescence Correlation Spectroscopy. Theory and applications.* R. Rigler & E.S. Elson, eds., p. 360. Springer Verlag: Berlin.
12. Schwille P., Oehlenschläger F. and Walter N. (1996). Analysis of RNA-DNA hybridization kinetics by fluorescence correlation spectroscopy, *Biochemistry* **35**:10182.
13. FLIM | Fluorescence Lifetime Imaging Microscopy: Fluorescence, fluorophore chemical imaging, confocal emission microspectroscopy, FRET, cross-correlation fluorescence microspectroscopy (http://www.nikoninstruments.com/infocenter.php?n=FLIM).
14. FLIM Applications: (http://www.nikoninstruments.com/infocenter.php?n=FLIM) "FLIM is able to discriminate between fluorescence emanating from different fluorophores and autoflorescing molecules in a specimen, even if their emission spectra are similar. It is, therefore, ideal for identifying fluorophores in multi-label studies. FLIM can also be used to measure intracellular ion concentrations without extensive calibration procedures (for example, Calcium Green) and to obtain information about the local environment of a fluorophore based on changes in its lifetime." FLIM is also often used in microspectroscopic/chemical imaging, or microscopic, studies to monitor spatial and temporal protein-protein interactions, properties of membranes and interactions with nucleic acids in living cells.
15. Gadella TW Jr., *FRET and FLIM techniques*, 33. Imprint: Elsevier, ISBN 978-0-08-054958-3. (2008) 560 pages
16. Langel FD, et al., Multiple protein domains mediate interaction between Bcl10 and Malt1, *J. Biol. Chem.*, (2008) 283(47):32419-31
17. Clayton AH. , The polarized AB plot for the frequency-domain analysis and representation of fluorophore rotation and resonance energy homotransfer. J *Microscopy*. (2008) 232(2):306-12
18. Clayton AH, et al., Predominance of activated EGFR higher-order oligomers on the cell surface. *Growth Factors* (2008) 20:1

19. Plowman et al., Electrostatic Interactions Positively Regulate K-Ras Nanocluster Formation and Function. *Molecular and Cellular Biology* (2008) 4377–4385
20. Belanis L, et al., Galectin-1 Is a Novel Structural Component and a Major Regulator of H-Ras Nanoclusters. *Molecular Biology of the Cell* (2008) 19:1404–1414
21. Van Manen HJ, Refractive index sensing of green fluorescent proteins in living cells using fluorescence lifetime imaging microscopy. Biophys J. (2008) 94(8):L67-9
22. Van der Krogt GNM, et al., A Comparison of Donor-Acceptor Pairs for Genetically Encoded FRET Sensors: Application to the Epac cAMP Sensor as an Example, PLoS ONE, (2008) 3(4):e1916
23. Dai X, et al., Fluorescence intensity and lifetime imaging of free and micellar-encapsulated doxorubicin in living cells. *Nanomedicine*. (2008) **4**(1):49-56.

## External links

- NIR Chemical Imaging in Pharmaceutical Industry (http://www.spectroscopyeurope.com/NIR_14_3.pdf)
- Pharmaceutical Process Analytical Technology: (http://www.fda.gov/cder/OPS/PAT.htm)
- NIR Chemical Imaging for Counterfeit Pharmaceutical Product Analysis (http://www.spectroscopymag.com/spectroscopy/Near-IR+Spectroscopy/NIR-Chemical-Imaging-for-Counterfeit-Pharmaceutica/ArticleStandard/Article/detail/406629)
- Chemical Imaging: Potential New Crime Busting Tool (http://www.sciencedaily.com/releases/2007/08/070802103435.htm)
- Applications of Chemical Imaging in Research (http://www3.imperial.ac.uk/vibrationalspectroscopyandchemicalimaging/research)

# Fluorescence microscopy

A **fluorescence microscope** (colloquially synonymous with *epifluorescence microscope*) is an optical microscope used to study properties of organic or inorganic substances using the phenomena of fluorescence and phosphorescence instead of, or in addition to, reflection and absorption.[1] [2]

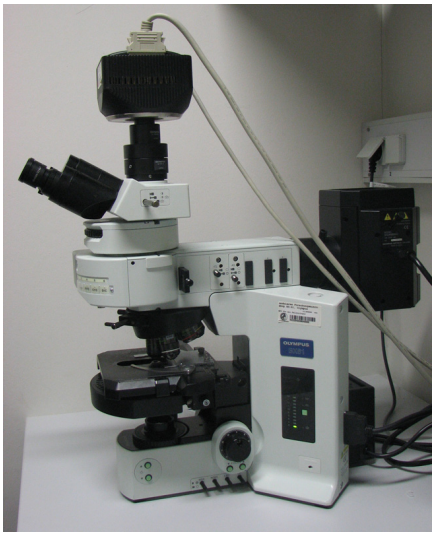

An upright fluorescence microscope (Olympus BX61) with the fluorescent filter cube turret above the objective lenses, coupled with a digital camera.

## Technique

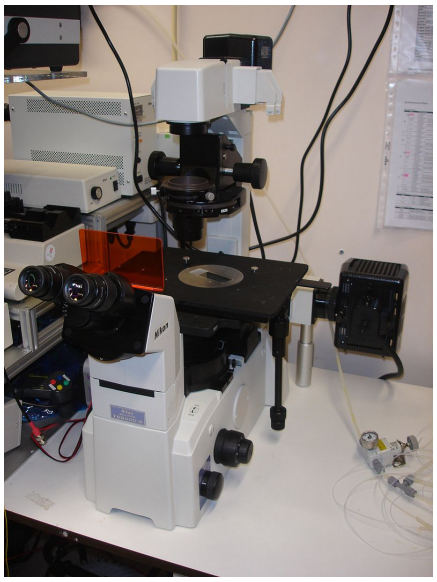

An inverted fluorescence microscope (Nikon TE2000) with the fluorescent filter cube turret below the stage. Note the orange plate that allows the user to look at a sample while protecting their eyes from the UV light.

In most cases, a component of interest in the specimen can be labeled specifically with a fluorescent molecule called a fluorophore (such as green fluorescent protein (GFP), fluorescein or DyLight 488).[1] The specimen is illuminated with light of a specific wavelength (or wavelengths) which is absorbed by the fluorophores, causing them to emit light of longer wavelengths (i.e. of a different color than the absorbed light). The illumination light is separated from the much weaker emitted fluorescence through the use of a spectral emission filter. Typical components of a fluorescence microscope are the light source (xenon arc lamp or mercury-vapor lamp), the excitation filter, the dichroic mirror (or dichromatic beamsplitter), and the emission filter (see figure below). The filters and the dichroic are chosen to match the spectral excitation and emission characteristics of the fluorophore used to label the specimen.[1] In this manner, the distribution of a single fluorophore (color) is imaged at a time. Multi-color images of several types of fluorophores must be composed by combining several single-color images.[1]

Most fluorescence microscopes in use are epifluorescence microscopes (i.e. excitation and observation of the fluorescence are from above (*epi–*) the specimen). These microscopes have become an important part in the field of biology, opening the doors for more advanced microscope designs, such as the confocal microscope and the total internal reflection fluorescence microscope (TIRF).

Fluorophores lose their ability to fluoresce as they are illuminated in a process called photobleaching. Special care must be taken to prevent photobleaching through the use of more robust fluorophores, by minimizing illumination, or by introducing a scavenger system to reduce the rate of photobleaching.

## Epifluorescence microscopy

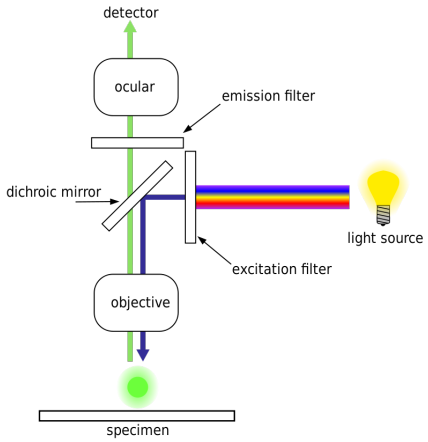


Schematic of a fluorescence microscope.

Epifluorescence microscopy is a method of fluorescence microscopy that is widely used in life sciences. The excitatory light is passed from above (or, for inverted microscopes, from below), through the objective lens and then onto the specimen instead of passing it first through the specimen. The fluorescence in the specimen gives rise to emitted light which is focused to the detector by the same objective that is used for the excitation. Since most of the excitatory light is transmitted through the specimen, only reflected excitatory light reaches the objective together with the emitted light and this method therefore gives an improved signal to noise ratio. An additional filter between the objective and the detector can filter out the remaining excitation light from fluorescent light. A common use in biology is to apply fluorescent or fluorochrome stains to the specimen in order to image distributions of proteins or other molecules of interest.

## Improvements and sub-diffraction techniques

The nature of light limits the size of the spot to which light can be focused. According to the diffraction limit a focused light distribution cannot be made smaller than approximately half of the wavelength of the used light. Uncovered in the 19th century by Ernst Abbe this has been a barrier of the achievable resolution of fluorescence light microscopes for a long time. While resolution is denoted by the ability to discern different objects of the same kind, localizing or tracking of single particles have been performed with a precision much below the diffraction limit.

Several improvements in microscopy techniques have been invented in the 20th century and have resulted in increased resolution and contrast to some extent. However they did not overcome the diffraction limit. In 1978 first theoretical ideas have been developed to break this barrier by using a 4Pi microscope as a confocal laser scanning fluorescence microscope where the light is focused ideally from all sides to a common focus which is used to scan the object by 'point-by-point' excitation combined with 'point-by-point' detection [3] . However, the first experimental demonstration of the 4pi microscope took place in 1994 [4] . The 4Pi microscopy is maximizing the amount of available focusing directions by using two opposing objective lenses or Multi-photon microscopy using redshifted light and multi-photon excitation.

The first technique to really achieve a sub-diffraction resolution was STED microscopy, proposed in 1994. This method and all techniques following the RESOLFT concept rely on a strong non-linear interaction between light and fluorescing molecules. The molecules are driven strongly between distinguishable molecular states at each specific location, so that finally light can be emitted at only a small fraction of space, hence an increased resolution.

As well in the 1990s another super resolution microscopy method based on wide field microscopy has been developed. Substantially improved size resolution of cellular nanostructures stained with a fluorescent marker was achieved by development of SPDM localization microscopy and the structured laser illumination (spatially modulated illumination, SMI) [5] . Combining the principle of SPDM with SMI resulted in the development of the Vertico SMI microscope [6] [7] . Single molecule detection of normal blinking fluorescent dyes like GFP can be achieved by using a further development of SPDM the so-called SPDMphymod technology which makes it possible to detect and count two different fluorescent molecule types at the molecular level (this technology is referred to as 2CLM, 2 Color Localization Microscopy) [8] .

Alternatively, the advent of photoactivated localization microscopy could achieve similar results by relying on blinking or switching of single molecules, where the fraction of fluorescing molecules is very small at each time. This stochastic response of molecules on the applied light corresponds also to a highly nonlinear interaction, leading to subdiffraction resolution.

## Gallery

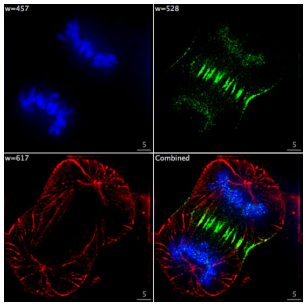


Epifluorescent imaging of the three components in a dividing human cancer cell. DNA is stained blue, a protein called INCENP is green, and the microtubules are red. Each fluorophore is imaged separately using a different combination of excitation and emission filters, and the images are captured sequentially using a digital CCD camera, then overlaid to give a complete image.

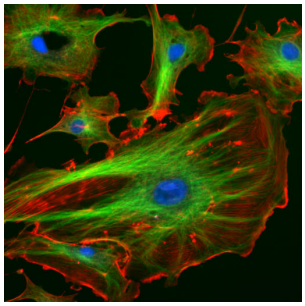

Endothelial cells under the microscope. Nuclei are stained blue with DAPI, microtubules are marked green by an antibody bound to FITC and actin filaments are labeled red with phalloidin bound to TRITC. Bovine pulmonary artery endothelial (BPAE) cells

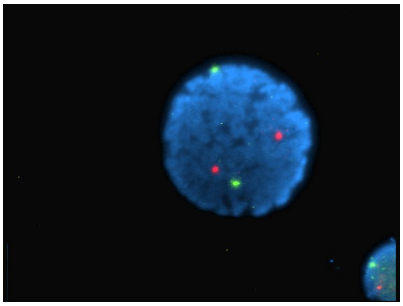

Human lymphocyte nucleus stained with DAPI with chromosome 13 (green) and 21 (red) centromere probes hybridized (Fluorescent in situ hybridization (FISH))

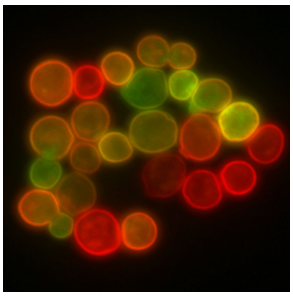

Yeast cell membrane visualized by some membrane proteins fused with RFP and GFP fluorescent markers. Imposition of light from both of markers results in yellow color.

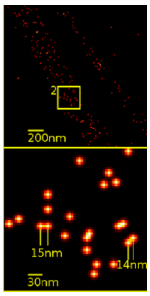


Super Resolution Microscopy: Single YFP molecule detection in a human cancer cell. Typical distance measurements in the 15 nm range (5 nm standard deviation) measured with a Vertico-SMI/SPDMphymod microscope

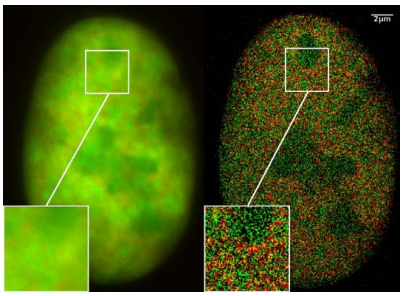


Super Resolution Microscopy: Co-localzation microscopy (2CLM) with GFP and RFP fusion proteins (nucleus of a bone cancer cell) 120.000 localized molecules in a wide-field area (470 $\mu m^2$) measured with a Vertico-SMI/SPDMphymod micrsocpe

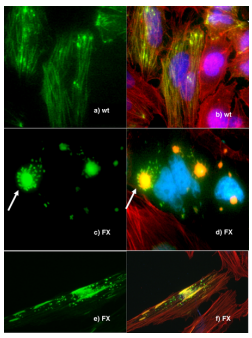


Fluorescence microscopy of DNA Expression in the Human Wild-Type and P239S Mutant Palladin.

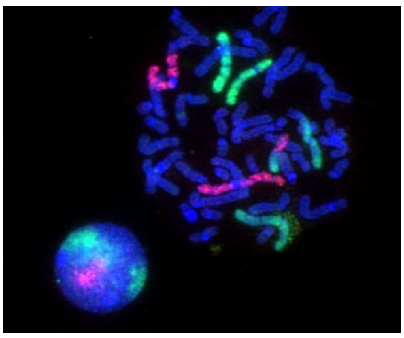

Fluorescence microscopy images of sun flares pathology in a blood cell showing the affected areas in red.

## See also

- Microscope
- Mercury-vapor lamp, Xenon arc lamp
- Stokes shift

## References

[1] Spring KR, Davidson MW. "Introduction to Fluorescence Microscopy" (http://www.microscopyu.com/articles/fluorescence/fluorescenceintro.html). *Nikon MicroscopyU*. . Retrieved 2008-09-28.

[2] "The Fluorescence Microscope" (http://nobelprize.org/educational_games/physics/microscopes/fluorescence/). *Microscopes—Help Scientists Explore Hidden Worlds*. The Nobel Foundation. . Retrieved 2008-09-28.

[3] >Considerations on a laser-scanning-microscope with high resolution and depth of field: C. Cremer and T. Cremer in M1CROSCOPICA ACTA VOL. 81 NUMBER 1 September,pp. 31—44 (1978)

[4] S.W. Hell, E.H.K. Stelzer, S. Lindek, C. Cremer (1994). "Confocal microscopy with an increased detection aperture: type-B 4Pi confocal microscopy" (http://www.opticsinfobase.org/viewmedia.cfm?uri=ol-19-3-222&seq=0). *Optics Letters* **19**: 222–224. doi:10.1364/OL.19.000222. .

[5] M. Hausmann, B. Schneider, J. Bradl, C. Cremer (1997): High-precision distance microscopy of 3D-nanostructures by a spatially modulated excitation fluorescence microscope. In: Optical Biopsies and Microscopic Techniques II (Edts Bigio IJ, Schneckenburger H, Slavik J, Svanberg K, Viallet PM), Proc. SPIE 3197: 217-222

[6] High precision structural analysis of subnuclear complexes in fixed and live cells via Spatially Modulated Illumination (SMI) microscopy: J. Reymann, D. Baddeley, P. Lemmer, W. Stadter, T. Jegou, K. Rippe, C. Cremer, U. Birk in CHROMOSOME RESEARCH, Vol. 16, pp. 367 –382 (2008)

[7] Nano-structure analysis using Spatially Modulated Illumination microscopy: D. Baddeley, C. Batram, Y. Weiland, C. Cremer, U.J. Birk in NATURE PROTOCOLS, Vol 2, pp. 2640 – 2646 (2007)

[8] Manuel Gunkel, Fabian Erdel, Karsten Rippe, Paul Lemmer, Rainer Kaufmann, Christoph Hörmann, Roman Amberger and Christoph Cremer: *Dual color localization microscopy of cellular nanostructures*. In: Biotechnology Journal, 2009, 4, 927-938. ISSN 1860-6768

## External links

- Fluorophores.org (http://www.fluorophores.org) - Database of fluorescent dyes.

# Fluorescence correlation spectroscopy

**Fluorescence correlation spectroscopy** (**FCS**) is a correlation analysis of fluctuation of the fluorescence intensity. The analysis provides parameters of the physics under the fluctuations. One of the interesting applications of this is an analysis of the concentration fluctuations of fluorescent particles (molecules) in solution. In this application, the fluorescence emitted from a very tiny space in solution containing a small number of fluorescent particles (molecules) is observed. The fluorescence intensity is fluctuating due to Brownian motion of the particles. In other words, the number of the particles in the sub-space defined by the optical system is randomly changing around the average number. The analysis gives the average number of fluorescent particles and average diffusion time, when the particle is passing through the space. Eventually, both the concentration and size of the particle (molecule) are determined. Since the method is observing a small number of molecule in a very tiny spot, it is a very sensitive analytical tool. Both parameters are important in biochemical research, biophysics, and chemistry. In contrast to other methods, such as HPLC analysis, FCS has no physical separation process and has a good spatial resolution determined by the optics. These are of great advantage. Moreover, the method enables us to observe fluorescence-tagged molecules in the biochemical pathway in intact living cells. This opens a new area, "in situ or in vivo biochemistry": tracing the biochemical pathway in intact cells and organs.

Commonly, FCS is employed in the context of optical microscopy, in particular confocal or two-photon microscopy. In these techniques light is focused on a sample and the measured fluorescence intensity fluctuations (due to diffusion, physical or chemical reactions, aggregation, etc.) are analyzed using the temporal autocorrelation. Because the measured property is essentially related to the magnitude and/or the amount of fluctuations, there is an optimum measurement regime at the level when individual species enter or exit the observation volume (or turn on and off in the volume). When too many entities are measured at the same time the overall fluctuations are small in comparison to the total signal and may not be resolvable – in the other direction, if the individual fluctuation-events are too sparse in time, one measurement may take prohibitively too long. FCS is in a way the fluorescent counterpart to dynamic light scattering, which uses coherent light scattering, instead of (incoherent) fluorescence.

When an appropriate model is known, FCS can be used to obtain quantitative information such as

- diffusion coefficients
- hydrodynamic radii
- average concentrations
- kinetic chemical reaction rates
- singlet-triplet dynamics

Because fluorescent markers come in a variety of colors and can be specifically bound to a particular molecule (e.g. proteins, polymers, metal-complexes, etc.), it is possible to study the behavior of individual molecules (in rapid succession in composite solutions). With the development of sensitive detectors such as avalanche photodiodes the detection of the fluorescence signal coming from individual molecules in highly dilute samples has become practical. With this emerged the possibility to conduct FCS experiments in a wide variety of specimens, ranging from materials science to biology. The advent of engineered cells with genetically tagged proteins (like green fluorescent protein) has made FCS a common tool for studying molecular dynamics in living cells.

## History

Signal-correlation techniques were first experimentally applied to fluorescence in 1972 by Magde, Elson, and Webb[1] , who are therefore commonly credited as the "inventors" of FCS. The technique was further developed in a group of papers by these and other authors soon after, establishing the theoretical foundations and types of applications.[2] [3] [4] See Thompson (1991)[5] for a review of that period.

Beginning in 1993[6] , a number of improvements in the measurement techniques—notably using confocal microscopy, and then two-photon microscopy—to better define the measurement volume and reject background—greatly improved the signal-to-noise ratio and allowed single molecule sensitivity.[7] [8] Since then, there has been a renewed interest in FCS, and as of August 2007 there have been over 3,000 papers using FCS found in Web of Science. See Krichevsky and Bonnet[9] for a recent review. In addition, there has been a flurry of activity extending FCS in various ways, for instance to laser scanning and spinning-disk confocal microscopy (from a stationary, single point measurement), in using cross-correlation (FCCS) between two fluorescent channels instead of autocorrelation, and in using Förster Resonance Energy Transfer (FRET) instead of fluorescence.

## Typical FCS setup

The typical FCS setup consists of a laser line (wavelengths ranging typically from 405–633 nm (cw), and from 690–1100 nm (pulsed)), which is reflected into a microscope objective by a dichroic mirror. The laser beam is focused in the sample, which contains fluorescent particles (molecules) in such high dilution, that only a few are within the focal spot (usually 1–100 molecules in one fL). When the particles cross the focal volume, they fluoresce. This light is collected by the same objective and, because it is red-shifted with respect to the excitation light it passes the dichroic mirror reaching a detector, typically a photomultiplier tube or avalanche photodiode detector. The resulting electronic signal can be stored either directly as an intensity versus time trace to be analyzed at a later point, or computed to generate the autocorrelation directly (which requires special acquisition cards). The FCS curve by itself only represents a time-spectrum. Conclusions on physical phenomena have to be extracted from there with appropriate models. The parameters of interest are found after fitting the autocorrelation curve to modeled functional forms. [10]

## The measurement volume

The measurement volume is a convolution of illumination (excitation) and detection geometries, which result from the optical elements involved. The resulting volume is described mathematically by the point spread function (or PSF), it is essentially the image of a point source. The PSF is often described as an ellipsoid (with unsharp boundaries) of few hundred nanometers in focus diameter, and almost one micrometre along the optical axis. The shape varies significantly (and has a large impact on the resulting FCS curves) depending on the quality of the optical elements (it is crucial to avoid astigmatism and to check the real shape of the PSF on the instrument). In the case of confocal microscopy, and for small pinholes (around one Airy unit), the PSF is well approximated by Gaussians:

$$PSF(r,z) = I_0 e^{-2r^2/\omega_{xy}^2} e^{-2z^2/\omega_z^2}$$

where $I_0$ is the peak intensity, r and z are radial and axial position, and $\omega_{xy}$ and $\omega_z$ are the radial and axial radii, and $\omega_z > \omega_{xy}$. This Gaussian form is assumed in deriving the functional form of the autocorrelation.

Typically $\omega_{xy}$ is 200–300 nm, and $\omega_z$ is **2–6** times larger.[11] One common way of calibrating the measurement volume parameters is to perform FCS on a species with known diffusion coefficient and concentration (see below). Diffusion coefficients for common fluorophores in water are given in a later section.

The Gaussian approximation works to varying degrees depending on the optical details, and corrections can sometimes be applied to offset the errors in approximation.[12]

## Autocorrelation function

The (temporal) autocorrelation function is the correlation of a time series with itself shifted by time $\tau$, as a function of $\tau$:

$$G(\tau) = \frac{\langle \delta I(t) \delta I(t+\tau) \rangle}{\langle I(t) \rangle^2} = \frac{\langle I(t) I(t+\tau) \rangle}{\langle I(t) \rangle^2} - 1$$

where $\delta I(t) = I(t) - \langle I(t) \rangle$ is the deviation from the mean intensity. The normalization (denominator) here is the most commonly used for FCS, because then the correlation at $\tau =$ (), *G*(0), is related to the average number of particles in the measurement volume.

## Interpreting the autocorrelation function

To extract quantities of interest, the autocorrelation data can be fitted, typically using a nonlinear least squares algorithm. The fit's functional form depends on the type of dynamics (and the optical geometry in question).

### Normal diffusion

The fluorescent particles used in FCS are small and thus experience thermal motions in solution. The simplest FCS experiment is thus normal 3D diffusion, for which the autocorrelation is:

$$G(\tau) = G(0) \frac{1}{(1 + (\tau/\tau_D))(1 + a^{-2}(\tau/\tau_D))^{1/2}} + G(\infty)$$

where $a = \omega_z / \omega_{xy}$ is the ratio of axial to radial $e^{-2}$radii of the measurement volume, and $\tau_D$ is the characteristic residence time. This form was derived assuming a Gaussian measurement volume. Typically, the fit would have three free parameters--G(0), $G(\infty)$, and $\tau_D$--from which the diffusion coefficient and fluorophore concentration can be obtained.
With the normalization used in the previous section, *G*(0) gives the mean number of diffusers in the volume <N>, or equivalently—with knowledge of the observation volume size—the mean concentration:

$$G(0) = \frac{1}{\langle N \rangle} = \frac{1}{V_{\text{eff}} \langle C \rangle},$$

where the effective volume is found from integrating the Gaussian form of the measurement volume and is given by:

$V_{\text{eff}} = \pi^{3/2} \omega_{xy}^2 \omega_z$.

$\tau_D$ gives the diffusion coefficient:

$D = \omega_{xy}^2 / 4\tau_D$.

### Anomalous diffusion

If the diffusing particles are hindered by obstacles or pushed by a force (molecular motors, flow, etc.) the dynamics is often not sufficiently well-described by the normal diffusion model, where the mean squared displacement (MSD) grows linearly with time. Instead the diffusion may be better described as anomalous diffusion, where the temporal dependenc of the MSD is non-linear as in the power-law:

$$MSD = 6 D_a t^{\alpha}$$

where $D_a$ is an anomalous diffusion coefficient. "Anomalous diffusion" commonly refers only to this very generic model, and not the many other possibilities that might be described as anomalous. Also, a power law is, in a strict sense, the expected form only for a narrow range of rigorously defined systems, for instance when the distribution of obstacles is fractal. Nonetheless a power law can be a useful approximation for a wider range of systems.
The FCS autocorrelation function for anomalous diffusion is:

$$G(\tau) = G(0)\frac{1}{(1+(\tau/\tau_D)^{\alpha})(1+a^{-2}(\tau/\tau_D)^{\alpha})^{1/2}} + G(\infty),$$

where the anomalous exponent $\alpha$ is the same as above, and becomes a free parameter in the fitting.

Using FCS, the anomalous exponent has been shown to be an indication of the degree of molecular crowding (it is less than one and smaller for greater degrees of crowding)[13].

## Polydisperse diffusion

If there are diffusing particles with different sizes (diffusion coefficients), it is common to fit to a function that is the sum of single component forms:

$$G(\tau) = G(0)\sum_i \frac{\alpha_i}{(1+(\tau/\tau_{D,i}))(1+a^{-2}(\tau/\tau_{D,i}))^{1/2}} + G(\infty)$$

where the sum is over the number different sizes of particle, indexed by i, and $\alpha_i$ gives the weighting, which is related to the quantum yield and concentration of each type. This introduces new parameters, which makes the fitting more difficult as a higher dimensional space must be searched. Nonlinear least square fitting typically becomes unstable with even a small number of $\tau_{D,i}$s. A more robust fitting scheme, especially useful for polydisperse samples, is the Maximum Entropy Method[14].

## Diffusion with flow

With diffusion together with a uniform flow with velocity $v$ in the lateral direction, the autocorrelation is[15]:

where $\tau_v = \omega_{xy}/v$ is the average residence time if there is only a flow (no diffusion).

## Chemical relaxation

A wide range of possible FCS experiments involve chemical reactions that continually fluctuate from equilibrium because of thermal motions (and then "relax"). In contrast to diffusion, which is also a relaxation process, the fluctuations cause changes between states of different energies. One very simple system showing chemical relaxation would be a stationary binding site in the measurement volume, where particles only produce signal when bound (e.g. by FRET, or if the diffusion time is much faster than the sampling interval). In this case the autocorrelation is:

$$G(\tau) = G(0)\exp(-\tau/\tau_B) + G(\infty)$$

where

$$\tau_B = (k_{\text{on}} + k_{\text{off}})^{-1}$$

is the relaxation time and depends on the reaction kinetics (on and off rates), and:

$$G(0) = \frac{1}{\langle N\rangle}\frac{k_{on}}{k_{off}} = \frac{1}{\langle N\rangle}K$$

is related to the equilibrium constant *K*.

Most systems with chemical relaxation also show measureable diffusion as well, and the autocorrelation function will depend on the details of the system. If the diffusion and chemical reaction are decoupled, the combined autocorrelation is the product of the chemical and diffusive autocorrelations.

## Triplet state correction

The autocorrelations above assume that the fluctuations are not due to changes in the fluorescent properties of the particles. However, for the majority of (bio)organic fluorophores--e.g. green fluorescent protein, rhodamine, Cy3 and Alexa Fluor dyes--some fraction of illuminated particles are excited to a triplet state (or other non-radiative decaying states) and then do not emit photons for a characteristic relaxation time $\tau_F$. Typically $\tau_F$ is on the order of microseconds, which is usually smaller than the dynamics of interest (e.g. $\tau_D$) but large enough to be measured. A

multiplicative term is added to the autocorrelation account for the triplet state. For normal diffusion:

where $F$ is the fraction of particles that have entered the triplet state and $\tau_F$ is the corresponding triplet state relaxation time. If the dynamics of interest are much slower than the triplet state relaxation, the short time component of the autocorrelation can simply be truncated and the triplet term is unnecessary.

## Common fluorescent probes

The fluorescent species used in FCS is typically a biomolecule of interest that has been tagged with a fluorophore (using immunohistochemistry for instance), or is a naked fluorophore that is used to probe some environment of interest (e.g. the cytoskeleton of a cell). The following table gives diffusion coefficients of some common fluorophores in water at room temperature, and their excitation wavelengths.

| Fluorescent dye | $D$ (×10$^{-10}$ m$^2$ s$^{-1}$) | Excitation wavelength (nm) | Reference |
|---|---|---|---|
| Rhodamine 6G | 2.8, 3.0, 4.14 ± 0.05 @ 25.00 °C | 514 | [16], [17], [18] |
| Rhodamine 110 | 2.7 | 488 | [19] |
| Tetramethyl rhodamine | 2.6 | 543 | |
| Cy3 | 2.8 | 543 | |
| Cy5 | 2.5, 3.7 ± 0.15 @ 25.00 °C | 633 | [20], [21] |
| carboxyfluorescein | 3.2 | 488 | |
| Alexa-488 | 1.96,4.35 @ 22.5±0.5 °C | 488 | [22] [23] |
| Atto655-maleimide | 4.07 ± 0.1 @ 25.00 °C | 663 | [24] |
| Atto655-carboxylicacid | 4.26 ± 0.08 @ 25.00 °C | 663 | [25] |
| 2′, 7′-difluorofluorescein (Oregon Green488) | 4.11 ± 0.06 @ 25.00 °C | 498 | [26] |

## Variations of FCS

FCS almost always refers to the single point, single channel, temporal autocorrelation measurement, although the term "fluorescence correlation spectroscopy" out of its historical scientific context implies no such restriction. FCS has been extended in a number of variations by different researchers, with each extension generating another name (usually an acronym).

### Fluorescence cross-correlation spectroscopy (FCCS)

FCS is sometimes used to study molecular interactions using differences in diffusion times (e.g. the product of an association reaction will be larger and thus have larger diffusion times than the reactants individually); however, FCS is relatively insensitive to molecular mass as can be seen from the following equation relating molecular mass to the diffusion time of globular particles (e.g. proteins):

$$\tau_D = \frac{3\pi\omega_{xy}^2\eta}{2kT}(M)^{1/3}$$

where $\eta$ is the viscosity of the sample and $M$ is the molecular mass of the fluorescent species. In practice, the diffusion times need to be sufficiently different--a factor of at least **1.6**--which means the molecular masses must differ by a factor of **4**.[27] Dual color fluorescence cross-correlation spectroscopy (FCCS) measures interactions by cross-correlating two or more fluorescent channels (one channel for each reactant), which distinguishes interactions more sensitively than FCS, particularly when the mass change in the reaction is small.

### Brightness analysis methods (N&B,[28] PCH,[29] FIDA,[30] Cumulant Analysis[31] )

Fluorescence cross correlation spectroscopy overcomes the weak dependence of diffusion rate on molecular mass by looking at multicolor coincidence. What about homo-interactions? The solution lies in brightness analysis. These methods use the heterogeneity in the intensity distribution of fluorescence to measure the molecular brightness of different species in a sample. Since dimers will contain twice the number of fluorescent labels as monomers, their molecular brightness will be approximately double that of monomers. As a result, the relative brightness is sensitive a measure of oligomerization. The average molecular brightness ( $\langle \epsilon \rangle$ ) is related to the variance ( $\sigma^2$) and the average intensity ( $\langle I \rangle$ ) as follows:[32]

$$\langle \varepsilon \rangle = \frac{\sigma^2 - \langle I \rangle}{\langle I \rangle} = \sum_i f_i \varepsilon_i$$

Here $f_i$ and $\epsilon_i$ are the fractional intensity and molecular brigthness, respectively, of species $i$ .

## Two- and three- photon FCS excitation

Several advantages in both spatial resolution and minimizing photodamage/photobleaching in organic and/or biological samples are obtained by two-photon or three-photon excitation FCS[33] [34] [35] [36] [37] .

### FRET-FCS

Another FCS based approach to studying molecular interactions uses fluorescence resonance energy transfer (FRET) instead of fluorescence, and is called FRET-FCS.[38] With FRET, there are two types of probes, as with FCCS; however, there is only one channel and light is only detected when the two probes are very close—close enough to ensure an interaction. The FRET signal is weaker than with fluorescence, but has the advantage that there is only signal during a reaction (aside from autofluorescence).

### Image correlation spectroscopy (ICS)

When the motion is slow (in biology, for example, diffusion in a membrane), getting adequate statistics from a single-point FCS experiment may take a prohibitively long time. More data can be obtained by performing the experiment in multiple spatial points in parallel, using a laser scanning confocal microscope. This approach has been called Image Correlation Spectroscopy (ICS)[39] . The measurements can then be averaged together.

Another variation of ICS performs a spatial autocorrelation on images, which gives information about the concentration of particles[40] . The correlation is then averaged in time.

A natural extension of the temporal and spatial correlation versions is spatio-temporal ICS (STICS) [41] . In STICS there is no explicit averaging in space or time (only the averaging inherent in correlation). In systems with non-isotropic motion (e.g. directed flow, asymmetric diffusion), STICS can extract the directional information. A variation that is closely related to STICS (by the Fourier transform) is *k*-space Image Correlation Spectroscopy (kICS).[42]

There are cross-correlation versions of ICS as well.[39]

### Scanning FCS variations

Some variations of FCS are only applicable to serial scanning laser microscopes. Image Correlation Spectroscopy and its variations all were implemented on a scanning confocal or scanning two photon microscope, but transfer to other microscopes, like a spinning disk confocal microscope. Raster ICS (RICS)[43] , and position sensitive FCS (PSFCS)[44] incorporate the time delay between parts of the image scan into the analysis. Also, low dimensional scans (e.g. a circular ring)[45] —only possible on a scanning system—can access time scales between single point and full image measurements. Scanning path has also been made to adaptively follow particles.[46]

### Spinning disk FCS, and spatial mapping

Any of the image correlation spectroscopy methods can also be performed on a spinning disk confocal microscope, which in practice can obtain faster imaging speeds compared to a laser scanning confocal microscope. This approach has recently been applied to diffusion in a spatially varying complex environment, producing a pixel resolution map of a diffusion coefficient.[47] . The spatial mapping of diffusion with FCS has subsequently been extended to the TIRF system.[48] Spatial mapping of dynamics using correlation techniques had been applied before, but only at sparse points[49] or at coarse resolution[41] .

### Total internal reflection FCS

Total internal reflection fluorescence (TIRF) is a microscopy approach that is only sensitive to a thin layer near the surface of a coverslip, which greatly minimizes background fluorscence. FCS has been extended to that type of microscope, and is called TIR-FCS[50] . Because the fluorescence intensity in TIRF falls off exponentially with distance from the coverslip (instead of as a Gaussian with a confocal), the autocorrelation function is different.

## Other fluorescent dynamical approaches

There are two main non-correlation alternatives to FCS that are widely used to study the dynamics of fluorescent species.

### Fluorescence recovery after photobleaching (FRAP)

In FRAP, a region is briefly exposed to intense light, irrecoverably photobleaching fluorophores, and the fluorescence recovery due to diffusion of nearby (non-bleached) fluorophores is imaged. A primary advantage of FRAP over FCS is the ease of interpreting qualitative experiments common in cell biology. Differences between cell lines, or regions of a cell, or before and after application of drug, can often be characterized by simple inspection of movies. FCS experiments require a level of processing and are more sensitive to potentially confounding influences like: rotational diffusion, vibrations, photobleaching, dependence on illumination and fluorescence color, inadequate statistics, etc. It is much easier to change the measurement volume in FRAP, which allows greater control. In practice, the volumes are typically larger than in FCS. While FRAP experiments are typically more qualitative, some researchers are studying FRAP quantitatively and including binding dynamics.[51] A disadvantage of FRAP in cell biology is the free radical perturbation of the cell caused by the photobleaching. It is also less versatile, as it cannot measure concentration or rotational diffusion, or co-localization. FRAP requires a significantly higher concentration of fluorophores than FCS.

### Particle tracking

In particle tracking, the trajectories of a set of particles are measured, typically by applying particle tracking algorithms to movies.[52] Particle tracking has the advantage that all the dynamical information is maintained in the measurement, unlike FCS where correlation averages the dynamics to a single smooth curve. The advantage is apparent in systems showing complex diffusion, where directly computing the mean squared displacement allows straightforward comparison to normal or power law diffusion. To apply particle tracking, the particles have to be distinguishable and thus at lower concentration than required of FCS. Also, particle tracking is more sensitive to noise, which can sometimes affect the results unpredictably.

## See also

- Confocal microscopy
- Fluorescence cross-correlation spectroscopy,FCCS
- FRET
- Dynamic light scattering
- Diffusion coefficient

## References


[1] Magde, D., Elson, E. L., Webb, W. W. Thermodynamic fluctuations in a reacting system: Measurement by fluorescence correlation spectroscopy,(1972) *Phys Rev Lett*, **29**, 705–708.

[2] Ehrenberg, M., Rigler, R. Rotational brownian motion and fluorescence intensity fluctuations,(1974) *Chem Phys*, **4**, 390–401.

[3] Elson, E. L., Magde, D. Fluorescence correlation spectroscopy I. Conceptual basis and theory,(1974) *Biopolymers*, **13**, 1–27.

[4] Magde, D., Elson, E. L., Webb, W. W. Fluorescence correlation spectroscopy II. An experimental realization,(1974) *Biopolymers*, **13**, 29–61.

[5] Thompson N L 1991 Topics in Fluorescence Spectroscopy Techniques vol 1, ed J R Lakowicz (New York: Plenum) pp 337–78

[6] Rigler, R, Ü. Mets1, J. Widengren and P. Kask. Fluorescence correlation spectroscopy with high count rate and low background: analysis of translational diffusion. European Biophysics Journal (1993) 22(3), 159.

[7] Eigen, M., Rigler, M. Sorting single molecules: application to diagnostics and evolutionary biotechnology,(1994) *Proc. Natl. Acad. Sci. USA*, **91**,5740–5747.

[8] Rigler, M. Fluorescence correlations, single molecule detection and large number screening. Applications in biotechnology,(1995) *J. Biotechnol.*, **41**,177–186.

[9] O. Krichevsky, G. Bonnet, "Fluorescence correlation spectroscopy: the technique and its applications," Rep. Prog. Phys. 65, 251–297 (2002).

[10] Medina, M. A., Schwille, P. Fluorescence correlation spectroscopy for the detection and study of single molecules in biology, (2002)*BioEssays*, **24**, 758–764.

[11] Mayboroda, O. A., van Remoortere, A., Tanke H. J., Hokke, C. H., Deelder, A. M., A new approach for fluorescence correlation spectroscopy (FCS) based immunoassays, (2003), *J. Biotechnol.*, **107**, 185–192.

[12] Hess, S.T., and W.W. Webb. 2002. Focal volume optics and experimental artifacts in confocal fluorescence correlation spectroscopy. Biophys. J. 83:2300–2317.

[13] Banks, D. S., and C. Fradin. 2005. Anomalous diffusion of proteins due to molecular crowding. Biophys. J. 89:2960–2971.

[14] Sengupta, P., K. Garai, J. Balaji, N. Periasamy, and S. Maiti. 2003. Measuring Size Distribution in Highly Heterogeneous Systems with Fluorescence Correlation Spectroscopy. Biophys. J. 84(3):1977–1984.

[15] Kohler, R.H., P. Schwille, W.W. Webb, and M.R. Hanson. 2000. Active protein transport through plastid tubules: velocity quantified by fluorescence correlation spectroscopy. J Cell Sci 113(22):3921–3930

[16] Magde, D., Elson, E. L., Webb, W. W. Fluorescence correlation spectroscopy II. An experimental realization,(1974) *Biopolymers*, **13**,29–61.

[17] Berland, K. M. Detection of specific DNA sequences using dual-color two-photon fluorescence correlation spectroscopy. (2004),*J. Biotechnol* ,**108(2)**, 127–136.

[18] Müller, C.B., Loman, A., Pacheco, V., Koberling, F., Willbold, D., Richtering, W., Enderlein, J. Precise measurement of diffusion by multi-color dual-focus fluorescence correlation spectroscopy (2008), *EPL*, **83**, 46001.

[19] Pristinski, D., Kozlovskaya, V., Sukhishvili, S. A. Fluorescence correlation spectroscopy studies of diffusion of a weak polyelectrolyte in aqueous solutions. (2005), *J. Chem. Phys.*, **122**, 014907.

[20] Widengren, J., Schwille, P., Characterization of photoinduced isomerization and back-isomerization of the cyanine dye Cy5 by fluorescence correlation spectroscopy. (2000), *J. Phys. Chem. A*, **104**, 6416–6428.

[21] Loman, A., Dertinger, T., Koberling, F., Enderlein, J. Comparison of optical saturation effects in conventional and dual-focus fluorescence correlation spectroscopy (2008), *Chem. Phys. Lett.*, **459**, 18–21.

[22] Pristinski, D., Kozlovskaya, V., Sukhishvili, S. A. Fluorescence correlation spectroscopy studies of diffusion of a weak polyelectrolyte in aqueous solutions. (2005), *J. Chem. Phys.*, **122**, 014907.

[23] Petráaek, Z. k.; Schwille, P., Precise Measurement of Diffusion Coefficients using Scanning Fluorescence Correlation Spectroscopy. Biophys. J. 2008, 94 (4), 1437-1448.

[24] Müller, C.B., Loman, A., Pacheco, V., Koberling, F., Willbold, D., Richtering, W., Enderlein, J. Precise measurement of diffusion by multi-color dual-focus fluorescence correlation spectroscopy (2008), *EPL*, **83**, 46001.

[25] Müller, C.B., Loman, A., Pacheco, V., Koberling, F., Willbold, D., Richtering, W., Enderlein, J. Precise measurement of diffusion by multi-color dual-focus fluorescence correlation spectroscopy (2008), *EPL*, **83**, 46001.

[26] Müller, C.B., Loman, A., Pacheco, V., Koberling, F., Willbold, D., Richtering, W., Enderlein, J. Precise measurement of diffusion by multi-color dual-focus fluorescence correlation spectroscopy (2008), *EPL*, **83**, 46001.

[27] Meseth, U., Wohland, T., Rigler, R., Vogel, H. Resolution of fluorescence correlation measurements. (1999) *Biophys. J.*, **76**, 1619–1631.

[28] Digman, M. A., R. Dalal, A. F. Horwitz, and E. Gratton. Mapping the number of molecules and brightness in the laser scanning microscope. (2008) *Biophys. J.* **94**, 2320–2332.

[29] Chen, Y., J. D. Müller, P. T. C. So, and E. Gratton. The photon counting histogram in fluorescence fluctuation spectroscopy. (1999) *Biophys. J.* **77**, 553–567.

[30] Kask, P., K. Palo, D. Ullmann, and K. Gall. Fluorescence-intensity distribution analysis and its application in biomolecular detection technology. (1999) *Proc. Natl. Acad. Sci. U. S. A.* **96**, 13756–13761.

[31] Müller, J. D. Cumulant analysis in fluorescence fluctuation spectroscopy. (2004) *Biophys. J.* **86**, 3981–3992.

[32] Qian, H., Elson, E.L. On the analysis of high order moments of fluorescence fluctuations. (1990) *Biophys. J.*, **57**, 375–380.

[33] Diaspro, A., and Robello, M. (1999). Multi-photon Excitation Microscopy to Study Biosystems. European Microscopy and Analysis., 5:5–7.

[34] Bagatolli, L.A., and Gratton, E. (2000). Two-photon fluorescence microscopy of coexisting lipid domains in giant unilamellar vesicles of binary phospholipid mixtures. Biophys J., 78:290–305.

[35] Schwille, P., Haupts, U., Maiti, S., and Webb. W.(1999). Molecular dynamics in living cells observed by fluorescence correlation spectroscopy with one- and two- photon excitation. *Biophysical Journal*, **77**(10):2251–2265.

[36] Near Infrared Microspectroscopy, Fluorescence Microspectroscopy,Infrared Chemical Imaging and High Resolution Nuclear Magnetic Resonance Analysis of Soybean Seeds, Somatic Embryos and Single Cells., Baianu, I.C. et al. 2004., In *Oil Extraction and Analysis.*, D. Luthria, Editor pp.241–273, AOCS Press., Champaign, IL.

[37] Single Cancer Cell Detection by Near Infrared Microspectroscopy, Infrared Chemical Imaging and Fluorescence Microspectroscopy.2004.I. C. Baianu, D. Costescu, N. E. Hofmann and S. S. Korban, q-bio/0407006 (July 2004) (http://arxiv.org/abs/q-bio/0407006)

[38] K. Remaut, B. Lucas, K. Braeckmans, N.N. Sanders, S.C. De Smedt and J. Demeester, FRET-FCS as a tool to evaluate the stability of oligonucleotide drugs after intracellular delivery, J Control Rel 103 (2005) (1), pp. 259–271.

[39] Wiseman, P. W., J. A. Squier, M. H. Ellisman, and K. R. Wilson. 2000. Two-photon video rate image correlation spectroscopy (ICS) and image cross-correlation spectroscopy (ICCS). J. Microsc. 200:14–25.

[40] Petersen, N. O., P. L. Ho¨ddelius, P. W. Wiseman, O. Seger, and K. E. Magnusson. 1993. Quantitation of membrane receptor distributions by image correlation spectroscopy: concept and application. Biophys. J. 65:1135–1146. (http://dx.doi.org/10.1016/S0006-3495(93)81173-1)

[41] Hebert, B., S. Constantino, and P. W. Wiseman. 2005. Spatio-temporal image correlation spectroscopy (STICS): theory, verification and application to protein velocity mapping in living CHO cells. Biophys. J. 88:3601–3614. (http://dx.doi.org/10.1529/biophysj.104.054874)

[42] Kolin, D.L., D. Ronis, and P.W. Wiseman. 2006. *k*-Space Image Correlation Spectroscopy: A Method for Accurate Transport Measurements Independent of Fluorophore Photophysics. Biophys. J. 91(8):3061–3075. (http://dx.doi.org/10.1529/biophysj.106.082768)

[43] Digman, M.A., P. Sengupta, P.W. Wiseman, C.M. Brown, A.R. Horwitz, and E. Gratton. 2005. Fluctuation Correlation Spectroscopy with a Laser-Scanning Microscope: Exploiting the Hidden Time Structure. Biophys. J. 88(5):L33–36.

[44] Skinner, J.P., Y. Chen, and J.D. Mueller. 2005. Position-Sensitive Scanning Fluorescence Correlation Spectroscopy. Biophys. J.:biophysj.105.060749. (http://dx.doi.org/10.1529/biophysj.105.060749)

[45] Ruan, Q., M.A. Cheng, M. Levi, E. Gratton, and W.W. Mantulin. 2004. Spatial-temporal studies of membrane dynamics: scanning fluorescence correlation spectroscopy (SFCS). Biophys. J. 87:1260–1267.

[46] A. Berglund and H. Mabuchi, "Tracking-FCS: Fluorescence correlation spectroscopy of individual particles," Opt. Express 13, 8069–8082 (2005).

[47] Sisan, D.R., R. Arevalo, C. Graves, R. McAllister, and J.S. Urbach. 2006. Spatially resolved fluorescence correlation spectroscopy using a spinning disk confocal microscope. Biophysical Journal 91(11):4241–4252. (http://dx.doi.org/10.1529/biophysj.106.084251)

[48] Kannan, B., L. Guo, T. Sudhaharan, S. Ahmed, I. Maruyama, and T. Wohland. 2007. Spatially resolved total internal reflection fluorescence correlation microscopy using an electron multiplying charge-coupled device camera. Analytical Chemistry 79(12):4463–4470

[49] Wachsmuth, M., W. Waldeck, and J. Langowski. 2000. Anomalous diffusion of fluorescent probes inside living cell nuclei investigated by spatially-resolved fluorescence correlation spectroscopy. J. Mol. Biol. 298(4):677–689.

[50] Lieto, A.M., and N.L. Thompson. 2004. Total Internal Reflection with Fluorescence Correlation Spectroscopy: Nonfluorescent Competitors. Biophys. J. 87(2):1268–1278.

[51] Sprague, B.L., and J.G. McNally. 2005. FRAP analysis of binding: proper and fitting. Trends in Cell Biology 15(2):84–91.

[52] http://www.physics.emory.edu/~weeks/idl/

## Further reading


- Rigler R. and Widengren J. (1990). Ultrasensitive detection of single molecules by fluorescence correlation spectroscopy, *BioScience* (Ed. Klinge & Owman) p.180
- Oehlenschläger F., Schwille P. and Eigen M. (1996). Detection of HIV-1 RNA by nucleic acid sequence-based amplification combined with fluorescence correlation spectroscopy, *Proc. Natl. Acad. Sci. USA* **93**:1281.


## External links

- Single-molecule spectroscopic methods (http://dx.doi.org/10.1016/j.sbi.2004.09.004)
- FCS Classroom (http://www.fcsxpert.com/classroom)
- Stowers Institute FCS Tutorial (http://research.stowers-institute.org/microscopy/external/Technology/FCS/index.htm)
- Cell Migration Consortium FCS Tutorial (http://www.cellmigration.org/resource/imaging/imaging_approaches_correlation_microscopy.shtml)

# Fluorescence cross-correlation spectroscopy

**Fluorescence cross-correlation spectroscopy** (FCCS) was introduced by Eigen and Rigler in 1994 and experimentally realized by Schwille in 1997. It extends the fluorescence correlation spectroscopy (FCS) procedure by introducing high sensitivity for distinguishing fluorescent particles which have a similar diffusion coefficient. FCCS uses two species which are independently labelled with two spectrally separated fluorescent probes. These fluorescent probes are excited and detected by two different laser light sources and detectors commonly known as green and red respectively. Both laser light beams are focused into the sample and tuned so that they overlap to form a superimposed confocal observation volume.

The normalized cross-correlation function is defined for two fluorescent species $G$ and $R$ which are independent green, G and red, R channels as follows:

where differential fluorescent signals $\delta I_G$ at a specific time, $t$ and $\delta I_R$ at a delay time, $\tau$ later is correlated with each other.

## Modeling

Cross-correlation curves are modeled according to a slightly more complicated mathematical function than applied in FCS. First of all, the effective superimposed observation volume in which the G and R channels form a single observation volume, $V_{eff,RG}$ in the solution:

$$V_{eff,RG} = \pi^{3/2}(\omega_{xy,G}^2 + \omega_{xy,R}^2)(\omega_{z,G}^2 + \omega_{z,R}^2)^{1/2}/2^{3/2}$$

where $\omega_{xy,G}^2$ and $\omega_{xy,R}^2$ are radial parameters and $\omega_{z,G}$ and $\omega_{z,R}$ are the axial parameters for the G and R channels respectively.
The diffusion time, $\tau_{D,GR}$ for a doubly (G and R) fluorescent species is therefore described as follows:

$$\tau_{D,GR} = \frac{\omega_{xy,G}^2 + \omega_{xy,R}^2}{8D_{GR}}$$

where $D_{GR}$ is the diffusion coefficient of the doubly fluorescent particle.

The cross-correlation curve generated from diffusing doubly labelled fluorescent particles can be modelled in separate channels as follows:

$$G_G(\tau) = 1 + \frac{(< C_G > Diff_k(\tau) + < C_{GR} > Diff_k(\tau))}{V_{eff,GR}(< C_G > + < C_{GR} >)^2}$$

$$G_R(\tau) = 1 + \frac{(< C_R > Diff_k(\tau) + < C_{GR} > Diff_k(\tau))}{V_{eff,GR}(< C_R > + < C_{GR} >)^2}$$

In the ideal case, the cross-correlation function is proportional to the concentration of the doubly labeled fluorescent complex:

with $Diff_k(\tau) = \frac{1}{(1+\frac{\tau}{\tau_{D,i}})(1+a^{-2}(\frac{\tau}{\tau_{D,i}})^{1/2}}$

Contrary to FCS, the intercept of the cross-correlation curve does not yield information about the doubly labelled fluorescent particles in solution.

## See also

- Fluorescence correlation spectroscopy
- Dynamic light scattering
- Fluorescence spectroscopy
- Diffusion coefficient

## External links

- FCS Classroom [1]

## References

[1] http://www.fcsxpert.com/classroom

# Circular dichroism

First pioneered by Jean-Baptiste Biot, Augustin Fresnel, and Aimé Cotton [1] , **circular dichroism (CD)** refers to the differential absorption of left and right circularly polarized light.[2] [3] . This phenomenon is exhibited in the absorption bands of optically active chiral molecules. CD spectroscopy has a wide range of applications in many different fields. Most notably, UV CD is used to investigate the secondary structure of proteins[4] . UV/Vis CD is used to investigate charge-transfer transitions [5] . Near-infrared CD is used to investigate geometric and electronic structure by probing metal d→d transitions[6] . Vibrational circular dichroism, which uses light from the infrared energy region, is used for structural studies of small organic molecules, and most recently proteins and DNA[7] .

## Physical Principles

### Circular polarization of light

Electromagnetic radiation consists of an electric and magnetic field that oscillate perpendicular to one another and to the propagating direction [8] . While linearly polarized light occurs when the electric field vector oscillates only in one plane and changes in magnitude, circularly polarized light occurs when the electric field vector rotates about its propagation direction and retains constant magnitude. Hence, it forms a helix in space while propagating. For left circularly polarized light (LCP) with propagation towards the observer, the electric vector rotates counterclockwise[9] . For right circularly polarized light (RCP), the electric vector rotates clockwise.

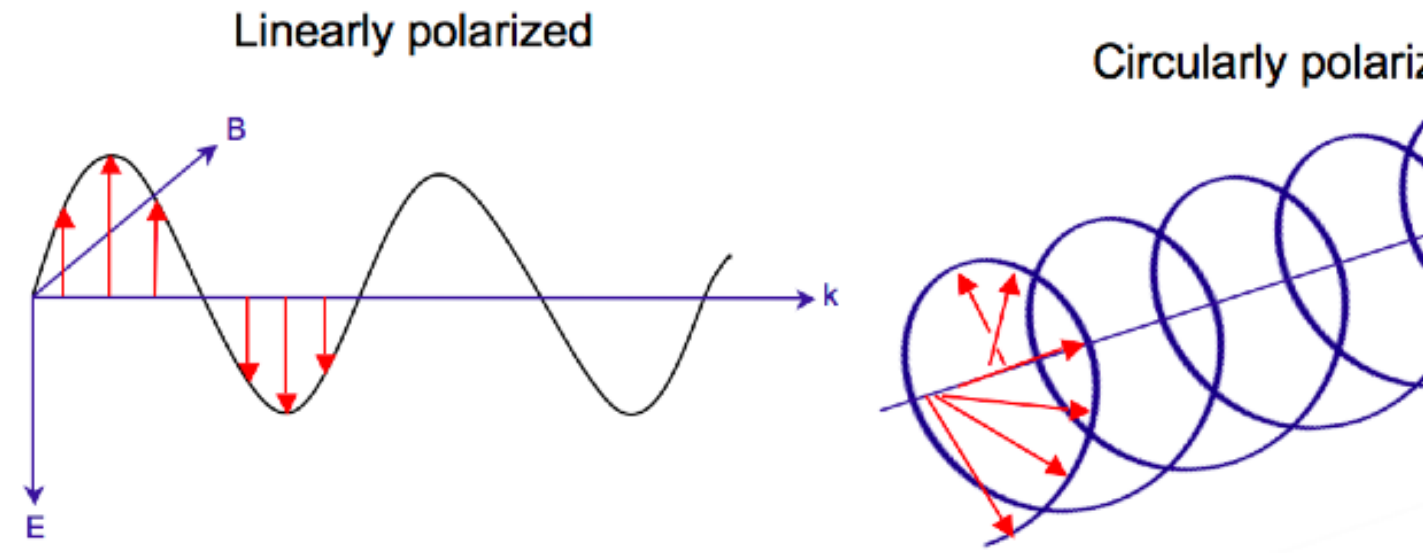


## Interaction of circularly polarized light with matter

When circularly polarized light passes through an absorbing optically active medium, the speeds between right and left polarizations differ ($c_L \neq c_R$) as well as their wavelength ($\lambda_L \neq \lambda_R$) and the extent to which they are absorbed ($\varepsilon_L \neq \varepsilon_R$). *Circular dichroism* is the difference $\Delta\varepsilon \equiv \varepsilon_L - \varepsilon_R$ [10] . The electric field of a light beam causes a linear displacement of charge when interacting with a molecule (electric dipole), whereas the magnetic field of it causes a circulation of charge (magnetic dipole). These two motions combined cause an excitation of an electron in a helical motion, which includes translation and rotation and their associated operators. The experimentally determined relationship between the rotational strength (R) of a sample and the Δε is given by

$$R_{exp} = \frac{3hc10^3 ln(10)}{32\pi^3 N_A} \int \frac{\Delta\epsilon}{\nu} d\nu$$

The rotational strength has also been determined theoretically,

We see from these two equations that in order to have non-zero $\triangle\epsilon$, the electric and magnetic dipole moment operators ( $\widehat{M}_{(elec.dipole)}$and $\widehat{M}_{(mag.dipole)}$) must transform as the same irreducible representation. $C_n$and $D_n$ are the only point groups where this can occur, making only chiral molecules CD active.

Simply put, since circularly polarized light itself is "chiral", it interacts differently with chiral molecules. That is, the two types of circularly polarized light are absorbed to different extents. In a CD experiment, equal amounts of left and right circularly polarized light of a selected wavelength are alternately radiated into a (chiral) sample. One of the two polarizations is absorbed more than the other one, and this wavelength-dependent difference of absorption is measured, yielding the CD spectrum of the sample. Due to the interaction with the molecule, the electric field vector of the light traces out an elliptical path after passing through the sample.

### Delta absorbance

By definition,

$$\Delta A = A_L - A_R$$

where ΔA (Delta Absorbance) is the difference between absorbance of left circularly polarized (LCP) and right circularly polarized (RCP) light (this is what is usually measured). ΔA is a function of wavelength, so for a measurement to be meaningful the wavelength at which it was performed must be known.

### Molar circular dichroism

It can also be expressed, by applying Beer's law, as:

$$\Delta A = (\epsilon_L - \epsilon_R)Cl$$

where

$\varepsilon_L$ and $\varepsilon_R$ are the molar extinction coefficients for LCP and RCP light,

$C$ is the molar concentration

$l$ is the path length in centimeters (cm).

Then

$$\Delta\epsilon = \epsilon_L - \epsilon_R$$

is the molar circular dichroism. This intrinsic property is what is usually meant by the circular dichroism of the substance. Since $\Delta\epsilon$ is a function of wavelength, a molar circular dichroism value ( $\Delta\epsilon$ ) must specify the wavelength at which it is valid.

### Extrinsic effects on circular dichroism

In many practical applications of circular dichroism (CD), as discussed below, the measured CD is not simply an intrinsic property of the molecule, but rather depends on the molecular conformation. In such a case the CD may also be a function of temperature, concentration, and the chemical environment, including solvents. In this case the reported CD value must also specify these other relevant factors in order to be meaningful.

### Molar ellipticity

Although ΔA is usually measured, for historical reasons most measurements are reported in degrees of ellipticity. Molar circular dichroism and molar ellipticity, [$\theta$], are readily interconverted by the equation:

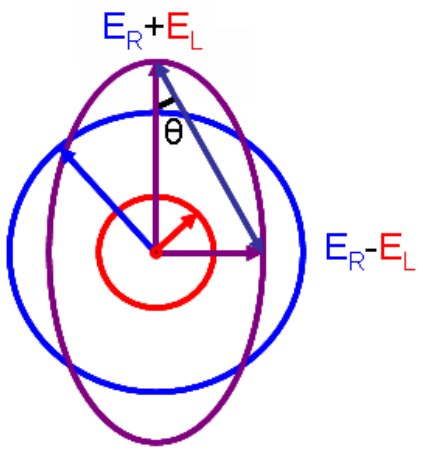


Elliptical polarized light (purple) is composed of unequal contributions of right (blue) and left (red) circular polarized light.

$$[\theta] = 3298.2\,\Delta\varepsilon.$$

This relationship is derived by defining the ellipticity of the polarization as:

$$\tan\theta = \frac{E_R - E_L}{E_R + E_L}$$

where

$E_R$ and $E_L$ are the magnitudes of the electric field vectors of the right-circularly and left-circularly polarized light, respectively.

When $E_R$ equals $E_L$ (when there is no difference in the absorbance of right- and left-circular polarized light), θ is 0° and the light is linearly polarized. When either $E_R$ or $E_L$ is equal to zero (when there is complete absorbance of the circular polarized light in one direction), θ is 45° and the light is circularly polarized.

Generally, the circular dichroism effect is small, so tanθ is small and can be approximated as θ in radians. Since the intensity or irradiance, I, of light is proportional to the square of the electric-field vector, the ellipticity becomes:

$$\theta(\text{radians}) = \frac{(I_R^{1/2} - I_L^{1/2})}{(I_R^{1/2} + I_L^{1/2})}$$

Then by substituting for I using Beer's law in natural logarithm form:

$$I = I_0 e^{-A \ln 10}$$

The ellipticity can now be written as:

$$\theta(\text{radians}) = \frac{(e^{\frac{-A_R}{2}\ln 10} - e^{\frac{-A_L}{2}\ln 10})}{(e^{\frac{-A_R}{2}\ln 10} + e^{\frac{-A_L}{2}\ln 10})} = \frac{e^{\Delta A \frac{\ln 10}{2}} - 1}{e^{\Delta A \frac{\ln 10}{2}} + 1}$$

Since $\Delta A << 1$, this expression can be approximated by expanding the exponentials in a Taylor series to first-order and then discarding terms of ΔA in comparison with unity and converting from radians to degrees:

$$\theta(\text{degrees}) = \Delta A \left(\frac{\ln 10}{4}\right)\left(\frac{180}{\pi}\right)$$

The linear dependence of solute concentration and pathlength is removed by defining molar ellipticity as,

$$[\theta] = \frac{100\theta}{\text{Cl}}$$

Then combining the last two expression with Beer's law, molar ellipticity becomes:

$$[\theta] = 100\,\Delta\varepsilon \left(\frac{\ln 10}{4}\right)\left(\frac{180}{\pi}\right) = 3298.2\,\Delta\varepsilon$$

**Mean residue ellipticity**

Methods for estimating secondary structure in polymers, proteins and polypeptides in particular, often require that the measured molar ellipticity spectrum be converted to a normalized value, specifically a value independent of the polymer length. Mean residue ellipticity is used for this purpose; it is simply the measured molar ellipticity of the molecule divided by the number of monomer units (residues) in the molecule.

## Application to biological molecules

In general, this phenomenon will be exhibited in absorption bands of any optically active molecule. As a consequence, circular dichroism is exhibited by biological molecules, because of their dextrorotary and levorotary components. Even more important is that a secondary structure will also impart a distinct CD to its respective molecules. Therefore, the alpha helix of proteins and the double helix of nucleic acids have CD spectral signatures representative of their structures. The capacity of CD to give a representative structural signature makes it a powerful tool in modern biochemistry with applications that can be found in virtually every field of study.

CD is closely related to the optical rotatory dispersion (ORD) technique, and is generally considered to be more advanced. CD is measured in or near the absorption bands of the molecule of interest, while ORD can be measured far from these bands. CD's advantage is apparent in the data analysis. Structural elements are more clearly distinguished since their recorded bands do not overlap extensively at particular wavelengths as they do in ORD. In principle these two spectral measurements can be interconverted through an integral transform (Kramers–Kronig

relation), if all the absorptions are included in the measurements.

The far-UV (ultraviolet) CD spectrum of proteins can reveal important characteristics of their secondary structure. CD spectra can be readily used to estimate the fraction of a molecule that is in the alpha-helix conformation, the beta-sheet conformation, the beta-turn conformation, or some other (e.g. random coil) conformation.[11] [12] These fractional assignments place important constraints on the possible secondary conformations that the protein can be in. CD cannot, in general, say where the alpha helices that are detected are located within the molecule or even completely predict how many there are. Despite this, CD is a valuable tool, especially for showing changes in conformation. It can, for instance, be used to study how the secondary structure of a molecule changes as a function of temperature or of the concentration of denaturing agents, e.g. Guanidinium hydrochloride or urea. In this way it can reveal important thermodynamic information about the molecule (such as the enthalpy and Gibbs free energy of denaturation) that cannot otherwise be easily obtained. Anyone attempting to study a protein will find CD a valuable tool for verifying that the protein is in its native conformation before undertaking extensive and/or expensive experiments with it. Also, there are a number of other uses for CD spectroscopy in protein chemistry not related to alpha-helix fraction estimation.

The near-UV CD spectrum (>250 nm) of proteins provides information on the tertiary structure. The signals obtained in the 250-300 nm region are due to the absorption, dipole orientation and the nature of the surrounding environment of the phenylalanine, tyrosine, cysteine (or S-S disulfide bridges) and tryptophan amino acids. Unlike in far-UV CD, the near-UV CD spectrum cannot be assigned to any particular 3D structure. Rather, near-UV CD spectra provide structural information on the nature of the prosthetic groups in proteins, e.g., the heme groups in hemoglobin and cytochrome c.

Visible CD spectroscopy is a very powerful technique to study metal–protein interactions and can resolve individual d-d electronic transitions as separate bands. CD spectra in the visible light region are only produced when a metal ion is in a chiral environment, thus, free metal ions in solution are not detected. This has the advantage of only observing the protein-bound metal, so pH dependence and stoichiometries are readily obtained. Optical activity in transition metal ion complexes have been attributed to configurational, conformational and the vicinal effects. Klewpatinond and Viles (2007) have produced a set of empirical rules for predicting the appearance of visible CD spectra for $Cu^{2+}$ and $Ni^{2+}$ square-planar complexes involving histidine and main-chain coordination.

CD gives less specific structural information than X-ray crystallography and protein NMR spectroscopy, for example, which both give atomic resolution data. However, CD spectroscopy is a quick method that does not require large amounts of proteins or extensive data processing. Thus CD can be used to survey a large number of solvent conditions, varying temperature, pH, salinity, and the presence of various cofactors.

CD spectroscopy is usually used to study proteins in solution, and thus it complements methods that study the solid state. This is also a limitation, in that many proteins are embedded in membranes in their native state, and solutions containing membrane structures are often strongly scattering. CD is sometimes measured in thin films.

## Experimental limitations

CD has also been studied in carbohydrates, but with limited success due to the experimental difficulties associated with measurement of CD spectra in the vacuum ultraviolet (VUV) region of the spectrum (100-200 nm), where the corresponding CD bands of unsubstituted carbohydrates lie. Substituted carbohydrates with bands above the VUV region have been successfully measured.

Measurement of CD is also complicated by the fact that typical aqueous buffer systems often absorb in the range where structural features exhibit differential absorption of circularly polarized light. Phosphate, sulfate, carbonate, and acetate buffers are generally incompatible with CD unless made extremely dilute e.g. in the 10-50 mM range. The TRIS buffer system should be completely avoided when performing far-UV CD. Borate and Onium compounds are often used to establish the appropriate pH range for CD experiments. Some experimenters have substituted fluoride for chloride ion because fluoride absorbs less in the far UV, and some have worked in pure water. Another,

almost universal, technique is to minimize solvent absorption by using shorter path length cells when working in the far UV, 0.1 mm path lengths are not uncommon in this work.

In addition to measuring in aqueous systems, CD, particularly far-UV CD, can be measured in organic solvents e.g. ethanol, methanol, trifluoroethanol (TFE). The latter has the advantage to induce structure formation of proteins, inducing beta-sheets in some and alpha helices in others, which they would not show under normal aqueous conditions. Most common organic solvents such as acetonitrile, THF, chloroform, dichloromethane are however, incompatible with far-UV CD.

It may be of interest to note that the protein CD spectra used in secondary structure estimation are related to the π to π*orbital absorptions of the amide bonds linking the amino acids. These absorption bands lie partly in the *so-called* vacuum ultraviolet (wavelengths less than about 200 nm). The wavelength region of interest is actually inaccessible in **air** because of the strong absorption of light by oxygen at these wavelengths. In practice these spectra are measured not in vacuum but in an oxygen-free instrument (filled with pure nitrogen gas).

Once oxygen has been eliminated, perhaps the second most important technical factor in working below 200 nm is to design the rest of the optical system to have low losses in this region. Critical in this regard is the use of aluminized mirrors whose coatings have been optimized for low loss in this region of the spectrum.

The usual light source in these instruments is a high pressure, short-arc xenon lamp. Ordinary xenon arc lamps are unsuitable for use in the low UV. Instead, specially constructed lamps with envelopes made from high-purity synthetic fused silica must be used.

Light from synchrotron sources has a much higher flux at short wavelengths, and has been used to record CD down to 160 nm. Recently the CD spectrometer at the electron storage ring facility ISA at the University of Aarhus in Denmark was used to record solid state CD spectra down to 120 nm.[13] At the quantum mechanical level, the information content of circular dichroism and optical rotation are identical.

## See also

- Circular polarization in nature
- Dichroism
- Linear dichroism
- Magnetic circular dichroism
- Optical activity
- Optical isomerism
- Optical rotation
- Optical rotatory dispersion
- Vibrational circular dichroism

## References

[1] G. D. Fasman (1996). Plenum Press. p. 3.
[2] P. Atkins and J. de Paula (2005). *Elements of Physical Chemistry, 4th ed.*. Oxford University Press.
[3] E. I. Solomon and A. B. P. Lever (2006). **1**. Wiley. p. 78.
[4] R. W. Woody (1994). K. Nakanishi, N. Berova, R. W. Woody. ed. VCH Publishers, Inc.. p. 473.
[5] Solomon, Neidig; A. T. Wecksler, G. Schenk, and T. R. Holman (2007). "Kinetic and Spectroscopic Studies of N694C Lipoxygenase: A Probe of the Substrate Activation Mechanism of a Nonheme Ferric Enzyme" (http://www.pubmedcentral.nih.gov/articlerender.fcgi?tool=pmcentrez&artid=2896304). *JACS* **129** (24): 7531–7537. doi:10.1021/ja068503d. PMID 17523638. PMC 2896304.
[6] E. I. Solomon and A. B. P. Lever (2006). **1**. Wiley. p. 78.
[7] K. Nakanishi, N. Berova, R. W. Woody, ed (1994). VCH Publishers, Inc..
[8] A. Rodger and B. Norden (1997). *Circular Dichroism and Linear Dichroism*. Oxford University Press.
[9] E. I. Solomon and A. B. P. Lever (2006). **1**. Wiley. p. 78.
[10] Woody,R.W.1994

[11] Whitmore L, Wallace BA (2008). "Protein secondary structure analyses from circular dichroism spectroscopy: methods and reference databases". *Biopolymers* **89** (5): 392–400. doi:10.1002/bip.20853. PMID 17896349.

[12] Greenfield NJ (2006). "Using circular dichroism spectra to estimate protein secondary structure" (http://www.pubmedcentral.nih.gov/articlerender.fcgi?tool=pmcentrez&artid=2728378). *Nature protocols* **1** (6): 2876–90. doi:10.1038/nprot.2006.202. PMID 17406547. PMC 2728378.

[13] U. Meierhenrich, J.J. Filippi, C. Meinert, J. H. Bredehöft, J. Takahashi, L. Nahon, N. C. Jones, S. V. Hoffmann (2010). "Circular Dichroism of Amino Acids in the Vacuum-Ultraviolet Region.". *Angewandte Chemie Int. Ed.* **49** (42): 7799–7802. doi:10.1002/anie.201003877.

## Further reading

1. Alison Rodger and Bengt Nordén, *Circular Dichroism and Linear Dichroism* (http://books.google.co.uk/books?hl=en&id=THeKGC99hJcC) (1997) Oxford University Press, Oxford, UK. ISBN 019855897X.
2. Fasman, G.D., *Circular Dichroism and the Conformational Analysis of Biomolecules* (1996) Plenum Press, New York.
3. Hecht, E., *Optics* 3rd Edition (1998) Addison Wesley Longman, Massachusetts.
4. Klewpatinond, M. and Viles, J.H. (2007) Empirical rules for rationalising visible circular dichroism of $Cu^{2+}$ and $Ni^{2+}$ histidine complexes: Applications to the prion protein. FEBS Letters 581, 1430-1434.

## External links

- Circular Dichroism explained (http://www.ap-lab.com/circular_dichroism.htm)
- Circular Dichroism at UMDNJ (http://www2.umdnj.edu/cdrwjweb/index.htm#software) - a good site for information on structure estimation software
- Electromagnetic waves (http://www.enzim.hu/~szia/cddemo/edemo1.htm) - Animated electromagnetic waves. The Emanim program is a teaching resource for helping students understand the nature of electromagnetic waves and their interaction with birefringent and dichroic samples
- An Introduction to Circular Dichroism Spectroscopy (http://www.photophysics.com/circulardichroism.php) - a very good tutorial on circular dichroism spectroscopy

# Vibrational spectroscopy

A **molecular vibration** occurs when atoms in a molecule are in periodic motion while the molecule as a whole has constant translational and rotational motion. The frequency of the periodic motion is known as a vibration frequency. The three atomic molecule have three modes of vibration irrespective of whether these are linear or nonlinear. The molecules with $n$(n must be greater than 3) atoms has $3n-6$ normal modes of vibration, whereas a *linear* molecule has $3n-5$ normal modes of vibration because rotation about its molecular axis is simply a rotation of the reference frame and cannot be observed[1] . A diatomic molecule thus has only one normal mode of vibration. The normal modes of vibration of polyatomic molecules are independent of each other, each involving simultaneous vibrations of different parts of the molecule.

A molecular vibration is excited when the molecule absorbs a quantum of energy, E, corresponding to the vibration's frequency, ν, according to the relation $E=h\nu$, where $h$ is Planck's constant. A fundamental vibration is excited when one such quantum of energy is absorbed by the molecule in its ground state. When two quanta are absorbed the first overtone is excited, and so on to higher overtones.

To a first approximation, the motion in a normal vibration can be described as a kind of simple harmonic motion. In this approximation, the vibrational energy is a quadratic function (parabola) with respect to the atomic displacements and the first overtone has twice the frequency of the fundamental. In reality, vibrations are anharmonic and the first overtone has a frequency that is slightly lower than twice that of the fundamental. Excitation of the higher overtones involves progressively less and less additional energy and eventually leads to dissociation of the molecule, as the potential energy of the molecule is more like a Morse potential.

The vibrational states of a molecule can be probed in a variety of ways. The most direct way is through infrared spectroscopy, as vibrational transitions typically require an amount of energy that corresponds to the infrared region of the spectrum. Raman spectroscopy, which typically uses visible light, can also be used to measure vibration frequencies directly.

Vibrational excitation can occur in conjunction with electronic excitation (vibronic transition), giving vibrational fine structure to electronic transitions, particularly with molecules in the gas state.

Simultaneous excitation of a vibration and rotations gives rise to vibration-rotation spectra.

## Vibrational coordinates

The coordinate of a normal vibration is a combination of *changes* in the positions of atoms in the molecule. When the vibration is excited the coordinate changes sinusoidally with a frequency ν, the frequency of the vibration.

### Internal coordinates

*Internal coordinates* are of the following types, illustrated with reference to the planar molecule ethylene,

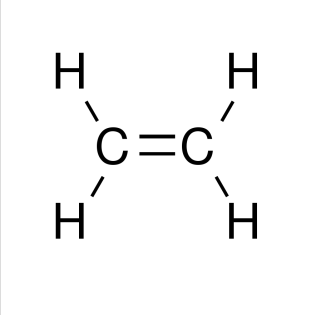


- Stretching: a change in the length of a bond, such as C-H or C-C
- Bending: a change in the angle between two bonds, such as the HCH angle in a methylene group

- Rocking: a change in angle between a group of atoms, such as a methylene group and the rest of the molecule.
- Wagging: a change in angle between the plane of a group of atoms, such as a methylene group and a plane through the rest of the molecule,
- Twisting: a change in the angle between the planes of two groups of atoms, such as a change in the angle between the two methylene groups.
- Out-of-plane: a change in the angle between any one of the C-H bonds and the plane defined by the remaining atoms of the ethylene molecule. Another example is in $BF_3$ when the boron atom moves in and out of the plane of the three fluorine atoms.

In a rocking, wagging or twisting coordinate the bond lengths within the groups involved do not change. The angles do. Rocking is distinguished from wagging by the fact that the atoms in the group stay in the same plane.

In ethene there are 12 internal coordinates: 4 C-H stretching, 1 C-C stretching, 2 H-C-H bending, 2 $CH_2$ rocking, 2 $CH_2$ wagging, 1 twisting. Note that the H-C-C angles cannot be used as internal coordinates as the angles at each carbon atom cannot all increase at the same time.

See infrared spectroscopy for some animated illustrations of internal coordinates.

## Symmetry-adapted coordinates

Symmetry-adapted coordinates may be created by applying a projection operator to a set of internal coordinates.[2] The projection operator is constructed with the aid of the character table of the molecular point group. For example, the four(un-normalised) C-H stretching coordinates of the molecule ethene are given by

$$Q_{s1} = q_1 + q_2 + q_3 + q_4$$
$$Q_{s2} = q_1 + q_2 - q_3 - q_4$$
$$Q_{s3} = q_1 - q_2 + q_3 - q_4$$
$$Q_{s4} = q_1 - q_2 - q_3 + q_4$$

where $q_1$ - $q_4$ are the internal coordinates for stretching of each of the four C-H bonds.

Illustrations of symmetry-adapted coordinates for most small molecules can be found in Nakamoto.[3]

## Normal coordinates

The normal coordinates, denoted as $Q$, refer to the positions of atoms away from their equilibrium positions, with respect to a normal mode of vibration. Each normal mode is assigned a single normal coordinate, and so the normal coordinate refers to the "progress" along that normal mode at any given time. Formally, normal modes are determined by solving a secular determinant, and then the normal coordinates (over the normal modes) can be expressed as a summation over the cartesian cordinates (over the atom positions). The advantage of working in normal modes is that they diagonalize the matrix governing the molecular vibrations, so each normal mode is an independent molecular vibration, associated with its own spectrum of quantum mechanical states. If the molecule possesses symmetries, it will belong to a point group, and the normal modes will "transform as" an irreducible representation under that group. The normal modes can then be qualitatively determined by applying group theory and projecting the irreducible representation onto the cartesian coordinates. For example, when this treatment is applied to $CO_2$, it is found that the C=O stretches are not independent, but rather there is a O=C=O symmetric stretch and an O=C=O asymmetric stretch.

- symmetric stretching: the sum of the two C-O stretching coordinates; the two C-O bond lengths change by the same amount and the carbon atom is stationary. $Q = q_1 + q_2$
- asymmetric stretching: the difference of the two C-O stretching coordinates; one C-O bond length increases while the other decreases. $Q = q_1 - q_2$

When two or more normal coordinates belong to the same irreducible representation of the molecular point group (colloquially, have the same symmetry) there is "mixing" and the coefficients of the combination cannot be

determined *a priori*. For example, in the linear molecule hydrogen cyanide, HCN, The two stretching vibrations are

1. principally C-H stretching with a little C-N stretching; $Q_1 = q_1 + a\, q_2$ ($a << 1$)
2. principally C-N stretching with a little C-H stretching; $Q_2 = b\, q_1 + q_2$ ($b << 1$)

The coefficients a and b are found by performing a full normal coordinate analysis by means of the Wilson GF method.[4]

## Newtonian mechanics

Perhaps surprisingly, molecular vibrations can be treated using Newtonian mechanics to calculate the correct vibration frequencies. The basic assumption is that each vibration can be treated as though it corresponds to a spring. In the harmonic approximation the spring obeys Hooke's law: the force required to extend the spring is proportional to the extension. The proportionality constant is known as a *force constant, k*. The anharmonic oscillator is considered elsewhere.[5]

$$\text{Force} = -kQ$$

By Newton's second law of motion this force is also equal to a "mass", *m*, times acceleration.

$$\text{Force} = m\frac{d^2Q}{dt^2}$$

Since this is one and the same force the ordinary differential equation follows.

$$m\frac{d^2Q}{dt^2} + kQ = 0$$

The solution to this equation of simple harmonic motion is

$$Q(t) = A\cos(2\pi\nu t); \quad \nu = \frac{1}{2\pi}\sqrt{\frac{k}{m}}.$$

*A* is the maximum amplitude of the vibration coordinate *Q*. It remains to define the "mass", *m*. In a homonuclear diatomic molecule such as $N_2$, it is half the mass of one atom. In a heteronuclear diatomic molecule, AB, it is the reduced mass, $\mu$ given by

$$\frac{1}{\mu} = \frac{1}{m_A} + \frac{1}{m_B}.$$

The use of the reduced mass ensures that the centre of mass of the molecule is not affected by the vibration. In the harmonic approximation the potential energy of the molecule is a quadratic function of the normal coordinate. It follows that the force-constant is equal to the second derivative of the potential energy.

$$k = \frac{\partial^2 V}{\partial Q^2}$$

When two or more normal vibrations have the same symmetry a full normal coordinate analysis must be performed (see GF method). The vibration frequencies, $\nu_i$ are obtained from the eigenvalues, $\lambda_i$, of the matrix product $\boldsymbol{GF}$. $\boldsymbol{G}$ is a matrix of numbers derived from the masses of the atoms and the geometry of the molecule.[4] $\boldsymbol{F}$ is a matrix derived from force-constant values. Details concerning the determination of the eigenvalues can be found in [6].

## Quantum mechanics

In the harmonic approximation the potential energy is a quadratic function of the normal coordinates. Solving the Schrödinger wave equation, the energy states for each normal coordinate are given by

$$E_n = \left(n + \frac{1}{2}\right) h \frac{1}{2\pi} \sqrt{\frac{k}{m}},$$

where *n* is a quantum number that can take values of 0, 1, 2 ... The difference in energy when *n* changes by 1 are therefore equal to the energy derived using classical mechanics. See quantum harmonic oscillator for graphs of the first 5 wave functions. Knowing the wave functions, certain selection rules can be formulated. For example, for a harmonic oscillator transitions are allowed only when the quantum number *n* changes by one,

$$\Delta n = \pm 1$$

but this does not apply to an anharmonic oscillator; the observation of overtones is only possible because vibrations are anharmonic. Another consequence of anharmonicity is that transitions such as between states *n*=2 and *n*=1 have slightly less energy than transitions between the ground state and first excited state. Such a transition gives rise to a hot band.

### Intensities

In an infrared spectrum the intensity of an absorption band is proportional to the derivative of the molecular dipole moment with respect to the normal coordinate.[7] The intensity of Raman bands depends on polarizability.

## See also

- Infrared spectroscopy
- Near infrared spectroscopy
- Raman spectroscopy
- Resonance Raman spectroscopy
- Coherent anti-Stokes Raman spectroscopy
- Eckart conditions
- FG method
- Fermi resonance
- Lennard-Jones potential
- Transition dipole moment

## References

[1] Landau LD and Lifshitz EM (1976) *Mechanics*, 3rd. ed., Pergamon Press. ISBN 0-08-021022-8 (hardcover) and ISBN 0-08-029141-4 (softcover)

[2] F.A. Cotton *Chemical applications of group theory*, Wiley, 1962, 1971

[3] K. Nakamoto *Infrared and Raman spectra of inorganic and coordination compounds,* 5th. edition, Part A, Wiley, 1997

[4] E.B. Wilson, J.C. Decius and P.C. Cross, *Molecular vibrations*, McGraw-Hill, 1955. (Reprinted by Dover 1980)

[5] S. Califano, *Vibrational states*, Wiley, 1976

[6] P. Gans, *Vibrating molecules*, Chapman and Hall, 1971

[7] D. Steele, *Theory of vibrational spectroscopy*, W.B. Saunders, 1971

## Further reading

- P.M.A. Sherwood, *Vibrational spectroscopy of solids*, Cambridge University Press, 1972

## External links

- Free Molecular Vibration code developed by Zs. Szabó and R. Scipioni (http://www.evtsz.bme.hu/web/staff/szabo/web_molecular_vibration/molec_vib_code.html)
- Molecular vibration and absorption (http://www.lsbu.ac.uk/water/vibrat.html)
- small explanation of vibrational spectra and a table including force constants (http://hyperphysics.phy-astr.gsu.edu/Hbase/molecule/vibspe.html).
- Character tables for chemically important point groups (http://symmetry.jacobs-university.de/)

# Vibrational circular dichroism

**Vibrational circular dichroism** (VCD) is a spectroscopic technique which detects differences in attenuation of left and right circularly polarized light passing through a sample. It is basically circular dichroism spectroscopy in the infrared and near infrared ranges[1] .

Because VCD is sensitive to the mutual orientation of distinct groups in a molecule, it provides three-dimensional structural information. Thus, it is a powerful technique as VCD spectra of enantiomers can be simulated using *ab initio* calculations, thereby allowing the identification of absolute configurations of small molecules in solution from VCD spectra. Among such quantum computations of VCD spectra resulting from the chiral properties of small organic molecules are those based on density functional theory (DFT) and gauge-invariant atomic orbitals (GIAO). As a simple example of the experimental results that were obtained by VCD are the spectral data obtained within the carbon-hydrogen (C-H) stretching region of 21 amino acids in heavy water solutions. Measurements of vibrational optical activity (VOA) have thus numerous applications, not only for small molecules, but also for large and complex biopolymers such as muscle proteins (myosin, for example) and DNA.

## Vibrational modes

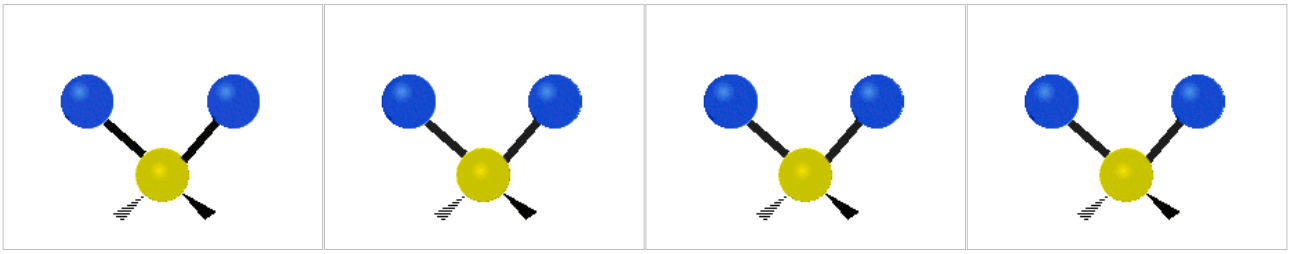

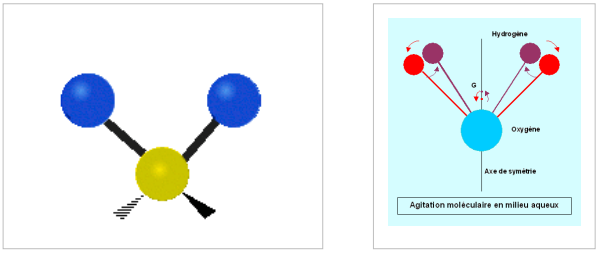

## Theory of VCD

While the fundamental quantity associated with the infrared absorption is the dipole strength, the differential absorption is proportional also to the rotational strength, a quantity which depends on both the electric and magnetic dipole transition moments. Sensitivity of the handedness of a molecule toward circularly polarized light results from the form of the rotational strength.

## VCD of peptides and proteins

Extensive VCD studies have been reported for both polypeptides and several proteins in solution[2] [3] [4] ; several recent reviews were also compiled[5] [6] [7] [8] . An extensive but not comprehensive VCD publications list is also provided in the "References" section. The published reports over the last 22 years have established VCD as a powerful technique with improved results over those previously obtained by visible/UV circular dichroism (CD) or optical rotatory dispersion (ORD) for proteins and nucleic acids.

## Amino acid and polypeptide structures

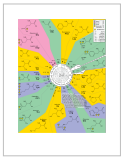

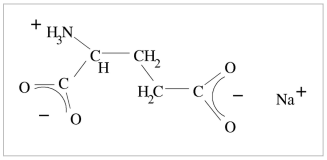

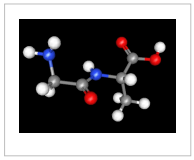

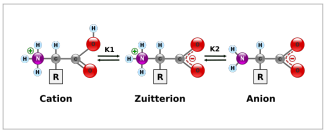


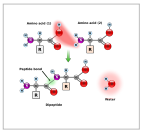

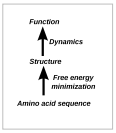


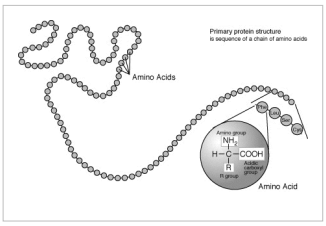


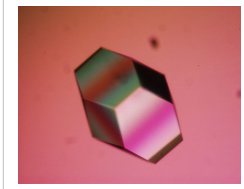

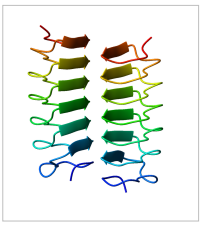

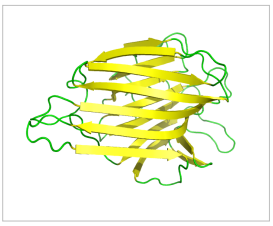

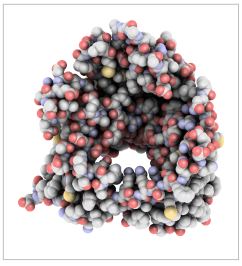

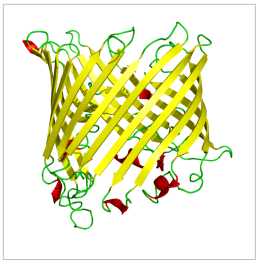

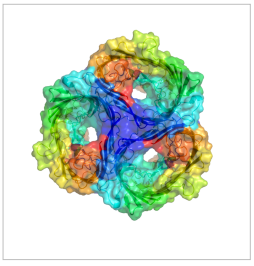

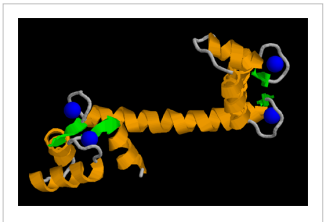

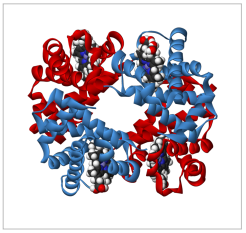

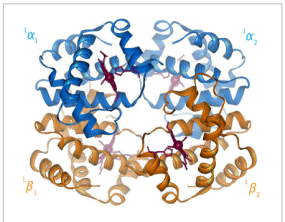

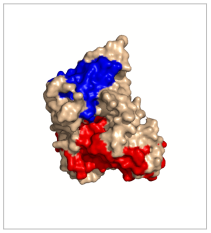

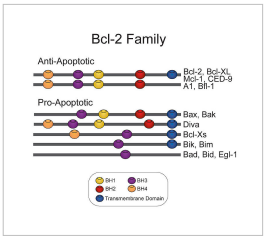


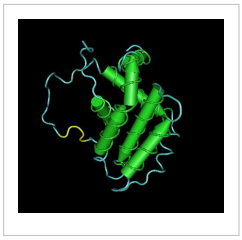

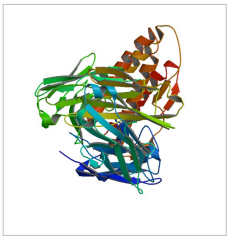

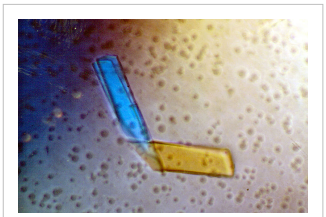

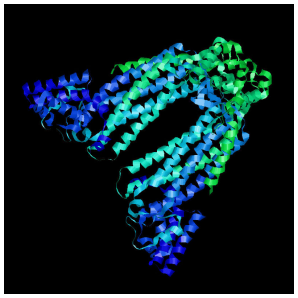

## VCD of nucleic acids

VCD spectra of nucleotides, synthetic polynucleotides and several nucleic acids, including DNA, have been reported and assigned in terms of the type and number of helices present in A- , B-, and Z- DNA.

## VCD Instrumentation

For biopolymers such as proteins and nucleic acids, the difference in absorbance between the levo- and dextro-configurations is five orders of magnitude smaller than the corresonding (unpolarized) absorbance. Therefore, VCD of biopolymers requires the use of very sensitive, specially built instrumentation as well as time-averaging over relatively long intervals of time even with such sensitive VCD spectrometers. Most CD instruments produce left- and right- circularly polarized light which is then either sine-wave or square-wave modulated, with subsequent phase-sensitive detection and lock-in amplification of the detected signal. In the case of FT-VCD, a photo-elastic modulator (PEM) is employed in conjunction with an FT-IR interferometer set-up. An example is that of a Bomem model MB-100 FT-IR interferometer equipped with additional polarizing optics/ accessories needed for recording VCD spectra. A parallel beam emerges through a side port of the interferometer which passes first through a wire grid linear polarizer and then through an octagonal-shaped ZnSe crystal PEM which modulates the polarized beam at a fixed, lower frequency such as 37.5 kHz. A mechanically stressed crystal such as ZnSe exhibits birefringence when stressed by an adjacent piezoelectric transducer. The linear polarizer is positioned close to, and at 45 degrees, with respect to the ZnSe crystal axis. The polarized radiation focused onto the detector is doubly modulated, both by the PEM and by the interferometer setup. A very low noise detector, such as MCT (HgCdTe), is also selected for the VCD signal phase-sensitive detection. The first dedicated VCD spectrometer brought to market was the ChiralIR from Bomem/BioTools, Inc. in 1997. Today, Thermo-Electron, Bruker, Jasco and BioTools offer either VCD accessories or stand-alone instrumentation.[9] To prevent detector saturation an appropriate, long wave pass filter is placed before the very low noise MCT detector, which allows only radiation below 1750 $cm^{-1}$ to reach the MCT detector; the latter however measures radiation only down to 750 $cm^{-1}$. FT-VCD spectra accumulation of the selected sample solution is then carried out, digitized and stored by an in-line computer. Published reviews that compare various VCD methods are also available.[10] [11]

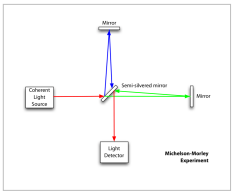
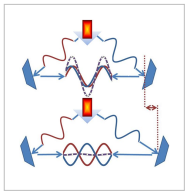
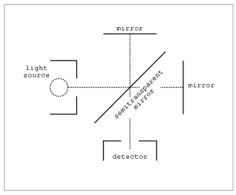
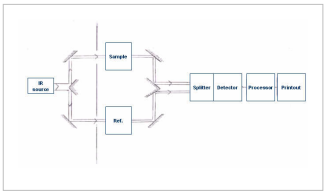

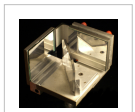
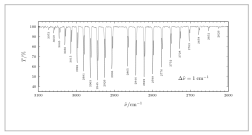
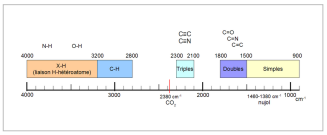
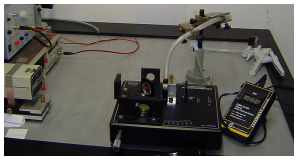
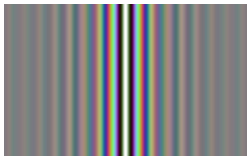
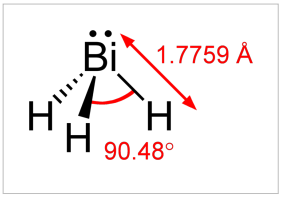

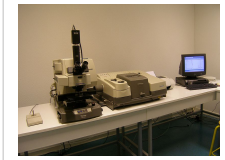

## Magnetic VCD

VCD spectra have also been reported in the presence of an applied external magnetic field[12] . This method can enhance the VCD spectral resolution for small molecules[13] [14] [15] [16] [17] .

## Raman optical activity (ROA)

ROA is a technique complementary to VCD especially useful in the 50—1600 $cm^{-1}$ spectral region; it is considered as the technique of choice for determining optical activity for photon energies less than 600 $cm^{-1}$.

## Notes

[1] http://planetphysics.org/?op=getobj;from=objects;id=410 Principles of IR and NIR Spectroscopy

[2] *"Vibrational Circular Dichroism of Polypeptides XII. Re-evaluation of the Fourier Transform Vibrational Circular Dichroism of Poly-gamma-Benzyl-L-Glutamate," P. Malon, R. Kobrinskaya, T. A. Keiderling, Biopolymers 27, 733-746 (1988).

[3] *"Vibrational Circular Dichroism of Biopolymers," T. A. Keiderling, S. C. Yasui, U. Narayanan, A. Annamalai, P. Malon, R. Kobrinskaya, L. Yang, in *Spectroscopy of Biological Molecules New Advances* ed. E. D. Schmid, F. W. Schneider, F. Siebert, p. 73-76 (1988).

[4] *"Vibrational Circular Dichroism of Polypeptides and Proteins," S. C. Yasui, T. A. Keiderling, *Mikrochimica Acta*, II, 325-327, (1988).

[5] *"Vibrational Circular Dichroism of Proteins Polysaccharides and Nucleic Acids" T. A. Keiderling, Chapter 8 in *Physical Chemistry of Food Processes, Vol. 2 Advanced Techniques, Structures and Applications.*, eds. I.C. Baianu, H. Pessen, T. Kumosinski, Van Norstrand--Reinhold, New York (1993), pp 307-337.

[6] "Spectroscopic characterization of Unfolded peptides and proteins studied with infrared absorption and vibrational circular dichroism spectra" T. A. Keiderling and Qi Xu, Advances in Protein Chemistry Volume 62, [Unfolded Proteins, Dedicated to John Edsall, Ed.: George Rose, Academic Press:New York] (2002), pp. 111-161.

[7] *"Protein and Peptide Secondary Structure and Conformational Determination with Vibrational Circular Dichroism " Timothy A. Keiderling, *Current Opinions in Chemical Biology* (Ed. Julie Leary and Mark Arnold) 6, 682-688 (2002).

[8] *Review: Conformational Studies of Peptides with Infrared Techniques. Timothy A. Keiderling and R. A. G. D. Silva, in Synthesis of Peptides and Peptidomimetics, Ed. M. Goodman and G. Herrman, Houben-Weyl, Vol 22Eb, Georg Thiem Verlag, New York (2002) pp. 715-738, (written and accepted in 2000).

[9] "Vibrational Circular Dichroism: A New Tool for the Solution-State Determination of the Structure and Absolute Configuration of Chiral Natural Product Molecules" Laurence A. Nafie, Natural Product Communications 3(3), 451-466 (2008)

[10] "Polarization Modulation Fourier Transform Infrared Spectroscopy with Digital SignalProcessing: Comparison of Vibrational Circular Dichroism Methods." Jovencio Hilario, DavidDrapcho, Raul Curbelo, Timothy A. Keiderling, Applied Spectroscopy 55, 1435-1447(2001)--

[11] "Vibrational circular dichroism of biopolymers. Summary of methods and applications.", Timothy A. Keiderling, Jan Kubelka, Jovencio Hilario, in *Vibrational spectroscopy of polymers and biological systems*, Ed. Mark Braiman, Vasilis Gregoriou, Taylor&Francis, Atlanta (CRC Press, Boca Raton, FL) (2006) pp. 253-324 (originally written in 2000, updated in 2003)

[12] "Observation of Magnetic Vibrational Circular Dichroism," T. A. Keiderling, Journal of Chemical Physics, 75, 3639-41 (1981).

[13] "Vibrational Spectral Assignment and Enhanced Resolution Using Magnetic Vibrational Circular Dichroism," T. R. Devine and T. A. Keiderling, *Spectrochimica Acta*, 43A, 627-629 (1987).

[14] "Magnetic Vibrational Circular Dichroism with an FTIR" P. V. Croatto, R. K. Yoo, T. A. Keiderling, SPIE Proceedings 1145 (7th International Conference on FTS, ed. D. G. Cameron) 152-153 (1989).

[15] "Direct Measurement of the Rotational g-Value in the Ground State of Acetylene by Magnetic Vibrational Circular Dichroism." C. N. Tam and T. A. Keiderling, Chemical Physics Letters, 243, 55-58 (1995).

[16] . "Ab initio calculation of the vibrational magnetic dipole moment" P. Bour, C. N. Tam, T. A. Keiderling, Journal of Physical Chemistry 99, 17810-17813 (1995)

[17] "Rotationally Resolved Magnetic Vibrational Circular Dichroism. Experimental Spectra and Theoretical Simulation for Diamagnetic Molecules." P. Bour, C. N. Tam, B. Wang, T. A. Keiderling, *Molecular Physics* 87, 299-318, (1996).

# References

## Peptides and proteins

- Huang R, Wu L, McElheny D, Bour P, Roy A, Keiderling TA. Cross-Strand Coupling and Site-Specific Unfolding Thermodynamics of a Trpzip beta-Hairpin Peptide Using (13)C Isotopic Labeling and IR Spectroscopy. *The journal of physical chemistry. B*. 2009 Apr;113(16):5661-74.
- "Vibrational Circular Dichroism of Poly alpha-Benzyl-L-Glutamate," R. D. Singh, and T. A. Keiderling, Biopolymers, 20, 237-40 (1981).
- "Vibrational Circular Dichroism of Polypeptides II. Solution Amide II and Deuteration Results," A. C. Sen and T. A. Keiderling, Biopolymers, 23, 1519-32 (1984).
- "Vibrational Circular Dichroism of Polypeptides III. Film Studies of Several alpha-Helical and ß-Sheet Polypeptides," A. C. Sen and T. A. Keiderling, Biopolymers, 23, 1533-46 (1984).
- "Vibrational Circular Dichroism of Polypeptides IV. Film Studies of L-Alanine Homo Oligopeptides," U. Narayanan, T. A. Keiderling, G. M. Bonora, and C. Toniolo, *Biopolymers* 24, 1257-63 (1985).
- "Vibrational Circular Dichroism of Polypeptides, T. A. Keiderling, S. C. Yasui, A. C. Sen, C. Toniolo, G. M. Bonora, in Peptides Structure and Function, Proceedings of the 9th American Peptide Symposium," ed. C. M. Deber, K. Kopple, V. Hruby; Pie rce Chemical: Rockford, IL; 167-172 (1985).
- "Vibrational Circular Dichroism of Polypeptides V. A Study of 310 Helical-Octapeptides" S. C. Yasui, T. A. Keiderling, G. M. Bonora, C. Toniolo, Biopolymers 25, 79-89 (1986).
- "Vibrational Circular Dichroism of Polypeptides VI. Polytyrosine alpha-helical and Random Coil Results," S. C. Yasui and T. A. Keiderling, Biopolymers 25, 5-15 (1986).
- "Vibrational Circular Dichroism of Polypeptides VII. Film and Solution Studies of alpha-forming Homo-Oligopeptides," U. Narayanan, T. A. Keiderling, G. M. Bonora, C. Toniolo, *Journal of the American Chemical Society*, 108, 2431-2437 (1986).
- "Vibrational Circular Dichroism of Polypeptides VIII. Poly Lysine Conformations as a Function of pH in Aqueous Solution," S. C. Yasui, T. A. Keiderling, Journal of the American Chemical Society, 108, 5576-5581 (1986).
- "Vibrational Circular Dichroism of Polypeptides IX. A Study of Chain Length Dependence for 310-Helix Formation in Solution." S. C. Yasui, T. A. Keiderling, F. Formaggio, G. M. Bonora, C. Toniolo, Journal of the American Chemical Society 108, 4988-499 3 (1986).
- "Vibrational Circular Dichroism of Biopolymers." T. A. Keiderling, *Nature*, 322, 851-852 (1986).
- "Vibrational Circular Dichroism of Polypeptides X. A Study of alpha-Helical Oligopeptides in Solution." S. C. Yasui, T. A. Keiderling, R. Katachai, Biopolymers 26, 1407-1412 (1987).
- "Vibrational Circular Dichroism of Polypeptides XI. Conformation of Poly(L-Lysine(Z)-L-Lysine(Z)-L-1-Pyrenylalanine) and Poly(L-Lysine(Z)-L-Lysine(Z)-L-1-Napthylala-nine) in Solution" S. C. Yasui, T. A. Keiderling, and M. Sisido, *Macromolecules* 20, 2 403-2406 (1987).
- "Vibrational Circular Dichroism of Biopolymers" T. A. Keiderling, S. C. Yasui, A. C. Sen, U. Narayanan, A. Annamalai, P. Malon, R. Kobrinskaya, L. Yang, in "F.E.C.S. Second International Conference on Circular

Dichroism, Conference Proceedings," ed. M. Kajtar, L. Eötvös Univ., Budapest, 1987, p. 155-161.

- "Vibrational Circular Dichroism of Poly-L-Proline and Other Helical Poly-peptides," R. Kobrinskaya, S. C. Yasui, T. A. Keiderling, in "Peptides: Chemistry and Biology, Proceedings of the 10th American Peptide Symposium," ed. G. R. Marshall, ESCOM, L eiden, 1988, p. 65-67.
- "Vibrational Circular Dichroism of Polypeptides with Aromatic Side Chains," S. C. Yasui, T. A. Keiderling, in "Peptides: Chemistry and Biology, Proceedings of the 10th American Peptide Symposium," ed. G. R. Marshall, ESCOM, Leiden, 1988, p. 90-92.
- "Vibrational Circular Dichroism of Polypeptides XII. Re-evaluation of the Fourier Transform Vibrational Circular Dichroism of Poly-gamma-Benzyl-L-Glutamate," P. Malon, R. Kobrinskaya, T. A. Keiderling, Biopolymers 27, 733-746 (1988).
- "Vibrational Circular Dichroism of Biopolymers," T. A. Keiderling, S. C. Yasui, U. Narayanan, A. Annamalai, P. Malon, R. Kobrinskaya, L. Yang, in *Spectroscopy of Biological Molecules New Advances* ed. E. D. Schmid, F. W. Schneider, F. Siebert, p. 73-76 (1988).
- "Vibrational Circular Dichroism of Polypeptides and Proteins," S. C. Yasui, T. A. Keiderling, *Mikrochimica Acta*, II, 325-327, (1988).
- "(1R,7R)-7-Methyl-6,9,-Diazatricyclo[6,3,0,01,6]Tridecanne-5,10-Dione, A Tricyclic Spirodilactam Containing Non-planar Amide Groups: Synthesis, NMR, Crystal Structure, Absolute Configuration, Electronic and Vibrational Circular Dichroism" P. Malon, C . L. Barness, M. Budesinsky, R. K. Dukor, D. van der Helm, T. A. Keiderling, Z. Koblicova, F. Pavlikova, M. Tichy, K. Blaha, Collections of Czechoslovak Chemical Communications 53, 2447-2472 (1988).
- "Vibrational Circular Dichroism of Poly Glutamic Acid" R. K. Dukor, T. A. Keiderling, in *Peptides 1988* (ed. G. Jung, E. Bayer) Walter de Gruyter, Berlin (1989) pp 519–521.
- "Biopolymer Conformational Studies with Vibrational Circular Dichroism" T. A. Keiderling, S. C. Yasui, P. Pancoska, R. K. Dukor, L. Yang, SPIE Proceeding 1057, ("Biomolecular Spectroscopy," ed. H. H. Mantsch, R. R. Birge) 7-14 (1989).
- "Vibrational Circular Dichroism. Comparison of Techniques and Practical Considerations" T. A. Keiderling, in "Practical Fourier Transform Infrared Spectroscopy. Industrial and Laboratory Chemical Analysis," ed. J. R. Ferraro, K. Krishnan (Academic Press, San Diego, 1990) p. 203-284.
- "Vibrational Circular Dichroism Study of Unblocked Proline Oligomers," R. K. Dukor, T. A. Keiderling, V. Gut, *International Journal of Peptide and Protein Research*, 38, 198-203 (1991).
- "Reassessment of the Random Coil Conformation. Vibrational CD Study of Proline Oligopeptides and Related Polypeptides" R. K. Dukor and T. A. Keiderling, Biopolymers 31 1747-1761 (1991).
- "Vibrational CD of the Amide II band in Some Model Polypeptides and Proteins" V. P. Gupta, T. A. Keiderling, Biopolymers 32 239-248 (1992).
- "Vibrational Circular Dichroism of Proteins Polysaccharides and Nucleic Acids" T. A. Keiderling, Chapter 8 in *Physical Chemistry of Food Processes, Vol. 2 Advanced Techniques, Structures and Applications.*, eds. I.C. Baianu, H. Pessen, T. Kumosinski, Van Norstrand—Reinhold, New York (1993), pp 307–337.
- "Structural Studies of Biological Macromolecules using Vibrational Circular Dichroism" T. A. Keiderling, P. Pancoska, Chapter 6 in Advances in Spectroscopy Vol. 21, *Biomolecular Spectroscopy Part B* eds. R. E. Hester, R. J. H. Clarke, John W iley Chichester (1993) pp 267–315.
- "Ab Initio Simulations of the Vibrational Circular Dichroism of Coupled Peptides" P. Bour and T. A. Keiderling, Journal of the American Chemical Society 115 9602-9607 (1993).
- "Ab initio Simulations of Coupled Peptide Vibrational Circular Dichroism" P. Bour, T. A. Keiderling in "Fifth International Conference on The Spectroscopy of Biological Molecules" Th. Theophanides, J. Anastassopoulou, N. Fotopoulos (Eds), Kluwen Aca demic Publ., Dortrecht, 1993, p. 29-30.
- "Vibrational Circular Dichroism Spectroscopy of Peptides and Proteins" T. A. Keiderling, in "Circular Dichroism Interpretations and Applications," K. Nakanishi, N. Berova, R. Woody, Eds., VCH Publishers, New York, (1994)

pp 497–521.

- "Conformational Study of Sequential Lys-Leu Based Polymers and Oligomers using Vibrational and Electronic Circular Dichroism Spectra" V. Baumruk, D. Huo, R. K. Dukor, T. A. Keiderling, D. LeLeivre and A. Brack Biopolymers 34, 1115-1121 (1994).
- "Vibrational Optical Activity of Oligopeptides" T. B. Freedman, L. A. Nafie, T. A. Keiderling *Biopolymers* (Peptide Science) 37 (ed. C. Toniolo) 265-279 (1995).
- "Characterization of ß-bend ribbon spiral forming peptides using electronic and vibrational circular dichroism" G. Yoder, T. A. Keiderling, F. Formaggio, M. Crisma, C. Toniolo Biopolymers 35, 103-111 (1995).
- "Vibrational Circular Dichroism as a Tool for Determination of Peptide Secondary Structure" P. Bour, T. A. Keiderling, P. Malon, in "Peptides 1994 (Proceedings of the 23rd European Peptide Symposium,1994," (H.L.S. Maia, ed.), Escom, Le iden 1995, p. 517-518.
- "Helical Screw Sense of homo-oligopeptides of C-alpha-methylated alpha-amino acids as Determined with Vibrational Circular Dichroism." G. Yoder, T. A. Keiderling, M. Crisma, F. Formaggio, C. Toniolo, J. Kamphuis, Tetrahedron Asymmetry 6, 687 -690 (1995).
- "Conformational Study of Linear Alternating and Mixed D- and L-Proline Oligomers Using Electronic and Vibrational CD and Fourier Transform IR." W. M&#228stle, R. K. Dukor, G. Yoder, T. A. Keiderling *Biopolymers* 36, 623-631 (1995).
- Review: "Vibrational Circular Dichroism Applications to Conformational Analysis of Biomolecules" T. A. Keiderling in *Circular Dichroism and the Conformational Analysis of Biomolecules* ed. G. D. Fasman, Plenum, New York (1996) p. 555-585.
- "Mutarotation studies of Poly L-Proline using FT-IR, Electronic and Vibrational Circular Dichroism" R. K. Dukor, T. A. Keiderling, Biospectroscopy 2, 83-100 (1996).
- "Vibrational Circular Dichroism Applications in Proteins and Peptides" T. A. Keiderling, Proceedings of the NATO ASI in Biomolecular Structure and Dynamics, Loutrakii Greece, May 1996, Ed. G. Vergoten (delayed second volume to 1998).
- "Transfer of Molecular Property Tensors in Cartesian Coordinates: A new algorithm for simulation of vibrational spectra" Petr Bour, Jana Sopkova, Lucie Bednarova, Petr Malon, T. A. Keiderling, *Journal of Computational Chemistry* 18, 6 46-659 (1997).
- "Vibrational Circular Dichroism Characterization of Alanine-Rich Peptides." Gorm Yoder and Timothy A. Keiderling, "Spectroscopy of Biological Molecules: Modern Trends," Ed. P. Carmona, R. Navarro, A. Hernanz, Kluwer Acad. Pub., Netherlands (1997) p p. 27-28.
- "Ionic strength effect on the thermal unfolding of alpha-spectrin peptides." D. Lusitani, N. Menhart, T.A. Keiderling and L. W. M. Fung. *Biochemistry* 37(1998)16546-16554.
- "In search of the earliest events of hCGb folding: structural studies of the 60-87 peptide fragment" S. Sherman, L. Kirnarsky, O. Prakash, H. M. Rogers, R.A.G.D. Silva, T.A. Keiderling, D. Smith, A.M. Hanly, F. Perini, and R.W. Ruddon, American Pep tide Symposium Proceedings, 1997.
- "Cold Denaturation Studies of (LKELPKEL)n Peptide Using Vibrational Circular Dichroism and FT-IR". R. A. G. D. Silva, Vladimir Baumruk, Petr Pancoska, T. A. Keiderling, Eric Lacassie, and Yves Trudelle, American Peptide Symposium Proceedings, 1997.
- "Simulations of oligopeptide vibrational CD. Effects of isotopic labeling." Petr Bour, Jan Kubelka,T. A. Keiderling Biopolymers 53, 380-395 (2000).
- "Site specific conformational determination in thermal unfolding studies of helical peptides using vibrational circular dichroism with isotopic substitution" R. A. G. D. Silva, Jan Kubelka, Petr Bour, Sean M. Decatur, Timothy A. Keiderling, *Proceedings of the National Academy of Sciences* (PNAS:USA) 97, 8318-8323 (2000).
- "Folding studies on the human chorionic gonadotropin b -subunit using optical spectroscopy of peptide fragments" R. A. G. D. Silva, S. A. Sherman, F. Perini, E. Bedows, T. A. Keiderling, Journal of the American Chemical Society, 122, 8623-8630 (2000).

- "Peptide and Protein Conformational Studies with Vibrational Circular Dichroism and Related Spectroscopies", Timothy A. Keiderling, (Revised and Expanded Chapter) In Circular Dichroism: Principles and Applications, 2nd Edition. (Eds. K. Nakanishi, N. Berova and R. A. Woody, John Wiley & Sons, New York (2000) p. 621-666.
- "Conformation studies with Optical Spectroscopy of peptides taken from hairpin sequences in the Human Chorionic Gonadotropin " R. A. G. D. Silva, S. A. Sherman, E. Bedows, T. A. Keiderling, Peptides for the New Millenium [*sic?*], Proceedings of the 16th American Peptide Symposium, (June, 1999 Minneapolis, MN) Ed.G. B. Fields, J. P. Tam, G. Barany, Kluwer Acad. Pub., Dordrecht,(2000) p. 325-326.
- "Analysis of Local Conformation within Helical Peptides via Isotope-Edited Vibrational Spectroscopy." S. M. Decatur, T. A. Keiderling, R. A. G. D.Silva, and P. Bour, Peptides for the New Millenium [*sic?*], Proceedings of the 16th American Peptide Symposium, (June, 1999 Minneapolis, MN) Ed. Ed.G. B. Fields, J. P. Tam, G. Barany, Kluwer Acad. Pub., Dordrecht, (2000) p. 414-416.
- "The anomalous infrared amide I intensity distribution in C-13 isotopically labeled peptide beta-sheets comes from extended, multiple stranded structures. An *Ab Initio* study." Jan Kubelka and T. A. Keiderling , *Journal of the American Chemical Society.* 123, 6142-6150 (2001).
- "Vibrational Circular Dichroism of Peptides and Proteins: Survey of Techniques, Qualitative and Quantitative Analyses, and Applications" Timothy A. Keiderling, Chapter in Infrared and Raman Spectroscopy of Biological Materials, Ed. Bing Yan and H.-U. Gremlich, Marcel Dekker, New York (2001) p. 55-100.
- "Chirality in peptide vibrations. Ab initio computational studies of length, solvation, hydrogen bond, dipole coupling and isotope effects on vibrational CD. " Jan Kubelka, Petr Bour, R. A. Gangani D. Silva, Sean M. Decatur, Timothy A. Keiderling, ACS Symposium Series 810, ["Chirality: Physical Chemistry," (Ed. Janice Hicks) American Chemical Society, Washington, DC] (2002), pp. 50–64.
- "Spectroscopic Characterization of Selected b-Sheet Hairpin Models", J. Hilario, J. Kubelka, F. A. Syud, S. H. Gellman, and T. A. Keiderling. Biopolymers (Biospectroscopy) 67: 233-236 (2002)
- " Discrimination between peptide $3_{10}$- and alpha-helices. Theoretical analysis of the impact of alpha-methyl substitution on experimental spectra " Jan Kubelka, R. A. Gangani D. Silva, and T. A. Keiderling, *Journal of the American Chemical Society*, 124, 5325-5332 (2002).
- "*Ab Initio* Quantum Mechanical Models of Peptide Helices and their Vibrational Spectra" Petr Bour, Jan Kubelka and T. A. Keiderling, Biopolymers 65, 45-59 (2002).
- "Discriminating $3_{10}$- from alpha-helices. Vibrational and electronic CD and IR Absorption study of related Aib-containing oligopeptides" R. A. Gangani D. Silva, Sritana Yasui, Jan Kubelka, Fernando Formaggio, Marco Crisma, Claudio Toniolo, and Timothy A. Keiderling, Biopolymers 65, 229-243 (2002).
- "Spectroscopic characterization of Unfolded peptides and proteins studied with infrared absorption and vibrational circular dichroism spectra" T. A. Keiderling and Qi Xu, Advances in Protein Chemistry Volume 62, [Unfolded Proteins, Dedicated to John Edsall, Ed.: George Rose, Academic Press:New York] (2002), pp. 111–161.
- "Protein and Peptide Secondary Structure and Conformational Determination with Vibrational Circular Dichroism " Timothy A. Keiderling, *Current Opinions in Chemical Biology* (Ed. Julie Leary and Mark Arnold) 6, 682-688 (2002).
- Review: Conformational Studies of Peptides with Infrared Techniques. Timothy A. Keiderling and R. A. G. D. Silva, in Synthesis of Peptides and Peptidomimetics, Ed. M. Goodman and G. Herrman, Houben-Weyl, Vol 22Eb, Georg Thiem Verlag, New York (2002) pp. 715–738, (written and accepted in 2000).
- "Spectroscopic Studies of Structural Changes in Two beta-Sheet Forming Peptides Show an Ensemble of Structures That Unfold Non-Cooperatively" Serguei V. Kuznetsov, Jovencio Hilario, T. A. Keiderling, Anjum Ansari, *Biochemistry*, 42 :4321-4332, (2003).
- "Optical spectroscopic investigations of model beta-sheet hairpins in aqueous solution" Jovencio Hilario, Jan Kubelka, T. A. Keiderling, *Journal of the American Chemical Society* 125, 7562-7574 (2003).

- "Synthesis and conformational study of homopeptides based on (S)-Bin, a C2-symmetric binapthyl-derived Caa-disubstituted glycine with only axial chirality" J.-P. Mazaleyrat, K. Wright, A. Gaucher, M. Wakselman, S. Oancea, F. Formaggio, C. Toniolo, V. Setnicka, J. Kapitan, T. A. Keiderling, Tetrahedron Asymmetry, 14, 1879-1893 (2003).
- "Empirical modeling of the peptide amide I band IR intensity in water solution," Petr Bour, Timothy A. Keiderling, *Journal of Chemical Physics*, 119, 11253-11262 (2003)
- "The Nature of Vibrational Coupling in Helical Peptides: An Isotope Labeling Study" by R. Huang, J. Kubelka, W. Barber-Armstrong, R. A. G. D Silva, S. M. Decatur, and T. A. Keiderling, *Journal of the American Chemical Society*, 126, 2346-2354 (2004).
- "The Complete Chirospectroscopic Signature of the Peptide $3_{10}$ Helix in Aqueous Solution" Claudio Toniolo, Fernando Formaggio, Sabrina Tognon, Quirinus B. Broxterman, Bernard Kaptein, Rong Huang, Vladimir Setnicka, Timothy A. Keiderling, Iain H. McColl, Lutz Hecht, Laurence D. Barron, Biopolymers 75, 32-45 (2004).
- "Induced axial chirality in the biphenyl core for the Ca-tetrasubstituted a-amino acid residue Bip and subsequent propagation of chirality in (Bip)n/Val oligopeptides" J.-P. Mazaleyrat, K. Wright, A. Gaucher, N. Toulemonde, M. Wakselman, S. Oancea, C. Peggion, F. Formaggio, V. Setnicka, T. A. Keiderling, C. Toniolo, *Journal of the American Chemical Society* 126; 12874-12879 (2004).
- *Ab initio* modeling of amide I coupling in anti-parallel b-sheets and the effect of the 13C isotopic labeling on vibrational spectra" Petr Bour, Timothy A. Keiderling, *Journal of Physical Chemistry B*, 109, 5348-5357 (2005)
- Solvent Effects on IR And VCD Spectra of Helical Peptides: Insights from Ab Initio Spectral Simulations with Explicit Water" Jan Kubelka and Timothy A. Keiderling, Journal of Physical Chemistry B 109, 8231-8243 (2005)
- IR Study of Cross-Strand Coupling in a beta-Hairpin Peptide Using Isotopic Labels., Vladimir Setnicka, Rong Huang, Catherine L. Thomas, Marcus A. Etienne, Jan Kubelka, Robert P. Hammer, Timothy A. Keiderling *Journal of the American Chemical Society* 127, 4992-4993 (2005).
- Vibrational spectral simulation for peptides of mixed secondary structure: Method comparisons with the trpzip model hairpin. Petr Bour and Timothy A. Keiderling, *Journal of Physical Chemistry B* 109, 232687-23697 (2005).
- Isotopically labeled peptides provide site-resolved structural data with infrared spectra. Probing the structural limit of optical spectroscopy, Timothy A. Keiderling, Rong Huang, Jan Kubelka, Petr Bour, Vladimir Setnicka, Robert P. Hammer, Marcus *A. Etienne, R. A. Gangani D. Silva, Sean M. Decatur Collections Symposium Series, 8, 42-49 (2005)—["Biologically Active Peptides" IXth Conference, Prague Czech Republic, April 20-22, 2005.

## Nucleic acids and polynucleotides

- "Application of Vibrational Circular Dichroism to Synthetic Polypeptides and Polynucleic Acids" T. A. Keiderling, S. C. Yasui, R. K. Dukor, L. Yang, Polymer Preprints 30, 423-424 (1989).
- "Vibrational Circular Dichroism of Polyribonucleic Acids. A Comparative Study in Aqueous Solution." A. Annamalai and T. A. Keiderling, *Journal of the American Chemical Society*, 109, 3125-3132 (1987).
- "Conformational phase transitions (A-B and B-Z) of DNA and models using vibrational circular dichroism" L. Wang, L. Yang, T. A. Keiderling in *Spectroscopy of Biological Molecules.*, eds. R. E. Hester, R. B. Girling, Special Publication 94 Roya l Society of Chemistry, Cambridge (1991) p. 137-38.
- "Vibrational Circular Dichroism of Proteins Polysaccharides and Nucleic Acids" T. A. Keiderling, Chapter 8 in *Physical Chemistry of Food Processes, Vol. 2 Advanced Techniques, Structures and Applications* eds. I. C. Baianu, H. Pessen, T. Kumosinski, Van Norstrand—Reinhold, New York (1993) pp. 307–337.
- "Structural Studies of Biological Macromolecules using Vibrational Circular Dichroism" T. A. Keiderling, P. Pancoska, Chapter 6 in Advances in Spectroscopy Vol. 21, "Biomolecular Spectroscopy Part B" ed. R. E. Hester, R. J. H. Clarke, John W iley Chichester (1993) pp 267–315.

- "Detection of Triple Helical Nucleic Acids with Vibrational Circular Dichroism," L. Wang, P. Pancoska, T. A. Keiderling in "Fifth International Conference on The Spectroscopy of Biological Molecules" Th. Theophanides, J. Anastassopoulou, N. Fotopoul os (Eds), Kluwen Academic Publ., Dortrecht, 1993, p. 81-82.
- "Helical Nature of Poly (dI-dC) • Poly (dI-dC). Vibrational Circular Dichroism Results" L. Wang and T. A. Keiderling Nucleic Acids Research 21 4127-4132 (1993).
- "Detection and Characterization of Triple Helical Pyrimidine-Purine-Pyrimidine Nucleic Acids with Vibrational Circular Dichroism" L. Wang, P. Pancoska, T. A. Keiderling, Biochemistry 33 8428-8435 (1994).
- "Vibrational Circular Dichroism of A-, B- and Z- form Nucleic Acids in the PO2- Stretching Region" L. Wang, L. Yang, T. A. Keiderling, Biophysical Journal 67, 2460-2467 (1994).
- "Studies of multiple stranded RNA and DNA with FTIR, vibrational and electronic circular dichroism," Zhihua Huang, Lijiang Wang and Timothy A. Keiderling, in Spectrosopy of Biological Molecules, Ed. J. C. Merlin, Kluwer Acad. Pub., Dordrecht, 1995, pp . 321-322.
- "Vibrational Circular Dichroism Applications to Conformational Analysis of Biomolecules" T. A. Keiderling in "Circular Dichroism and the Conformational Analysis of Biomolecules" ed G. D. Fasman, Plenum, New York (1996) pp. 555–598.
- "Vibrational Circular Dichroism Techniques and Application to Nucleic Acids" T. A. Keiderling, In "Biomolecular Structure and Dynamics", NATO ASI series, Series E: Applied Sciences- Vol.342, Eds: G. Vergoten and T. Theophanides, Kluwer Academ ic Publishers, Dordrecht, The Netherlands,pp. 299–317 (1997).


## See also

- Circular dichroism
- Birefringence
- Optical rotatory dispersion
- IR spectroscopy
- Polarization
- Proteins
- Nucleic Acids
- DNA
- Molecular models of DNA
- DNA structure
- Protein structure
- Amino acids
- Density functional theory
- Quantum chemistry
- Raman optical activity (ROA)

# Raman spectroscopy

**Raman spectroscopy** (named after C. V. Raman, pronounced /ˈrɑːmən/) is a spectroscopic technique used to study vibrational, rotational, and other low-frequency modes in a system.[1] It relies on inelastic scattering, or Raman scattering, of monochromatic light, usually from a laser in the visible, near infrared, or near ultraviolet range. The laser light interacts with molecular vibrations, phonons or other excitations in the system, resulting in the energy of the laser photons being shifted up or down. The shift in energy gives information about the phonon modes in the system. Infrared spectroscopy yields similar, but complementary, information.

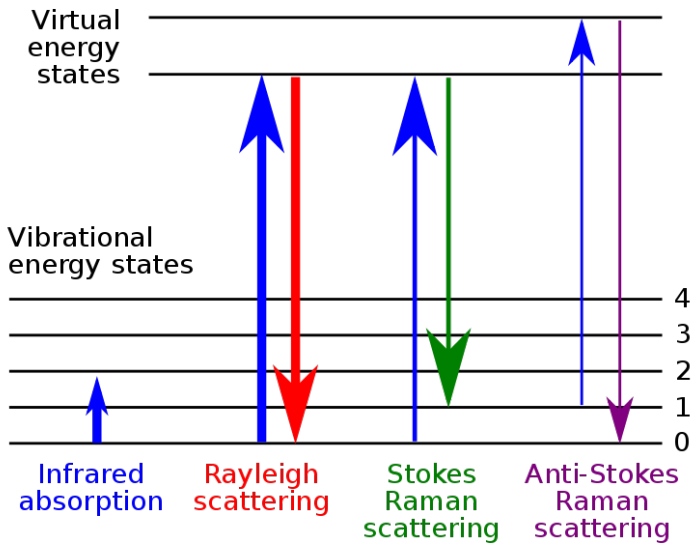


Energy level diagram showing the states involved in Raman signal. The line thickness is roughly proportional to the signal strength from the different transitions.

Typically, a sample is illuminated with a laser beam. Light from the illuminated spot is collected with a lens and sent through a monochromator. Wavelengths close to the laser line, due to elastic Rayleigh scattering, are filtered out while the rest of the collected light is dispersed onto a detector.

Spontaneous Raman scattering is typically very weak, and as a result the main difficulty of Raman spectroscopy is separating the weak inelastically scattered light from the intense Rayleigh scattered laser light. Historically, Raman spectrometers used holographic gratings and multiple dispersion stages to achieve a high degree of laser rejection. In the past, photomultipliers were the detectors of choice for dispersive Raman setups, which resulted in long acquisition times. However, modern instrumentation almost universally employs notch or edge filters for laser rejection and spectrographs (either axial transmissive (AT), Czerny-Turner (CT) monochromator) or FT (Fourier transform spectroscopy based), and CCD detectors.

There are a number of advanced types of Raman spectroscopy, including surface-enhanced Raman, resonance Raman, tip-enhanced Raman, polarised Raman, stimulated Raman (analogous to stimulated emission), transmission Raman, spatially-offset Raman, and hyper Raman.

## Basic theory

The Raman effect occurs when light impinges upon a molecule and interacts with the electron cloud and the bonds of that molecule. For the spontaneous Raman effect, which is a form of scattering, a photon excites the molecule from the ground state to a virtual energy state. When the molecule relaxes it emits a photon and it returns to a different rotational or vibrational state. The difference in energy between the original state and this new state leads to a shift in the emitted photon's frequency away from the excitation wavelength. The Raman effect, which is a light scattering phenomenon, should not be confused with absorption (as with fluorescence) where the molecule is excited to a discrete (not virtual) energy level.

If the final vibrational state of the molecule is more energetic than the initial state, then the emitted photon will be shifted to a lower frequency in order for the total energy of the system to remain balanced. This shift in frequency is designated as a Stokes shift. If the final vibrational state is less energetic than the initial state, then the emitted

photon will be shifted to a higher frequency, and this is designated as an Anti-Stokes shift. Raman scattering is an example of inelastic scattering because of the energy transfer between the photons and the molecules during their interaction.

A change in the molecular polarization potential — or amount of deformation of the electron cloud — with respect to the vibrational coordinate is required for a molecule to exhibit a Raman effect. The amount of the polarizability change will determine the Raman scattering intensity. The pattern of shifted frequencies is determined by the rotational and vibrational states of the sample.

## History

Although the inelastic scattering of light was predicted by Adolf Smekal in 1923, it is not until 1928 that it was observed in practice. The Raman effect was named after one of its discoverers, the Indian scientist Sir C. V. Raman who observed the effect by means of sunlight (1928, together with K. S. Krishnan and independently by Grigory Landsberg and Leonid Mandelstam).[1] Raman won the Nobel Prize in Physics in 1930 for this discovery accomplished using sunlight, a narrow band photographic filter to create monochromatic light and a "crossed" filter to block this monochromatic light. He found that light of changed frequency passed through the "crossed" filter.

Systematic pioneering theory of the Raman effect was developed by Czechoslovak physicist George Placzek between 1930 and 1934.[2] The mercury arc became the principal light source, first with photographic detection and then with spectrophotometric detection. At the present time, lasers are used as light sources.

## Raman spectra

Raman spectra are typically expressed in wavenumbers, which have units of inverse length. In order to convert between spectral wavelength and wavenumbers of shift in the Raman spectrum, the following formula can be used:

$$\Delta w = \left( \frac{1}{\lambda_0} - \frac{1}{\lambda_1} \right) \ ,$$

where $\Delta w$ is the Raman shift expressed in wavenumber, $\lambda_0$ is the excitation wavelength, and $\lambda_1$ is the Raman spectrum wavelength. Most commonly, the units chosen for expressing wavenumber in Raman spectra is inverse centimeters ($cm^{-1}$). Since wavelength is often expressed in units of nanometers (nm), the formula above can scale for this units conversion explicitly, giving

$$\Delta w(\mathrm{cm}^{-1}) = \left( \frac{1}{\lambda_0(\mathrm{nm})} - \frac{1}{\lambda_1(\mathrm{nm})} \right) \times 10^7 \frac{(\mathrm{nm})}{(\mathrm{cm})},$$

## Applications

Raman spectroscopy is commonly used in chemistry, since vibrational information is specific to the chemical bonds and symmetry of molecules. Therefore, it provides a fingerprint by which the molecule can be identified. For instance, the vibrational frequencies of SiO, $Si_2O_2$, and $Si_3O_3$ were identified and assigned on the basis of normal coordinate analyses using infrared and Raman spectra.[3] The fingerprint region of organic molecules is in the (wavenumber) range 500–2000 $cm^{-1}$. Another way that the technique is used to study changes in chemical bonding, e.g., when a substrate is added to an enzyme.

Raman gas analyzers have many practical applications. For instance, they are used in medicine for real-time monitoring of anaesthetic and respiratory gas mixtures during surgery.

In solid state physics, spontaneous Raman spectroscopy is used to, among other things, characterize materials, measure temperature, and find the crystallographic orientation of a sample. As with single molecules, a given solid material has characteristic phonon modes that can help an experimenter identify it. In addition, Raman spectroscopy can be used to observe other low frequency excitations of the solid, such as plasmons, magnons, and

superconducting gap excitations. The spontaneous Raman signal gives information on the population of a given phonon mode in the ratio between the Stokes (downshifted) intensity and anti-Stokes (upshifted) intensity.

Raman scattering by an anisotropic crystal gives information on the crystal orientation. The polarization of the Raman scattered light with respect to the crystal and the polarization of the laser light can be used to find the orientation of the crystal, if the crystal structure (to be specific, its point group) is known.

Raman active fibers, such as aramid and carbon, have vibrational modes that show a shift in Raman frequency with applied stress. Polypropylene fibers also exhibit similar shifts. The radial breathing mode is a commonly used technique to evaluate the diameter of carbon nanotubes. In nanotechnology, a Raman microscope can be used to analyze nanowires to better understand the composition of the structures.

Spatially-offset Raman spectroscopy (SORS), which is less sensitive to surface layers than conventional Raman, can be used to discover counterfeit drugs without opening their internal packaging, and for non-invasive monitoring of biological tissue.[4] Raman spectroscopy can be used to investigate the chemical composition of historical documents such as the Book of Kells and contribute to knowledge of the social and economic conditions at the time the documents were produced.[5] This is especially helpful because Raman spectroscopy offers a non-invasive way to determine the best course of preservation or conservation treatment for such materials.

Raman spectroscopy is being investigated as a means to detect explosives for airport security.[6]

Raman spectroscopy has also been used to confirm the prediction of existence of low-frequency phonons [7] in proteins and DNA (see, e.g., [8] [9] [10] [11] greatly stimulating the studies of low-frequency collective motion in proteins and DNA and their biological functions.[12] [13]

## Microspectroscopy

Raman spectroscopy offers several advantages for microscopic analysis. Since it is a scattering technique, specimens do not need to be fixed or sectioned. Raman spectra can be collected from a very small volume (< 1 μm in diameter); these spectra allow the identification of species present in that volume. Water does not generally interfere with Raman spectral analysis. Thus, Raman spectroscopy is suitable for the microscopic examination of minerals, materials such as polymers and ceramics, cells and proteins. A Raman microscope begins with a standard optical microscope, and adds an excitation laser, a monochromator, and a sensitive detector (such as a charge-coupled device (CCD), or photomultiplier tube (PMT)). FT-Raman has also been used with microscopes.

In *direct imaging*, the whole field of view is examined for scattering over a small range of wavenumbers (Raman shifts). For instance, a wavenumber characteristic for cholesterol could be used to record the distribution of cholesterol within a cell culture.

The other approach is *hyperspectral imaging* or *chemical imaging*, in which thousands of Raman spectra are acquired from all over the field of view. The data can then be used to generate images showing the location and amount of different components. Taking the cell culture example, a hyperspectral image could show the distribution of cholesterol, as well as proteins, nucleic acids, and fatty acids. Sophisticated signal- and image-processing techniques can be used to ignore the presence of water, culture media, buffers, and other interferents.

Raman microscopy, and in particular confocal microscopy, has very high spatial resolution. For example, the lateral and depth resolutions were 250 nm and 1.7 μm, respectively, using a confocal Raman microspectrometer with the 632.8 nm line from a Helium-Neon laser with a pinhole of 100 μm diameter. Since the objective lenses of microscopes focus the laser beam to several micrometres in diameter, the resulting photon flux is much higher than achieved in conventional Raman setups. This has the added benefit of enhanced fluorescence quenching. However, the high photon flux can also cause sample degradation, and for this reason some setups require a thermally conducting substrate (which acts as a heat sink) in order to mitigate this process.

By using Raman microspectroscopy, *in vivo* time- and space-resolved Raman spectra of microscopic regions of samples can be measured. As a result, the fluorescence of water, media, and buffers can be removed. Consequently

*in vivo* time- and space-resolved Raman spectroscopy is suitable to examine proteins, cells and organs.

Raman microscopy for biological and medical specimens generally uses near-infrared (NIR) lasers (785 nm diodes and 1064 nm Nd:YAG are especially common). This reduces the risk of damaging the specimen by applying higher energy wavelengths. However, the intensity of NIR Raman is low (owing to the $\omega^4$ dependence of Raman scattering intensity), and most detectors required very long collection times. Recently, more sensitive detectors have become available, making the technique better suited to general use. Raman microscopy of inorganic specimens, such as rocks and ceramics and polymers, can use a broader range of excitation wavelengths.[14]

## Polarized analysis

The polarization of the Raman scattered light also contains useful information. This property can be measured using (plane) polarized laser excitation and a polarization analyzer. Spectra acquired with the analyzer set at both perpendicular and parallel to the excitation plane can be used to calculate the depolarization ratio. Study of the technique is useful in teaching the connections between group theory, symmetry, Raman activity, and peaks in the corresponding Raman spectra.

The spectral information arising from this analysis gives insight into molecular orientation and vibrational symmetry. In essence, it allows the user to obtain valuable information relating to the molecular shape, for example in synthetic chemistry or polymorph analysis. It is often used to understand macromolecular orientation in crystal lattices, liquid crystals or polymer samples.[15]

## Variations

Several variations of Raman spectroscopy have been developed. The usual purpose is to enhance the sensitivity (e.g., surface-enhanced Raman), to improve the spatial resolution (Raman microscopy), or to acquire very specific information (resonance Raman).

- **Surface Enhanced Raman Spectroscopy (SERS)** - Normally done in a silver or gold colloid or a substrate containing silver or gold. Surface plasmons of silver and gold are excited by the laser, resulting in an increase in the electric fields surrounding the metal. Given that Raman intensities are proportional to the electric field, there is large increase in the measured signal (by up to $10^{11}$). This effect was originally observed by Martin Fleischmann but the prevailing explanation was proposed by Van Duyne in 1977.[16] A comprehensive theory of the effect is that given by Lombardi and Birke in 2008 called the a Unified Approach to Surface-Enhanced Raman Spectroscopy.[17]
- **Resonance Raman spectroscopy** - The excitation wavelength is matched to an electronic transition of the molecule or crystal, so that vibrational modes associated with the excited electronic state are greatly enhanced. This is useful for studying large molecules such as polypeptides, which might show hundreds of bands in "conventional" Raman spectra. It is also useful for associating normal modes with their observed frequency shifts.[18]
- **Surface-Enhanced Resonance Raman Spectroscopy (SERRS)** - A combination of SERS and resonance Raman spectroscopy that uses proximity to a surface to increase Raman intensity, and excitation wavelength matched to the maximum absorbance of the molecule being analysed.
- **Hyper Raman** - A non-linear effect in which the vibrational modes interact with the second harmonic of the excitation beam. This requires very high power, but allows the observation of vibrational modes that are normally "silent". It frequently relies on SERS-type enhancement to boost the sensitivity.[19]
- **Spontaneous Raman Spectroscopy** - Used to study the temperature dependence of the Raman spectra of molecules.
- **Optical Tweezers Raman Spectroscopy (OTRS)** - Used to study individual particles, and even biochemical processes in single cells trapped by optical tweezers.

- **Stimulated Raman Spectroscopy** - A spatially coincident, two color pulse (with polarization either parallel or perpendicular) transfers the population from ground to a rovibrationally excited state, if the difference in energy corresponds to an allowed Raman transition, and if neither frequency corresponds to an electronic resonance. Two photon UV ionization, applied after the population transfer but before relaxation, allows the intra-molecular or inter-molecular Raman spectrum of a gas or molecular cluster (indeed, a given conformation of molecular cluster) to be collected. This is a useful molecular dynamics technique.
- **Spatially Offset Raman Spectroscopy (SORS)** - The Raman scatter is collected from regions laterally offset away from the excitation laser spot, leading to significantly lower contributions from the surface layer than with traditional Raman spectroscopy.[20]
- **Coherent anti-Stokes Raman spectroscopy (CARS)** - Two laser beams are used to generate a coherent anti-Stokes frequency beam, which can be enhanced by resonance.
- **Raman optical activity (ROA)** - Measures vibrational optical activity by means of a small difference in the intensity of Raman scattering from chiral molecules in right- and left-circularly polarized incident light or, equivalently, a small circularly polarized component in the scattered light.[21]
- **Transmission Raman** - Allows probing of a significant bulk of a turbid material, such as powders, capsules, living tissue, etc. It was largely ignored following investigations in the late 1960s[22] but was rediscovered in 2006 as a means of rapid assay of pharmaceutical dosage forms.[23] There are also medical diagnostic applications.[24]
- **Inverse Raman spectroscopy**.
- **Tip-Enhanced Raman Spectroscopy (TERS)** - Uses a metallic (usually silver-/gold-coated AFM or STM) tip to enhance the Raman signals of molecules situated in its vicinity. The spatial resolution is approximately the size of the tip apex (20-30 nm). TERS has been shown to have sensitivity down to the single molecule level.

# References


[1] Gardiner, D.J. (1989). *Practical Raman spectroscopy*. Springer-Verlag. ISBN 978-0387502540.

[2] Placzek G.: "Rayleigh Streeung und Raman Effekt", In: Hdb. der Radiologie, Vol. VI., 2, 1934, p. 209

[3] Khanna, R.K. (1981). "Raman-spectroscopy of oligomeric SiO species isolated in solid methane". *Journal of Chemical Physics* **74**: 2108. doi:10.1063/1.441393.

[4] "Fake drugs caught inside the pack" (http://news.bbc.co.uk/2/hi/health/6314287.stm). BBC News. 2007-01-31. . Retrieved 2008-12-08.

[5] Irish classic is still a hit (in calfskin, not paperback) - New York Times (http://www.nytimes.com/2007/05/28/world/europe/28kells.html), nytimes.com

[6] Ben Vogel (29 August 2008). "Raman spectroscopy portends well for standoff explosives detection" (http://www.janes.com/news/transport/business/jar/jar080829_1_n.shtml). Jane's. . Retrieved 2008-08-29.

[7] Kuo-Chen Chou and Nian-Yi Chen (1977) The biological functions of low-frequency phonons. Scientia Sinica, 20, 447-457.

[8] Urabe, H., Tominaga, Y. and Kubota, K. (1983) Experimental evidence of collective vibrations in DNA double helix Raman spectroscopy. Journal of Chemical Physics, 78, 5937-5939.

[9] Chou, K.C. (1983) Identification of low-frequency modes in protein molecules. Biochemical Journal, 215, 465-469.

[10] Chou, K.C. (1984) Low-frequency vibration of DNA molecules. Biochemical Journal, 221, 27-31.

[11] Urabe, H., Sugawara, Y., Ataka, M. and Rupprecht, A. (1998) Low-frequency Raman spectra of lysozyme crystals and oriented DNA films: dynamics of crystal water. Biophys J, 74, 1533-1540.

[12] Kuo-Chen Chou (1988) Review: Low-frequency collective motion in biomacromolecules and its biological functions. Biophysical Chemistry, 30, 3-48.

[13] Chou, K.C. (1989) Low-frequency resonance and cooperativity of hemoglobin. Trends in Biochemical Sciences, 14, 212.

[14] Ellis DI, Goodacre R (August 2006). "Metabolic fingerprinting in disease diagnosis: biomedical applications of infrared and Raman spectroscopy". *Analyst* **131** (8): 875–85. doi:10.1039/b602376m. PMID 17028718.

[15] Khanna, R.K. (1957). *Evidence of ion-pairing in the polarized Raman spectra of a Ba2+CrO doped KI single crystal*. John Wiley & Sons, Ltd. doi:10.1002/jrs.1250040104.

[16] Jeanmaire DL, van Duyne RP (1977). "Surface Raman Electrochemistry Part I. Heterocyclic, Aromatic and Aliphatic Amines Adsorbed on the Anodized Silver Electrode". *Journal of Electroanalytical Chemistry* (Elsevier Sequouia S.A.) **84**: 1–20. doi:10.1016/S0022-0728(77)80224-6.

[17] Lombardi JR, Birke RL (2008). "A Unified Approach to Surface-Enhanced Raman Spectroscopy". *[Journal of Physical Chemistry C]* (American Chemical Society) **112**: 5605–5617. doi:10.1021/jp800167 CCC.

[18] Chao RS, Khanna RK, Lippincott ER (1974). "Theoretical and experimental resonance Raman intensities for the manganate ion". *J Raman Spectroscopy* **3**: 121. doi:10.1002/jrs.1250030203.

[19] Kneipp K, *et al.* (1999). "Surface-Enhanced Non-Linear Raman Scattering at the Single Molecule Level". *Chem. Phys.* **247**: 155–162. doi:10.1016/S0301-0104(99)00165-2.

[20] Matousek P, Clark IP, Draper ERC, *et al.* (2005). "Subsurface Probing in Diffusely Scattering Media using Spatially Offset Raman Spectroscopy". *Applied Spectroscopy* **59** (12): 393. doi:10.1366/000370205775142548. PMID 16390587.

[21] Barron LD, Hecht L, McColl IH, Blanch EW (2004). "Raman optical activity comes of age". *Molec. Phys.* **102** (8): 731–744. doi:10.1080/00268970410001704399.

[22] B. Schrader, G. Bergmann, Fresenius. Z. (1967). *Anal. Chem.*: 225–230.

[23] P. Matousek, A. W. Parker (2006). "Bulk Raman Analysis of Pharmaceutical Tablets". *Applied Spectroscopy* **60** (12): 1353–1357. doi:10.1366/000370206779321463. PMID 17217583.

[24] P. Matousek, N. Stone (2007). "Prospects for the diagnosis of breast cancer by noninvasive probing of calcifications using transmission Raman spectroscopy". *Journal of Biomedical Optics* **12** (2): 024008. doi:10.1117/1.2718934. PMID 17477723.

## External links

- Raman FAQs (frequently asked questions) (http://www.horiba.com/scientific/products/raman-spectroscopy/tutorial-faqs/raman-faqs/), horiba.com
- Raman on SiGe Superlattice (http://content.piacton.com/Uploads/Princeton/Documents/Library/UpdatedLibrary/Raman_on_SiGe_Superlattice_Using_TriVista.pdf), princetoninstruments.com
- An introduction to Raman spectroscopy (http://www.horiba.com/scientific/products/raman-spectroscopy/raman-resource/raman-tutorial/), horiba.com
- Raman Application examples (http://www.horiba.com/scientific/products/raman-spectroscopy/application-notes/), horiba.com
- An introduction on Raman Scattering (http://www.d3technologies.co.uk/en/10371.aspx), d3technologies.co.uk
- Raman Spectroscopy Applications (http://www.renishaw.com/en/raman-spectroscopy-applications--6259), renishaw.com
- Raman Data Search and Storage (http://ramandata.sourceforge.net) - The free application with a wonderful database of Raman data (vibrations, assignment) with storage function and Raman spectra (discussions) with search function. ramandata.sourceforge.net
- Romanian Database of Raman Spectroscopy (http://rdrs.uaic.ro) - This database contains mineral species (natural and synthetic) with description of crystal structure, sample image, number of sample, origin, Raman spectrum and vibrations, Raman discussion and references. Also, this site contains artefacts sample with sample image and pigment spectrum; black, red, white or blue pigment. rdrs.uaic.ro
- Chemical Imaging Without Dyeing (http://witec.de/en/download/Raman/ImagingMicroscopy04.pdf), witec.de
- DoITPoMS Teaching and Learning Package - Raman Spectroscopy (http://www.doitpoms.ac.uk/tlplib/raman/index.php) - an introduction, aimed at undergraduate level. doitpoms.ac.uk
- Raman Spectroscopy Tutorial (http://161.58.205.25/Raman_Spectroscopy/rtr-ramantutorial.php?ss=800) - A detailed explanation of Raman Spectroscopy including Resonance-Enhanced Raman Scattering and Surface-Enhanced Raman Scattering. 161.25.205.25
- The Science Show, ABC Radio National (http://www.abc.net.au/rn/science/ss/stories/s1581469.htm) - Interview with Scientist on NASA funded project to build Raman Spectrometer for the 2009 Mars mission: a cellular phone size device to detect almost any substance known, with commercial <USD$5000 commercial spin-off, prototyped by June 2006. abc.net.au/rn
- Raman spectroscopy for medical diagnosis (http://pubs.acs.org/subscribe/journals/ancham/79/i11/pdf/0607feature_griffiths.pdf) from the June 1, 2007 issue of *Analytical Chemistry* (http://pubs3.acs.org/acs/journals/toc.page?incoden=ancham&indecade=0&involume=79&inissue=11), pubs.acs.org

- Spontaneous Raman Scattering (SRS) (http://www.lavision.de/en/techniques/raman-scattering.php), lavision.de
- Painless laser device could spot early signs of disease (http://www.bbc.co.uk/news/science-environment-11390951), BBC News, 2010-09-26

# Microscope image processing

**Microscope image processing** is a broad term that covers the use of digital image processing techniques to process, analyze and present images obtained from a microscope. Such processing is now commonplace in a number of diverse fields such as medicine, biological research, cancer research, drug testing, metallurgy, etc. A number of manufacturers of microscopes now specifically design in features that allow the microscopes to interface to an image processing system.

## Image acquisition

Until the early 1990s, most image acquisition in video microscopy applications was typically done with an analog video camera, often simply closed circuit TV cameras. While this required the use of a frame grabber to digitize the images, video cameras provided images at full video frame rate (25-30 frames per second) allowing live video recording and processing. While the advent of solid state detectors yielded several advantages, the real-time video camera was actually superior in many respects.

Today, acquisition is usually done using a CCD camera mounted in the optical path of the microscope. The camera may be full colour or monochrome. Very often, very high resolution cameras are employed to gain as much direct information as possible. Cryogenic cooling is also common, to minimise noise. Often digital cameras used for this application provide pixel intensity data to a resolution of 12-16 bits, much higher than is used in consumer imaging products.

Ironically, in recent years, much effort has been put into acquiring data at video rates, or higher (25-30 frames per second or higher). What was once easy with off-the-shelf video cameras now requires special, high speed electronics to handle the vast digital data bandwidth.

Higher speed acquisition allows dynamic processes to be observed in real time, or stored for later playback and analysis. Combined with the high image resolution, this approach can generate vast quantities of raw data, which can be a challenge to deal with, even with a modern computer system.

It should be observed that while current CCD detectors allow very high image resolution, often this involves a trade-off because, for a given chip size, as the pixel count increases, the pixel size decreases. As the pixels get smaller, their well depth decreases, reducing the number of electrons that can be stored. In turn, this results in a poorer signal to noise ratio.

For best results, one must select an appropriate sensor for a given application. Because microscope images have an intrinsic limiting resolution, it often makes little sense to use a noisy, high resolution detector for image acquisition. A more modest detector, with larger pixels, can often produce much higher quality images because of reduced noise. This is especially important in low-light applications such as fluorescence microscopy.

Moreover, one must also consider the temporal resolution requirements of the application. A lower resolution detector will often have a significantly higher acquisition rate, permitting the observation of faster events. Conversely, if the observed object is motionless, one may wish to acquire images at the highest possible spatial resolution without regard to the time required to acquire a single image.

## 2D image techniques

Image processing for microscopy application begins with fundamental techniques intended to most accurately reproduce the information contained in the microscopic sample. This might include adjusting the brightness and contrast of the image, averaging images to reduce image noise and correcting for illumination non-uniformities. Such processing involves only basic arithmetic operations between images (i.e. addition, subtraction, multiplication and division). The vast majority of processing done on microscope image is of this nature.

Another class of common 2D operations called image convolution are often used to reduce or enhance image details. Such "blurring" and "sharpening" algorithms in most programs work by altering a pixel's value based on a weighted sum of that and the surrounding pixels. (a more detailed description of kernel based convolution deserves an entry for itself).

Other basic two dimensional techniques include operations such as image rotation, warping, color balancing etc.

At times, advanced techniques are employed with the goal of "undoing" the distortion of the optical path of the microscope, thus eliminating distortions and blurring caused by the instrumentation. This process is called deconvolution, and a variety of algorithms have been developed, some of great mathematical complexity. The end result is an image far sharper and clearer than could be obtained in the optical domain alone. This is typically a 3-dimensional operation, that analyzes a volumetric image (i.e. images taken at a variety of focal planes through the sample) and uses this data to reconstruct a more accurate 3-dimensional image. vaya mudura kalutha vaya

## 3D image techniques

Another common requirement is to take a series of images at a fixed position, but at different focal depths. Since most microscopic samples are essentially transparent, and the depth of field of the focused sample is exceptionally narrow, it is possible to capture images "through" a three-dimensional object using 2D equipment like confocal microscopes. Software is then able to reconstruct a 3D model of the original sample which may be manipulated appropriately. The processing turns a 2D instrument into a 3D instrument, which would not otherwise exist. In recent times this technique has led to a number of scientific discoveries in cell biology.

## Analysis

Analysis of images will vary considerably according to application. Typical analysis includes determining where the edges of an object are, counting similar objects, calculating the area, perimeter length and other useful measurements of each object. A common approach is to create an image mask which only includes pixels that match certain criteria, then perform simpler scanning operations on the resulting mask. It is also possible to label objects and track their motion over a series of frames in a video sequence.

## References

Russ, John C. (2006-12-19) [1992]. *The Image Processing Handbook* (5th edition ed.). CRC Press. ISBN 0849372542.

- Jan-Mark Geusebroek, Color and Geometrical Structure in Images, Applications in Microscopy, ISBN 90-5776-057-6
- Young Ian T., Not just pretty pictures: Digital quantitative microscopy, Proc. Royal Microscopical Society, 1996, 31(4), pp. 311-313.
- Young Ian T., Quantitative Microscopy, IEEE Engineering in Medicine and Biology, 1996, 15(1), pp. 59-66.
- Young Ian T., Sampling density and quantitative microscopy, Analytical and Quantitative Cytology and Histology, vol. 10, 1988, pp. 269-275

## See also

- Image processing
- Endrov
- GemIdent

## External links

- Quantitative Microscopy [1]
- 3-D Image Processing in Microscopy [2]
- Sampling theorem [3] - Nyquist sampling in digital microscopy

## References

[1] http://www.ph.tn.tudelft.nl/People/young/manuscripts/QM/QM.html
[2] http://www.med.uni-giessen.de/ipl/iplcourse.html
[3] http://www.vanosta.be/pcrnyq.htm

# Electron microscopy

An **electron microscope** is a type of microscope that produces an electronically-magnified image of a specimen for detailed observation. The electron microscope (EM) uses a particle beam of electrons to illuminate the specimen and create a magnified image of it. The microscope has a greater resolving power than a light-powered optical microscope, because it uses electrons that have wavelengths about 100,000 times shorter than visible light (photons), and can achieve magnifications of up to 2,000,000x, whereas ordinary, non-confocal light microscopes are limited to 2000x magnification.

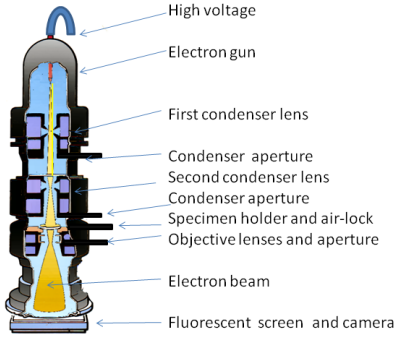


Diagram of a transmission electron microscope

The electron microscope uses electrostatic and electromagnetic "lenses" to control the electron beam and focus it to form an image. These lenses are analogous to, but different from the glass lenses of an optical microscope that form a magnified image by focusing light on or through the specimen. In transmission, the electron beam is first diffracted by the specimen, and then, the electron microscope “lenses" re-focus the beam into a Fourier-transformed image of the diffraction pattern for the selected area of investigation. The real image thus formed is a highly `magnified' image by a factor of several million, and can be then recorded on a special photographic plate, or viewed on a detecting screen. Electron microscopes are used to observe a wide range of biological and inorganic specimens including microorganisms, cells, large molecules, biopsy samples, metals, and crystals. Industrially, the electron microscope is primarily used for quality control and failure analysis in semiconductor device fabrication.

An electron microscope's advantages over X-ray crystallography are that the specimen need not be a single crystal or even a polycrystalline powder, and also that the Fourier transform reconstruction of the object's magnified structure occurs physically and thus avoids the need for solving the phase problem faced by the X-ray crystalographers after obatining their X-ray diffraction patterns of a single crystal or polycrystalline powder. The transmission electron microscope's major `disadvantage' is the need for extremely thin sections of the specimens, typically less than 10 nanometers. For biological specimens it also requires biological sample special `staining' with heavy atom labels in order to achieve the required contrast, and then chemical fixation as well as encasing with a polymer resin to stabilize the biological specimen which is thin sectioned.

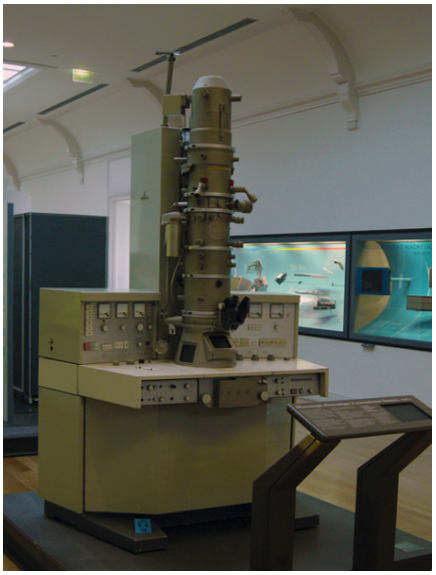

A 1973 Siemens electron microscope, Musée des Arts et Métiers, Paris

## History

In 1931, the German physicist Ernst Ruska and German electrical engineer Max Knoll constructed the prototype electron microscope, capable of four-hundred-power magnification; the apparatus was a practical application of the principles of electron microscopy.[1] Two years later, in 1933, Ruska built an electron microscope that exceeded the resolution attainable with an optical (lens) microscope.[1] Moreover, Reinhold Rudenberg, the scientific director of Siemens-Schuckertwerke, obtained the patent for the electron microscope in May 1931. Family illness compelled the electrical engineer to devise an electrostatic microscope, because he wanted to make visible the poliomyelitis virus.

In 1937, the Siemens company financed the development work of Ernst Ruska and Bodo von Borries, and employed Helmut Ruska (Ernst's brother) to develop applications for the microscope, especially with biologic specimens.[1] [2] Also in 1937, Manfred von Ardenne pioneered the scanning electron microscope.[3] The first *practical* electron microscope was constructed in 1938, at the University of Toronto, by Eli Franklin Burton and students Cecil Hall, James Hillier, and Albert Prebus; and Siemens produced the first *commercial* Transmission Electron Microscope (TEM) in 1939.[4] Although contemporary electron microscopes are capable of two million-power magnification, as scientific instruments, they remain based upon Ruska's prototype.

Electron microscope constructed by Ernst Ruska in 1933

# Types

### Transmission electron microscope (TEM)

The original form of electron microscope, the transmission electron microscope (TEM) uses a high voltage electron beam to create an image. The electrons are emitted by an electron gun, commonly fitted with a tungsten filament cathode as the electron source. The electron beam is accelerated by an anode typically at +100 keV (40 to 400 keV) with respect to the cathode, focused by electrostatic and electromagnetic lenses, and transmitted through the specimen that is in part transparent to electrons and in part scatters them out of the beam. When it emerges from the specimen, the electron beam carries information about the structure of the specimen that is magnified by the objective lens system of the microscope. The spatial variation in this information (the "image") is viewed by projecting the magnified electron image onto a fluorescent viewing screen coated with a phosphor or scintillator material such as zinc sulfide. The image can be photographically recorded by exposing a photographic film or plate directly to the electron beam, or a high-resolution phosphor may be coupled by means of a lens optical system or a fibre optic light-guide to the sensor of a CCD (charge-coupled device) camera. The image detected by the CCD may be displayed on a monitor or computer.

Resolution of the TEM is limited primarily by spherical aberration, but a new generation of aberration correctors have been able to partially overcome spherical aberration to increase resolution. Hardware correction of spherical aberration for the High Resolution TEM (HRTEM) has allowed the production of images with resolution below 0.5 Ångström (50 picometres)[5] at magnifications above 50 million times.[6] The ability to determine the positions of atoms within materials has made the HRTEM an important tool for nano-technologies research and development.[7]

### Scanning electron microscope (SEM)

Unlike the TEM, where electrons of the high voltage beam carry the image of the specimen, the electron beam of the Scanning Electron Microscope (SEM)[8] does not at any time carry a complete image of the specimen. The SEM produces images by probing the specimen with a focused electron beam that is scanned across a rectangular area of the specimen (raster scanning). At each point on the specimen the incident electron beam loses some energy, and that lost energy is converted into other forms, such as heat, emission of low-energy secondary electrons, light emission (cathodoluminescence) or x-ray emission. The display of the SEM maps the varying intensity of any of these signals into the image in a position corresponding to the position of the beam on the specimen when the signal was generated. In the SEM image of an ant shown at right, the image was constructed from signals produced by a secondary electron detector, the normal or conventional imaging mode in most SEMs.

An image of an ant in a scanning electron microscope

Generally, the image resolution of an SEM is about an order of magnitude poorer than that of a TEM. However, because the SEM image relies on surface processes rather than transmission, it is able to image bulk samples up to many centimetres in size and (depending on instrument design and settings) has a great depth of field, and so can produce images that are good representations of the three-dimensional shape of the sample.

### Reflection electron microscope (REM)

In the **Reflection Electron Microscope** (REM) as in the TEM, an electron beam is incident on a surface, but instead of using the transmission (TEM) or secondary electrons (SEM), the reflected beam of elastically scattered electrons is detected. This technique is typically coupled with Reflection High Energy Electron Diffraction (RHEED) and *Reflection high-energy loss spectrum (RHELS)*. Another variation is Spin-Polarized Low-Energy Electron Microscopy (SPLEEM), which is used for looking at the microstructure of magnetic domains.[9]

### Scanning transmission electron microscope (STEM)

The STEM rasters a focused incident probe across a specimen that (as with the TEM) has been thinned to facilitate detection of electrons scattered *through* the specimen. The high resolution of the TEM is thus possible in STEM. The focusing action (and aberrations) occur before the electrons hit the specimen in the STEM, but afterward in the TEM. The STEMs use of SEM-like beam rastering simplifies annular dark-field imaging, and other analytical techniques, but also means that image data is acquired in serial rather than in parallel fashion.

### Low voltage electron microscope (LVEM)

The low voltage electron microscope (LVEM) is a combination of SEM, TEM and STEM in one instrument, which operates at relatively low electron accelerating voltage of 5 kV. Low voltage increases image contrast which is especially important for biological specimens. This increase in contrast significantly reduces, or even eliminates the need to stain. Sectioned samples generally need to be thinner than they would be for conventional TEM (20-65 nm). Resolutions of a few nm are possible in TEM, SEM and STEM modes.[10] [11]

## Sample preparation

Materials to be viewed under an electron microscope may require processing to produce a suitable sample. The technique required varies depending on the specimen and the analysis required:

An insect coated in gold for viewing with a scanning electron microscope.

- *Chemical fixation* for biological specimens aims to stabilize the specimen's mobile macromolecular structure by chemical crosslinking of proteins with aldehydes such as formaldehyde and glutaraldehyde, and lipids with osmium tetroxide.
- *Cryofixation* – freezing a specimen so rapidly, to liquid nitrogen or even liquid helium temperatures, that the water forms vitreous (non-crystalline) ice. This preserves the specimen in a snapshot of its solution state. An entire field called cryo-electron microscopy has branched from this technique. With the development of cryo-electron microscopy of vitreous sections (CEMOVIS), it is now possible to observe samples from virtually any biological specimen close to its native state.
- *Dehydration* – freeze drying, or replacement of water with organic solvents such as ethanol or acetone, followed by critical point drying or infiltration with embedding resins.
- *Embedding, biological specimens* – after dehydration, tissue for observation in the transmission electron microscope is embedded so it can be sectioned ready for viewing. To do this the tissue is passed through a 'transition solvent' such as epoxy propane and then infiltrated with a resin such as Araldite epoxy resin; tissues may also be embedded directly in water-miscible acrylic resin. After the resin has been polymerised (hardened) the sample is thin sectioned (ultrathin sections) and stained - it is then ready for viewing.
- *Embedding, materials* - after embedding in resin, the specimen is usually ground and polished to a mirror-like finish using ultra-fine abrasives. The polishing process must be performed carefully to minimize scratches and

other polishing artifacts that reduce image quality.

- *Sectioning* – produces thin slices of specimen, semitransparent to electrons. These can be cut on an ultramicrotome with a diamond knife to produce ultrathin slices about 60-90 nm thick. Disposable glass knives are also used because they can be made in the lab and are much cheaper.
- *Staining* – uses heavy metals such as lead, uranium or tungsten to scatter imaging electrons and thus give contrast between different structures, since many (especially biological) materials are nearly "transparent" to electrons (weak phase objects). In biology, specimens are can be stained "en bloc" before embedding and also later after sectioning. Typically thin sections are stained for several minutes with an aqueous or alcoholic solution of uranyl acetate followed by aqueous lead citrate.
- *Freeze-fracture or freeze-etch* – a preparation method particularly useful for examining lipid membranes and their incorporated proteins in "face on" view. The fresh tissue or cell suspension is frozen rapidly (cryofixed), then fractured by simply breaking or by using a microtome while maintained at liquid nitrogen temperature. The cold fractured surface (sometimes "etched" by increasing the temperature to about −100 °C for several minutes to let some ice sublime) is then shadowed with evaporated platinum or gold at an average angle of 45° in a high vacuum evaporator. A second coat of carbon, evaporated perpendicular to the average surface plane is often performed to improve stability of the replica coating. The specimen is returned to room temperature and pressure, then the extremely fragile "pre-shadowed" metal replica of the fracture surface is released from the underlying biological material by careful chemical digestion with acids, hypochlorite solution or SDS detergent. The still-floating replica is thoroughly washed from residual chemicals, carefully fished up on fine grids, dried then viewed in the TEM.
- *Ion Beam Milling* – thins samples until they are transparent to electrons by firing ions (typically argon) at the surface from an angle and sputtering material from the surface. A subclass of this is Focused ion beam milling, where gallium ions are used to produce an electron transparent membrane in a specific region of the sample, for example through a device within a microprocessor. Ion beam milling may also be used for cross-section polishing prior to SEM analysis of materials that are difficult to prepare using mechanical polishing.
- *Conductive Coating* – an ultrathin coating of electrically-conducting material, deposited either by high vacuum evaporation or by low vacuum sputter coating of the sample. This is done to prevent the accumulation of static electric fields at the specimen due to the electron irradiation required during imaging. Such coatings include gold, gold/palladium, platinum, tungsten, graphite etc. and are especially important for the study of specimens with the scanning electron microscope. Another reason for coating, even when there is more than enough conductivity, is to improve contrast, a situation more common with the operation of a FESEM (field emission SEM).

## Disadvantages

Electron microscopes are expensive to build and maintain, but the capital and running costs of confocal light microscope systems now overlaps with those of basic electron microscopes. They are dynamic rather than static in their operation, requiring extremely stable high-voltage supplies, extremely stable currents to each electromagnetic coil/lens, continuously-pumped high- or ultra-high-vacuum systems, and a cooling water supply circulation through the lenses and pumps. As they are very sensitive to vibration and external magnetic fields, microscopes designed to achieve high resolutions must be housed in stable buildings (sometimes underground) with special services such as magnetic field cancelling systems. Some desktop low voltage electron microscopes have TEM capabilities at very low voltages (around 5 kV) without stringent voltage supply, lens coil current, cooling water or vibration isolation requirements and as such are much less expensive to buy and far easier to install and maintain, but do not have the same ultra-high (atomic scale) resolution capabilities as the larger instruments.

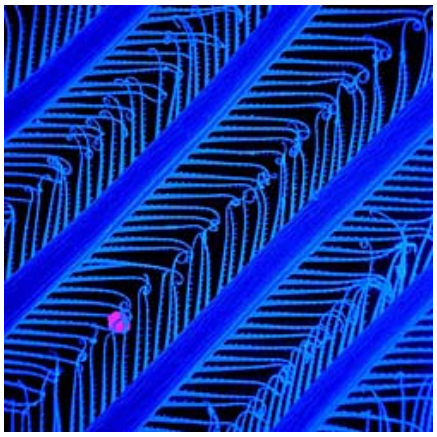

False-color SEM image of the filter setae of an Antarctic krill. (Raw electron microscope images carry no color information.)
**Pictured:** First degree filter setae with V-shaped second degree setae pointing towards the inside of the feeding basket. The purple ball is 1 μm in diameter.

The samples largely have to be viewed in vacuum, as the molecules that make up air would scatter the electrons. One exception is the environmental scanning electron microscope, which allows hydrated samples to be viewed in a low-pressure (up to 20 Torr/2.7 kPa), wet environment.

Scanning electron microscopes usually image conductive or semi-conductive materials best. Non-conductive materials can be imaged by an environmental scanning electron microscope. A common preparation technique is to coat the sample with a several-nanometer layer of conductive material, such as gold, from a sputtering machine; however, this process has the potential to disturb delicate samples.

Small, stable specimens such as carbon nanotubes, diatom frustules and small mineral crystals (asbestos fibres, for example) require no special treatment before being examined in the electron microscope. Samples of hydrated materials, including almost all biological specimens have to be prepared in various ways to stabilize them, reduce their thickness (ultrathin sectioning) and increase their electron optical contrast (staining). These processes may result in *artifacts*, but these can usually be identified by comparing the results obtained by using radically different specimen preparation methods. It is generally believed by scientists working in the field that as results from various preparation techniques have been compared and that there is no reason that they should all produce similar artifacts, it is reasonable to believe that electron microscopy features correspond with those of living cells. In addition, higher-resolution work has been directly compared to results from X-ray crystallography, providing independent confirmation of the validity of this technique. Since the 1980s, analysis of cryofixed, vitrified specimens has also become increasingly used by scientists, further confirming the validity of this technique.[12] [13] [14]

## Applications

Semiconductor and data storage

- Circuit edit
- Defect analysis
- Failure analysis

**Biology and life sciences**

- Diagnostic electron microscopy
- Cryobiology
- Protein localization
- Electron tomography
- Cellular tomography
- Cryo-electron microscopy
- Toxicology
- Biological production and viral load monitoring
- Particle analysis
- Pharmaceutical QC
- Structural biology
- 3D tissue imaging
- Virology
- Vitrification

Research

- Electron beam-induced deposition
- Materials qualification
- Materials and sample preparation
- Nanoprototyping
- Nanometrology
- Device testing and characterization

Industry

- High-resolution imaging
- 2D & 3D micro-characterization
- Macro sample to nanometer metrology
- Particle detection and characterization
- Direct beam-writing fabrication
- Dynamic materials experiments
- Sample preparation
- Forensics
- Mining (mineral liberation analysis)
- Chemical/Petrochemical

## See also

- Category:Electron microscope images
- Electron energy loss spectroscopy (EELS)
- Energy filtered transmission electron microscopy (EFTEM)
- Field emission microscope
- HiRISE
- High-resolution transmission electron microscopy (HRTEM)
- Scanning tunneling microscope
- Scanning confocal electron microscopy
- Scanning electron microscope (SEM)
- Scanning transmission electron microscope (STEM)
- Transmission Electron Aberration-corrected Microscope
- Electron diffraction
- X-ray diffraction
- X-ray microscope
- X-ray crystallography
- X-ray photoelectron spectroscopy (XPS)
- Microscope image processing
- Microscopy
- Acronyms in microscopy
- Nanoscience
- Nanotechnology
- Surface science
- *Ultramicroscopy* (journal)

## References


[1] Ernst Ruska (1986). "Ernst Ruska Autobiography" (http://nobelprize.org/nobel_prizes/physics/laureates/1986/ruska-autobio.html). Nobel Foundation. . Retrieved 2010-01-31.

[2] Kruger DH, Schneck P, Gelderblom HR (May 2000). "Helmut Ruska and the visualisation of viruses" (http://linkinghub.elsevier.com/retrieve/pii/S0140673600022509). *Lancet* **355** (9216): 1713–7. doi:10.1016/S0140-6736(00)02250-9. PMID 10905259. .

[3] M von Ardenne and D Beischer (1940). "Untersuchung von metalloxyd-rauchen mit dem universal-elektronenmikroskop" (in German). *Zeitschrift Electrochemie* **46**: 270–277.

[4] "James Hillier" (http://web.mit.edu/Invent/iow/hillier.html). *Inventor of the Week: Archive*. 2003-05-01. . Retrieved 2010-01-31.

[5] Erni, Rolf; Rossell, MD; Kisielowski, C; Dahmen, U (2009). "Atomic-Resolution Imaging with a Sub-50-pm Electron Probe". *Physical Review Letters* **102** (9): 096101. doi:10.1103/PhysRevLett.102.096101. PMID 19392535.

[6] "The Scale of Things" (http://www.sc.doe.gov/bes/scale_of_things.html). Office of Basic Energy Sciences, U.S. Department of Energy. 2006-05-26. . Retrieved 2010-01-31.

[7] O'Keefe MA, Allard LF (pdf). *Sub-Ångstrom Electron Microscopy for Sub-Ångstrom Nano-Metrology* (http://www.osti.gov/bridge/servlets/purl/821768-E3YVgN/native/821768.pdf). Information Bridge: DOE Scientific and Technical Information - Sponsored by OSTI. . Retrieved 2010-01-31.

[8] McMullan D (1993). "Scanning Electron Microscopy, 1928 - 1965" (http://www-g.eng.cam.ac.uk/125/achievements/mcmullan/mcm.htm). . Cincinnati, OH. . Retrieved 2010-01-31.

[9] "SPLEEM" (http://ncem.lbl.gov/frames/spleem.html). National Center for Electron Microscopy (NCEM). . Retrieved 2010-01-31.

[10] Nebesářová1, Jana; Vancová, Marie (2007). "How to Observe Small Biological Objects in Low Voltage Electron Microscope" (http://journals.cambridge.org/abstract_S143192760708124X). *Microscopy and Microanalysis* **13** (3): 248–249. .

[11] Drummy, Lawrence, F.; Yang, Junyan; Martin, David C. (2004). "Low-voltage electron microscopy of polymer and organic molecular thin films". *Ultramicroscopy* **99** (4): 247–256. doi:10.1016/j.ultramic.2004.01.011. PMID 15149719.

[12] Adrian, Marc; Dubochet, Jacques; Lepault, Jean; McDowall, Alasdair W. (1984). "Cryo-electron microscopy of viruses". *Nature* **308** (5954): 32–36. doi:10.1038/308032a0. PMID 6322001.

[13] Sabanay, I.; Arad, T.; Weiner, S.; Geiger, B. (1991). "Study of vitrified, unstained frozen tissue sections by cryoimmunoelectron microscopy" (http://jcs.biologists.org/cgi/content/abstract/100/1/227). *Journal of Cell Science* **100** (1): 227–236. PMID 1795028. .

[14] Kasas, S.; Dumas, G.; Dietler, G.; Catsicas, S.; Adrian, M. (2003). "Vitrification of cryoelectron microscopy specimens revealed by high-speed photographic imaging". *Journal of Microscopy* **211** (1): 48–53. doi:10.1046/j.1365-2818.2003.01193.x.


## External links

- Science Aid: Electron Microscopy (http://scienceaid.co.uk/biology/cell/analysingcells.html) High School (GCSE, A Level) resource
- Cell Centered Database - Electron microscopy data (http://ccdb.ucsd.edu/sand/main?typeid=4&event=showMPByType&start=1)

### General

- Nanohedron.com|Nano image gallery (http://www.nanohedron.com/) beautiful images generated with electron microscopes.
- electron microscopy (http://www.microscopy.ethz.ch) Website of the ETH Zurich: Very good graphics and images, which illustrate various procedures.
- Environmental Scanning Electron Microscope (ESEM) (http://www.danilatos.com)
- X-ray element analysis in electron microscope (http://www.microanalyst.net/index_e.phtml) – Information portal with X-ray microanalysis and EDX contents

### History

- John H.L. Watson: Very early Electron Microscopy in the Department of Physics, the University of Toronto – A personal recollection (http://www.physics.utoronto.ca/overview/history/microsco)
- Rubin Borasky Electron Microscopy Collection, 1930-1988 (http://americanhistory.si.edu/archives/d8452.htm) Archives Center, National Museum of American History, Smithsonian Institution.

### Other

- The Royal Microscopical Society, Electron Microscopy Section (UK) (http://www.rms.org.uk/em.shtml)
- Albert Lleal micrograph. Scanning Electron Micrograph Coloured SEM (http://www.albertlleal.com/microphotography.html)

# Diagnostic electron microscopy

The transmission electron microscope (TEM) is used as an important diagnostic tool to screen human tissues at high magnification (the ultrastructural level), often in conjunction with other methods, particularly light microscopy and immunofluorescence techniques. The TEM was first used extensively for this purpose in the 1980s, especially for identifying the markers of cell differentiation to identify tumours, and in renal disease. Immunolabelling techniques are now generally used instead of the TEM for tumour diagnosis but the technique retains a critical role in the diagnosis of renal disease and a range of other conditions.

Specifically, TEM should be used for diagnostic purposes when it: (1) provides useful (complementary) information in the context of a carefully considered differential diagnosis; (2) provides an 'improved' diagnosis that results in better treatment strategies and; (3) is time & cost effective in respect to alternative techniques. For diagnostic purposes solid tissues are prepared for TEM in the same way as other biological tissues, they are fixed in glutaraldehyde and osmium tetroxide then dehydrated and embedded in epoxy resin. The epoxy resin block is trimmed and the target tissue is selected using a light microscope by viewing semithin sections stained with toluidine blue. The block is then retrimmed and the specific area for observation is ultrathin sectioned, preferably using a diamond knife. The ultrathin sections are collected on 3mm copper (mesh) grids and stained with uranyl acetate and lead citrate to make the contents of the tissue electron dense (and thus visible in the electron microscope).[1]

## References

[1] Woods AE, Stirling JW. 2008. Electron microscopy. In, Theory and Practice of Histological Techniques. Eds, Bancroft JD and Gamble M. 6th edition. Churchill Livingstone: pages 601-640

## External links

The Association of Clinical Electron Microscopists (UK) (http://www.acem.org.uk/)

# HiRISE

**High Resolution Imaging Science Experiment** is a camera on board the Mars Reconnaissance Orbiter. The 65 kg (143 lb), $40 million (USD) instrument was built under the direction of the University of Arizona's Lunar and Planetary Laboratory by Ball Aerospace & Technologies Corp.. It consists of a 0.5 m (19.7 in) aperture reflecting telescope, the largest of any deep space mission, which allows it to take pictures of Mars with resolutions up to 0.3 m/pixel, resolving objects below a meter across.

By 2010, HiRISE mapped about 1 percent of Martian surface at this quality.[1]

A worker prepares HiRISE before it is shipped for attachment to the spacecraft

## History

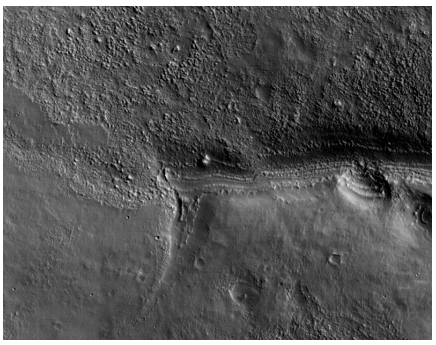

Crop of first image of Mars from the HiRISE camera

In the late 1980s, Alan Delamere of Ball Aerospace began planning the kind of high-resolution imaging needed to support sample return and surface exploration of Mars. In early 2001 he teamed up with Alfred McEwen of the University of Arizona to propose such a camera for the Mars Reconnaissance Orbiter (MRO), and NASA formally accepted it November 9, 2001.[2]

Ball Aerospace was given the responsibility to build the camera and they delivered HiRISE to NASA on December 6, 2004, for integration with the rest of the spacecraft.[3] It was prepared for launch on board the MRO on August 12, 2005, to the cheers of the HiRISE team who were present.[4]

During the cruise phase of MRO, HiRISE took several calibration shots including several of the Moon and the Jewel Box cluster. These images helped to calibrate the camera and prepare it for taking pictures of Mars.

On March 10, 2006, MRO achieved Martian orbit and primed HiRISE to acquire some initial images of Mars.[5] The instrument had two opportunities to take pictures of Mars (the first was on March 24, 2006) before MRO entered aerobraking, during which time the camera was turned off for six months.[6] It was turned on successfully September 27, and took its first high-resolution pictures of Mars on September 29.

Artist's rendition of HiRISE at Mars

On October 6, 2006 HiRISE took the first image of Victoria Crater, a site which is also under study by the Opportunity rover.[7]

In February 2007 seven detectors showed signs of degradation, with one IR channel almost completely degraded, and one other showing advanced signs of degradation. The problems appear to disappear when higher temperatures are used to take pictures with the camera.[8] As of March, the degradation appeared to have stabilized, but the underlying cause remained unknown.[9] Subsequent experiments with the Engineering Model (EM) at Ball Aerospace provided definitive evidence for the cause: contamination in the analog-to-digital converters (ADCs) which results in flipping bits to create the apparent noise or bad data in the images, combined with design flaws leading to delivery of poor analog waveforms to the ADCs. Further work showed that the degradation can be reversed by heating the ADCs.

On 2007-10-03, HiRISE was turned toward Earth, and took a picture of it and the Moon. In a full-resolution color image, Earth was 90 pixels across and the Moon was 24 pixels across from a distance of 142 million km.[10]

On May 25, 2008, HiRISE imaged NASA's Mars Phoenix Lander parachuting down to Mars. It was the first time that a spacecraft imaged the final descent of another spacecraft onto a planetary body.[11]

On April 1, 2010, NASA released the first images under the HiWish program in which just plain folk suggested places for HiRISE to photograph. One of the eight locations was Aureum Chaos.[12] The first image below gives a wide view of the area. The next two images are from the HiRISE image.[13]

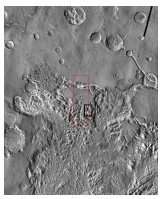

THEMIS image of wide view of following HiRISE images. Black box shows approximate location of HiRISE images. This image is just a part of the vast area know as Aureum Chaos. Click on image to see more details.

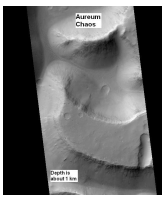


Aureum Chaos, as seen by HiRISE, under the HiWish program. Image is located in Margaritifer Sinus quadrangle.

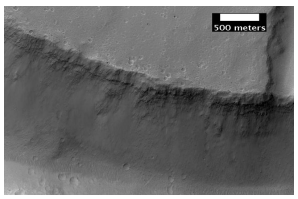


Close up view of previous image, as seen by HiRISE under HiWish program. Small round dots are boulders.

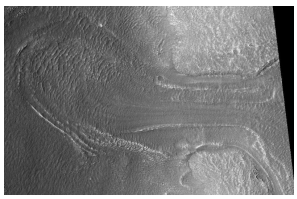

Probable glacier as seen by HiRISE under HiWish program. Radar studies have found that it is made up of almost completely pure ice. It appears to be moving from the high ground (a mesa) on the right. Location is Ismenius Lacus quadrangle.

## Purpose

The HiRISE camera is designed to view surface features of Mars in greater detail than has previously been possible.[14] This allows for the study of the age of Martian features, looking for landing sites for future Mars landers, and in general, seeing the Martian surface in far greater detail than has previously been done from orbit. By doing so, it is allowing better studies of Martian channels and valleys, volcanic landforms, possible former lakes and oceans, and other surface landforms as they exist on the Martian surface.[15]

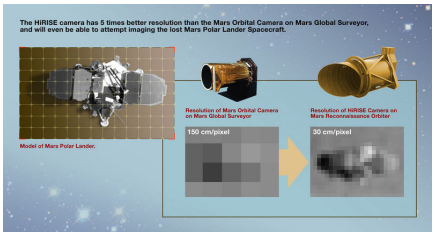


Comparison of resolution of MRO HiRISE camera with predecessor, the MOC aboard MGS

The general public will soon be allowed to request sites for the HiRISE camera to capture. For this reason, and due to the unprecedented access of pictures to the general public, shortly after they have been received and processed, the camera has been given the philosophy, "The People's Camera".[16]

## Design

HiRISE was designed to be a High Resolution camera from the beginning. It consists of a large mirror, as well as a large CCD camera. Because of this, it achieves a resolution of 1 microradian, or 0.3 meter at a height of 300 km. (For comparison purposes, satellite images on Google Maps are available to 1 meter.[17] ) It can image in three color bands, 400–600 nm (blue-green or B-G), 550–850 nm (red) and 800–1,000 nm (near infrared or NIR).[18]

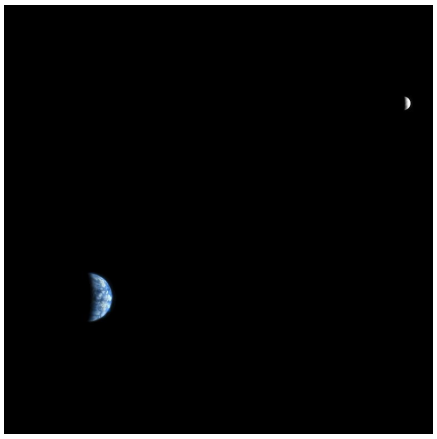

Earth and Moon from Mars Reconnaissance Orbiter taken by HiRISE

HiRISE incorporates a 0.5-meter primary mirror, the largest optical telescope ever sent beyond Earth's orbit. The mass of the instrument is 64.2 kg.[19]

Red color images are at 20,048 pixels wide (6 km in a 300 km orbit), and Green-Blue and NIR are at 4,048 pixels wide (1.2 km). HiRISE's onboard computer reads out these lines in time with the orbiter's ground speed, meaning the images are potentially unlimited in height. Practically this is limited by the onboard computer's 28 Gb memory capacity. The nominal maximum size of red images (compressed to 8 bits per pixel) is about 20,000 × 126,000 pixels, or 2520 megapixels and 4,000 × 126,000 pixels (504 megapixels) for the narrower images of the B-G and NIR bands. A single uncompressed image uses up to 28 Gb. However, these images are transmitted compressed,with a typical max size of 11.2 Gigabits. These images are released to the general public on the HiRISE website via a new format called JPEG 2000.[20] [21]

To facilitate the mapping of potential landing sites, HiRISE can produce stereo pairs of images from which the topography can be measured to an accuracy of 0.25 meter.

## Images naming conventions

HIRISE images are available to the public, so it can be useful to know how they are named. This is an excerpt from the official documentation [22]:

```
Name:
ppp_oooooo_tttt_ffff_c.IMG
```

```
ppp = Mission Phase:
  INT = Integration and Testing
  CAL = Calibration Observations
  ATL = ATLO Observations
  KSC = Kennedy Space Center Observations
  SVT = Sequence Verification Test
  LAU = Launch
  CRU = Cruise Observations
  APR = Mars Approach Observations
  AEB = Aerobraking Phase
  TRA = Transition Phase
  PSP = Primary Science Orbit (nov 2006-nov 2008)
  REL = Relay phase
  E01 = 1st Extended Mission Phase if needed
  Exx = Additional extended Missions if needed
```

```
oooooo = MRO orbit number
```

```
tttt = Target code
```

```
ffff Filter/CCD designation:
RED0-RED9 - Red filter CCDs
IR10-IR11 - Near-Infrared filter CCDs
BG12-BG13 - Blue-Green filter CCDs
```

```
c = Channel number of CCD (0 or 1)
```

The target code refers to the latitudinal position of the center of the planned observation relative to the start of orbit. The start of orbit is located at the equator on the descending side (night side) of the orbit. A target code of 0000 refers to the start of orbit. The target code increases in value along the orbit track ranging from 0000 to 3595. This convention allows the file name ordering to be time sequential. The first three digits refers to the number of whole degrees from the start of orbit, the fourth digit refers to the fractional degrees rounded to the nearest 0.5 degrees. Values greater than 3595 identify observations as off-Mars or special observations.

Examples of target code:

```
0000 - planned observation at the equator on descending side of orbit.
0900 - planned observation at the south pole.
1800 - planned observation at the equator on the ascending side (day side) of the orbit.
2700 - planned observation at the north pole.
```

Off-Mars and Special Observations Values:

```
4000 - Star Observation
4001 - Phobos Observation
4002 - Deimos Observation
4003 - Special Calibration Observation
```

# Footnotes


[1] **Microsoft and NASA Bring Mars Down to Earth Through the WorldWide Telescope** (07.12.10) - NASA (http://www.nasa.gov/topics/nasalife/features/microsoft_ww_telescope.html)

[2] UANews (2001-11-09). "UA-Led Team's Ultra-High Resolution Camera Selected for 2005 Launch to Mars" (http://uanews.org/cgi-bin/WebObjects/UANews.woa/4/wa/MainStoryDetails?ArticleID=4493). Press release. . Retrieved 2006-06-08.

[3] UANews (2004-12-06). "Ultra-sharp, Mars-Bound HiRISE Camera Delivered" (http://uanews.org/cgi-bin/WebObjects/UANews.woa/4/wa/MainStoryDetails?ArticleID=10192). Press release. . Retrieved 2006-06-08.

[4] UANews (2005-08-08). "UA Team Cheers Launch of Mars Reconnaissance Orbiter, HiRISE" (http://uanews.org/cgi-bin/WebObjects/UANews.woa/4/wa/MainStoryDetails?ArticleID=11437). Press release. . Retrieved 2006-06-08.

[5] "Mars Reconnaissance Orbiter Successfully Enters Orbit Around Mars!" (http://web.archive.org/web/20060603061811/http://mars.jpl.nasa.gov/mro/mission/orbiter_update.html). *NASA MRO website*. Archived from the original (http://mars.jpl.nasa.gov/mro/mission/orbiter_update.html) on 2006-06-03. . Retrieved 2006-06-08.

[6] NASA (2006-03-24). "UA Team Cheers Launch of Mars Reconnaissance Orbiter, HiRISE" (http://mars.jpl.nasa.gov/mro/newsroom/pressreleases/20060324a.html). Press release. . Retrieved 2006-06-08.

[7] HiRISE | Victoria Crater at Meridiani Planum (TRA_000873_1780) (http://hiroc.lpl.arizona.edu/images/TRA/TRA_000873_1780/)

[8] NASA (2007-02-07). "Spacecraft Set to Reach Milestone, Reports Technical Glitches" (http://www.jpl.nasa.gov/news/news.cfm?release=2007-013). Press release. . Retrieved 2007-03-06.

[9] Shiga, David (16 March 2007). "Ailing Mars camera is stable – for now" (http://space.newscientist.com/article/dn11402-ailing-mars-camera-is-stable--for-now.html). NewScientist.com news service. . Retrieved 2007-03-18.

[10] "Earth and Moon as Seen from Mars" (http://www.nasa.gov/mission_pages/MRO/multimedia/mro20080303earth.html). NASA. 2008-03-03. . Retrieved 2008-06-21.

[11] "Camera on Mars Orbiter Snaps Phoenix During Landing" (http://www.jpl.nasa.gov/news/phoenix/release.php?ArticleID=1714). *JPL website*. . Retrieved 2008-05-28.

[12] http://uahirise.org/releases/hiwish-captions.php
[13] http://hirise.lpl.arizona.edu/ESP_016869_1775
[14] Alan Delamere (2003) (PDF). *MRO HiRISE: Instrument Development* (http://marsoweb.nas.nasa.gov/HiRISE/papers/6th_int_mars_conf/Delamere_HiRISE_InstDev.pdf). 6th International Mars Conference. . Retrieved 2008-05-25.
[15] "Science Goals" (http://hirise.lpl.arizona.edu). Lunar and Planetary Laboratory, University of Arizona. . Retrieved June 7, 2006.
[16] "HiRISE" (http://hirise.lpl.arizona.edu). Lunar and Planetary Laboratory, University of Arizona. . Retrieved 19 March 2006.
[17] " Google Earth FAQ (http://earth.google.com/faq.html#4)" *Google Earth Website*.
[18] "MRO HiRISE Camera Specifications" (http://marsoweb.nas.nasa.gov/HiRISE/instrument.html#components). *HiRISE website*. . Retrieved 2 January 2006.
[19] Mission to Mars: the HiRISE camera on-board MRO (http://cat.inist.fr/?aModele=afficheN&cpsidt=20649610), *Focal plane arrays for space telescopes III,* 27–28 August 2007, San Diego, California, USA
[20] "HiRISE: Instrument Development" (http://marsoweb.nas.nasa.gov/HiRISE/papers/6th_int_mars_conf/Delamere_HiRISE_InstDev.pdf) (PDF). *NASA Ames Research Center website*. . Retrieved 7 February 2006.
[21] "Fact Sheet: HiRISE" (http://www.nasm.si.edu/research/ceps/cepsicons/highlights/fact_sheet_front.pdf) (PDF). *National Air and Space Museum*. . Retrieved 18 February 2006.
[22] http://hirise.lpl.arizona.edu/pdf/HiRISE_EDR_SIS_2007_03_15.pdf

## External links

- HiRISE official website (http://hirise.lpl.arizona.edu/)
- HiBlog, the official HiRISE blog (http://hirise.lpl.arizona.edu/HiBlog/)
- Help NASA categorize images taken by HiRISE (http://clickworkers.arc.nasa.gov/hirise)
- Patterns of Mars - 12 High Resolution Photos by HiRISE on www.time.com (http://feeds.feedburner.com/~r/time/topstories/~3/365740126/0,29307,1827176,00.html)
- Browse Map of Images (http://global-data.mars.asu.edu/bin/hirise.pl) from ASU.

# Scanning confocal electron microscopy

**Scanning confocal electron microscopy** (**SCEM**) is an electron microscopy technique analogous to scanning confocal optical microscopy (SCOM). In this technique, the studied sample is illuminated by a focussed electron beam, as in other scanning microscopy techniques, such as scanning transmission electron microscopy or scanning electron microscopy. However, in SCEM, the collection optics is arranged symmetrically to the illumination optics to gather only the electrons that pass the beam focus. This results in superior depth resolution of the imaging. The technique is relatively new and is being actively developed.

## History

The idea of SCEM logically follows from SCOM and thus is rather old. However, practical design and construction of scanning confocal electron microscope is a complex problem first solved by Nestor J. Zaluzec.[1] [2] [3] [4] His first scanning confocal electron microscope demonstrated the 3D properties of the SCEM, but have not realized the sub-nanometer lateral spatial resolution achievable with high-energy electrons (lateral resolution of only ~80 nm has been demonstrated). Several groups are currently working on construction of atomic resolution SCEM.[5] In particular, atomically resolved SCEM images have already been obtained [6] [7]

## Operation

The sample is illuminated by a focussed electron beam, and the beam is re-focussed on the detector, thus collecting only electrons passing through the focus. In order to produce an image, the beam should be laterally scanned. In the original design, this was achieved by placing synchronized scanning and descanning deflectors. Such design is complex and only a few custom-built setups exist. Another approach is to use stationary illumination and collection, but perform scan by moving the sample with a high-precision piezo-controlled holder. Such holders are readily available and can fit into most commercial electron microscopes thereby realizing the SCEM mode. As a practical demonstration, atomically resolved SCEM images have been recorded.[6] [7]

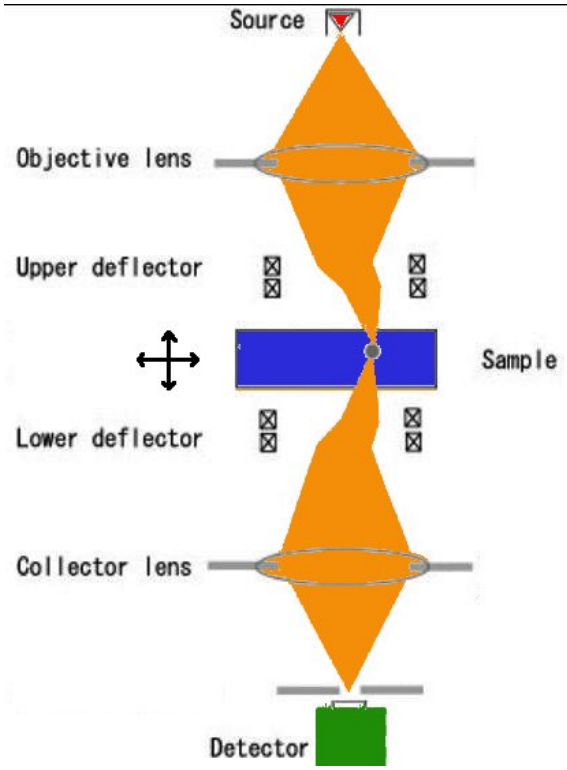

Schematic of SCEM

## Advantages of SCEM

High energies of incident particles (200 keV electrons vs. 2 eV photons) result in much higher spatial resolution of SCEM as compared to SCOM (lateral resolution <1 nm vs. >400 nm).

As compared to conventional electron microscopy (TEM, STEM, SEM), SCEM offers 3-dimensional imaging. 3D imaging in SCEM was expected from the confocal geometry of SCEM, and it has recently been confirmed by theoretical modeling.[8] In particular, it is predicted that a heavy layer (gold) can be identified in light matrix (aluminum) with ~10 nm precision in depth; this depth resolution is limited by the convergence angle of the electron beam and could be improved to a few nanometers in next-generation electron microscopes equipped with two fifth-order spherical aberration correctors.[9] [10]

## References

[1] N.J. Zaluzec, US Patent # 6,548,810 -0, 2003

[2] N.J. Zaluzec (2003). "The Scanning Confocal Electron Microscope" (http://www.amc.anl.gov/Docs/ANL/SCEM/MToday-SCEM-Article.pdf). *Microsc. Today* **6**: 8. .

[3] N.J. Zaluzec (2007). "Scanning Confocal Electron Microscopy". *Microsc. Microanal.* **13**: 1560. doi:10.1017/S1431927607074004.

[4] S.P. Frigo, Z.H. Levine, N.J. Zaluzec (2002). "Submicron imaging of buried integrated circuit structures using scanning confocal electron microscopy" (http://link.aip.org/link/?APPLAB/81/2112/1). *Appl. Phys. Lett.* **81**: 2112. doi:10.1063/1.1506010. .

[5] "Dr. Peter Nellist" (http://www.materials.ox.ac.uk/peoplepages/nellist.html). . Retrieved 2009-06-06.

[6] A. Hashimoto *et al.* (2008). "Development of Stage-scanning System for Confocal Scanning Transmission Electron Microscopy" (http://www.jstage.jst.go.jp/article/ejssnt/6/0/111/_pdf). *E-J. Surf. Sci. Nanotech.* **6**: 111–114. doi:10.1380/ejssnt.2008.111. .

[7] M. Takeguchi *et al.* (2008). *J. Elec. Microscopy* **57**: 123.

[8] K. Mitsuishi *et al.* (2008). "Bloch wave-based calculation of imaging properties of high-resolution scanning confocal electron microscopy". *Ultramicroscopy* **108** (9): 981. doi:10.1016/j.ultramic.2008.04.005. PMID 18519159.

[9] P. D. Nellist *et al.* (=2006). "Confocal operation of a transmission electron microscope with two aberration correctors" (http://link.aip.org/link/?APPLAB/89/124105/1). *Appl. Phys. Lett.* **89**: 124105. .

[10] *Jeol News* **39** (1). 2004.

## See also

- Confocal microscopy
- Confocal laser scanning microscopy
- Electron microscopy
- Scanning electron microscope
- Scanning transmission electron microscopy
- Transmission electron microscopy

# Acronyms in microscopy

List of materials analysis methods:

**Contents:** Top · 0–9 · A B C D E F G H I J K L M N O P Q R S T U V W X Y Z

- **μSR** - see Muon spin spectroscopy
- **χ** - see Magnetic susceptibility

## A

- **Analytical ultracentrifugation** - Analytical ultracentrifugation
- **AAS** - Atomic absorption spectroscopy
- **AED** - Auger electron diffraction
- **AES** - Auger electron spectroscopy
- **AFM** - Atomic force microscopy
- **AFS** - Atomic fluorescence spectroscopy
- **APFIM** - Atom probe field ion microscopy
- **APS** - Appearance potential spectroscopy
- **ARPES** - Angle resolved photoemission spectroscopy
- **ARUPS** - Angle resolved ultraviolet photoemission spectroscopy
- **ATR** - Attenuated total reflectance

## B

- **BET** - BET surface area measurement (BET from Brunauer, Emmett, Teller)
- **BiFC** - Bimolecular fluorescence complementation
- **BKD** - Backscatter Kikuchi diffraction, see **EBSD**
- **BRET** - Bioluminescence resonance energy transfer
- **BSED** - Back scattered electron diffraction, see **EBSD**

## C

- **CAICISS** - Coaxial impact collision ion scattering spectroscopy
- **CARS** - Coherent anti-Stokes Raman spectroscopy
- **CBED** - Convergent beam electron diffraction
- **CCM** - Charge collection microscopy
- **CDI** - Coherent diffraction imaging
- **CE** - Capillary electrophoresis
- **CET** - Cryo-electron tomography
- **CL** - Cathodoluminescence
- **CLSM** - Confocal laser scanning microscopy
- **COSY** - Correlation spectroscopy
- **Cryo-EM** - Cryo-electron microscopy
- **CV** - Cyclic voltammetry

## D

- **DE(T)A** - Dielectric thermal analysis
- **dHvA** - De Haas-van Alphen effect
- **DIC** - Differential interference contrast microscopy
- **Dielectric spectroscopy** - Dielectric spectroscopy
- **DLS** - Dynamic light scattering
- **DLTS** - Deep-level transient spectroscopy
- **DMA** - Dynamic mechanical analysis
- **DPI** - Dual polarisation interferometry
- **DRS** - Differential reflectance spectroscopy
- **DSC** - Differential scanning calorimetry
- **DTA** - Differential thermal analysis
- **DVS** - Dynamic vapour sorption

## E

- **EBIC** - Electron beam induced current (and see IBIC: ion beam induced charge)
- **EBS** - Elastic (non-Rutherford) backscattering spectrometry (see RBS)
- **EBSD** - Electron backscatter diffraction
- **ECOSY** - Exclusive correlation spectroscopy
- **ECT** - Electrical capacitance tomography
- **EDAX** - Energy-dispersive analysis of x-rays
- **EDMR** - Electrically Detected Magnetic Resonance, see ESR or EPR
- **EDS** - Energy Dispersive Spectroscopy
- **EDX** - Energy dispersive X-ray spectroscopy
- **EELS** - Electron energy loss spectroscopy
- **EFTEM** - Energy filtered transmission electron microscopy
- **EID** - Electron induced desorption
- **EIT** and **ERT** - Electrical impedance tomography and Electrical resistivity tomography
- **EL** - Electroluminescence
- **Electron crystallography** - Electron crystallography
- **ELS** - Electrophoretic light scattering
- **ENDOR** - Electron nuclear double resonance, see ESR or EPR

- **EPMA** - Electron probe microanalysis
- **EPR** - Electron paramagnetic resonance spectroscopy
- **ERD** or **ERDA** - Elastic recoil detection or Elastic recoil detection analysis
- **ESCA** - Electron spectroscopy for chemical analysis* **see XPS**
- **ESD** - Electron stimulated desorption
- **ESEM** - Environmental scanning electron microscopy
- **ESI-MS** or **ES-MS** - Electrospray ionization mass spectrometry or Electrospray mass spectrometry
- **ESR** - Electron spin resonance spectroscopy
- **ESTM** - Electrochemical scanning tunneling microscopy
- **EXAFS** - Extended X-ray absorption fine structure
- **EXSY** - Exchange spectroscopy

## F

- **FCS** - Fluorescence correlation spectroscopy
- **FCCS** - Fluorescence cross-correlation spectroscopy
- **FEM** - Field emission microscopy
- **FIB** - Focused ion beam microscopy
- **FIM-AP** - Field ion microscopy–atom probe
- **Flow birefringence** - Flow birefringence
- **Fluorescence anisotropy** - Fluorescence anisotropy
- **FLIM** - Fluorescence lifetime imaging
- **Fluorescence microscopy** - Fluorescence microscopy
- **FRET** - Fluorescence resonance energy transfer
- **FRS** - Forward Recoil Spectrometry, a synonym of ERD
- **FTICR** or **FT-MS** - Fourier transform ion cyclotron resonance or Fourier transform mass spectrometry
- **FTIR** - Fourier transform infrared spectroscopy

## G

- **GC-MS** - Gas chromatography-mass spectrometry
- **GDMS** - Glow discharge mass spectrometry
- **GDOS** - Glow discharge optical spectroscopy
- **GISAXS** - Grazing incidence small angle X-ray scattering
- **GIXD** - Grazing incidence X-ray diffraction
- **GIXR** - Grazing incidence X-ray reflectivity
- **GLC** - Gas-liquid chromatography

## H

- **HAADF** - high angle annular dark-field imaging
- **HAS** - Helium atom scattering
- **HPLC** - High performance liquid chromatography
- **HREELS** - High resolution electron energy loss spectroscopy
- **HREM** - High-resolution electron microscopy
- **HRTEM** - High-resolution transmission electron microscopy

## I

- **IAES** - Ion induced Auger electron spectroscopy
- **IBA** - Ion beam analysis
- **IBIC** - Ion beam induced charge microscopy
- **ICP-AES** - Inductively_coupled_plasma_atomic_emission_spectroscopy
- **ICP-MS** - Inductively coupled plasma mass spectrometry
- **Immunofluorescence** - Immunofluorescence
- **ICR** - Ion cyclotron resonance
- **IETS** - Inelastic electron tunneling spectroscopy
- **IGA** - Intelligent gravimetric analysis
- **IIX** - Ion induced X-ray analysis: See Particle induced X-ray emission
- **INS** - Ion neutralization spectroscopy
  Inelastic neutron scattering
- **IRS** - Infrared spectroscopy
- **ISS** - Ion scattering spectroscopy
- **ITC** - Isothermal titration calorimetry
- **IVEM** - Intermediate voltage electron microscopy

## L

- List of materials analysis methods (deliberate self-link)
- **LALLS** - Low-angle laser light scattering
- **LC-MS** - Liquid chromatography-mass spectrometry
- **LEED** - Low-energy electron diffraction
- **LEEM** - Low-energy electron microscopy
- **LEIS** - Low-energy ion scattering
- **LIBS** - Laser induced breakdown spectroscopy
- **LOES** - Laser optical emission spectroscopy
- **LS** - Light (Raman) scattering

## M

- **MALDI** - Matrix-assisted laser desorption/ionization
- **MBE** - Molecular beam epitaxy
- **MEIS** - Medium energy ion scattering
- **MFM** - Magnetic force microscopy
- **MIT** - Magnetic induction tomography
- **MPM** - Multiphoton fluorescence microscopy
- **MRFM** - Magnetic resonance force microscopy
- **MRI** - Magnetic resonance imaging
- **MS** - Mass spectrometry
- **MS/MS** - Tandem mass spectrometry
- **Mössbauer spectroscopy** - Mössbauer spectroscopy
- **MTA** - Microthermal analysis

## N

- **NAA** - Neutron activation analysis
- **Nanovid microscopy** - Nanovid microscopy
- **ND** - Neutron diffraction
- **NDP** - Neutron depth profiling
- **NEXAFS** - Near edge X-ray absorption fine structure
- **NIS** - Nuclear inelastic scattering/absorption
- **NMR** - Nuclear magnetic resonance spectroscopy
- **NOESY** - Nuclear Overhauser effect spectroscopy
- **NRA** - Nuclear reaction analysis
- **NSOM** - Near-field optical microscopy

## O

- **OBIC** - Optical beam induced current
- **ODNMR** - Optically detected magnetic resonance, see ESR or EPR
- **OES** - Optical emission spectroscopy
- **Osmometry** - Osmometry

## P

- **PAS** - Positron annihilation spectroscopy
- **Photoacoustic spectroscopy** - Photoacoustic spectroscopy
- **PAT** or **PACT** - Photoacoustic tomography or photoacoustic computed tomography
- **PAX** - Photoemission of adsorbed xenon
- **PC or PCS** - Photocurrent spectroscopy
- **Phase contrast microscopy** - Phase contrast microscopy
- **PhD** - Photoelectron diffraction
- **PD** - Photodesorption
- **PDEIS** - Potentiodynamic electrochemical impedance spectroscopy
- **PDS** - Photothermal deflection spectroscopy
- **PED** - Photoelectron diffraction
- **PEELS** - parallel electron energy loss spectroscopy

- **PES** - Photoelectron spectroscopy
- **PINEM** - photon-induced near-field electron microscopy
- **PIGE** - Particle (or proton) induced gamma-ray spectroscopy, see Nuclear reaction analysis
- **PIXE** - Particle (or proton) induced X-ray spectroscopy
- **PL** - Photoluminescence
- **Porosimetry** - Porosimetry
- **Powder diffraction** - Powder diffraction
- **PTMS** - Photothermal microspectroscopy
- **PTS** - Photothermal spectroscopy

## Q

- **QENS** - Quasi-elastic neutron scattering

## R

- **Raman** - Raman spectroscopy
- **RAXRS** - Resonant anomalous X-ray scattering
- **RBS** - Rutherford backscattering spectrometry
- **REM** - Reflection electron microscopy
- **RDS** - Reflectance Difference Spectroscopy
- **RHEED** - Reflection high energy electron diffraction
- **RIXS** - Resonant inelastic X-ray scattering
- **RR spectroscopy** - Resonance Raman spectroscopy

## S

- **SAD** - Selected area diffraction
- **SAED** - Selected area electron diffraction
- **SAM** - Scanning Auger microscopy
- **SANS** - Small angle neutron scattering
- **SAXS** - Small angle X-ray scattering
- **SCANIIR** - Surface composition by analysis of neutral species and ion-impact radiation
- **SCEM** - Scanning confocal electron microscopy
- **SE** - Spectroscopic ellipsometry
- **SEC** - Size exclusion chromatography
- **SEIRA** - Surface enhanced infrared absorption spectroscopy
- **SEM** - Scanning electron microscopy
- **SERS** - Surface enhanced Raman spectroscopy
- **SERRS** - Surface enhanced resonance Raman spectroscopy
- **SEXAFS** - Surface extended X-ray absorption fine structure
- **SICM** - Scanning ion-conductance microscopy
- **SIL** - Solid immersion lens
- **SIM** - Solid immersion mirror
- **SIMS** - Secondary ion mass spectrometry
- **SNMS** - Sputtered neutral species mass spectroscopy
- **SNOM** - Scanning near-field optical microscopy
- **SPECT** - Single photon emission computed tomography
- **SPM** - Scanning probe microscopy

- **SRM-CE/MS** - Selected-reaction-monitoring capillary-electrophoresis mass-spectrometry
- **SSNMR** - Solid-state nuclear magnetic resonance
- **Stark spectroscopy** - Stark spectroscopy
- **STED** - Stimulated Emission Depletion microscopy
- **STEM** - Scanning transmission electron microscopy
- **STM** - Scanning tunneling microscopy
- **STS** - Scanning tunneling spectroscopy
- **SXRD** - Surface X-ray Diffraction (SXRD)

## T

- **TAT** or **TACT** - Thermoacoustic tomography or thermoacoustic computed tomography (see also photoacoustic tomography - PAT)
- **TEM** - transmission electron microscope/microscopy
- **TGA** - Thermogravimetric analysis
- **TIKA** - Transmitting ion kinetic analysis
- **TIRFM** - Total internal reflection fluorescence microscopy
- **TLS** - Photothermal lens spectroscopy, a type of Photothermal spectroscopy
- **TMA** - Thermomechanical analysis
- **TOF-MS** - Time-of-flight mass spectrometry
- **Two-photon excitation microscopy** - Two-photon excitation microscopy
- **TXRF** - Total reflection X-ray fluorescence analysis

## U

- **Ultrasound attenuation spectroscopy** - Ultrasound attenuation spectroscopy
- **Ultrasonic testing** - Ultrasonic testing
- **UPS** - UV-photoelectron spectroscopy

## V

- **VEDIC** - Video-enhanced differential interference contrast microscopy
- **Voltammetry** - Voltammetry

## W

- **WAXS** - Wide angle X-ray scattering
- **WDX or WDS** - Wavelength dispersive X-ray spectroscopy

## X

- **XAES** - X-ray induced Auger electron spectroscopy
- **XANES** - XANES, synonymous with NEXAFS (Near edge X-ray absorption fine structure)
- **XAS** - X-ray absorption spectroscopy
- **X-CTR** - X-ray crystal truncation rod scattering
- **X-ray crystallography** - X-ray crystallography
- **XDS** - X-ray diffuse scattering
- **XPEEM** - X-ray photoelectron emission microscopy
- **XPS** - X-ray photoelectron spectroscopy
- **XRD** - X-ray diffraction

- **XRES** - X-ray resonant exchange scattering
- **XRF** - X-ray fluorescence analysis
- **XRR** - X-ray reflectivity
- **XRS** - X-ray Raman scattering
- **XSW** - X-ray standing wave technique

## References


- Callister, WD (2000). *Materials Science and Engineering - An Introduction*. *John Wiley and Sons* : London. ISBN 0-471-32013-7.
- Yao, N, ed (2007). *Focused Ion Beam Systems: Basics and Applications*. *Cambridge University Press* : Cambridge, UK. ISBN 978-052183-1994.


# Nanoscience

Part of a series of articles on

History
Implications
Applications
Regulation
Organizations
Popular culture
List of topics

**Nanomaterials**

Fullerene
Carbon Nanotubes
Nanoparticles

**Nanomedicine**

Nanotoxicology
Nanosensor

**Molecular self-assembly**

Self-assembled monolayer
Supramolecular assembly
DNA nanotechnology

**Nanoelectronics**

Molecular electronics
Nanolithography

**Scanning probe microscopy**

Atomic force microscope
Scanning tunneling microscope

**Molecular nanotechnology**

Molecular assembler
Nanorobotics
Mechanosynthesis

**Nanotechnology Portal**

**Nanotechnology**, shortened to "**nanotech**", is the study of manipulating matter on an atomic and molecular scale. Generally nanotechnology deals with structures sized between 1 to 100 nanometer in at least one dimension, and involves developing materials or devices within that size. Quantum mechanical effects are very important at this scale.

Nanotechnology is very diverse, ranging from extensions of conventional device physics to completely new approaches based upon molecular self-assembly, from developing new materials with dimensions on the nanoscale to investigating whether we can directly control matter on the atomic scale.

There is much debate on the future implications of nanotechnology. Nanotechnology may be able to create many new materials and devices with a vast range of applications, such as in medicine, electronics, biomaterials and energy production. On the other hand, nanotechnology raises many of the same issues as any new technology, including concerns about the toxicity and environmental impact of nanomaterials,[1] and their potential effects on global economics, as well as speculation about various doomsday scenarios. These concerns have led to a debate among advocacy groups and governments on whether special regulation of nanotechnology is warranted.

## Origins

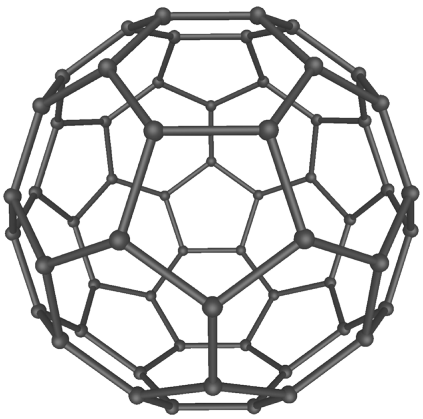

Buckminsterfullerene $C_{60}$, also known as the buckyball, is a representative member of the carbon structures known as fullerenes. Members of the fullerene family are a major subject of research falling under the nanotechnology umbrella.

The first use of the concepts found in 'nano-technology' (but pre-dating use of that name) was in "There's Plenty of Room at the Bottom", a talk given by physicist Richard Feynman at an American Physical Society meeting at Caltech on December 29, 1959. Feynman described a process by which the ability to manipulate individual atoms and molecules might be developed, using one set of precise tools to build and operate another proportionally smaller set, and so on down to the needed scale. In the course of this, he noted, scaling issues would arise from the changing magnitude of various physical phenomena: gravity would become less important, surface tension and van der Waals attraction would become increasingly more significant, etc. This basic idea appeared plausible, and exponential assembly enhances it with parallelism to produce a useful quantity of end products. The term "nanotechnology" was defined by Tokyo Science University Professor Norio Taniguchi in a 1974 paper[2] as follows: "'Nano-technology' mainly consists of the processing of, separation, consolidation, and deformation of materials by one atom or by one molecule." In the 1980s the basic idea of this definition was explored in much more depth by Dr. K. Eric Drexler, who promoted the technological significance of nano-scale phenomena and devices through speeches and the books Engines of Creation: The Coming Era of Nanotechnology (1986) and *Nanosystems: Molecular Machinery, Manufacturing, and Computation*,[3] and so the term acquired its current sense. Engines of Creation: The Coming Era of Nanotechnology is considered the first book on the topic of nanotechnology. Nanotechnology and nanoscience got started in the early 1980s with two major developments; the birth of cluster science and the invention of the scanning tunneling microscope (STM). This development led to the discovery of fullerenes in 1985 and carbon nanotubes a few years later. In another development, the synthesis and properties of semiconductor nanocrystals was studied; this led to a fast increasing number of metal and metal oxide nanoparticles and quantum dots. The atomic force microscope (AFM or SFM) was invented six years after the STM was invented. In 2000, the United States National Nanotechnology Initiative was founded to coordinate Federal nanotechnology research and development and is evaluated by the President's Council of Advisors on Science and Technology.

## Fundamental concepts

One nanometer (nm) is one billionth, or $10^{-9}$, of a meter. By comparison, typical carbon-carbon bond lengths, or the spacing between these atoms in a molecule, are in the range 0.12–0.15 nm, and a DNA double-helix has a diameter around 2 nm. On the other hand, the smallest cellular life-forms, the bacteria of the genus Mycoplasma, are around 200 nm in length.

To put that scale in another context, the comparative size of a nanometer to a meter is the same as that of a marble to the size of the earth.[4] Or another way of putting it: a nanometer is the amount an average man's beard grows in the time it takes him to raise the razor to his face.[4]

Two main approaches are used in nanotechnology. In the "bottom-up" approach, materials and devices are built from molecular components which assemble themselves chemically by principles of molecular recognition. In the "top-down" approach, nano-objects are constructed from larger entities without atomic-level control.[5]

Areas of physics such as nanoelectronics, nanomechanics, nanophotonics and nanoionics have evolved during the last few decades to provide a basic scientific foundation of nanotechnology.

### Larger to smaller: a materials perspective

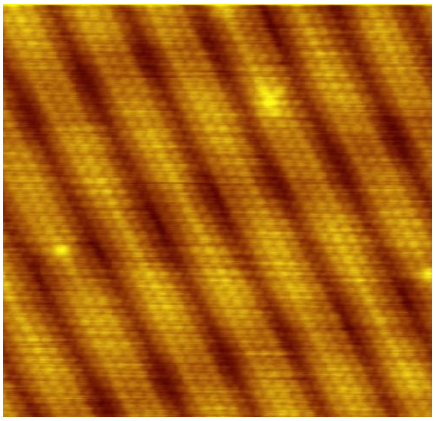

Image of reconstruction on a clean Gold(100) surface, as visualized using scanning tunneling microscopy. The positions of the individual atoms composing the surface are visible.

A number of physical phenomena become pronounced as the size of the system decreases. These include statistical mechanical effects, as well as quantum mechanical effects, for example the “quantum size effect” where the electronic properties of solids are altered with great reductions in particle size. This effect does not come into play by going from macro to micro dimensions. However, quantum effects become dominant when the nanometer size range is reached, typically at distances of 100 nanometers or less, the so called quantum realm. Additionally, a number of physical (mechanical, electrical, optical, etc.) properties change when compared to macroscopic systems. One example is the increase in surface area to volume ratio altering mechanical, thermal and catalytic properties of materials. Diffusion and reactions at nanoscale, nanostructures materials and nanodevices with fast ion transport are generally referred to nanoionics. *Mechanical* properties of nanosystems are of interest in the nanomechanics research. The catalytic activity of nanomaterials also opens potential risks in their interaction with biomaterials.[6]

Materials reduced to the nanoscale can show different properties compared to what they exhibit on a macroscale, enabling unique applications. For instance, opaque substances become transparent (copper); stable materials turn combustible (aluminum); insoluble materials become soluble (gold). A material such as gold, which is chemically inert at normal scales, can serve as a potent chemical catalyst at nanoscales. Much of the fascination with nanotechnology stems from these quantum and surface phenomena that matter exhibits at the nanoscale.[7]

### Simple to complex: a molecular perspective

Modern synthetic chemistry has reached the point where it is possible to prepare small molecules to almost any structure. These methods are used today to manufacture a wide variety of useful chemicals such as pharmaceuticals or commercial polymers. This ability raises the question of extending this kind of control to the next-larger level, seeking methods to assemble these single molecules into supramolecular assemblies consisting of many molecules arranged in a well defined manner.

These approaches utilize the concepts of molecular self-assembly and/or supramolecular chemistry to automatically arrange themselves into some useful conformation through a bottom-up approach. The concept of molecular

recognition is especially important: molecules can be designed so that a specific configuration or arrangement is favored due to non-covalent intermolecular forces. The Watson–Crick basepairing rules are a direct result of this, as is the specificity of an enzyme being targeted to a single substrate, or the specific folding of the protein itself. Thus, two or more components can be designed to be complementary and mutually attractive so that they make a more complex and useful whole.

Such bottom-up approaches should be capable of producing devices in parallel and be much cheaper than top-down methods, but could potentially be overwhelmed as the size and complexity of the desired assembly increases. Most useful structures require complex and thermodynamically unlikely arrangements of atoms. Nevertheless, there are many examples of self-assembly based on molecular recognition in biology, most notably Watson–Crick basepairing and enzyme-substrate interactions. The challenge for nanotechnology is whether these principles can be used to engineer new constructs in addition to natural ones.

## Molecular nanotechnology: a long-term view

Molecular nanotechnology, sometimes called molecular manufacturing, describes engineered nanosystems (nanoscale machines) operating on the molecular scale. Molecular nanotechnology is especially associated with the molecular assembler, a machine that can produce a desired structure or device atom-by-atom using the principles of mechanosynthesis. Manufacturing in the context of productive nanosystems is not related to, and should be clearly distinguished from, the conventional technologies used to manufacture nanomaterials such as carbon nanotubes and nanoparticles.

When the term "nanotechnology" was independently coined and popularized by Eric Drexler (who at the time was unaware of an earlier usage by Norio Taniguchi) it referred to a future manufacturing technology based on molecular machine systems. The premise was that molecular scale biological analogies of traditional machine components demonstrated molecular machines were possible: by the countless examples found in biology, it is known that sophisticated, stochastically optimised biological machines can be produced.

It is hoped that developments in nanotechnology will make possible their construction by some other means, perhaps using biomimetic principles. However, Drexler and other researchers[8] have proposed that advanced nanotechnology, although perhaps initially implemented by biomimetic means, ultimately could be based on mechanical engineering principles, namely, a manufacturing technology based on the mechanical functionality of these components (such as gears, bearings, motors, and structural members) that would enable programmable, positional assembly to atomic specification.[9] The physics and engineering performance of exemplar designs were analyzed in Drexler's book *Nanosystems*.

In general it is very difficult to assemble devices on the atomic scale, as all one has to position atoms on other atoms of comparable size and stickiness. Another view, put forth by Carlo Montemagno,[10] is that future nanosystems will be hybrids of silicon technology and biological molecular machines. Yet another view, put forward by the late Richard Smalley, is that mechanosynthesis is impossible due to the difficulties in mechanically manipulating individual molecules.

This led to an exchange of letters in the ACS publication Chemical & Engineering News in 2003.[11] Though biology clearly demonstrates that molecular machine systems are possible, non-biological molecular machines are today only in their infancy. Leaders in research on non-biological molecular machines are Dr. Alex Zettl and his colleagues at Lawrence Berkeley Laboratories and UC Berkeley. They have constructed at least three distinct molecular devices whose motion is controlled from the desktop with changing voltage: a nanotube nanomotor, a molecular actuator,[12] and a nanoelectromechanical relaxation oscillator.[13]

An experiment indicating that positional molecular assembly is possible was performed by Ho and Lee at Cornell University in 1999. They used a scanning tunneling microscope to move an individual carbon monoxide molecule (CO) to an individual iron atom (Fe) sitting on a flat silver crystal, and chemically bound the CO to the Fe by applying a voltage.

# Current research

## Nanomaterials

The nanomaterials field includes subfields which develop or study materials having unique properties arising from their nanoscale dimensions.[15]

- Interface and colloid science has given rise to many materials which may be useful in nanotechnology, such as carbon nanotubes and other fullerenes, and various nanoparticles and nanorods. Nanomaterials with fast ion transport are related also to nanoionics and nanoelectronics.
- Nanoscale materials can also be used for bulk applications; most present commercial applications of nanotechnology are of this flavor.
- Progress has been made in using these materials for medical applications; see Nanomedicine.
- Nanoscale materials are sometimes used in solar cells which combats the cost of traditional Silicon solar cells
- Development of applications incorporating semiconductor nanoparticles to be used in the next generation of products, such as display technology, lighting, solar cells and biological imaging; see quantum dots.

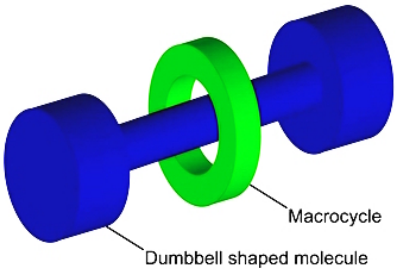


Graphical representation of a rotaxane, useful as a molecular switch.

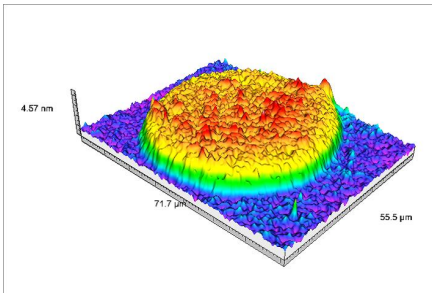


Sarfus image of a DNA biochip elaborated by bottom-up approach.

## Bottom-up approaches

These seek to arrange smaller components into more complex assemblies.

- DNA nanotechnology utilizes the specificity of Watson–Crick basepairing to construct well-defined structures out of DNA and other nucleic acids.
- Approaches from the field of "classical" chemical synthesis also aim at designing molecules with well-defined shape (e.g. bis-peptides[16] ).
- More generally, molecular self-assembly seeks to use concepts of supramolecular chemistry, and molecular recognition in particular, to cause single-molecule components to automatically arrange themselves into some useful conformation.
- Atomic force microscope tips can be used as a nanoscale "write head" to deposit a chemical upon a surface in a desired pattern in a process called dip pen nanolithography. This technique fits into the larger subfield of nanolithography.

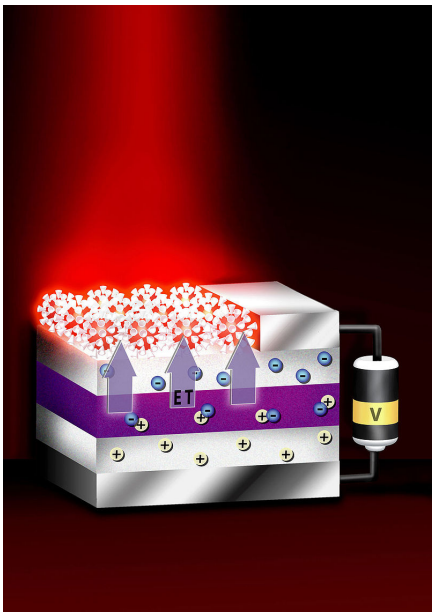


This device transfers energy from nano-thin layers of quantum wells to nanocrystals above them, causing the nanocrystals to emit visible light.[14]

## Top-down approaches

These seek to create smaller devices by using larger ones to direct their assembly.

- Many technologies that descended from conventional solid-state silicon methods for fabricating microprocessors are now capable of creating features smaller than 100 nm, falling under the definition of nanotechnology. Giant magnetoresistance-based hard drives already on the market fit this description,[17] as do atomic layer deposition (ALD) techniques. Peter Grünberg and Albert Fert received the Nobel Prize in Physics in 2007 for their discovery of Giant magnetoresistance and contributions to the field of spintronics.[18]
- Solid-state techniques can also be used to create devices known as nanoelectromechanical systems or NEMS, which are related to microelectromechanical systems or MEMS.
- Focused ion beams can directly remove material, or even deposit material when suitable pre-cursor gasses are applied at the same time. For example, this technique is used routinely to create sub-100 nm sections of material for analysis in Transmission electron microscopy.
- Atomic force microscope tips can be used as a nanoscale "write head" to deposit a resist, which is then followed by a etching process to remove material in a top-down method.

## Functional approaches

These seek to develop components of a desired functionality without regard to how they might be assembled.

- Molecular electronics seeks to develop molecules with useful electronic properties. These could then be used as single-molecule components in a nanoelectronic device.[19] For an example see rotaxane.
- Synthetic chemical methods can also be used to create synthetic molecular motors, such as in a so-called nanocar.

## Biomimetic approaches

- Bionics or biomimicry seeks to apply biological methods and systems found in nature, to the study and design of engineering systems and modern technology. Biomineralization is one example of the systems studied.
- Bionanotechnology the use of biomolecules for applications in nanotechnology, including use of viruses.[20]

## Speculative

These subfields seek to anticipate what inventions nanotechnology might yield, or attempt to propose an agenda along which inquiry might progress. These often take a big-picture view of nanotechnology, with more emphasis on its societal implications than the details of how such inventions could actually be created.

- Molecular nanotechnology is a proposed approach which involves manipulating single molecules in finely controlled, deterministic ways. This is more theoretical than the other subfields and is beyond current capabilities.
- Nanorobotics centers on self-sufficient machines of some functionality operating at the nanoscale. There are hopes for applying nanorobots in medicine,[21] [22] [23] but it may not be easy to do such a thing because of several drawbacks of such devices.[24] Nevertheless, progress on innovative materials and methodologies has been demonstrated with some patents granted about new nanomanufacturing devices for future commercial applications, which also progressively helps in the development towards nanorobots with the use of embedded nanobioelectronics concepts.[25] [26]
- Productive nanosystems are "systems of nanosystems" which will be complex nanosystems that produce atomically precise parts for other nanosystems, not necessarily using novel nanoscale-emergent properties, but well-understood fundamentals of manufacturing. Because of the discrete (i.e. atomic) nature of matter and the possibility of exponential growth, this stage is seen as the basis of another industrial revolution. Mihail Roco, one of the architects of the USA's National Nanotechnology Initiative, has proposed four states of nanotechnology that seem to parallel the technical progress of the Industrial Revolution, progressing from passive nanostructures to active nanodevices to complex nanomachines and ultimately to productive nanosystems.[27]
- Programmable matter seeks to design materials whose properties can be easily, reversibly and externally controlled though a fusion of information science and materials science.

- Due to the popularity and media exposure of the term nanotechnology, the words picotechnology and femtotechnology have been coined in analogy to it, although these are only used rarely and informally.

## Tools and techniques

There are several important modern developments. The atomic force microscope (AFM) and the Scanning Tunneling Microscope (STM) are two early versions of scanning probes that launched nanotechnology. There are other types of scanning probe microscopy, all flowing from the ideas of the scanning confocal microscope developed by Marvin Minsky in 1961 and the scanning acoustic microscope (SAM) developed by Calvin Quate and coworkers in the 1970s, that made it possible to see structures at the nanoscale. The tip of a scanning probe can also be used to manipulate nanostructures (a process called positional assembly). Feature-oriented scanning-positioning methodology suggested by Rostislav Lapshin appears to be a promising way to implement these nanomanipulations in automatic mode. However, this is still a slow process because of low scanning velocity of the microscope. Various techniques of nanolithography such as optical lithography, X-ray lithography dip pen nanolithography, electron beam lithography or nanoimprint lithography were also developed. Lithography is a top-down fabrication technique where a bulk material is reduced in size to nanoscale pattern.

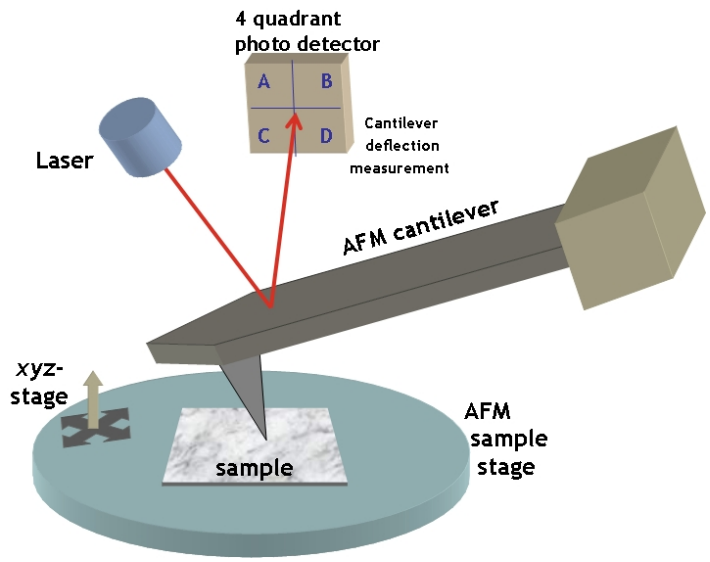


Typical AFM setup. A microfabricated cantilever with a sharp tip is deflected by features on a sample surface, much like in a phonograph but on a much smaller scale. A laser beam reflects off the backside of the cantilever into a set of photodetectors, allowing the deflection to be measured and assembled into an image of the surface.

Another group of nanotechnological techniques include those used for fabrication of nanowires, those used in semiconductor fabrication such as deep ultraviolet lithography, electron beam lithography, focused ion beam machining, nanoimprint lithography, atomic layer deposition, and molecular vapor deposition, and further including molecular self-assembly techniques such as those employing di-block copolymers. However, all of these techniques preceded the nanotech era, and are extensions in the development of scientific advancements rather than techniques which were devised with the sole purpose of creating nanotechnology and which were results of nanotechnology research.

The top-down approach anticipates nanodevices that must be built piece by piece in stages, much as manufactured items are made. Scanning probe microscopy is an important technique both for characterization and synthesis of nanomaterials. Atomic force microscopes and scanning tunneling microscopes can be used to look at surfaces and to move atoms around. By designing different tips for these microscopes, they can be used for carving out structures on surfaces and to help guide self-assembling structures. By using, for example, feature-oriented scanning-positioning approach, atoms can be moved around on a surface with scanning probe microscopy techniques. At present, it is expensive and time-consuming for mass production but very suitable for laboratory experimentation.

In contrast, bottom-up techniques build or grow larger structures atom by atom or molecule by molecule. These techniques include chemical synthesis, self-assembly and positional assembly. Dual polarisation interferometry is one tool suitable for characterisation of self assembled thin films. Another variation of the bottom-up approach is

molecular beam epitaxy or MBE. Researchers at Bell Telephone Laboratories like John R. Arthur. Alfred Y. Cho, and Art C. Gossard developed and implemented MBE as a research tool in the late 1960s and 1970s. Samples made by MBE were key to the discovery of the fractional quantum Hall effect for which the 1998 Nobel Prize in Physics was awarded. MBE allows scientists to lay down atomically precise layers of atoms and, in the process, build up complex structures. Important for research on semiconductors, MBE is also widely used to make samples and devices for the newly emerging field of spintronics.

However, new therapeutic products, based on responsive nanomaterials, such as the ultradeformable, stress-sensitive Transfersome vesicles, are under development and already approved for human use in some countries.

## Applications

As of August 21, 2008, the Project on Emerging Nanotechnologies estimates that over 800 manufacturer-identified nanotech products are publicly available, with new ones hitting the market at a pace of 3–4 per week.[28] The project lists all of the products in a publicly accessible online.[29] Most applications are limited to the use of "first generation" passive nanomaterials which includes titanium dioxide in sunscreen, cosmetics and some food products; Carbon allotropes used to produce gecko tape; silver in food packaging, clothing, disinfectants and household appliances; zinc oxide in sunscreens and cosmetics, surface coatings, paints and outdoor furniture varnishes; and cerium oxide as a fuel catalyst.[30]

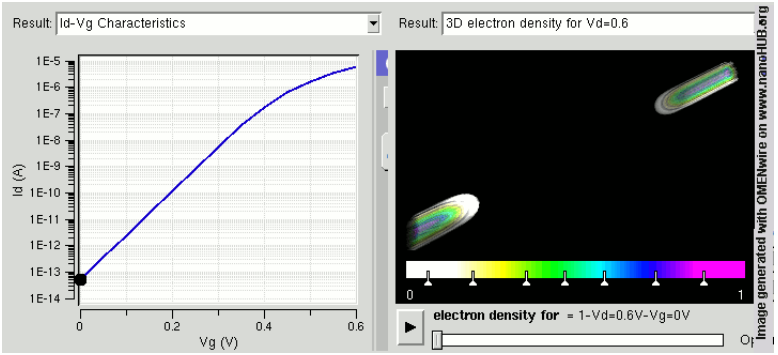


One of the major application of nanotechnology is in the area of nanoelectronics with MOSFET's being made of small nanowires ~10 nm in length. Here is a simulation of such a nanowire

The National Science Foundation (a major distributor for nanotechnology research in the United States) funded researcher David Berube to study the field of nanotechnology. His findings are published in the monograph Nano-Hype: The Truth Behind the Nanotechnology Buzz.[31] This study concludes that much of what is sold as “nanotechnology” is in fact a recasting of straightforward materials science, which is leading to a “nanotech industry built solely on selling nanotubes, nanowires, and the like” which will “end up with a few suppliers selling low margin products in huge volumes." Further applications which require actual manipulation or arrangement of nanoscale components await further research. Though technologies branded with the term 'nano' are sometimes little related to and fall far short of the most ambitious and transformative technological goals of the sort in molecular manufacturing proposals, the term still connotes such ideas. According to Berube, there may be a danger that a "nano bubble" will form, or is forming already, from the use of the term by scientists and entrepreneurs to garner funding, regardless of interest in the transformative possibilities of more ambitious and far-sighted work.[32]

# Implications

Because of the far-ranging claims that have been made about potential applications of nanotechnology, a number of serious concerns have been raised about what effects these will have on our society if realized, and what action if any is appropriate to mitigate these risks.

There are possible dangers that arise with the development of nanotechnology. The Center for Responsible Nanotechnology suggests that new developments could result, among other things, in untraceable weapons of mass destruction, networked cameras for use by the government, and weapons developments fast enough to destabilize arms races ("Nanotechnology Basics").

One area of concern is the effect that industrial-scale manufacturing and use of nanomaterials would have on human health and the environment, as suggested by nanotoxicology research. Groups such as the Center for Responsible Nanotechnology have advocated that nanotechnology should be specially regulated by governments for these reasons. Others counter that overregulation would stifle scientific research and the development of innovations which could greatly benefit mankind.

Other experts, including director of the Woodrow Wilson Center's Project on Emerging Nanotechnologies David Rejeski, have testified[33] that successful commercialization depends on adequate oversight, risk research strategy, and public engagement. Berkeley, California is currently the only city in the United States to regulate nanotechnology;[34] Cambridge, Massachusetts in 2008 considered enacting a similar law,[35] but ultimately rejected this.[36]

## Health and environmental concerns

Some of the recently developed nanoparticle products may have unintended consequences. Researchers have discovered that silver nanoparticles used in socks only to reduce foot odor are being released in the wash with possible negative consequences.[37] Silver nanoparticles, which are bacteriostatic, may then destroy beneficial bacteria which are important for breaking down organic matter in waste treatment plants or farms.[38]

A study at the University of Rochester found that when rats breathed in nanoparticles, the particles settled in the brain and lungs, which led to significant increases in biomarkers for inflammation and stress response.[39] A study in China indicated that nanoparticles induce skin aging through oxidative stress in hairless mice.[40] [41]

A two-year study at UCLA's School of Public Health found lab mice consuming nano-titanium dioxide showed DNA and chromosome damage to a degree "linked to all the big killers of man, namely cancer, heart disease, neurological disease and aging".[42]

A major study published more recently in Nature Nanotechnology suggests some forms of carbon nanotubes – a poster child for the “nanotechnology revolution” – could be as harmful as asbestos if inhaled in sufficient quantities. Anthony Seaton of the Institute of Occupational Medicine in Edinburgh, Scotland, who contributed to the article on carbon nanotubes said "We know that some of them probably have the potential to cause mesothelioma. So those sorts of materials need to be handled very carefully."[43] In the absence of specific nano-regulation forthcoming from governments, Paull and Lyons (2008) have called for an exclusion of engineered nanoparticles from organic food.[44] A newspaper article reports that workers in a paint factory developed serious lung disease and nanoparticles were found in their lungs.[45]

## Regulation

Calls for tighter regulation of nanotechnology have occurred alongside a growing debate related to the human health and safety risks associated with nanotechnology.[46] Furthermore, there is significant debate about who is responsible for the regulation of nanotechnology. While some non-nanotechnology specific regulatory agencies currently cover some products and processes (to varying degrees) – by “bolting on” nanotechnology to existing regulations – there are clear gaps in these regimes.[47] In "Nanotechnology Oversight: An Agenda for the Next Administration,"[48]

former EPA deputy administrator J. Clarence (Terry) Davies lays out a clear regulatory roadmap for the next presidential administration and describes the immediate and longer term steps necessary to deal with the current shortcomings of nanotechnology oversight.

Stakeholders concerned by the lack of a regulatory framework to assess and control risks associated with the release of nanoparticles and nanotubes have drawn parallels with bovine spongiform encephalopathy ('mad cow's disease), thalidomide, genetically modified food,[49] nuclear energy, reproductive technologies, biotechnology, and asbestosis. Dr. Andrew Maynard, chief science advisor to the Woodrow Wilson Center's Project on Emerging Nanotechnologies, concludes (among others) that there is insufficient funding for human health and safety research, and as a result there is currently limited understanding of the human health and safety risks associated with nanotechnology.[50] As a result, some academics have called for stricter application of the precautionary principle, with delayed marketing approval, enhanced labelling and additional safety data development requirements in relation to certain forms of nanotechnology.[51]

The Royal Society report[52] identified a risk of nanoparticles or nanotubes being released during disposal, destruction and recycling, and recommended that "manufacturers of products that fall under extended producer responsibility regimes such as end-of-life regulations publish procedures outlining how these materials will be managed to minimize possible human and environmental exposure" (p.xiii). Reflecting the challenges for ensuring responsible life cycle regulation, the Institute for Food and Agricultural Standards [53] has proposed standards for nanotechnology research and development should be integrated across consumer, worker and environmental standards. They also propose that NGOs and other citizen groups play a meaningful role in the development of these standards.

In October 2008, the Department of Toxic Substances Control (DTSC), within the California Environmental Protection Agency, announced its intent to request information regarding analytical test methods, fate and transport in the environment, and other relevant information from manufacturers of carbon nanotubes.[54] The purpose of this information request will be to identify information gaps and to develop information about carbon nanotubes, an important emerging nanomaterial.

## See also

- Bionanoscience
- Energy applications of nanotechnology
- List of emerging technologies
- List of software for nanostructures modeling
- Materiomics
- Molecular design software
- Molecular mechanics
- Nanoengineering
- Nanobiotechnology
- Nanofluidics
- Nanohub
- Nanometrology
- Nanoscale networks
- Nanotechnology education
- Nanotechnology in water treatment
- Nanothermite
- Nanoweapons
- Top-down and bottom-up
- Translational research

- Virtual Institute of Nano Films

# References


[1] Cristina Buzea, Ivan Pacheco, and Kevin Robbie (2007). "Nanomaterials and Nanoparticles: Sources and Toxicity" (http://scitation.aip.org/getabs/servlet/GetabsServlet?prog=normal&id=BJIOBN00000200000400MR17000001&idtype=cvips&gifs=Yes). *Biointerphases* **2**: MR17. .

[2] N. Taniguchi (1974). *On the Basic Concept of 'Nano-Technology*. Proc. Intl. Conf. Prod. London, Part II British Society of Precision Engineering.

[3] Eric Drexler (1991). *Nanosystems: Molecular Machinery, Manufacturing, and Computation. MIT PhD thesis* (http://www.e-drexler.com/d/06/00/Nanosystems/toc.html). New York: Wiley. ISBN 0471575186. .

[4] Kahn, Jennifer (2006). "Nanotechnology". *National Geographic* **2006** (June): 98–119.

[5] Rodgers, P. (2006). "Nanoelectronics: Single file". *Nature Nanotechnology*. doi:10.1038/nnano.2006.5.

[6] 22

[7] Lubick, N. (2008). Silver socks have cloudy lining. Environ Sci Technol. 42(11):3910

[8] Nanotechnology: Developing Molecular Manufacturing (http://www.crnano.org/developing.htm)

[9] "Some papers by K. Eric Drexler" (http://www.imm.org/PNAS.html). .

[10] California NanoSystems Institute (http://www.cnsi.ucla.edu/institution/personnel?personnel_id=105488)

[11] C&En: Cover Story - Nanotechnology (http://pubs.acs.org/cen/coverstory/8148/8148counterpoint.html)

[12] Regan, BC; Aloni, S; Jensen, K; Ritchie, RO; Zettl, A (2005). "Nanocrystal-powered nanomotor." (http://www.physics.berkeley.edu/research/zettl/pdf/312.NanoLett5regan.pdf). *Nano letters* **5** (9): 1730–3. doi:10.1021/nl0510659. PMID 16159214. .

[13] Regan, B. C.; Aloni, S.; Jensen, K.; Zettl, A. (2005). "Surface-tension-driven nanoelectromechanical relaxation oscillator" (http://www.lbl.gov/Science-Articles/Archive/sabl/2005/May/Tiniest-Motor.pdf). *Applied Physics Letters* **86**: 123119. doi:10.1063/1.1887827. .

[14] Wireless nanocrystals efficiently radiate visible light (http://www.sandia.gov/news-center/news-releases/2004/micro-nano/well.html)

[15] Clarkson, AJ; Buckingham, DA; Rogers, AJ; Blackman, AG; Clark, CR (2004). "Nanostructured Ceramics in Medical Devices: Applications and Prospects". *JOM* **56** (10): 38–43. doi:10.1007/s11837-004-0289-x. PMID 11196953.

[16] Levins, Christopher G.; Schafmeister, Christian E. (2006). "The Synthesis of Curved and Linear Structures from a Minimal Set of Monomers.". *ChemInform* **37**. doi:10.1002/chin.200605222.

[17] "Applications/Products" (http://www.nano.gov/html/facts/appsprod.html). National Nanotechnology Initiative. . Retrieved 2007-10-19.

[18] "The Nobel Prize in Physics 2007" (http://nobelprize.org/nobel_prizes/physics/laureates/2007/index.html). Nobelprize.org. . Retrieved 2007-10-19.

[19] Das S, Gates AJ, Abdu HA, Rose GS, Picconatto CA, Ellenbogen JC. (2007). "Designs for Ultra-Tiny, Special-Purpose Nanoelectronic Circuits". *IEEE Transactions on Circuits and Systems I* **54** (11): 2528–2540. doi:10.1109/TCSI.2007.907864.

[20] C.Michael Hogan. 2010. *Virus*. Encyclopedia of Earth. National Council for Science and the Environment (http://www.eoearth.org/article/Virus?topic=49496). eds. S.Draggan and C.Cleveland

[21] Ghalanbor Z, Marashi SA, Ranjbar B (2005). "Nanotechnology helps medicine: nanoscale swimmers and their future applications". *Med Hypotheses* **65** (1): 198–199. doi:10.1016/j.mehy.2005.01.023. PMID 15893147.

[22] Kubik T, Bogunia-Kubik K, Sugisaka M. (2005). "Nanotechnology on duty in medical applications". *Curr Pharm Biotechnol.* **6** (1): 17–33. PMID 15727553.

[23] Leary, SP; Liu, CY; Apuzzo, ML (2006). "Toward the Emergence of Nanoneurosurgery: Part III-Nanomedicine: Targeted Nanotherapy, Nanosurgery, and Progress Toward the Realization of Nanoneurosurgery". *Neurosurgery* **58** (6): 1009–1026. doi:10.1227/01.NEU.0000217016.79256.16. PMID 16723880.

[24] Shetty RC (2005). "Potential pitfalls of nanotechnology in its applications to medicine: immune incompatibility of nanodevices". *Med Hypotheses* **65** (5): 998–9. doi:10.1016/j.mehy.2005.05.022. PMID 16023299.

[25] Cavalcanti A, Shirinzadeh B, Freitas RA Jr., Kretly LC. (2007). "Medical Nanorobot Architecture Based on Nanobioelectronics". *Recent Patents on Nanotechnology* (http://bentham.org/nanotec/). **1** (1): 1–10. doi:10.2174/187221007779814745.

[26] Boukallel M, Gauthier M, Dauge M, Piat E, Abadie J. (2007). "Smart microrobots for mechanical cell characterization and cell convoying". *IEEE Trans. Biomed. Eng.* **54** (8): 1536–40. doi:10.1109/TBME.2007.891171. PMID 17694877.

[27] "International Perspective on Government Nanotechnology Funding in 2005" (http://www.nsf.gov/crssprgm/nano/reports/mcr_05-0526_intpersp_nano.pdf). .

[28] Project on Emerging Nanotechnologies. (2008). Analysis: This is the first publicly available on-line inventory of nanotechnology-based consumer products. (http://www.nanotechproject.org/inventories/consumer/analysis_draft/)

[29] Nanotechproject.org (http://www.nanotechproject.org/inventories/consumer/)

[30] Applications for Nanotechnology (http://www.americanelements.com/nanotech.htm)

[31] Prometheusbooks.com (http://www.prometheusbooks.com/index.php?main_page=product_info&products_id=1822/)

[32] Berube, David. Nano=Hype: The Truth Behind the Nanotechnology Buzz, Amherst, NY: Prometheus Books, 2006

[33] Testimony of David Rejeski for U.S. Senate Committee on Commerce, Science and Transportation (http://www.nanotechproject.org/news/archive/successful_commercialization_depends_on/) Project on Emerging Nanotechnologies. Retrieved on 2008-3-7.

[34] Berkeley considering need for nano safety (Rick DelVecchio, Chronicle Staff Writer) Friday, November 24, 2006 (http://www.sfgate.com/cgi-bin/article.cgi?file=/c/a/2006/11/24/MNGP9MJ4KI1.DTL)
[35] Cambridge considers nanotech curbs - City may mimic Berkeley bylaws (By Hiawatha Bray, Boston Globe Staff) January 26, 2007 (http://boston.com/business/technology/articles/2007/01/26/cambridge_considers_nanotech_curbs/)
[36] Recommendations for a Municipal Health & Safety Policy for Nanomaterials: A Report to the Cambridge City Manager. July 2008. (http://www.nanolawreport.com/Cambridge.pdf)
[37] Lubick, N. (2008). Silver socks have cloudy lining. (http://pubs.acs.org/subscribe/journals/esthag-w/2008/apr/science/nl_nanosocks.html)
[38] Murray R.G.E., Advances in Bacterial Paracrystalline Surface Layers (Eds.: T. J. Beveridge, S. F. Koval). Plenum pp. 3 ± 9. [9]
[39] Elder, A. (2006). Tiny Inhaled Particles Take Easy Route from Nose to Brain. (http://www.urmc.rochester.edu/pr/news/story.cfm?id=1191)
[40] Wu, J; Liu, W; Xue, C; Zhou, S; Lan, F; Bi, L; Xu, H; Yang, X *et al*. (2009). "Toxicity and penetration of TiO2 nanoparticles in hairless mice and porcine skin after subchronic dermal exposure.". *Toxicology letters* **191** (1): 1–8. doi:10.1016/j.toxlet.2009.05.020. PMID 19501137.
[41] Jonaitis, TS; Card, JW; Magnuson, B (2010). "Concerns regarding nano-sized titanium dioxide dermal penetration and toxicity study.". *Toxicology letters* **192** (2): 268–9. doi:10.1016/j.toxlet.2009.10.007. PMID 19836437.
[42] Schneider, Andrew, "Amid Nanotech's Dazzling Promise, Health Risks Grow" (http://www.aolnews.com/nanotech/article/amid-nanotechs-dazzling-promise-health-risks-grow/19401235), March 24, 2010.
[43] Weiss, R. (2008). Effects of Nanotubes May Lead to Cancer, Study Says. (http://www.washingtonpost.com/wp-dyn/content/article/2008/05/20/AR2008052001331.html?hpid=sec-health&sid=ST2008052100104)
[44] Paull, J. & Lyons, K. (2008). "Nanotechnology: The Next Challenge for Organics" (http://orgprints.org/13569/1/13569.pdf). *Journal of Organic Systems* **3**: 3-22. .
[45] Smith, Rebecca (August 19, 2009). "Nanoparticles used in paint could kill, research suggests" (http://www.telegraph.co.uk/health/healthnews/6016639/Nanoparticles-used-in-paint-could-kill-research-suggests.html). London: Telegraph. . Retrieved May 19, 2010.
[46] Kevin Rollins (Nems Mems Works, LLC). "Nanobiotechnology Regulation: A Proposal for Self-Regulation with Limited Oversight" (http://www.nanolabweb.com/index.cfm/action/main.default.viewArticle/articleID/290/CFID/3564274/CFTOKEN/43473772/index.html). *Volume 6 - Issue 2*. . Retrieved 2 September 2010.
[47] Bowman D, and Hodge G (2006). "Nanotechnology: Mapping the Wild Regulatory Frontier". *Futures* **38**: 1060–1073. doi:10.1016/j.futures.2006.02.017.
[48] Davies, JC. (2008). Nanotechnology Oversight: An Agenda for the Next Administration (http://www.nanotechproject.org/publications/archive/pen13/).
[49] Rowe G, Horlick-Jones T, Walls J, Pidgeon N, (2005). "Difficulties in evaluating public engagement initiatives: reflections on an evaluation of the UK GM Nation?". *Public Understanding of Science* (http://pus.sagepub.com/cgi/content/abstract/14/4/331). **14**: 333.
[50] Maynard, A. Testimony by Dr. Andrew Maynard for the U.S. House Committee on Science and Technology (http://www.science.house.gov/publications/Testimony.aspx?TID=12957). (2008-4-16). Retrieved on 2008-11-24.
[51] Faunce TA et al. Sunscreen Safety: The Precautionary Principle, The Australian Therapeutic Goods Administration and Nanoparticles in Sunscreens Nanoethics (2008) 2:231–240 DOI 10.1007/s11569-008-0041-z. Thomas Faunce & Katherine Murray & Hitoshi Nasu & Diana Bowman (published online: 24 July 2008). "Sunscreen Safety: The Precautionary Principle, The Australian Therapeutic Goods Administration and Nanoparticles in Sunscreens" (http://law.anu.edu.au/StaffUploads/236-Nanoethics Sunscreens 2008.pdf). Springer Science + Business Media B.V. . Retrieved 18 June 2009.
[52] Royal Society and Royal Academy of Engineering (2004). *Nanoscience and nanotechnologies: opportunities and uncertainties* (http://www.nanotec.org.uk/finalReport.htm). . Retrieved 2008-05-18.
[53] https://www.msu.edu/~ifas/
[54] *Nanotechnology web page* (http://www.dtsc.ca.gov/TechnologyDevelopment/Nanotechnology/index.cfm). Department of Toxic Substances Control. 2008. .

## Further reading

- " Basic Concepts of Nanotechnology (http://www.inanot.com/)" History of Nano-Technology, News, Materials, Potential Risks and Important People.
- "About Nanotechnology - An Introduction to Nanotech from The Project on Emerging Nanotechnologies" (http://www.nanotechproject.org/topics/nano101/). Nanotechproject.org. Retrieved 2009-11-24.
- "Nanotechnology Introduction Pages" (http://www.nanotech-now.com/nano_intro.htm). Nanotech-now.com. Retrieved 2009-11-24.
- Medicalnanotec.com (http://www.medicalnanotec.com), Introduction to applications of Nanotechnology in Medicine.
- Maynard, Andrew, "The Twinkie Guide to Nanotechnology • News Archive • Nanotechnology Project" (http://www.nanotechproject.org/news/archive/the_twinkie_guide_to_nanotechnology/). Nanotechproject.org.

2007-10-22. Retrieved 2009-11-24. Woodrow Wilson International Center for Scholars. 2007. - "..a friendly, funny, 25-minute travel guide to the technology"

- "Nanotechnology Basics: For Students and Other Learners". Center for Responsible Nanotechnology - World Care. 11 November 2008.
- Fritz Allhoff and Patrick Lin (eds.), *Nanotechnology & Society: Current and Emerging Ethical Issues* (http://www.springer.com/philosophy/ethics/book/978-1-4020-6208-7) (Dordrecht: Springer, 2008).
- Fritz Allhoff, Patrick Lin, James Moor, and John Weckert (eds.) "Nanoethics: The Ethical and Societal Implications of Nanotechnology" (http://www.wiley.com/WileyCDA/WileyTitle/productCd-0470084170.html). John Wiley & Sons. 2007. "Wiley" (http://www.nanoethics.org/wiley.html).
- J. Clarence Davies, EPA and Nanotechnology: Oversight for the 21st Century (http://www.nanotechproject.org/publications/archive/epa_nanotechnology_oversight_for_21st/), *Project on Emerging Nanotechnologies*, PEN 9, May 2007.
- Carl Marziali, "Little Big Science," (http://www.usc.edu/uscnews/stories/13316.html) USC Trojan Family Magazine, Winter 2007.
- William Sims Bainbridge: *Nanoconvergence: The Unity of Nanoscience, Biotechnology, Information Technology and Cognitive Science*, June 27, 2007, Prentice Hall, ISBN 0-13-244643-X
- Lynn E. Foster: *Nanotechnology: Science, Innovation, and Opportunity*, December 21, 2005, Prentice Hall, ISBN 0-13-192756-6
- *Impact of Nanotechnology on Biomedical Sciences: Review of Current Concepts on Convergence of Nanotechnology With Biology* (http://www.azonano.com/details.asp?ArticleID=1242) by Herbert Ernest and Rahul Shetty, from AZojono, May 2005.
- Hunt, G & Mehta, M (eds)(2008) Nanotechnology: Risk, Ethics & Law, Earthscan, London.
- Andrew Schneider, The Nanotech Gamble (http://www.aolnews.com/category/nanotech/), Growing Health Risks from Nanomaterials in Food and Medicine, First in a Three-Part Series, AOL News Special Report, March 24, 2010.
- Hari Singh Nalwa (2004), Encyclopedia of Nanoscience and Nanotechnology (10-Volume Set), American Scientific Publishers. ISBN 1-58883-001-2
- Michael Rieth and Wolfram Schommers (2006), Handbook of Theoretical and Computational Nanotechnology (10-Volume Set), American Scientific Publishers. ISBN 1-58883-042-X
- Akhlesh Lakhtakia (ed) (2004). *The Handbook of Nanotechnology. Nanometer Structures: Theory, Modeling, and Simulation*. SPIE Press, Bellingham, WA, USA. ISBN 0-8194-5186-X.
- Fei Wang & Akhlesh Lakhtakia (eds) (2006). *Selected Papers on Nanotechnology—Theory & Modeling (Milestone Volume 182)*. SPIE Press, Bellingham, WA, USA. ISBN 0-8194-6354-X.
- Jumana Boussey, Georges Kamarinos, Laurent Montès (editors) (2003), Towards Nanotechnology (http://www.lavoisier.fr/notice/fr2746208580.html), "Nano et Micro Technologies", Hermes Sciences Publ., Paris, ISBN 2-7462-0858-X.
- The Silicon Valley Toxics Coalition (April, 2008), Regulating Emerging Technologies in Silicon Valley and Beyond (http://www.svtc.org/svtc_nanotech)
- Genetic Engineering & Biotechnology News (http://www.genengnews.com) (January, 2008), Getting a Handle on Nanobiotech Products (http://www.genengnews.com/articles/chitem.aspx?aid=2325) Regulators and Companies Are Laying the Groundwork for a Predicted Bright Future
- Suh WH, Suslick KS, Stucky GD, Suh YH (2009). "Nanotechnology, nanotoxicology, and neuroscience" (http://www.pubmedcentral.nih.gov/articlerender.fcgi?tool=pmcentrez&artid=2728462). *Progress in Neurobiology* **87** (3): 133–70. doi:10.1016/j.pneurobio.2008.09.009. PMID 18926873. PMC 2728462.

## External links

- What is Nanotechnology? (http://www.vega.org.uk/video/programme/3) (A Vega/BBC/OU Video Discussion).
- Nanotec Expo (http://www.nanotecexpo.com.br/english) - Fair and Congress Latin American of Nanotechnology
- "Nanotechnology Basics: For Students and Other Learners." (http://www.crnano.org/basics.htm) Center for Responsible Nanotechnology. World Care. 11 Nov. 2008.
- Nanotechnology (http://www.dmoz.org/Science/Technology/Nanotechnology//) at the Open Directory Project
- Course on *Introduction to Nanotechnology* (http://nanohub.org/resources/6583)
- The Nano Age (http://www.thenanoage.com)

# Nanotechnology

| Part of a series of articles on |
|---|
| History<br>Implications<br>Applications<br>Regulation<br>Organizations<br>Popular culture<br>List of topics |
| **Nanomaterials** |
| Fullerene<br>Carbon Nanotubes<br>Nanoparticles |
| **Nanomedicine** |
| Nanotoxicology<br>Nanosensor |
| **Molecular self-assembly** |
| Self-assembled monolayer<br>Supramolecular assembly<br>DNA nanotechnology |
| **Nanoelectronics** |
| Molecular electronics<br>Nanolithography |
| **Scanning probe microscopy** |
| Atomic force microscope<br>Scanning tunneling microscope |
| **Molecular nanotechnology** |
| Molecular assembler<br>Nanorobotics<br>Mechanosynthesis |
| **Nanotechnology Portal** |

**Nanotechnology**, shortened to "**nanotech**", is the study of manipulating matter on an atomic and molecular scale. Generally nanotechnology deals with structures sized between 1 to 100 nanometer in at least one dimension, and involves developing materials or devices within that size. Quantum mechanical effects are very important at this scale.

Nanotechnology is very diverse, ranging from extensions of conventional device physics to completely new approaches based upon molecular self-assembly, from developing new materials with dimensions on the nanoscale to investigating whether we can directly control matter on the atomic scale.

There is much debate on the future implications of nanotechnology. Nanotechnology may be able to create many new materials and devices with a vast range of applications, such as in medicine, electronics, biomaterials and energy production. On the other hand, nanotechnology raises many of the same issues as any new technology, including concerns about the toxicity and environmental impact of nanomaterials,[1] and their potential effects on global economics, as well as speculation about various doomsday scenarios. These concerns have led to a debate among advocacy groups and governments on whether special regulation of nanotechnology is warranted.

## Origins

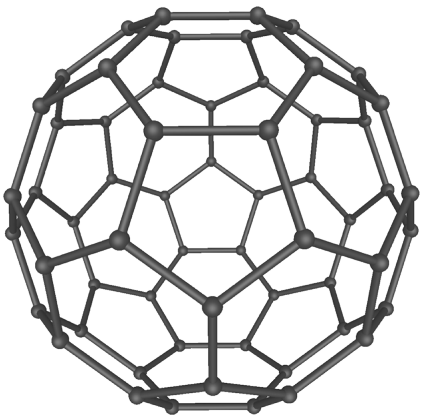

Buckminsterfullerene $C_{60}$, also known as the buckyball, is a representative member of the carbon structures known as fullerenes. Members of the fullerene family are a major subject of research falling under the nanotechnology umbrella.

The first use of the concepts found in 'nano-technology' (but pre-dating use of that name) was in "There's Plenty of Room at the Bottom", a talk given by physicist Richard Feynman at an American Physical Society meeting at Caltech on December 29, 1959. Feynman described a process by which the ability to manipulate individual atoms and molecules might be developed, using one set of precise tools to build and operate another proportionally smaller set, and so on down to the needed scale. In the course of this, he noted, scaling issues would arise from the changing magnitude of various physical phenomena: gravity would become less important, surface tension and van der Waals attraction would become increasingly more significant, etc. This basic idea appeared plausible, and exponential assembly enhances it with parallelism to produce a useful quantity of end products. The term "nanotechnology" was defined by Tokyo Science University Professor Norio Taniguchi in a 1974 paper[2] as follows: "'Nano-technology' mainly consists of the processing of, separation, consolidation, and deformation of materials by one atom or by one molecule." In the 1980s the basic idea of this definition was explored in much more depth by Dr. K. Eric Drexler, who promoted the technological significance of nano-scale phenomena and devices through speeches and the books Engines of Creation: The Coming Era of Nanotechnology (1986) and *Nanosystems: Molecular Machinery, Manufacturing, and Computation*,[3] and so the term acquired its current sense. Engines of Creation: The Coming Era of Nanotechnology is considered the first book on the topic of nanotechnology. Nanotechnology and nanoscience got started in the early 1980s with two major developments; the birth of cluster science and the invention of the scanning tunneling microscope (STM). This development led to the discovery of fullerenes in 1985 and carbon nanotubes a few years later. In another development, the synthesis and properties of semiconductor nanocrystals was studied; this led to a fast increasing number of metal and metal oxide nanoparticles and quantum dots. The atomic force microscope (AFM or SFM) was invented six years after the STM was invented. In 2000, the United States National Nanotechnology Initiative was founded to coordinate Federal nanotechnology research and development and is evaluated by the President's Council of Advisors on Science and Technology.

## Fundamental concepts

One nanometer (nm) is one billionth, or $10^{-9}$, of a meter. By comparison, typical carbon-carbon bond lengths, or the spacing between these atoms in a molecule, are in the range 0.12–0.15 nm, and a DNA double-helix has a diameter around 2 nm. On the other hand, the smallest cellular life-forms, the bacteria of the genus Mycoplasma, are around 200 nm in length.

To put that scale in another context, the comparative size of a nanometer to a meter is the same as that of a marble to the size of the earth.[4] Or another way of putting it: a nanometer is the amount an average man's beard grows in the time it takes him to raise the razor to his face.[4]

Two main approaches are used in nanotechnology. In the "bottom-up" approach, materials and devices are built from molecular components which assemble themselves chemically by principles of molecular recognition. In the "top-down" approach, nano-objects are constructed from larger entities without atomic-level control.[5]

Areas of physics such as nanoelectronics, nanomechanics, nanophotonics and nanoionics have evolved during the last few decades to provide a basic scientific foundation of nanotechnology.

### Larger to smaller: a materials perspective

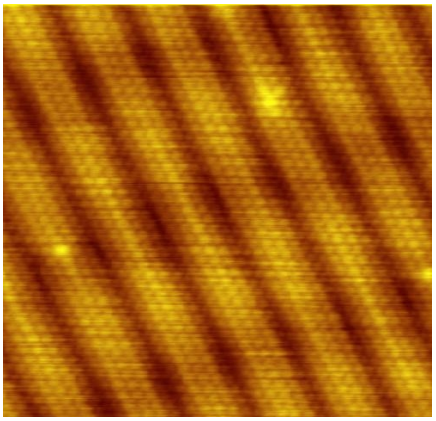

Image of reconstruction on a clean Gold(100) surface, as visualized using scanning tunneling microscopy. The positions of the individual atoms composing the surface are visible.

A number of physical phenomena become pronounced as the size of the system decreases. These include statistical mechanical effects, as well as quantum mechanical effects, for example the “quantum size effect” where the electronic properties of solids are altered with great reductions in particle size. This effect does not come into play by going from macro to micro dimensions. However, quantum effects become dominant when the nanometer size range is reached, typically at distances of 100 nanometers or less, the so called quantum realm. Additionally, a number of physical (mechanical, electrical, optical, etc.) properties change when compared to macroscopic systems. One example is the increase in surface area to volume ratio altering mechanical, thermal and catalytic properties of materials. Diffusion and reactions at nanoscale, nanostructures materials and nanodevices with fast ion transport are generally referred to nanoionics. *Mechanical* properties of nanosystems are of interest in the nanomechanics research. The catalytic activity of nanomaterials also opens potential risks in their interaction with biomaterials.[6]

Materials reduced to the nanoscale can show different properties compared to what they exhibit on a macroscale, enabling unique applications. For instance, opaque substances become transparent (copper); stable materials turn combustible (aluminum); insoluble materials become soluble (gold). A material such as gold, which is chemically inert at normal scales, can serve as a potent chemical catalyst at nanoscales. Much of the fascination with nanotechnology stems from these quantum and surface phenomena that matter exhibits at the nanoscale.[7]

### Simple to complex: a molecular perspective

Modern synthetic chemistry has reached the point where it is possible to prepare small molecules to almost any structure. These methods are used today to manufacture a wide variety of useful chemicals such as pharmaceuticals or commercial polymers. This ability raises the question of extending this kind of control to the next-larger level, seeking methods to assemble these single molecules into supramolecular assemblies consisting of many molecules arranged in a well defined manner.

These approaches utilize the concepts of molecular self-assembly and/or supramolecular chemistry to automatically arrange themselves into some useful conformation through a bottom-up approach. The concept of molecular

recognition is especially important: molecules can be designed so that a specific configuration or arrangement is favored due to non-covalent intermolecular forces. The Watson–Crick basepairing rules are a direct result of this, as is the specificity of an enzyme being targeted to a single substrate, or the specific folding of the protein itself. Thus, two or more components can be designed to be complementary and mutually attractive so that they make a more complex and useful whole.

Such bottom-up approaches should be capable of producing devices in parallel and be much cheaper than top-down methods, but could potentially be overwhelmed as the size and complexity of the desired assembly increases. Most useful structures require complex and thermodynamically unlikely arrangements of atoms. Nevertheless, there are many examples of self-assembly based on molecular recognition in biology, most notably Watson–Crick basepairing and enzyme-substrate interactions. The challenge for nanotechnology is whether these principles can be used to engineer new constructs in addition to natural ones.

## Molecular nanotechnology: a long-term view

Molecular nanotechnology, sometimes called molecular manufacturing, describes engineered nanosystems (nanoscale machines) operating on the molecular scale. Molecular nanotechnology is especially associated with the molecular assembler, a machine that can produce a desired structure or device atom-by-atom using the principles of mechanosynthesis. Manufacturing in the context of productive nanosystems is not related to, and should be clearly distinguished from, the conventional technologies used to manufacture nanomaterials such as carbon nanotubes and nanoparticles.

When the term "nanotechnology" was independently coined and popularized by Eric Drexler (who at the time was unaware of an earlier usage by Norio Taniguchi) it referred to a future manufacturing technology based on molecular machine systems. The premise was that molecular scale biological analogies of traditional machine components demonstrated molecular machines were possible: by the countless examples found in biology, it is known that sophisticated, stochastically optimised biological machines can be produced.

It is hoped that developments in nanotechnology will make possible their construction by some other means, perhaps using biomimetic principles. However, Drexler and other researchers[8] have proposed that advanced nanotechnology, although perhaps initially implemented by biomimetic means, ultimately could be based on mechanical engineering principles, namely, a manufacturing technology based on the mechanical functionality of these components (such as gears, bearings, motors, and structural members) that would enable programmable, positional assembly to atomic specification.[9] The physics and engineering performance of exemplar designs were analyzed in Drexler's book *Nanosystems*.

In general it is very difficult to assemble devices on the atomic scale, as all one has to position atoms on other atoms of comparable size and stickiness. Another view, put forth by Carlo Montemagno,[10] is that future nanosystems will be hybrids of silicon technology and biological molecular machines. Yet another view, put forward by the late Richard Smalley, is that mechanosynthesis is impossible due to the difficulties in mechanically manipulating individual molecules.

This led to an exchange of letters in the ACS publication Chemical & Engineering News in 2003.[11] Though biology clearly demonstrates that molecular machine systems are possible, non-biological molecular machines are today only in their infancy. Leaders in research on non-biological molecular machines are Dr. Alex Zettl and his colleagues at Lawrence Berkeley Laboratories and UC Berkeley. They have constructed at least three distinct molecular devices whose motion is controlled from the desktop with changing voltage: a nanotube nanomotor, a molecular actuator,[12] and a nanoelectromechanical relaxation oscillator.[13]

An experiment indicating that positional molecular assembly is possible was performed by Ho and Lee at Cornell University in 1999. They used a scanning tunneling microscope to move an individual carbon monoxide molecule (CO) to an individual iron atom (Fe) sitting on a flat silver crystal, and chemically bound the CO to the Fe by applying a voltage.

# Current research

## Nanomaterials

The nanomaterials field includes subfields which develop or study materials having unique properties arising from their nanoscale dimensions.[15]

- Interface and colloid science has given rise to many materials which may be useful in nanotechnology, such as carbon nanotubes and other fullerenes, and various nanoparticles and nanorods. Nanomaterials with fast ion transport are related also to nanoionics and nanoelectronics.
- Nanoscale materials can also be used for bulk applications; most present commercial applications of nanotechnology are of this flavor.
- Progress has been made in using these materials for medical applications; see Nanomedicine.
- Nanoscale materials are sometimes used in solar cells which combats the cost of traditional Silicon solar cells
- Development of applications incorporating semiconductor nanoparticles to be used in the next generation of products, such as display technology, lighting, solar cells and biological imaging; see quantum dots.

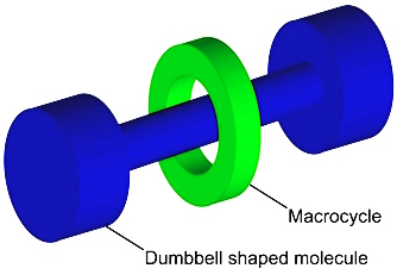


Graphical representation of a rotaxane, useful as a molecular switch.

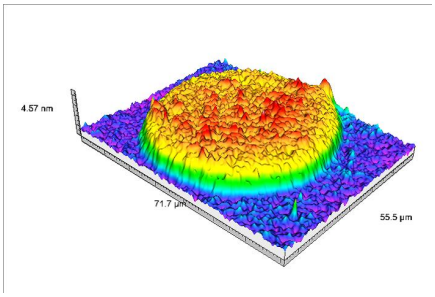


Sarfus image of a DNA biochip elaborated by bottom-up approach.

## Bottom-up approaches

These seek to arrange smaller components into more complex assemblies.

- DNA nanotechnology utilizes the specificity of Watson–Crick basepairing to construct well-defined structures out of DNA and other nucleic acids.
- Approaches from the field of "classical" chemical synthesis also aim at designing molecules with well-defined shape (e.g. bis-peptides[16] ).
- More generally, molecular self-assembly seeks to use concepts of supramolecular chemistry, and molecular recognition in particular, to cause single-molecule components to automatically arrange themselves into some useful conformation.
- Atomic force microscope tips can be used as a nanoscale "write head" to deposit a chemical upon a surface in a desired pattern in a process called dip pen nanolithography. This technique fits into the larger subfield of nanolithography.

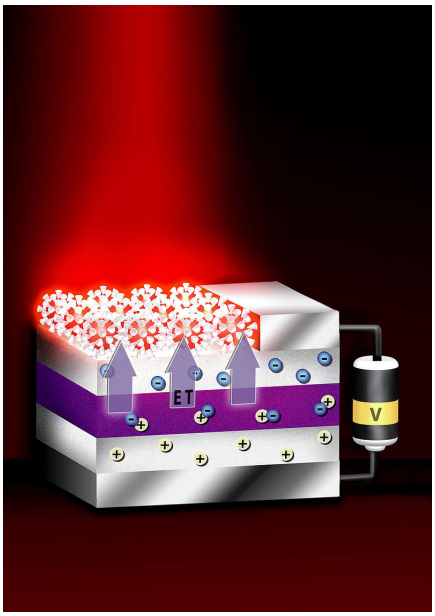


This device transfers energy from nano-thin layers of quantum wells to nanocrystals above them, causing the nanocrystals to emit visible light.[14]

## Top-down approaches

These seek to create smaller devices by using larger ones to direct their assembly.

- Many technologies that descended from conventional solid-state silicon methods for fabricating microprocessors are now capable of creating features smaller than 100 nm, falling under the definition of nanotechnology. Giant magnetoresistance-based hard drives already on the market fit this description,[17] as do atomic layer deposition (ALD) techniques. Peter Grünberg and Albert Fert received the Nobel Prize in Physics in 2007 for their discovery of Giant magnetoresistance and contributions to the field of spintronics.[18]
- Solid-state techniques can also be used to create devices known as nanoelectromechanical systems or NEMS, which are related to microelectromechanical systems or MEMS.
- Focused ion beams can directly remove material, or even deposit material when suitable pre-cursor gasses are applied at the same time. For example, this technique is used routinely to create sub-100 nm sections of material for analysis in Transmission electron microscopy.
- Atomic force microscope tips can be used as a nanoscale "write head" to deposit a resist, which is then followed by a etching process to remove material in a top-down method.

## Functional approaches

These seek to develop components of a desired functionality without regard to how they might be assembled.

- Molecular electronics seeks to develop molecules with useful electronic properties. These could then be used as single-molecule components in a nanoelectronic device.[19] For an example see rotaxane.
- Synthetic chemical methods can also be used to create synthetic molecular motors, such as in a so-called nanocar.

## Biomimetic approaches

- Bionics or biomimicry seeks to apply biological methods and systems found in nature, to the study and design of engineering systems and modern technology. Biomineralization is one example of the systems studied.
- Bionanotechnology the use of biomolecules for applications in nanotechnology, including use of viruses.[20]

## Speculative

These subfields seek to anticipate what inventions nanotechnology might yield, or attempt to propose an agenda along which inquiry might progress. These often take a big-picture view of nanotechnology, with more emphasis on its societal implications than the details of how such inventions could actually be created.

- Molecular nanotechnology is a proposed approach which involves manipulating single molecules in finely controlled, deterministic ways. This is more theoretical than the other subfields and is beyond current capabilities.
- Nanorobotics centers on self-sufficient machines of some functionality operating at the nanoscale. There are hopes for applying nanorobots in medicine,[21] [22] [23] but it may not be easy to do such a thing because of several drawbacks of such devices.[24] Nevertheless, progress on innovative materials and methodologies has been demonstrated with some patents granted about new nanomanufacturing devices for future commercial applications, which also progressively helps in the development towards nanorobots with the use of embedded nanobioelectronics concepts.[25] [26]
- Productive nanosystems are "systems of nanosystems" which will be complex nanosystems that produce atomically precise parts for other nanosystems, not necessarily using novel nanoscale-emergent properties, but well-understood fundamentals of manufacturing. Because of the discrete (i.e. atomic) nature of matter and the possibility of exponential growth, this stage is seen as the basis of another industrial revolution. Mihail Roco, one of the architects of the USA's National Nanotechnology Initiative, has proposed four states of nanotechnology that seem to parallel the technical progress of the Industrial Revolution, progressing from passive nanostructures to active nanodevices to complex nanomachines and ultimately to productive nanosystems.[27]
- Programmable matter seeks to design materials whose properties can be easily, reversibly and externally controlled though a fusion of information science and materials science.

- Due to the popularity and media exposure of the term nanotechnology, the words picotechnology and femtotechnology have been coined in analogy to it, although these are only used rarely and informally.

## Tools and techniques

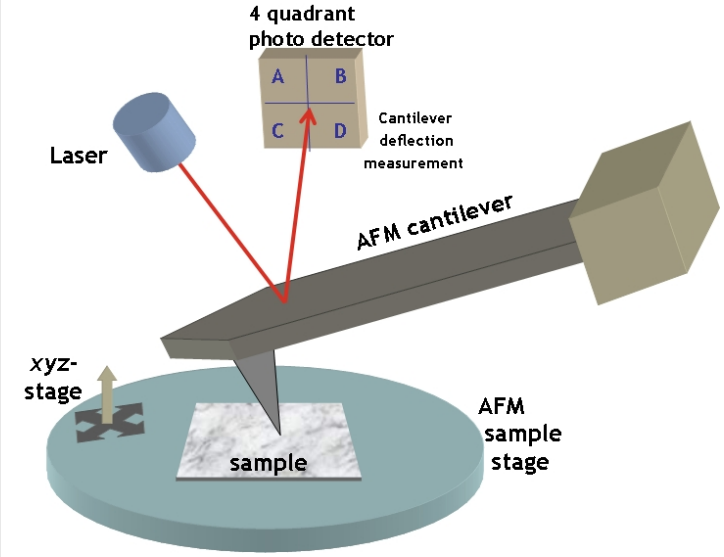


Typical AFM setup. A microfabricated cantilever with a sharp tip is deflected by features on a sample surface, much like in a phonograph but on a much smaller scale. A laser beam reflects off the backside of the cantilever into a set of photodetectors, allowing the deflection to be measured and assembled into an image of the surface.

There are several important modern developments. The atomic force microscope (AFM) and the Scanning Tunneling Microscope (STM) are two early versions of scanning probes that launched nanotechnology. There are other types of scanning probe microscopy, all flowing from the ideas of the scanning confocal microscope developed by Marvin Minsky in 1961 and the scanning acoustic microscope (SAM) developed by Calvin Quate and coworkers in the 1970s, that made it possible to see structures at the nanoscale. The tip of a scanning probe can also be used to manipulate nanostructures (a process called positional assembly). Feature-oriented scanning-positioning methodology suggested by Rostislav Lapshin appears to be a promising way to implement these nanomanipulations in automatic mode. However, this is still a slow process because of low scanning velocity of the microscope. Various techniques of nanolithography such as optical lithography, X-ray lithography dip pen nanolithography, electron beam lithography or nanoimprint lithography were also developed. Lithography is a top-down fabrication technique where a bulk material is reduced in size to nanoscale pattern.

Another group of nanotechnological techniques include those used for fabrication of nanowires, those used in semiconductor fabrication such as deep ultraviolet lithography, electron beam lithography, focused ion beam machining, nanoimprint lithography, atomic layer deposition, and molecular vapor deposition, and further including molecular self-assembly techniques such as those employing di-block copolymers. However, all of these techniques preceded the nanotech era, and are extensions in the development of scientific advancements rather than techniques which were devised with the sole purpose of creating nanotechnology and which were results of nanotechnology research.

The top-down approach anticipates nanodevices that must be built piece by piece in stages, much as manufactured items are made. Scanning probe microscopy is an important technique both for characterization and synthesis of nanomaterials. Atomic force microscopes and scanning tunneling microscopes can be used to look at surfaces and to move atoms around. By designing different tips for these microscopes, they can be used for carving out structures on surfaces and to help guide self-assembling structures. By using, for example, feature-oriented scanning-positioning approach, atoms can be moved around on a surface with scanning probe microscopy techniques. At present, it is expensive and time-consuming for mass production but very suitable for laboratory experimentation.

In contrast, bottom-up techniques build or grow larger structures atom by atom or molecule by molecule. These techniques include chemical synthesis, self-assembly and positional assembly. Dual polarisation interferometry is one tool suitable for characterisation of self assembled thin films. Another variation of the bottom-up approach is

molecular beam epitaxy or MBE. Researchers at Bell Telephone Laboratories like John R. Arthur. Alfred Y. Cho, and Art C. Gossard developed and implemented MBE as a research tool in the late 1960s and 1970s. Samples made by MBE were key to the discovery of the fractional quantum Hall effect for which the 1998 Nobel Prize in Physics was awarded. MBE allows scientists to lay down atomically precise layers of atoms and, in the process, build up complex structures. Important for research on semiconductors, MBE is also widely used to make samples and devices for the newly emerging field of spintronics.

However, new therapeutic products, based on responsive nanomaterials, such as the ultradeformable, stress-sensitive Transfersome vesicles, are under development and already approved for human use in some countries.

## Applications

As of August 21, 2008, the Project on Emerging Nanotechnologies estimates that over 800 manufacturer-identified nanotech products are publicly available, with new ones hitting the market at a pace of 3–4 per week.[28] The project lists all of the products in a publicly accessible online.[29] Most applications are limited to the use of "first generation" passive nanomaterials which includes titanium dioxide in sunscreen, cosmetics and some food products; Carbon allotropes used to produce gecko tape; silver in food packaging, clothing, disinfectants and household appliances; zinc oxide in sunscreens and cosmetics, surface coatings, paints and outdoor furniture varnishes; and cerium oxide as a fuel catalyst.[30]

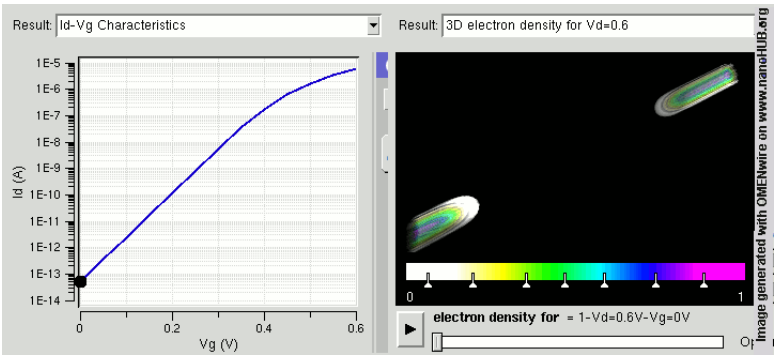


One of the major application of nanotechnology is in the area of nanoelectronics with MOSFET's being made of small nanowires ~10 nm in length. Here is a simulation of such a nanowire

The National Science Foundation (a major distributor for nanotechnology research in the United States) funded researcher David Berube to study the field of nanotechnology. His findings are published in the monograph Nano-Hype: The Truth Behind the Nanotechnology Buzz.[31] This study concludes that much of what is sold as “nanotechnology” is in fact a recasting of straightforward materials science, which is leading to a “nanotech industry built solely on selling nanotubes, nanowires, and the like” which will “end up with a few suppliers selling low margin products in huge volumes." Further applications which require actual manipulation or arrangement of nanoscale components await further research. Though technologies branded with the term 'nano' are sometimes little related to and fall far short of the most ambitious and transformative technological goals of the sort in molecular manufacturing proposals, the term still connotes such ideas. According to Berube, there may be a danger that a "nano bubble" will form, or is forming already, from the use of the term by scientists and entrepreneurs to garner funding, regardless of interest in the transformative possibilities of more ambitious and far-sighted work.[32]

# Implications

Because of the far-ranging claims that have been made about potential applications of nanotechnology, a number of serious concerns have been raised about what effects these will have on our society if realized, and what action if any is appropriate to mitigate these risks.

There are possible dangers that arise with the development of nanotechnology. The Center for Responsible Nanotechnology suggests that new developments could result, among other things, in untraceable weapons of mass destruction, networked cameras for use by the government, and weapons developments fast enough to destabilize arms races ("Nanotechnology Basics").

One area of concern is the effect that industrial-scale manufacturing and use of nanomaterials would have on human health and the environment, as suggested by nanotoxicology research. Groups such as the Center for Responsible Nanotechnology have advocated that nanotechnology should be specially regulated by governments for these reasons. Others counter that overregulation would stifle scientific research and the development of innovations which could greatly benefit mankind.

Other experts, including director of the Woodrow Wilson Center's Project on Emerging Nanotechnologies David Rejeski, have testified[33] that successful commercialization depends on adequate oversight, risk research strategy, and public engagement. Berkeley, California is currently the only city in the United States to regulate nanotechnology;[34] Cambridge, Massachusetts in 2008 considered enacting a similar law,[35] but ultimately rejected this.[36]

## Health and environmental concerns

Some of the recently developed nanoparticle products may have unintended consequences. Researchers have discovered that silver nanoparticles used in socks only to reduce foot odor are being released in the wash with possible negative consequences.[37] Silver nanoparticles, which are bacteriostatic, may then destroy beneficial bacteria which are important for breaking down organic matter in waste treatment plants or farms.[38]

A study at the University of Rochester found that when rats breathed in nanoparticles, the particles settled in the brain and lungs, which led to significant increases in biomarkers for inflammation and stress response.[39] A study in China indicated that nanoparticles induce skin aging through oxidative stress in hairless mice.[40] [41]

A two-year study at UCLA's School of Public Health found lab mice consuming nano-titanium dioxide showed DNA and chromosome damage to a degree "linked to all the big killers of man, namely cancer, heart disease, neurological disease and aging".[42]

A major study published more recently in Nature Nanotechnology suggests some forms of carbon nanotubes – a poster child for the “nanotechnology revolution” – could be as harmful as asbestos if inhaled in sufficient quantities. Anthony Seaton of the Institute of Occupational Medicine in Edinburgh, Scotland, who contributed to the article on carbon nanotubes said "We know that some of them probably have the potential to cause mesothelioma. So those sorts of materials need to be handled very carefully."[43] In the absence of specific nano-regulation forthcoming from governments, Paull and Lyons (2008) have called for an exclusion of engineered nanoparticles from organic food.[44] A newspaper article reports that workers in a paint factory developed serious lung disease and nanoparticles were found in their lungs.[45]

## Regulation

Calls for tighter regulation of nanotechnology have occurred alongside a growing debate related to the human health and safety risks associated with nanotechnology.[46] Furthermore, there is significant debate about who is responsible for the regulation of nanotechnology. While some non-nanotechnology specific regulatory agencies currently cover some products and processes (to varying degrees) – by “bolting on” nanotechnology to existing regulations – there are clear gaps in these regimes.[47] In "Nanotechnology Oversight: An Agenda for the Next Administration,"[48]

former EPA deputy administrator J. Clarence (Terry) Davies lays out a clear regulatory roadmap for the next presidential administration and describes the immediate and longer term steps necessary to deal with the current shortcomings of nanotechnology oversight.

Stakeholders concerned by the lack of a regulatory framework to assess and control risks associated with the release of nanoparticles and nanotubes have drawn parallels with bovine spongiform encephalopathy ('mad cow's disease), thalidomide, genetically modified food,[49] nuclear energy, reproductive technologies, biotechnology, and asbestosis. Dr. Andrew Maynard, chief science advisor to the Woodrow Wilson Center's Project on Emerging Nanotechnologies, concludes (among others) that there is insufficient funding for human health and safety research, and as a result there is currently limited understanding of the human health and safety risks associated with nanotechnology.[50] As a result, some academics have called for stricter application of the precautionary principle, with delayed marketing approval, enhanced labelling and additional safety data development requirements in relation to certain forms of nanotechnology.[51]

The Royal Society report[52] identified a risk of nanoparticles or nanotubes being released during disposal, destruction and recycling, and recommended that "manufacturers of products that fall under extended producer responsibility regimes such as end-of-life regulations publish procedures outlining how these materials will be managed to minimize possible human and environmental exposure" (p.xiii). Reflecting the challenges for ensuring responsible life cycle regulation, the Institute for Food and Agricultural Standards [53] has proposed standards for nanotechnology research and development should be integrated across consumer, worker and environmental standards. They also propose that NGOs and other citizen groups play a meaningful role in the development of these standards.

In October 2008, the Department of Toxic Substances Control (DTSC), within the California Environmental Protection Agency, announced its intent to request information regarding analytical test methods, fate and transport in the environment, and other relevant information from manufacturers of carbon nanotubes.[53] The purpose of this information request will be to identify information gaps and to develop information about carbon nanotubes, an important emerging nanomaterial.

## See also

- Bionanoscience
- Energy applications of nanotechnology
- List of emerging technologies
- List of software for nanostructures modeling
- Materiomics
- Molecular design software
- Molecular mechanics
- Nanoengineering
- Nanobiotechnology
- Nanofluidics
- Nanohub
- Nanometrology
- Nanoscale networks
- Nanotechnology education
- Nanotechnology in water treatment
- Nanothermite
- Nanoweapons
- Top-down and bottom-up
- Translational research

- Virtual Institute of Nano Films

# References


[1] Cristina Buzea, Ivan Pacheco, and Kevin Robbie (2007). "Nanomaterials and Nanoparticles: Sources and Toxicity" (http://scitation.aip.org/getabs/servlet/GetabsServlet?prog=normal&id=BJIOBN00000200000400MR17000001&idtype=cvips&gifs=Yes). *Biointerphases* **2**: MR17. .

[2] N. Taniguchi (1974). *On the Basic Concept of 'Nano-Technology*. Proc. Intl. Conf. Prod. London, Part II British Society of Precision Engineering.

[3] Eric Drexler (1991). *Nanosystems: Molecular Machinery, Manufacturing, and Computation. MIT PhD thesis* (http://www.e-drexler.com/d/06/00/Nanosystems/toc.html). New York: Wiley. ISBN 0471575186. .

[4] Kahn, Jennifer (2006). "Nanotechnology". *National Geographic* **2006** (June): 98–119.

[5] Rodgers, P. (2006). "Nanoelectronics: Single file". *Nature Nanotechnology*. doi:10.1038/nnano.2006.5.

[6] 22

[7] Lubick, N. (2008). Silver socks have cloudy lining. Environ Sci Technol. 42(11):3910

[8] Nanotechnology: Developing Molecular Manufacturing (http://www.crnano.org/developing.htm)

[9] "Some papers by K. Eric Drexler" (http://www.imm.org/PNAS.html). .

[10] California NanoSystems Institute (http://www.cnsi.ucla.edu/institution/personnel?personnel_id=105488)

[11] C&En: Cover Story - Nanotechnology (http://pubs.acs.org/cen/coverstory/8148/8148counterpoint.html)

[12] Regan, BC; Aloni, S; Jensen, K; Ritchie, RO; Zettl, A (2005). "Nanocrystal-powered nanomotor." (http://www.physics.berkeley.edu/research/zettl/pdf/312.NanoLett5regan.pdf). *Nano letters* **5** (9): 1730–3. doi:10.1021/nl0510659. PMID 16159214. .

[13] Regan, B. C.; Aloni, S.; Jensen, K.; Zettl, A. (2005). "Surface-tension-driven nanoelectromechanical relaxation oscillator" (http://www.lbl.gov/Science-Articles/Archive/sabl/2005/May/Tiniest-Motor.pdf). *Applied Physics Letters* **86**: 123119. doi:10.1063/1.1887827. .

[14] Wireless nanocrystals efficiently radiate visible light (http://www.sandia.gov/news-center/news-releases/2004/micro-nano/well.html)

[15] Clarkson, AJ; Buckingham, DA; Rogers, AJ; Blackman, AG; Clark, CR (2004). "Nanostructured Ceramics in Medical Devices: Applications and Prospects". *JOM* **56** (10): 38–43. doi:10.1007/s11837-004-0289-x. PMID 11196953.

[16] Levins, Christopher G.; Schafmeister, Christian E. (2006). "The Synthesis of Curved and Linear Structures from a Minimal Set of Monomers.". *ChemInform* **37**. doi:10.1002/chin.200605222.

[17] "Applications/Products" (http://www.nano.gov/html/facts/appsprod.html). National Nanotechnology Initiative. . Retrieved 2007-10-19.

[18] "The Nobel Prize in Physics 2007" (http://nobelprize.org/nobel_prizes/physics/laureates/2007/index.html). Nobelprize.org. . Retrieved 2007-10-19.

[19] Das S, Gates AJ, Abdu HA, Rose GS, Picconatto CA, Ellenbogen JC. (2007). "Designs for Ultra-Tiny, Special-Purpose Nanoelectronic Circuits". *IEEE Transactions on Circuits and Systems I* **54** (11): 2528–2540. doi:10.1109/TCSI.2007.907864.

[20] C.Michael Hogan. 2010. *Virus*. Encyclopedia of Earth. National Council for Science and the Environment (http://www.eoearth.org/article/Virus?topic=49496). eds. S.Draggan and C.Cleveland

[21] Ghalanbor Z, Marashi SA, Ranjbar B (2005). "Nanotechnology helps medicine: nanoscale swimmers and their future applications". *Med Hypotheses* **65** (1): 198–199. doi:10.1016/j.mehy.2005.01.023. PMID 15893147.

[22] Kubik T, Bogunia-Kubik K, Sugisaka M. (2005). "Nanotechnology on duty in medical applications". *Curr Pharm Biotechnol.* **6** (1): 17–33. PMID 15727553.

[23] Leary, SP; Liu, CY; Apuzzo, ML (2006). "Toward the Emergence of Nanoneurosurgery: Part III-Nanomedicine: Targeted Nanotherapy, Nanosurgery, and Progress Toward the Realization of Nanoneurosurgery". *Neurosurgery* **58** (6): 1009–1026. doi:10.1227/01.NEU.0000217016.79256.16. PMID 16723880.

[24] Shetty RC (2005). "Potential pitfalls of nanotechnology in its applications to medicine: immune incompatibility of nanodevices". *Med Hypotheses* **65** (5): 998–9. doi:10.1016/j.mehy.2005.05.022. PMID 16023299.

[25] Cavalcanti A, Shirinzadeh B, Freitas RA Jr., Kretly LC. (2007). "Medical Nanorobot Architecture Based on Nanobioelectronics". *Recent Patents on Nanotechnology* (http://bentham.org/nanotec/). **1** (1): 1–10. doi:10.2174/187221007779814745.

[26] Boukallel M, Gauthier M, Dauge M, Piat E, Abadie J. (2007). "Smart microrobots for mechanical cell characterization and cell convoying". *IEEE Trans. Biomed. Eng.* **54** (8): 1536–40. doi:10.1109/TBME.2007.891171. PMID 17694877.

[27] "International Perspective on Government Nanotechnology Funding in 2005" (http://www.nsf.gov/crssprgm/nano/reports/mcr_05-0526_intpersp_nano.pdf). .

[28] Project on Emerging Nanotechnologies. (2008). Analysis: This is the first publicly available on-line inventory of nanotechnology-based consumer products. (http://www.nanotechproject.org/inventories/consumer/analysis_draft/)

[29] Nanotechproject.org (http://www.nanotechproject.org/inventories/consumer/)

[30] Applications for Nanotechnology (http://www.americanelements.com/nanotech.htm)

[31] Prometheusbooks.com (http://www.prometheusbooks.com/index.php?main_page=product_info&products_id=1822/)

[32] Berube, David. Nano=Hype: The Truth Behind the Nanotechnology Buzz, Amherst, NY: Prometheus Books, 2006

[33] Testimony of David Rejeski for U.S. Senate Committee on Commerce, Science and Transportation (http://www.nanotechproject.org/news/archive/successful_commercialization_depends_on/) Project on Emerging Nanotechnologies. Retrieved on 2008-3-7.

[34] Berkeley considering need for nano safety (Rick DelVecchio, Chronicle Staff Writer) Friday, November 24, 2006 (http://www.sfgate.com/cgi-bin/article.cgi?file=/c/a/2006/11/24/MNGP9MJ4KI1.DTL)

[35] Cambridge considers nanotech curbs - City may mimic Berkeley bylaws (By Hiawatha Bray, Boston Globe Staff) January 26, 2007 (http://boston.com/business/technology/articles/2007/01/26/cambridge_considers_nanotech_curbs/)

[36] Recommendations for a Municipal Health & Safety Policy for Nanomaterials: A Report to the Cambridge City Manager. July 2008. (http://www.nanolawreport.com/Cambridge.pdf)

[37] Lubick, N. (2008). Silver socks have cloudy lining. (http://pubs.acs.org/subscribe/journals/esthag-w/2008/apr/science/nl_nanosocks.html)

[38] Murray R.G.E., Advances in Bacterial Paracrystalline Surface Layers (Eds.: T. J. Beveridge, S. F. Koval). Plenum pp. 3 ± 9. [9]

[39] Elder, A. (2006). Tiny Inhaled Particles Take Easy Route from Nose to Brain. (http://www.urmc.rochester.edu/pr/news/story.cfm?id=1191)

[40] Wu, J; Liu, W; Xue, C; Zhou, S; Lan, F; Bi, L; Xu, H; Yang, X *et al*. (2009). "Toxicity and penetration of TiO2 nanoparticles in hairless mice and porcine skin after subchronic dermal exposure.". *Toxicology letters* **191** (1): 1–8. doi:10.1016/j.toxlet.2009.05.020. PMID 19501137.

[41] Jonaitis, TS; Card, JW; Magnuson, B (2010). "Concerns regarding nano-sized titanium dioxide dermal penetration and toxicity study.". *Toxicology letters* **192** (2): 268–9. doi:10.1016/j.toxlet.2009.10.007. PMID 19836437.

[42] Schneider, Andrew, "Amid Nanotech's Dazzling Promise, Health Risks Grow" (http://www.aolnews.com/nanotech/article/amid-nanotechs-dazzling-promise-health-risks-grow/19401235), March 24, 2010.

[43] Weiss, R. (2008). Effects of Nanotubes May Lead to Cancer, Study Says. (http://www.washingtonpost.com/wp-dyn/content/article/2008/05/20/AR2008052001331.html?hpid=sec-health&sid=ST2008052100104)

[44] Paull, J. & Lyons, K. (2008). "Nanotechnology: The Next Challenge for Organics" (http://orgprints.org/13569/1/13569.pdf). *Journal of Organic Systems* **3**: 3-22. .

[45] Smith, Rebecca (August 19, 2009). "Nanoparticles used in paint could kill, research suggests" (http://www.telegraph.co.uk/health/healthnews/6016639/Nanoparticles-used-in-paint-could-kill-research-suggests.html). London: Telegraph. . Retrieved May 19, 2010.

[46] Kevin Rollins (Nems Mems Works, LLC). "Nanobiotechnology Regulation: A Proposal for Self-Regulation with Limited Oversight" (http://www.nanolabweb.com/index.cfm/action/main.default.viewArticle/articleID/290/CFID/3564274/CFTOKEN/43473772/index.html). *Volume 6 - Issue 2*. . Retrieved 2 September 2010.

[47] Bowman D, and Hodge G (2006). "Nanotechnology: Mapping the Wild Regulatory Frontier". *Futures* **38**: 1060–1073. doi:10.1016/j.futures.2006.02.017.

[48] Davies, JC. (2008). Nanotechnology Oversight: An Agenda for the Next Administration (http://www.nanotechproject.org/publications/archive/pen13/).

[49] Rowe G, Horlick-Jones T, Walls J, Pidgeon N, (2005). "Difficulties in evaluating public engagement initiatives: reflections on an evaluation of the UK GM Nation?". *Public Understanding of Science* (http://pus.sagepub.com/cgi/content/abstract/14/4/331). **14**: 333.

[50] Maynard, A. Testimony by Dr. Andrew Maynard for the U.S. House Committee on Science and Technology (http://www.science.house.gov/publications/Testimony.aspx?TID=12957). (2008-4-16). Retrieved on 2008-11-24.

[51] Faunce TA et al. Sunscreen Safety: The Precautionary Principle, The Australian Therapeutic Goods Administration and Nanoparticles in Sunscreens Nanoethics (2008) 2:231–240 DOI 10.1007/s11569-008-0041-z. Thomas Faunce & Katherine Murray & Hitoshi Nasu & Diana Bowman (published online: 24 July 2008). "Sunscreen Safety: The Precautionary Principle, The Australian Therapeutic Goods Administration and Nanoparticles in Sunscreens" (http://law.anu.edu.au/StaffUploads/236-Nanoethics Sunscreens 2008.pdf). Springer Science + Business Media B.V. . Retrieved 18 June 2009.

[52] Royal Society and Royal Academy of Engineering (2004). *Nanoscience and nanotechnologies: opportunities and uncertainties* (http://www.nanotec.org.uk/finalReport.htm). . Retrieved 2008-05-18.

[53] *Nanotechnology web page* (http://www.dtsc.ca.gov/TechnologyDevelopment/Nanotechnology/index.cfm). Department of Toxic Substances Control. 2008. .

## Further reading

- " Basic Concepts of Nanotechnology (http://www.inanot.com/)" History of Nano-Technology, News, Materials, Potential Risks and Important People.
- "About Nanotechnology - An Introduction to Nanotech from The Project on Emerging Nanotechnologies" (http://www.nanotechproject.org/topics/nano101/). Nanotechproject.org. Retrieved 2009-11-24.
- "Nanotechnology Introduction Pages" (http://www.nanotech-now.com/nano_intro.htm). Nanotech-now.com. Retrieved 2009-11-24.
- Medicalnanotec.com (http://www.medicalnanotec.com), Introduction to applications of Nanotechnology in Medicine.
- Maynard, Andrew, "The Twinkie Guide to Nanotechnology • News Archive • Nanotechnology Project" (http://www.nanotechproject.org/news/archive/the_twinkie_guide_to_nanotechnology/). Nanotechproject.org.

2007-10-22. Retrieved 2009-11-24. Woodrow Wilson International Center for Scholars. 2007. - "..a friendly, funny, 25-minute travel guide to the technology"

- "Nanotechnology Basics: For Students and Other Learners". Center for Responsible Nanotechnology - World Care. 11 November 2008.
- Fritz Allhoff and Patrick Lin (eds.), *Nanotechnology & Society: Current and Emerging Ethical Issues* (http://www.springer.com/philosophy/ethics/book/978-1-4020-6208-7) (Dordrecht: Springer, 2008).
- Fritz Allhoff, Patrick Lin, James Moor, and John Weckert (eds.) "Nanoethics: The Ethical and Societal Implications of Nanotechnology" (http://www.wiley.com/WileyCDA/WileyTitle/productCd-0470084170.html). John Wiley & Sons. 2007. "Wiley" (http://www.nanoethics.org/wiley.html).
- J. Clarence Davies, EPA and Nanotechnology: Oversight for the 21st Century (http://www.nanotechproject.org/publications/archive/epa_nanotechnology_oversight_for_21st/), *Project on Emerging Nanotechnologies*, PEN 9, May 2007.
- Carl Marziali, "Little Big Science," (http://www.usc.edu/uscnews/stories/13316.html) USC Trojan Family Magazine, Winter 2007.
- William Sims Bainbridge: *Nanoconvergence: The Unity of Nanoscience, Biotechnology, Information Technology and Cognitive Science*, June 27, 2007, Prentice Hall, ISBN 0-13-244643-X
- Lynn E. Foster: *Nanotechnology: Science, Innovation, and Opportunity*, December 21, 2005, Prentice Hall, ISBN 0-13-192756-6
- *Impact of Nanotechnology on Biomedical Sciences: Review of Current Concepts on Convergence of Nanotechnology With Biology* (http://www.azonano.com/details.asp?ArticleID=1242) by Herbert Ernest and Rahul Shetty, from AZojono, May 2005.
- Hunt, G & Mehta, M (eds)(2008) Nanotechnology: Risk, Ethics & Law, Earthscan, London.
- Andrew Schneider, The Nanotech Gamble (http://www.aolnews.com/category/nanotech/), Growing Health Risks from Nanomaterials in Food and Medicine, First in a Three-Part Series, AOL News Special Report, March 24, 2010.
- Hari Singh Nalwa (2004), Encyclopedia of Nanoscience and Nanotechnology (10-Volume Set), American Scientific Publishers. ISBN 1-58883-001-2
- Michael Rieth and Wolfram Schommers (2006), Handbook of Theoretical and Computational Nanotechnology (10-Volume Set), American Scientific Publishers. ISBN 1-58883-042-X
- Akhlesh Lakhtakia (ed) (2004). *The Handbook of Nanotechnology. Nanometer Structures: Theory, Modeling, and Simulation*. SPIE Press, Bellingham, WA, USA. ISBN 0-8194-5186-X.
- Fei Wang & Akhlesh Lakhtakia (eds) (2006). *Selected Papers on Nanotechnology—Theory & Modeling (Milestone Volume 182)*. SPIE Press, Bellingham, WA, USA. ISBN 0-8194-6354-X.
- Jumana Boussey, Georges Kamarinos, Laurent Montès (editors) (2003), Towards Nanotechnology (http://www.lavoisier.fr/notice/fr2746208580.html), "Nano et Micro Technologies", Hermes Sciences Publ., Paris, ISBN 2-7462-0858-X.
- The Silicon Valley Toxics Coalition (April, 2008), Regulating Emerging Technologies in Silicon Valley and Beyond (http://www.svtc.org/svtc_nanotech)
- Genetic Engineering & Biotechnology News (http://www.genengnews.com) (January, 2008), Getting a Handle on Nanobiotech Products (http://www.genengnews.com/articles/chitem.aspx?aid=2325) Regulators and Companies Are Laying the Groundwork for a Predicted Bright Future
- Suh WH, Suslick KS, Stucky GD, Suh YH (2009). "Nanotechnology, nanotoxicology, and neuroscience" (http://www.pubmedcentral.nih.gov/articlerender.fcgi?tool=pmcentrez&artid=2728462). *Progress in Neurobiology* **87** (3): 133–70. doi:10.1016/j.pneurobio.2008.09.009. PMID 18926873. PMC 2728462.

## External links

- What is Nanotechnology? (http://www.vega.org.uk/video/programme/3) (A Vega/BBC/OU Video Discussion).
- Nanotec Expo (http://www.nanotecexpo.com.br/english) - Fair and Congress Latin American of Nanotechnology
- "Nanotechnology Basics: For Students and Other Learners." (http://www.crnano.org/basics.htm) Center for Responsible Nanotechnology. World Care. 11 Nov. 2008.
- Nanotechnology (http://www.dmoz.org/Science/Technology/Nanotechnology//) at the Open Directory Project
- Course on *Introduction to Nanotechnology* (http://nanohub.org/resources/6583)
- The Nano Age (http://www.thenanoage.com)

# Surface science

**Surface science** is the study of physical and chemical phenomena that occur at the interface of two phases, including solid-liquid interfaces, solid-gas interfaces, solid-vacuum interfaces, and liquid-gas interfaces. It includes the fields of *surface chemistry* and *surface physics*.[1] Some related practical applications are classed as surface engineering. The science encompasses concepts such as heterogeneous catalysis, semiconductor device fabrication, fuel cells, self-assembled monolayers, and adhesives. Surface science is closely related to interface and colloid science.[2] Interfacial chemistry and physics are common subjects for both. The methods are different. In addition, interface and colloid science studies macroscopic phenomena that occur in heterogeneous systems due to peculiarities of interfaces.

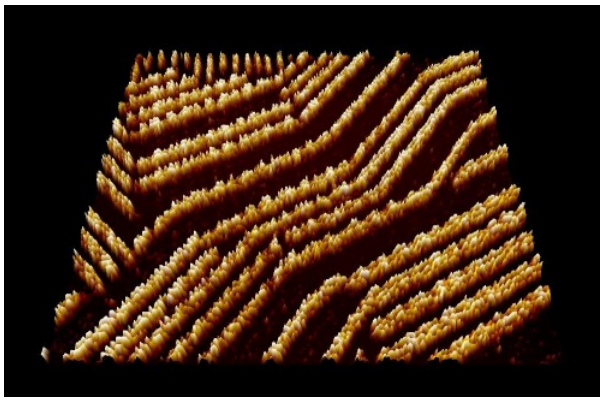

STM image of a Quinacridone adsorbate. The self-assembled supramolecular chains of the organic semiconductor are adsorbed on a Graphite surface.

## History

The field of surface chemistry started with heterogeneous catalysis pioneered by Paul Sabatier on hydrogenation and Fritz Haber on the Haber process.[3] Irving Langmuir was also one of the founders of this field, and the scientific journal on surface science, *Langmuir*, bears his name. The Langmuir adsorption equation is used to model monolayer adsorption where all surface adsorption sites have the same affinity for the adsorbing species. Gerhard Ertl in 1974 described for the first time the adsorption of hydrogen on a palladium surface using a novel technique called LEED.[4] Similar studies with platinum,[5] nickel,[6] [7] and iron [8] followed. Most recent developments in surface sciences include the 2007 Nobel Prize of Chemistry winner Gerhard Ertl's advancements in surface chemistry, specifically his investigation of the interaction between carbon monoxide molecules and platinum surfaces.

## Surface chemistry

Surface chemistry can be roughly defined as the study of chemical reactions at interfaces. It is closely related to surface engineering, which aims at modifying the chemical composition of a surface by incorporation of selected elements or functional groups that produce various desired effects or improvements in the properties of the surface or interface. Surface chemistry also overlaps with electrochemistry. Surface science is of particular importance to the field of heterogeneous catalysis.

The adhesion of gas or liquid molecules to the surface is known as adsorption. This can be due to either chemisorption or by physisorption. These too are included in surface chemistry.

The behavior of a solution based interface is affected by the surface charge, dipoles, energies, and their distribution within the electrical double layer.

## Surface physics

Surface physics can be roughly defined as the study of physical changes that occur at interfaces. It overlaps with surface chemistry. Some of the things investigated by surface physics include surface states, surface diffusion, surface reconstruction, surface phonons and plasmons, epitaxy and surface enhanced Raman scattering, the emission and tunneling of electrons, spintronics, and the self-assembly of nanostructures on surface.

## Analysis techniques

The study and analysis of surfaces involves both physical and chemical analysis techniques.

Several modern methods probe the topmost 1−10 nm of the of surfaces exposed to vacuum. These include X-ray photoelectron spectroscopy, Auger electron spectroscopy, low-energy electron diffraction, electron energy loss spectroscopy, thermal desorption spectroscopy, ion scattering spectroscopy, secondary ion mass spectrometry, and other surface analysis methods included in the list of materials analysis methods. Many of these techniques require vacuum as they rely on the detection of electrons or ions emitted from the surface under study. Moreover, in general ultra high vacuum, in the range of $10^{-7}$ pascal pressure or better, is necessary to reduce surface contamination by residual gas, by reducing the number of molecules reaching the sample over a given time period. At 0.1 mPa ($10^{-6}$ Torr), it only takes 1 second to cover a surface with a contaminant, so much lower pressures are needed for measurements.

Purely optical techniques can be used to study interfaces under a wide variety of conditions. Reflection-absorption infrared, dual polarisation interferometry, surface enhanced Raman, and sum frequency generation spectroscopies can be used to probe solid-vacuum as well as solid-gas, solid-liquid, and liquid-gas surfaces.

Modern physical analysis methods include scanning-tunneling microscopy (STM) and a family of methods descended from it. These microscopies have considerably increased the ability and desire of surface scientists to measure the physical structure of many surfaces. This increase is related to a more general interest in nanotechnology.

## See also

- Surface modification
- Surface finishing
- Tribology
- Micromeritics
- Kelvin probe force microscope

## References

[1] Prutton, Martin (1994). *Introduction to Surface Physics*. Oxford University Press. ISBN 0198-53476-0.

[2] Luklema, J. (1995–2005). *Fundamentals of Interface and Colloid Science*. **1–5**. Academic Press.

[3] Wennerström, Håkan; Lidin, Sven. "*Scientific Background on the Nobel Prize in Chemistry 2007 Chemical Processes on Solid Surfaces*" (http://nobelprize.org/nobel_prizes/chemistry/laureates/2007/chemadv07.pdf) (pdf). .

[4] Conrad, H.; Ertl, G.; Latta, E.E. (February 1974). "Adsorption of hydrogen on palladium single crystal surfaces". *Surface Science* **41** (2): 435–446. doi:10.1016/0039-6028(74)90060-0.

[5] Christmann, K.; Ertl, G.; Pignet, T. (February 1976). "Adsorption of hydrogen on a Pt(111) surface". *Surface Science* **54** (2): 365–392. doi:10.1016/0039-6028(76)90232-6.

[6] Christmann, K.; Schober, O.; Ertl, G.; Neumann, M. (June 1, 1974). "Adsorption of hydrogen on nickel single crystal surfaces". *The Journal of Chemical Physics* **60** (11): 4528–4540. doi:10.1063/1.1680935.

[7] Christmann, K.; Behm, R. J.; Ertl, G.; Van Hove, M. A.; Weinberg, W. H. (May 1, 1979). "Chemisorption geometry of hydrogen on Ni(111): Order and disorder". *The Journal of Chemical Physics* **70** (9): 4168–4184. doi:10.1063/1.438041.

[8] Imbihl, R.; Behm, R. J.; Christmann, K.; Ertl, G.; Matsushima, T. (May 2, 1982). "Phase transitions of a two-dimensional chemisorbed system: H on Fe(110)". *Surface Science* **117**: 257–266. doi:10.1016/0039-6028(82)90506-4.

## External links

- "Ram Rao Materials and Surface Science" (http://www.vega.org.uk/video/programme/24), a video from the Vega Science Trust
- Surface Chemistry Discoveries (http://www.surfchem.net)

# Electron tomography

**Electron Tomography** (**ET**) is a tomography technique for obtaining detailed 3D structures of subcellular macromolecular objects. Electron tomography is an extension of traditional transmission electron microscopy and uses a transmission electron microscope to collect the data. In the process, a beam of electrons is passed through the sample at incremental degrees of rotation around the center of the target sample. This information is collected and used to assemble a three dimensional image of the target. Current resolutions of ET systems are in the 5-20 nm range, suitable for examining supra-molecular multi-protein structures, although not the secondary and tertiary structure of an individual protein or polypeptide.

## ADF-STEM Tomography

In the field of biology, bright-field transmission electron microscopy (BF-TEM) and high-resolution TEM (HRTEM) are the primary imaging methods for tomography tilt series acquisition. However, there are two issues associated with BF-TEM and HRTEM. First, acquiring an interpretable 3D tomogram requires that the projected image intensities vary monotonically with material thickness. This condition is difficult to guarantee in BF/HRTEM, where image intensities are dominated by phase-contrast with the potential for multiple contrast reversals with thickness, making it difficult to distinguish voids from high-density inclusions.[1] Second, the contrast transfer function of BF-TEM is essentially a high-pass filter – information at low spatial frequencies is significantly suppressed – resulting in an exaggeration of sharp features. However, the technique of annular dark field scanning transmission electron microscopy (ADF-STEM) more effectively suppresses phase and diffraction contrast, providing image intensities that vary with the projected mass-thickness of samples up to microns thick for materials with low atomic number. ADF-STEM also acts as a low-pass filter, eliminating the edge-enhancing artifacts common in BF/HRTEM. Thus, provided that the features can be resolved, ADF-STEM tomography can yield a reliable reconstruction of the underlying specimen which is extremely important for its application in material science.[2] Some applications of ADF-STEM tomography in material science and physics can be found in refs.[3] [4] [5] [6] . So far, the best resolving power of a single-axis ADF-STEM tomography is 0.5±0.1×0.5±0.1×0.7±0.2 nm^3 as reported in[7] .

### Different tilting methods

The most popular tilting methods are the single-axis and the dual-axis tilting methods. Dual-axis tomography is sometimes referred to as conical tomography as well. By using dual-axis tilting, the elongation effect is reduced by a factor of $\sqrt{2}$however, twice as many of images need to be taken.

## See also

- Positron emission tomography
- Three dimensional transmission electron microscopy

## External links

- Feature article on electron tomography [8] from November 1, 2007 issue of *Analytical Chemistry* [9]

## References

[1] Bals, S; Kisielowski, C F; Croitoru, M; Tendeloo, G Van (2005). "Annular Dark Field Tomography in TEM". *Microscopy and Microanalysis* **11**. doi:10.1017/S143192760550117X.

[2] Midgley, P; Weyland, M (2003). "3D electron microscopy in the physical sciences: the development of Z-contrast and EFTEM tomography". *Ultramicroscopy* **96** (3-4): 413. doi:10.1016/S0304-3991(03)00105-0. PMID 12871805.

[3] Midgley, Paul A.; Dunin-Borkowski, Rafal E. (2009). "Electron tomography and holography in materials science". *Nature Materials* **8** (4): 271. doi:10.1038/nmat2406. PMID 19308086.

[4] Ercius, Peter; Weyland, Matthew; Muller, David A.; Gignac, Lynne M. (2006). "Three-dimensional imaging of nanovoids in copper interconnects using incoherent bright field tomography". *Applied Physics Letters* **88**: 243116. doi:10.1063/1.2213185.

[5] Li, H.; Xin, H. L.; Muller, D. A.; Estroff, L. A. (2009). "Visualizing the 3D Internal Structure of Calcite Single Crystals Grown in Agarose Hydrogels". *Science* **326** (5957): 1244. doi:10.1126/science.1178583. PMID 19965470.

[6] Xin, Huolin L.; Ercius, Peter; Hughes, Kevin J.; Engstrom, James R.; Muller, David A. (2010). "Three-dimensional imaging of pore structures inside low-κ dielectrics". *Applied Physics Letters* **96**: 223108. doi:10.1063/1.3442496.

[7] Xin, Huolin L.; Ercius, Peter; Hughes, Kevin J.; Engstrom, James R.; Muller, David A. (2010). "Three-dimensional imaging of pore structures inside low-κ dielectrics". *Applied Physics Letters* **96**: 223108. doi:10.1063/1.3442496.

[8] http://pubs.acs.org/doi/abs/10.1021/ac071982u

[9] http://pubs3.acs.org/acs/journals/toc.page?incoden=ancham&indecade=0&involume=79&inissue=21

# Virtopsy

**Virtopsy** is a portmanteau of virtual and autopsy. It is a way of performing a non- or minimally-invasive autopsy by scanning a corpse. Virtopsy is a registered name of the research team in Bern, Switzerland.

## Virtopsies in popular culture

- In the *CSI: Miami* episode “Deep Freeze”, Dr. Woods performs a virtopsy on a recently murdered athlete to prevent damaging it so that he could be cryogenically frozen.
- In the *CSI: NY* episode “Veritas”, Sid does a virtual autopsy on Derek, showing Stella that the bullet that killed him entered through his cheek.

## See also

- Autopsy
- Magnetic resonance imaging
- Medical imaging
- Multislice spiral computer tomography

## External links

- The virtopsy website [1] at the University of Bern
- An article on virtopsies [2] by Popular Science
- An article on virtopsies [3] by the New York Times
- The Virtual Autopsy Table [4]

## References

[1] http://www.virtopsy.com/
[2] http://www.popsci.com/popsci/medicine/5196c4522fa84010vgnvcm1000004eecbccdrcrd.html
[3] http://www.nytimes.com/2004/12/12/magazine/12VIRTOPSY.html
[4] http://www.vimeo.com/6866296

# Xenon-enhanced CT scanning

**Xenon-enhanced CT scanning** is a method of computed tomography (CT scanning) used for neuroimaging in which the subject inhales xenon gas while CT images are made.[1] The method can be used to assess changes in cerebral blood flow in the period shortly after a traumatic brain injury.[1] The diffusion of the gas into the tissues shows how much blood flow each area is getting.[1]

## References

[1] Zink BJ (March 2001). "Traumatic brain injury outcome: Concepts for emergency care". *Ann Emerg Med* **37** (3): 318–32. doi:10.1067/mem.2001.113505. PMID 11223769.

# X-ray microtomography

**Microtomography** (commonly known as Industrial CT Scanning), like tomography, uses x-rays to create cross-sections of a 3D-object that later can be used to recreate a virtual model without destroying the original model. The term *micro* is used to indicate that the pixel sizes of the cross-sections are in the micrometer range.[1] These pixel sizes have also resulted in the terminology micro-computed tomography, micro-ct, micro-computer tomography, high resolution x-ray tomography, and similar terminologies. All of these names generally represent the same class of instruments.

This also means that the machine is much smaller in design compared to the human version and is used to model smaller objects. In general, there are two types of scanner setups. In one setup, the X-ray source and detector are typically stationary during the scan while the sample/animal rotates. The second setup, much more like a clinical CT scanner, is gantry based where the animal/specimen is stationary in space while the X-ray tube and detector rotate around. These scanners are typically used for small animals (in-vivo scanners), biomedical samples, foods, microfossils, and other studies for which minute detail is desired.

The first X-ray microtomography system was conceived and built by Jim Elliott in the early 1980s. The first published X-ray microtomographic images were reconstructed slices of a small tropical snail, with pixel size about 50 micrometers.[2] Many believe that the technology did not really take off until the advent of the cone beam reconstruction algorithm originally authored by Lee Feldkamp.

# Working principle

- **Imaging system**

  **Fan beam reconstruction**

  The fan-beam system is based on a 1-dimensional x-ray detector and an electronic x-ray source, creating 2-dimensional cross-sections of the object. Typically used in human Computed tomography systems.

  **Cone beam reconstruction**

  The cone-beam system is based on a 2-dimensional x-ray detector (camera) and an electronic x-ray source, creating projection images that later will be used to reconstruct the image cross-sections.

- **Open/Closed systems**

  **Open x-ray system**

  In an open system, x-rays may escape or leak out, thus the operator must stay behind a shield, have special protective clothing, or operate the scanner from a distance or a different room. Typical examples of these scanners are the human versions, or designed for big objects.

  **Closed x-ray system**

  In a closed system, x-ray shielding is put around the scanner so the operator can put the scanner on a desk or special table. Although the scanner is shielded, care must be taken and the operator usually carries a dose meter, since x-rays have a tendency to be absorbed by metal and then re-emitted like an antenna. Although a typical scanner will produce a relatively harmless volume of x-rays, repeated scannings in a short timeframe could pose a danger.

  Closed systems tend to become very heavy because lead is used to shield the x-rays. Therefore, the smaller scanners only have a small space for samples.

# Three-dimensional (3D) image reconstruction

## The principle

Because microtomography scanners offer isotropic, or near isotropic, resolution, display of images does not need to be restricted to the conventional axial images. Instead, it is possible for a software program to build a volume by 'stacking' the individual slices one on top of the other. The program may then display the volume in an alternative manner.

## Volume rendering

Volume rendering is a technique used to display a 2D projection of a 3D discretely sampled data set, as produced by a microtomography scanner. Usually these are acquired in a regular pattern (e.g., one slice every millimeter) and usually have a regular number of image pixels in a regular pattern. This is an example of a regular volumetric grid, with each volume element, or voxel represented by a single value that is obtained by sampling the immediate area surrounding the voxel.

### Image segmentation

Where different structures have similar threshold density, it can become impossible to separate them simply by adjusting volume rendering parameters. The solution is called segmentation, a manual or automatic procedure that can remove the unwanted structures from the image.

## Typical use

- **Biomedical**
  - Both in vitro and in vivo small animal imaging
  - Human skin samples
  - Bone samples, ranging in size from rodents to human biopsies
  - Lung imaging using respiratory gating
  - Cardiovascular imaging using cardiac gating
  - Tumor imaging (may require contrast agents)
  - Soft tissue imaging (may require contrast agents)
- **Electronics**

  Small electronic components. E.g. DRAM IC in plastic case.
- **Microdevices**

  E.g. spray nozzle
- **Composite materials and metallic foams**

  E.g. composite material with glass fibers 10 to 12 micrometres in diameter
- **Polymers, plastics**
- **Diamonds**

  E.g. detecting defects in a diamond and finding the best way to cut it.
- **Food and seeds**
  - E.g. piece of chocolate cake, cookies
  - 3-D Imaging of Foods Using X-Ray Microtomography[3]
- **Wood and paper**

  E.g. piece of wood to visualize year periodicity and cell structure
- **Building materials**

  E.g. concrete after loading.
- **Geology**
  - E.g. sandstone
  - porosity and flow studies
- **Microfossils**

  E.g. bentonic foraminifers
- **Space**

  E.g. Locating Stardust-like particles in aerogel using x-ray techniques[4]
- **Others**
- **Stereo images**

  Visualizing with blue and green or blue filters to see depth

## Publications

- MicroComputed Tomography: Methodology and Applications [5]
- Synchrotron and non synchrotron X-ray microtomography threedimensional representation of bone ingrowth in calcium phosphate biomaterials [6]
- Microfocus X-ray Computer Tomography in Materials Research [7]
- Locating Stardust-like particles in aerogel using x-ray techniques [8]
- 3-D Imaging of Foods Using X-Ray Microtomography [9]
- Use of micro CT to study kidney stones [10]
- Application of the Gatan X-ray Ultramicroscope (XuM) to the Investigation of Material and Biological Samples [11]
- 3D Synchrotron X-ray microtomography of paint samples [12]

## References

[1] MeSH *X-Ray+Microtomography* (http://www.nlm.nih.gov/cgi/mesh/2009/MB_cgi?mode=&term=X-Ray+Microtomography)
[2] JC Elliott and SD Dover. X-ray microtomography. J. Microscopy 126, 211-213, 1982.
[3] http://www.cb.uu.se/~cris/Documents/GIT2003.pdf
[4] http://www.lpi.usra.edu/meetings/lpsc2003/pdf/1228.pdf
[5] http://www.crcpress.com/product/isbn/9781420058765
[6] http://www.ecmjournal.org/journal/supplements/vol009supp01/pdf/v009supp01a24.pdf
[7] http://www.ndt.net/article/wcndt00/papers/idn399/idn399.htm
[8] http://www.lpi.usra.edu/meetings/lpsc2003/pdf/1228.pdf
[9] http://www.cb.uu.se/~cris/Documents/GIT2003.pdf
[10] http://www.pubmedcentral.nih.gov/articlerender.fcgi?artid=544194
[11] http://www.gatan.com/files/PDF/products/XuMMTNov08Paper.pdf
[12] http://sls.web.psi.ch/view.php/beamlines/tomcat/publications/2009_Ferreira_SPIE.pdf

# Positron emission tomography

**Positron emission tomography** (**PET**) is a nuclear medicine imaging technique which produces a three-dimensional image or picture of functional processes in the body. The system detects pairs of gamma rays emitted indirectly by a positron-emitting radionuclide (tracer), which is introduced into the body on a biologically active molecule. Images of tracer concentration in 3-dimensional or 4-dimensional space (the 4th dimension being time) within the body are then reconstructed by computer analysis. In modern scanners, this reconstruction is often accomplished with the aid of a CT X-ray scan performed on the patient during the same session, in the same machine.

Image of a typical positron emission tomography (PET) facility

If the biologically active molecule chosen for PET is FDG, an analogue of glucose, the concentrations of tracer imaged then give tissue metabolic activity, in terms of regional glucose uptake. Although use of this tracer results in the most common type of PET scan, other tracer molecules are used in PET to image the tissue concentration of many other types of molecules of interest.

PET/CT-System with 16-slice CT; the ceiling mounted device is an injection pump for CT contrast agent

## History

The concept of emission and transmission tomography was introduced by David E. Kuhl and Roy Edwards in the late 1950s. Their work later led to the design and construction of several tomographic instruments at the University of Pennsylvania. Tomographic imaging techniques were further developed by Michel Ter-Pogossian, Michael E. Phelps and others at the Washington University School of Medicine.[1] [2]

Work by Gordon Brownell, Charles Burnham and their associates at the Massachusetts General Hospital beginning in the 1950s contributed significantly to the development of PET technology and included the first demonstration of annihilation radiation for medical imaging.[3] Their innovations, including the use of light pipes, and volumetric analysis have been important in the deployment of PET imaging. In 1961, James Robertson and his associates at Brookhaven National Laboratory built the first single-plane PET scan, nicknamed the "head-shrinker." [4]

It is interesting that one of the factors most responsible for the acceptance of positron imaging was the development of radiopharmaceuticals. In particular, the development of labeled 2-fluorodeoxy-D-glucose (2FDG) by the Brookhaven group under the direction of Al Wolf and Joanna Fowler was a major factor in expanding the scope of PET imaging.[5] The compound was first administered to two normal human volunteers by Abass Alavi in August 1976 at the University of Pennsylvania. Brain images obtained with an ordinary (non-PET) nuclear scanner demonstrated the concentration of FDG in that organ. Later, the substance was used in dedicated positron tomographic scanners, to yield the modern procedure.

The logical extension of positron instrumentation was a design using two 2-dimensional arrays. PC-I was the first instrument using this concept and was designed in 1968, completed in 1969 and reported in 1972. The first applications of PC-I in tomographic mode as distinguished from the computed tomographic mode were reported in 1970.[6] It soon became clear to many of those involved in PET development that a circular or cylindrical array of detectors was the logical next step in PET instrumentation. Although many investigators took this approach, James Robertson [7] and Z.H. Cho[8] were the first to propose a ring system which has become the prototype of the current shape of PET.

The PET/CT scanner, attributed to Dr David Townsend and Dr Nutt was named by TIME Magazine as the medical invention of the year in 2000.

# Description

## Operation

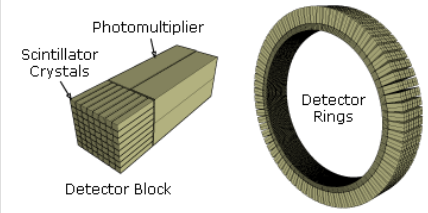

Schematic view of a detector block and ring of a PET scanner

To conduct the scan, a short-lived radioactive tracer isotope is injected into the living subject (usually into blood circulation). The tracer is chemically incorporated into a biologically active molecule. There is a waiting period while the active molecule becomes concentrated in tissues of interest; then the subject is placed in the imaging scanner. The molecule most commonly used for this purpose is fluorodeoxyglucose (FDG), a sugar, for which the waiting period is typically an hour. During the scan a record of tissue concentration is made as the tracer decays.

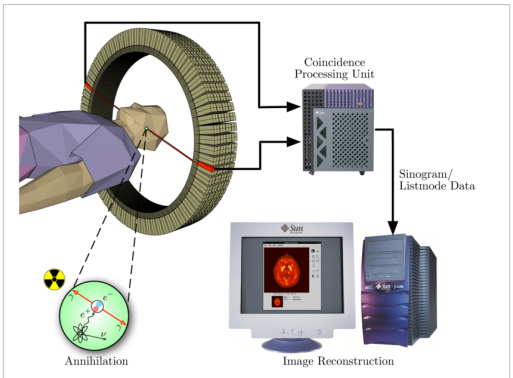

Schema of a PET acquisition process

As the radioisotope undergoes positron emission decay (also known as positive beta decay), it emits a positron, an antiparticle of the electron with opposite charge. The emitted positron travels in tissue for a short distance (typically less than 1 mm, but dependent on the isotope[9] ), during which time it loses kinetic energy, until it decelerates to a point where it can interact with an electron.[10] The encounter annihilates both electron and positron, producing a pair of annihilation (gamma) photons moving in approximately opposite directions. These are detected when they reach a scintillator in the scanning device, creating a burst of light which is detected by photomultiplier tubes or silicon avalanche photodiodes (Si APD). The technique depends on simultaneous or coincident detection of the pair of photons moving in approximately opposite direction (it would be exactly opposite in their center of mass frame, but the scanner has no way to know this, and so has a built-in slight direction-error tolerance). Photons that do not arrive in temporal "pairs" (i.e. within a timing-window of a few nanoseconds) are ignored.

## Localization of the positron annihilation event

The most significant fraction of electron-positron decays result in two 511 keV gamma photons being emitted at almost 180 degrees to each other; hence it is possible to localize their source along a straight line of coincidence (also called formally the **line of response** or **LOR**). In practice the LOR has a finite width as the emitted photons are not exactly 180 degrees apart. If the resolving time of the detectors is less than 500 picoseconds rather than about 10 nanoseconds, it is possible to localize the event to a segment of a chord, whose length is determined by the detector timing resolution. As the timing resolution improves, the signal-to-noise ratio (SNR) of the image will improve, requiring fewer events to achieve the same image quality. This technology is not yet common, but it is available on

some new systems.[11]

## Image reconstruction using coincidence statistics

More commonly, a technique much like the reconstruction of computed tomography (CT) and single photon emission computed tomography (SPECT) data is used, although the data set collected in PET is much poorer than CT, so reconstruction techniques are more difficult (see Image reconstruction of PET).

Using statistics collected from tens-of-thousands of coincidence events, a set of simultaneous equations for the total activity of each parcel of tissue along many LORs can be solved by a number of techniques, and thus a map of radioactivities as a function of location for parcels or bits of tissue (also called voxels), may be constructed and plotted. The resulting map shows the tissues in which the molecular tracer has become concentrated, and can be interpreted by a nuclear medicine physician or radiologist in the context of the patient's diagnosis and treatment plan.

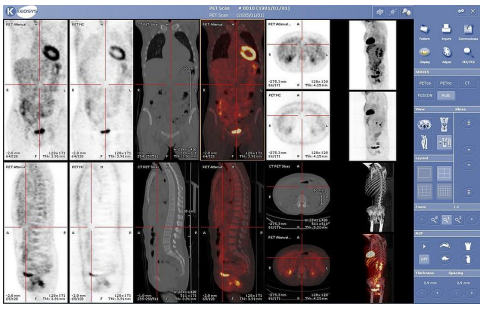

A complete body PET / CT Fusion image

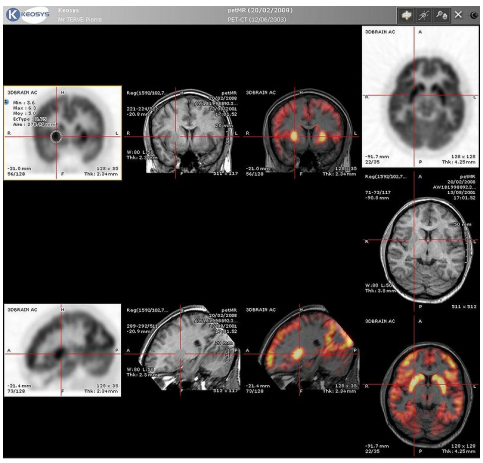

A Brain PET / MRI Fusion image

## Combination of PET with CT or MRI

PET scans are increasingly read alongside CT or magnetic resonance imaging (MRI) scans, the combination ("co-registration") giving both anatomic and metabolic information (i.e., what the structure is, and what it is doing biochemically). Because PET imaging is most useful in combination with anatomical imaging, such as CT, modern PET scanners are now available with integrated high-end multi-detector-row CT scanners. Because the two scans can be performed in immediate sequence during the same session, with the patient not changing position between the two types of scans, the two sets of images are more-precisely registered, so that areas of abnormality on the PET imaging can be more perfectly correlated with anatomy on the CT images. This is very useful in showing detailed views of moving organs or structures with higher anatomical variation, which is more common outside the brain.

At the Jülich Institute of Neurosciences and Biophysics, the world's largest PET/MRI device began operation in April 2009: a 9.4-tesla magnetic resonance tomograph (MRT) combined with a positron emission tomograph (PET). Presently, only the head and brain can be imaged at these high magnetic field strengths.[12]

## Radionuclides

Radionuclides used in PET scanning are typically isotopes with short half lives such as carbon-11 (~20 min), nitrogen-13 (~10 min), oxygen-15 (~2 min), and fluorine-18 (~110 min). These radionuclides are incorporated either into compounds normally used by the body such as glucose (or glucose analogues), water or ammonia, or into molecules that bind to receptors or other sites of drug action. Such labelled compounds are known as radiotracers. It is important to recognize that PET technology can be used to trace the biologic pathway of any compound in living humans (and many other species as well), provided it can be radiolabeled with a PET isotope. Thus the specific processes that can be probed with PET are virtually limitless, and radiotracers for new target molecules and processes are being synthesized all the time; as of this writing there are already dozens in clinical use and hundreds

applied in research. Presently, however, by far the most commonly used radiotracer in clinical PET scanning is FDG, an analogue of glucose that is labeled with fluorine-18 .

Due to the short half lives of most radioisotopes, the radiotracers must be produced using a cyclotron in close proximity to the PET imaging facility. The half life of fluorine-18 is long enough that radiotracers labeled with fluorine-18 can be manufactured commercially at offsite locations and shipped to imaging centers.

## Limitations

The minimization of radiation dose to the subject is an attractive feature of the use of short-lived radionuclides. Besides its established role as a diagnostic technique, PET has an expanding role as a method to assess the response to therapy, in particular, cancer therapy,[13] where the risk to the patient from lack of knowledge about disease progress is much greater than the risk from the test radiation.

Limitations to the widespread use of PET arise from the high costs of cyclotrons needed to produce the short-lived radionuclides for PET scanning and the need for specially adapted on-site chemical synthesis apparatus to produce the radiopharmaceuticals. Few hospitals and universities are capable of maintaining such systems, and most clinical PET is supported by third-party suppliers of radiotracers which can supply many sites simultaneously. This limitation restricts clinical PET primarily to the use of tracers labelled with fluorine-18, which has a half life of 110 minutes and can be transported a reasonable distance before use, or to rubidium-82, which can be created in a portable generator and is used for myocardial perfusion studies. Nevertheless, in recent years a few on-site cyclotrons with integrated shielding and hot labs have begun to accompany PET units to remote hospitals. The presence of the small on-site cyclotron promises to expand in the future as the cyclotrons shrink in response to the high cost of isotope transportation to remote PET machines [14]

Because the half-life of fluorine-18 is about two hours, the prepared dose of a radiopharmaceutical bearing this radionuclide will undergo multiple half-lives of decay during the working day. This necessitates frequent recalibration of the remaining dose (determination of activity per unit volume) and careful planning with respect to patient scheduling.

## Image reconstruction

The raw data collected by a PET scanner are a list of 'coincidence events' representing near-simultaneous detection (typically, within a window of 6 to 12 nanoseconds of each other) of annihilation photons by a pair of detectors. Each coincidence event represents a line in space connecting the two detectors along which the positron emission occurred. Modern systems with a higher time resolution (roughly 3 nanoseconds) also use a technique (called "Time-of-flight") where they more precisely decide the difference in time between the detection of the two photons and can thus localize the point of origin of the annihilation event between the two detectors to within 10 cm.

Coincidence events can be grouped into projection images, called sinograms. The sinograms are sorted by the angle of each view and tilt (for 3D images). The sinogram images are analogous to the projections captured by computed tomography (CT) scanners, and can be reconstructed in a similar way. However, the statistics of the data are much worse than those obtained through transmission tomography. A normal PET data set has millions of counts for the whole acquisition, while the CT can reach a few billion counts. As such, PET data suffer from scatter and random events much more dramatically than CT data does.

In practice, considerable pre-processing of the data is required - correction for random coincidences, estimation and subtraction of scattered photons, detector dead-time correction (after the detection of a photon, the detector must "cool down" again) and detector-sensitivity correction (for both inherent detector sensitivity and changes in sensitivity due to angle of incidence).

Filtered back projection (FBP) has been frequently used to reconstruct images from the projections. This algorithm has the advantage of being simple while having a low requirement for computing resources. However, shot noise in the raw data is prominent in the reconstructed images and areas of high tracer uptake tend to form streaks across the

image. Also, FBP treats the data deterministically - it does not account for the inherent randomness associated with PET data, thus requiring all the pre-reconstruction corrections described above.

Iterative expectation-maximization algorithms are now the preferred method of reconstruction. These algorithms compute an estimate of the likely distribution of annihilation events that led to the measured data, based on statistical principles. The advantage is a better noise profile and resistance to the streak artifacts common with FBP, but the disadvantage is higher computer resource requirements.

**Attenuation correction**: As different LORs must traverse different thicknesses of tissue, the photons are attenuated differentially. The result is that structures deep in the body are reconstructed as having falsely low tracer uptake. Contemporary scanners can estimate attenuation using integrated x-ray CT equipment, however earlier equipment offered a crude form of CT using a gamma ray (positron emitting) source and the PET detectors.

While attenuation-corrected images are generally more faithful representations, the correction process is itself susceptible to significant artifacts. As a result, both corrected and uncorrected images are always reconstructed and read together.

**2D/3D reconstruction**: Early PET scanners had only a single ring of detectors, hence the acquisition of data and subsequent reconstruction was restricted to a single transverse plane. More modern scanners now include multiple rings, essentially forming a cylinder of detectors.

There are two approaches to reconstructing data from such a scanner: 1) treat each ring as a separate entity, so that only coincidences within a ring are detected, the image from each ring can then be reconstructed individually (2D reconstruction), or 2) allow coincidences to be detected between rings as well as within rings, then reconstruct the entire volume together (3D).

3D techniques have better sensitivity (because more coincidences are detected and used) and therefore less noise, but are more sensitive to the effects of scatter and random coincidences, as well as requiring correspondingly greater computer resources. The advent of sub-nanosecond timing resolution detectors affords better random coincidence rejection, thus favoring 3D image reconstruction.

## Applications

PET is both a medical and research tool. It is used heavily in clinical oncology (medical imaging of tumors and the search for metastases), and for clinical diagnosis of certain diffuse brain diseases such as those causing various types of dementias. PET is also an important research tool to map normal human brain and heart function.

PET is also used in pre-clinical studies using animals, where it allows repeated investigations into the same subjects. This is particularly valuable in cancer research, as it results in an increase in the statistical quality of the data (subjects can act as their own control) and substantially reduces the numbers of animals required for a given study.

Alternative methods of scanning include x-ray computed tomography (CT), magnetic resonance imaging (MRI) and functional magnetic resonance imaging (fMRI), ultrasound and single photon emission computed tomography (SPECT).

While some imaging scans such as CT and MRI isolate organic anatomic changes in the body, PET and SPECT are capable of detecting areas of molecular biology detail (even prior to anatomic change). PET scanning does this using radiolabelled molecular probes that have different rates of uptake depending on the type and function of tissue involved. Changing of regional blood flow in various anatomic structures (as a measure of the injected positron emitter) can be visualized and relatively quantified with a PET scan.

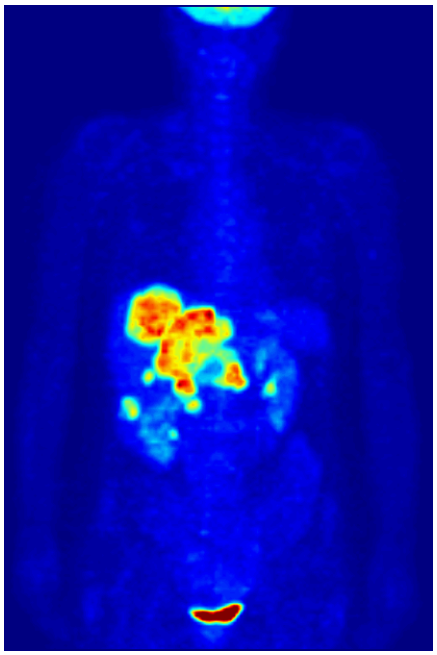

Maximum intensity projection (MIP) of a F-18 FDG wholebody PET acquisition; liver metastases of a colorectal tumor are clearly visible within the abdominal region of the image. Normal physiological isotope uptake is seen in the brain, renal collection systems and bladder. In this animation, it is important to view the subject as rotating clockwise (note liver position).

PET imaging is best performed using a dedicated PET scanner. However, it is possible to acquire PET images using a conventional dual-head gamma camera fitted with a coincidence detector. The quality of gamma-camera PET is considerably lower, and acquisition is slower. However, for institutions with low demand for PET, this may allow on-site imaging, instead of referring patients to another center, or relying on a visit by a mobile scanner.

PET is a valuable technique for some diseases and disorders, because it is possible to target the radio-chemicals used for particular bodily functions.

1. Oncology: PET scanning with the tracer fluorine-18 (F-18) fluorodeoxyglucose (FDG), called FDG-PET, is widely used in clinical oncology. This tracer is a glucose analog that is taken up by glucose-using cells and phosphorylated by hexokinase (whose mitochondrial form is greatly elevated in rapidly growing malignant tumours). A typical dose of FDG used in an oncological scan is 200-400 MBq for an adult human. Because the oxygen atom which is replaced by F-18 to generate FDG is required for the next step in glucose metabolism in all cells, no further reactions occur in FDG. Furthermore, most tissues (with the notable exception of liver and kidneys) cannot remove the phosphate added by hexokinase. This means that FDG is trapped in any cell which takes it up, until it decays, since phosphorylated sugars, due to their ionic charge, cannot exit from the cell. This results in intense radiolabeling of tissues with high glucose uptake, such as the brain, the liver, and most cancers. As a result, FDG-PET can be used for diagnosis, staging, and monitoring treatment of cancers, particularly in Hodgkin's lymphoma, non-Hodgkin lymphoma, and lung cancer. Many other types of solid tumors will be found to be very highly labeled on a case-by-case basis—a fact which becomes especially useful in searching for tumor metastasis, or for recurrence after a known highly active primary tumor is removed. Because individual PET scans are more expensive than "conventional" imaging with computed tomography (CT) and magnetic resonance imaging (MRI), expansion of FDG-PET in cost-constrained health services will depend on proper health

technology assessment; this problem is a difficult one because structural and functional imaging often cannot be directly compared, as they provide different information. Oncology scans using FDG make up over 90% of all PET scans in current practice.

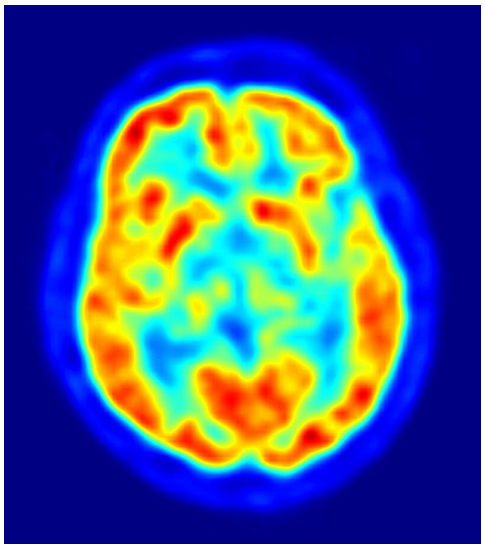

PET scan of the human brain.

Neurology: PET neuroimaging is based on an assumption that areas of high radioactivity are associated with brain activity. What is actually measured indirectly is the flow of blood to different parts of the brain, which is generally believed to be correlated, and has been measured using the tracer oxygen-15. However, because of its 2-minute half-life O-15 must be piped directly from a medical cyclotron for such uses, and this is difficult. In practice, since the brain is normally a rapid user of glucose, and since brain pathologies such as Alzheimer's disease greatly decrease brain metabolism of both glucose and oxygen in tandem, standard FDG-PET of the brain, which measures regional glucose use, may also be successfully used to differentiate Alzheimer's disease from other dementing processes, and also to make early diagnosis of Alzheimer's disease. The advantage of FDG-PET for these uses is its much wider availability. PET imaging with FDG can also be used for localization of seizure focus: A seizure focus will appear as hypometabolic during an interictal scan. Several radiotracers (i.e. radioligands) have been developed for PET that are ligands for specific neuroreceptor subtypes such as [$^{11}$C] raclopride and [$^{18}$F] fallypride for dopamine D2/D3 receptors, [$^{11}$C]McN 5652 and [$^{11}$C]DASB for serotonin transporters, or enzyme substrates (e.g. 6-FDOPA for the AADC enzyme). These agents permit the visualization of neuroreceptor pools in the context of a plurality of neuropsychiatric and neurologic illnesses. A novel probe developed at the University of Pittsburgh termed PIB (Pittsburgh compound B) permits the visualization of amyloid plaques in the brains of Alzheimer's patients. This technology could assist clinicians in making a positive clinical diagnosis of AD pre-mortem and aid in the development of novel anti-amyloid therapies. [$^{11}$C]PMP (N-[$^{11}$C]methylpiperidin-4-yl propionate) is a novel radiopharmaceutical used in PET imaging to determine the activity of the acetylcholinergic neurotransmitter system by acting as a substrate for acetylcholinesterase. Post-mortem examination of AD patients have shown decreased levels of acetylcholinesterase. [$^{11}$C]PMP is used to map the acetylcholinesterase activity in the brain which could allow for pre-mortem diagnosis of AD and help to monitor AD treatments.[15] Avid Radiopharmaceuticals of Philadelphia has developed a compound called 18F-AV-45 that uses the longer-lasting radionuclide fluorine-18 to detect amyloid plaques using PET scans.[16]

3. Cardiology, atherosclerosis and vascular disease study: In clinical cardiology, FDG-PET can identify so-called "hibernating myocardium", but its cost-effectiveness in this role versus SPECT is unclear. Recently, a role has been suggested for FDG-PET imaging of atherosclerosis to detect patients at risk of stroke [17].
4. Neuropsychology / Cognitive neuroscience: To examine links between specific psychological processes or disorders and brain activity.
5. Psychiatry: Numerous compounds that bind selectively to neuroreceptors of interest in biological psychiatry have been radiolabeled with C-11 or F-18. Radioligands that bind to dopamine receptors (D1,D2, reuptake transporter), serotonin receptors (5HT1A, 5HT2A, reuptake transporter) opioid receptors (mu) and other sites have been used successfully in studies with human subjects. Studies have been performed examining the state of these receptors in patients compared to healthy controls in schizophrenia, substance abuse, mood disorders and other psychiatric conditions.
6. Pharmacology: In pre-clinical trials, it is possible to radiolabel a new drug and inject it into animals. Such scans are referred to as biodistribution studies. The uptake of the drug, the tissues in which it concentrates, and its

eventual elimination, can be monitored far more quickly and cost effectively than the older technique of killing and dissecting the animals to discover the same information. Much more commonly, however, drug occupancy at a purported site of action can be inferred indirectly by competition studies between unlabeled drug and radiolabeled compounds known apriori to bind with specificity to the site. A single radioligand can be used this way to test many potential drug candidates for the same target. A related technique involves scanning with radioligands that compete with an endogenous (naturally occurring) substance at a given receptor to demonstrate that a drug causes the release of the natural substance.

7. PET technology for small animal imaging: A miniature PET tomograph has been constructed that is small enough for a fully conscious and mobile rat to wear on its head while walking around.[18] This RatCAP (Rat Conscious Animal PET) allows animals to be scanned without the confounding effects of anesthesia. PET scanners designed specifically for imaging rodents or small primates are marketed for academic and pharmaceutical research.
8. Musculo-Skeletal Imaging: PET has been shown to be a feasible technique for studying skeletal muscles during exercises like walking.[19] One of the main advantages of using PET is that it can also provide muscle activation data about deeper lying muscles such as the vastus intermedialis and the gluteus minimus, as compared to other muscle studying techniques like Electromyography, which can only be used on superficial muscles (i.e. directly under the skin). A clear disadvantage, however, is that PET provides no timing information about muscle activation, because it has to be measured after the exercise is completed. This is due to the time it takes for FDG to accumulate in the activated muscles.

## Safety

PET scanning is non-invasive, but it does involve exposure to ionizing radiation. The total dose of radiation is not insignificant, usually around 5–7 mSv. However, in modern practice, a combined PET/CT scan is almost always performed, and for PET/CT scanning, the radiation exposure may be substantial - around 23-26 mSv (for a 70 kg person - dose is likely to be higher for higher body weights).[20] When compared to the classification level for radiation workers in the UK, of 6 mSv it can be seen that PET scans need proper justification. This can also be compared to 2.2 mSv average annual background radiation in the UK, 0.02 mSv for a chest x-ray and 6.5 - 8 mSv for a CT scan of the chest, according to the Chest Journal and ICRP.[21] [22] A policy change suggested by the IFALPA member associations in year 1999 mentioned that an aircrew member is likely to receive a radiation dose of 4–9 mSv per year.[23]

## See also

- Diffuse optical imaging
- Hot cell (Equipment used to produce the radiopharmaceuticals used in PET)
- Molecular Imaging

## References

[1] Ter-Pogossian, M.M.; M.E. Phelps, E.J. Hoffman, N.A. Mullani (1975). "A positron-emission transaxial tomograph for nuclear imaging (PET)" (http://www.osti.gov/energycitations/product.biblio.jsp?osti_id=4251398). *Radiology* **114** (1): 89–98. .

[2] Phelps, M.E.; E.J. Hoffman, N.A. Mullani, M.M. Ter-Pogossian (March 1, 1975). "Application of annihilation coincidence detection to transaxial reconstruction tomography" (http://jnm.snmjournals.org/cgi/content/abstract/16/3/210). *Journal of Nuclear Medicine* **16** (3): 210–224. PMID 1113170. .

[3] Sweet, W.H.; G.L. Brownell (1953). "Localization of brain tumors with positron emitters". *Nucleonics* **11**: 40–45.

[4] *A Vital Legacy: Biological and Environmental Research in the Atomic Age,* U.S. Department of Energy, The Office of Biological and Environmental Research, September 1997, p 25-26

[5] IDO, T., C-N. WAN, V. CASELLA, J.S. FOWLER, A.P. WOLF, M. REIVICH, and D.E. KUHL, ``Labeled 2-deoxy-D-glucose analogs. -labeled 2-deoxy-2-fluoro-D-glucose, 2-deoxy-2-fluoro-D-mannose and C-14-2-deoxy-2-fluoro-D-glucose*, The Journal of Labelled Compounds and Radiopharmaceuticals 1978; 14:175-182.*

[6] BROWNELL G.L., C.A. BURNHAM, B. HOOP JR., and D.E. BOHNING, ``Quantitative dynamic studies using short-lived radioisotopes and positron detection *in Proceedings of the Symposium on Dynamic Studies with Radioisotopes in Medicine, Rotterdam. August 31 - September 4, 1970. IAEA. Vienna. 1971. pp. 161-172.*

[7] ROBERTSON J.S., MARR R.B., ROSENBLUM M., RADEKA V., and YAMAMOTO Y.L., ``32-Crystal positron transverse section detector*, in Tomographic Imaging in Nuclear Medicine, Freedman GS, Editor. 1973, The Society of Nuclear Medicine: New York. pp. 142-153.*

[8] CHO, Z. H., ERIKSSON L., and CHAN J.K., ``A circular ring transverse axial positron camera *in Reconstruction Tomography in Diagnostic Radiology and Nuclear Medicine, Ed. Ter-Pogossian MM., University Park Press: Baltimore, 1975.*

[9] Michael E. Phelps (2006). *PET: physics, instrumentation, and scanners*. Springer. pp. 8–10.

[10] "PET Imaging" (http://www.medcyclopaedia.com/library/topics/volume_i/p/pet_imaging.aspx). GE Healthcare. .

[11] "Invitation to Cover: Advancements in "Time-of-Flight" Technology Make New PET/CT Scanner at Penn a First in the World" (http://www.uphs.upenn.edu/news/News_Releases/jun06/PETCTITC.htm). University of Pennsylvania. June 15, 2006. . Retrieved February 22, 2010.

[12] "A Close Look Into the Brain" (http://www.fz-juelich.de/portal/index.php?index=1172). Jülich Research Centre. 29 April 2009. . Retrieved 2009-04-29.

[13] Young H, Baum R, Cremerius U, *et al.* (1999). "Measurement of clinical and subclinical tumour response using [18F]-fluorodeoxyglucose and positron emission tomography: review and 1999 EORTC recommendations.". *European Journal of Cancer* **35** (13): 1773–1782. doi:10.1016/S0959-8049(99)00229-4. PMID 10673991.

[14] Technology | July 2003: Trends in MRI | Medical Imaging (http://www.medicalimagingmag.com/issues/articles/2003-07_05.asp)

[15] D. E. Kuhl, R. A. Koeppe, S. Minoshima, S. E. Snyder, E. P. Ficaro, N. L. Foster, K. A. Frey and M. R. Kilbourn (1999) In vivo mapping of cerebral acetylcholinesterase activity in aging and Alzheimer's disease (http://www.neurology.org/cgi/content/abstract/52/4/691) Neurology (http://www.neurology.org/)

[16] Kolata, Gina. "Promise Seen for Detection of Alzheimer's" (http://www.nytimes.com/2010/06/24/health/research/24scans.html), *The New York Times*, June 23, 2010. Accessed June 23, 2010.

[17] http://circ.ahajournals.org/cgi/content/abstract/105/23/2708

[18] Rat Conscious Animal PET (http://www.chemistry.bnl.gov/ratcap/gallery.html)

[19] Oi et al., *FDG-PET imaging of lower extremity muscular activity during level walking*, Journal of Orthopaedic Science 2003(8):55-61

[20] G. Brix, U Lechel, G Glatting, SI Ziegler, W Münzing, SP Müller and T Beyer (2005) Radiation Exposure of Patients Undergoing Whole-Body Dual-Modality 18F-FDG PET/CT Examinations (http://jnm.snmjournals.org/cgi/content/full/46/4/608) Journal of Nuclear Medicine (http://jnm.snmjournals.org/)

[21] (http://google.com/search?q=cache:0_m8_v25lbEJ:www.icrp.org/downloadDoc.asp?document=docs/ICRP_87_CT_s.pps+chest+ct+dose+msv&cd=1&hl=en&ct=clnk&gl=uk&client=firefox-a), ICRP, 30/10/09.

[22] (http://chestjournal.chestpubs.org/content/133/5/1289.full), [Chest Journal], 30/10/09.

[23] Air crew radiation exposure—An overview (http://www.ans.org/pubs/magazines/nn/docs/2000-1-3.pdf), Susan Bailey, Nuclear News (a publication of American Nuclear Society), January 2000.

## Further reading

- Bustamante E. and Pedersen P.L. (1977). "High aerobic glycolysis of rat hepatoma cells in culture: role of mitochondrial hexokinase.". *Proceedings of the National Academy of Sciences USA* **74** (9): 3735–3739. doi:10.1073/pnas.74.9.3735.
- Dumit Joseph, *Picturing Personhood: Brain Scans and Biomedical Identity*, Princeton University Press, 2004
- Herman, Gabor T. (2009). *Fundamentals of Computerized Tomography: Image Reconstruction from Projections* (2nd ed.). Springer. ISBN 978-1-85233-617-2..
- Klunk WE, Engler H, Nordberg A, Wang Y, Blomqvist G, Holt DP, Bergstrom M, Savitcheva I, Huang GF, Estrada S, Ausen B, Debnath ML, Barletta J, Price JC, Sandell J, Lopresti BJ, Wall A, Koivisto P, Antoni G, Mathis CA, and Langstrom B. (2004). "Imaging brain amyloid in Alzheimer's disease with Pittsburgh Compound-B". *Annals of Neurology* **55** (3): 306–319. doi:10.1002/ana.20009. PMID 14991808.

## External links

- PET Images (http://rad.usuhs.edu/medpix/master.php3?mode=image_finder&action=search&srchstr=&srch_type=all&labels=&details=2&no_filter=2&plane_id=&capt_id=-4&filter_m=modality&filter_o=&acr_pre=&filter_p=&acr_post=#top) Search MedPix(r)
- Seeing is believing: In vivo functional real-time imaging of transplanted islets using positron emission tomography (PET)(a protocol) (http://www.natureprotocols.com/2006/12/21/seeing_is_believing_in_vivo_fu_1.php), Nature Protocols, from Nature Medicine - 12, 1423 - 1428 (2006).
- The nuclear medicine and molecular medicine podcast (http://nuccast.com) - Podcast
- Positron Emission Particle Tracking (http://www.np.ph.bham.ac.uk/pic/pept.htm) (PEPT) - engineering analysis tool based on PET that is able to track single particles in 3D within mixing systems or fluidised beds. Developed at the University of Birmingham, UK.
- CMS coverage of PET scans (http://www.hematologytimes.com/ht/p_article.do?id=948)
- PET-CT atlas Harvard Medical School (http://www.med.harvard.edu/JPNM/chetan/)

# Raman microscopy

**Raman spectroscopy** (named after C. V. Raman, pronounced /ˈrɑːmən/) is a spectroscopic technique used to study vibrational, rotational, and other low-frequency modes in a system.[1] It relies on inelastic scattering, or Raman scattering, of monochromatic light, usually from a laser in the visible, near infrared, or near ultraviolet range. The laser light interacts with molecular vibrations, phonons or other excitations in the system, resulting in the energy of the laser photons being shifted up or down. The shift in energy gives information about the phonon modes in the system. Infrared spectroscopy yields similar, but complementary, information.

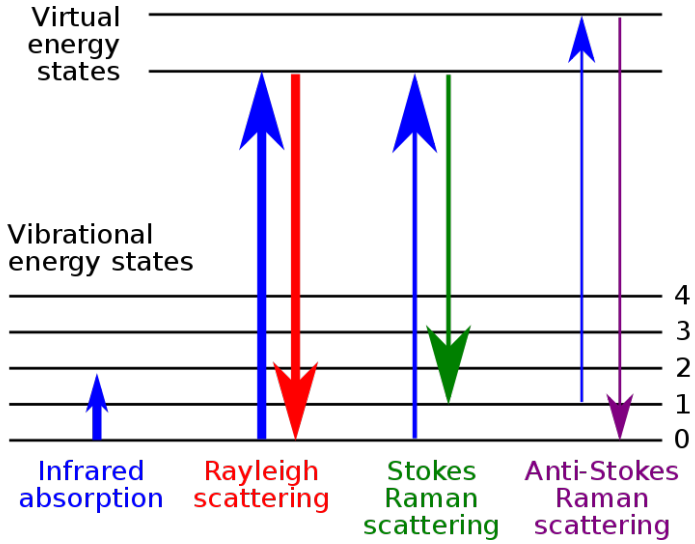


Energy level diagram showing the states involved in Raman signal. The line thickness is roughly proportional to the signal strength from the different transitions.

Typically, a sample is illuminated with a laser beam. Light from the illuminated spot is collected with a lens and sent through a monochromator. Wavelengths close to the laser line, due to elastic Rayleigh scattering, are filtered out while the rest of the collected light is dispersed onto a detector.

Spontaneous Raman scattering is typically very weak, and as a result the main difficulty of Raman spectroscopy is separating the weak inelastically scattered light from the intense Rayleigh scattered laser light. Historically, Raman spectrometers used holographic gratings and multiple dispersion stages to achieve a high degree of laser rejection. In the past, photomultipliers were the detectors of choice for dispersive Raman setups, which resulted in long acquisition times. However, modern instrumentation almost universally employs notch or edge filters for laser rejection and spectrographs (either axial transmissive (AT), Czerny-Turner (CT) monochromator) or FT (Fourier transform spectroscopy based), and CCD detectors.

There are a number of advanced types of Raman spectroscopy, including surface-enhanced Raman, resonance Raman, tip-enhanced Raman, polarised Raman, stimulated Raman (analogous to stimulated emission), transmission Raman, spatially-offset Raman, and hyper Raman.

## Basic theory

The Raman effect occurs when light impinges upon a molecule and interacts with the electron cloud and the bonds of that molecule. For the spontaneous Raman effect, which is a form of scattering, a photon excites the molecule from the ground state to a virtual energy state. When the molecule relaxes it emits a photon and it returns to a different rotational or vibrational state. The difference in energy between the original state and this new state leads to a shift in the emitted photon's frequency away from the excitation wavelength. The Raman effect, which is a light scattering phenomenon, should not be confused with absorption (as with fluorescence) where the molecule is excited to a discrete (not virtual) energy level.

If the final vibrational state of the molecule is more energetic than the initial state, then the emitted photon will be shifted to a lower frequency in order for the total energy of the system to remain balanced. This shift in frequency is designated as a Stokes shift. If the final vibrational state is less energetic than the initial state, then the emitted photon will be shifted to a higher frequency, and this is designated as an Anti-Stokes shift. Raman scattering is an example of inelastic scattering because of the energy transfer between the photons and the molecules during their interaction.

A change in the molecular polarization potential — or amount of deformation of the electron cloud — with respect to the vibrational coordinate is required for a molecule to exhibit a Raman effect. The amount of the polarizability change will determine the Raman scattering intensity. The pattern of shifted frequencies is determined by the rotational and vibrational states of the sample.

## History

Although the inelastic scattering of light was predicted by Adolf Smekal in 1923, it is not until 1928 that it was observed in practice. The Raman effect was named after one of its discoverers, the Indian scientist Sir C. V. Raman who observed the effect by means of sunlight (1928, together with K. S. Krishnan and independently by Grigory Landsberg and Leonid Mandelstam).[1] Raman won the Nobel Prize in Physics in 1930 for this discovery accomplished using sunlight, a narrow band photographic filter to create monochromatic light and a "crossed" filter to block this monochromatic light. He found that light of changed frequency passed through the "crossed" filter.

Systematic pioneering theory of the Raman effect was developed by Czechoslovak physicist George Placzek between 1930 and 1934.[2] The mercury arc became the principal light source, first with photographic detection and then with spectrophotometric detection. At the present time, lasers are used as light sources.

## Raman spectra

Raman spectra are typically expressed in wavenumbers, which have units of inverse length. In order to convert between spectral wavelength and wavenumbers of shift in the Raman spectrum, the following formula can be used:

$$\Delta w = \left( \frac{1}{\lambda_0} - \frac{1}{\lambda_1} \right) \ ,$$

where $\Delta w$ is the Raman shift expressed in wavenumber, $\lambda_0$ is the excitation wavelength, and $\lambda_1$ is the Raman spectrum wavelength. Most commonly, the units chosen for expressing wavenumber in Raman spectra is inverse centimeters ($cm^{-1}$). Since wavelength is often expressed in units of nanometers (nm), the formula above can scale for this units conversion explicitly, giving

$$\Delta w(\mathrm{cm}^{-1}) = \left( \frac{1}{\lambda_0(\mathrm{nm})} - \frac{1}{\lambda_1(\mathrm{nm})} \right) \times 10^7 \frac{(\mathrm{nm})}{(\mathrm{cm})},$$

## Applications

Raman spectroscopy is commonly used in chemistry, since vibrational information is specific to the chemical bonds and symmetry of molecules. Therefore, it provides a fingerprint by which the molecule can be identified. For instance, the vibrational frequencies of SiO, $Si_2O_2$, and $Si_3O_3$ were identified and assigned on the basis of normal coordinate analyses using infrared and Raman spectra.[3] The fingerprint region of organic molecules is in the (wavenumber) range 500–2000 $cm^{-1}$. Another way that the technique is used to study changes in chemical bonding, e.g., when a substrate is added to an enzyme.

Raman gas analyzers have many practical applications. For instance, they are used in medicine for real-time monitoring of anaesthetic and respiratory gas mixtures during surgery.

In solid state physics, spontaneous Raman spectroscopy is used to, among other things, characterize materials, measure temperature, and find the crystallographic orientation of a sample. As with single molecules, a given solid material has characteristic phonon modes that can help an experimenter identify it. In addition, Raman spectroscopy can be used to observe other low frequency excitations of the solid, such as plasmons, magnons, and superconducting gap excitations. The spontaneous Raman signal gives information on the population of a given phonon mode in the ratio between the Stokes (downshifted) intensity and anti-Stokes (upshifted) intensity.

Raman scattering by an anisotropic crystal gives information on the crystal orientation. The polarization of the Raman scattered light with respect to the crystal and the polarization of the laser light can be used to find the orientation of the crystal, if the crystal structure (to be specific, its point group) is known.

Raman active fibers, such as aramid and carbon, have vibrational modes that show a shift in Raman frequency with applied stress. Polypropylene fibers also exhibit similar shifts. The radial breathing mode is a commonly used technique to evaluate the diameter of carbon nanotubes. In nanotechnology, a Raman microscope can be used to analyze nanowires to better understand the composition of the structures.

Spatially-offset Raman spectroscopy (SORS), which is less sensitive to surface layers than conventional Raman, can be used to discover counterfeit drugs without opening their internal packaging, and for non-invasive monitoring of biological tissue.[4] Raman spectroscopy can be used to investigate the chemical composition of historical documents such as the Book of Kells and contribute to knowledge of the social and economic conditions at the time the documents were produced.[5] This is especially helpful because Raman spectroscopy offers a non-invasive way to determine the best course of preservation or conservation treatment for such materials.

Raman spectroscopy is being investigated as a means to detect explosives for airport security.[6]

Raman spectroscopy has also been used to confirm the prediction of existence of low-frequency phonons [7] in proteins and DNA (see, e.g., [8] [9] [10] [11] greatly stimulating the studies of low-frequency collective motion in proteins and DNA and their biological functions.[12] [13]

## Microspectroscopy

Raman spectroscopy offers several advantages for microscopic analysis. Since it is a scattering technique, specimens do not need to be fixed or sectioned. Raman spectra can be collected from a very small volume (< 1 μm in diameter); these spectra allow the identification of species present in that volume. Water does not generally interfere with Raman spectral analysis. Thus, Raman spectroscopy is suitable for the microscopic examination of minerals, materials such as polymers and ceramics, cells and proteins. A Raman microscope begins with a standard optical microscope, and adds an excitation laser, a monochromator, and a sensitive detector (such as a charge-coupled device (CCD), or photomultiplier tube (PMT)). FT-Raman has also been used with microscopes.

In *direct imaging*, the whole field of view is examined for scattering over a small range of wavenumbers (Raman shifts). For instance, a wavenumber characteristic for cholesterol could be used to record the distribution of cholesterol within a cell culture.

The other approach is *hyperspectral imaging* or *chemical imaging*, in which thousands of Raman spectra are acquired from all over the field of view. The data can then be used to generate images showing the location and amount of different components. Taking the cell culture example, a hyperspectral image could show the distribution of cholesterol, as well as proteins, nucleic acids, and fatty acids. Sophisticated signal- and image-processing techniques can be used to ignore the presence of water, culture media, buffers, and other interferents.

Raman microscopy, and in particular confocal microscopy, has very high spatial resolution. For example, the lateral and depth resolutions were 250 nm and 1.7 μm, respectively, using a confocal Raman microspectrometer with the 632.8 nm line from a Helium-Neon laser with a pinhole of 100 μm diameter. Since the objective lenses of microscopes focus the laser beam to several micrometres in diameter, the resulting photon flux is much higher than achieved in conventional Raman setups. This has the added benefit of enhanced fluorescence quenching. However, the high photon flux can also cause sample degradation, and for this reason some setups require a thermally conducting substrate (which acts as a heat sink) in order to mitigate this process.

By using Raman microspectroscopy, *in vivo* time- and space-resolved Raman spectra of microscopic regions of samples can be measured. As a result, the fluorescence of water, media, and buffers can be removed. Consequently *in vivo* time- and space-resolved Raman spectroscopy is suitable to examine proteins, cells and organs.

Raman microscopy for biological and medical specimens generally uses near-infrared (NIR) lasers (785 nm diodes and 1064 nm Nd:YAG are especially common). This reduces the risk of damaging the specimen by applying higher energy wavelengths. However, the intensity of NIR Raman is low (owing to the $\omega^4$ dependence of Raman scattering intensity), and most detectors required very long collection times. Recently, more sensitive detectors have become available, making the technique better suited to general use. Raman microscopy of inorganic specimens, such as rocks and ceramics and polymers, can use a broader range of excitation wavelengths.[14]

## Polarized analysis

The polarization of the Raman scattered light also contains useful information. This property can be measured using (plane) polarized laser excitation and a polarization analyzer. Spectra acquired with the analyzer set at both perpendicular and parallel to the excitation plane can be used to calculate the depolarization ratio. Study of the technique is useful in teaching the connections between group theory, symmetry, Raman activity, and peaks in the corresponding Raman spectra.

The spectral information arising from this analysis gives insight into molecular orientation and vibrational symmetry. In essence, it allows the user to obtain valuable information relating to the molecular shape, for example in synthetic chemistry or polymorph analysis. It is often used to understand macromolecular orientation in crystal lattices, liquid crystals or polymer samples.[15]

## Variations

Several variations of Raman spectroscopy have been developed. The usual purpose is to enhance the sensitivity (e.g., surface-enhanced Raman), to improve the spatial resolution (Raman microscopy), or to acquire very specific information (resonance Raman).

- **Surface Enhanced Raman Spectroscopy (SERS)** - Normally done in a silver or gold colloid or a substrate containing silver or gold. Surface plasmons of silver and gold are excited by the laser, resulting in an increase in the electric fields surrounding the metal. Given that Raman intensities are proportional to the electric field, there is large increase in the measured signal (by up to $10^{11}$). This effect was originally observed by Martin Fleischmann but the prevailing explanation was proposed by Van Duyne in 1977.[16] A comprehensive theory of the effect is that given by Lombardi and Birke in 2008 called the a Unified Approach to Surface-Enhanced Raman Spectroscopy.[17]

- **Resonance Raman spectroscopy** - The excitation wavelength is matched to an electronic transition of the molecule or crystal, so that vibrational modes associated with the excited electronic state are greatly enhanced. This is useful for studying large molecules such as polypeptides, which might show hundreds of bands in "conventional" Raman spectra. It is also useful for associating normal modes with their observed frequency shifts.[18]
- **Surface-Enhanced Resonance Raman Spectroscopy (SERRS)** - A combination of SERS and resonance Raman spectroscopy that uses proximity to a surface to increase Raman intensity, and excitation wavelength matched to the maximum absorbance of the molecule being analysed.
- **Hyper Raman** - A non-linear effect in which the vibrational modes interact with the second harmonic of the excitation beam. This requires very high power, but allows the observation of vibrational modes that are normally "silent". It frequently relies on SERS-type enhancement to boost the sensitivity.[19]
- **Spontaneous Raman Spectroscopy** - Used to study the temperature dependence of the Raman spectra of molecules.
- **Optical Tweezers Raman Spectroscopy (OTRS)** - Used to study individual particles, and even biochemical processes in single cells trapped by optical tweezers.
- **Stimulated Raman Spectroscopy** - A spatially coincident, two color pulse (with polarization either parallel or perpendicular) transfers the population from ground to a rovibrationally excited state, if the difference in energy corresponds to an allowed Raman transition, and if neither frequency corresponds to an electronic resonance. Two photon UV ionization, applied after the population transfer but before relaxation, allows the intra-molecular or inter-molecular Raman spectrum of a gas or molecular cluster (indeed, a given conformation of molecular cluster) to be collected. This is a useful molecular dynamics technique.
- **Spatially Offset Raman Spectroscopy (SORS)** - The Raman scatter is collected from regions laterally offset away from the excitation laser spot, leading to significantly lower contributions from the surface layer than with traditional Raman spectroscopy.[20]
- **Coherent anti-Stokes Raman spectroscopy (CARS)** - Two laser beams are used to generate a coherent anti-Stokes frequency beam, which can be enhanced by resonance.
- **Raman optical activity (ROA)** - Measures vibrational optical activity by means of a small difference in the intensity of Raman scattering from chiral molecules in right- and left-circularly polarized incident light or, equivalently, a small circularly polarized component in the scattered light.[21]
- **Transmission Raman** - Allows probing of a significant bulk of a turbid material, such as powders, capsules, living tissue, etc. It was largely ignored following investigations in the late 1960s[22] but was rediscovered in 2006 as a means of rapid assay of pharmaceutical dosage forms.[23] There are also medical diagnostic applications.[24]
- **Inverse Raman spectroscopy**.
- **Tip-Enhanced Raman Spectroscopy (TERS)** - Uses a metallic (usually silver-/gold-coated AFM or STM) tip to enhance the Raman signals of molecules situated in its vicinity. The spatial resolution is approximately the size of the tip apex (20-30 nm). TERS has been shown to have sensitivity down to the single molecule level.

## References


[1] Gardiner, D.J. (1989). *Practical Raman spectroscopy*. Springer-Verlag. ISBN 978-0387502540.

[2] Placzek G.: "Rayleigh Streeung und Raman Effekt", In: Hdb. der Radiologie, Vol. VI., 2, 1934, p. 209

[3] Khanna, R.K. (1981). "Raman-spectroscopy of oligomeric SiO species isolated in solid methane". *Journal of Chemical Physics* **74**: 2108. doi:10.1063/1.441393.

[4] "Fake drugs caught inside the pack" (http://news.bbc.co.uk/2/hi/health/6314287.stm). BBC News. 2007-01-31. . Retrieved 2008-12-08.

[5] Irish classic is still a hit (in calfskin, not paperback) - New York Times (http://www.nytimes.com/2007/05/28/world/europe/28kells.html), nytimes.com

[6] Ben Vogel (29 August 2008). "Raman spectroscopy portends well for standoff explosives detection" (http://www.janes.com/news/transport/business/jar/jar080829_1_n.shtml). Jane's. . Retrieved 2008-08-29.

[7] Kuo-Chen Chou and Nian-Yi Chen (1977) The biological functions of low-frequency phonons. Scientia Sinica, 20, 447-457.

[8] Urabe, H., Tominaga, Y. and Kubota, K. (1983) Experimental evidence of collective vibrations in DNA double helix Raman spectroscopy. Journal of Chemical Physics, 78, 5937-5939.

[9] Chou, K.C. (1983) Identification of low-frequency modes in protein molecules. Biochemical Journal, 215, 465-469.

[10] Chou, K.C. (1984) Low-frequency vibration of DNA molecules. Biochemical Journal, 221, 27-31.

[11] Urabe, H., Sugawara, Y., Ataka, M. and Rupprecht, A. (1998) Low-frequency Raman spectra of lysozyme crystals and oriented DNA films: dynamics of crystal water. Biophys J, 74, 1533-1540.

[12] Kuo-Chen Chou (1988) Review: Low-frequency collective motion in biomacromolecules and its biological functions. Biophysical Chemistry, 30, 3-48.

[13] Chou, K.C. (1989) Low-frequency resonance and cooperativity of hemoglobin. Trends in Biochemical Sciences, 14, 212.

[14] Ellis DI, Goodacre R (August 2006). "Metabolic fingerprinting in disease diagnosis: biomedical applications of infrared and Raman spectroscopy". *Analyst* **131** (8): 875–85. doi:10.1039/b602376m. PMID 17028718.

[15] Khanna, R.K. (1957). *Evidence of ion-pairing in the polarized Raman spectra of a Ba2+CrO doped KI single crystal*. John Wiley & Sons, Ltd. doi:10.1002/jrs.1250040104.

[16] Jeanmaire DL, van Duyne RP (1977). "Surface Raman Electrochemistry Part I. Heterocyclic, Aromatic and Aliphatic Amines Adsorbed on the Anodized Silver Electrode". *Journal of Electroanalytical Chemistry* (Elsevier Sequouia S.A.) **84**: 1–20. doi:10.1016/S0022-0728(77)80224-6.

[17] Lombardi JR, Birke RL (2008). "A Unified Approach to Surface-Enhanced Raman Spectroscopy". *[Journal of Physical Chemistry C]* (American Chemical Society) **112**: 5605–5617. doi:10.1021/jp800167 CCC.

[18] Chao RS, Khanna RK, Lippincott ER (1974). "Theoretical and experimental resonance Raman intensities for the manganate ion". *J Raman Spectroscopy* **3**: 121. doi:10.1002/jrs.1250030203.

[19] Kneipp K, *et al.* (1999). "Surface-Enhanced Non-Linear Raman Scattering at the Single Molecule Level". *Chem. Phys.* **247**: 155–162. doi:10.1016/S0301-0104(99)00165-2.

[20] Matousek P, Clark IP, Draper ERC, *et al.* (2005). "Subsurface Probing in Diffusely Scattering Media using Spatially Offset Raman Spectroscopy". *Applied Spectroscopy* **59** (12): 393. doi:10.1366/000370205775142548. PMID 16390587.

[21] Barron LD, Hecht L, McColl IH, Blanch EW (2004). "Raman optical activity comes of age". *Molec. Phys.* **102** (8): 731–744. doi:10.1080/00268970410001704399.

[22] B. Schrader, G. Bergmann, Fresenius. Z. (1967). *Anal. Chem.*: 225–230.

[23] P. Matousek, A. W. Parker (2006). "Bulk Raman Analysis of Pharmaceutical Tablets". *Applied Spectroscopy* **60** (12): 1353–1357. doi:10.1366/000370206779321463. PMID 17217583.

[24] P. Matousek, N. Stone (2007). "Prospects for the diagnosis of breast cancer by noninvasive probing of calcifications using transmission Raman spectroscopy". *Journal of Biomedical Optics* **12** (2): 024008. doi:10.1117/1.2718934. PMID 17477723.


## External links

- Raman FAQs (frequently asked questions) (http://www.horiba.com/scientific/products/raman-spectroscopy/tutorial-faqs/raman-faqs/), horiba.com
- Raman on SiGe Superlattice (http://content.piacton.com/Uploads/Princeton/Documents/Library/UpdatedLibrary/Raman_on_SiGe_Superlattice_Using_TriVista.pdf), princetoninstruments.com
- An introduction to Raman spectroscopy (http://www.horiba.com/scientific/products/raman-spectroscopy/raman-resource/raman-tutorial/), horiba.com
- Raman Application examples (http://www.horiba.com/scientific/products/raman-spectroscopy/application-notes/), horiba.com
- An introduction on Raman Scattering (http://www.d3technologies.co.uk/en/10371.aspx), d3technologies.co.uk

- Raman Spectroscopy Applications (http://www.renishaw.com/en/raman-spectroscopy-applications--6259), renishaw.com
- Raman Data Search and Storage (http://ramandata.sourceforge.net) - The free application with a wonderful database of Raman data (vibrations, assignment) with storage function and Raman spectra (discussions) with search function. ramandata.sourceforge.net
- Romanian Database of Raman Spectroscopy (http://rdrs.uaic.ro) - This database contains mineral species (natural and synthetic) with description of crystal structure, sample image, number of sample, origin, Raman spectrum and vibrations, Raman discussion and references. Also, this site contains artefacts sample with sample image and pigment spectrum; black, red, white or blue pigment. rdrs.uaic.ro
- Chemical Imaging Without Dyeing (http://witec.de/en/download/Raman/ImagingMicroscopy04.pdf), witec.de
- DoITPoMS Teaching and Learning Package - Raman Spectroscopy (http://www.doitpoms.ac.uk/tlplib/raman/index.php) - an introduction, aimed at undergraduate level. doitpoms.ac.uk
- Raman Spectroscopy Tutorial (http://161.58.205.25/Raman_Spectroscopy/rtr-ramantutorial.php?ss=800) - A detailed explanation of Raman Spectroscopy including Resonance-Enhanced Raman Scattering and Surface-Enhanced Raman Scattering. 161.25.205.25
- The Science Show, ABC Radio National (http://www.abc.net.au/rn/science/ss/stories/s1581469.htm) - Interview with Scientist on NASA funded project to build Raman Spectrometer for the 2009 Mars mission: a cellular phone size device to detect almost any substance known, with commercial <USD$5000 commercial spin-off, prototyped by June 2006. abc.net.au/rn
- Raman spectroscopy for medical diagnosis (http://pubs.acs.org/subscribe/journals/ancham/79/i11/pdf/0607feature_griffiths.pdf) from the June 1, 2007 issue of *Analytical Chemistry* (http://pubs3.acs.org/acs/journals/toc.page?incoden=ancham&indecade=0&involume=79&inissue=11), pubs.acs.org
- Spontaneous Raman Scattering (SRS) (http://www.lavision.de/en/techniques/raman-scattering.php), lavision.de
- Painless laser device could spot early signs of disease (http://www.bbc.co.uk/news/science-environment-11390951), BBC News, 2010-09-26

# Neutron spin echo

**Neutron spin echo** spectroscopy is an inelastic neutron scattering technique invented by Ferenc Mezei in the 1970's, and developed in collaboration with John Hayter. [1] In recognition of his work and in other areas, Mezei was awarded the first Walter Haelg Prize [2] in 1999.

The spin-echo spectrometer possesses an extremely high energy resolution (roughly one part in 100,000). Additionally, it measures the density-density correlation (or intermediate scattering function) F(Q,t) as a function of momentum transfer Q and time. Other neutron scattering techniques measure the dynamic structure factor S(Q,ω), which can be converted to F(Q,t) by a Fourier transform, which may be difficult in practice. For weak inelastic features S(Q,ω) is better suited, however, for (slow) relaxations the natural representation is given by F(Q,t). Because of its extraordinary high effective energy resolution compared to other neutron scattering techniques, NSE is an ideal method to observe [3] overdamped internal dynamic modes (relaxations)and other diffusive processes in materials such as a polymer blends, alkane chains, or microemulsions. The extraordinary power of NSE spectrometry was further demonstrated recently[4] [5] by the direct observation of coupled internal protein domain dynamics in the proteins NHERF1 and Taq polymerase, allowing the direct visualization of protein nanomachinery in motion.

## How it works

Basically NSE is a time-of-flight technique. Concerning the neutron spins it has a strong analogy to the so-called Hahn echo,[6] well known in the field of NMR. In both cases the loss of polarization (magnetization) due to dephasing of the spins in time is restored by an effective time reversal operation, that leads to a restituation of polarization (rephasing). In NMR the dephasing happens due to variation in the local fields at positions of the nuclei, in NSE the dephasing is due to different neutron velocities in the incoming neutron beam. The Larmor precession of the neutron spin in a preparation zone with a magnetic field before the sample encodes the individual velocities of neutrons in the beam into precession angles. Close to the sample the time reversal is effected by a so-called flipper. A symmetric decoding zone follows such that at its end the precession angle accumulated in the preparation zone is exactly compensated (provided the sample did not change the neutron velocity, i.e. elastic scattering), all spins rephase to form the "spin-echo". Ideally the full polarization is restored. This effect does not depend on the velocity/energy/wavelength of the incomning neutron. If the scattering at the sample is not elastic but changes the neutron velocity, the rephasing will become incomplete and a loss of final polarization results, which depends on the distribution of differences in the time, which the neutrons need to fly through the symmetric first (coding) and second (decoding)precession zones. The time differences occur due to a velocity change acquired by non-elastic scattering at the sample. The distribution of these time differences is proportional (in the linearization approximation which is appropriate for quasi-elastic high resolution spectroscopy) to the spectral part of the scattering function S(Q,ω). The effect on the measured beam polarization is proportional to the cos-Fourier transform of the spectral function, the intermediate scattering function F(Q,t). The time parameter depends on the neutron wavelength and the factor connecting precession angle with (reciprocal) velocity, which can e.g. be controlled by setting a certain magnetic field in the preparation and decoding zones. Scans of t may then be performed by variing the magnetic field. For some further explanations pertaining the NSE principle with animations see: pathfinder.neutron-eu.net [7].

**It is important to note: all the spin manipulations are just a means to detect velocity changes of the neutron**, which influence --for technical reasons-- in terms of a Fourier transform of the spectral function in the measured intensity. The velocity changes of the neutrons convey the physical information which is available by using NSE, i.e.

$I(Q,t) \propto S(Q) + \int \cos(\omega t)\, S(Q,\omega)\, dt$ where $\omega \propto \Delta v$ and $t \propto B \times \lambda^3$.

B denotes the precession field strength, λ the (average) neutron wavelength and Δv the neutron velocity change upon scattering at the sample.

The main reason for using NSE is that by the above means it can reach Fourier times of up to many 100ns, which corresponds to energy resolutions in the neV range. The closest approach to this resolution by a spectroscopic neutron instrument type, namely the backscattering spectrometer (BSS), is in the range of 0.5 to 1 μeV. The spin-echo trick allows to use an intense beam of neutrons with a wavelength distribution of 10% or more and at the same time to be sensitive to velocity changes in the range of less than $10^{-4}$.

Note: the above explanations assumes the generic NSE configuration --as first utilized by the IN11 instrument at the Institut Laue–Langevin (ILL)--. Other approaches are possible like the resonance spin-echo, NRSE with concentrated a DC field and a RF field in the flippers at the end of preparation and decoding zones which then are without magnetic field (zero field). In principle these approaches are equivalent concerning the connection of the final intensity signal with the intermediate scattering function. Due to technical difficulties until now they have not reached the same level of performance than the generic (IN11) NSE types.

## What it can measure

In soft matter research the structure of macromolecular objects is often investigated by small angle neutron scattering, SANS. The exchange of hydrogen with deuterium in some of the molecules creates scattering contrast between even equal chemical species. The SANS diffraction pattern—if interpreted in real space—corresponds to a snapshot picture of the molecular arrangement. Neutron spin echo instruments can analyze the inelastic broadening of the SANS intensity and thereby analyze the motion of the macromolecular objects. [8] A coarse analogy would be a photo with a certain opening time instead of the SANS like snapshot. The opening time corresponds to the Fourier time which depends on the setting of the NSE spectrometer, it is proportional to the magnetic field (integral) and to the third power of the neutron wavelength. Values up to several hundreds of nanoseconds are available. Note that the spatial resolution of the scattering experiment is in the nanometer range, which means that a time range of e.g. 100 ns corresponds to effective molecular motion velocities of 1 nm/100 ns = 1 cm/s. This may be compared to the typical neutron velocity of 200..1000 m/s used in these type of experiments.

## NSE and spin-incoherent scattering (from protons)

Many inelastic studies that use normal time-of-flight (TOF) or backscattering spectrometers rely on the huge incoherent neutron scattering cross section of protons. The scattering signal is dominated by the corresponding contribution, which represents the (average) self-correlation function (in time) of the protons.

For NSE spin incoherent scattering has the disadvantage that it flips the neutron spins during scattering with a probability of 2/3. Thus converting 2/3 of the scattering intensity into "non-polarized" background and putting a factor of -1/3 in front of the cos-Fourier integral contribution pertaining the incoherent intensity. This signal subtracts from the coherent echo signal. The result may be a complicated combination which cannot be decomposed if only NSE is employed. However, in pure cases, i.e. when there is an overwhelming intensity contribution due to protons, NSE can be used to measure their incoherent spectrum.

The intensity situation of NSE --for e.g. soft-matter samples-- is the same as in small angle scattering (SANS). Which means that molecular objects with coherent scattering contrast at low Q (momentum transfer) show a much larger intensity as the incoherent contribution (which is the background level). But at larger Q usually somewhere around Q=0.3 $A^{-1}$ the incoherent scattering becomes stronger than the coherent part. At least for hydrogen containing systems contrast requires the presense of some protons and even pure deuterated samples show spin-incoherent scattering from deuterons, however, 40 times weaker than the proton scattering.

Fully protonated samples allow successful measurements but at intensities of the order of the SANS background level. [9] This requires correspondingly long counting times.

Note: This interference with the spin manipulation of the NSE technique occurs only with **spin-incoherent** scattering. Isotopic incoherent scattering yields a "normal" NSE signal.

## Existing spectrometers

- IN11 [10] (Institut Laue-Langevin,ILL [11], Grenoble, France)
- IN15 [12] (Institut Laue-Langevin,ILL [11], Grenoble, France)
- J-NSE (Juelich Centre for Neutron Science JCNS [13], Juelich, Germany, hosted by FRMII [14], Munich (Garching), Germany)
- NG5-NSE (NIST CNRF [15], Gaithersburg, USA)
- NSE@SNS (JCNS [16] SNS, Oak Ridge [17])
- RESEDA (FRM II Munich FRMII [14], Munich, Germany
- V5/SPAN (Hahn-Meitner Institut [18], Berlin, Germany)
- C2-2 (ISSP [19], Tokai, Japan)

## See also

- Biological small-angle scattering
- Larmor precession
- Neutron resonance spin echo
- Neutron scattering
- NMR
- Protein domain
- SAXS
- Soft matter
- Spin echo

## References

[1] Mezei, F., ed (1980). *Neutron Spin Echo*. Lecture Notes in Physics Vol. 128. Springer.

[2] http://neutron.neutron-eu.net/n_ensa/Prize

[3] B. Farago (2006). "Neutron spin echo study of well organized soft matter systems". *Physica B: Condensed matter* **385-386**: 688–691. doi:10.1016/j.physb.2006.05.292.

[4] B. Farago , Li J, Cornilescu G, Callaway DJE, Bu Z (November 2010). "Activation of Nanoscale Allosteric Protein Domain Motion Revealed by Neutron Spin Echo Spectroscopy" (http://linkinghub.elsevier.com/retrieve/pii/S0006-3495(10)01208-7). *Biophysical Journal* **99** (10): 3473–3482. doi:10.1016/j.bpj.2010.09.058. PMID 21081097. .

[5] Bu Z, Biehl R, Monkenbusch M, Richter D, Callaway DJE (2005). "Coupled protein domain motion in Taq polymerase revealed by neutron spin-echo spectroscopy" (http://www.pubmedcentral.nih.gov/articlerender.fcgi?tool=pmcentrez&artid=1345721). *Proc Natl Acad Sci USA* **102** (49): 17646–17651. doi:10.1073/pnas.0503388102. PMID 16306270. PMC 1345721.

[6] E.L. Hahn (1950). "Spin Echoes". *Physical Review* **80**: 580.

[7] http://pathfinder.neutron-eu.net/idb/methods/spin-echo

[8] M. Monkenbusch and D. Richter (2007). "High resolution neutron spectroscopy - a tool for the investigation of dynamics of polymers and soft matter". *Comptes Rendus Physique* **8**: 845-864.

[9] A. Wischnewski and M. Monkenbusch and L. Willner and D. Richter and G. Kali (2003). "Direct observation of the transition from free to constrained single-segment motion in entangled polymer melts". *Physical Review Letters* **90**: 058302.

[10] http://www.ill.eu/in11/

[11] http://www.ill.fr

[12] http://www.ill.eu/in15/

[13] http://www.jcns.info

[14] http://wwwnew.frm2.tum.de

[15] http://www.ncnr.nist.gov

[16] http://www.jcns.info/jcns_nse_sns

[17] http://neutrons.ornl.gov/instruments/SNS/NSE/

[18] http://www.hmi.de

[19] http://www.issp.u-tokyo.ac.jp

# Article Sources and Contributors

**Crystal** *Source*: http://en.wikipedia.org/w/index.php?oldid=399853456 *Contributors*: - ), 119, 13creek13, 2over0, 84user, 99of9, A Macedonian, A Softer Answer, AGK, AHM, Aaronbrick, Abc518, Abeg92, Acdx, Acroterion, AdjustShift, Ael 2, Ahoerstemeier, Aitias, Ajaxkroon, Alansohn, Alfie66, Altenmann, Alxeedo, Ambarsande, Andrew Levine, Angr, Angusmclellan, Animum, Ann Stouter, Anna Lincoln, Antandrus, Archer7, Arthena, Ask123, Audioiv, Awickert, Aymatth2, Az1568, B9 hummingbird hovering, Backslash Forwardslash, Badseed, Banano03, Bantman, Bauke, Bballerc28, Beaumont, Beland, Ben-Zin, Bencherlite, BlackHak, Bluezy, Bmg916, Bob Doubles, Bob f it, Bobo192, Boccobrock, Bomac, Bonez22, Bongwarrior, BrianKnez, Bronzephoenix, Butane Goddess, CIreland, Caitlincookegroup565, Call me Bubba, Caltas, Calvin 1998, CambridgeBayWeather, Can't sleep, clown will eat me, Capricorn42, Captain-n00dle, CardinalDan, Carlosguitar, Cdnc, Centrx, Cherryalexandra, Chlstal, Chowbok, Chris 73, Chrishastoes, Chzz, Clicketyclack, Closedmouth, Cmichael, Cms13foreverandalways, Cnguyen123, Cody574, Cometstyles, Complexica, Conversion script, Courcelles, Cpj0788, Crysandlg, Crystal whacker, Crystall94, Cutler, DCM, DJ Clayworth, DVD R W, Daarznieks, Dana Ashkenazi, Dancinstar, Daniel Case, Danski14, Darigan, Davewho2, David.Monniaux, DeadEyeArrow, Debresser, Deglr6328, DeltaQuad, Dengero, DerHexer, Devshoppe, Dgrant, Digon3, Discospinster, Doctormatt, Doctorshim, Dolphinholmer, DrBob, Dreadstar, Ds13, Dschwen, Duckone, Dweller, Dylan Lake, Dysepsion, Eclecticology, El C, El aprendelenguas, ElusiveByte, Emerson7, Emote, Enviroboy, Epbr123, Espetkov, Euryalus, Everyking, Excirial, FaerieInGrey, Faradayplank, FastLizard4, Fastilysock, Favonian, Fieldday-sunday, Finavon, FoRgEtFuLxLuV94, Foobar, Freestyle-69, GDonato, Galoubet, Gcm, Gentgeen, George The Dragon, Giftlite, Gilliam, Glen, Gobonobo, Godwine1994, Gogo Dodo, Govany, Gowtham99.9, Gradbrad, Graham87, Grayshi, GregorB, Gscshoyru, Gtstricky, Gunmetal Angel, Gurch, Gzkn, Hadal, Hagedis, Headbomb, Hellbus, Hempelmann, Hornlitz, Hurricanehink, Husond, Hut 8.5, Huw Powell, Hydrogen Iodide, Icairns, Iempleh, Immunize, Insanity Incarnate, Intelati, Isnow, J.delanoy, J04n, Jamm.T, Janejellyroll, January, Jaxl, Jay Litman, Jeff G., Jennavecia, Jiy, Jleela14, Jmath666, Jmundo, JoJan, John Stewart, John254, JohnCD, Jojhutton, Jon K4, Jonere, Jose77, Junglecat, Jurema Oliveira, Jusdafax, KSmrq, Kaivosukeltaja, Kandar, Karol Langner, Kemiv, Kevin Murray, Kiernanscott, Kiia15, Kingykongy, KnowledgeOfSelf, Knuckles, Knulclunk, Kocoumlovesyou, Korg, Krawi, Kubigula, L Kensington, LAAFan, Latifshaikh20, Laurap414, Lazyboi69, LeaveSleaves, LedgendGamer, Lemchesvej, Lights, Lisatwo, Logger9, Lotje, Lowellian, Luckas Blade, MER-C, MPerel, Magister Mathematicae, Major.T, Majorly, Mani1, Marie Poise, Matdrodes, MaterialsScientist, Materialscientist, Mav, Maxim, Mbz1, McSly, MeStevo, Meaningful Username, Melaen, Mentifisto, Michael Hardy, Michaeldu, MickMacNee, Mike Rosoft, Mild Bill Hiccup, Minesweeper, Miquonranger03, Mirwin, Miscibleliquids, Mr. Lefty, Mr.pieface, Musashi miyamoto, N96, Namazu-tron, NawlinWiki, Netalarm, NewEnglandYankee, NiallMcQueen, No Guru, Norm, Ochib, Oda Mari, Olivier, Olof, Omegatron, Optakeover, Ouishoebean, Outsider1994, Oxymoron83, PandaSaver, Pelo12354, Perdygal90210, Pharaoh of the Wizards, Philip Trueman, Physchim62, Piano non troppo, Pinethicket, Plangent, Poeloq, Polluks, Pontificake, PreRaphaelite, PrestonH, Puckly, PuppyGirl1508, PuzzletChung, Pyrospirit, Rachack, Radon210, RainbowOfLight, Rapidfyre, RazorICE, Rdsmith4, Reciproc08, Recognizance, Recurring dreams, ReikiEssentials, RememberMe?, ResearchRave, Rettetast, Rhanyeia, Rian-Koo, Ridge Runner, Rifleman 82, Riotrocket8676, Rocket000, Rocksrocksrockagh, Romanm, Ronhjones, RoyBoy, Rror, RyGuy17, SEWilco, SMC, Sahil shark, Samsara, Saperaud, Sarvil, Sasquatch, Savant13, Sceptre, Sean William, Secrets.of.the.skies, Selket, Sem-mem, Sergay, Shawnhath, Siim, Sir Arver, Sjakkalle, Slon02, Smack, Snowolf, Snowynight, Some jerk on the Internet, Sonic3KMaster, SonichuCWC, SorryGuy, Soumyasch, Springnuts, Stephane29, Stephenb, Stevertigo, Strongbadmanofme, Sublimehypocrisy, Suisui, Superdvd, Superm401, Swerdnaneb, T g7, TUF-KAT, Taemyr, Tagsontiago, Tantalate, TantalumTelluride, Tardigrade13, Tbone55, Techman224, Tekkenmasterbrendan, Tellyaddict, The Thing That Should Not Be, The undertow, TheCheeseManCan, TheWeakWilled, Thegreatdr, Thehelpfulone, This lousy t-shirt, Thrind, Tiddly Tom, Tide rolls, Tinkerbellkait, Tinkerperson, Tiptoety, Tom harrison, Tonmad, Tpb, Transisto, Traxs7, TreasuryTag, Ttony21, TutterMouse, UbUb, Ultatri, Una Smith, Upholder, Ut Libet, VI, Vanzpunk0676, Vary, VasilievVV, Ve4ernik, Vegaswikian, Veinor, Velella, Versus22, Vicki Rosenzweig, Vipinhari, Virusbetax, Voyagerfan5761, Vsmith, Vuong Ngan Ha, Wafflescakes, Walkerma, Wars, Wayne Slam, Weiguxp, Wenli, WikiLaurent, Willworkforicecream, Wisterlane, Wizard191, Wizardman, Wmahan, Wyatt915, Xanzzibar, YKWSG, Yamamoto Ichiro, Yidisheryid, Youandme, Z.E.R.O., ZX81, Zack, Zamphuor, Zap Rowsdower, Zsendukas, Zzuuzz, Білецький В.С., Куллер, 1073 anonymous edits

**Diffraction** *Source*: http://en.wikipedia.org/w/index.php?oldid=398346220 *Contributors*: 2over0, A1call, Abiermans, Across.The.Synapse, AdjustShift, Afrine, Ahmed1994, Alai, Alan Joe Skarda, Aleas, Ali, Amaltheus, Amosnomore, Andre Engels, AnnaFrance, Anoko moonlight, Anonymous Dissident, Army1987, Arnero, Arun Sapkota, Atlant, Av99, Barney-12-3, Bazzargh, Bbatsell, Bcrowell, Beetstra, BenFrantzDale, Birge, Bmicomp, Bongwarrior, Bryan Derksen, Buttseckks, CVIMG, Cambridgeincolour, Can't sleep, clown will eat me, Cdnc, Charles Matthews, Charmed4ever, Complexica, Conversion script, Cpl Syx, Crowsnest, Cuardin, Cwenger, Cwkmail, D-Kuru, DMacks, Decibert, DerHexer, Dicklyon, Dino, DrBob, DrJolo, Egil, Ellywa, Enormousdude, Epzcaw, Erguvan7, Erudecorp, Eurion, FDominec, Falcon8765, Flowersofnight, Francs2000, Fredbauder, Fresheneesz, Garagebarrage27, Gfutia, Gholam, Giftlite, Gludwiczak, GregRM, Hadal, Headbomb, Hillbrand, Howabout1, Hunterd, Icez, Igoldste, Instinct, Isnow, Ivarravi1, J.delanoy, JCraw, JForget, Jaganath, Jaxl, Jeff Dahl, Jermor, Jhbdel, Jjron, Jm smits, Jmartinsson, Karol Langner, Kdliss, KristianMolhave, Kurykh, L Kensington, LMB, La goutte de pluie, Largesock, Laserheinz, Le Scarlet Douche, Light current, Lightmouse, Linus M., Lotje, MER-C, Macpherson123, Magnus Manske, Mani1, Materialscientist, Maxdlink, Mbz1, Mejor Los Indios, Michael Hardy, Mikewax, Moe Epsilon, Moletrouser, Mortense, Moumouza, Mufka, MuthuKutty, Nailbiter, Narvalo, NawlinWiki, Neparis, Ngebbett, Nghtwlkr, Nikai, Nk, Nuno Tavares, Odedee, OlavN, Olv 26, Omer88f, Orionus, OwenX, Oysteinp, P100011011, Pakaran, Peterlewis, Pfaletra, Pfalstad, Pflatau, Pinethicket, Pps, ProhibitOnions, Pschemp, Quadell, RG2, Radiant chains, Ram-Man, Rbj, Reddi, RenamedUser2, Revilo314, Rgu.bhagyamma, Riceman3, Rnt20, Robert L, Ronbus, Rosuna, Rspanton, Rtcoles, RyanCross, Sakurambo, Sam Hocevar, Sango123, Saperaud, Seapalling3, SebastianHelm, Sebrofb, Seraphimblade, Shadowjams, Shim'on, Shoessss, Siddhant, SimonP, Skarebo, Skippy le Grand Gourou, Skoch3, Some jerk on the Internet, Srleffler, Steve Quinn, Stirling Newberry, Stou, Strait, Sudiarta, SunCreator, Sverdrup, TakuyaMurata, Teapotgeorge, TechnoFaye, The Anome, Thermochap, Tomruen, Trevorcox, Undying Flame, V81, Vanished User 1004, Wideofthemark, WikHead, Wikiborg, Wikid77, Wingchi, Wolfkeeper, Wtshymanski, Wyklety, Xiahou, YxTay, Yyy, ﻝﻱﻕﻉ ﻑﺵﺍﻙ, 百家姓之四, 305 anonymous edits

**Uniform theory of diffraction** *Source*: http://en.wikipedia.org/w/index.php?oldid=329320806 *Contributors*: CanadianCaesar, Difference engine, Edwin Carter, Jitse Niesen, Kalle, Mild Bill Hiccup, PEHowland, Paul D. Anderson, Pjvpjv, RHaworth, Red Act, Ryachris, Thubing, Zscout370, 6 anonymous edits

**Crystallography** *Source*: http://en.wikipedia.org/w/index.php?oldid=397349562 *Contributors*: 168..., 2over0, Addere, Afrankwiki, Ahoerstemeier, Alansohn, Alphachimp, Ambarsande, Baldhur, Berland, BlindEagle42, Bluemask, C quest000, Cadmium, Cchoongcc, Cdnc, Cherlin, Christopherlin, Chuunen Baka, Ck lostsword, Commander Nemet, Connormah, Constructive editor, Conversion script, Coolguy92591, Crystal whacker, Cstras, Cutler, Daarznieks, Dcirovic, Dhollm, Drue, Duncan.france, Gcm, Geologyguy, GeorgeLouis, Giftlite, Gilliam, Glenn, Gobonobo, Gombang, Gyrofrog, Headbomb, Heron, Hugh2414, Hugo-cs, Invitatious, J.delanoy, Jimfbleak, Jitse Niesen, Jittat, JohnOwens, Julesd, KSmrq, Kafuffle, Kalpanaiitm, Karol Langner, Kcordina, Kdliss, Kkmurray, Kokoriko, Krauss, Kurykh, Leonard G., Linas, Ling.Nut, Luna Santin, M stone, Mahlerite, Malcolm Farmer, Marciajeanne, Materialscientist, Maxdlink, Menchi, Mentifisto, Mhaitham.shammaa, Michael Hardy, MikeW25, Mikenorton, Mirokado, Mkosmul, Moonshiner, Mxpule, Olof, Oneforlogic, Oysteinp, Patrick, PhilKnight, Phys, Piano non troppo, Pion, Polyparadigm, Profjohn, PsiStar, Puchiko, Quantockgoblin, Quickbeam, Reciproc08, Rob Hooft, Robinh, Romaioi, Sahehco, SchfiftyThree, Seanwal111111, Siim, Simesa, Steve Quinn, Substatique, Suisui, TantalumTelluride, TenOfAllTrades, Terrace4, Triops, Uber-Nerd, Van helsing, Vsmith, Walkerma, Walkiped, Wik, Zundark, Zzuuzz, 132 anonymous edits

**Paracrystalline** *Source*: http://en.wikipedia.org/w/index.php?oldid=355175151 *Contributors*: Akulo, Bci2, Carlog3, CharlotteWebb, Furmanj, Giftlite, Pax85, Sting au, Venny85, Warut, 2 anonymous edits

**Quantum optics** *Source*: http://en.wikipedia.org/w/index.php?oldid=399644830 *Contributors*: A. B., Agge1000, Alansohn, AmarChandra, Asfarer, Assedo, Austin Maxwell, Bakrivan, Benevolentkoi, Beowulf333, Brazmyth, Charles Matthews, ChicXulub, Chub, Crmrmurphy, DARTH SIDIOUS 2, David Newton, DavidGrayson, Dekona, Dicklyon, Dolbin, Eng.ahmedsamy, Fabrictramp, Gabroni, Gaius Cornelius, Gerd Breitenbach, GermanX, Gfutia, HappyCamper, Harold f, Hess88, J S Lundeen, John Belushi, Knotwork, Laurascudder, LeonWhite, Linas, Lysdexia, Matt McIrvin, Mechanical digger, MykReeve, Nerone, Pgabolde, Pizza1512, Pjvpjv, Pmokeefe, Pvvni, REwhite, RPaschotta, RobinK, Sanders muc, Sapphic, SchillerStephan, Sijokjoseph, Srleffler, Staz69uk, SteinAlive, Sylgeist, Synergy, Thingg, Thunderhead, Tomatoman, Waxigloo, WikiDan61, Zarniwoot, ZorkFox, 55 anonymous edits

**X-rays** *Source*: http://en.wikipedia.org/w/index.php?oldid=175484653 *Contributors*: (jarbarf), 0, 21655, 2D, 2over0, 5 albert square, A Softer Answer, A8UDI, ACupOfCoffee, AGToth, Aarchiba, Academic Challenger, Adam1213, Adambro, Aditya, AdjustShift, Afiller, Agentilini, Ahoerstemeier, Ajraddatz, Alansohn, Aleator, Alesnormales, Alex.tan, Alfio, Alphachimp, Amir hmn2002, AnakngAraw, Anandgnanaraj, AndKemp, Andonic, Andrei Stroe, Anitajayy, Anna Lincoln, Anonymous Dissident, Anseljh, Antagonist, Antonio Lopez, Anwar saadat, Arakunem, Arcadian, Arctic Night, Aribex, Arru, Art Carlson, Art LaPella, Ashmoo, Atif.t2, Atmoz, Average Earthman, AxelBoldt, Axl, Aza, B0at, Baa, Backslash Forwardslash, Badgernet, Baggio10, Bahamut Star, Bangvang, Barkjon, Bart133, Beetstra, Bemoeial, BenFrantzDale, Bender235, Benkruisdijk, Bensaccount, Bentu, Bert Hickman, Betacommand, Bhadani, BiT, Bigbear bh, Bige1977, BillC, Binksternet, Blabbyblabby, Blackangel25, Blechnic, BlueDevil, Bobblewik, Bobjonhson1234567890, Bobmack89x, Bobo192, Bodybagger, Boing! said Zebedee, Bongwarrior, Bouncingmolar, Bowlhover, Brandon5485, BrendanRyan, BrianOfRugby, Britney901, Btunell, Bulatyk, Bullzeye, Butane Goddess, Bwilkins, Cairan, Calestyo, Calvin1509, Camw, Can't sleep, clown will eat me, Canadian-Bacon, Capricorn42, Carlj7, Cburnett, Cdang, Cgingold, Cgmusselman, Chairman S., CharlotteWebb, Chem-awb, ChemNerd, Chetvorno, ChicXulub, Chicago god, Chinju, Chris5858, ChrisGriswold, Ckatz, Clam0p, Clamalosal, Closedmouth, Cls465, Cohan, Conversion script, Coofjdf, Cool Blue, Coolth, CorvetteZ51, Courcelles, Cqouliinnn, Craigloomis, Crohnie, Cs-wolves, CurranH, Cybercobra, Cycotic, Cyon, D o z y, DARTH SIDIOUS 2, DD7990, DHN, DMacks, DV8 2XL, DVD R W, DaL33T, Daniel5127, DanielCD, Dave souza, Davehi1, David R. Ingham, David.Monniaux, Davidjk, Dazeley, Deenoe, Deglr6328, Dekisugi, Delengar, DerHexer, Dhesi, Digger3000, DimosthenisS, Dirac66, DirkvdM, Discospinster, Dlh-stablelights, Dlohcierekim, Dnvrfantj, Doctorevil64, Dododerek, Dohey, Donarreiskoffer, DrBob, DrSHaber, Dragomiloff, Drchessman, Drgeorgek, DuO, Dulciana, Dupdater, Dureo, Dusti, Earlypsychosis, Egg, Egil, Ejquant, El C, ElPeste, Elektron, Emijrp, Emperorbma, Englishnerd, Enormousdude, Enviroboy, Epbr123, Everyking, Evil saltine, Excirial, Faithlessthewonderboy, Fang 23, Farahead, Fastfission, FayssalF, Feezo, FelisSchrödingeris, Femto, Ffooxx33, Fieldday-sunday, FireSinger, Flewis, Focus mankind, Foochar, Fordan, Forteblast, Franetjust, Frostyboy27, Frymaster, Fundistraction, Fvw, Fëaluinix, GHe, Gail, Gaius Cornelius, Garrythefish, Gejigeji, Gene Nygaard, Geneva2007, Giftlite, Gilliam, Glane23, Glyn carter, Go229, Gobonobo, Gogo Dodo, GrGr, GraemeL, Graham87, Greg L, Greggydude, Gregory Merchan, Griffinofwales, Groudon185, Gscshoyru, Gseryakov, Gsmgm, Gurch, Gökhan, Hadal, Haikupoet, Hairy Dude, HamburgerRadio, Hammer1980, Harland1, Headbomb, Hellbus, Helloworld2007, HenrikP, Hephaestos, Heron, Herostratus, Hiijin47, Hmrox, Hobartimus, Hodgson-Burnett's Secret Garden, Homerjay, Horoporo, Hst43, Hu12, Huga, Hugh Davey, HumphreyW, Huntthetroll, Hydrargyrum, I B Wright, I own in the bed, I.M.S., Icairns, Icarus3, Igoldste, Immunize, Inkypaws, Insanity Incarnate, Inzy, Ionactive, Iridescent, Irishguy, Irrawaddy, Ixfd64, J.delanoy, JForget, Jacek Kendysz, Jackol, Jaknouse, Jaraalbe, Jarash, Javierito92, Jclerman, Jdrewitt, Jeff Dahl, Jeff G., Jeppy2,

Jeronimo, Jfdwolff, Jh51681, Jimfbleak, Jj137, Jmh649, John of Reading, JohnOwens, Johnbod, Jonah Saltzman, Jonverve, Joriki, Jose77, Jovianeye, Jumping cheese, Jusjih, Kate, Kathreen8, Kbk, Kdliss, Kdp2004, Keenan Pepper, Keilana, Kellogg257, Kevin B12, Kgf0, Khaled hosny, Khalid hassani, Khoikhoi, Kicking222, Kieff, King of Hearts, Kingpin13, Klar sagen, Kowey, Kram9, Krawi, Ktulu6, Kungfuadam, Kzollman, LAAFan, LOL, Larryisgood, Lars Lindberg Christensen, Lcolson, LeaveSleaves, Lee, LegitimateAndEvenCompelling, Lesonyrra, LibLord, Lightmouse, Ligulem, Limulus, LinDrug, Lindmere, LittleOldMe old, Ljb999, Logan, Looxix, Lord Emsworth, Loren.wilton, LorenzoB, Lotje, Lradrama, Lui1014, Luna Santin, MBisanz, MER-C, MMS2013, MONGO, Maias, MarcoTolo, Mariemontwarrirors, Marshallsumter, MastCell, Matt Whyndham, Matthewpppp, Mav, Mav12321, Maximus Rex, Mdog22, Mentifisto, Merope, Michael Daly, MichaelMouat, Micky bang, Mikalwilliams, Mike Serfas, Mikelk3, Mild Bill Hiccup, Milkbreath, Minston, Miquonranger03, MisterDie, Mmxx, Mnolf, Mohammed269, Money Machine, Moonkeymasta, Mschlindwein, Mufka, Muhammad2692, My Core Competency is Competency, MyNameIsNorris, NJ, Naddy, Nagsv, Nbishop, Neelix, Nehrams2020, Nevfennas, Nibuod, Nick C, Nihiltres, Niteowlneils, Nmnogueira, Noommos, NorwegianBlue, Notary137, Nsaa, Nzgabriel, Old Moonraker, Omegatron, Oxymoron83, Ozuma, Paleorthid, Pang-hung.liu, Paolo.dL, Paul August, Perardi, Percy Jackson, PerryS, Peter bertok, Petersam, Pflatau, Phaedriel, Pharaoh of the Wizards, PhilHibbs, Philip Trueman, PhilipBembridge, Philipcosson, Philipp Wetzlar, Piano non troppo, Pieter Kuiper, Pigsonthewing, Pince Nez, Pinethicket, Pizza Puzzle, Polonium, Pornstar12345, Poupoune5, PrestonH, Princemackenzie, Puchiko, Pyfan, Qrsdogg, Quacha, Quadell, Quandaryus, Quennbee3150, Quintote, Quixeh, Qwertyus, Qxz, R'n'B, R.J. Croton, RB972, RColbeth, Radon210, Raelx, Ragib, Rapidcreek, RaseaC, RazorICE, Rdsmith4, Reach Out to the Truth, Rebecca, Rebroad, Reconsider the static, RedLinks, Reddi, Redthoreau, Retinoblastoma, RetiredUser2, RexNL, Ricardo monteiro, Rich Farmbrough, RichardBartle, Rixs2010, Rjwilmsi, Rlee0001, Rmhermen, Rob.bastholm, RobertFritzius, RobertG, Robertgreer, Rod57, Rohitphy, Ronz, RoseWill, RoyBoy, Rror, Ruud Koot, Rwmshopping, Ryancormack, S Roper, S3000, Salty!, Salvio giuliano, Sam Korn, Samwb123, Savage1881, SchfiftyThree, Scwlong, Seervoitek, Sengkang, Serie, SeteboS, Shaddack, Shadowjams, Shai-kun, Shalom Yechiel, Shankrxn8111, Shannon bohle, Sherool, Shewlett95, Shizhao, Shmuel Benezra, Shoessss, SimonP, Sjschen, Skier Dude, Skippy le Grand Gourou, Sky Attacker, Skysmith, Sleigh, SlimVirgin, Slon02, Smack, Snottily, Snowolf, Soarhead77, Sodium, Soundray, Spitfire, Srleffler, Stephen Bain, Stephenb, Steve Hart, Stevenfruitsmaak, Stirling Newberry, Stretch 135, Stuart Wimbush, Suh004757, Suicidalhamster, Sumersethi, SuperHamster, Superbeecat, SusanLesch, Svick, SwirlBoy39, Symane, THEQUEST410, TJ, TMN, Tango, Tannim101, Tarotcards, Tarquin, Tasfhkl, Tawker, Tektoon, Teles, Tellthepeople, Template namespace initialisation script, TestPilot, Tetracube, That Guy, From That Show!, The Anome, The Thing That Should Not Be, The editor1, The monkey likes pie, Thekingkiller, Think outside the box, Thunderlord, Tiddly Tom, Tide rolls, Tiny plastic Grey Knight, Tiptoety, Tleave2000, TobiWanKenobi, Tom harrison, Tomayres, Tone, TopCat99, Torchwood5, Toreau, Tpbradbury, Travisbrady, Traxs7, Tristanb, Trumpet marietta 45750, Tsr, Twooars, Tyler, Tyw7, Ugur Basak, Uphill12345, Ursa Gamma, Utcursch, Uucp, Van helsing, Variable, Vary, Velella, Versus22, Vgranucci, Victor Chmara, Vipinhari, Virak, Vishnava, Viskonsas, Volland, Voyagerfan5761, Vsmith, Waggers, Waleran, Walterdevries, Wantdouble, Warfreak, Wavelength, Wavemaster447, Weatherman100, WellsSt, WereSpielChequers, Werson, Whatever404, Whiner01, White Shadows, Wikibofh, Wikieditor06, Wikipedia brown, William Avery, Wireless Keyboard, Wjbeaty, Wolfkeeper, Wouterstomp, Wwwwolf, WxGopher, Xenophrenic, Xihr, Xmastree, Xrayuploader, Yidisheryid, Yintan, YuanY, Yworo, Yyy, Zaita, ZakuSage, Zaphraud, Zhou Yu, ZiyaA, Zrogerz69, Zundark, Zzzzzzzzzzz, Александър, 百家姓之四, 1523 anonymous edits

**Electron** *Source*: http://en.wikipedia.org/w/index.php?oldid=399815631 *Contributors*: (aeropagitica), 16@r, A. di M., A4, ABF, AVand, Aarchiba, Abutorsam007, Acalamari, Acelor, AcidHelmNun, Acrinym, Acroterion, Adam Rock, Ahoerstemeier, Aitias, Akamad, Al Wiseman, Ale jrb, AlexiusHoratius, AllyUnion, Almcaeobtac, Amakuru, Anaraug, Andre Engels, Andres, Andrewlp1991, Anonymous Dissident, Antonio Lopez, Ap, Ardonik, Army1987, Arpingstone, Art LaPella, Artichoker, Asierra, AstroNomer, Atjesse, AtomicDragon, Avoided, AxelBoldt, AzaToth, Bagel7, Bakanov, Bambaiah, Bart133, Bbbl67, Bdesham, Beetle B., BenRG, Benjadow, Benjah-bmm27, Bennybp, Bensaccount, BernardH, Bert Hickman, BillC, Blainster, Bobo192, Bondslave777, Bongwarrior, Booba5, Brews ohare, Brian0918, Bryan Derksen, Bvcrist, C.Bluck, CYD, Calair, Caltas, Camembert, CanadianLinuxUser, Cantras, CardinalDan, Ceranthor, Chamal N, Chekaz, ChemGardener, Chetvorno, Chill doubt, Chizkiyahuavraham, Christian75, Christopher Parham, ChristopherWillis, Chymicus, CircafuciX, Ckatz, Cometstyles, Complexica, Confusedmiked, Conversion script, Cool Blue, Correcting nonesense, CosineKitty, Crohnie, Csilcock, Curps, D, DARTH SIDIOUS 2, DMacks, DV8 2XL, DVdm, Da monster under your bed, Dabomb87, Dadude3320, Daniel.Cardenas, DannyWilde, Dar-Ape, DarthVader, Darthgriz98, Dauto, David Hochron, David edwards, DavidStern, Dawn Bard, December21st2012Freak, Deh, Deryck Chan, Diberri, Dina, Dineshextreeme, Dirac66, Discospinster, Dispenser, Dissident, Dmn, Dmr2, DonJStevens, Donarreiskoffer, Droll, Drondent, Dude1818, Długosz, E23, EJF, Eadon-com, EagleFalconn, Ealdgyth, Earle Martin, Ed Poor, Edgar181, Edward Z. Yang, Egil, Ehrenkater, El C, Eleassar, Eleassar777, Elroch, Enviroboy, Epbr123, Equendil, Eric B, Eric-Wester, Euchanels, Evgeny, Ezhuttukari, Fastfission, FeralDruid, Ferkelparade, Fizicist, FreplySpang, Fruge, Funnybunny, Fæ, GDonato, Gaius Cornelius, Galmicmi, Gary King, Gdo01, Gdr, Gef756, Gene Nygaard, Generalguy11, Gentgeen, GeometryGirl, GianniG46, Giftlite, Gil987, Gilgamesh, Glenn, Goplat, GorillaWarfare, GrahamColm, Graymornings, GreenSpigot, Greg L, GregU, GrouchyDan, Gtstricky, Gzuckier, H2g2bob, Hadal, HaeB, HappyVR, Harddk, HcorEric X, Headbomb, Heavy bolter, Heimstern, Herbee, Heron, Hidaspal, Hongthay, Hoo man, Hqb, Hurleymann1, Hveziris, IRP, Icairns, Icalanise, Ilikepie2221, Imaninjapirate, Inala, Incnis Mrsi, Iridescent, IrishChemistPride, IrishChemistPride2, Itub, Ixfd64, J Di, J-stan, J.Sarfatti, J.delanoy, JLaTondre, JSpudeman, JabberWok, Jackal irl, Jacksccsi, Jaganath, James Trotter, Jamyricks, Jaques O. Carvalho, Jaxl, JayMars, Jebba, Jeff3000, JimQ, Jimp, Jjasharpe, Jncraton, JoanneB, JoeMarfice, John5955, JohnArmagh, JohnOwens, Joizashmo, Joncam, Jonnyapple, Jordi Burguet Castell, Joshmt, Jrockley, Jusdafax, Jusjih, KPH2293, Kaiba, Kalivd, Kan8eDie, Karol Langner, Kingpin13, Kingturtle, Kjoonlee, KnowledgeOfSelf, Knutux, KrakatoaKatie, Kriak, Krich, Kriscotta, Kuririmo, Kurtcobain321, Kurykh, Kurzon, Kwekubo, Lathrop, Latka, Leuko, Light current, Lightmouse, Linas, Lissajous, Lkruijsw, Llort, LouisBB, LovesMacs, Lucinos, Lunchscale, Lycaon, LyleHoward, MEJG, Maliz, Malo, Mani1, Markhurd, Martial75, MasterOfHisOwnDomain, Materialscientist, Mattfont, Mav, Maximus Rex, Mbell, McVities, Mcmonsterbrothers, Megaboz, Melchoir, Melibarr05, Mermaid from the Baltic Sea, Merovingian, MetsFan76, Mgaarafan, Michael Devore, Michael H 34, Michael Hardy, Mike Peel, Mike Rosoft, Mild Bill Hiccup, Mindmatrix, Mindspillage, MinicheddarsandelephantsFTW, Miquonranger03, Mitch Ames, Mlouns, Mni9791, Monkey Bounce, Mote, Mpulier, Mr. Hallman, MrZap, Mrhellcool, Ms2ger, Muhends, Mxn, Mydickishuge24, Nabla, Narayanese, NativeForeigner, Naturalnumber, Neparis, Nergaal, Nergality, Neurolysis, NewEnglandYankee, Newone, Nihiltres, Noel Streatfield, Noisalt, Nonagonal Spider, NovaDog, Nrcprm2026, NuclearWarfare, NuclearWinner, Numbo3, Nwbeeson, Obradovic Goran, Ocatecir, Odatus, Omega21, Omegatron, Omnedon, Omnipedian, Opelio, Optiguy54, Ori.livneh, Owlbuster, Ozielke, PEBill, Paine Ellsworth, Palica, Pandion auk, Patrick, Patrick L. Goes, Pcarbonn, Pcorty, Pearle, Percommode, Persian Poet Gal, Peter G Werner, Peter470, PeterisP, Peterlin, Peyna, Philip Trueman, PhilipO, Phillycheesesteaks, PhySusie, Physchim62, Piano non troppo, Pieter Kuiper, Piledhigheranddeeper, Pinethicket, PingPongBoy, Pingveno, Pnacitum, PoliticalJunkie, Ponyo, Potekhin, Prestonmag, Priceracks, Pt, RAlafriz, RG2, RJHall, RadicalOne, RainbowOfLight, Rajeevmass, RandomTREES, Ravedave, Raynor42, Rbdebole, RedRollerskate, Reddi, Rednblu, Redvers, Restu20, Retired username, RetiredUser2, RexNL, Reywas92, Rgoodermote, Riana, Rich Farmbrough, RichBlinne, Richerman, Ricky81682, Rightly, Rjwilmsi, RobertAustin, Ronhjones, Rotational, RoyBoy, Royalguard11, Roybb95, Rurik3, Ruslik0, RyanOrdemann, Ryrivard, S0aasdf2sf, SCZenz, Sadi Carnot, Salsb, Sanders muc, SandyGeorgia, Sbyrnes321, Scarian, Schapel, Sean William, Secretlondon, Sergeanthuggy, Shaadow, Shaddack, Sheliak, Sheogorath, Shootbamboo, SimonP, Sjodenenator, Skymt, Slartibartfast1992, Slowking Man, Smith Jones, SmoothK, Sohaib360, Spencer, Spike Wilbury, SpookyMulder, SpuriousQ, Srleffler, Ssd, Ssilvers, Stepa, Stepheng3, Steve Quinn, Stevertigo, StradivariusTV, Strait, StuTheSheep, Suisui, Surv1v4l1st, Susvolans, Swifterthenyou, Swimallday, THEN WHO WAS PHONE?, Tcncv, Tellyaddict, Thadaddy3233, TheChrisD, Thecurran, Theonlyedge, Thereen, Thermochap, Thingg, Thisisborin9, Tide rolls, Tim Starling, TimothyRias, Timwi, TomasBat, Tomdobb, TonyHagale, Tonyfey, Tonyrex, Travelbird, TriTertButoxy, Trojancowboy, Tyco.skinner, UPS Truck Driver, UberCryxic, Uncle G, Unclevortex, Uruk2008, User A1, Utility Monster, V1adis1av, Vanished User 0001, Ventolin, Versus22, Vespristiano, VictorP, Visionholder, Voltron Hax, Voorlandt, Voyajer, Vsmith, WFPM, WMSwiki, Waggers, Wavelength, Wayne Slam, Wayward, Wereon, West Brom 4ever, Wigie, WikHead, Wikiborg, WikipedianMarlith, William Avery, Wilt, WingkeeLEE, WizendraW, WolfmanSF, Wolfmankurd, X!, Xantolus, Xerxes314, Xplat, Yamamoto Ichiro, Yath, Yoos, Yzmo, Zazaban, Zazou, Zeamays, ZeroOne, Zigger, ~K, 百家姓之四, 998 anonymous edits

**Neutron** *Source*: http://en.wikipedia.org/w/index.php?oldid=399424502 *Contributors*: 2D, 5 albert square, A. di M., ABigGreenHippo, Aadal, Aarchiba, Abce2, Abd, Abdullais4u, Abhinav paulite, Acalamari, AdjustShift, Aecarol, Agesworth, Ahoerstemeier, AlDragon, Alansohn, Alchie1, Aldaron, AnakngAraw, Andre Engels, Andrea105, Andres, Andrewa, Animum, AnonGuy, Antixt, Anyeverybody, Arjen Dijksman, ArnoLagrange, Art Carlson, Aruton, Astavats, AstroNomer, Asyndeton, Attilios, AxelBoldt, AySz88, Badseed, Bambaiah, Bender235, Bensaccount, Bluerasberry, Bobo192, Brainblaster52, Brazmyth, Bryan Derksen, Bsimmons666, Burntsauce, CDN99, Cabb99, Caiyern, Calypso, Can't sleep, clown will eat me, CanisRufus, Capricorn42, Cenarium, Cglassey, Chasingsol, Chenyu, Christofurio, Church of emacs, Citicat, Complexica, Conversion script, Copper.nanotube, CosineKitty, Cyp, DFriend, DV8 2XL, Danny, Dark Mage, Darrell cosare, Dbiel, Deanlsinclair, Demicx, Denni, DerHexer, Dev 176, DoctorPiouk, Donarreiskoffer, Doughboy, Doulos Christos, Dr.Science, Drilnoth, Dycedarg, Długosz, Ecko15, Eddideigel, Edgar181, El C, Ellywa, Enviroboy, Epbr123, Epicstonemason, Everyking, Extransit, Falcorian, Fasettle, Favonian, Femto, Forteblast, Frau Holle, Fredrik, FreeFull, Gaius Cornelius, Gentgeen, Geoking66, GianniG46, Giftlite, Gimmetrow, Glenn, Gogo Dodo, GoingBatty, Goods21, Goostyyy, Gopal81, Gordonrox24, Goudzovski, Graham87, Green Day143, Hans Moravec, Hdehuer, Headbomb, Heavens is the world, HenryLi, Herbee, Husond, Hyray, Icairns, Icek, Illdz, Industrieman, Interiot, Ironnickel, Ixfd64, J.delanoy, JBukon, JWB, JaGa, Jakew, Jaknouse, JamesBWatson, JarlaxleArtemis, Jdrewitt, Jeff G., JerrySteal, JetLover, Jimmy be, Joelholdsworth, Jorge Stolfi, Joshmt, Jrockley, Ju7kik8ol568r, Juancnuno, Julesd, Jusdafax, Karenjc, Karol Langner, Kbk, Kdliss, Keilana, Ketiltrout, King of Hearts, Kjkolb, Kjoonlee, Kkmurray, Knutux, KunalKathuria, Kuyabribri, KyleDantarin, LarryFrank, LexCorp, Lokal Profil, Looxix, Lord Shivan, LorenzoB, M1ss1ontomars2k4, Magister Mathematicae, MagnInd, Marek69, Marshallsumter, Martin451, Mav, Maximus Rex, Maxis ftw, Melchoir, Mennoblaauw, Merovingian, MetsFan76, Mike Rosoft, Mike Serfas, Mikez, Mkweise, Mocirne, Montazmeahii, Morgrimm, Mosaffa, Mother.earth, Mr. Wheely Guy, Mviduka4197, Mwtoews, N5iln, Nakon, Naturalnumber, Naturespace, NawlinWiki, Ncmvocalist, Nebulosus, Neparis, Nergaal, Newone, Nick Y., NickMartin, Nicklcms, Nightscream, Nihiltres, Nikai, Nsaa, NuclearWinner, O18, Obradovic Goran, Olivier, Oo64eva, Oxymoron83, PL290, Paine Ellsworth, Patrick, Patstuart, Patsw, Paul Erik, Paula Pilcher, Pcorty, Persian Poet Gal, Peter bertok, Phantomsteve, Phydend, Pilotguy, Pinethicket, Possum, Poupoune5, Prashanthns, Psturm, RG2, RJHall, RadiantRay, RadicalOne, Rajeevmass, Rangek, Raven1977, Renafaye77, Reyk, Riana, Richard Arthur Norton (1958- ), Rmrfstar, Roadrunner, Robert Johnson 10, Romanm, Ronebofh, Ronhjones, Roomyt, Rursus, Rwflammang, SDC, Safalra, Salsb, Samwb123, Satan's Kitchen, Sbharris, Sbowers3, Scarymaryfwfc, SchfiftyThree, Scottfisher, Seattle Skier, Sega381, Shadowjams, Shoeofdeath, Sjkimminau, SkyLined, Slakr, Soarhead77, SouthernMan, Sparky2002b, SpeedyGonsales, Spencer, Spute, Srleffler, Starkiller88, Stephenb, Strait, Subash.chandran007, Susvolans, TSO1D, TakuyaMurata, Tarosan, Tchaika, Teles, The Anome, The High Fin Sperm Whale, The Thing That Should Not Be, TheEditrix2, Thedjatclubrock, Tide rolls, Tiptoety, Tobias Hoevekamp, Tohd8BohaithuGh1, TomasBat, TraceyR, Trelvis, Triple333, Tsogo3, Tupungato, Unkenruf, Unyoyega, Valery Beaud, Vboo-belarus, Versus22, VictorianMutant, Voidxor, Vsmith, Vuo, W1k13rh3nry, Wafulz, WaveEtherSniffer, Whitepaw, Wigren, Wiki Tiki God, Wiki alf, WikiSlasher, Wikipelli, Wknight94, XJamRastafire, Xaonon, Xerxes314, Yyy, Zfr, Zhou Yu, Велетень, لی‌قی‌ع فش‌اک, 513 anonymous edits

**Muon** *Source*: http://en.wikipedia.org/w/index.php?oldid=399046291 *Contributors*: 217.126.156.xxx, 24.93.53.xxx, 5Q5, A. di M., Ahoerstemeier, Andrew Carlssin, Angela, Anonymous Dissident, Anthony Appleyard, Army1987, AxelBoldt, Bambaiah, BarretBonden, Belg4mit, Bennetto, Bermy88, Bkell, Bkellihan, Bm gub, Bodhitha, Bryan Derksen, Bubba73, CYD, Can't sleep, clown will eat me, CapitalR, Ceyockey, Cjxc92, Conversion script, Coppertwig, Corpx, CrniBombarder!!!, Dane Sorensen, DannyWilde, Dauto, Deglr6328, Diberri, DnetSvg, Donarreiskoffer, DoubleBlue, Dougluce, DragonflySixtyseven, Eb.hoop, EddEdmondson, Ehrenkater, Eog1916, Falcorian, Giftlite, Goudzovski, Graham87, Graymornings, HEL, Headbomb, Herbee, Icalanise, JabberWok, Jarry1250, Jdrewitt, JorisvS, Kariteh, Keenan Pepper, Ken Gallager, Kjoonlee, Kotika98, Larryisgood, LiDaobing, Looxix, Mani1, Mav, Melchoir, Merovingian, Mihaip, Mike Peel, Milledit, Millosh, Misterigloo, Mother.earth, Nono64, Ojigiri, Paine Ellsworth, Pcarbonn, Pjacobi, Puzl bustr, RDR, Ravedave, Rholton, Rich Farmbrough, Roadrunner, Rob Hooft, RobPlatt,

Roentgenium111, Roscoe x, Rotiro, Ruakh, SCZenz, STGM, SalomonCeb, Salsb, Saritepe, Sbharris, Sbyrnes321, SchmittM, Scottfisher, Sheliak, Spencer, Srleffler, StewartMH, Stifle, Strait, Tarotcards, Tetracube, The Epopt, Thecinimod, Tigerhawkvok, Tim Starling, Vanderdecken, VasilievVV, Wavelength, Whiner01, Woohookitty, Xerxes314, Xinghuei, Yevgeny Kats, Youandme, Zundark, 150 anonymous edits

**X-ray diffraction** *Source*: http://en.wikipedia.org/w/index.php?oldid=394572358 *Contributors*: 168..., 2over0, Aboalbiss, Alxmel, Annabel, BevVincent, Bkraabel, Bullet2010, Cgingold, Coops1974, Crystal whacker, Darkstar78, Drbreznjev, EdJohnston, Gertlex, GregorB, Haimingli, Irene Ringworm, Jcwf, Jdrewitt, Jeff Dahl, Kbh3rd, Kdliss, Kkmurray, La Pianista, Localshop, M.Arjeneh, Mikaey, Mspraveen, Nanotech18, Neparis, NerdyNSK, Nitrofev, Paul Henning, Pieter Kuiper, RadXman, Rb82, RexNL, Rifleman 82, Rixs2010, Romaioi, Runeuser, S030100000408, Selket, SellusGravius, Skier Dude, Slinky Puppet, Spellcast, Steve Quinn, Taras, Tpikonen, Uvainio, VTBushyTail, Webridge, Wickey-nl, Xstreamsys, יש דוד, 61 anonymous edits

**Electron diffraction** *Source*: http://en.wikipedia.org/w/index.php?oldid=397487657 *Contributors*: AB, Achoacho, Allycatblues, Andrei Stroe, Average Earthman, D3, Daniel.Cardenas, Excirial, Frecklefoot, Grimlock, Headbomb, Hyleelyh, Icairns, Ideal gas equation, Iridescent, Jag123, Jamelan, Jusjih, Karol Langner, Keilana, Kkmurray, Kristof vt, Linas, Michael Hardy, Mnmngb, Mpatel, Nikai, Oysteinp, Parvindsastry, Perditax, Rb82, Rob Hooft, Skoch3, That Guy, From That Show!, Thermochap, User A1, Zoicon5, 百家姓之四, 58 anonymous edits

**Neutron diffraction** *Source*: http://en.wikipedia.org/w/index.php?oldid=398531474 *Contributors*: Ahoerstemeier, Andre Engels, Andrewcwalters, Andyfaff, Appraiser, Benjah-bmm27, Brim, Doradus, Eco76, Eno-ja, Gene Nygaard, GoOhm, Gonzo fan2007, Hellbus, Jag123, Jaraalbe, Jcwf, Jdrewitt, John, Judge Nutmeg, Karol Langner, Kdliss, Kipmaster, Lawrie.skinner, Metabolizer, Mnmngb, Nafradi, PV=nRT, PhilBentley, Pietrow, Puppy8800, R'n'B, Rod57, Romaioi, Saber girl08, SimonD, Soarhead77, Sophus Bie, Sword, Tassedethe, Tomer shalev, V81, YK Times, Zoicon5, Սահակ, 51 anonymous edits

**Neutron scattering** *Source*: http://en.wikipedia.org/w/index.php?oldid=394415595 *Contributors*: Agesworth, Andyfaff, Anonymous Dissident, Calltl, Cardamon, Chipmonker, Dougluce, EBlackburn, Goochelaar, Grj23, Hellbus, J bellingham, Jdrewitt, Joachim Wuttke, Karol Langner, Kdliss, Kiyabg, Low-frequency internal, Marie Poise, Msiebuhr, NSR, Nitrous x, Paula Pilcher, PhilBentley, PranksterTurtle, Qwerty Binary, Sam8, Sanders muc, Sbharris, Soarhead77, 14 anonymous edits

**Inelastic neutron scattering** *Source*: http://en.wikipedia.org/w/index.php?oldid=353840878 *Contributors*: Chris the speller, D-rew, Jdrewitt, Joachim Wuttke, Kukini, Mkresch, Paradoxsociety, Paula Pilcher, 9 anonymous edits

**Ionization cooling** *Source*: http://en.wikipedia.org/w/index.php?oldid=188728045 *Contributors*: Chrisrogers1234, Reyk

**Deep inelastic scattering** *Source*: http://en.wikipedia.org/w/index.php?oldid=386381678 *Contributors*: Alansohn, Anthony Appleyard, Batmanand, Charles Matthews, D.H, DerHexer, Dna-webmaster, E2m, Epbr123, Julesd, Majorly, Nbach, Neparis, Peter Harriman, PeterReid, Phe, Quietly, SCZenz, Saga City, T@nn, Vb, 17 anonymous edits

**Timeline of microphysics** *Source*: http://en.wikipedia.org/w/index.php?oldid=326033832 *Contributors*: 0, 5.41, AjAldous, Aspects, Attilios, Bookalign, Bryan Derksen, Charles Matthews, Colonies Chris, Cutler, D6, DO'Neil, DannyWilde, Dave souza, DavidLevinson, Dirac66, Dstudent, EdH, Elektron, Elliskev, Fibonacci, Gareth Owen, Gregnguyen, Gretyl, HappyCamper, Harp, Headbomb, Hidaspal, Isomorphic, J.delanoy, JeffBobFrank, JeffW, Jheald, Kierano, L Kensington, Laurascudder, LeYaYa, Likebox, Looxix, Macumba, Michael Devore, Michael Zimmermann, MimirZero, Mr impossible, ObsidianOrder, Okedem, Onionmon, Paulleake, Physicistjedi, Piil, Pjacobi, Radagast83, RayTomes, Rmhermen, Ruud Koot, Safalra, Saga City, Selket, Smack, Steve Quinn, Stone, Tabletop, Tassedethe, Taxman, Timwi, Urhixidur, Vegaswikian, XJamRastafire, Yamara, 37 anonymous edits

**Automatic calculation of particle interaction or decay** *Source*: http://en.wikipedia.org/w/index.php?oldid=388034483 *Contributors*: Calwiki, Cricketgirl, Eurekaman, Freacafe, Headbomb, JaGa, PigFlu Oink, Rhebus, SGGH, Sophus Bie, Tassedethe, Victor Lopes, 9 anonymous edits

**S-matrix** *Source*: http://en.wikipedia.org/w/index.php?oldid=376223237 *Contributors*: Abdull, Adjusting, Akriasas, AugPi, Bakken, Berto, Bodera, BradBeattie, Businessman332211, Charles Matthews, Filemon, Giftlite, Hammer Raccoon, Headbomb, Hfastedge, Jeff3000, Likebox, Lumidek, MFH, Maedin, Maliz, Matiasleoni, Michael Hardy, Ntsimp, Oleg Alexandrov, Pearle, Phys, PhysicsBob, Poli, QFT, RJFJR, Reuqr, Rich Farmbrough, Safalra, Secfan, SeventyThree, StephenWeber, StevenJohnston, Tbackstr, TimothyRias, Tothebarricades.tk, Tsiaojian lee, Tweet Tweet, 32 anonymous edits

**List of materials analysis methods** *Source*: http://en.wikipedia.org/w/index.php?oldid=397461654 *Contributors*: Amaltheus, Arbasli, Askewmind, Bvcrist, C.jeynes, Cardamon, CharlesC, ChrisHodgesUK, Coloradoauthor, Danski14, Dreampursuer, EdC2, Ein hesse, Excaliburhorn, Excirial, Fredericks, Freecat, Garion96, Gimme danger, Gurch, HYPN2457, Hubble618, IanOsgood, IceKarma, JackSeoul, Jcwf, Jlacount, Kanzure, Karnesky, Karthikc123, Khatru2, Kkmurray, Korg, Materialscientist, Michael Hardy, Mjmerriknight, Murray.booth, Neparis, Ohthelameness, Open2universe, Pegship, Pharmacomancer, Pythagoruz, Rixs2010, Runningamok19, Topbanana, Twisp, Woogee, XPh6, Yanwen, Yaotsan, 102 anonymous edits

**List of neutrino experiments** *Source*: http://en.wikipedia.org/w/index.php?oldid=394407884 *Contributors*: BD2412, DrCLN, Headbomb, Henbo, Hugo999, Morgan wascko, Neutrinoless, Pjacobi, Puttybrain, V1adis1av, 12 anonymous edits

**Optical microscope** *Source*: http://en.wikipedia.org/w/index.php?oldid=398948491 *Contributors*: 2over0, 3dnatureguy, A Karley, AJim, Aaagmnr, Aazn, Ajraddatz, Alansohn, Alipson, Amaltheus, Andonee, Andy Nestl, Archer3, Arnero, Axl, Beetstra, Bigboyslam, Bobo192, Bochica, Boing! said Zebedee, Brian the Editor, Bryan Derksen, Can't sleep, clown will eat me, Cancun771, Captain-tucker, Chizeng, Chris the speller, ChrisCork, Chrisjj, Ckatz, Clearly kefir, Cmprince, CommonsDelinker, Coolbrdr, Cyrillic, Czforums, Danh, DeadEyeArrow, DerBorg, Dicklyon, Dietzel65, Dina, DoITPoMS, Domitori, Dr bab, Dreadstar, Edward Z. Yang, Egil, El Muñeco Shakes It Up, Baby, Ellergodt, EntertainU, Erkcan, Escape Orbit, EyeTrawl, Favonian, Femto, Fountains of Bryn Mawr, Fritzpoll, G. C. Hood, Gaff, Gaius Cornelius, Galoubet, Ganjil213, Gerry Ashton, Goodparley, Grafen, HaeB, Haiqu, HalfShadow, Hao2lian, Haydood23, HeartofaDog, Hema 030, Heron, HexaChord, HiraV, Hmains, Hu12, Hugh2414, Huntthetroll, Hurricanehink, Iridescent, J.delanoy, JTN, Jagged 85, Jakehuston, Jasper33, Jeff G., Jmlk17, John Nevard, John254, JohnCD, Julius Sahara, Keyence, Kkmurray, Klapi, Knight1993, Kopeliovich, Kosebamse, Kyle1278, L Kensington, Larryisgood, LeaveSleaves, Leonard G., Lexic 4712, Liamdarga, Lotje, MJD86, Madhero88, Magnus Manske, Majorclanger, MarcoTolo, Marshman, Materialscientist, MauriceJFox3, Mav, Maypigeon of Liberty, Meeples, Megaman en m, Mentifisto, Merrimoles, Michael Daly, Microscopist, Mikael Häggström, Mike2vil, Mild Bill Hiccup, Mintleaf, Monedula, Mpe, Mr.Z-man, Ncross35, Neutrality, Nineteenninetyfour, Nmedard, Nonagonal Spider, Numbo3, Okedem, Oliver12, Omicronpersei8, Overney, Oxymoron83, Pb30, Peter G Werner, Peter XX, Peterlewis, PhilKnight, Philip Trueman, Philopp, Piano non troppo, Pichote, Plastikspork, Psyche825, Puchiko, Pxma, Quigabyte, Quinsareth, R'n'B, RJHall, Rcej, Res2216firestar, Rettetast, Rigadoun, RockMFR, RokasT, Sagaci, Sangak, Sarindam7, Scarian, Scotto001, Sebhaase, Sentausa, Shadowjams, Slooj, Snigbrook, Squidonius, Srleffler, Sruzin, Stephenchou0722, SunCreator, Sunray, Superweapons, Svance, Tamasflex, Tameeria, Tellyaddict, Thelb4, Topory, Trabelsiismail, TutterMouse, Uncle Dick, Velella, W0lfie, WLU, Wawong, Wayne Slam, Webmaster5000, WikHead, WingkeeLEE, Woohookitty, Yamamoto Ichiro, Yosri, Zaphraud, Zephyr2k, Zephyris, Zzuuzz, 428 anonymous edits

**Confocal microscope** *Source*: http://en.wikipedia.org/w/index.php?oldid=47017285 *Contributors*: 9eyedeel, Aaguerri, Axelv, Beland, Blechnic, Butterfly reflections, Carrasmith, Celephicus, Chewie, ChrisHodgesUK, Ciphers, ColinEberhardt, Donarreiskoffer, Drdaveng, Dyuku, EpiVictor, EronMain, Femto, Ff5166, Flameviper, Franco3450, H2g2bob, Ian Glenn, Jaeger5432, Joechao, Jumboman, Laportechicago, LegitimateAndEvenCompelling, Lexic 4712, MarcoTolo, Martious, Matanbz, MetrologyMan, MicroBio Hawk, Ncross35, Nikevich, Nonantum, OlavN, OttoTheFish, Plantsurfer, Pyo, Remyrem1, Rjwilmsi, Sandsturm, Sjock, Skookumdad, Smartse, Smith609, Srleffler, Tabascoj, TenOfAllTrades, Trilarion, Umangagarwal, User A1, Utbg2008, Vanillacreem, Whosasking, Xorx, Zephyris, 71 anonymous edits

**Atomic force microscope** *Source*: http://en.wikipedia.org/w/index.php?oldid=342015215 *Contributors*: .:Ajvol:., A13ean, Aaagmnr, Admartch, Ahram, Ahram-kim, Alansohn, Allentchang, Alvestrand, Ambios, Ams627, Angela, Anthonydelaware, Antony-22, Arcfrk, Ase (usurped), Askewmind, Average Earthman, Beatnik8983, Bendzh, Bfollinprm, Bibble, Bobblewik, Bochica, Bryan Derksen, Canjth, Cdnc, Chuckiesdad, Chych, CommonsDelinker, Courcelles, Creepin475, Crm2kmsu, Crystallina, Cucumberslumber, Cybercobra, Cyrus Grisham, Davidcastro, Dgrant, Doulos Christos, Edward, El C, Fdu.uiuc, Femto, Flipperinu, Fontissophy, Frosty0814snowman, Fuhghettaboutit, Gaijinpl, Gene Nygaard, Gene93k, Geodesic42, Graphene, Grmf, HYPN2457, Halibutt, Hodja Nasreddin, Iwan Novirion, Jatosado, Jaxl, Jcwf, Jmorgan, Jni, Joechao, Joeyfox10, John, John Dalton, Jpeaton, Kamukwam, Kariteh, Keenan Pepper, Kiracofe8, Koavf, KristianMolhave, LMB, Lauranrg, Leifisme, Materialscientist, Maximus Rex, Mephistophelian, Mikespedia, Mormegil, NanoMamaForReal, Nanoguy123, Ngebbett, Nmnogueira, Nuujinn, Oreo Priest, Orphan Wiki, Ouji-fin, Phancy Physicist, PhilKnight, Physicistjedi, Pieter Kuiper, Qef, Quadell, Qxz, Raymondwinn, Rezecib, Rhandley123, Rich Farmbrough, RoB, Rob Hooft, Ronz, Rostislav Lapshin, Rostislav V. Lapshin, Ruder, SJP, Sasquatch, Satish.murthy, Sbharris, Sbyrnes321, SecretDisc, Seraphchoir, Shniken1, Sisyphos happy man, Skier Dude, Smartse, Solsikche, Ssola, Switchsonic, Tai89ch, The wub, Think outside the box, Thumperward, Tim Starling, Trabelsiismail, Uglygizmo, Vfranceschi, Welkin.Shibboleth, Wiki alf, Wikiborg, William Avery, Yapete, Yurko, Yyy, Zeamays, Zureks, 217 anonymous edits

**Electron microscope** *Source*: http://en.wikipedia.org/w/index.php?oldid=399818495 *Contributors*: 007 n1, 5Q5, A. Carty, A3RO, ABF, Aaronsharpe, Acdx, Acroterion, Activist, Adam Mihalyi, Adambiswanger1, Adijr, AdjustShift, Aillema, Aitias, Alan012, Alansohn, Albany NY, Alex Klotz, Amaltheus, Andre Engels, Andrei Stroe, Antonio Lopez, Apparition11, ArchonMagnus, Aurelius173, Average Earthman, Backslash Forwardslash, Banus, Bci2, Bencherlite, Bender235, Bensaccount, Blanchardb, Blechnic, Bobo192, Bongwarrior, Borgx, Brianga, Bydand, C0nanPayne, Calabraxthis, Camembert, Can't sleep, clown will eat me, CanisRufus, Capricorn42, Captain-tucker, Cbj77, Cetcher1159, Ceyockey, Cgarber, Chai, Chem-awb, Chris G, Chrislk02, Christian75, Chuunen Baka, Chych, Closenplay, Conversion script, Corpx, Csown, D, DSRH, DVD R W, Daniel, DarkFalls, Darth Panda, Davewild, David R. Ingham, Davidbaca, Dcoetzee, Deglr6328, DeltaMicroscopyStudent, DerHexer, Dexarouskies, Dexter prog, Dgrant, Diaa abdelmoneim, Dicklyon, Dlohcierekim, Docu, Dogposter, DoubleBlue, Doyley, DrFO.Jr.Tn, DrMikeF, Drago27218, Drpickem, Dvratnam, Edal, Editor2020, El aprendelenguas, Elearning2000, Enchanter, Epbr123, Ephram Shizgal, Esem0, Evan1991, EyeSerene, FF2010, Fabricationary, Fallboy, Felipeavb, Ferengi, Fieldday-sunday, Fireice, Frank, Frank A, Frankatca, Frankenpuppy, Fueled, Funnybunny, Gaius Cornelius, Gary King, Gene Nygaard, George Burgess, Gh5046,

Giftlite, Gogo Dodo, Golfguy220-, GrahamColm, GregorB, Grey Shadow, Ground, Hat'nCoat, Hedgemonkey, Heron, Hitmanjon, Hornlitz, Horselover Frost, Hu, Hugo-cs, Hurricane Angel, Hydrogen Iodide, II MusLiM HyBRiD II, ILike2BeAnonymous, INkubusse, Ian Pitchford, IanOsgood, Igoldste, Imaninjapirate, Irfanhasmit, Isaac yagmoor, Itai, J.delanoy, JNighthawk, JRodeng, JTN, JaGa, Jaccardi, Jacopo Werther, JamesBWatson, Jared lap, Jeff G., Jeremiah, Jimp, Jjmatt33, Joelholdsworth, JohnOwens, JorgeGG, Joshua.morgan, Jungy111, Jusdafax, Karnesky, Karol Langner, Keilana, Kesac, Kils, Kingpin13, Kissavos, KnowledgeOfSelf, Konsu, Kpjas, KristianMolhave, Kukini, Kuru, Kusunose, KyraVixen, Kzollman, LeilaniLad, Leuko, Liferulez, LilHelpa, Lindmere, Lotje, Luna Santin, MER-C, Magnus Manske, Makingwiththeparticles, MarcoTolo, Marek69, Mark.murphy, Maro91eg, Materialscientist, Maurice Carbonaro, Mayapur, McSly, Mhazard9, Mhmolitor, Mikaey, Minimac, Mmxx, Monkeyknife, MoogleFan, MrOllie, Mschlindwein, Mwtoews, Myscrnnm, N5iln, Nate1481, Nath87, Ncemer, Netkinetic, Neurolysis, NewEnglandYankee, Nickfor1, Nihiltres, Nikai, Nmnogueira, Novalis, Oceano30, Oysteinp, Paulhaiti, Pdcook, Pengo, Perfecto, Pharaoh of the Wizards, Philip Trueman, Piano non troppo, Pip2andahalf, Plantsurfer, Plasticup, Pliable, PrestonH, Quadell, R.rommel, RUL3R, RainbowOfLight, Rajah, Rich Farmbrough, Richard Arthur Norton (1958- ), Riflemann, Risk one, Rjwilmsi, RobHarding, Rror, Rsrikanth05, Rurik3, Rustavo, S0uj1r0, STHayden, Sceptre, Sciurinæ, Sean William, Selket, Shirulashem, Sikkema, Silsor, Simon Shek, Simonmn, SkyLineRxx, Sludtke42, Snowmanradio, Snoyes, Sodium, Spbrandom, Spearhead, Speedyboy, Srdomingue, Srnec, Stahlkocher1, Staxringold, Steff, StephenBuxton, Steven Zhang, Stokerm, Sub-Angstrom, Subversive.sound, Svdmolen, Tacvek, Tahirulislam, Tapir Terrific, Terrace4, Tetraedycal, The Anome, Thedjatclubrock, Thermochap, Thingg, Tijadr, Til.Bartel, TimVickers, Tjmayerinsf, Tmopkisn, Travelbird, Twisted86, Tylersosmart, Tyrol5, Ulfbastel, Utcursch, Vossman, WahreJakob, Waldir, Wavelength, Willking1979, Wtmitchell, Zephyris, Zzuuzz, Кодекс, გიგა, 781 anonymous edits

**Synchrotron** *Source*: http://en.wikipedia.org/w/index.php?oldid=399552629 *Contributors*: Alvinwc, Animum, Aottley, Benbest, Besselfunctions, Bevo, Bewebste, Boris Barowski, Brockert, BrokenSegue, BryanD, Cantus, Casey56, Choochus, Cirejcon, ConradPino, DFRussia, DV8 2XL, Dan100, Darkgecko, David.Monniaux, Dee Earley, Dlenmn, Drakmyth, E2m, EdwardEMeyer, Eju77, Elwell, Emerson7, Enquire, Estel, Eubulides, Excirial, Fantasi, Fredrik, Gbleem, Gene Nygaard, Gentooligan, Gogo Dodo, Headbomb, JabberWok, Jaganath, Jeff G., Jjron, Jotamar, Jotel, Justpastalaska, Kdliss, Klaus, LSTech, Larkster, Laurascudder, Leonard G., Linas, Lokster, Macaddct1984, Mancune2001, MarioFanNo1, MarkSweep, Mike Rosoft, Mjamja, Mjspe1, Mongerhedron, Mrpeauk, Mrstonky, Mullet, Nahum Reduta, Nikai, Nunh-huh, Olee007@gmail.com, P7lejo, PRehse, Palfrey, Pizza1512, Pj.de.bruin, Ptomato, Pwesolowski, Quantum.wells, RoyBoy, Rufua, RupertMillard, SDC4004, SSRF CHINA, SallyForth123, Septuagent, Shadowfax0, Smithbrenon, Stevenj, TPK, Teddybearspicnic, TheMaster42, Thinko, Timo Honkasalo, TimothyPilgrim, Tpikonen, Uvainio, Vicarious, WLU, Whitt35, Wolfkeeper, Xtreambar, Yk13, Zondor, Zowie, Zzedar, 朝彦, 179 anonymous edits

**X-ray microscope** *Source*: http://en.wikipedia.org/w/index.php?oldid=399826238 *Contributors*: AB, AndyBQ, Bci2, Birge, Bouncingmolar, Can't sleep, clown will eat me, Cgingold, Chamal N, Deglr6328, Discospinster, Dratman, EbozMoore, Heron, Icairns, JTN, Loopunrolling, Marshman, NHSavage, Pmokeefe, Ptfptf, R'n'B, Rl, RoyBoy, Sommacal Alfonso, Stepp-Wulf, Stirling Newberry, The Anome, Томми Нёрд, 29 anonymous edits

**Field emission microscope** *Source*: http://en.wikipedia.org/w/index.php?oldid=219566021 *Contributors*: Creepin475, Djr32, Fargo21, Karnesky, RGForbes, Rror, Wopp

**Scanning tunneling microscope** *Source*: http://en.wikipedia.org/w/index.php?oldid=399258986 *Contributors*: .:Ajvol:., 198.133.22.xxx, 5Q5, Abrech, Adailton, Aiken drum, Aleks-eng, Alki, Ambios, Anastasius zwerg, Angela, Anthonydelaware, Antony-22, Apple white8888888, Aqptech, Arcfrk, Arch dude, ArmyOfFluoride, AxelBoldt, Banaticus, Beatnik8983, Ben Webber, BillWSmithJr, BobDole4Prez, Bobblewik, Bryan Derksen, Btilm, Caltas, Captain panda, Carlog3, Cato82, Cdnc, Chinesecomponents, Chotchki, Connormah, Conversion script, Crowsnest, Cycloptic squirrel, DGG, DMCer, Darth Panda, DerHexer, Dispenser, Dmsar, Duncan.france, Electron9, Electronegativity, Ellywa, Enteris, ErikvDijk, Erwinrossen, EvilFred, Eynar, Fawcett5, Femto, Finemann, FloNight, FourBlades, GChriss, Gaff, Gene Nygaard, Graham Jones, Grungebox, Gruntler, Hadal, Halibutt, Heron, IanOsgood, Into The Fray, Iridescent, Jarry1250, Jcarkeys, Jhjensen, Jkl, Joefaust, Kallew4, Kariteh, Kataloveno, Kero584, Kingpin13, KnowledgeOfSelf, Kpjas, KristianMolhave, Kukini, LMB, Luna Santin, Lupin, M0RHI, MER-C, Masa-aiz, Materialscientist, Mejor Los Indios, Mephistophelian, MesserWoland, Mhaesen, Mimihitam, N5iln, Nanotrix, OlEnglish, Omegatron, On the sixth day God created MANchester, Pb30, Perl, Pflodo, Photodude, Phpistasty, Pinethicket, Pintuiitb, Pion, Rajkashana, Redlen, Rettetast, Rob Lindsey, Robert L, Robma, Rostislav V. Lapshin, RuM, Satish.murthy, Sbyrnes321, Sceptre, Schatman, Schneelocke, SchuminWeb, Sean D Martin, Shadow demon, Shinmawa, Siddhant, Simetrical, Sir Nicholas de Mimsy-Porpington, Spiralhighway, Splash, Stikonas, Storybear, Surya Prakash.S.A., Taemyr, TheAndypriced, Tobinmarcus, Tom mullany, Trabelsiismail, Ultraexactzz, Varano, Vrenator, Vuo, White Shadows, WikiDao, Zeamays, Zvika, Zwilson, 261 anonymous edits

**Transmission Electron Aberration-corrected Microscope** *Source*: http://en.wikipedia.org/w/index.php?oldid=390706505 *Contributors*: AJim, Achris51, Average Earthman, Avoran, Bobblewik, CSWarren, CommonsDelinker, Doradus, Eaolson, Hellbus, JTN, Keraunos, Lumos3, Materialscientist, Minimac, Smartse, Wavelength, 11 anonymous edits

**ISIS** *Source*: http://en.wikipedia.org/w/index.php?oldid=242282562 *Contributors*: 23skidoo, Aboutrob, Agent 86, Alexhp, Alexliamw, AnakngAraw, Andrew Dalby, Andrew c, ArchangelMichael, Arcoro01, BD2412, BrightLights, Brynic, Camerong, CatherineMunro, Ceyockey, Christopherlin, Clare LC, Coso, Dmol, Dogru144, Dominus, Dysmorodrepanis, EALacey, Eequor, En21b, Fariel, Feinoha, Fernandobouregard, FuriousFreddy, Grey Shadow, GuillaumeTell, HERB, HJ Mitchell, Ikara, Ioeth, Ironholds, Islander, J73, JamesMLane, Jdrewitt, Jecowa, Jll, Johnatx, Jpbowen, Kevin Ryde, Laurascudder, Lmaltier, Mathursuhas, Maurauth, Maxis ftw, Mdnavman, Michaelrawi, Miguelfms, Mike Garcia, Mingleima, Miyagawa, Mlm42, Morning star, Mwtoews, Nedrutland, Nekura, Nigelbeameniii, Notreallydavid, Philip Cross, PigFlu Oink, Polluks, Propaniac, Psycho Chicken, Pt, QWerk, Queen Elizabeth II's Little Spy, Qwfp, Rabo3, RaptorZX3, Rd232, Regushee, Ricky81682, Roger McCoy, Rwendland, S.baumann, Scbarry, Seegoon, SlackerMom, Snek01, TheoClarke, Tverbeek, Twilsonb, Ugmedia, Uker, Vchimpanzee, Waldir, Wikiacc, Wolf-Dieter, Wurzeller, 60 anonymous edits

**ISIS neutron source** *Source*: http://en.wikipedia.org/w/index.php?oldid=398642909 *Contributors*: 2over0, Andreww, Benjaminevans82, BigDukeSix, Bobblewik, CarolGray, Croquant, Florentino floro, Inglebat, Islander, J bellingham, Jll, Marshallsumter, Mhockey, Orlady, RLMCG, Shaddack, Stwalkerster, Superborsuk, Tikiwont, Tpikonen, Whiner01, Wurzeller, XR2TT, 19 anonymous edits

**Sudbury Neutrino Observatory** *Source*: http://en.wikipedia.org/w/index.php?oldid=394131797 *Contributors*: Bearcat, Blotto adrift, Boardhead, Bryan Derksen, CDN99, Ceyockey, Conversion script, Cstaffa, CyclePat, DMcanada, DonovanHawkins, Duk, Euchiasmus, Falcorian, Fleurot, Flup, Flying fish, Gene Nygaard, Golfcam, HEL, Hadal, Headbomb, Hooperbloob, Hunor, Icalanise, Jag123, Jht4060, Jiminy pop, Joseph Dwayne, Judge Nutmeg, Kelapstick, Kmccarty, Korandder, Linas, Looxix, M@sk, Maury Markowitz, Mindmatrix, Montrealais, Msh210, NeilFraser, Neparis, PeregrineAY, Qui1che, Rich Farmbrough, Rnt20, Rotiro, RoySmith, Safalra, Sbharris, Scorbatt, ShakingSpirit, Shanes, Silsor, Stepa, Strait, Taxman, Tevatron, Tikiwont, Turtlejuice, Varnav, WISo, Wikibob, Wilmot1, 65 anonymous edits

**ATLAS experiment** *Source*: http://en.wikipedia.org/w/index.php?oldid=397684841 *Contributors*: 84user, AB, AcademyAD, Akamad, Amapelli, AndrewWatt, Andrius.v, Apis O-tang, Bcrowell, Bobblewik, Bovineone, Bridgeplayer, Bunchofgrapes, Bzzybee13, Charles Matthews, Ciphers, Col. Hauler, Cowman109, Curps, Cyberia23, Cynicism addict, Davdde, Djinn65, DragonflySixtyseven, Ehn, Erkcan, Flying fish, Francphy5, Francs2000, Freakofnurture, Frencheigh, GangofOne, Gene Nygaard, Gregb, Gurch, Harp, Harryboyles, Headbomb, Herr apa, Ida Shaw, Jag123, Jmnbatista, Joopercoopers, Juhanson, Khukri, Kozuch, Kyurkewicz, Laurascudder, LeoNomis, Linas, Loodog, Lumidek, Lupin, MagdaGa, Mako098765, Mallorn, Mandavi, Manfalk, Martijn Hoekstra, Master z0b, Matt Crypto, Maxkramer, Mets501, Mithridates, Mjaekel, Neparis, Nick Number, O. Harris, Orion11M87, Pediadeep, PeterMcCready, Plasticup, Rama, Rich Farmbrough, Rjwilmsi, Rob.derosa, SCZenz, SandyGeorgia, Sdedeo, Sfdan, Sheliak, SimonP, SinWin, Spellmaster, Splash, Ssayler, Suruena, Susvolans, The wub, Tm1729, Tony1, Tushar.bhatnagar, V9, Vald, WISo, Wayward, Wiki alf, Woodrowr, Z6, Zondor, 123 anonymous edits

**Microscopy** *Source*: http://en.wikipedia.org/w/index.php?oldid=398971658 *Contributors*: 02aifisher, 2D, 65.68.87.xxx, Abstraktn, AdjustShift, Aleksi Peltola, Alessandro Esposito, Alexandrov, Alexburke, AlphaEta, Altenmann, Amaltheus, Andy Nestl, AnnaFrance, Appraiser, Art LaPella, Arthena, Ash, Awien, AxelBoldt, Azo bob, BenFrantzDale, Bensaccount, Bernard Macdougall, Binary TSO, Blankfaze, Bobo192, Brian24545, Bsadowski1, CZ Micha, Caco de vidro, Capricorn42, Cashewnut761, Ceyockey, Chazerizer, Closedmouth, Conversion script, Coolbrdr, Cpeditorial, Da Joe, David Levy, Default007, Deglr6328, Dicklyon, Dietzel65, Domitori, Donarreiskoffer, Drphilharmonic, Dumeineguete, Egelberg, El C, Ellywa, Epbr123, Esprit15d, Ewen, Fbarw, FireBrandon, Fungicord, Galoubet, Gcm, Gerry Ashton, GirasoleDE, Gnomeselby, Goodnightmush, Graeme Bartlett, Greetings, Earthling, H2g2bob, HYPN2457, Hede2000, Hetar, Hqb, Hu12, Hugh2414, IEQParticles, Iamnotareplicatorat, Isoxyl, J.delanoy, JTN, JWSchmidt, Jaccardi, Jfdwolff, Jhpbroeke, John Elson, Jpbowen, Karekare0, Karnesky, Karol Langner, Keramamide, Khoikhoi, Kierongreen, Killiondude, Kkmurray, Kleopatra, Kubigula, Leuko, Lexic 4712, Loren.wilton, Lorhenzso 02, MarcoTolo, Marshman, Maurreen, Mboverload, Mercenario97, Michael Hardy, Microbiologyprocedure.com, Mikael Häggström, Mike.lifeguard, Molsmith, Moonriddengirl, MrGodot, MrOllie, Mrs Trellis, Mwfn, Mwfn1, Nick Number, Nigholith, Nitishmalik, OlavN, Oliver12, OttoTheFish, Oxymoron83, PFHLai, PascaleP, Paulburnett, Pearle, Peruvianllama, Peter G Werner, Peterlewis, Phoenix Hacker, Pinky127, Pvosta, RH, Radagast83, Reedy, Reelrt, Rflrob, Rjwilmsi, Rmosler2100, Rnt20, Robert M. Hunt, Rotational, Rubin joseph 10, Samjlord, Scharks, Serpent's Choice, Silverchemist, Siphiro, Sir Vicious, Sjakkalle, Skomorokh, Slicky, Snowmanradio, Snowolfd4, Spellcast, Srleffler, Srnec, Sumanesh Chakraborty, Sunray, TenOfAllTrades, Tevildo, Theresa knott, Thiseye, TimVickers, Tombomp, Trevor MacInnis, Troyrock, Untionic, Utbg2008, Utcursch, Uther Dhoul, Van helsing, Velella, Vgranucci, VivaEmilyDavies, Vsmith, WahreJakob, Warut, Wavelength, Weihao.chiu, WeoMoe, WereSpielChequers, Whisperingdrop, Wik, Witkacy, Wood Thrush, Woohookitty, Xezbeth, Zephyris, आशीष भटनागर, 293 anonymous edits

**X-ray crystallography** *Source*: http://en.wikipedia.org/w/index.php?oldid=399630875 *Contributors*: 168..., 2over0, 84user, ABiochemist, Adacus12, Adenosine, Almostfly, Anna Lincoln, Anthony Duff, Awadewit, BarretBonden, Bassophile, Beatnik8983, Ben.c.roberts, Bfiene, BlastOButter42, Bobblehead, BokicaK, C. Foultz, C.Fred, Cacycle, Cadmium, Capecodeph, Carcharoth, CardinalDan, Carstensen, Castor canadensis, Cdang, Cgingold, Chem-awb, ChemGrrl, ChemicalBit, Christopherlin, Chrumps, Cmura, Cometstyles, Conversion script, Cryptophile, Crystal whacker, D4g0thur, Dark link, Dewhastme, Dspoel, EdChem, EdJohnston, Eequor, ElBenevolente, Enochlau, Evil Monkey, Foobar, Fourchannel, Gcm, Gene Nygaard, Geni, Genisock2, Gertlex, Giraffedata, Glen, Graeme Bartlett, Graham87, Gurch, Harrydance, Headbomb, Hodja Nasreddin, Ian Pitchford, Icek, Ike9898, IowaStateUniversity, Irene Ringworm, Itub, JLaTondre, JMatthews, Jaapkroe, Jcwf, Jdrewitt, Jeff Dahl, Jevinsweval, Jjron, Jmath666, Joachim Wuttke, JoeAnderson, John, Jonathan Drain, Kaluza, Karelj, Karol Langner, Kazkaskazkasako, Kdliss, Keenan Pepper, Kevin Cowtan, Kjaergaard, Koavf, Kznf, Leonard G., Lightmouse, Lintze, Lipuju, Liveste, LostLucidity, Lotje, M stone, Maneesh, MarcoTolo, Marj Tiefert, MartinSchneebeli, Mashford, Materialscientist, Maxim, Melamed katz, Memenen, Michael Devore, Michael Hardy, Mikeyrocksya, Mitartep, Moink, Mr Stephen, Msebast, Mxn, N p holmes, Naudefj, NerdyNSK, Nihiltres, O RLY?, Oeffner, Opabinia regalis, Oysteinp, Paolo.dL, Paul Henning, Pdcook, Ph.eyes, Phe, Philip Trueman, Pilatus, Pjacobi, Polyparadigm, Prashanthns, Protonk, Quantockgoblin,

Quantumobserver, Quickbeam, Quixeh, Qwertyrandomnumber, RJHall, RadXman, Ravi22, Reciproc08, Riana, Rifleman 82, Rmhermen, Romaioi, Ruppweb, S Levchenkov, STHayden, Sasakthi, Seans Potato Business, ShadE04, Shenme, Silly rabbit, SimonP, Sintaku, Soarhead77, Spamicles, Splette, Srleffler, Ssteinz13, Starnestommy, Stewartadcock, TBChem, Tasfhkl, Tassedethe, Tempodivalse, The Special Six, Thincat, TimVickers, TomWeirich, Tpikonen, Tralala, TreeSmiler, V8rik, Voorlandt, Vossman, Vsmith, WahreJakob, Wavelength, WaysToEscape, Webridge, Wheedhee, Wickey-nl, Wildcat07, Will Beback Auto, WillowW, Wimvandorst, Xcomradex, Yardgnome, Yyy, 264 anonymous edits

**X-ray scattering techniques** *Source*: http://en.wikipedia.org/w/index.php?oldid=397626188 *Contributors*: 168..., 2over0, Aboalbiss, Alxmel, Annabel, BevVincent, Bkraabel, Bullet2010, Cgingold, Coops1974, Crystal whacker, Darkstar78, Drbreznjev, EdJohnston, Gertlex, GregorB, Haimingli, Irene Ringworm, Jcwf, Jdrewitt, Jeff Dahl, Kbh3rd, Kdliss, Kkmurray, La Pianista, Localshop, M.Arjeneh, Mikaey, Mspraveen, Nanotech18, Neparis, NerdyNSK, Nitrofev, Paul Henning, Pieter Kuiper, RadXman, Rb82, RexNL, Rifleman 82, Rixs2010, Romaioi, Runeuser, S030100000408, Selket, SellusGravius, Skier Dude, Slinky Puppet, Spellcast, Steve Quinn, Taras, Tpikonen, Uvainio, VTBushyTail, Webridge, Wickey-nl, Xstreamsys, יש דוד, 61 anonymous edits

**Fourier transform spectroscopy** *Source*: http://en.wikipedia.org/w/index.php?oldid=396945624 *Contributors*: 123Mike456Winston789, AJim, Asterion, Bci2, Bersbers, Berserkerus, BigFatBuddha, Bobby1011, Christopherlin, Conversion script, Damian Yerrick, Deglr6328, E104421, EndersJ, Epbr123, Graeme Bartlett, Graham87, Greggklein, Guillom, Hankwang, Harold f, Haydarkustu, HelgeStenstrom, Jaraalbe, Jcwf, John.lindner, Jonathan F, Kcordina, Kingpin13, Kkmurray, Martyjmch, Matanbz, Materialscientist, Michael Hardy, Nikai, Nitrogen15, PBSurf, Peter, Peterlewis, Publicly Visible, Quibik, Rifleman 82, Rnt20, Ronningt, Roybb95, Sbyrnes321, Seidenstud, Skier Dude, Slapidus, Smeyer1, Stannered, Stepan Roucka, Stokerm, Sverdrup, Taw, Thinkinnng, Tim Starling, Vataro, Veinor, Victorsong, Vsmith, Whasmith, 81 anonymous edits

**Hyperspectral imaging** *Source*: http://en.wikipedia.org/w/index.php?oldid=398218579 *Contributors*: Adoniscik, Andrew c, Bagaulin, Bci2, BodkinDesign1968, Caerbannog, Cm the p, Cuaxdon, Dhaluza, Ehn, Gcrisford, Geologicharka, GreatWhiteNortherner, Hankwang, Headbomb, Hyperspectral, Hyperspectralman, Johanume, Jprikkel, Lantonov, Materialscientist, Mboverload, Moin95, Oldtimer1820, Rnakatsuji, Tbandit, Tperrien, Victorsong, Whaa?, عين‌ام, 42 anonymous edits

**2D-FT NMRI and Spectroscopy** *Source*: http://en.wikipedia.org/w/index.php?oldid=376470276 *Contributors*: Bci2

**NMR microscopy** *Source*: http://en.wikipedia.org/w/index.php?oldid=375431439 *Contributors*: Basawala, Bobblewik, Gloy, Joechao, Mindmatrix, STHayden, Simon12, Woohookitty, 6 anonymous edits

**Chemical imaging** *Source*: http://en.wikipedia.org/w/index.php?oldid=379265863 *Contributors*: Alansohn, Andyphil, AngelOfSadness, Annabel, Banus, Batykefer, Bci2, BierHerr, Chris the speller, Closedmouth, D6, Davewild, Editore99, Fgnievinski, Gabi bart, GeeJo, Grafen, HYPN2457, Iridescent, JIP, Jim.henderson, Kkmurray, Larryloz, Materialscientist, Mdd, Mkansiz, Natalie Erin, QCRsolutionsCorp, R'n'B, Skysmith, Stone, Tassedethe, Ultraexactzz, Wilson003, 40 anonymous edits

**Fluorescence microscopy** *Source*: http://en.wikipedia.org/w/index.php?oldid=48762017 *Contributors*: Andy Nestl, Antony-22, Bci2, Bwbrian, Ch'marr, Cnickelfr, Coccyx Bloccyx, DO11.10, DerHexer, Eugene-elgato, Ferh2os, Firehox, Gbleem, Graham87, Hetar, IlyaV, JSpung, Jerrykim, Joechao, John, Kupirijo, Kymacpherson, Lexic 4712, Llbbl, MarcoTolo, Materialscientist, Microscopist, Minna Sora no Shita, Mysid, Nick Number, Nicolae Coman, Nmnogueira, Omar35880, OttoTheFish, Paultmoon, Pjvpjv, Pvosta, Radagast83, Rifleman 82, Scrabbler, Stepa, SubwayEater, TenOfAllTrades, Utbg2008, Vokey588, Will-moore-dundee, Wimox, Wtmitchell, Yerpo, Zeldaoot, Zephyris, 65 anonymous edits

**Fluorescence correlation spectroscopy** *Source*: http://en.wikipedia.org/w/index.php?oldid=397340951 *Contributors*: Antony-22, Arjen Dijksman, Bci2, BenFrantzDale, Berky, Danrs, Dkkim, Fatiguehop, Gogowitsch, Graik, Hbayat, Jcwf, John, Karol Langner, Lightmouse, Maartend8, Michael Hardy, NathanHagen, Nikevich, ST47, Skier Dude, Tizeff, Unruhj, Wisdom89, Yidehuren, 与謝野鋼管, 37 anonymous edits

**Fluorescence cross-correlation spectroscopy** *Source*: http://en.wikipedia.org/w/index.php?oldid=355567003 *Contributors*: Bci2, Clicketyclack, Maartend8, Steve Quinn, 4 anonymous edits

**Circular dichroism** *Source*: http://en.wikipedia.org/w/index.php?oldid=397183432 *Contributors*: AJim, Andrew Rodland, Atlant, Bci2, Bensaccount, Biophysik, Bjsamelsonjones, Bryan Derksen, ChemGardener, Christopherlin, Crystal whacker, Dave3457, DeadEyeArrow, Dirac66, DrEricYH, Dwmyers, Element16, Evercat, Fru1tbat, Grgjou, Herr blaschke, ILike2BeAnonymous, Icairns, Jammedshut, Jeodesic, Jfitzger, Johann Wolfgang, Kapgains, Karol Langner, Kinlee, Kjaergaard, Kkmurray, Loohcsnuf, LostLucidity, Maartend8, Mark Oakley, Materialscientist, Mboverload, Michael Hardy, Miguel Andrade, Mikaduki, Mikegretes, Mklewpatinond, Nakane, Nikai, Noosentaal, Obradovic Goran, PaddyM, Paolo.dL, PierreAbbat, RASnyder, Steve Quinn, Synchronism, The wub, Thorwald, Tldcollins, V8rik, WillowW, Zen Mind, 87 anonymous edits

**Vibrational spectroscopy** *Source*: http://en.wikipedia.org/w/index.php?oldid=100013831 *Contributors*: Akriasas, Arnero, Baccyak4H, Bendzh, Berland, Cybercobra, Effeietsanders, Forever Amber, Giftlite, Gobonobo, Grimlock, Hankwang, HappyCamper, Itub, Ivan Štambuk, Kbrose, Keilana, Kent.carey, Kkmurray, Larryloz, Martyjmch, Nenyedi, P.wormer, Petergans, Pol098, Punctilius, Rdmsgl, Riana, SGGH, Shalom Yechiel, Silvem, Steinpilz, Steve Quinn, Tercer, The Anome, Veinor, 43 anonymous edits

**Vibrational circular dichroism** *Source*: http://en.wikipedia.org/w/index.php?oldid=394484119 *Contributors*: Aktsu, Auntof6, Bci2, Buurma, Dave3457, Jmbj, Jndurand, LilHelpa, Nick Number, Petulda, R'n'B, Slaweks, Wnt, Zeitlupe, 3 anonymous edits

**Raman spectroscopy** *Source*: http://en.wikipedia.org/w/index.php?oldid=397480953 *Contributors*: 1richard7, AJim, ARBradley4015, Afrine, Akv, Andrewavalon, Annabel, ArepoEn, Asfarer, Birdbrainscan, Blind cyclist, Brat32, Bullraker, Cdegallo, Charles Matthews, Christopherlin, Cyblor, D.Wardle, D3 TECHNOLOGIES, David Eppstein, Dazzaling69, Dch312, Dfbaum, Drphilharmonic, Editore99, Enquire, Fang Aili, Ferini, GT, Gabi bart, Gaius Cornelius, Galoubet, Gene Nygaard, Gene s, Gentgeen, Gerkleplex, GermanX, Giftlite, Gioto, Gumby600, Gunnar Larsson, Hankwang, Jaeger5432, Jaganath, Jameslh, Janke, Jll, Jmameren, Jofox, John of Reading, Jonnyapple, Judenicholson, Keramamide, Kkmurray, Koavf, Kraftlos, Kwamikagami, Latch.r, LilHelpa, LordDamorcro, Loreshadow, LostLucidity, Lotje, Low-frequency internal, MARKELLOS, MICKYGAL007, Magicalsaumy, Mahendra Kulkarni, Manulinho72, MarcoTolo, Martin Hedegaard, Measly Swan, Merope, Michbich, Mill haru, Minored, Mippi283, Moxfyre, Mythealias, NathanHagen, Nihonjoe, Nikai, Nmnogueira, Paszczakowna, Paul August, Paul venter, Pavlina2.0, Pcarbonn, Pericles899, Petergans, Piano non troppo, Pixeltoo, Pro crast in a tor, Quantumobserver, RTC, Ravi khanna, Redleaf, Rich Farmbrough, Rob Hooft, Ronningt, Rossheth, Rulie123, Shashang, Shreevatsa, Smalljim, Srosie68, TDogg310, Tantalate, Teabelle, Tha Stunna, The number c, The wub, Thue, Tillwe, Tmb4bd, Tomatoman, Tomgally, Tzontonel, Uther Dhoul, Whisperingdrop, Will4235, Wilson003, Yasuakinaito, Zylorian, 180 anonymous edits

**Microscope image processing** *Source*: http://en.wikipedia.org/w/index.php?oldid=397319574 *Contributors*: 1ForTheMoney, Altenmann, Anniebiogirl, Bryan Derksen, Cmdrjameson, DavidWBrooks, GRAHAMUK, Hosse, JTN, Jackol, Karnesky, LeaveSleaves, Mahogny, Mdd, Orderud, Pvosta, Rubik-wuerfel, Schmiteye, Seabhcan, Skarebo, Snow Shoes, Tdi1, The Anome, Tristanb, Watts52, Way4thesub, 33 anonymous edits

**Electron microscopy** *Source*: http://en.wikipedia.org/w/index.php?oldid=15996062 *Contributors*: 007 n1, 5Q5, A. Carty, A3RO, ABF, Aaronsharpe, Acdx, Acroterion, Activist, Adam Mihalyi, Adambiswanger1, Adijr, AdjustShift, Aillema, Aitias, Alan012, Alansohn, Albany NY, Alex Klotz, Amaltheus, Andre Engels, Andrei Stroe, Antonio Lopez, Apparition11, ArchonMagnus, Aurelius173, Average Earthman, Backslash Forwardslash, Banus, Bci2, Bencherlite, Bender235, Bensaccount, Blanchardb, Blechnic, Bobo192, Bongwarrior, Borgx, Brianga, Bydand, C0nanPayne, Calabraxthis, Camembert, Can't sleep, clown will eat me, CanisRufus, Capricorn42, Captain-tucker, Cbj77, Cetcher1159, Ceyockey, Cgarber, Chai, Chem-awb, Chris G, Chrislk02, Christian75, Chuunen Baka, Chych, Closenplay, Conversion script, Corpx, Csown, D, DSRH, DVD R W, Daniel, DarkFalls, Darth Panda, Davewild, David R. Ingham, Davidbaca, Dcoetzee, Deglr6328, DeltaMicroscopyStudent, DerHexer, Dexarouskies, Dexter prog, Dgrant, Diaa abdelmoneim, Dicklyon, Dlohcierekim, Docu, Dogposter, DoubleBlue, Doyley, DrFO.Jr.Tn, DrMikeF, Drago27218, Drpickem, Dvratnam, Edal, Editor2020, El aprendelenguas, Elearning2000, Enchanter, Epbr123, Ephram Shizgal, Esem0, Evan1991, EyeSerene, FF2010, Fabricationary, Fallboy, Felipeavb, Ferengi, Fieldday-sunday, Fireice, Frank, Frank A, Frankatca, Frankenpuppy, Fueled, Funnybunny, Gaius Cornelius, Gary King, Gene Nygaard, George Burgess, Gh5046, Giftlite, Gogo Dodo, Golfguy220-, GrahamColm, GregorB, Grey Shadow, Ground, Hat'nCoat, Hedgemonkey, Heron, Hitmanjon, Hornlitz, Horselover Frost, Hu, Hugo-cs, Hurricane Angel, Hydrogen Iodide, II MusLiM HyBRiD II, ILike2BeAnonymous, INkubusse, Ian Pitchford, IanOsgood, Igoldste, Imaninjapirate, Irfanhasmit, Isaac yagmoor, Itai, J.delanoy, JNighthawk, JRodeng, JTN, JaGa, Jaccardi, Jacopo Werther, JamesBWatson, Jared lap, Jeff G., Jeremiah, Jimp, Jjmatt33, Joelholdsworth, JohnOwens, JorgeGG, Joshua.morgan, Jungy111, Jusdafax, Karnesky, Karol Langner, Keilana, Kesac, Kils, Kingpin13, Kissavos, KnowledgeOfSelf, Konsu, Kpjas, KristianMolhave, Kukini, Kuru, Kusunose, KyraVixen, Kzollman, LeilaniLad, Leuko, Liferulez, LilHelpa, Lindmere, Lotje, Luna Santin, MER-C, Magnus Manske, Makingwiththeparticles, MarcoTolo, Marek69, Mark.murphy, Maro91eg, Materialscientist, Maurice Carbonaro, Mayapur, McSly, Mhazard9, Mhmolitor, Mikaey, Minimac, Mmxx, Monkeyknife, MoogleFan, MrOllie, Mschlindwein, Mwtoews, Myscrnnm, N5iln, Nate1481, Nath87, Ncemer, Netkinetic, Neurolysis, NewEnglandYankee, Nickfor1, Nihiltres, Nikai, Nmnogueira, Novalis, Oceano30, Oysteinp, Paulhaiti, Pdcook, Pengo, Perfecto, Pharaoh of the Wizards, Philip Trueman, Piano non troppo, Pip2andahalf, Plantsurfer, Plasticup, Pliable, PrestonH, Quadell, R.rommel, RUL3R, RainbowOfLight, Rajah, Rich Farmbrough, Richard Arthur Norton (1958- ), Riflemann, Risk one, Rjwilmsi, RobHarding, Rror, Rsrikanth05, Rurik3, Rustavo, S0uj1r0, STHayden, Sceptre, Sciurinæ, Sean William, Selket, Shirulashem, Sikkema, Silsor, Simon Shek, Simonmn, SkyLineRxx, Sludtke42, Snowmanradio, Snoyes, Sodium, Spbrandom, Spearhead, Speedyboy, Srdomingue, Srnec, Stahlkocher1, Staxringold, Steff, StephenBuxton, Steven Zhang, Stokerm, Sub-Angstrom, Subversive.sound, Svdmolen, Tacvek, Tahirulislam, Tapir Terrific, Terrace4, Tetraedycal, The Anome, Thedjatclubrock, Thermochap, Thingg, Tijadr, Til.Bartel, TimVickers, Tjmayerinsf, Tmopkisn, Travelbird, Twisted86, Tylersosmart, Tyrol5, Ulfbastel, Utcursch, Vossman, WahreJakob, Waldir, Wavelength, Willking1979, Wtmitchell, Zephyris, Zzuuzz, Кодекс, გიგა, 781 anonymous edits

**Diagnostic electron microscopy** *Source*: http://en.wikipedia.org/w/index.php?oldid=343526257 *Contributors*: D6, Fabrictramp, Hedgemonkey, Itub, Jack1956, Katharineamy, 1 anonymous edits

**HiRISE** *Source*: http://en.wikipedia.org/w/index.php?oldid=397707101 *Contributors*: Adoniscik, BatteryIncluded, Bazzy J, BerserkerBen, Bricktop, Bryan Derksen, Cassioli, Chris the speller, ChrisCork, CommonsDelinker, DJBarney24, Emesee, Fotaun, Geoffrey.landis, HiDrNick, It's-is-not-a-genitive, Japkebab, Jawed, Jimmarsmars, Johnpacklambert, Jtmichcock, Kitch, Kukini, LilHelpa, MECU, Mild Bill Hiccup, Mjamja, Mlm42, Nahum Reduta, Planetary, RSStockdale, Ravedave, Rjwilmsi, Sardanaphalus, Sdsds, Stassats, Tinwelint, Tuvas, VT hawkeye, White Cat, Wikielwikingo, Will.i.am, Willhsmit, 33 anonymous edits

**Scanning confocal electron microscopy** *Source*: http://en.wikipedia.org/w/index.php?oldid=373937945 *Contributors*: Hmmst, M-le-mot-dit, Materialscientist, THEN WHO WAS PHONE?, 1 anonymous edits

**Acronyms in microscopy** *Source*: http://en.wikipedia.org/w/index.php?oldid=240161472 *Contributors*: Amaltheus, Arbasli, Askewmind, Bvcrist, C.jeynes, Cardamon, CharlesC, ChrisHodgesUK, Coloradoauthor, Danski14, Dreampursuer, EdC2, Ein hesse, Excaliburhorn, Excirial, Fredericks, Freecat, Garion96, Gimme danger, Gurch, HYPN2457, Hubble618, IanOsgood, IceKarma, JackSeoul, Jcwf, Jlacount, Kanzure, Karnesky, Karthikc123, Khatru2, Kkmurray, Korg, Materialscientist, Michael Hardy, Mjmerriknight, Murray.booth, Neparis, Ohthelameness, Open2universe, Pegship, Pharmacomancer, Pythagoruz, Rixs2010, Runningamok19, Topbanana, Twisp, Woogee, XPh6, Yanwen, Yaotsan, 102 anonymous edits

**Nanoscience** *Source*: http://en.wikipedia.org/w/index.php?oldid=321435914 *Contributors*: 04spicerc, 1234eatmoore, 144.132.75.xxx, 1836311903, 200.191.188.xxx, 2D, 2over0, 450hondarider, 84user, 9.172, A Real Live One, A. B., A.Ou, ADM, Abune, Academic Challenger, AcademyAD, Actinman, AdamRetchless, AdamWeeden, Adashiel, Addihockey10, Addshore, Adecoco, AdjustShift, Admiral Roo, AdnanSa, Aerothorn, Ahoerstemeier, Aim Here, AirBa, Airplaneman, Ajdecon, AkSahota312, Akaala, Akendall, Alansohn, AlexTheScot, Alexius08, Alexnye, Ali, AllanHainey, Allmightyduck, Almonit, Alsandro, Altenmann, Amaurea, Anaraug, Andonic, Andreareinhardt, AndreiDukhin, Andrewpmk, Andrewrp, AngelOfSadness, Anirudh51, Anna Lincoln, AnnaFrance, Anonymous editor, Anoxonian, Ant12344321, Ant123456789, Antandrus, Antipoff, Antonrojo, Antony-22, Antorourke, Apalaria, Apoorvbadami, Arabani, Arcendet, ArglebargleIV, Ariasne, Arifhussaintm, Arion 3x3, Arnoutf, Arpingstone, Art LaPella, Arthur Rubin, Asbian513, Asmeurer, Aude, Avenged Eightfold, Average Earthman, Ayaazzz, Azlib77, B33R, Badgernet, Balsone1990, BananaFiend, Barbara Shack, Barticus88, Bathosrex, Baz.77.243.99.32, Bbatsell, Beatnik8983, Bedrokdamian, Beepu, Beetstra, Belovedfreak, Ben Wraith, Benstown, Bibliomaniac15, Big Bird, Bikenyakr, BlastOButter42, Blechnic, Blobglob, Blue520, Blueelectricstorm, Bmeguru, Bob, Bob rulz, Bob123456788, Bobblewik, Bobo The Ninja, Bobo192, Bobzchemist, Bogdanb, Bongwarrior, Bookandcoffee, Bornhj, Bornslippy, BradBeattie, Briaboru, Brianga, Bryan Derksen, Bschott, Burgundavia, Bushsf, Butros, Bücherwürmlein, CNicol, CY3AHHA, Cacycle, Caddcreativity, Caiaffa, Cal 1234, Calair, Caltas, Calvin 1998, Camw, Can't sleep, clown will eat me, CanadianLinuxUser, Candy-Panda, Canthusus, Cantus, Capitalistroadster, Capricorn42, Captain-tucker, CardinalDan, Carlos-alberto-teixeira, Carlosguitar, CarolineFThornPhD, Catgut, Caulde, CecilPL, Cedars, Ceyockey, Ch'an, Chamal N, CharlesC, Charliebigpotatoes, CharlotteWebb, Chcknwnm, Cheaptubes, ChemGardener, Chicken Wing, Chill doubt, Chimpman, Chinofireball, Chodges, Chooyimooyi, ChrassLovesEmma, Chris Roy, ChrisViper, ChrisfromHouston, Chrislk02, Christopher Connor, Christopher Parham, Chubbychunk, Chun-hian, Chymicus, Chzz, Clicketyclack, Closedmouth, Cmarz, Cole141299, Cometstyles, Con0002, Connormah, Conversion script, Corvidaecorvus, CotyXD, Coumarin, Cp111, Cpichardo, Cpl Syx, Cpuwhiz11, CranfieldSAS, Cruitbuck, Cryonic07, Csjoiner, Css, CtotheC, Cubic Hour, Cugerbrant, Cww, Cyberevil, Cyberman, DASonnenfeld, DLH, DV8 2XL, DVD R W, Da monster under your bed, Dado, Dag556, Damicatz, Dan100, Dancter, Daniel C, Daniel Shanefield, Dark Gaia, DarkFalls, Daveydweeb, David Levy, David.Monniaux, David44357, Davidfstr, Davidrforrest, Dbfirs, Dbsherman, DeadEyeArrow, Deb, Deeb, Deligeyik, Delldot, Dennis Valeev, DennisRobinson, Deor, DerHexer, Deselliers, Desiromeo107, Desplesda, Despotuli, Dethme0w, Devonmbr, Dexterousg, Dhappe, Dhp1080, Dibbity Dan, Dicklyon, Dina, Discospinster, Djr32, Dkrogers, Dll99, Dmberube, Dmerrill, DouglasGreen, Dr SHOEB82, Dr-b-m, DrMikeF, Drat, Dreaded Walrus, DriveMySol, Dskluz, Dynaflow, Dysepsion, E Wing, EBY3221, ERK, ESkog, EVGroup, Eclecticology, Ecleveland, EdBever, Edcolins, Edison, Edkarpov, Eecon, Eequor, Efbfweborg, Efiiamagus, Ehn, Eivind, El C, Elamere, Electricitylikesme, Eliz81, Elmmapleoakpine, Elwhy, Emiles93, Environ1561, Epastore, Epbr123, Eric Holloway, Erpreeti, Ertugrul.Bülbül, Escape Orbit, Esmash, Ettrig, Etxrge, Eve Hall, Everyking, Evlekis, Excirial, Exeunt, Fabrictramp, Fadierulez999, Falcorian, Fartherred, Fauncet, FayssalF, Femto, Feydey, Figarow, Filmz, Finlay McWalter, Firebladed, Fireplace, Firesnake1995, Flatline, Flewis, Floodamanny, FlyingToaster, Fock, Fox, Frank 76, Frankie1969, Frecklefoot, FreeKresge, FreplySpang, Fuhghettaboutit, FullMetal Falcon, Fvw, Fæ, G.A.S, GChriss, GDonato, GJeffery, GVnayR, Gaff, Gail, Gakrivas, Garion96, Gatorguy13, Gchriss, Gcm, Gdo01, Geoffreyhunt, Georgewilliamherbert, GermanX, Gheinen, Ghewgill, Giftlite, Gilliam, Gioto, Gjd001, Glane23, Gleeson 44, Glen, Glenn, Glloq, Globalhealth, Gogo Dodo, Graham87, Granla, Greennature2, Gulhar, Gurch, Guyzero, Gwernol, H0D G, H0riz0n, HPSLPP, Hadal, Hanacy, HandyAndy, HappyCamper, Happysailor, Harry2big4u, Headbomb, Henry Flower, Hephaestos, Herbythyme, Heron, HexaChord, Hoborobo234, Hojmatt, Honeyzjj, Howard547, Howcheng, Howdoesthiswo, Hreinn, Hu12, Hubert Wan, Hulagutten, Human.v2.0, Hupselipup, Husond, II MusLiM HyBRiD II, IRP, IVila, Iain99, Iam, Ian13, IanOsgood, Iandotcom, Icairns, Icarus, Ice Cold Beer, Iceni6, Ida Shaw, IddoGenuth, Ilikepie121, Illustria, Im a hustla, Imaninjapirate, ImperfectlyInformed, Imroy, Infinium, InsertNameHere, Intelligentsium, Inwind, Ira Ko, Irishguy, Islander, IstvanWolf, Itschris, Itsmine, Iwilker, Ixfd64, J.delanoy, JCOwens, JForget, JHMM13, Jaccardi, Jackol, Jaganath, Jamesmorrison, Jamesontai, Jamesooders, JanGlaenzer, Janastasopoulo, Jasbirsingheng, Jauhienij, Jaxonowens, Jbw2, Jeffnichols, Jeffrey Mall, Jeffwarnica, Jenita JJ, Jfdwolff, JimVC3, Jj137, Jmanigold, Joachim Schrod, Joan-of-arc, JoanneB, Joao.caprivi, Joeschmoe360, John.parkes007, Johnnyb82, Johntex, Jon seah, Jose77, Joseph Solis in Australia, Jpeob, Jrockley, Jrsheehan, Jrugordon, Judicatus, Junglecat, Jusdafax, KKul, Kaerondaes, Kami, Kamil101, Kamleshshah21, Karenjc, Karnesky, Katula, Kbdank71, Kcordina, Keenan Pepper, Keith D, Kenneth M Burke, Kenyon, Khaydarian, Killdevil, Kim Bruning, Kingpin13, Kiran b e, Kirsted, Kishan88, Kkmurray, Kku, Kmg90, Knotnic, KnowledgeOfSelf, Kokopellimama, KoshVorlon, Kosigrim, Koyo123, KrakatoaKatie, KramarDanIkabu, Krawi, KristianMolhave, Ktsquare, Kubigula, Kukini, Kuru, Kuunavang, L Hamm, LC, Lady BlahDeBlah, Laogooli, Larry laptop, Latka, Laurascudder, Law, LeaveSleaves, Legeres, Les boys, Leuko, Lfatehi, Lifeboatpres, Lights, Lightspeedchick, Ligulem, Likemike232, Lilgoni, Lizz379, Logger9, Looscan, Loupeter, Lowellian, Lstanley, Lucid, Luckyleafus, Luna Santin, Lunalona, Luvleme, M stone, MER-C, MITBeaverRocks, MMc, Mac, Mac Davis, MacGyverMagic, MacMed, Macewindu, Maercli, Maha ts, Malerin, Malzees, Mandarax, Maniraptor, Manmantong2000, Manufacturing, Maqayum, Marashie, MarsRover, Masschaos123, Master of Puppets, Matau, Materialscientist, Mateuszica, Math Champion, Mathiasoutraegus, Mattcuk, Matticus78, Mattjharrison, Mauron, Mav, Maximus Rex, Mayooresan, Mboverload, McGeddon, McVities, Mdebets, Meco, Meelosh, Melsaran, Memset, Menchi, Mentifisto, Metmathos, Mfsxkseb, Miami33139, Michael Devore, Michael Hardy, Michael93555, Michaelas10, Michelle Roberts, Michellecrisp, Micke-sv, Mikastu, Mike Rosoft, Mike Treder, Mikeb87, Milesrulez, Mills89, Mimzy1990, Mindmatrix, Minipieper, Minna Sora no Shita, Miranda, Mirondella, Missing Ace, MisterSheik, Misza13, Mmm, Moink, MoonGod, Morgan-92, Mormegil, Morven, Motor, Mr Bound, Mr strain, Mr. Random, MrArt, MrOllie, Mrannanj, Mrmattyboy, Mschel, Mugless, Mwanner, Mww113, Mxb design, Mxn, Mysterymadman, NAHID, NHL09addict, NJGW, Nabeth, Naddy, Nakon, NanoIQP, NanoTechReader, NanoWorld, Nanobug, Nanodic, Nanoink1, Nanojames, Nanoorg, Nanoshel, Nanotechthefuture, Naught101, Nauticashades, Naveenlingam, NawlinWiki, Nayvik, Ndenison, Neko-chan, Neverquick, NewEnglandYankee, Newtownrocks, Nick Boulevard, Nickvalcke, Night Stalker, Nips, Nmedard, Nmnogueira, NoIdeaNick, Noah Salzman, Noclevername, Noosphere, Nopetro, Notheruser, November05, Nsaa, Nuno Tavares, Nwerk, Obedium, Oda Mari, Ohnoitsjamie, Oklahombre, Oldoneeye, Oleg Alexandrov, OllieFury, Omicronpersei8, Opelio, Optimale, Ouji-fin, OwenX, Oxymoron83, P4k, P99am, Palapa, Palpatine, Paranoid, ParisianBlade, Passw0rd, Pat010, Patchiemoo, Paul August, Paulk4, Pavan maddali, Pb30, Pechotat, Pedant17, Pedantic of Purley, Pegasus1138, Penubag, Peripitus, Perl, Persian Poet Gal, Peruvianllama, Peter.C, Petri Krohn, Pgan002, Phantomsteve, Philip Trueman, Phillipedison1891, Phound14, Physicist, Piano non troppo, Picaroon, Pip2andahalf, Piperh, Pizza1512, Plastic, Plastikspork, Pmccray, Pmccray1, Porno, PranksterTurtle, Prettyperky, Primetime, Prolog, Prozhen, Quantpole, Quarl, Quintote, R'n'B, RDF, RG2, RHaworth, RMFan1, RadicalBender, Radon210, Raeky, Rajamouli2000, Rama's Arrow, RaseaC, Raterman, Raul654, Raven4x4x, Rbarreira, Reaver789, RedHillian, Reimarspohr, Remember, Remi0o, Rettetast, RexNL, ReyBrujo, Rholton, Rice888, Rich Farmbrough, Richard001, RichardF, Rifleman 82, Rknasc, Rlee1185, Rob-nick, Robert Merkel, RobertBradbury, Rocky rawstern, Rodolfou, Rogena, Rollerblade, Rollinsk, RonUSMC, Ronaldo wanna b, Ronhjones, Ronz, RosaWeber, Rostislav Lapshin, Rothfuss, Roux-HG, RoyBoy, Royboycrashfan, Rrburke, RxS, RyanCross, Ryanmcdaniel, Ryt, Ryulong, Ryza0708, SFClancy, SFKatUMO, SJP, ST47, Sachinrocks, Saeed5252, Salih, Salsb, Sameerhansda, Sander123, Sandrider, Sarahmcd, Sarangdutt, Sarbruis, Saturday, Savidan, Scarian, Sceptre, Schneediener, SchubertCommunications, Scibaby, Scientific American, Scilit, Scorpionman, Scoutersig, Scullin, Sean122, Seb az86556, Seddon, Seidenstud, Selket, Shadowjams, Shanes, Shd, SheffGruff, Shinels12, Shinseki, Shirulashem, Shmay, Shoeofdeath, Siliconov, Simon rjh, SiobhanHansa, Sionus, Sir Paul, Sir Vicious, Sirveaux, Sjö, SkerHawx, Skier Dude, Skysmith, Slaphappie, Smevy, Smilecolorsan, Smokefoot, Smokizzy, Snarkosis, Snowolf, Snoyes, Socialjest404, Solipsist, Sonett72, Soonerman1, Soxwon, Sp3ct3r, SpaceFlight89, Speedoflightning, SpencerWilson, Spirallingspirit, SpuriousQ, Srividyakripakar, Srleffler, Staeiou, Stannered, Stardotboy, StephenBuxton, Stephenb, Stevage, SteveKSmith, Sthubertus, StimsonsGhetto1, SudhirP, Sumo42, Sumthin, Superstuntguy, SusanLesch, Sverdrup, Swaroopsr, Sweet2, Sweetpea2007, Scythos, Syke22, T-borg, TNTfan101, Tabletop, Tamarkot, Tapir Terrific, Tarkovsky, TeamZissou, Tec2tec, Techguru, Tellyaddict, Template namespace initialisation script, Tempodivalse, Tennesboy, Texture, That Guy, From That Show!, The 888th Avatar, The Evil Spartan, The Rambling Man, The Thing That Should Not Be, The Ungovernable Force, The wub, TheBilly, TheRanger, Thingg, Thunderstix, Thuresson, Tiddly Tom, Tide rolls, Tiggerjay, Tikar aurum, Tilla, TimVickers, Timspencer1, Tirkfl, Tisdalepardi, Tjmayerinsf, Tme42, Tohd8BohaithuGh1, Tom harrison, Tomshen, Tonym88, Torakuro, TotalSpaceshipGuy3, Tothebarricades.tk, Touchstone42, Traal, TreasuryTag, Treisijs, Triona, Triwbe, Troels Arvin, Trounce, Trovatore, Tubedogg, Tuffshagga, Twocentsplain, UberScienceNerd, Ukexpat, Unconscious, Unixer, Uri, Useight, Utcursch, Uvi, VI, Vanished User 0001, Vanished user 03, Vary, Vasiliy Faronov, Vegasciencetrust, Veinor, Vera Cruz, Verarapuajay, Vgy7ujm, Vimal samuthiravel, Vinodm, Violentbob, Vipuser, Viriditas, Viva dsk, VladimirKorablin, Vrenator, Vssun, Vuo, W bausman, WLU, WadeSimMiser, Walker-IFR, Wangi, WarthogDemon, Wavelength, Waxigloo, Wazza28, WearyTraveller, WhatisFeelings?, Whitesaint, Whkoh, Wiki Raja, Wiki man55, WikiED, Wikiborg, Wikipelli, Wikkrockiana, WillWare, Wizkid291, Wmaster, Woohookitty, WpZurp, Wælgæst wæfre, Xcaliburn, Xen0phile, Yamamoto Ichiro, Ybbor, Ycarcomed, YellowMonkey, Yintan, Yngvarr, Ynhockey, Youandme, Youssefsan, Yst, Yupik, Zealotii, Zenith87, Zigger, Zundark, Zybez, Zygomorph, 3157 anonymous edits

**Nanotechnology** *Source*: http://en.wikipedia.org/w/index.php?oldid=398315214 *Contributors*: 04spicerc, 1234eatmoore, 144.132.75.xxx, 1836311903, 200.191.188.xxx, 2D, 2over0, 450hondarider, 84user, 9.172, A Real Live One, A. B., A.Ou, ADM, Abune, Academic Challenger, AcademyAD, Actinman, AdamRetchless, AdamWeeden, Adashiel, Addihockey10, Addshore, Adecoco, AdjustShift, Admiral Roo, AdnanSa, Aerothorn, Ahoerstemeier, Aim Here, AirBa, Airplaneman, Ajdecon, AkSahota312, Akaala, Akendall, Alansohn, AlexTheScot, Alexius08, Alexnye, Ali, AllanHainey, Allmightyduck, Almonit, Alsandro, Altenmann, Amaurea, Anaraug, Andonic, Andreareinhardt, AndreiDukhin, Andrewpmk, Andrewrp, AngelOfSadness, Anirudh51, Anna Lincoln, AnnaFrance, Anonymous editor, Anoxonian, Ant12344321, Ant123456789, Antandrus, Antipoff, Antonrojo, Antony-22, Antorourke, Apalaria, Apoorvbadami, Arabani, Arcendet, ArglebargleIV, Ariasne, Arifhussaintm, Arion 3x3, Arnoutf, Arpingstone, Art LaPella, Arthur Rubin, Asbian513, Asmeurer, Aude, Avenged Eightfold, Average Earthman, Ayaazzz, Azlib77, B33R, Badgernet, Balsone1990, BananaFiend, Barbara Shack, Barticus88, Bathosrex, Baz.77.243.99.32, Bbatsell, Beatnik8983, Bedrokdamian, Beepu, Beetstra, Belovedfreak, Ben Wraith, Benstown, Bibliomaniac15, Big Bird, Bikenyakr, BlastOButter42, Blechnic, Blobglob, Blue520, Blueelectricstorm, Bmeguru, Bob, Bob rulz, Bob123456788, Bobblewik, Bobo The Ninja, Bobo192, Bobzchemist, Bogdanb, Bongwarrior, Bookandcoffee, Bornhj, Bornslippy, BradBeattie, Briaboru, Brianga, Bryan Derksen, Bschott, Burgundavia, Bushsf, Butros, Bücherwürmlein, CNicol, CY3AHHA, Cacycle, Caddcreativity, Caiaffa, Cal 1234, Calair, Caltas, Calvin 1998, Camw, Can't sleep, clown will eat me, CanadianLinuxUser, Candy-Panda, Canthusus, Cantus, Capitalistroadster, Capricorn42, Captain-tucker, CardinalDan, Carlos-alberto-teixeira, Carlosguitar, CarolineFThornPhD, Catgut, Caulde, CecilPL, Cedars, Ceyockey, Ch'an, Chamal N, CharlesC, Charliebigpotatoes, CharlotteWebb, Chcknwnm, Cheaptubes, ChemGardener, Chicken Wing, Chill doubt, Chimpman, Chinofireball, Chodges, Chooyimooyi, ChrassLovesEmma, Chris Roy,

**Surface science** *Source*: http://en.wikipedia.org/w/index.php?oldid=379714046 *Contributors*: Amaltheus, Amp, AndreiDukhin, Bcmille, Bduke, Brianjd, BryanG, Bvcrist, Cardamon, Carlofnetcong, Discospinster, Dllahr, DonSiano, Dr-b-m, Duccio, Eno-ja, Ethmatl, Gaius Cornelius, Gentgeen, GianniG46, Gsp8181, HappyCamper, Headbomb, Humanist, IvanLanin, Karol Langner, Knights who say ni, Lantonov, Lightmouse, LilHelpa, Marj Tiefert, Materialscientist, Michael Hardy, Nanotrix, Nimur, Occhanikov, OldakQuill, Pieter Kuiper, Pjvpjv, Proepro, QTCaptain, Quuxplusone, RMFan1, Runningamok19, Sbertazzo, Scott.spillman, Trigger hippie77, V8rik, Yannjp, 43 anonymous edits

**Electron tomography** *Source*: http://en.wikipedia.org/w/index.php?oldid=399684972 *Contributors*: Editsalot, Elzzup, Flyingidiot, Gaius Cornelius, GreatMizuti, Icelight, Materialscientist, RoyBoy, User A1, 26 anonymous edits

**Virtopsy** *Source*: http://en.wikipedia.org/w/index.php?oldid=399724432 *Contributors*: GregorB, Hellosandimas, Nyttend, Philippe Nicolai-Dashwood, Sandstein, Synetech, Tameamseo, TenPoundHammer, Tophtucker, 2 anonymous edits

**Xenon-enhanced CT scanning** *Source*: http://en.wikipedia.org/w/index.php?oldid=255655707 *Contributors*: Delldot

**X-ray microtomography** *Source*: http://en.wikipedia.org/w/index.php?oldid=397746082 *Contributors*: Amxitsa, Arcadian, Bakashi10, Bantman, Bmasscha, Bobblewik, C777, Colonies Chris, Egallois, Feydey, Hymiegladstone, Iweber2003, JaGa, JasWilliams, Kkmurray, La goutte de pluie, Loopunrolling, Louisa Tattersfield, Massestephanie, Master of Puppets, Materialscientist, Mbell, Meganckj, MeltBanana, Nikki311, Obaeyens, Open2universe, Paul venter, Psychomanu, Still, Twisp, Xraynano, 32 anonymous edits

**Positron emission tomography** *Source*: http://en.wikipedia.org/w/index.php?oldid=399817430 *Contributors*: A314268, Alansohn, Alex Spade, Alex.tan, Anastrophe, Andre Engels, Andrel, Andrew73, Andrewa, Anna Lincoln, Arcadian, Ask123, Astuishin, Atlant, AxelBoldt, Axl, Bdekker, Benjaminevans82, Bertrus, Bfg67, Bfong, Bhindibhagee, BlueEvo2, Blueduck99, Bobblewik, Bradhegg, CallipygianSchoolGirl, Caltas, Captainj, Cburnett, Ccohalan, Cflm001, CharlesC, Chetanr, Chirality, Chtito, ChumpusRex, Conversion script, Crampedson, Crud302, DMacks, Da Joe, Damato, David Martland, Db099221, Deglr6328, Delta G, Dharmalens, Discospinster, DocWatson42, Doradus, Dougher, Doulos Christos, Download, Dratman, Drgarden, Dricherby, Duedilly, Electron9, Epbr123, Fivepints, Fizzy, Flapdragon, Fnielsen, Frederickhoyles, Gaius Cornelius, Galoubet, Garrettcarpenter10, Gaussgauss, Graham87, GyroMagician, Harsh Stone White, Headbomb, Hehkuviini, Hg6996, Hssp, Hu12, I K Brunel, Ilgiz, Improv, J.delanoy, JForget, JMumford, JamesMLane, Jascii, JdeJ, Jebus989, Jeremy Butler, Jiang, Jk91185, Jmarchn, Jsmit317, Junior Brian, Kaobear, Karada, Kazkaskazkasako, Khalid hassani, King Spadina, Kjkolb, Klar sagen, Kostmo, Kubanczyk, Kygkim, Lambiam, Larham, Lcolson, LostIntel, MAlvis, Magnus Manske, Makemi, Malcolm Farmer, Manzilla86, Mark PEA, Markssss, Mathewbrowne, Mco44, Michael Hardy, Mike Dill, MrBell, Mrdambro, Mrs.meganmmc, Munkel Davidson, Naffer, NawlinWiki, Neparis, Neutrality, NikNakk, Nmullani, Nunquam Dormio, OlEnglish, Oliphaunt, On the sixth day God created MANchester, PETUSER, Patrick, Permacultura, Pernambuco, Pgk, Phdplayahatadegree, Phil Boswell, Purple Paint, R.a.o.u.l.d.a.l., RTC, Ralph Saroyan, Raschal, Recognizance, Riwiener, Rjwilmsi, Rl, Rmhermen, RodC, Ropcat, Rsabbatini, Salsa Shark, Salvadorjo, Sayeth, Sbharris, Schneelocke, Sduncan53, SeanMack, Shirt58, Shlomke, SineWave, Sjayanthi, Slakhan, Slakr, Slon02, SnowflakeHolocaust, SoWhy, Spellmaster, Stevesg, Suffusion of Yellow, T.j.chryssikos, Tekhnofiend, TenOfAllTrades, Tevonic, The Anome, Thecheesykid, Themfromspace, Tide rolls, Tito4000, Tony46, TonySt, Toolator, Vasil', Vaughan, Voyagerfan5761, Was a bee, Wikid, Will Beback Auto, Wisdom89, Wolfgangamadeus, Yeti7, Yhseo, Zereshk, Δ, 298 anonymous edits

**Raman microscopy** *Source*: http://en.wikipedia.org/w/index.php?oldid=149168064 *Contributors*: 1richard7, AJim, ARBradley4015, Afrine, Akv, Andrewavalon, Annabel, ArepoEn, Asfarer, Birdbrainscan, Blind cyclist, Brat32, Bullraker, Cdegallo, Charles Matthews, Christopherlin, Cyblor, D.Wardle, D3 TECHNOLOGIES, David Eppstein, Dazzaling69, Dch312, Dfbaum, Drphilharmonic, Editore99, Enquire, Fang Aili, Ferini, GT, Gabi bart, Gaius Cornelius, Galoubet, Gene Nygaard, Gene s, Gentgeen, Gerkleplex, GermanX, Giftlite, Gioto, Gumby600, Gunnar Larsson, Hankwang, Jaeger5432, Jaganath, Jameslh, Janke, Jll, Jmameren, Jofox, John of Reading, Jonnyapple, Judenicholson, Keramamide, Kkmurray, Koavf, Kraftlos, Kwamikagami, Latch.r, LilHelpa, LordDamorcro, Loreshadow, LostLucidity, Lotje, Low-frequency internal, MARKELLOS, MICKYGAL007, Magicalsaumy, Mahendra Kulkarni, Manulinho72, MarcoTolo, Martin Hedegaard, Measly Swan, Merope, Michbich, Mill haru, Minored, Mippi283, Moxfyre, Mythealias, NathanHagen, Nihonjoe, Nikai, Nmnogueira, Paszczakowna, Paul August, Paul venter, Pavlina2.0, Pcarbonn, Pericles899, Petergans, Piano non troppo, Pixeltoo, Pro crast in a tor, Quantumobserver, RTC, Ravi khanna, Redleaf, Rich Farmbrough, Rob Hooft, Ronningt, Rossheth,

Rulie123, Shashang, Shreevatsa, Smalljim, Srosie68, TDogg310, Tantalate, Teabelle, Tha Stunna, The number c, The wub, Thue, Tillwe, Tmb4bd, Tomatoman, Tomgally, Tzontonel, Uther Dhoul, Whisperingdrop, Will4235, Wilson003, Yasuakinaito, Zylorian, 180 anonymous edits

**Neutron spin echo** *Source*: http://en.wikipedia.org/w/index.php?oldid=399373882 *Contributors*: Ben Paltrow, Bender235, Eugene-elgato, Kurt Schmidt, Localoptimum, M.monkenbusch, Paula Pilcher, R'n'B, Satarsa, Shimgray, Tibor Horvath, Tpikonen, 12 anonymous edits

# Image Sources, Licenses and Contributors

**File:Unknown Quartz crystal 66.JPG** *Source*: http://en.wikipedia.org/w/index.php?title=File:Unknown_Quartz_crystal_66.JPG *License*: GNU Free Documentation License *Contributors*: User:Digon3

**File:Insulincrystals.jpg** *Source*: http://en.wikipedia.org/w/index.php?title=File:Insulincrystals.jpg *License*: Public Domain *Contributors*: Chrumps, Jurema Oliveira, Photohound

**File:Halite(Salt)USGOV.jpg** *Source*: http://en.wikipedia.org/w/index.php?title=File:Halite(Salt)USGOV.jpg *License*: Public Domain *Contributors*: ARTE, Mschel, Pavlo Chemist, Quadro, Saperaud, Selphy, Str4nd, Urutseg, 11 anonymous edits

**File:Monocristal dsc03676.jpg** *Source*: http://en.wikipedia.org/w/index.php?title=File:Monocristal_dsc03676.jpg *License*: Creative Commons Attribution-Sharealike 2.0 *Contributors*: User:David.Monniaux

**File:Gallium1 640x480.jpg** *Source*: http://en.wikipedia.org/w/index.php?title=File:Gallium1_640x480.jpg *License*: unknown *Contributors*: -

**File:Ice crystals.jpg** *Source*: http://en.wikipedia.org/w/index.php?title=File:Ice_crystals.jpg *License*: GNU Free Documentation License *Contributors*: Mila Zinkova

**File:A fossil shell with calcite.jpg** *Source*: http://en.wikipedia.org/w/index.php?title=File:A_fossil_shell_with_calcite.jpg *License*: Creative Commons Attribution-Sharealike 3.0 *Contributors*: Mila

**Image:Square diffraction.jpg** *Source*: http://en.wikipedia.org/w/index.php?title=File:Square_diffraction.jpg *License*: unknown *Contributors*: V81, from the English Wikipedia

**File:Two-Slit Diffraction.png** *Source*: http://en.wikipedia.org/w/index.php?title=File:Two-Slit_Diffraction.png *License*: GNU Free Documentation License *Contributors*: Glenn, Peo, SharkD, Snaily

**Image:Diffraction pattern in spiderweb.JPG** *Source*: http://en.wikipedia.org/w/index.php?title=File:Diffraction_pattern_in_spiderweb.JPG *License*: Creative Commons Attribution-Sharealike 3.0 *Contributors*: Mila Zinkova

**Image:Solar glory at the steam from hot spring.jpg** *Source*: http://en.wikipedia.org/w/index.php?title=File:Solar_glory_at_the_steam_from_hot_spring.jpg *License*: Creative Commons Attribution-Sharealike 3.0 *Contributors*: Mila Zinkova

**Image:Young Diffraction.png** *Source*: http://en.wikipedia.org/w/index.php?title=File:Young_Diffraction.png *License*: Public Domain *Contributors*: DrKiernan, Glenn, Quatar

**Image:Single-slit-diffraction-ripple-tank.jpg** *Source*: http://en.wikipedia.org/w/index.php?title=File:Single-slit-diffraction-ripple-tank.jpg *License*: BSD *Contributors*: Original uploader was A3XX at it.wikipedia

**Image:Wave Diffraction 4Lambda Slit.png** *Source*: http://en.wikipedia.org/w/index.php?title=File:Wave_Diffraction_4Lambda_Slit.png *License*: Public Domain *Contributors*: Original uploader was Dicklyon at en.wikipedia

**Image:diffraction1.png** *Source*: http://en.wikipedia.org/w/index.php?title=File:Diffraction1.png *License*: unknown *Contributors*: Denniss, Rosarinagazo, Tony Wills, 2 anonymous edits

**File:Diffraction2vs5.jpg** *Source*: http://en.wikipedia.org/w/index.php?title=File:Diffraction2vs5.jpg *License*: GNU Free Documentation License *Contributors*: Original uploader was Bcrowell at en.wikipedia

**File:Diffraction-red laser-diffraction grating PNr°0126.jpg** *Source*: http://en.wikipedia.org/w/index.php?title=File:Diffraction-red_laser-diffraction_grating_PNr°0126.jpg *License*: unknown *Contributors*: D-Kuru, GianniG46

**File:Diffraction 150 slits.jpg** *Source*: http://en.wikipedia.org/w/index.php?title=File:Diffraction_150_slits.jpg *License*: Creative Commons Attribution 3.0 *Contributors*: User:Shim'on

**Image:Airy-pattern.svg** *Source*: http://en.wikipedia.org/w/index.php?title=File:Airy-pattern.svg *License*: Public Domain *Contributors*: User:Sakurambo

**Image:Airy2.gif** *Source*: http://en.wikipedia.org/w/index.php?title=File:Airy2.gif *License*: Creative Commons Attribution-Sharealike 3.0 *Contributors*: MuthuKutty, Prim Ethics

**Image:zboo lucky image 1pc.png** *Source*: http://en.wikipedia.org/w/index.php?title=File:Zboo_lucky_image_1pc.png *License*: Public Domain *Contributors*: Mike Peel, Rnt20, Werckmeister

**File:Diffraction on elliptic aperture with fft.png** *Source*: http://en.wikipedia.org/w/index.php?title=File:Diffraction_on_elliptic_aperture_with_fft.png *License*: GNU Free Documentation License *Contributors*: User:FDominec

**Image:X-ray diffraction pattern 3clpro.jpg** *Source*: http://en.wikipedia.org/w/index.php?title=File:X-ray_diffraction_pattern_3clpro.jpg *License*: Creative Commons Attribution-Sharealike 3.0 *Contributors*: User:Jeff Dahl

**File:Stohrem.jpg** *Source*: http://en.wikipedia.org/w/index.php?title=File:Stohrem.jpg *License*: GNU Free Documentation License *Contributors*: User:Materialscientist

**File:Fcc lattice 4.JPG** *Source*: http://en.wikipedia.org/w/index.php?title=File:Fcc_lattice_4.JPG *License*: GNU Free Documentation License *Contributors*: Cdang, David Eppstein, Thierry Dugnolle

**File:Silica.svg** *Source*: http://en.wikipedia.org/w/index.php?title=File:Silica.svg *License*: Public Domain *Contributors*: Silica.jpg:

**File:Electromagnetic-Spectrum.png** *Source*: http://en.wikipedia.org/w/index.php?title=File:Electromagnetic-Spectrum.png *License*: Creative Commons Attribution-Sharealike 2.5 *Contributors*: Belfer00, Materialscientist, Penubag

**File:Roentgen-x-ray-von-kollikers-hand.jpg** *Source*: http://en.wikipedia.org/w/index.php?title=File:Roentgen-x-ray-von-kollikers-hand.jpg *License*: Public Domain *Contributors*: Wilhelm Conrad Röntgen

**File:Laprascopy-Roentgen.jpg** *Source*: http://en.wikipedia.org/w/index.php?title=File:Laprascopy-Roentgen.jpg *License*: Public Domain *Contributors*: User:HenrikP

**File:Brain CT scan.jpg** *Source*: http://en.wikipedia.org/w/index.php?title=File:Brain_CT_scan.jpg *License*: Creative Commons Attribution-Sharealike 3.0 *Contributors*: Afiller, Explicit, Fastily, Materialscientist, 3 anonymous edits

**Image:preg xray.jpg** *Source*: http://en.wikipedia.org/w/index.php?title=File:Preg_xray.jpg *License*: Public Domain *Contributors*: anon

**File:X-ray diffraction pattern 3clpro.jpg** *Source*: http://en.wikipedia.org/w/index.php?title=File:X-ray_diffraction_pattern_3clpro.jpg *License*: Creative Commons Attribution-Sharealike 3.0 *Contributors*: User:Jeff Dahl

**File:X-RayOfNeedlefish-1.jpg** *Source*: http://en.wikipedia.org/w/index.php?title=File:X-RayOfNeedlefish-1.jpg *License*: Creative Commons Attribution 3.0 *Contributors*: Dazeley

**File:WaterCooledXrayTube.svg** *Source*: http://en.wikipedia.org/w/index.php?title=File:WaterCooledXrayTube.svg *License*: Public Domain *Contributors*: User:Coolth, User:Hmilch

**File:Historical X-ray nci-vol-1893-300.jpg** *Source*: http://en.wikipedia.org/w/index.php?title=File:Historical_X-ray_nci-vol-1893-300.jpg *License*: Public Domain *Contributors*: Unknown photographer/artist

**File:Moon in x-rays.gif** *Source*: http://en.wikipedia.org/w/index.php?title=File:Moon_in_x-rays.gif *License*: unknown *Contributors*: Bkell, Deglr6328, Melesse, Skier Dude, Stan Shebs, 2 anonymous edits

**File:Schattenkreuzröhre-in use-lateral view-standing cross.jpg** *Source*: http://en.wikipedia.org/w/index.php?title=File:Schattenkreuzröhre-in_use-lateral_view-standing_cross.jpg *License*: unknown *Contributors*: D-Kuru, GianniG46, RJHall

**File:Cyclotron motion wider view.jpg** *Source*: http://en.wikipedia.org/w/index.php?title=File:Cyclotron_motion_wider_view.jpg *License*: GNU Free Documentation License *Contributors*: User:Sfu

**File:Bohr atom model English.svg** *Source*: http://en.wikipedia.org/w/index.php?title=File:Bohr_atom_model_English.svg *License*: Creative Commons Attribution-Sharealike 2.5 *Contributors*: User:Brighterorange

**File:Orbital s1.png** *Source*: http://en.wikipedia.org/w/index.php?title=File:Orbital_s1.png *License*: Creative Commons Attribution-Sharealike 3.0 *Contributors*: User:RJHall

**File:Standard Model of Elementary Particles.svg** *Source*: http://en.wikipedia.org/w/index.php?title=File:Standard_Model_of_Elementary_Particles.svg *License*: Creative Commons Attribution 3.0 *Contributors*: User:MissMJ

**File:Asymmetricwave2.png** *Source*: http://en.wikipedia.org/w/index.php?title=File:Asymmetricwave2.png *License*: Creative Commons Attribution 3.0 *Contributors*: User:TimothyRias

**File:Virtual pairs near electron.png** *Source*: http://en.wikipedia.org/w/index.php?title=File:Virtual_pairs_near_electron.png *License*: GNU Free Documentation License *Contributors*: User:RJHall

**File:Lorentz force.svg** *Source*: http://en.wikipedia.org/w/index.php?title=File:Lorentz_force.svg *License*: GNU Free Documentation License *Contributors*: User:Jaro.p

**File:Bremsstrahlung.svg** *Source*: http://en.wikipedia.org/w/index.php?title=File:Bremsstrahlung.svg *License*: Public Domain *Contributors*: Journey234, Pieter Kuiper, RJHall

**File:Hydrogen Density Plots.png** *Source*: http://en.wikipedia.org/w/index.php?title=File:Hydrogen_Density_Plots.png *License*: unknown *Contributors*: PoorLeno (talk)

**File:Lightning over Oradea Romania cropped.jpg** *Source*: http://en.wikipedia.org/w/index.php?title=File:Lightning_over_Oradea_Romania_cropped.jpg *License*: Public Domain *Contributors*: User:Lucas

**File:Lorentz factor.svg** *Source*: http://en.wikipedia.org/w/index.php?title=File:Lorentz_factor.svg *License*: Public Domain *Contributors*: User:Trassiorf, User:egg

**File:Pairproduction.png** *Source*: http://en.wikipedia.org/w/index.php?title=File:Pairproduction.png *License*: GNU Free Documentation License *Contributors*: Original uploader was Davidhorman at en.wikipedia. Later version(s) were uploaded by Falcorian at en.wikipedia.

**File:AirShower.svg** *Source*: http://en.wikipedia.org/w/index.php?title=File:AirShower.svg *License*: Creative Commons Attribution 3.0 *Contributors*: User:Mpfiz

**File:Aurore australe - Aurora australis.jpg** *Source*: http://en.wikipedia.org/w/index.php?title=File:Aurore_australe_-_Aurora_australis.jpg *License*: unknown *Contributors*: Diti, Ehquionest

**File:GPN-2000-003012.png** *Source*: http://en.wikipedia.org/w/index.php?title=File:GPN-2000-003012.png *License*: Public Domain *Contributors*: NASA

**Image:Quark structure neutron.svg** *Source*: http://en.wikipedia.org/w/index.php?title=File:Quark_structure_neutron.svg *License*: Creative Commons Attribution-Sharealike 2.5 *Contributors*: User:Harp

**Image:Beta Negative Decay.svg** *Source*: http://en.wikipedia.org/w/index.php?title=File:Beta_Negative_Decay.svg *License*: Public Domain *Contributors*: User:Joelholdsworth

**File:Institut Laue–Langevin (ILL) in Grenoble, France.jpg** *Source*: http://en.wikipedia.org/w/index.php?title=File:Institut_Laue–Langevin_(ILL)_in_Grenoble,_France.jpg *License*: Creative Commons Attribution 3.0 *Contributors*: User:Tupungato

**Image:fusion rxnrate.svg** *Source*: http://en.wikipedia.org/w/index.php?title=File:Fusion_rxnrate.svg *License*: Creative Commons Attribution 2.5 *Contributors*: User:Dstrozzi

**Image:Sasahara.svg** *Source*: http://en.wikipedia.org/w/index.php?title=File:Sasahara.svg *License*: GNU Free Documentation License *Contributors*: Original uploader was JWB at en.wikipedia

**Image:Moons shodow in muons.gif** *Source*: http://en.wikipedia.org/w/index.php?title=File:Moons_shodow_in_muons.gif *License*: Trademarked *Contributors*: Deglr6328, Headbomb, Stifle, Vanderdecken, 1 anonymous edits

**Image:Muon Decay.png** *Source*: http://en.wikipedia.org/w/index.php?title=File:Muon_Decay.png *License*: Public Domain *Contributors*: User:Thymo

**Image:Simple-TEM-beam-path.jpg** *Source*: http://en.wikipedia.org/w/index.php?title=File:Simple-TEM-beam-path.jpg *License*: GNU Free Documentation License *Contributors*: Original uploader was Oysteinp at en.wikipedia

**Image:DifraccionElectronesMET.jpg** *Source*: http://en.wikipedia.org/w/index.php?title=File:DifraccionElectronesMET.jpg *License*: GNU Free Documentation License *Contributors*: Original uploader was Oysteinp at en.wikipedia

**Image:inelastic-neutron-scattering-basics.png** *Source*: http://en.wikipedia.org/w/index.php?title=File:Inelastic-neutron-scattering-basics.png *License*: Public Domain *Contributors*: Joachim Wuttke

**Image:DIS.svg** *Source*: http://en.wikipedia.org/w/index.php?title=File:DIS.svg *License*: Public Domain *Contributors*: User:E2m

**Image:Optical microscope nikon alphaphot +.jpg** *Source*: http://en.wikipedia.org/w/index.php?title=File:Optical_microscope_nikon_alphaphot_+.jpg *License*: GNU Free Documentation License *Contributors*: Moisey

**Image:Microscope And Digital Camera.JPG** *Source*: http://en.wikipedia.org/w/index.php?title=File:Microscope_And_Digital_Camera.JPG *License*: GNU Free Documentation License *Contributors*: User:Zephyris

**Image:Stelluti bees1630.jpg** *Source*: http://en.wikipedia.org/w/index.php?title=File:Stelluti_bees1630.jpg *License*: Public Domain *Contributors*: Francesco Stelluti

**Image:Optical microscope nikon alphaphot.jpg** *Source*: http://en.wikipedia.org/w/index.php?title=File:Optical_microscope_nikon_alphaphot.jpg *License*: Public Domain *Contributors*: GcG(jawp)

**File:Leica EpifluorescenceMicroscope ObjectiveLens.jpg** *Source*: http://en.wikipedia.org/w/index.php?title=File:Leica_EpifluorescenceMicroscope_ObjectiveLens.jpg *License*: GNU Free Documentation License *Contributors*: User:Zephyris

**Image:Microscope-optical path.svg** *Source*: http://en.wikipedia.org/w/index.php?title=File:Microscope-optical_path.svg *License*: GNU Free Documentation License *Contributors*: Adjustit, Dietzel65

**Image:Paper_Micrograph_Bright.png** *Source*: http://en.wikipedia.org/w/index.php?title=File:Paper_Micrograph_Bright.png *License*: Creative Commons Attribution-Sharealike 3.0 *Contributors*: User:Zephyris

**Image:Paper_Micrograph_Cross-Polarised.png** *Source*: http://en.wikipedia.org/w/index.php?title=File:Paper_Micrograph_Cross-Polarised.png *License*: Creative Commons Attribution-Sharealike 3.0 *Contributors*: User:Zephyris

**Image:Paper_Micrograph_Dark.png** *Source*: http://en.wikipedia.org/w/index.php?title=File:Paper_Micrograph_Dark.png *License*: Creative Commons Attribution-Sharealike 3.0 *Contributors*: User:Zephyris

**Image:Paper_Micrograph_Phase.png** *Source*: http://en.wikipedia.org/w/index.php?title=File:Paper_Micrograph_Phase.png *License*: Creative Commons Attribution-Sharealike 3.0 *Contributors*: User:Zephyris

**Image:2008Computex DnI Award AnMo Dino-Lite Digital Microscope.jpg** *Source*: http://en.wikipedia.org/w/index.php?title=File:2008Computex_DnI_Award_AnMo_Dino-Lite_Digital_Microscope.jpg *License*: unknown *Contributors*: User:BrockF5

**Image:Confocalprinciple.svg** *Source*: http://en.wikipedia.org/w/index.php?title=File:Confocalprinciple.svg *License*: GNU Free Documentation License *Contributors*: Danh

**File:Minsky Confocal Reflection Microscope.png** *Source*: http://en.wikipedia.org/w/index.php?title=File:Minsky_Confocal_Reflection_Microscope.png *License*: Public Domain *Contributors*: Marvin Minsky (inventor), Ameter & Levy (Attorneys)

**File:Tetrachimena_Beta_Tubulin.png** *Source*: http://en.wikipedia.org/w/index.php?title=File:Tetrachimena_Beta_Tubulin.png *License*: Creative Commons Attribution-Sharealike 3.0 *Contributors*: User:Pjasnos

**File:Confocal measurement of 1-euro-star 3d and euro.png** *Source*: http://en.wikipedia.org/w/index.php?title=File:Confocal_measurement_of_1-euro-star_3d_and_euro.png *License*: Creative Commons Attribution-Sharealike 3.0 *Contributors*: User:Ssolbergj, User:Xorx

**File:Confocal measurement of 1-euro-star 3d Reflection.png** *Source*: http://en.wikipedia.org/w/index.php?title=File:Confocal_measurement_of_1-euro-star_3d_Reflection.png *License*: Creative Commons Attribution-Sharealike 3.0 *Contributors*: User:Xorx

**File:Confocal measurement of 1-euro-star 3d profile 200.svg** *Source*: http://en.wikipedia.org/w/index.php?title=File:Confocal_measurement_of_1-euro-star_3d_profile_200.svg *License*: Creative Commons Attribution-Sharealike 3.0 *Contributors*: User:Xorx

**Image:Atomic force microscope by Zureks.jpg** *Source*: http://en.wikipedia.org/w/index.php?title=File:Atomic_force_microscope_by_Zureks.jpg *License*: Creative Commons Attribution-Sharealike 3.0 *Contributors*: User:Zureks

**Image:Atomic force microscope block diagram.svg** *Source*: http://en.wikipedia.org/w/index.php?title=File:Atomic_force_microscope_block_diagram.svg *License*: Public Domain *Contributors*: OverlordQ, Ssola, Twisp

**file:AFM (used) cantilever in Scanning Electron Microscope, magnification 1000x.JPG** *Source*: http://en.wikipedia.org/w/index.php?title=File:AFM_(used)_cantilever_in_Scanning_Electron_Microscope,_magnification_1000x.JPG *License*: Creative Commons Attribution-Sharealike 3.0 *Contributors*: User:Materialscientist, User:SecretDisc

**file:AFM (used) cantilever in Scanning Electron Microscope, magnification 3000x.JPG** *Source*: http://en.wikipedia.org/w/index.php?title=File:AFM_(used)_cantilever_in_Scanning_Electron_Microscope,_magnification_3000x.JPG *License*: Creative Commons Attribution-Sharealike 3.0 *Contributors*: User:Materialscientist, User:SecretDisc

**Image:AFM noncontactmode.jpg** *Source*: http://en.wikipedia.org/w/index.php?title=File:AFM_noncontactmode.jpg *License*: Creative Commons Attribution-Sharealike 3.0 *Contributors*: User:Creepin475

**Image:Single-Molecule-Under-Water-AFM-Tapping-Mode.jpg** *Source*: http://en.wikipedia.org/w/index.php?title=File:Single-Molecule-Under-Water-AFM-Tapping-Mode.jpg *License*: Attribution *Contributors*: User:Yurko

**Image:AFM beamdetection.jpg** *Source*: http://en.wikipedia.org/w/index.php?title=File:AFM_beamdetection.jpg *License*: Creative Commons Attribution-Sharealike 3.0 *Contributors*: User:Creepin475

**Image:Atomic Force Microscope Science Museum London.jpg** *Source*: http://en.wikipedia.org/w/index.php?title=File:Atomic_Force_Microscope_Science_Museum_London.jpg *License*: GNU Free Documentation License *Contributors*: John Dalton

**File:Electron Microscope.png** *Source*: http://en.wikipedia.org/w/index.php?title=File:Electron_Microscope.png *License*: Public Domain *Contributors*: GrahamColm

**File:Siemens-electron-microscope.jpg** *Source*: http://en.wikipedia.org/w/index.php?title=File:Siemens-electron-microscope.jpg *License*: Creative Commons Attribution-Sharealike 3.0 *Contributors*: User:Edal

**File:Ernst Ruska Electron Microscope - Deutsches Museum - Munich-edit.jpg** *Source*: http://en.wikipedia.org/w/index.php?title=File:Ernst_Ruska_Electron_Microscope_-_Deutsches_Museum_-_Munich-edit.jpg *License*: GNU Free Documentation License *Contributors*: J Brew, uploaded on the English-speaking Wikipedia by .

**File:Ant SEM.jpg** *Source*: http://en.wikipedia.org/w/index.php?title=File:Ant_SEM.jpg *License*: unknown *Contributors*: Fanghong, Howcheng, Kersti Nebelsiek, Mattes, NEON ja, Neil916, Olei, Romary, Steff, 1 anonymous edits

**File:Golden insect 01 Pengo.jpg** *Source*: http://en.wikipedia.org/w/index.php?title=File:Golden_insect_01_Pengo.jpg *License*: unknown *Contributors*: Pengo, Waldir

**File:Krillfilter2kils.jpg** *Source*: http://en.wikipedia.org/w/index.php?title=File:Krillfilter2kils.jpg *License*: GNU Free Documentation License *Contributors*: User:uwe kils

**Image:Schéma de principe du synchrotron.jpg** *Source*: http://en.wikipedia.org/w/index.php?title=File:Schéma_de_principe_du_synchrotron.jpg *License*: Attribution *Contributors*: EPSIM 3D/JF Santarelli, Synchrotron Soleil

**Image:Aust.-Synchrotron-Interior-Panorama,-14.06.2007.jpg** *Source*: http://en.wikipedia.org/w/index.php?title=File:Aust.-Synchrotron-Interior-Panorama,-14.06.2007.jpg *License*: GNU Free Documentation License *Contributors*: User:Jjron

**Image:SOLEIL le 01 juin 2005.jpg** *Source*: http://en.wikipedia.org/w/index.php?title=File:SOLEIL_le_01_juin_2005.jpg *License*: Attribution *Contributors*: David.Monniaux, Pieter Kuiper

**Image:Hohlraum irradiation on NOVA laser.jpg** *Source*: http://en.wikipedia.org/w/index.php?title=File:Hohlraum_irradiation_on_NOVA_laser.jpg *License*: Public Domain *Contributors*: Deglr6328, DynV, Gumby600, Monkeybait

**Image:Be foil square.jpg** *Source*: http://en.wikipedia.org/w/index.php?title=File:Be_foil_square.jpg *License*: GNU Free Documentation License *Contributors*: Original uploader was Deglr6328 at en.wikipedia

**Image:FEM.JPG** *Source*: http://en.wikipedia.org/w/index.php?title=File:FEM.JPG *License*: Creative Commons Attribution-Sharealike 3.0 *Contributors*: User:Creepin475

**File:Atomic resolution Au100.JPG** *Source*: http://en.wikipedia.org/w/index.php?title=File:Atomic_resolution_Au100.JPG *License*: Public Domain *Contributors*: Erwinrossen, Filnik, Liftarn, Mormegil, Nemissimo, Pieter Kuiper, WikipediaMaster, 7 anonymous edits

**File:Chiraltube.gif** *Source*: http://en.wikipedia.org/w/index.php?title=File:Chiraltube.gif *License*: Public Domain *Contributors*: Taner Yildirim (The National Institute of Standards and Technology - NIST)

**File:Stmsample.jpg** *Source*: http://en.wikipedia.org/w/index.php?title=File:Stmsample.jpg *License*: Creative Commons Attribution-Sharealike 2.5 *Contributors*: User:M0RHI

**File:ScanningTunnelingMicroscope schematic.png** *Source*: http://en.wikipedia.org/w/index.php?title=File:ScanningTunnelingMicroscope_schematic.png *License*: Creative Commons Attribution-Sharealike 2.0 *Contributors*: User:schmid

**File:Cens nanomanipulation3d Trixler.jpg** *Source*: http://en.wikipedia.org/w/index.php?title=File:Cens_nanomanipulation3d_Trixler.jpg *License*: Creative Commons Attribution 3.0 *Contributors*: Frank Trixler, LMU/CeNS: Organic Semiconductor Nanostructures

**Image:ISISLogo.png** *Source*: http://en.wikipedia.org/w/index.php?title=File:ISISLogo.png *License*: unknown *Contributors*: Islander

**Image:ISIS_exptal_hall.jpg** *Source*: http://en.wikipedia.org/w/index.php?title=File:ISIS_exptal_hall.jpg *License*: unknown *Contributors*: wurzeller

**Image:ISIS_neutron_hall.jpg** *Source*: http://en.wikipedia.org/w/index.php?title=File:ISIS_neutron_hall.jpg *License*: Creative Commons Attribution-Sharealike 3.0 *Contributors*: User:Sandig

**Image:Sudbury Neutrino Observatory.artist concept of detector.jpg** *Source*: http://en.wikipedia.org/w/index.php?title=File:Sudbury_Neutrino_Observatory.artist_concept_of_detector.jpg *License*: unknown *Contributors*: Bearcat, Duk, Joseph Dwayne, 1 anonymous edits

**File:Sudbury sno.jpg** *Source*: http://en.wikipedia.org/w/index.php?title=File:Sudbury_sno.jpg *License*: Public Domain *Contributors*: Original uploader was Srbauer at de.wikipedia

**Image:LHC.svg** *Source*: http://en.wikipedia.org/w/index.php?title=File:LHC.svg *License*: Creative Commons Attribution-Sharealike 2.5 *Contributors*: User:Harp

**Image:ATLAS-logo.jpg** *Source*: http://en.wikipedia.org/w/index.php?title=File:ATLAS-logo.jpg *License*: unknown *Contributors*: Andrius.v, Melesse

**Image:CERN Atlas Caverne.jpg** *Source*: http://en.wikipedia.org/w/index.php?title=File:CERN_Atlas_Caverne.jpg *License*: GNU Free Documentation License *Contributors*: Nikolai Schwerg

**Image:gg to ttH.jpg** *Source*: http://en.wikipedia.org/w/index.php?title=File:Gg_to_ttH.jpg *License*: Public Domain *Contributors*: Ephraim33, Harp, Helix84, Joelholdsworth, Perhelion, Pieter Kuiper, Setreset

**Image:ATLAS TRT.jpg** *Source*: http://en.wikipedia.org/w/index.php?title=File:ATLAS_TRT.jpg *License*: GNU Free Documentation License *Contributors*: Gorgo, Harp

**Image:ATLAS HCal.jpg** *Source*: http://en.wikipedia.org/w/index.php?title=File:ATLAS_HCal.jpg *License*: GNU Free Documentation License *Contributors*: Mdd, Pieter Kuiper, Skaller, 1 anonymous edits

**Image:CERN-Rama-33.jpg** *Source*: http://en.wikipedia.org/w/index.php?title=File:CERN-Rama-33.jpg *License*: Creative Commons Attribution-Sharealike 2.0 *Contributors*: User:Rama

**Image:ATLAS Above.jpg** *Source*: http://en.wikipedia.org/w/index.php?title=File:ATLAS_Above.jpg *License*: GNU Free Documentation License *Contributors*: Gorgo, Harp

**Image:Atlas detector CERN feb2007.jpg** *Source*: http://en.wikipedia.org/w/index.php?title=File:Atlas_detector_CERN_feb2007.jpg *License*: Public Domain *Contributors*: Sindre Skrede

**Image:Misc pollen.jpg** *Source*: http://en.wikipedia.org/w/index.php?title=File:Misc_pollen.jpg *License*: Public Domain *Contributors*: Dartmouth Electron Microscope Facility, Dartmouth College

**Image:Optical stereo microscope nikon smz10.jpg** *Source*: http://en.wikipedia.org/w/index.php?title=File:Optical_stereo_microscope_nikon_smz10.jpg *License*: Public Domain *Contributors*: GcG(jawp)

**Image:Hypertrophic Zone of Epiphyseal Plate.jpg** *Source*: http://en.wikipedia.org/w/index.php?title=File:Hypertrophic_Zone_of_Epiphyseal_Plate.jpg *License*: Public Domain *Contributors*: User:Robert M. Hunt

**File:Single_YFP_molecule_superresolution_microscopy.tif** *Source*: http://en.wikipedia.org/w/index.php?title=File:Single_YFP_molecule_superresolution_microscopy.tif *License*: unknown *Contributors*: -

**File:GFP Superresolution Christoph Cremer.JPG** *Source*: http://en.wikipedia.org/w/index.php?title=File:GFP_Superresolution_Christoph_Cremer.JPG *License*: GNU Free Documentation License *Contributors*: User:Andy Nestl

**File:3D-SIM-1 NPC Confocal vs 3D-SIM detail.jpg** *Source*: http://en.wikipedia.org/w/index.php?title=File:3D-SIM-1_NPC_Confocal_vs_3D-SIM_detail.jpg *License*: Creative Commons Attribution-Sharealike 3.0 *Contributors*: Changes in layout by the uploader. Only the creator of the original (Lothar Schermelleh) should be credited.

**File:3D-SIM-1_NPC_Confocal_vs_3D-SIM.jpg** *Source*: http://en.wikipedia.org/w/index.php?title=File:3D-SIM-1_NPC_Confocal_vs_3D-SIM.jpg *License*: Creative Commons Attribution-Sharealike 3.0 *Contributors*: Lothar Schermelleh

**File:3D-SIM-2_Nucleus prophase 3d_rotated.jpg** *Source*: http://en.wikipedia.org/w/index.php?title=File:3D-SIM-2_Nucleus_prophase_3d_rotated.jpg *License*: Creative Commons Attribution-Sharealike 3.0 *Contributors*: Lothar Schermelleh

**File:3D-SIM-3_Prophase 3 color.jpg** *Source*: http://en.wikipedia.org/w/index.php?title=File:3D-SIM-3_Prophase_3_color.jpg *License*: Creative Commons Attribution-Sharealike 3.0 *Contributors*: Lothar Schermelleh

**File:3D-SIM-4_Anaphase 3 color.jpg** *Source*: http://en.wikipedia.org/w/index.php?title=File:3D-SIM-4_Anaphase_3_color.jpg *License*: Creative Commons Attribution-Sharealike 3.0 *Contributors*: Lothar Schermelleh

**File:Phase-Phase Contrast.jpg** *Source*: http://en.wikipedia.org/w/index.php?title=File:Phase-Phase_Contrast.jpg *License*: Creative Commons Attribution-Sharealike 3.0 *Contributors*: User:Egelberg

**Image:Housebeemouth100x.jpg** *Source*: http://en.wikipedia.org/w/index.php?title=File:Housebeemouth100x.jpg *License*: GNU Free Documentation License *Contributors*: John Alan Elson

**Image:RiceStemcs400x1.jpg** *Source*: http://en.wikipedia.org/w/index.php?title=File:RiceStemcs400x1.jpg *License*: GNU Free Documentation License *Contributors*: John Alan Elson

**Image:Rabbitttestis100x2.jpg** *Source*: http://en.wikipedia.org/w/index.php?title=File:Rabbitttestis100x2.jpg *License*: GNU Free Documentation License *Contributors*: John Alan Elson

**Image:FernProthallium400x.jpg** *Source*: http://en.wikipedia.org/w/index.php?title=File:FernProthallium400x.jpg *License*: GNU Free Documentation License *Contributors*: John Alan Elson

**File:Zeolite-ZSM-5-3D-vdW.png** *Source*: http://en.wikipedia.org/w/index.php?title=File:Zeolite-ZSM-5-3D-vdW.png *License*: Public Domain *Contributors*: Benjah-bmm27, Ephemeronium

**File:Kepler conjecture 1.jpg** *Source*: http://en.wikipedia.org/w/index.php?title=File:Kepler_conjecture_1.jpg *License*: Public Domain *Contributors*: Ragesoss

**File:Snowflake8.png** *Source*: http://en.wikipedia.org/w/index.php?title=File:Snowflake8.png *License*: Public Domain *Contributors*: Nauticashades, Saperaud, WillowW

**File:3D model hydrogen bonds in water.jpg** *Source*: http://en.wikipedia.org/w/index.php?title=File:3D_model_hydrogen_bonds_in_water.jpg *License*: GNU Free Documentation License *Contributors*: User:snek01

**File:Bragg diffraction.png** *Source*: http://en.wikipedia.org/w/index.php?title=File:Bragg_diffraction.png *License*: GNU General Public License *Contributors*: user:hadmack

**File:Diamond and graphite2.jpg** *Source*: http://en.wikipedia.org/w/index.php?title=File:Diamond_and_graphite2.jpg *License*: GNU Free Documentation License *Contributors*: User:Itub, User:Materialscientist

**File:penicillin.png** *Source*: http://en.wikipedia.org/w/index.php?title=File:Penicillin.png *License*: Creative Commons Attribution 2.5 *Contributors*: User:Bassophile

**File:Myoglobin.png** *Source*: http://en.wikipedia.org/w/index.php?title=File:Myoglobin.png *License*: Public Domain *Contributors*: User:AzaToth

**File:X ray diffraction.png** *Source*: http://en.wikipedia.org/w/index.php?title=File:X_ray_diffraction.png *License*: Creative Commons Attribution-Sharealike 3.0 *Contributors*: Thomas Splettstoesser

**File:Protein crystal.jpg** *Source*: http://en.wikipedia.org/w/index.php?title=File:Protein_crystal.jpg *License*: Public Domain *Contributors*: Monkeybait, TimVickers

**File:CrystalDrops.svg** *Source*: http://en.wikipedia.org/w/index.php?title=File:CrystalDrops.svg *License*: Creative Commons Attribution-Sharealike 3.0 *Contributors*: User:Adenosine

**File:X Ray Diffractometer.JPG** *Source*: http://en.wikipedia.org/w/index.php?title=File:X_Ray_Diffractometer.JPG *License*: GNU Free Documentation License *Contributors*: Ff02::3, Pieter Kuiper

**File:eden.png** *Source*: http://en.wikipedia.org/w/index.php?title=File:Eden.png *License*: Creative Commons Attribution 2.5 *Contributors*: User:Bassophile

**File:Spectrum of blue flame.svg** *Source*: http://en.wikipedia.org/w/index.php?title=File:Spectrum_of_blue_flame.svg *License*: GNU Free Documentation License *Contributors*: user:Deglr6328 on english wikipedia. Recreated from orginal data

**File:Ftir-interferogram.png** *Source*: http://en.wikipedia.org/w/index.php?title=File:Ftir-interferogram.png *License*: GNU Free Documentation License *Contributors*: User:Butenbremer

**Image:Interferometer.svg** *Source*: http://en.wikipedia.org/w/index.php?title=File:Interferometer.svg *License*: GNU Free Documentation License *Contributors*: User:Stannered

**Image:HyperspectralCube.jpg** *Source*: http://en.wikipedia.org/w/index.php?title=File:HyperspectralCube.jpg *License*: Public Domain *Contributors*: Dr. Nicholas M. Short, Sr.

**Image:MultispectralComparedToHyperspectral.jpg** *Source*: http://en.wikipedia.org/w/index.php?title=File:MultispectralComparedToHyperspectral.jpg *License*: Public Domain *Contributors*: Dr. Nicholas M. Short, Sr.

**Image:Modern 3T MRI.JPG** *Source*: http://en.wikipedia.org/w/index.php?title=File:Modern_3T_MRI.JPG *License*: Creative Commons Attribution-Sharealike 2.5 *Contributors*: User:KasugaHuang

**Image:FIRST measurement of SF6 and NH3.jpg** *Source*: http://en.wikipedia.org/w/index.php?title=File:FIRST_measurement_of_SF6_and_NH3.jpg *License*: Creative Commons Attribution-Sharealike 3.0 *Contributors*: Andre Villemaire

**Image:Fluorescence microscop.jpg** *Source*: http://en.wikipedia.org/w/index.php?title=File:Fluorescence_microscop.jpg *License*: Creative Commons Attribution-Sharealike 2.5 *Contributors*: Dietzel65, Masur

**Image:Inverted microscope.jpg** *Source*: http://en.wikipedia.org/w/index.php?title=File:Inverted_microscope.jpg *License*: Creative Commons Attribution-Sharealike 2.5 *Contributors*: Nuno Nogueira (Nmnogueira at en.wikipedia

**Image:FluorescenceFilters 2008-09-28.svg** *Source*: http://en.wikipedia.org/w/index.php?title=File:FluorescenceFilters_2008-09-28.svg *License*: GNU Free Documentation License *Contributors*: User:Wimox

**Image:Dividing Cell Fluorescence.jpg** *Source*: http://en.wikipedia.org/w/index.php?title=File:Dividing_Cell_Fluorescence.jpg *License*: GNU Free Documentation License *Contributors*: transfert on commons by F Lamiot

**Image:FluorescentCells.jpg** *Source*: http://en.wikipedia.org/w/index.php?title=File:FluorescentCells.jpg *License*: Public Domain *Contributors*: Amada44, DO11.10, Emijrp, Hannes Röst, NEON ja, Origamiemensch, Splette, Tolanor, 6 anonymous edits

**Image:FISH 13 21.jpg** *Source*: http://en.wikipedia.org/w/index.php?title=File:FISH_13_21.jpg *License*: Public Domain *Contributors*: Gregor1976

**Image:Yeast membrane proteins.jpg** *Source*: http://en.wikipedia.org/w/index.php?title=File:Yeast_membrane_proteins.jpg *License*: Creative Commons Attribution 2.5 *Contributors*: User:Masur

**File:Expression of Human Wild-Type and P239S Mutant Palladin.png** *Source*: http://en.wikipedia.org/w/index.php?title=File:Expression_of_Human_Wild-Type_and_P239S_Mutant_Palladin.png *License*: unknown *Contributors*: see above

**File:Bloodcell sun flares pathology.jpeg** *Source*: http://en.wikipedia.org/w/index.php?title=File:Bloodcell_sun_flares_pathology.jpeg *License*: Public Domain *Contributors*: Birindand, Karelj, NEON ja, 1 anonymous edits

**Image:Linearly_pol.png** *Source*: http://en.wikipedia.org/w/index.php?title=File:Linearly_pol.png *License*: Public Domain *Contributors*: RASnyder

**Image:Circularly_pol.png** *Source*: http://en.wikipedia.org/w/index.php?title=File:Circularly_pol.png *License*: Public Domain *Contributors*: RASnyder

**Image:Electric Vectors 1.png** *Source*: http://en.wikipedia.org/w/index.php?title=File:Electric_Vectors_1.png *License*: unknown *Contributors*: BokicaK, Pieter Kuiper

**Image:Ethylene.svg** *Source*: http://en.wikipedia.org/w/index.php?title=File:Ethylene.svg *License*: Public Domain *Contributors*: User:Bryan Derksen

**File:Symmetrical stretching.gif** *Source*: http://en.wikipedia.org/w/index.php?title=File:Symmetrical_stretching.gif *License*: Public Domain *Contributors*: Tiago Becerra Paolini, 2 anonymous edits

**File:Asymmetrical stretching.gif** *Source*: http://en.wikipedia.org/w/index.php?title=File:Asymmetrical_stretching.gif *License*: Public Domain *Contributors*: Tiago Becerra Paolini

**File:Scissoring.gif** *Source*: http://en.wikipedia.org/w/index.php?title=File:Scissoring.gif *License*: Public Domain *Contributors*: Tiago Becerra Paolini

**File:Twisting.gif** *Source*: http://en.wikipedia.org/w/index.php?title=File:Twisting.gif *License*: Public Domain *Contributors*: Tiago Becerra Paolini

**File:Wagging.gif** *Source*: http://en.wikipedia.org/w/index.php?title=File:Wagging.gif *License*: Public Domain *Contributors*: Tiago Becerra Paolini

**File:Agitation moléculaire en milieu aqueux.PNG** *Source*: http://en.wikipedia.org/w/index.php?title=File:Agitation_moléculaire_en_milieu_aqueux.PNG *License*: Creative Commons Attribution-Sharealike 3.0 *Contributors*: User:H'arnet

**File:GeneticCode21.svg** *Source*: http://en.wikipedia.org/w/index.php?title=File:GeneticCode21.svg *License*: unknown *Contributors*: Original uploader was Kosigrim at en.wikipedia

**File:Monosodium-glutamate.png** *Source*: http://en.wikipedia.org/w/index.php?title=File:Monosodium-glutamate.png *License*: GNU Free Documentation License *Contributors*: Cacycle, Leyo, Rob Hooft, Samulili

**File:H-Gly-Ala-OH.jpg** *Source*: http://en.wikipedia.org/w/index.php?title=File:H-Gly-Ala-OH.jpg *License*: Creative Commons Attribution-Sharealike 2.5 *Contributors*: Csatazs

**File:Zuiterrionball.svg** *Source*: http://en.wikipedia.org/w/index.php?title=File:Zuiterrionball.svg *License*: Public Domain *Contributors*: user:YassineMrabet

**File:Peptidformationball.svg** *Source*: http://en.wikipedia.org/w/index.php?title=File:Peptidformationball.svg *License*: Public Domain *Contributors*: Karol007, Marek M, PatríciaR, Rocket000, YassineMrabet, 2 anonymous edits

**File:Aa structure function.svg** *Source*: http://en.wikipedia.org/w/index.php?title=File:Aa_structure_function.svg *License*: Public Domain *Contributors*: Jonathan

**File:Protein Dynamics Cytochrome C 2NEW smaller.gif** *Source*: http://en.wikipedia.org/w/index.php?title=File:Protein_Dynamics_Cytochrome_C_2NEW_smaller.gif *License*: GNU Free Documentation License *Contributors*: Original uploader was Zephyris at en.wikipedia

**File:Protein-primary-structure.png** *Source*: http://en.wikipedia.org/w/index.php?title=File:Protein-primary-structure.png *License*: Public Domain *Contributors*: National Human Genome Research Institute (NHGRI)

**File:Lysozyme crystal1.JPG** *Source*: http://en.wikipedia.org/w/index.php?title=File:Lysozyme_crystal1.JPG *License*: Creative Commons Attribution-Sharealike 2.0 *Contributors*: Chrumps, Lode

**File:1ezg Tenebrio molitor.png** *Source*: http://en.wikipedia.org/w/index.php?title=File:1ezg_Tenebrio_molitor.png *License*: GNU Free Documentation License *Contributors*: Original uploader was WillowW at en.wikipedia

**File:Concanavalin A.png** *Source*: http://en.wikipedia.org/w/index.php?title=File:Concanavalin_A.png *License*: Public Domain *Contributors*: User:Lijealso

**File:Porin.qutemol.ao.png** *Source*: http://en.wikipedia.org/w/index.php?title=File:Porin.qutemol.ao.png *License*: Creative Commons Attribution-Sharealike 2.5 *Contributors*: ALoopingIcon

**File:Sucrose porin 1a0s.png** *Source*: http://en.wikipedia.org/w/index.php?title=File:Sucrose_porin_1a0s.png *License*: GNU Free Documentation License *Contributors*: Opabinia regalis

**File:Sucrose specific porin 1A0S.png** *Source*: http://en.wikipedia.org/w/index.php?title=File:Sucrose_specific_porin_1A0S.png *License*: GNU Free Documentation License *Contributors*: Snow64

**File:StrictosidineSynthase.png** *Source*: http://en.wikipedia.org/w/index.php?title=File:StrictosidineSynthase.png *License*: Creative Commons Attribution-Sharealike 3.0 *Contributors*: User:Hannes Röst

**File:Calmodulin 1CLL.png** *Source*: http://en.wikipedia.org/w/index.php?title=File:Calmodulin_1CLL.png *License*: Public Domain *Contributors*: Joolz, Lateiner, LeaMaimone, Lode, 1 anonymous edits

**File:Haemoglobin-3D-ribbons.png** *Source*: http://en.wikipedia.org/w/index.php?title=File:Haemoglobin-3D-ribbons.png *License*: Public Domain *Contributors*: Benjah-bmm27, Ephemeronium, Grafite

**File:Hemoglobin t-r state ani.gif** *Source*: http://en.wikipedia.org/w/index.php?title=File:Hemoglobin_t-r_state_ani.gif *License*: GNU Free Documentation License *Contributors*: User:Habj

**File:Clostridium perfringens Alpha Toxin Rotate.rsh.gif** *Source*: http://en.wikipedia.org/w/index.php?title=File:Clostridium_perfringens_Alpha_Toxin_Rotate.rsh.gif *License*: Public Domain *Contributors*: Ramin Herati

**File:Bcl-2 Family.jpg** *Source*: http://en.wikipedia.org/w/index.php?title=File:Bcl-2_Family.jpg *License*: unknown *Contributors*: Hoffmeier

**File:Bcl-2 3D.jpg** *Source*: http://en.wikipedia.org/w/index.php?title=File:Bcl-2_3D.jpg *License*: GNU Free Documentation License *Contributors*: CN3D

**File:PBB Protein THPO image.jpg** *Source*: http://en.wikipedia.org/w/index.php?title=File:PBB_Protein_THPO_image.jpg *License*: Public Domain *Contributors*: www.pdb.org

**File:Bence Jones Protein MLE1.jpg** *Source*: http://en.wikipedia.org/w/index.php?title=File:Bence_Jones_Protein_MLE1.jpg *License*: Public Domain *Contributors*: Alex McPherson, University of California, Irvine

**File:Duck Delta 1 Crystallin.jpg** *Source*: http://en.wikipedia.org/w/index.php?title=File:Duck_Delta_1_Crystallin.jpg *License*: Public Domain *Contributors*: Ragesoss

**File:Michelson-morley.png** *Source*: http://en.wikipedia.org/w/index.php?title=File:Michelson-morley.png *License*: GNU Free Documentation License *Contributors*: user:bighead

**File:Interferometer.JPG** *Source*: http://en.wikipedia.org/w/index.php?title=File:Interferometer.JPG *License*: Creative Commons Attribution-Sharealike 3.0 *Contributors*: User:Brews ohare

**File:Michelson interferometer schematic.png** *Source*: http://en.wikipedia.org/w/index.php?title=File:Michelson_interferometer_schematic.png *License*: GNU Free Documentation License *Contributors*: Teebeutel

**File:IR spectroscopy apparatus.jpg** *Source*: http://en.wikipedia.org/w/index.php?title=File:IR_spectroscopy_apparatus.jpg *License*: GNU Free Documentation License *Contributors*: Ewen, Matthias M., Pieter Kuiper

**File:IR spectrometer.jpg** *Source*: http://en.wikipedia.org/w/index.php?title=File:IR_spectrometer.jpg *License*: Public Domain *Contributors*: S.Levchenkov

**File:Michelson Interferometer.jpg** *Source*: http://en.wikipedia.org/w/index.php?title=File:Michelson_Interferometer.jpg *License*: unknown *Contributors*: Falcorian, Juiced lemon, Teebeutel

**File:Ir hcl rot-vib mrtz.svg** *Source*: http://en.wikipedia.org/w/index.php?title=File:Ir_hcl_rot-vib_mrtz.svg *License*: Creative Commons Attribution-Sharealike 2.5 *Contributors*: mrtz

**File:BandeIR.png** *Source*: http://en.wikipedia.org/w/index.php?title=File:BandeIR.png *License*: GNU Free Documentation License *Contributors*: User:Grimlock

**File:Michelsoninterferometer.jpg** *Source*: http://en.wikipedia.org/w/index.php?title=File:Michelsoninterferometer.jpg *License*: unknown *Contributors*: Juiced lemon, Skygazer, Tano4595, Teebeutel, Umherirrender, Xorx

**File:Michelson couleur.jpg** *Source*: http://en.wikipedia.org/w/index.php?title=File:Michelson_couleur.jpg *License*: Creative Commons Attribution-Sharealike 2.5 *Contributors*: NicoB, Teebeutel

**File:Bismuthine-2D-IR-MMW-dimensions.png** *Source*: http://en.wikipedia.org/w/index.php?title=File:Bismuthine-2D-IR-MMW-dimensions.png *License*: Public Domain *Contributors*: Ben Mills

**File:Infrared spectrometer.jpg** *Source*: http://en.wikipedia.org/w/index.php?title=File:Infrared_spectrometer.jpg *License*: GNU Free Documentation License *Contributors*: ishikawa

**Image:Raman energy levels.svg** *Source*: http://en.wikipedia.org/w/index.php?title=File:Raman_energy_levels.svg *License*: Creative Commons Attribution-Sharealike 3.0 *Contributors*: User:Moxfyre

**Image:MRO HiRISE.jpg** *Source*: http://en.wikipedia.org/w/index.php?title=File:MRO_HiRISE.jpg *License*: Public Domain *Contributors*: Bricktop

**Image:MRO-First Image-crop.jpg** *Source*: http://en.wikipedia.org/w/index.php?title=File:MRO-First_Image-crop.jpg *License*: Public Domain *Contributors*: Bryan Derksen, Conscious, Wisi

**Image:Hirise at mars.jpg** *Source*: http://en.wikipedia.org/w/index.php?title=File:Hirise_at_mars.jpg *License*: Public Domain *Contributors*: JPG-GR, Shell Kinney, Tuvas

**Image:Aureum Chaos wide context.JPG** *Source*: http://en.wikipedia.org/w/index.php?title=File:Aureum_Chaos_wide_context.JPG *License*: Public Domain *Contributors*: Jim Secosky modified nasa image

**Image:Aureum Chaos wide view.JPG** *Source*: http://en.wikipedia.org/w/index.php?title=File:Aureum_Chaos_wide_view.JPG *License*: Public Domain *Contributors*: Jim Secosky modified nasa image.

**Image:Aureum Chaos HiWish.JPG** *Source*: http://en.wikipedia.org/w/index.php?title=File:Aureum_Chaos_HiWish.JPG *License*: Public Domain *Contributors*: Jim Secosky modified nasa image.

**Image:Lobate feature with hiwish.JPG** *Source*: http://en.wikipedia.org/w/index.php?title=File:Lobate_feature_with_hiwish.JPG *License*: Public Domain *Contributors*: Jim Secosky modified nasa image

**Image:MRO HiRISE comparison.jpg** *Source*: http://en.wikipedia.org/w/index.php?title=File:MRO_HiRISE_comparison.jpg *License*: Public Domain *Contributors*: Bricktop

**Image:The Earth and the Moon photographed from Mars orbit.jpg** *Source*: http://en.wikipedia.org/w/index.php?title=File:The_Earth_and_the_Moon_photographed_from_Mars_orbit.jpg *License*: Public Domain *Contributors*: NASA/JPL-Caltech/University of Arizona

**Image:SCEM.JPG** *Source*: http://en.wikipedia.org/w/index.php?title=File:SCEM.JPG *License*: Creative Commons Attribution-Sharealike 3.0 *Contributors*: User:Materialscientist

**Image:C60a.png** *Source*: http://en.wikipedia.org/w/index.php?title=File:C60a.png *License*: GNU Free Documentation License *Contributors*: Original uploader was Mstroeck at en.wikipedia Later versions were uploaded by Bryn C at en.wikipedia.

**Image:Atomic resolution Au100.JPG** *Source*: http://en.wikipedia.org/w/index.php?title=File:Atomic_resolution_Au100.JPG *License*: Public Domain *Contributors*: Erwinrossen, Filnik, Liftarn, Mormegil, Nemissimo, Pieter Kuiper, WikipediaMaster, 7 anonymous edits

**Image:Rotaxane cartoon.jpg** *Source*: http://en.wikipedia.org/w/index.php?title=File:Rotaxane_cartoon.jpg *License*: GNU Free Documentation License *Contributors*: Original uploader was M Stone at en.wikipedia Later versions were uploaded by M stone at en.wikipedia.

**File:Sarfus.DNABiochip.jpg** *Source*: http://en.wikipedia.org/w/index.php?title=File:Sarfus.DNABiochip.jpg *License*: Creative Commons Attribution-Sharealike 3.0 *Contributors*: Nanolane

**Image:Achermann7RED.jpg** *Source*: http://en.wikipedia.org/w/index.php?title=File:Achermann7RED.jpg *License*: Public Domain *Contributors*: Marc Achermann

**Image:AFMsetup.jpg** *Source*: http://en.wikipedia.org/w/index.php?title=File:AFMsetup.jpg *License*: Creative Commons Attribution 2.5 *Contributors*: Kristian Mølhave

**Image:Threshold_formation.gif** *Source*: http://en.wikipedia.org/w/index.php?title=File:Threshold_formation.gif *License*: Public Domain *Contributors*: Saumitra R Mehrotra & Gerhard Klimeck

**Image:Selfassembly Organic Semiconductor Trixler LMU.jpg** *Source*: http://en.wikipedia.org/w/index.php?title=File:Selfassembly_Organic_Semiconductor_Trixler_LMU.jpg *License*: Creative Commons Attribution-Sharealike 3.0 *Contributors*: Frank Trixler; adapted from LMU/CeNS: Organic Semiconductor Nanostructures

**Image:ECAT-Exact-HR--PET-Scanner.jpg** *Source*: http://en.wikipedia.org/w/index.php?title=File:ECAT-Exact-HR--PET-Scanner.jpg *License*: Public Domain *Contributors*: Jens Langner (http://www.jens-langner.de/)

**File:16slicePETCT.jpg** *Source*: http://en.wikipedia.org/w/index.php?title=File:16slicePETCT.jpg *License*: Public Domain *Contributors*: User:Hg6996

**Image:PET-detectorsystem 2.png** *Source*: http://en.wikipedia.org/w/index.php?title=File:PET-detectorsystem_2.png *License*: Public Domain *Contributors*: User:Kjkolb

**Image:PET-schema.png** *Source*: http://en.wikipedia.org/w/index.php?title=File:PET-schema.png *License*: Public Domain *Contributors*: Jens Langner (http://www.jens-langner.de/)

**File:Viewer medecine nucleaire keosys.JPG** *Source*: http://en.wikipedia.org/w/index.php?title=File:Viewer_medecine_nucleaire_keosys.JPG *License*: Public Domain *Contributors*: User:Mco44

**Image:PET-MR2-Head-Keosys.JPG** *Source*: http://en.wikipedia.org/w/index.php?title=File:PET-MR2-Head-Keosys.JPG *License*: Public Domain *Contributors*: User:Mco44

**Image:PET-MIPS-anim.gif** *Source*: http://en.wikipedia.org/w/index.php?title=File:PET-MIPS-anim.gif *License*: Public Domain *Contributors*: Jens Langner (http://www.jens-langner.de/)

**Image:PET-image.jpg** *Source*: http://en.wikipedia.org/w/index.php?title=File:PET-image.jpg *License*: Public Domain *Contributors*: Jens Langner (http://www.jens-langner.de/)

# License